

**Development of synthetic strategies towards libraries
of heterocyclic and bicyclic inhibitors of Cdc25A
&
Development of solid phase synthesis of cyclic peptides**

Von der Naturwissenschaftlichen Fakultät der
Gottfried Wilhelm Leibniz Universität Hannover

zur Erlangung des Grades

Doktor der Naturwissenschaften (Dr. rer. nat.)

genehmigte Dissertation

von

Dipl.-Chem. Hao Luo

geboren am 15.06.1982 in Chongqing, China

[2015]

Referent: Prof. Dr. Markus Kalesse

Korreferent: Prof. Dr. Andreas Kirschning

Tag der Promotion: 19.05.2015

Abstract (english)

Hao Luo

Development of synthetic strategies for libraries of heterocyclic and bicyclic inhibitors of Cdc25A

&

Development of solid phase synthesis of cyclic peptides

Key words: Cdc25A, Hantzsch pyrrole synthesis, Hantzsch thiazole synthesis, Paar-Knorr pyrrole synthesis, 1,3-dipolar cycloaddition, Native chemical ligation (NCL), cysteine, Fmoc solid phase peptide synthesis (Fmoc-SPPS), latent thioester linker, cyclization.

Cdc25A is a phosphatase, which is treated as a novel target for tumor therapy. Dr. R. Frank and Dr. I. Hoffmann recently proposed lead structures of two new Cdc25A inhibitors, which were acquired from combinatorial chemical methods. The detailed SAR studies of these new Cdc25A inhibitors have to be done in order to elucidate the mode of action. For the SAR studies, in this work, a library containing a large number of Cdc25A inhibitor derivatives is accessed by conventional organic chemical methods. The synthesis of these heterocyclic Cdc25A inhibitors consists of two major steps: formation of the thiazole from an α -halo ketone and a thioamide through a classical Hantzsch thiazole synthesis and the conjugated pyrrole ring was formed either by a modified Hantzsch pyrrole synthesis or by classical Paal-Knorr pyrrole synthesis. The important pyrrolidine ring system of the lead structure of the bicyclic Cdc25A inhibitor was straightforwardly constructed by a 1,3-dipolar cycloaddition from the north fragment and the south fragment.

Native chemical ligation is a method, which joins two peptides through an amide bond between an N-terminal cysteine and a C-terminal amino acid without any coupling reagents. The C-terminal peptide thioester, which is required for NCL, could be synthesized exclusively by the Boc-SPPS method, but utilization of this method is relatively inconvenient. Unfortunately, the C-terminal peptide thioester is not accessible by the Fmoc-SPPS. To apply the Fmoc-SPPS anyway, in this work, a latent thioester linker strategy was used. The C-terminal peptide ester, which contains a special linker, was prepared by Fmoc-SPPS. This special linker allows the C-terminal thioester to be formed *in situ* from the C-terminal peptide ester precursor and facilitates the NCL transformation. A few linear model sequences containing the latent thioester linker were prepared in this work, followed by the study of on-resin NCL-cyclization of these linear model sequences. After initial investigations, some important factors, which manipulate the quality of the NCL cyclization, were identified. So far, the overall yield of model reactions were generally poor and thus further studies and optimizations are necessary.

Kurzfassung (Deutsch)

Hao Luo

Entwicklung von Synthesestrategien für Bibliotheken von heterocyclischen und bicyclischen Cdc25A-Inhibitoren

&

Entwicklung der Festphasensynthese der cyclischen Peptide

Schlagworte: Cdc25A, Hantzsch-Pyrrol-Synthese, Hantzsch-Thioazol-Synthese, Paal-Knorr-Pyrrol-Synthese, 1,3-dipolare Cycloaddition, Native chemical ligation (NCL), Cystein, Fmoc-Festphasenpeptidsynthese (Fmoc-SPPS), latente Thioester-Linker, Cyclisierung.

Das Cdc25A ist eine Phosphatase, welche wird seit Jahrzehnten als neues Target für die Tumorthherapie intensiv erforscht. Vor kurzer Zeit wurden zwei neue Leitstrukturen von Cdc25A-Inhibitoren von Dr. R. Frank und Dr. I. Hoffmann vorgeschlagen. Die Leitstrukturen sind frisch aus den kombinatorischen chemischen Methoden erworben, daher muss die SAR-Studie von Cdc25A-Inhibitoren noch durchgeführt werden, damit der Wirkungsmechanismus aufgeklärt werden kann. Für die SAR-Studie, in dieser Arbeit wird die Bibliothek, welche eine große Anzahl von Cdc25A-Inhibitor-Derivaten umfasst, durch herkömmliche organisch-chemische Methoden zugänglich gemacht. Die Synthese von heterocyclischen Cdc25A-Inhibitoren besteht aus zwei Hauptschritten: die Bildung des Thiazols sollte aus einem α -Halogen-Keton und einem Thioamid über eine klassische Hantzsch-Thiazol-Synthese dargestellt werden. Danach wurde der konjugierte Pyrrol-Ring entweder durch eine modifizierte Hantzsch-Pyrrol-Synthese oder durch die klassische Paal-Knorr-Pyrrol-Synthese gebildet. Das wichtige Pyrrolidin-Ringsystem von der Leitstruktur des bicyclischen Cdc25A-Inhibitors konnte problemlos durch eine 1,3-dipolare Cycloaddition aus Nordhälfte und Südhälfte konstruiert werden.

Die Native Chemical Ligation ist eine Methode, die zwei Peptide durch eine Amidbindung zwischen einem N-terminalen Cystein und einer beliebigen C-terminalen Aminosäure ohne Kupplungsreagenzien kuppl. Der für die NCL benötigte C-terminale Peptidthioester könnte ausschließlich durch die relativ unbequeme Boc-SPPS Methode synthetisiert werden. Um die Fmoc-Festphasenpeptidsynthese anzuwenden, wurde in dieser Arbeit eine latente Thioester-Linker-Strategie verwendet. Der C-terminale Peptidester wurde durch die Fmoc-SPPS dargestellt. Dieser C-terminale Peptidester enthält einen speziellen Linker, welcher den C-terminalen Peptidthioester *in situ* bildet, um die NCL zu ermöglichen. Durch die Fmoc-SPPS-Methode wurden einige Model-Sequenzen dargestellt, welche auch den latenten Thioester-Linker enthielten. Danach erfolgte die Untersuchung der NCL-Cyclisierung auf dem Harz der verschiedenen linearen Peptide. Nach den anfänglichen Untersuchungen wurden einige wichtigen Faktoren festgestellt. Weitere Studien und Optimierungen zur Erhöhung der bisher generell sehr niedrigen Ausbeuten sind nötig.

Table of Contents

A. Theoretical part

Part I. Development of synthetic strategies for libraries of heterocyclic and bicyclic inhibitors of Cdc25A.....	16
1. Introduction.....	16
1.1 Heterocyclic compounds.....	16
1.1.1 Notable 5-membered heterocyclic compounds.....	17
1.1.2 Notable 6-membered heterocyclic compounds.....	19
1.1.3 Heterocyclic compounds in medicinal field.....	20
1.2 Combinatorial chemistry in the drug discovery.....	21
1.2.2 Discovery of the lead structure through the combinatorial chemistry.....	24
1.2.3 Structure-activity relationship (SAR) study.....	25
1.2.4 Quantitative structure-activity relationship (QSAR).....	27
1.3 Cancer and the Cdc25s inhibitors.....	27
2. The retro synthetic analysis and the design of the synthetic route.....	32
2.1 Retro synthetic analysis of the heterocyclic inhibitor.....	32
2.1.1 The initial synthetic plan of the heterocyclic inhibitor.....	32
2.1.2 An alternative synthetic plan for the heterocyclic inhibitor.....	34
2.2. The retro synthetic analysis of the bicyclic inhibitor.....	35
2.2.1 The synthetic plan of the bicyclic inhibitor.....	35
2.3. Outline of the construction of further derivatives.....	37
2.3.1 Derivatization of heterocyclic inhibitor.....	37
3. Results and discussion.....	39
3.1 Commencing with the initial plan toward the heterocyclic inhibitor.....	39
3.1.1 Synthesis of 5	39
3.1.2 Synthesis of thiophene-2-carbothioamide (6).....	39
3.1.3 Synthesis of 1-(2-(thiophene-2-yl)thiazol-4-yl)ethanone (9).....	39
3.1.4 Synthesis of 2-bromo-1-(2-(thiophen-2-yl)thiazol-4-yl)ethanone (2).....	40
3.2 Change of the tactic.....	40
3.2.1 Synthesis of dibrominediketone 10	41
3.2.2 The second approach towards 2-bromo-1-(2-(thiophene-2-yl)thiazol-4-yl)ethanone (2)...	41
3.2.3 The synthesis of (Z)-ethyl 3-((tetrahydrofuran-2-yl)methylamino)but-2-enoate (12).....	41
3.2.4 The synthesis of ethyl 2-methyl-1-((tetrahydrofuran-2-yl)methyl)-5-(2-(thiophene-2-yl)thiazol-4-yl)-1H-pyrrole-3-carboxylate (13).....	42

3.2.5 The final steps toward the lead structure 19	43
3.2.6 The synthesis of various amides derived from 19	43
3.3 The alternative route to achieve the pyrrole ring	44
3.3.1 The synthesis of 1,4-diolester 14	44
3.3.2 The approach to 13 through the Paal-Knorr synthesis	44
3.3.3 The generation of pyrrol with different substitutions	45
3.3.4 From the intermediates 15 and 16 to the final products	46
3.4 Extension of the library by derivatization on designated positions	46
3.4.1 Derivatization of the far right end with other heterocyclic compounds.....	46
3.4.2. Derivatization at the 5 position in the pyrrole ring system.....	50
3.4.3 Supplement of the library through further N-substituted pyrrole derivatives	55
3.5 Synthesis of the bicyclic compounds and its derivatives	58
3.5.1 Synthesis of the lead structure of the bicyclic compounds	58
3.5.2 Derivatization at the <i>para</i> -position of the aniline.....	58
4. Summary and conclusion.....	64

Part II. Development of solid phase synthesis of cyclic peptides 66

1 Introduction.....	66
1.1 Conventional and native chemical ligation methods of peptide synthesis.....	66
1.1.1 Conventional methods of peptide synthesis	66
1.1.2 Native chemical ligation (NCL).....	68
1.2 Development of the solid phase peptide synthesis (SPPS)	72
1.2.1 Development of the Merrifield resin	72
1.2.2 Development of more advanced resins and methods	74
1.3 Latent thioester linker strategy.....	78
1.3.1 O to S acyl transfer	79
1.3.2 N to S acyl transfer	80
1.4 NCL cyclization in solution and solid phase.....	81
1.5 Polymeric support.....	83
2. Plan for the prove-of-concept on-resin NCL cyclization study	86
2.1 Motivation of development of the methodology.....	86
2.2 Cyclization through on-resin Native Chemical Ligation	88
2.3 Choice of proper polymeric support and sulfhydryl protecting group.....	89
3. Results and discussion.....	92

3.1 Organic synthetic chemistry.....	92
3.1.1 Initial attempt of generation of the latent thioester linker 4	92
3.1.2 Attempt of formation of depsi-peptide building block 6 in solution.....	94
3.1.3. First attempt of generation of the sequence 10 through Fmoc-SPPS.....	95
3.1.4 Modification of the linker 4 and repeating of the Fmoc-SPPS.....	100
3.2 Investigation of solution phase NCL cyclization.....	103
3.2.1 Investigation of solution phase NCL cyclization of 14	103
3.2.2 Modification of the sequence 14 and investigation of the new sequence 16	107
3.2.3 Investigation of CWSSL 16 with alternating stereochemistry.....	109
3.2.5 Investigation of solution phase NCL cyclization of 16 with thiol additive.....	110
3.2.6 Reinvestigation of the solution phase NCL cyclization of 14 at low temperatures.....	111
3.2.6 Shift of the investigation subject to the sequence 19	112
3.2.7 Determination of the ideal TCEP concentration in the buffer mixture.....	115
3.2.8 Investigation of solution phase NCL cyclization of 20	116
3.3 Investigation of on-resin NCL cyclization.....	117
3.3.1 On-resin NCL cyclization of fully protected sequence 21	117
3.3.2 Investigation of on-resin NCL cyclization of sequence 19	119
3.3.3 Investigation of on-resin NCL cyclization of further model sequences.....	121
4. Summary and outlook.....	134

B. Experimental section

Experimental section.....	138
Part I. Development of synthetic strategies for libraries of heterocyclic and bicyclic inhibitors Cdc25A.....	138
1 General details.....	138
2 Synthesis of the lead structure 13 and its amide derivatives 20 and 21 through Hantzsch method.....	140
2.1. 1,4-dibromobutane-2,3-dione (10).....	140
2.2 Thiophene-2-carbothioamide (6).....	140
2.3. 2-bromo-1-(2-(thiophen-2-yl)thiazol-4-yl)ethanone (2).....	141
2.4 (Z)-ethyl 3-(((tetrahydrofuran-2-yl)methyl)amino)but-2-enoate (12).....	142
2.5 Ethyl 2-methyl-1-((tetrahydrofuran-2-yl)methyl)-5-(2-(thiophen-2-yl)thiazol-4-yl)-1H-pyrrole-3-carboxylate (13).....	143
2.6 2-methyl-1-((tetrahydrofuran-2-yl)methyl)-5-(2-(thiophen-2-yl)thiazol-4-yl)-1H-pyrrole-3-carboxylic acid (18).....	144

2.7 2-methyl-1-((tetrahydrofuran-2-yl)methyl)-5-(2-(thiophen-2-yl)thiazol-4-yl)-1H-pyrrole-3-carboxamide (19).....	144
2.8 <i>N</i> ,2-dimethyl-1-((tetrahydrofuran-2-yl)methyl)-5-(2-(thiophen-2-yl)thiazol-4-yl)-1H-pyrrole-3-carboxamide (20)	145
2.9 <i>N,N</i> ,2-trimethyl-1-((tetrahydrofuran-2-yl)methyl)-5-(2-(thiophen-2-yl)thiazol-4-yl)-1H-pyrrole-3-carboxamide (21)	146
3 Syntheses of <i>N</i> -substituted pyrrole derivatives through the Paar-Knorr pyrrole synthesis route	147
3.1 Ethyl 2-acetyl-4-oxo-4-(2-(thiophen-2-yl)thiazol-4-yl)butanoate (14).....	147
General procedure of generation of <i>N</i> -substituted pyrrole derivatives.....	148
3.2 Ethyl 2-methyl-1-((tetrahydrofuran-2-yl)methyl)-5-(2-(thiophen-2-yl)thiazol-4-yl)-1H-pyrrole-3-carboxylate (13)	148
3.3 Ethyl 1-benzyl-2-methyl-5-(2-(thiophen-2-yl)thiazol-4-yl)-1H-pyrrole-3-carboxylate (15)...	149
3.4 Ethyl 1-(3-fluoro-4-methylphenyl)-2-methyl-5-(2-(thiophen-2-yl)thiazol-4-yl)-1H-pyrrole-3-carboxylate (16).....	149
3.5 Ethyl 1-(2-fluorophenyl)-2-methyl-5-(2-(thiophen-2-yl)thiazol-4-yl)-1H-pyrrole-3-carboxylate (51)	150
3.6 Ethyl 1-(3-fluorophenyl)-2-methyl-5-(2-(thiophen-2-yl)thiazol-4-yl)-1H-pyrrole-3-carboxylate (52).....	151
3.7 Ethyl 1-(4-fluorophenyl)-2-methyl-5-(2-(thiophen-2-yl)thiazol-4-yl)-1H-pyrrole-3-carboxylate (53).....	152
3.8 Ethyl 1-(2-methoxyphenyl)-2-methyl-5-(2-(thiophen-2-yl)thiazol-4-yl)-1H-pyrrole-3-carboxylate (54).....	152
3.9 Ethyl 1-(3-methoxyphenyl)-2-methyl-5-(2-(thiophen-2-yl)thiazol-4-yl)-1H-pyrrole-3-carboxylate (55).....	153
3.10 Ethyl 1-(4-methoxyphenyl)-2-methyl-5-(2-(thiophen-2-yl)thiazol-4-yl)-1H-pyrrole-3-carboxylate (56).....	154
3.11 Ethyl 1-(3-fluorobenzyl)-2-methyl-5-(2-(thiophen-2-yl)thiazol-4-yl)-1H-pyrrole-3-carboxylate (57).....	154
3.12 Ethyl 1-(4-fluorobenzyl)-2-methyl-5-(2-(thiophen-2-yl)thiazol-4-yl)-1H-pyrrole-3-carboxylate (58).....	155
3.13 1-benzyl-2-methyl-5-(2-(thiophen-2-yl)thiazol-4-yl)-1H-pyrrole-3-carboxylic acid (15')....	156
3.14 1-(3-fluoro-4-methylphenyl)-2-methyl-5-(2-(thiophen-2-yl)thiazol-4-yl)-1H-pyrrole-3-carboxylic acid (16')	156
3.15 1-(2-fluorophenyl)-2-methyl-5-(2-(thiophen-2-yl)thiazol-4-yl)-1H-pyrrole-3-carboxylic acid (51')	156
3.16 1-(3-fluorophenyl)-2-methyl-5-(2-(thiophen-2-yl)thiazol-4-yl)-1H-pyrrole-3-carboxylic acid (52')	157

3.17 1-(4-fluorophenyl)-2-methyl-5-(2-(thiophen-2-yl)thiazol-4-yl)-1 <i>H</i> -pyrrole-3-carboxylic acid (53')	157
3.18 1-(2-methoxyphenyl)-2-methyl-5-(2-(thiophen-2-yl)thiazol-4-yl)-1 <i>H</i> -pyrrole-3-carboxylic acid (54')	157
3.19 1-(3-methoxyphenyl)-2-methyl-5-(2-(thiophen-2-yl)thiazol-4-yl)-1 <i>H</i> -pyrrole-3-carboxylic acid (55')	158
3.20 1-(4-methoxyphenyl)-2-methyl-5-(2-(thiophen-2-yl)thiazol-4-yl)-1 <i>H</i> -pyrrole-3-carboxylic acid (56')	158
3.21 1-(3-fluorobenzyl)-2-methyl-5-(2-(thiophen-2-yl)thiazol-4-yl)-1 <i>H</i> -pyrrole-3-carboxylic acid (57')	158
3.22 1-(4-fluorobenzyl)-2-methyl-5-(2-(thiophen-2-yl)thiazol-4-yl)-1 <i>H</i> -pyrrole-3-carboxylic acid (58')	159
3.23 1-benzyl-2-methyl-5-(2-(thiophen-2-yl)thiazol-4-yl)-1 <i>H</i> -pyrrole-3-carboxamide (23)	159
3.24 1-(3-fluoro-4-methylphenyl)-2-methyl-5-(2-(thiophen-2-yl)thiazol-4-yl)-1 <i>H</i> -pyrrole-3-carboxamide (24)	160
3.25 1-(2-fluorophenyl)-2-methyl-5-(2-(thiophen-2-yl)thiazol-4-yl)-1 <i>H</i> -pyrrole-3-carboxamide (59)	161
3.26 1-(3-fluorophenyl)- <i>N</i> ,2-dimethyl-5-(2-(thiophen-2-yl)thiazol-4-yl)-1 <i>H</i> -pyrrole-3-carboxamide (60)	161
3.27 1-(4-fluorophenyl)-2-methyl-5-(2-(thiophen-2-yl)thiazol-4-yl)-1 <i>H</i> -pyrrole-3-carboxamide (63)	162
3.28 1-(4-fluorophenyl)- <i>N</i> ,2-dimethyl-5-(2-(thiophen-2-yl)thiazol-4-yl)-1 <i>H</i> -pyrrole-3-carboxamide (64)	163
3.29 1-(2-methoxyphenyl)-2-methyl-5-(2-(thiophen-2-yl)thiazol-4-yl)-1 <i>H</i> -pyrrole-3-carboxamide (65)	164
3.30 1-(2-methoxyphenyl)- <i>N</i> ,2-dimethyl-5-(2-(thiophen-2-yl)thiazol-4-yl)-1 <i>H</i> -pyrrole-3-carboxamide (66)	164
3.31 1-(3-methoxyphenyl)-2-methyl-5-(2-(thiophen-2-yl)thiazol-4-yl)-1 <i>H</i> -pyrrole-3-carboxamide (67)	165
3.32 1-(3-methoxyphenyl)- <i>N</i> ,2-dimethyl-5-(2-(thiophen-2-yl)thiazol-4-yl)-1 <i>H</i> -pyrrole-3-carboxamide (68)	166
3.33 1-(4-methoxyphenyl)-2-methyl-5-(2-(thiophen-2-yl)thiazol-4-yl)-1 <i>H</i> -pyrrole-3-carboxamide (69)	166
3.3.4 1-(4-methoxyphenyl)- <i>N</i> ,2-dimethyl-5-(2-(thiophen-2-yl)thiazol-4-yl)-1 <i>H</i> -pyrrole-3-carboxamide (70)	167
3.3.5 1-(3-fluorobenzyl)-2-methyl-5-(2-(thiophen-2-yl)thiazol-4-yl)-1 <i>H</i> -pyrrole-3-carboxamide (71)	168
3.3.6 1-(4-fluorobenzyl)-2-methyl-5-(2-(thiophen-2-yl)thiazol-4-yl)-1 <i>H</i> -pyrrole-3-carboxamide (72)	169

4 Synthesis of the derivative with N-methyl pyrrole on the right side.....	169
4.1 1-methyl-1 <i>H</i> -pyrrole-2-carbothioamide (26)	169
4.2 2-bromo-1-(2-(1-methyl-1 <i>H</i> -pyrrol-2-yl)thiazol-4-yl)ethanone (29).....	170
4.3 Ethyl 2-methyl-5-(2-(1-methyl-1 <i>H</i> -pyrrol-2-yl)thiazol-4-yl)-1-((tetrahydrofuran-2-yl)methyl)-1 <i>H</i> -pyrrole-3-carboxylate (31).....	171
4.4 2-methyl-5-(2-(1-methyl-1 <i>H</i> -pyrrol-2-yl)thiazol-4-yl)-1-((tetrahydrofuran-2-yl)methyl)-1 <i>H</i> -pyrrole-3-carboxylic acid (33)	172
4.5 2-methyl-5-(2-(1-methyl-1 <i>H</i> -pyrrol-2-yl)thiazol-4-yl)-1-((tetrahydrofuran-2-yl)methyl)-1 <i>H</i> -pyrrole-3-carboxamide (35).....	172
4.6 <i>N</i> ,2-dimethyl-5-(2-(1-methyl-1 <i>H</i> -pyrrol-2-yl)thiazol-4-yl)-1-((tetrahydrofuran-2-yl)methyl)-1 <i>H</i> -pyrrole-3-carboxamide (36).....	173
5 Synthesis of derivative with N-methyl indole on the right side.	174
5.1 1-methyl-1 <i>H</i> -indole (27).....	174
5.2 1-methyl-1 <i>H</i> -indole-3-carbothioamide (28).....	175
5.3 2-bromo-1-(2-(1-methyl-1 <i>H</i> -indol-3-yl)thiazol-4-yl)ethanone (30)	175
5.4 Ethyl 2-methyl-5-(2-(1-methyl-3 <i>a</i> ,7 <i>a</i> -dihydro-1 <i>H</i> -indol-3-yl)thiazol-4-yl)-1-((tetrahydrofuran-2-yl)methyl)-1 <i>H</i> -pyrrole-3-carboxylate (32)	176
5.5 2-methyl-5-(2-(1-methyl-3 <i>a</i> ,7 <i>a</i> -dihydro-1 <i>H</i> -indol-3-yl)thiazol-4-yl)-1-((tetrahydrofuran-2-yl)methyl)-1 <i>H</i> -pyrrole-3-carboxylic acid (34)	177
5.6 2-methyl-5-(2-(1-methyl-3 <i>a</i> ,7 <i>a</i> -dihydro-1 <i>H</i> -indol-3-yl)thiazol-4-yl)-1-((tetrahydrofuran-2-yl)methyl)-1 <i>H</i> -pyrrole-3-carboxamide (37).....	177
6 Synthesis of 2-trifluoromethyl pyrrole derivative.	178
6.1 Ethyl 4,4,4-trifluoro-3-oxo-2-(2-oxo-2-(2-(thiophen-2-yl)thiazol-4-yl)ethyl)butanoate (41)	178
6.2 Ethyl 1-((tetrahydrofuran-2-yl)methyl)-5-(2-(thiophen-2-yl)thiazol-4-yl)-2-(trifluoromethyl)-1 <i>H</i> -pyrrole-3-carboxylate (40).....	179
6.3 1-((tetrahydrofuran-2-yl)methyl)-5-(2-(thiophen-2-yl)thiazol-4-yl)-2-(trifluoromethyl)-1 <i>H</i> -pyrrole-3-carboxylic acid (42)	180
6.4 1-((tetrahydrofuran-2-yl)methyl)-5-(2-(thiophen-2-yl)thiazol-4-yl)-2-(trifluoromethyl)-1 <i>H</i> -pyrrole-3-carboxamide (43).....	180
6.5 <i>N</i> -methyl-1-((tetrahydrofuran-2-yl)methyl)-5-(2-(thiophen-2-yl)thiazol-4-yl)-2-(trifluoromethyl)-1 <i>H</i> -pyrrole-3-carboxamide (44).....	181
7 Synthesis of 2-methoxymethyl pyrrole derivative.....	183
7.1 Ethyl 4-methoxy-3-oxo-2-(2-oxo-2-(2-(thiophen-2-yl)thiazol-4-yl)ethyl)butanoate (46)	183
7.2 Ethyl 2-(methoxymethyl)-1-((tetrahydrofuran-2-yl)methyl)-5-(2-(thiophen-2-yl)thiazol-4-yl)-1 <i>H</i> -pyrrole-3-carboxylate (47).....	184
7.3 Ethyl 2-(methoxymethyl)-1-((tetrahydrofuran-2-yl)methyl)-5-(2-(thiophen-2-yl)thiazol-4-yl)-1 <i>H</i> -pyrrole-3-carboxylate (48).....	185

7.4 2-(methoxymethyl)-1-((tetrahydrofuran-2-yl)methyl)-5-(2-(thiophen-2-yl)thiazol-4-yl)-1 <i>H</i> -pyrrole-3-carboxamide (49).....	185
7.5 2-(methoxymethyl)- <i>N</i> -methyl-1-((tetrahydrofuran-2-yl)methyl)-5-(2-(thiophen-2-yl)thiazol-4-yl)-1 <i>H</i> -pyrrole-3-carboxamide (50)	186
8 Synthesis of the lead structure of the bicyclic inhibitor	187
8.1 1-(4-acetylphenyl)-1 <i>H</i> -pyrrole-2,5-dione (75).....	187
8.2 (<i>S,E</i>)-methyl 4-methyl-2-(2-methylbenzylideneamino)pentanoate (78)	188
8.3 (1 <i>S</i>)-methyl 5-(4-acetylphenyl)-1-isobutyl-4,6-dioxo-3- <i>o</i> -tolyl-octahydropyrrolo[3,4- <i>c</i>]pyrrole-1-carboxylate (79)	188
Part II. Development of solid phase synthesis of cyclic peptides	190
1 General details	190
2 Procedure of preparing ion exchange column.....	192
2.1 Preparation of (H ⁺) exchange column.....	192
2.2 Preparation of (CH ₃ COO ⁻) exchange column.....	192
3 Procedure of Kaiser test to determine the free amino groups.....	192
4 Determination of the loading through Fmoc release UV assay	193
5 Preparation of the latent thioester linker 12	193
5.1 2-hydroxy-3-mercaptopropanoic acid (3)	193
5.2 3-(<i>tert</i> -butyldisulfanyl)-2-hydroxypropanoic acid (4)	194
5.3 2-(<i>tert</i> -butyldimethylsilyloxy)-3-(<i>tert</i> -butyldisulfanyl)propanoic acid (12)	195
6 General procedure of loading of the linker 12 onto the Tentagel NH ₂ resin.....	196
7 TBAF deprotection and the coupling of the first amino acid through the esterification	197
8 Post SPPS work-up and deprotection of the various protecting groups	197
9 General procedure of the on-resin NCL cyclization.....	198
9.1 Cyclo Cys-Ser-Ser-Leu-Gly (19')	198
9.2 Cyclo Cys-Ser-Ser-Leu-Phe (20')	199
9.3 Cyclo Cys-Ser-Typ-Leu-Gly (22').....	199
9.4 Cyclo Cys-Ala-Ala-Leu-Gly (24')	200
9.5 Cyclo Cys-Ser-Leu-Leu-Phe-Gly (25').....	201
9.6 Cyclo Cys-Ser-Trp-Leu-Phe-Gly (26').....	202
9.7 Cyclo Cys-Ala-Ala-Ser-Ser-Leu-Gly (27')	203
C. Reference list.....	204
D. Appendix	210

Abbreviation

Å	angstrom (100 pm)	DMG	dimethylglycine
AA	amino acid	DMSO	dimethyl sulfoxide
Ac	acetyl	DKFZ	Deutsches Krebsforschungszentrum
ACN	acetonitrile	Dtt	dithiothreitol
AcOH	acetic acid	EDC	1-ethyl-3-(3-dimethylaminopropyl)carbodiimide
ADMET	Absorption, Distribution, Metabolism and Excretion	Et	ethyl
Ala	alanine	<i>et. al.</i>	<i>et alias</i>
AlMe ₃	trimethylaluminium	EtOH	ethanol
Ar	aryl	F	fluorine
Arg	arginine	Fmoc chloride	fluorenylmethyloxycarbonyl
BHA	benzylhydramine	GdmCl	guanidium chloride
Boc	<i>tert</i> -butylcarboxylic	Gly	glycine
Br	bromine	HATU	1-[bis(dimethylamino)methylene]-1 <i>H</i> -1,2,3-triazolo[4,5- <i>b</i>]pyridinium 3-oxid hexafluorophosphate
Bzl	benzyl	HBt	benzotriazole
Cbz	carboxybenzyl	HBTU	<i>N,N,N',N'</i> -tetramethyl- <i>O</i> -(1 <i>H</i> -benzotriazol-1-yl)uronium hexafluorophosphate
Cdc	cell division cycle	HCl	hydrogen chloride
CDI	carbonyldiimidazole	HF	hydrogen fluoride
Cdk1	cyclin dependent-kinase 1	HOBt	hydroxybenzotriazole
CLEAR	cross-linked ethoxylate acrylate	HPLC	high performance liquid chromatography
CNG	center nerve system	HR	high-resolution
Cys	cysteine	Ile	isoleucine
DCC	<i>N,N</i> -dicyclohexylcarbodiimide	HZI	Helmholtz Centre for Infection Research
DCM	dichloromethane	I	iodine
DIC	<i>N,N'</i> -diisopropylcarbodiimide	iPrMgCl·LiCl	isopropylmagnesium chloride lithium chloride
DIPEA	<i>N,N</i> -diisopropylethylamine		
DMAP	4-dimethylaminopyridine		
DME	1,2-dimethoxyethane		
DMF	<i>N,N'</i> -dimethylformamide		

<i>J</i>	coupling constant	ppm	<i>parts per million</i>
KOH	potassium hydroxide	PS	polystyrene
KSCN	potassium thiocyanate	PS-POE	polyethylene glycol-polystyrene
L	liter	PTM	post-translational modifications
Leu	leucine	RAM	Rink amide
LC-MS	liquid chromatography–mass spectrometry	RP	reverse phase
M	molar	QSAR	quantitative structure activity relationship
MBHA	4-methylbenzhydrylamine	R _f	retention factor
mM	millimolar	RT	ambient temperature
Me	methyl	SAR	structure-activity relationship
MeI	methyl iodide	SPPS	solid phase peptide synthesis
MeMgBr	methylmagnesium bromide	<i>t</i> Bu	<i>tert</i> -butyl sulfide
MeOH	methanol	TAMPAL	trityl-associated-mercaptopropionic acid-leucine
MESNa	2-sulfanyethanesulfonate	TBS	<i>tert</i> -butyldimethylsilyl
MPAA	(4-carboxymethyl)thiophenol	TBTU	<i>O</i> -(Benzotriazol-1-yl)- <i>N,N,N',N'</i> -tetramethyluronium tetrafluoroborate
MSA	methanesulfonic acid	<i>t</i> -BuOH	<i>tert</i> -Butyl alcohol
MTB ether	methyl <i>tert</i> -butyl ether	TECP	tris(2-carboxyethyl)phosphine
NaBH ₄	sodium borohydride	TFA	trifluoroacetic acid
NCL	native chemical ligation	TFMSA	trifluoromethanesulfonic acid
NH ₃	ammonia	THF	tetrahydrofuran
NMP	<i>N</i> -methyl-2-pyrrolidone	TLC	thin layer chromatography
NMR	nuclear magnetic resonance	TLC	thin layer chromatography
PAM	phenylacetamidomethyl	<i>t</i> _R	retention time
PEG	polyethylene glycol	Tyr	thyronine
PEGA <i>N,N</i> -	polyethylene glycol-polydimethylacrylamide	UV	ultraviolet
PEG-PS	poly(ethylene glycol)-polystyrene		
PG	protecting group		
Ph	phenyl		

Part I. Development of synthetic strategies for libraries of heterocyclic and bicyclic inhibitors of Cdc25A

1. Introduction

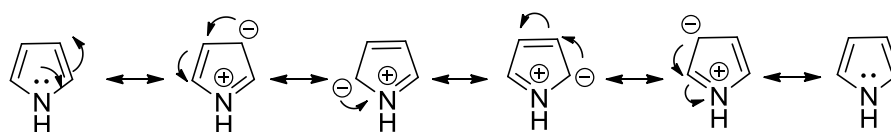
1.1 Heterocyclic compounds

The carbocyclic compounds like benzene, cyclopentane and cyclohexane are very common in the day-to-day organic chemistry routines. The chemists are usually familiar with these carbocyclic compounds since they are well presented almost everywhere: as solvents, reagents or catalysts. In case, one or more of the carbon atoms are replaced by other elements, they are considered as the heterocyclic compounds. The other elements involve in this replacement are regularly oxygen, nitrogen and sulfur, but not only restrict to these, other heterocyclic compounds bearing the boron, phosphorus and silicon could also be seen in rare cases.^[1] Over two centuries the heterocyclic compounds have been studied and the heterocyclic compounds family has been largely extended. Almost half of the known organic compounds are made of heterocycles.^[2] In general the heterocyclic compounds could be classified into two categories.^[3] The aromatic and aliphatic heterocyclic compounds. The determination of aromatic and aliphatic heterocyclic compounds complies with the Hückel's rule. The aliphatic heterocyclic compounds are commonly considered as the cyclic derivative of the ether, thioether and amine while the aromatic heterocyclic compounds behave themselves in the similar way like the benzene. The chemical properties of aliphatic heterocyclic compounds don't differ greatly from their linear counterparts, however the ring strain and steric factor of individual compounds could significantly change their chemical reactivity. Because the chemical properties of the aliphatic heterocyclic compounds are largely similar to their linear counterpart, the main research interest was focused on the study of the aromatic heterocyclic compounds. The ring size of heterocyclic compounds normally ranged between three and ten. The 3- and 4-membered heterocyclic compounds are relatively uncommon due to their strong ring strain. The mainstay of the heterocyclic compounds are these 5, 6 and 7-membered rings because of their suitable ring size. In order to systematically name these heterocyclic compounds, Hantzsch and Widman individually developed a similar nomenclature system,^[4] collectively called Hantzsch-Wideman nomenclature. The

assignment of heterocyclic compound with ring size smaller than ten follows this pattern. The heterocyclic compounds, which were already given the trivial names, do not follow this system. In the day-to-day organic chemistry the 5- and 6-membered heterocyclic compounds are well presented everywhere. Among them the most important heterocyclic compounds are these containing oxygen, nitrogen and sulfur atoms.

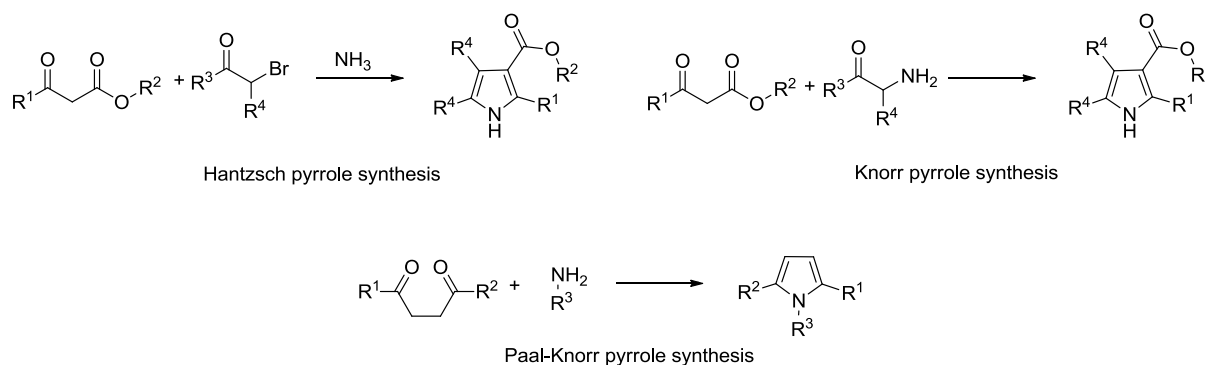
1.1.1 Notable 5-membered heterocyclic compounds

5-Membered heterocyclic compounds contain 5 atoms in the ring system, from which one or two atoms are heteroatoms. Frequently the unsaturated compounds are more stable due to the additional aromaticity, which they usually achieve. The notable 5 membered compounds are pyrrol, furan and thiophene and their saturated counterparts pyrrolidine, tetrahydrofuran and thiolane. These unsaturated 5 membered compounds fulfill the Hückel's rule through an unused free π -electron pair on the heteroatom and thus form the π -excessive ring.^[5] Their stability are rationalized by the valence bond resonance throughout the entire ring system (Scheme 1).



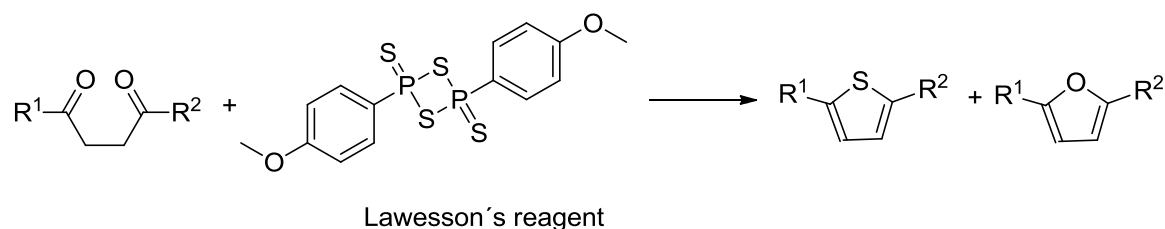
Scheme 1. Resonance of the pyrrole

Because of the resonance the carbon atoms within the ring often have a higher electron density compare to benzene and consequentially they could be easily attacked by electrophiles rather than nucleophiles. To generate these aromatic 5-membered heterocyclic compounds, many synthesis routes have been described. Pyrrole could be synthesis readily through Hantzsch-pyrrole synthesis,^[6] Knorr-pyrrole synthesis^[7] and Paal-Knorr synthesis.^[8] The latter is also applicable for synthesis of furan and thiophene (Scheme 2).



Scheme 2. Established methods for pyrrole synthesis

Classically, furan and thiophene can be obtained via the reaction of 1,4-diketones with Lawesson's reagent as main and side products^[9] (Scheme 3).



Scheme 3. Preparation of thiophene and furan from 1,4-diketone and Lawesson's reagent

Other notable 5-membered heterocyclic compounds are the thiazoline and thiazole, which especially the latter could be regularly saw in some special natural products (notably in vitamine B₁) as well as in the synthetic compounds. The thiazole contains two heteroatoms, the sulfur and nitrogen atoms in 1,3 positions, thus it belongs to the azole family. The structure is very similar to the imidazole. The thiazole is aromatic due to its π electron delocalization.

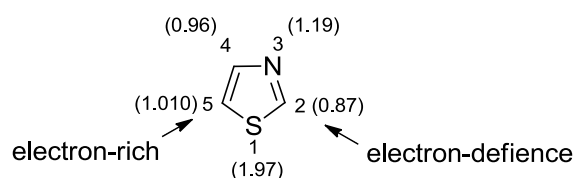
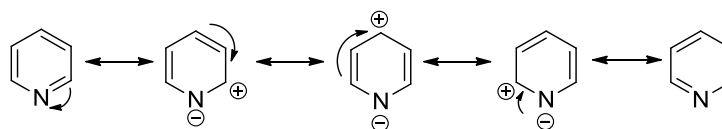


Figure 1. Electron density in thiazole

A strong aromatic ring current is developed as the consequence of the large delocalization and this changes the electron density within the ring. Among these carbon atoms, the C2 carbon atom is calculated strong electrophilic whereas the C5 is nucleophilic (Figure 1), therefore the thiazole can undergo different type of reactions. Classically the thiazole can be obtained through the Hantzsch thiazole synthesis,^[10] Robinson-Gabriel-synthesis^[11] and Cook-Heilbron thiazole synthesis.^[12] Moreover at present days 1,2,3-triazole gradually becomes the one of the most important 5-membered heterocyclic compounds due to its broad applications in medicinal chemistry^[13] and biological science.^[14] It can be readily synthesized through the 1,3-dipolar cycloaddition from an alkyne and an azide.

1.1.2 Notable 6-membered heterocyclic compounds

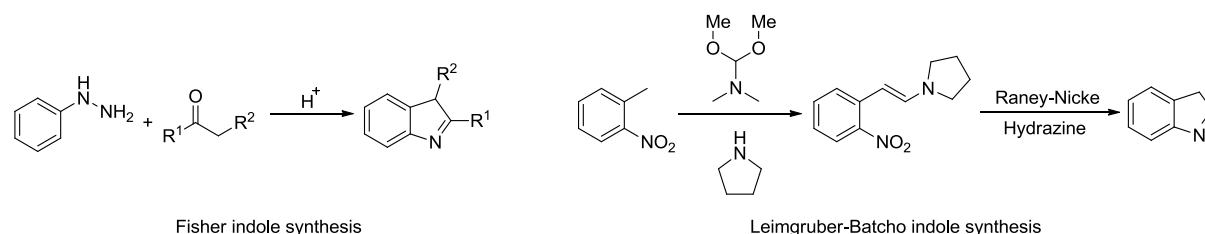
Import six-membered heterocyclic compounds are these bearing the nitrogen atom. The rings bear only one nitrogen atom are called the piperidine and pyridine, in which the piperidine is a sterical hindered base routinely used for the organic synthesis (notably in Fmoc peptide synthesis), its unsaturated form pyridine is an analogue to benzene, but its hexagonal ring system is slightly deformed due to the shorter C-N bond.



Scheme 4. Resonance form of the pyridine

Unlike its 5-membered counterpart pyrrole, it has a free electron pair totally unrelated to the aromaticity. It possesses a permanent dipole, in which the nitrogen atom bears the partial negative charge, while the 2, 4- and 6-carbon atom are electron-deficient (Scheme 4). The 3,5-positions are normally considered neutral. The nucleophilic attack would prefer to take place in these electron-deficient positions whereas the electrophilic substitution would initialize in the 3 and 5 positions. The heterocyclic compounds could derive from fusion with other rings either the carbocyclic ring or other heterocyclic ring to form the bicyclic or multicyclic systems. The practice of fusion of the different ring systems is often pharmacological active (quinoline, benzazepine). Indole is such classic example and a common precursor to many pharmaceuticals. It consists of one

pyrrole fused to one benzene ring and the new bicyclic system still retains the aromaticity. For a century many indole synthesis strategy has been emerged, among them the most significant methods are the original Fisher-indole synthesis,^[15] and Leimgruber–Batcho indole synthesis by using the Raney-Nickel and hydrazine as reductant^[16] (Scheme 5)



Scheme 5. Fisher and Leimgruber-Batcho indole synthesis

1.1.3 Heterocyclic compounds in medicinal field

Heterocyclic compounds are applicable in many areas especially in the medicinal field.^[5] These molecules containing the heterocyclic compound fragments often show more biological activity than their counterparts, which only carry the carbocyclic compounds. For this reason the heterocycles are often presented in a large range of the commercially available synthetic medicines including antibiotic (Penicillin G), antibacteria (Norfloxacin), antidepressant (Cymbalta), antimalarial (Chloroquine), antitumor, anti-HIV (Zidovudine), antidiabetic (Actos) drugs (Figure 2).

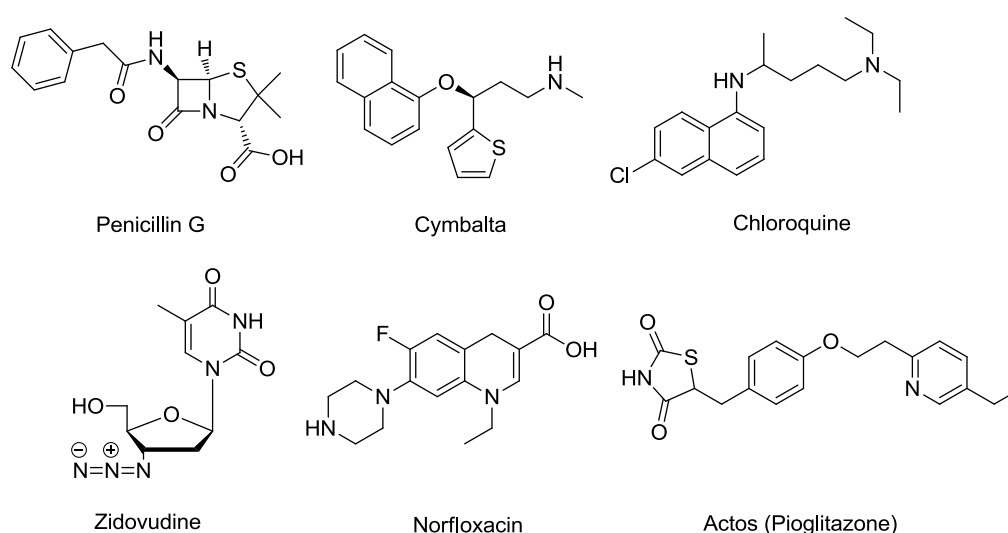


Figure 2. The common medicines containing heterocycles

The research interest of the indole and pyrrole is mainly focused on the medicinal area. Many indole containing compounds have been synthesized to treat various center nerve system (CNS) diseases.^[17] Furan ring is often contained in terpenoids and its derivative 2-(5H)furanone is the main scaffold of various antibiotic, anti-tumor agents,^[18] whereas pyridine is substantially involved in the treatment of muscular disorder (muscular rheumatism).^[19]

The natural occurring heterocyclic compounds are mainly alkaloids, from which many contain the nitrogen atoms. Ergotamine bears the indole backbone and inhibits antimigraine activity.^[20] Posaconazole is based on triazole scaffold and shows biological activity against microorganism *candida*.^[21] Cinchonine, which is a member of the quinolone family, inhibits high activity against malaria (Figure 3).^[22]

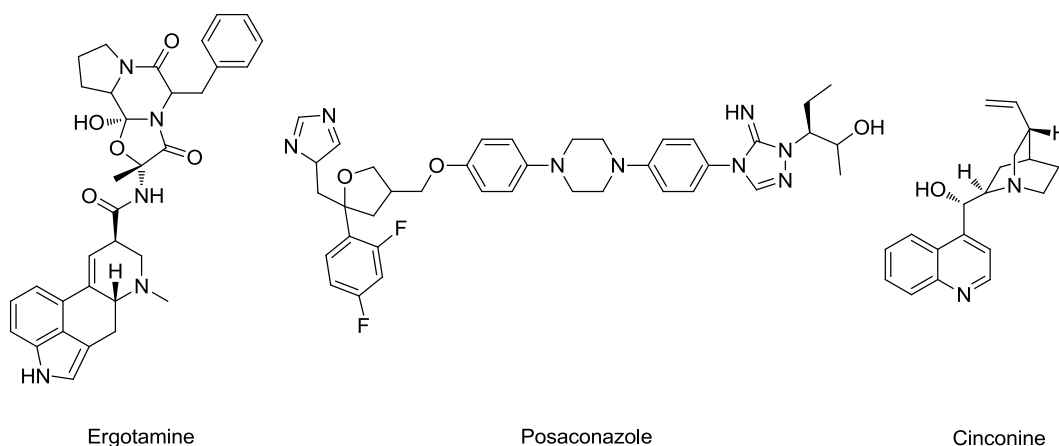


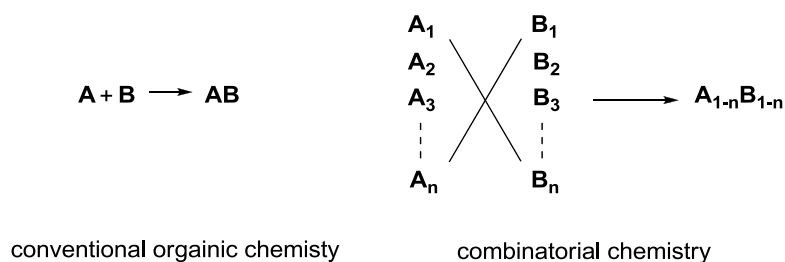
Figure 3. Heterocyclic compounds with large medicinal significance.

The large interest of developing novel heterocyclic compounds emerged in the past because of their wide pharmaceutical applicability. In the future, more biological active heterocyclic compounds will appear in one way or another while this interest still remains.

1.2 Combinatorial chemistry in the drug discovery

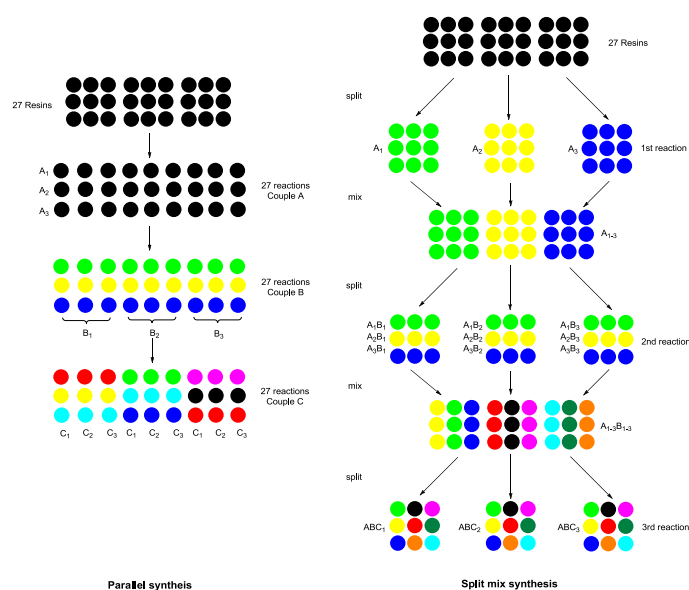
Today, in pharmaceutical research, the lead structures for drug design generally originate from two major sources: Natural occurring compounds and combinatorial chemistry. Combinatorial chemistry is a novel method, which is designed to reduce the time and cost in effective drug discovery.

In general, combinatorial chemistry generates a large collection of molecules, also called chemical library and the individual bioactivity of each molecule is determined by high throughput screening. Unlike the conventional organic chemistry, each single compound in this chemical library is not synthesized one after another but preferentially in parallel manner or in a one-pot reaction (Scheme 6). By doing this a lot of time can be saved and a huge quantity of compounds can be generated in short time.



Scheme 6. Two different ways of generation of chemical compounds.

In practice, there are several ways to effectively establish a chemical library, either chemically or biosynthetically. In the chemical approach, both the solution phase and the solid phase methods can be applicable. In solution phase the synthesis is performed on small scale, each vial in the array is filled with different reagents and various reactions of the same kind are allowed to take place simultaneously. Immediately after the reaction the unpurified products can be directly screened. The solid phase peptide synthesis has already been introduced by Merrifield back in the 1960's, but not until the early 1990's it was first deployed to generate a peptide library.^[23] The starting material in this case is anchored on the resin beads through coupling reactions, then the reagent is added to the solvent, after each reaction the by-product and the excess unreacted reagent can be easily washed out while the desired product still attaches to the resin. In the solid phase two different synthetic strategies are deployed, either parallel synthesis^[24] or the split and mix method (Scheme 7).^[25]



Scheme 7. Parallel synthesis vs. the split and mix strategy

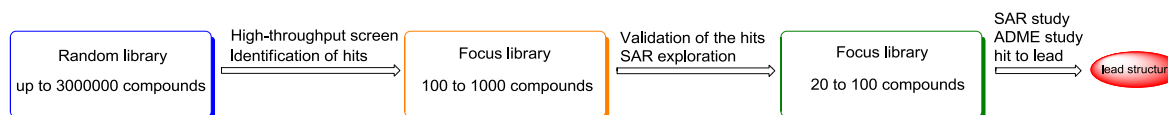
The parallel synthesis on solid phase is not much different than the parallel synthesis in the solution phase. The starting material fixed on the resin is partitioned to n ways, each portion reacts stepwise and simultaneously with different building blocks in a giving order and after the designed steps a new combinatorial library with high diversity are established. In the split and mix synthesis, the starting material is split to n portions in the beginning and each portion is allowed to react with different building blocks, then all resin beads will be recombined and again divided into n portion before the conversion with next building blocks begins (see scheme 4). In comparison to the parallel synthesis, a large combinatorial library could be much easier achieved by utilizing the split and mix method but some drawbacks limited the application of this method:

- The material could only be made in very small amount.
- Screening on the resin could be deceiving, highly active compound could be masked by less active compounds
- Highly complex mixture could be formed.

After the establishment the chemical library, the next immediate step is the determination of individual bioactivity through screening. There are two basic types of the screen methods:^[26]

- Random screening: detection of lead without knowing any structural information.
- Directed screening: evaluation of analogue of the lead to generation structure-activity-relationship. I

1.2.2 Discovery of the lead structure through the combinatorial chemistry



Scheme 8. Work-flow of the discovery of the lead structure

At the present days, the identification of the optimal molecule structure for the drug development within the framework of the combinatorial chemistry is achieved by following standard procedure:

1. A mixture contains large degree of diversity (normally 100,000 to 3,000,000 compounds), called random library, is generated either through high throughput parallel solution phase or combinatorial solid phase synthesis. This whole random library will be then high throughput screened to identify the hits.
2. If the screening identifies any hits, one focus library (contains 100 to 1000 compounds) will be established with the high throughput parallel solution phase synthesis to validate the hit and initially explore the Structure Activity Relationship (SAR).
3. The confirmed hit will be further optimized through the study of one smaller focus library (contains 20 to 100 compounds, which obtained from medicinal chemistry methods), after the study complete SAR, and ADMET (Absorption, Distribution, Metabolism, Excretion and Toxicity) properties of the lead structure will be elucidated.

1.2.3 Structure-activity relationship (SAR) study

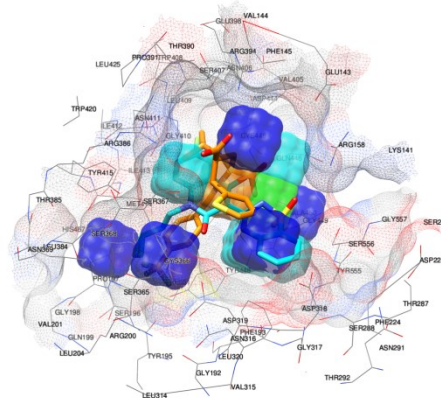


Figure 4. 3-D QSAR palm model.^[27]

The structure-activity relationship describes the connection between the structure and its biological activity. In drug discovery, the analogues with similar structure to original structure are often expected have similar biological activity but sometimes also comes up with undesired side effects.^[28] In order to determine which part of the compound (formally called: pharmacophore) is responsible to its beneficial biological activity, the structural difference between the original structure and its analogues is investigated. After the study, the information extracted from the investigation could be used to redesign the drug-like original compound to increase its beneficial biological activity and meanwhile reduce or even eliminate the undesired side effect. The SAR study assesses the influence of these analogues, which are derived from the original structures through some minor changes, on the biological activity. These minor changes may alter the biological activity, though the new analogue should still retain large structural, chemical and biochemical similarities to the original compounds.

Frequently three basic types of changes are conducted in the SAR study:

1. The change of size and shape of the carbon scaffold.
 - Additional methylene groups inside the chain or ring system could enlarge the size and respectively enhance the lipophilicity. The more lipophilic analogues may have better membrane penetration ability.
 - The number of the unsaturated carbon bonds could be adjusted. Removal of some C-C double bonds may make the resulted analogue conformational flexible and could be more fit onto the active or receptor

sites much easier but sometimes this could also cause the alternation of the biological activity of the analogue. Moreover, insertion of the double bonds in the carbon scaffold leads to *E*- and *Z*-isomers, which generally exhibit different biological activity.

- Introduction or removal of the alicyclic ring system could adjust the molecular size and make it better fit onto the binding pocket of the target. Additional aromatic rings will increase the rigidity of the analogue and may improve the resistance to metabolism.
2. Alternation of the substitution or change of the number of the substitutions. This change sometimes could substantially modify the biological properties and activity of the new analogues.
 - Introduction of the methyl group and the halogen would increase the lipophilicity and reduce the water solubility. Besides the methyl group could improve the binding of molecular to the pocket site, but meanwhile it could lead to the steric hindrance. Furthermore the methyl group has the considerable influence on the metabolism rate, depends on in which part of the molecular it is incorporated.
 - Insertion of the hydroxyl group will improve the water solubility but makes the new analogue less membrane penetrable. Meanwhile the binding to the target site could benefit from the new hydrogen bonds.
 - The basic groups in the molecule generally refer to various amines, these amines could be readily converted into salt form and thus the entire molecule is water soluble. Additional basic groups in the molecule would also vastly increase the water solubility.
 - Introduction of COOH and SO₃H groups could improve the binding to the target site through the hydrogen bond and acid base interaction.
 3. Change of the stereochemistry. The stereochemistry mainly regulates the binding affinity to the binding site. Different stereochemistry leads to the diverse biological activity.

Despite previous knowledge the effect on the biological activity of those changes are hardly predictable, in practice there are always exceptions, the investigation of the biological activity changes could only be concluded after the actual molecule is synthesized and tested.

1.2.4 Quantitative structure-activity relationship (QSAR)

In order to quantitatively describe the relationship between the biological activity and measurable pharmacological parameters a mathematic model is established through regression analysis. In this model the relationship between the activity and parameters is described by the mathematic equation:

$$\text{Biological activity} = f(\text{parameters})$$

The parameters (size, shape, electron distribution) are generally considered have major influence on the biological activity, and the biological activity is the value to the variable parameters. With help of this model, the activity could be predicted. By the defined range of activity the respond value of parameters could also be calculated, this could help the medicinal chemist to decide, which compounds need to be synthesized thus reduce the cost and time.

1.3 Cancer and the Cdc25s inhibitors

Cancer is a serious disease and associates closely to unregulated cell growth. It is a collective name of several deadly diseases. Annually it causes tens of millions fatalities and is the leading killer of the human beings reported by the World Health Organization (WHO) as of 2014.^[29] It is almost incurable in the past time but the situation has been changed since the introduction of the novel target therapy of tumor cell, different parts of tumor cell have been used as targets for tumor treatments

Even so the repression of the fast tumor cell growth remains as the difficult part of the tumor therapy. Recently the G₂ / mitosis transition phase within the cell division cycle aroused a great deal of interest of tumor therapy, if this transition could be efficiently blocked or repressed, the tumor cell might eventually cease to grow. The transition between G₂ and mitosis phases progresses only under the coordinated regulation of Cdk1 (cyclin dependent-kinase 1).^[30] The Cdk1 is a highly conserved protein, which functions as a serine / threonine kinase, and is vital for the G₂ / M transition. Commonly, the Cdk1 rests in its inactive state, because its threonine 14 and tyrosine 15 residues, which locate within the ATP binding loop, are phosphorylated by the WEE1 and MYT1 kinases (Figure 5).^[31]

In order to function as the G₂ / M transition regulator, Cdk1 must bind to the activator Cyclin B and form the complex Cdk1 / Cyclin B, upon formation of the

complex the active center of Cdk1 will open and available for the subsequent transformation.

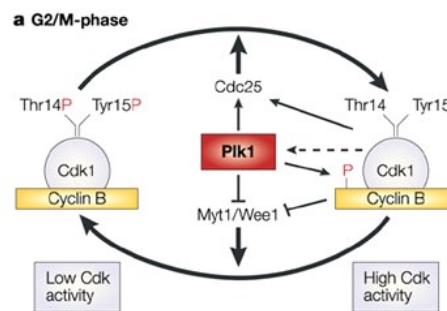
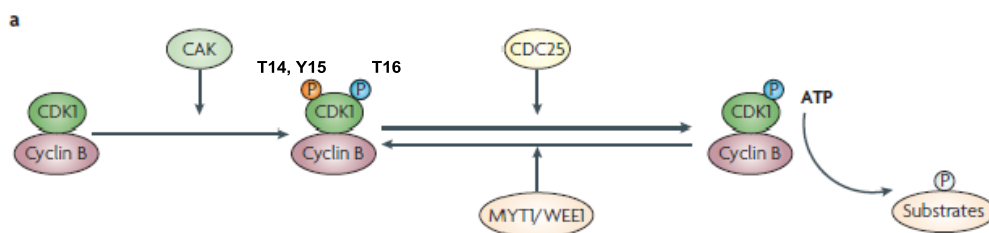


Figure 5. Cyclin A / CDK 1 complex.^[32]

During the entry phase of the G_2 / M transition, the Cdk1 / Cyclin B complex locates in the cytosol, whereas the threonine 14 and tyrosine 15 residues of Cdk1 are still phosphorylated, thus the complex shows no enzymatic activity. Subsequently, the relocation of the Cdk1 / Cyclin B complex to the nucleus takes place, meanwhile the threonine 16 residue of Cdk1 is activated through the phosphorylation by the Cdk-activating kinase (CAK; Cdk7 in metazoans). Sequentially the inhibitory threonine 14 (T14) and tyrosine 15 (Y15) residues of Cdk1 are dephosphorylated and consequently the Cdk 1 / Cyclin B complex is constitutionally active and this is followed immediately by condensation of the chromosome.^[33]



Scheme 6. Activation and deactivation of the CDK1 / Cyclin B complex.^[34]

The dephosphorylation of the T14 and Y15 residues is specifically regulated by a dual specific phosphatase cell division cycle 25 phosphatase homologue A (Cdc25A).

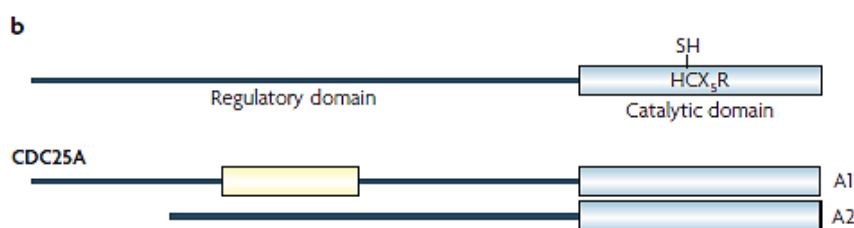


Figure 6. The Cdc25A phosphatase.^[34]

Cdc25A along with other two homologues B and C constitute the Cdc25 phosphatase family in the mammalian cells.^[35] The existence of human Cdc25 genes was firstly described by Sadhu^[36] then two main homologues A and B of Cdc25s were isolated and individually identified.^[37] The Cdc25 phosphatase contains two domains, from which one is the catalytic domain and the other is the regulatory domain (Figure 6). The catalytic domain is highly conserved, whereas the regulatory domain is more versatile, the phosphorylation / dephosphorylation of the regulatory domain changes the catalytic or inhibitory ability of the regulatory domain. The deactivated Cdk1 could bind additional Cyclin B in the cells while the Cdc25A is overexpressed, therefore the G₂ / M transition is promoted. In many cancer cases the expression or overexpression of the Cdc25A and Cdc25B was observed thus the Cdc25s especially the Cdc25A and Cdc25B are generally classified as oncogenes. Their overexpression often associates to the premature assemble and activation of the Cdk1 / Cyclin B complex and the acceleration of the cancer cells division. In these cases the overexpress of the Cdc25A or B is fatal, however through the slight interference of short hair-spin RNA, the Cdc25 phosphatases could be repressed and consequentially the amount of activated Cdk1 / Cyclin B complex would decrease. Lacking of Cdk1 / Cyclin B complex, the G₂ / M transition would not progress thus the cancer cell division ceases.

Since a decade, Cdc25A emerged as a new target for the tumor therapy due to its crucial role in the cell division. Besides the broad phosphatase inhibitors (Figure 7), a handful of novel small to middle sized molecules, which show inhibitory effects against Cdc25A, have already been tested and some were even released in the market for the further research.

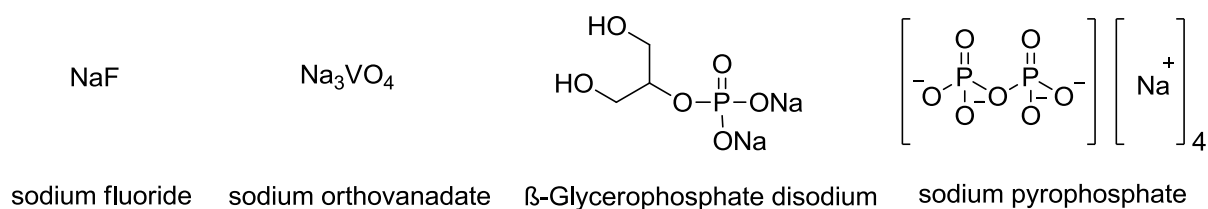


Figure 7. Common Ser / Thr, acidic and alkaline phosphatase inhibitors

Some commercially available inhibitors distinguished themselves with their notable inhibitory ability: NSC 95397,^[38] NSC 663284 (aka: Cdc25 Phosphatase Inhibitor II)^[39] as well as Cpd 5 (Figure 8).^[40] They are cell-permeable, 7-substituted quinolinedione compounds and function as the potent, irreversible, mixed competitive inhibitors of the Cdc25 phosphatase family. NSC 95397 and its monohydroxyl-NSC 95397, dihydroxyl-NSC 95397 derivatives showed inhibition of human hepatoma and breast cancer cells *in vitro*.

NSC 663284 blocks spreading of many human tumor cell lines and is usually deployed as an anti-proliferation reagent by inhibiting Cdc25s.^[41]

In rat hepatocytes both hepatoma cell growth and DNA synthesis are inhibited by Cpd5 *in vitro*.

Disadvantageously they are all broad Cdc25 inhibitors, so that they did not show sufficient inhibitory ability against Cdc25A.

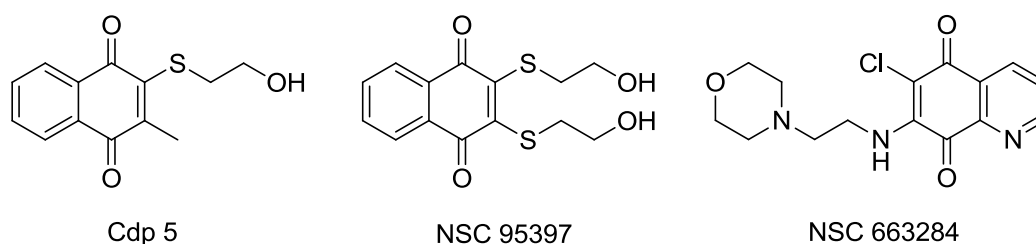


Figure 8. Some broad Cdc25 inhibitors in the market.

Furthermore a few compounds, which are derived from the yohimbine alkaloids have also been reported as Cdc25A inhibitors (Figure 9).^[42]

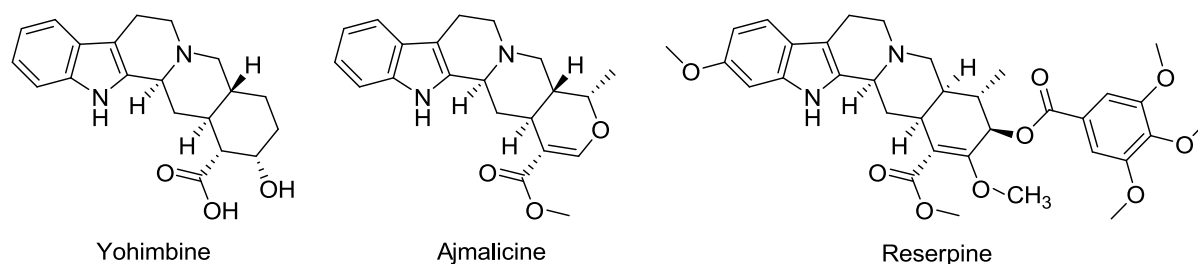


Figure 9. Structures of the yohimbine alkaloids Cdc25A inhibitors.

Most recently, two new selective Cdc25A inhibitors (Figure 8) have been synthesized and identified through the combinatorial chemical method and partially characterized by PD. Dr. Ingrid Hoffmann (DKFZ) and Dr. Ronald Frank (HZI). They identified the hits on the target Cdc25A and validated them through the previous procedures. However most biological and medicinal properties especially the structure-activity relationship (SAR) remains unknown. In order to get full spectra of details and eventually turn the hit to the lead, a library contains a small number (20-100) of diverse derivatives will be required, these carried out. But one effective chemical synthetic route toward these compounds prior to the intensive research must be needed, which becomes the main objective of this thesis.

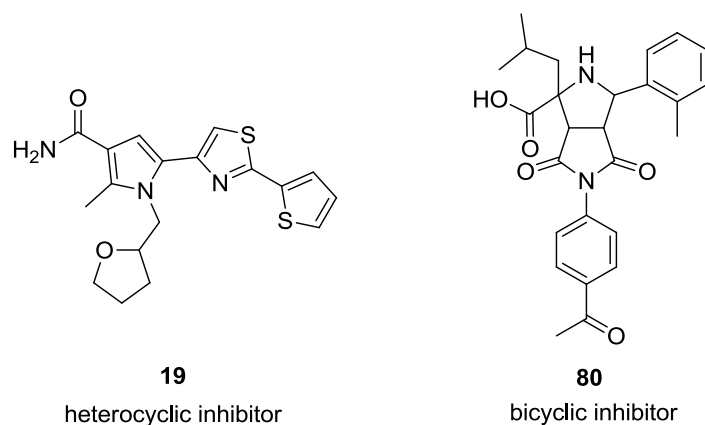
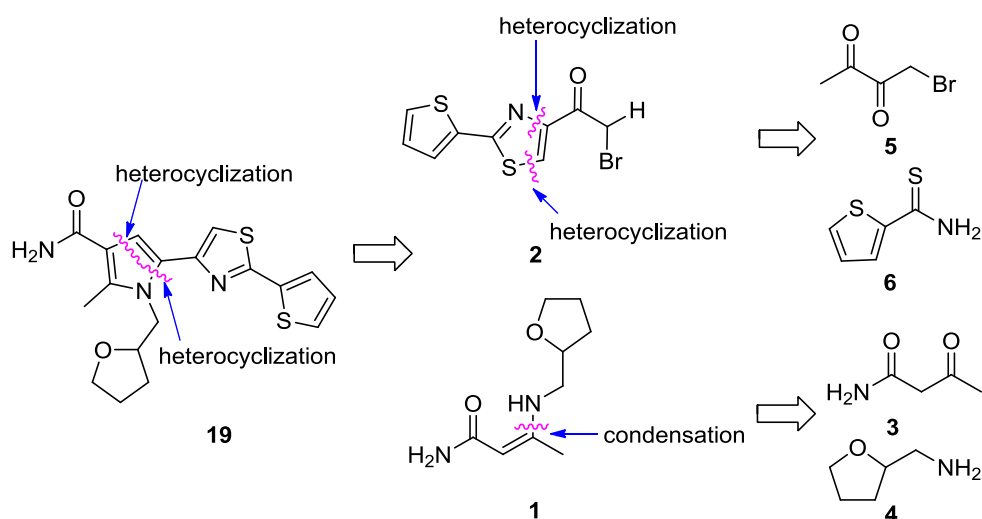


Figure 10. Two novel Cdc25A inhibitors

2. The retro synthetic analysis and the design of the synthetic route

2.1 Retro synthetic analysis of the heterocyclic inhibitor

This work starts with the synthesis of the heterocyclic inhibitor **19**. The synthesis towards compound **19** will encounter construction of the conjugated heterocyclic system. Two compounds (pyrrole and thiazole) are recognized to be the backbone of the inhibitor **19** and the synthesis of **19** will focus on the building of these two heterocyclic systems. The Hantzsch pyrrole synthesis is a classic method to furnish the pyrrole ring. Inspired by the classic Hantzsch pyrrole synthesis the pyrrole ring is commonly generated through the reaction between an α -halo ketone and an enamine, in which the enamine is formed *in situ*.^[6] But in this synthetic route the enamine **1**, which is needed for the heterocyclization, will be formed beforehand and then allowed to react with the α -halo ketone **2**. The enamine **1** could be readily obtained by condensation of the fragments **3** and **4**. The bromoketone **2**, which contains the thiazole ring, could be formed within the frame of Hantzsch thiazole synthesis^[10] from the respective haloketone **5** and thioamide **6** (Scheme 9).

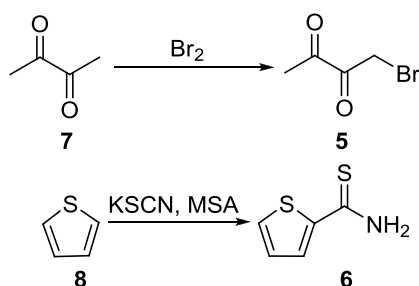


Scheme 9. Retro synthetic analysis of heterocyclic inhibitor

2.1.1 The initial synthetic plan of the heterocyclic inhibitor

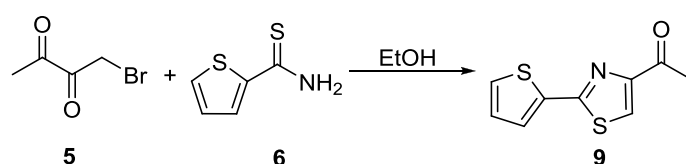
The fragments **3** and **4** are commercially available so the initial synthesis will concentrate on the syntheses of fragments **5** and **6**.

The monobromodiketone **5** was made through simple monobromination of the diketone **7**.^[43] Meanwhile the fragment thiophenethioamide **6** could be synthesized by an acidic catalyzed Fried-Crafts-acylation of the thiophene **8**.^[44]



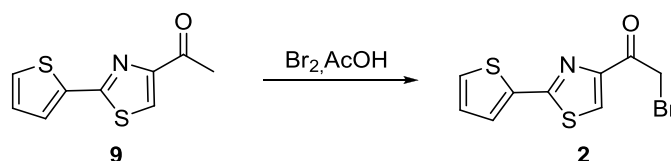
Scheme 10. Generation of starting materials **5** and **6**.

Afterwards the fragments **5** and **6** could be assembled into ketone **9** through the thiazole formation.^[45]



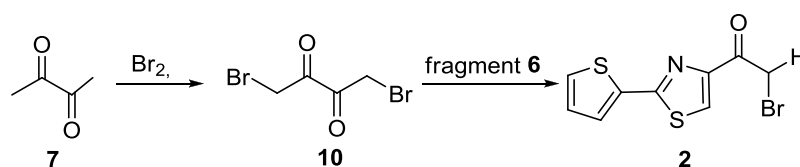
Scheme 11. Plan of generation of intermediate **9**

The intermediate **9** would then form fragment **2** through bromination.^[45]



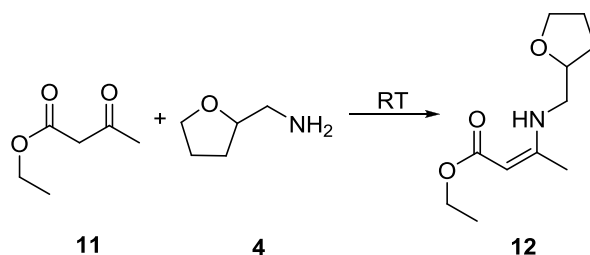
Scheme 12 Plan of bromination of intermediate **9**

In case of difficulties with the bromination of the intermediate **9**, a backup plan is also considered. In this case, the starting material **7** would be dibrominated to the dibromodiketone **10**,^[46] which then could also form fragment **2** through the same pathway.^[45]



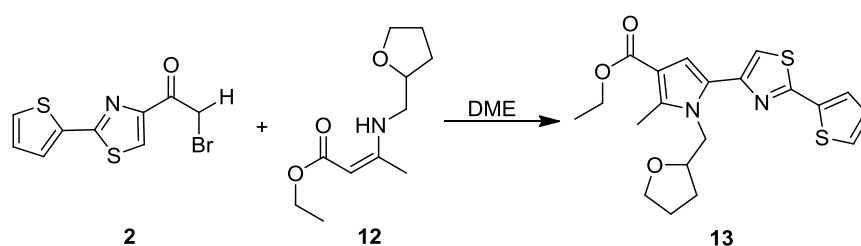
Scheme 13. The backup plan to achieve the intermediate **2**

In favor of further modifications, the original fragment **1** is deliberately replaced by new fragment enamineester **12**. Formation of the ester bond could be hydrolyzed to the carboxylic acid and enable to prepare various amides. The formation of the enamineester **12** could be achieved through a condensation of ketoester **11** and amine **4**,^[47] which are commercially available.



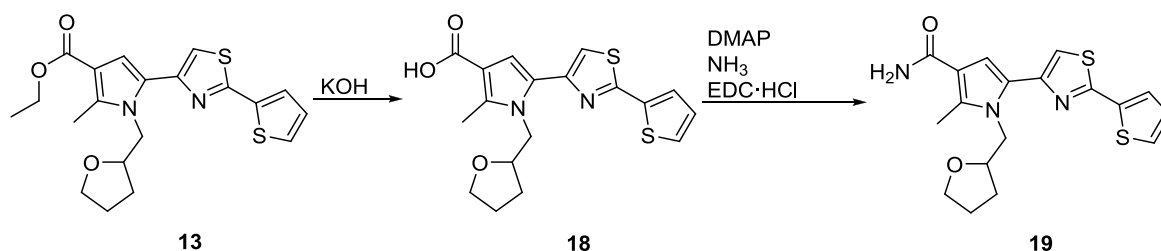
Scheme 14. Plan of formation of enamine ester **12**

The upcoming step is crucial in the synthetic route. The fragments **2** and **12** will be assembled to form the pyrrole ring system.^[48]



Scheme 15. Plan of formation of pyrrole ring

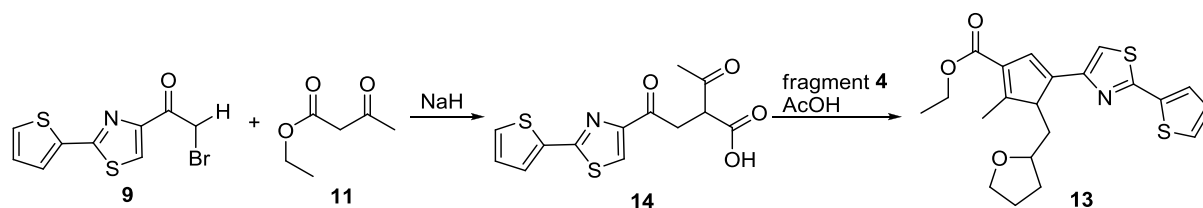
After the completion of the intermediate **13**, the conjugate cyclic ring system is established. The following steps will be generation of the amide bond: After the saponification of the intermediate **13**,^[49] the carboxylic acid **18** is converted to generate the lead structure **19**.^[50]



Scheme 16. Synthetic route through **13** to the final product **19**

2.1.2 An alternative synthetic plan for the heterocyclic inhibitor

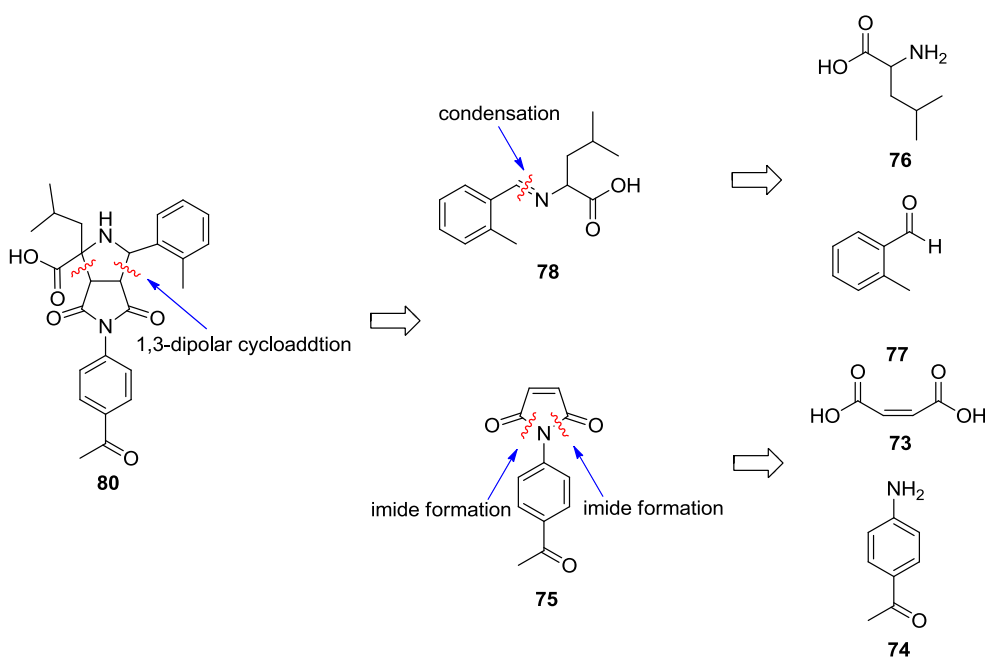
A secondary route to construct the pyrrole ring will also be taken into account, if the Hantzsch method is not successful. This alternative method is based on the Paal-Knorr pyrrole synthesis^[8] and can be applied immediately after the completion of fragment **2**. The changes are, instead of generating the enamine **12** the fragment **2** would be alkylated with ketone ester **11** at first^[51] and followed by the ring formation with fragment **4** to accomplish the pyrrole.^[52]



Scheme 17. The Paal-Knorr route to generate intermediate **13**

2.2. The retro synthetic analysis of the bicyclic inhibitor

The overall structure of the bicyclic inhibitor simply comprises of the pyrrolidine ring system and the imide moiety. The pyrrolidine ring is formed from part **78** and the southern segment **75** through the 1,3-dipolar cycloaddition. The imine fragment **78** is again formed from **76** and **77**, whereas the imide part is formed from fragment **73** and **74**. All fragments from **74** to **77** are commercially available. (Scheme 18).

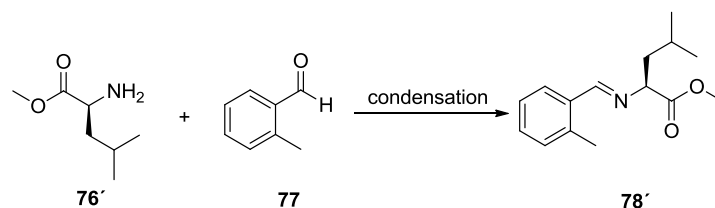


Scheme 18. Retro synthetic analysis of bicyclic inhibitor

2.2.1 The synthetic plan of the bicyclic inhibitor

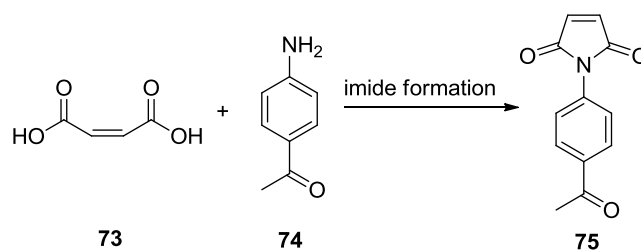
The synthesis of the bicyclic inhibitor **80** is straightforward, because all the basic fragments are commercially available. However, there were no details available about the stereochemistry, the compound **80** above is just a suggestion of the structure. Which specific configuration is beneficial to the biological activity remains unknown. At the beginning of the synthesis, this work will not aim on any specific stereochemistry but rather starts with any starting materials, which are available.

The upper fragment **78'** (fragment **78** with specific configuration) is made by condensation from L-Leucine methyl ester **76'** (the L configuration amino acid ester of fragment **76**) and 2-methylbenzaldehyde **77**.^[53]



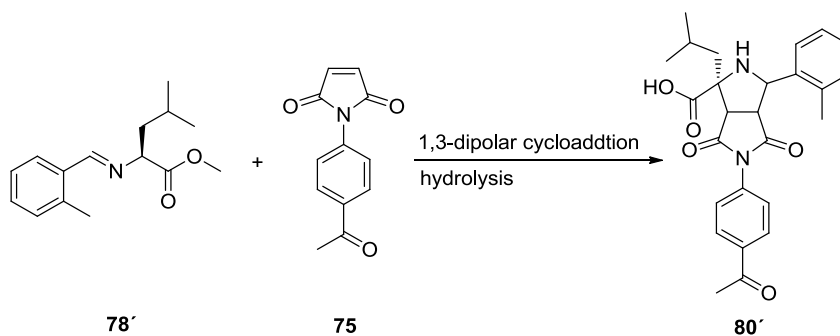
Scheme 19. Synthesis of fragment **78**

Fragment **75** could be furnished through imide formation from the maleic acid **73** and the 4-aminoacetophenone **74**.^[54]



Scheme 20. Synthesis of fragment **75**

The assembly of fragments **75** and **78'** is accomplished through a 1,3-dipolar cycloaddition^[55] and after the hydrolysis of the methyl ester, the first structure in this library will be formed.



Scheme 21. Synthesis of **80'**

2.3. Outline of the construction of further derivatives

2.3.1 Derivatization of heterocyclic inhibitor

In order to establish a library, a few further modifications on lead structure **19** have to be carried out. Retaining the backbones (pyrrole and thioazole rings) of the lead structure **19**, four areas can be modified (Figure 11).

1. The primary amide can be replaced by using *N*-substituted amines on the amide formation step.
2. The alkyl residue attached to the pyrrole ring can be varied by using ketone ester with different alkyl functionalities.
3. The nitrogen atom of the pyrrole ring is able to be connected to various aromatic or alicyclic moieties.
4. The thiophene on the far right side can be deliberately replaced through other heterocyclic compounds.

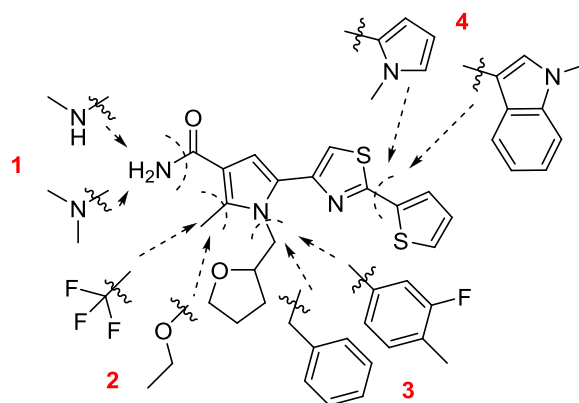


Figure 9. Derivatization plan of heterocyclic inhibitor

2.3.2 Derivatization of the bicyclic inhibitor

In the case of the bicyclic inhibitor, there are four possible positions, which could be derivatized (Figure 12).

1. The leucine could be replaced by different amino acids, of which both D, and L-amino acids should be contained.
2. The *o*-tolyl group from the upper right side might be substituted by various aromatic ring systems.
3. The carboxylic acid from the upper left side could be formed into diverse amides.
4. The substitution pattern of the aromatic residue can be expanded by halogens ethers or propionyl groups.

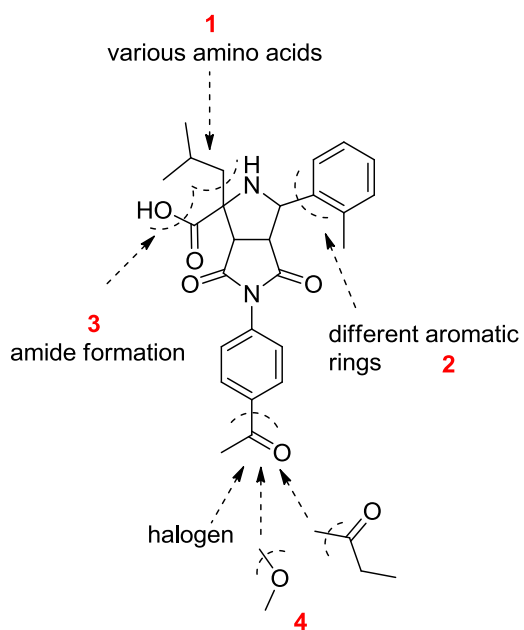
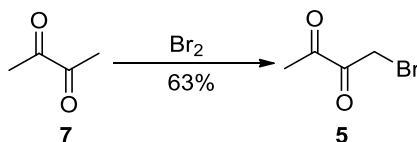


Figure 12. Derivatization plan of bicyclic inhibitor

3. Results and discussion

3.1 Commencing with the initial plan toward the heterocyclic inhibitor

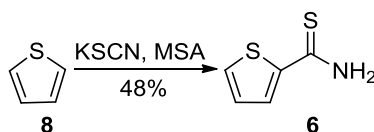
3.1.1 Synthesis of 5



Scheme 22. Monobromination of the starting material 7.

This experiment was carried out according to the procedure of reference.^[43] Diketone 7 was brominated with an equimolar amount of bromine. In order to avoid the formation of the dibrominated product, the rate of bromine drops was kept constantly slow, and the temperature inside the flask was maintained between 20 – 30 °C, and the final product was separated through fractional distillation with 63% yield.

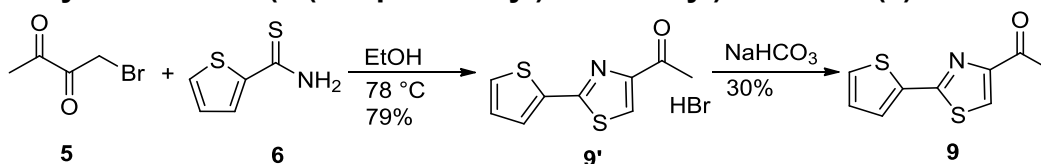
3.1.2 Synthesis of thiophene-2-carbothioamide (6)



Scheme 23. Preparation of thioamide 6.

The thioamide 6 was prepared by following the procedure of the reference.^[44] Thiophene 8 was thioacylated through a Friedel-Crafts acylation with help of methanesulfonic acid. After work the raw product was isolated in 48% yield by using flash chromatography. The total yield could be slightly improved (by 6%), when the water phase was also carefully extracted with chloroform and purified through flash chromatography.

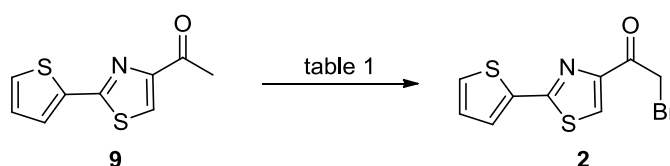
3.1.3 Synthesis of 1-(2-(thiophene-2-yl)thiazol-4-yl)ethanone (9)



Scheme 24. Formation of the ketone 9.

This experiment followed the instruction of the reference.^[43] Ketone **9** was successfully synthesized after two steps. The raw product was purified by using the flash chromatography with 30% yield over two steps. The yield is not satisfactory due to the existence of a large amount of by-product. The TLC analysis showed that the by-product was very polar, which suggested that it could be constructed through the polymerization of **5**.

3.1.4 Synthesis of 2-bromo-1-(2-(thiophen-2-yl)thiazol-4-yl)ethanone (**2**)



Scheme 23. Failed attempts to achieve the intermediate **2**.

Table 1. Monobromination under different conditions

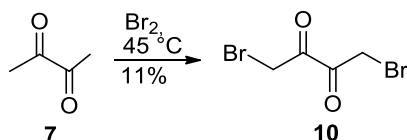
entry	solvent	temperature	catalyst	result
1	chloroform	RT	none	no product
2	chloroform	45 °C	AcOH	no product
3	DCM	RT	none	no product

The bromination of **9** was initially conducted in chloroform at RT^[45], but it was not successful. Afterwards two more brominations were attempted under slightly changed conditions (Table 1),^{[46][56]} unfortunately none of these experiments achieved the desired monobrominated product. In all three cases the starting material **9** was nearly fully recovered after the reaction, which indicated that the bromination did not take place at all.

3.2 Change of the tactic

Since the initial synthetic route could not achieve the desired product **2**, the bromination of the ketone was instead performed prior to the thiazole formation. Thereafter, the secondary synthetic plan using dibromineketone **10** as starting material was carried out.^[44]

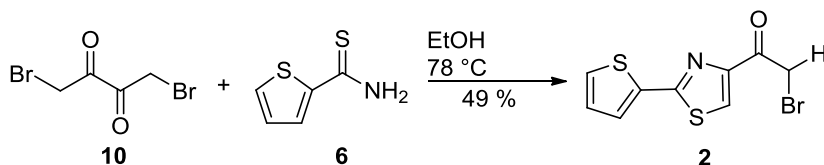
3.2.1 Synthesis of dibrominediketone 10



Scheme 26. Dibromination of the starting material **7**.

To diketone **7** was added two equivalent of bromine, and heated at 45°C until no more gas emerged from the reaction vessel. The raw product was purified by recrystallization in modest 11% isolated yield. The recrystallization of the raw product caused the huge loss of the substance, and the raw product was therefore applied without any purification.

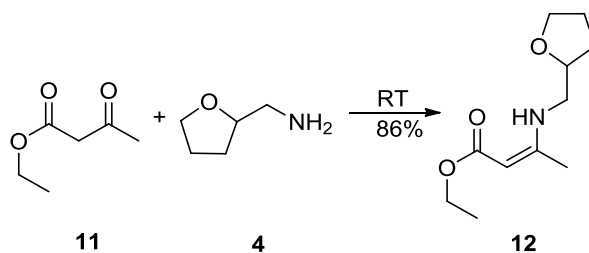
3.2.2 The second approach towards 2-bromo-1-(2-(thiophene-2-yl)thiazol-4-yl)ethanone (**2**)



Scheme 27. Successful synthesis of the **2** through the secondary route.

This step was carried out under the same conditions as the previous reaction of the synthesis of the intermediate **9'**.^[40] Bromoketone **2** was successfully synthesized and the difficult bromination step of **9'** was bypassed. The raw product was purified through flash chromatography in 49% yield. The thiazole formation from fragments **6** and **10** was more effective than thiazole formation at the section **3.1.3**, much less by-product was observed on the TLC plate during the experiment.

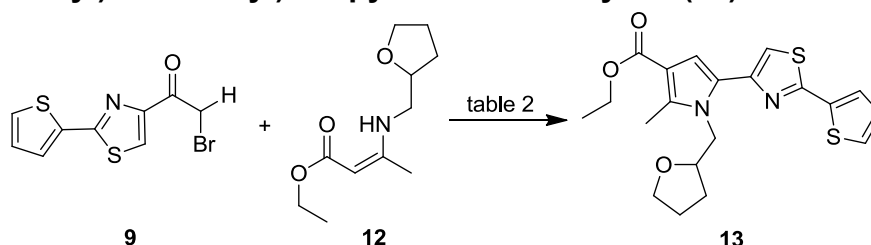
3.2.3 The synthesis of (Z)-ethyl 3-((tetrahydrofuran-2-yl)methylamino)but-2-enoate (**12**)



Scheme 28. The synthesis of the enamine ester **12**.

The synthesis was carried out at RT by following the same procedure of the reference,^[45] the raw product was isolated in 86% yield by using flash chromatography.

3.2.4 The synthesis of ethyl 2-methyl-1-((tetrahydrofuran-2-yl)methyl)-5-(2-(thiophene-2-yl)thiazol-4-yl)-1H-pyrrole-3-carboxylate (13)



Scheme 29. Formation of the pyrrole ring under optimized conditions

The pyrrole ring formation was achieved after a few attempts under various conditions.

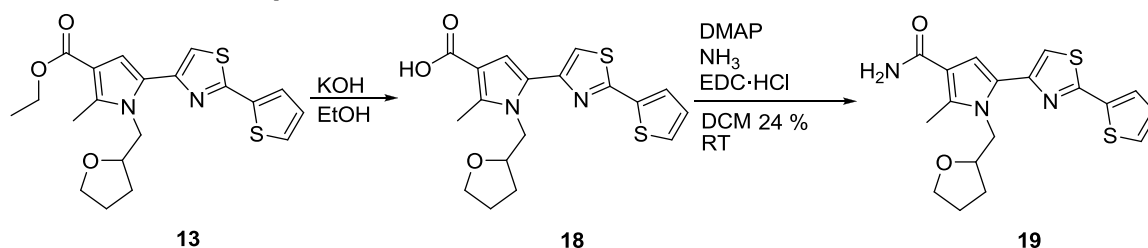
Table 2. pyrrole formation under various conditions.

entry	solvent	temperature	reactant	yield
3	toluene	RT	AcOH	no reaction
4	DMF	150 °C	DIPEA	no reaction
5	DME	85 °C	/	42%
6	DME	85 °C	DIPEA	32%

The reaction was firstly carried out in toluene with catalytic amount of acetic acid (Table 2, entry 3),^[57] no reaction took place. Acetic acid was a weak acid and apparently it did not initialize the reaction, besides RT may be too mild for this reaction and therefore, the reaction needs to be performed under more vigorous conditions. The reaction was again carried out overnight under reflux of DMF (150 °C) and with catalytic amount of DIPEA (Table 2, entry 4),^[58] unfortunately the temperature was too high and the starting materials were all destroyed just after 1 hour. Then the reaction was carried out under reflux of DME at relatively milder temperature (85 °C) (Table 2, entry 5),^[59] the desired product was formed and isolated in 42% yield. The reaction was then performed under the same conditions but with additional DIPEA (Table 2, entry 6), the DIPEA additive in this

case did not promote the yield, but instead diminished the yield by 10% when compared to the former experiment.

3.2.5 The final steps toward the lead structure 19



Scheme 30. Construction of the lead structure **19**.

Ester **13** was then subjected to saponification in 10% KOH ethanol,^[47] The acid **18** was successfully formed. The raw product was assessed by TLC and the conversion was quantitative. The raw intermediate **18** was then used for the final step without further purification. The formation of primary amide was achieved by using the common coupling reagent combinations (EDC / DMAP)^[48] and the reaction was accomplished after 5 hours, raw product was purified by flash chromatography. The formation of the primary amide under those conditions was not highly efficient, the final product came out only in 24% yield calculated over two steps.

3.2.6 The synthesis of various amides derived from 19

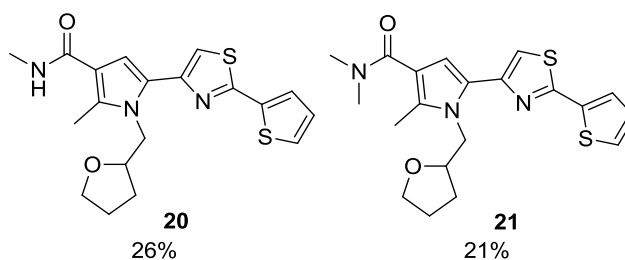


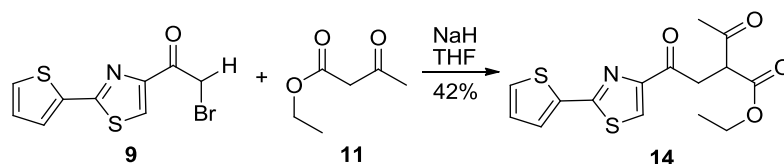
Figure 13. Different amide derivatives of the lead structure.

Furthermore two derivatives **20** and **21** with substituted amides were constructed in the same way^[48] with comparable yields to the lead structure **19**.

3.3 The alternative route to achieve the pyrrole ring

3.3.1 The synthesis of 1,4-diolester **14**

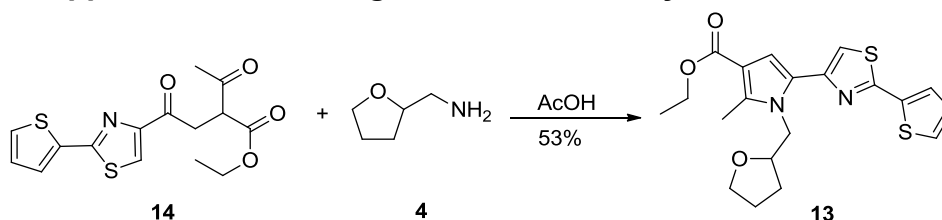
For comparison purpose, the secondary synthetic route based on the Paal-Knorr pyrrole synthesis was also investigated.



Scheme 31. Generation of the 1,4-dicarbonyl intermediate **14**.

The study of this route commenced with the alkylation of ketoester **11** with the already synthesized bromo-ketone **9**.^[51] After a few initial attempts, it was found that the reaction time must be kept short (within 10 min.), otherwise the polymerization started, which resulted in undesired polymeric products. The actual reaction concluded after 5 minutes and the product was separated in 42% yield through flash chromatography.

3.3.2 The approach to **13** through the Paal-Knorr synthesis

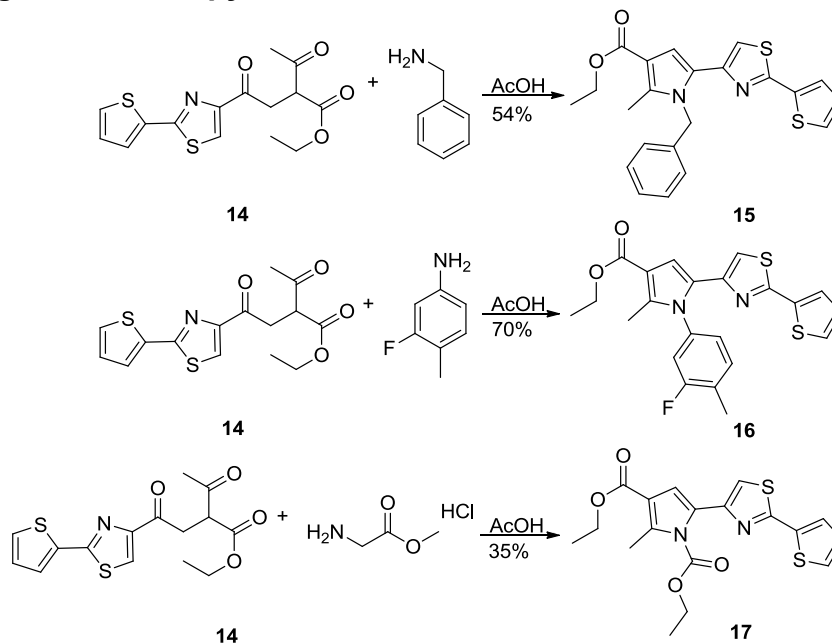


Scheme 32. The pyrrole formation through Paal-Knorr method.

The 1,4-diolester **14** and starting material **4** were condensed with assistance of acetic acid and the pyrrole ring subsequently formed through the ring closure with **4** (Scheme 32). The formed product **13** (53% yield) was identical to the product, which was formed through Hantzsch synthetic route. Combined with the previous step, the synthesis of 1,4-diolester **14**, the calculated yield over two steps was 22%, and apparently the Hantzsch route (42% yield) was advantageous over the Paal-Knorr route in term of the productivity. However

with the intermediate **14** in hand, the Paal-Knorr method is more versatile and facilitates the generation of a large number of derivatives in a short time.

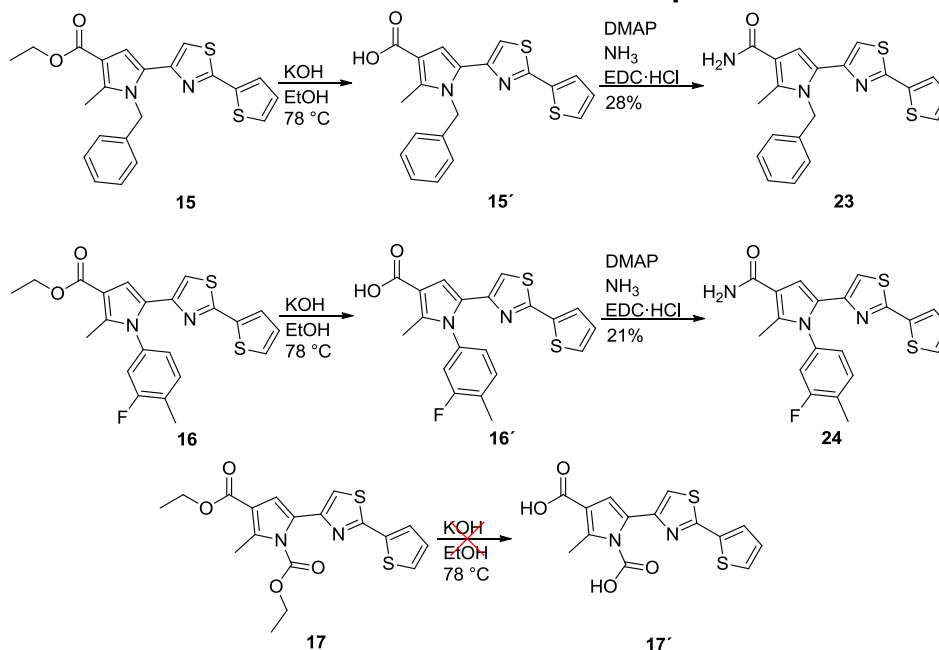
3.3.3 The generation of pyrrole with different substitutions



Scheme 33. Preparation of derivatives through the same method.

Afterwards three derivatives were constructed in the same way through the condensation of 1,4-diolester **14** with three different amines. The intermediates **15**, **16**, **17** were converted from 1,4-diolester **14** with phenylmethanamine, 3-fluoro-4-methylaniline or methyl 2-aminoacetate. All syntheses were successful, The highest yield was achieved in the case of **16** (70%).

3.3.4 From the intermediates 15 and 16 to the final products



Scheme 34. From intermediates to the final products.

After the completion of those intermediates, it was attempted to transform the intermediates **15** – **17** to amides through the same procedure of the construction of the lead structure **13** (Scheme 34). The intermediates **15** and **16** were successfully converted into the desired final product **23** and **24** in modest yield (28% and 21%). The intermediate **17** did not survive the saponification and resulted in a white solid, which was neither soluble in water nor in the organic solvent. Possibly both ester bonds were simultaneously saponificated to the carboxylic acids and then the intramolecular ring closure occurred while heating at 78°C and the intermediate **17** was finally converted into a cyclic acid anhydride compound.

3.4 Extension of the library by derivatization on designated positions

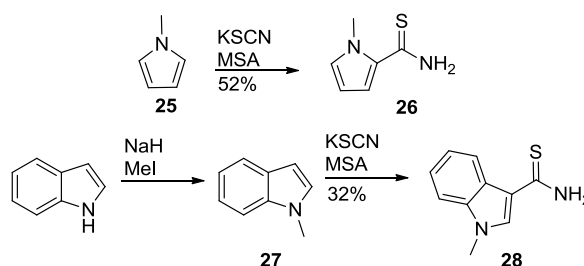
3.4.1 Derivatization of the far right end with other heterocyclic compounds

Comply with the initial synthetic plan, the thiophene on the far right end will be deliberately replaced by other heterocyclic compounds in order to determine, whether the thiophene residue contributes to biological activity of the lead structure. Nitrogen contained heterocyclic compounds will replace thiophene. One replacement for the thiophene is its nitrogen counterpart of thiophene,

pyrrole. A second candidate to replace thiophene is indole, which has a larger size and thus hopefully it could be more suitable to fit the binding pocket.

3.4.1.1 Formation of the N-methylated heterocyclic compounds

The sulfur atom of thiophene carries a free electron pair and thereby thiophene is an H-acceptor, but conversely both pyrrole and indole carry a hydrogen atom and present the character of the H-donor. When thiophene directly replaced by them, the biological property of the new formed derivatives will be substantially changed. In order not to alter the biological activity of the new derivatives in the opposite way, the nitrogen atom in both moieties will be masked by the methyl group and consequentially they are turned into the H-acceptors.

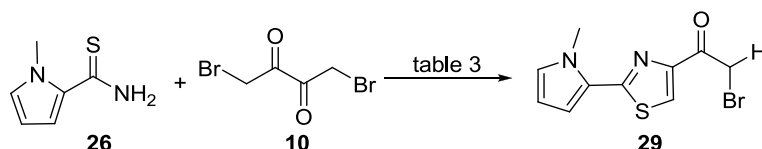


Scheme 35. Formation of the thioamides of further heterocyclic compounds.

N-methyl pyrrole was commercial purchased and the methylation of indole was accomplished by using the sodium hydride and methyl iodide.^[60] The methylated compounds were then utilized for the thioacylation without purification. Then the thioacylation were performed under previous used conditions^[42] and the raw product were isolated in moderate yield 52% (1-methyl-1H-pyrrole-2-carbothioamide (**26**)) and 32% (1-methyl-1H-indole-3-carbothioamide (**28**)) through the flash chromatography calculated over two steps.

3.4.1.2 Formation of the thiazole system from **26** containing *N*-methylated pyrrole.

The previous conditions were not directly applicable for the thiazole formation from the intermediate **26** and **28**, but rather experienced some modifications.



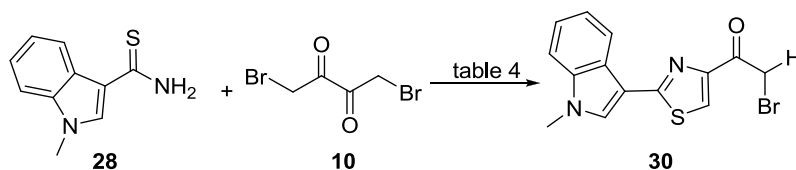
Scheme 36. Preparation of the **29** under various conditions

Table 3. Preparation of the **29** under various conditions

entry	solvent	temperature	reaction time	base	yield
8	EtOH	78 °C	1h	none	/
9	EtOH	RT	1h	none	/
10	THF	RT	2 h	DIPEA	/
11	THF	RT	15 min.	DIPEA	36%

In contrast to the previous reaction (section 3.2.2), the high temperature (78 °C) and protic solvent in this case were disadvantageous (Table 3, entry 8 and 9), in an aprotic solvent and with catalytic amount of DIPEA, the intermediate **29** was formed rapidly at RT within 15 minutes (Table 3, entry 11), a prolonged reaction duration was not beneficial, because after 2 hours the TLC analysis showed that the already formed product vanished (Table 3, entry 10).

3.4.1.3 Formation of the thiazole system form **28** containing *N*-methylated indole.



Scheme 37. Preparation of **30** under the optimized conditions.

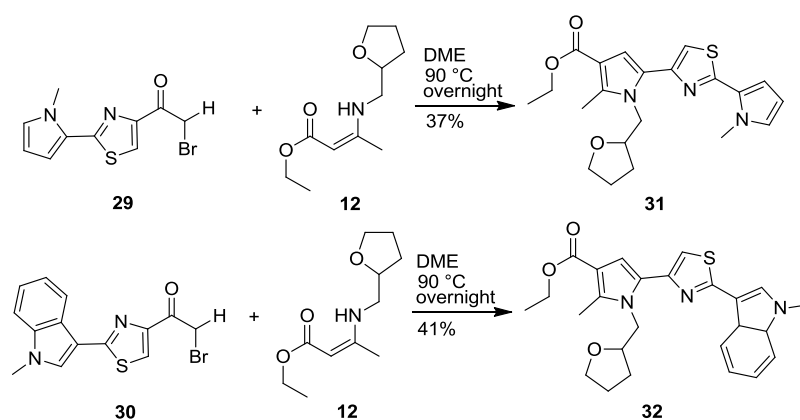
Table 4. Preparation of **30** under two conditions.

entry	solvent	temperature	reaction time	base	yield
12	THF	RT	20 min.	DIPEA	/
13	EtOH	RT	30 min	none	26%

Surprisingly the same conditions, by using which the intermediate **29** was successfully constructed, did not work in the case of synthesis of **30** (Table 4. entry 12). Instead intermediate **30** was generated in ethanol without DIPEA additive within 30 min in 26% isolated yield (Table 4. entry 13).

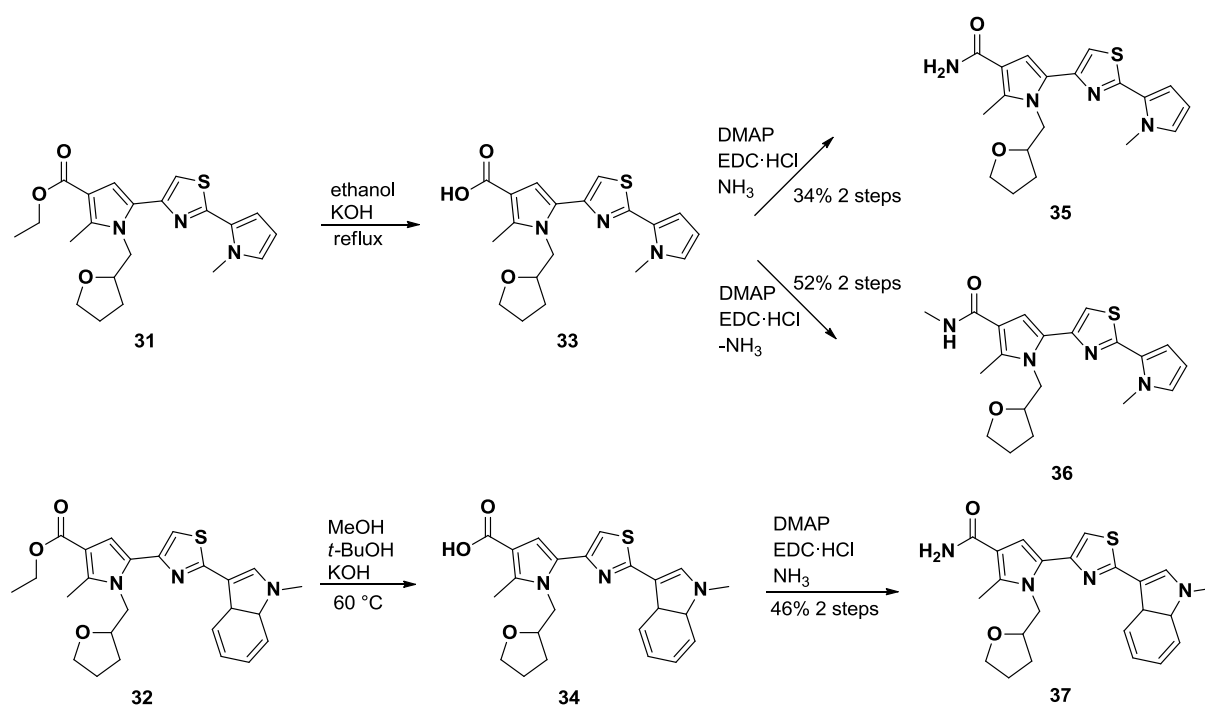
3.4.1.2 The route toward the final products **35**, **36** and **37**.

Both intermediates **29** and **30** were then allowed to react with fragment **12** to construct the pyrrole ring system. Under the established conditions both intermediates were respectively converted into the intermediate **31** and **32** with isolated yield 37% and 41%.



Scheme 38. Formation of the intermediate **31** and **32**.

Afterwards, intermediates **31** and **32** were supposed to be hydrolyzed into carboxylic acids by following the established conditions. However, the intermediate **32** was not soluble in ethanol and thus after 24 hours no reaction took place as judged by TLC. Instead it was dissolved in the mixture (MeOH:*t*-BuOH:40% KOH water solution = 2:2 :1) and then heated at 60 °C for 36 hours, then the TLC showed that the starting material was completely consumed and the carboxylic acid was formed thereafter. The hydrolysis of the compound **31** took four times longer (48 hours) than the established conditions (12 hours), but eventually the hydrolysis was accomplished. The unpurified carboxylic acids **33** and **34** were then directly transformed through the established method into the amides **35**, **36** and **37** respectively with isolated yield of 34%, 52% and 46% calculated for two steps.



Scheme 39. The finalization of the syntheses of the final products **35**, **36** and **37**.

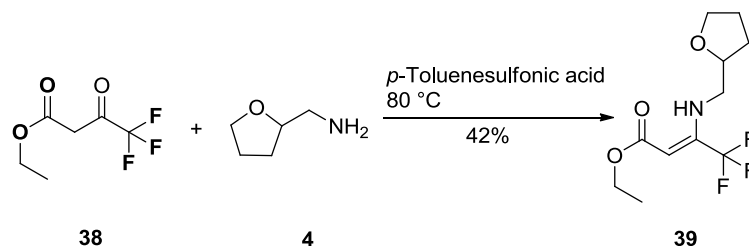
3.4.2. Derivatization at the 5 position in the pyrrole ring system

3.4.2.1 Derivatization at the 5 position with trifluoromethyl group

In this part of the synthesis, the 5'-methyl residue in the pyrrole ring system will be replaced by the strong electron withdrawing trifluoromethyl group in order to determine the contribution of this particular position to the whole biological activity.

Besides, based on the common knowledge, incorporation of fluorine atoms into the bioactive compounds often enhance its bioactivity and improve the pharmacological property.^[28] The fluorine atom could mimic the hydrogen atom. Since the trifluoromethyl group is not much larger than the methyl group but occupies more room than the isopropyl residue, and thus it could be better filled into the enzyme receptor site. Furthermore the fluorine sometimes blocks certain reactions and in such cases these compounds subsequently possess improved anti-cancer reactivity. The trifluoromethyl group significantly increases the lipophilicity of the bioactive compound and moreover the strong electronegativity of the fluorine changes the electron effect and thus enhances the thermal and oxidative resistance of the compound.

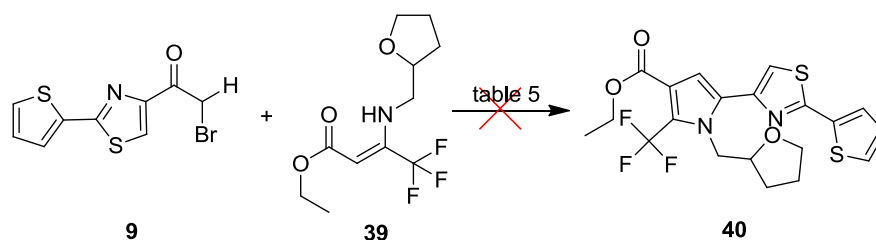
The synthesis commenced with the new starting material **38**, due to the additional trifluoromethyl group the desired enamine **39** could no longer be generated under the previous mild conditions (section 3.2.3). However with help of catalytic amount of the *p*-toluenesulfonic acid, the enamine acetyl ethyl ester **39** was still generated at 80 °C in moderate isolated yield (42%).^[61]



Scheme 40. The formation the enamine ester **39**.

3.4.2.1.1 Attempt of the formation of the pyrrole through the Hantzsch method

The intermediate **39** was allowed to react with the fragment **9** to form the pyrrole ring under various conditions.

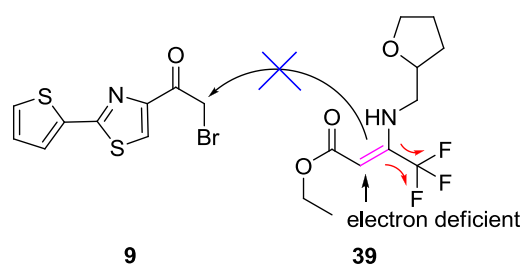


Scheme 41. Failed pyrrole ring formation through the initial method.

Table 5. Pyrrole formation under various conditions.

entry	solvent	temperature	reaction time	base	yield
14	DME	90 °C	overnight	none	/
15	DME	90 °C	overnight	DIPEA	/
16	DMF	140 °C	2 h	none	/
17	DMG	200 °C	2 h	none	/
18	diphenyl ether	200 °C	2 h	none	/

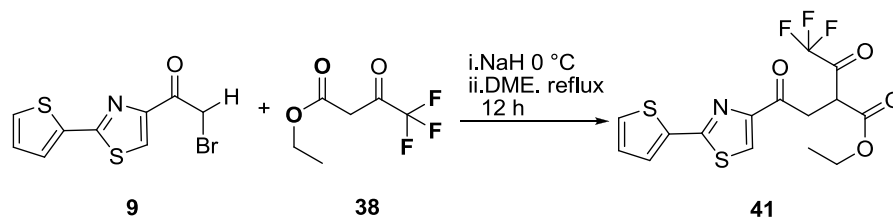
At first the reaction was carried out overnight under reflux of DME (Table 5. entry 14), but no product was formed. Then the reaction was repeated under same condition but with additional DIPEA, (Table 5. entry 15) the starting material decomposed overnight without traces of the desired product. Then the reaction was conducted in DMF, DMG and diphenyl ether and the reaction mixture was heated at 140 °C, 200 °C and 200 °C for two hours respectively (Table 5. entry 16, 17, 18). In all these cases, no reaction took place and the starting materials rapidly decomposed. The issue was caused by the additional strong electron-withdrawing fluorine atoms. The double bond of the enamine under the influence of the fluorine atoms is extremely electron deficient and could not initiate the nucleophilic substitution with the haloketone **9** and thereby no follow-up steps are expectable.

**Figure 14.** The trifluoromethyl group obstructed the pyrrole formation.

3.4.2.1.2 Attempt of the formation of pyrrole through the Paal-Knorr method

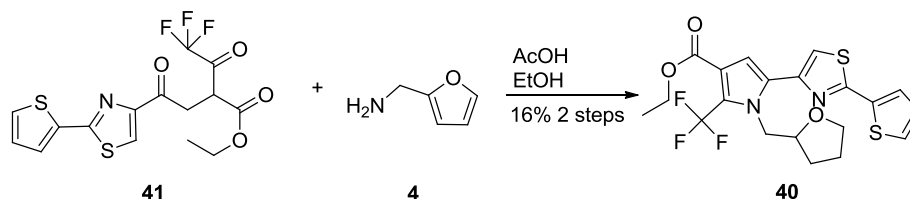
With no success of the pyrrole formation through the Hantzsch route, the Paal-Knorr method was examined.

The generation of the 1,4-dicarbonyl compound **41** from **38** and intermediate **9** as the first step of the new route was hereby investigated.



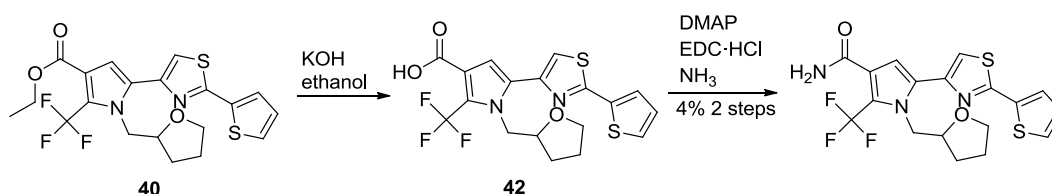
Scheme 42. Generation of the 1,4-dicarbonyl intermediate **41**

Again, due to the influence of the fluorine atoms, the α -carbon atom between two carbonyl groups is less nucleophilic and after the deprotonation, it could unlikely attack the haloketone **9** neither in acetone (reflux with KI)^[62] nor in DMF (at RT)^[63] and under these conditions the reaction did not occur even after 24 hours. Alternatively under reflux of DME, after 12 hours the 1,4-dicarbonyl compound **41** was quantitatively formed judged by the TLC and the raw product was directly converted without purification. (Scheme 42)

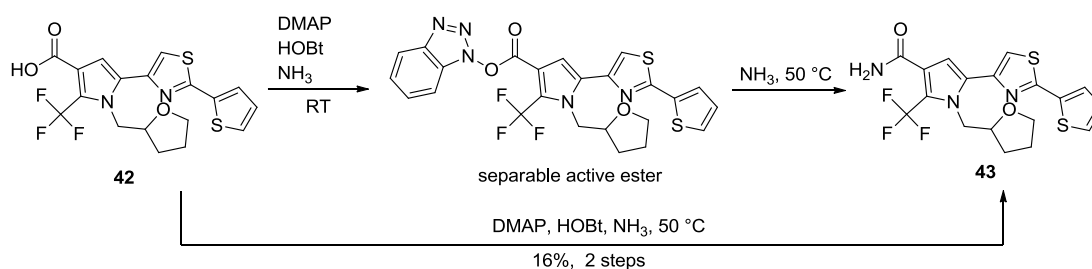


Scheme 43. Successful pyrrole formation through Paal-Knorr method.

The pyrrole ring formation from **41** and **4** through Paal-Knorr approach was successful through the previous established conditions (16% isolated yield over 2 steps) (Scheme 43), and followed by the hydrolysis of the intermediate **40** under the established conditions, then without purification converted to the amide **43** through the previous reaction (Scheme 44). The isolated yield over 2 steps was only 4% through the EDC / DMAP activation.



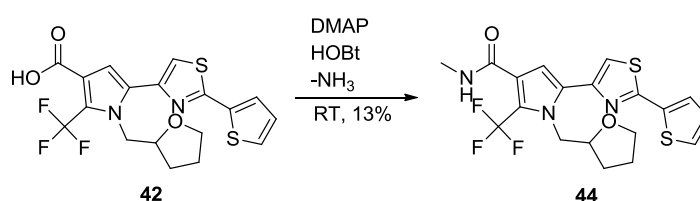
Scheme 44. Amide formation with EDC / DMAP activation.



Scheme 45. Amide formation with HOBt / DMAP activation.

For comparison, the amide formation was performed again by using the HOBt / EDC coupling reagent combination (Scheme 45).^[64] At first the coupling was conducted at RT, the reaction seemed to be finished after 1 h (TLC control), but surprisingly the isolated product was the active ester intermediate according to the NMR spectra. In this case the fluorine atoms possibly stabilize the active ester intermediate, which commonly exists only for an extremely short period. So in this case, the ammonia may need more energy to replace the HOBt residue to form the desired primary amide bond, accordingly the reaction was performed again at 50 °C with 10 folds of ammonia and after 4 hours the reaction concluded. This time the correct amide was formed with 16% isolated yield over 2 steps.

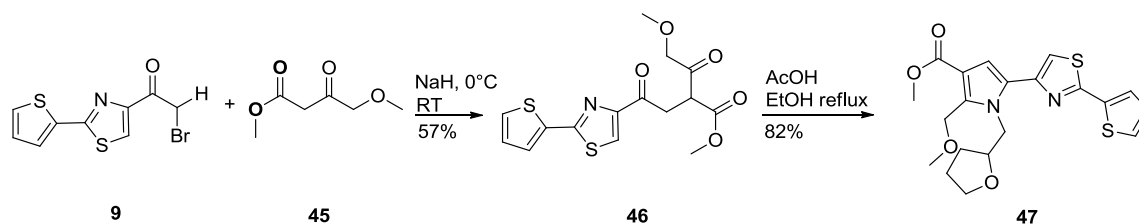
Simultaneously The N-methylated amide **44** was converted at RT from **42** with 13% yield over 2 steps.



Scheme 46. Formation of the **44** with HOBt / DMAP activation.

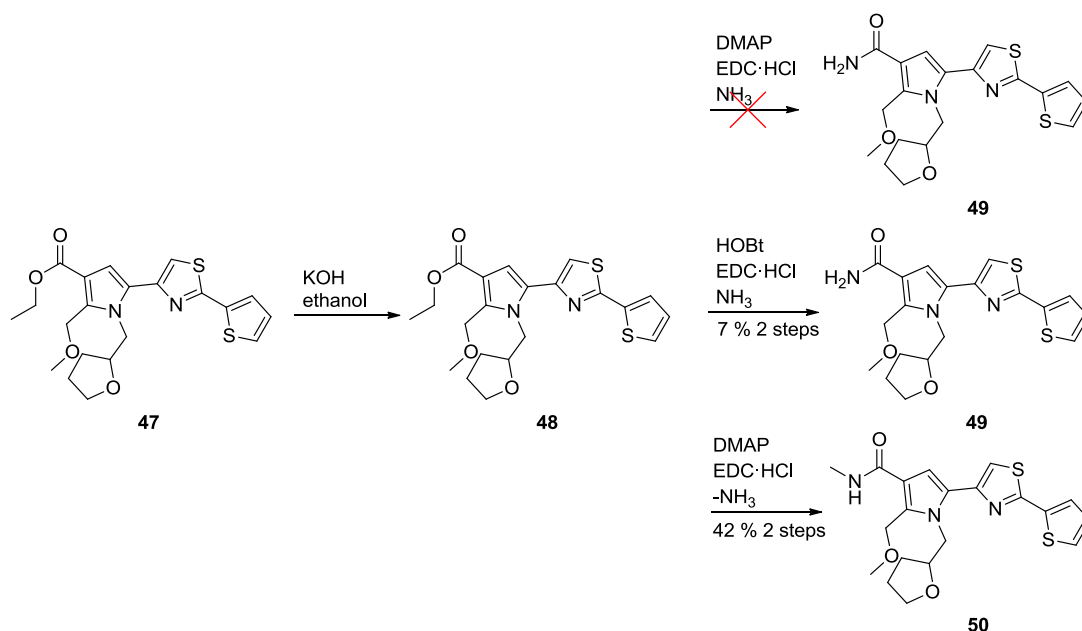
3.4.2.2 Derivatization in the 5 position with methoxyethyl residue

In order to transform the 5 position into an H-acceptor, a methoxyethyl group was introduced in place of the methyl residue. The synthesis still followed the Paal-Knorr method. The 1,4-dicarbonyl compound **46** was formed in 57% yield from starting material **45** and fragment **9** under the established conditions with slight adjustment of temperature. Then the compound **46** was smoothly converted into the compound **47** within an hour in 82% isolated yield (Scheme 47).



Scheme 47. Preparation of the intermediate **47**.

The compound **47** was then hydrolyzed with KOH to the carboxylic acid **48** and the unpurified carboxylic acid **48** was converted into both amide **49** and the N-methylated amide **50**. The formation of the amide **49** did not work with the coupling reagent combination EDC / DMAP, no desired product was isolated in this way, however with EDC / HOBt the product was obtained in poor yield (7% over 2 steps). The conversion to the N-methylated amide did not encounter large obstacles and the N-methylated amide was readily synthesized by using EDC / DMAP in 42% isolated yield over 2 steps (Scheme 48).

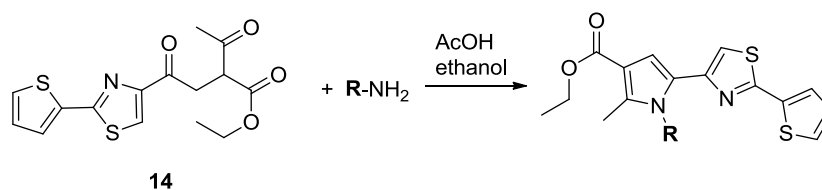


Scheme 48. The generation of the final products **49** and **50**.

3.4.3 Supplement of the library through further N-substituted pyrrole derivatives

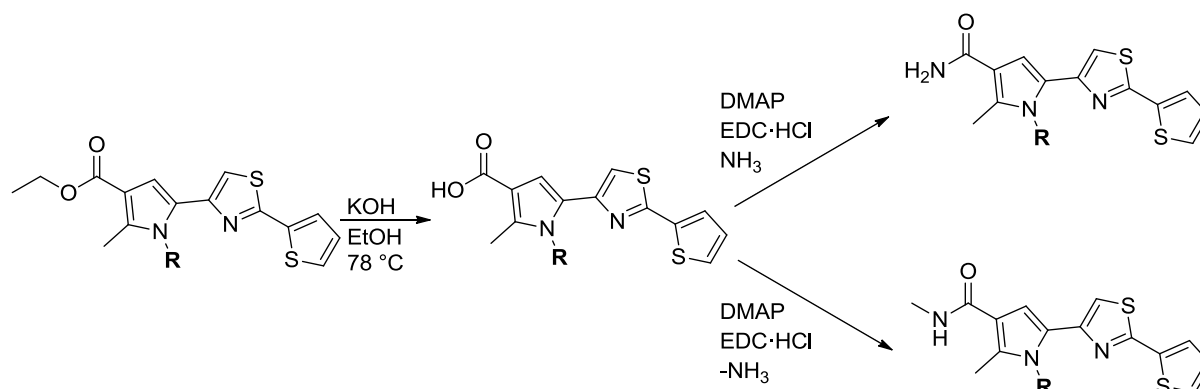
By following the previous examples (compounds **23** and **24**), more derivatives with N- substituted pyrrole ring systems were generated through the Paal-Knorr method to study the influence of the side chain on the overall bioactivity. The

originally attached 2-methyl tetrahydrofuranyl group in the following studies will be replaced by a few aromatic residues. Upon these changes the side chain will be enlarged due to the larger ring size of the benzene and these changes will increase the chance to bind to the binding site. Besides the benzene ring could enhance the rigidity of the bioactive compound and improve the metabolism resistance. Moreover the benzene ring itself could carry various substitutions and inhibit different pharmacological properties. The generation of ester precursors for these derivatives was straightforward from the 1,4-dicarbonyl compound **14** with different amines. The syntheses under the established reaction conditions were generally trouble-free (Table 6).



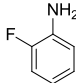
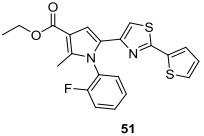
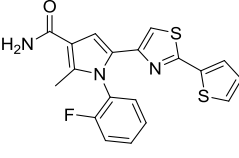
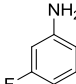
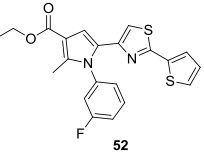
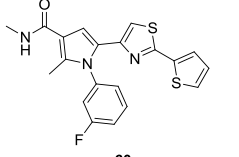
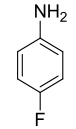
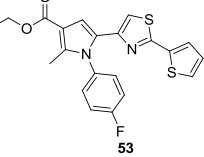
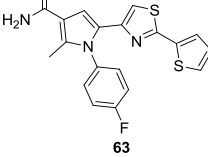
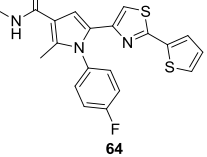
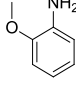
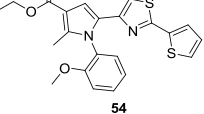
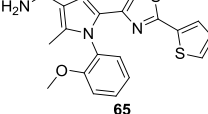
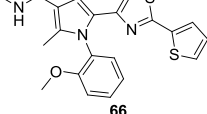
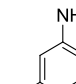
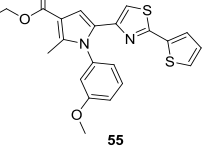
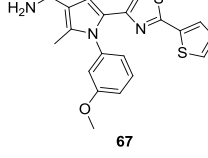
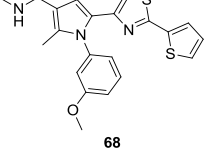
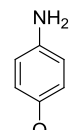
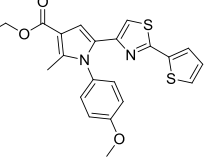
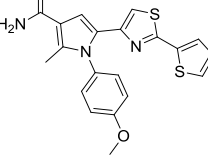
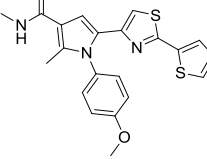
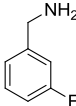
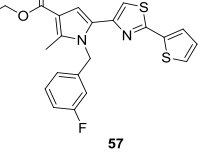
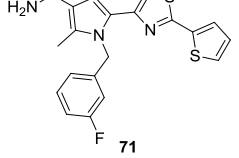
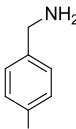
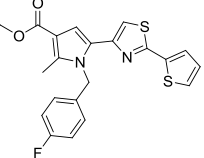
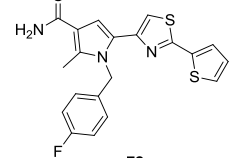
Scheme 49. General procedure of generation intermediate of N-substituted pyrrole derivatives

Then all intermediates were hydrolyzed and converted to the respective amides.



Scheme 50. General procedure of the generation of N-substituted pyrrole derivatives

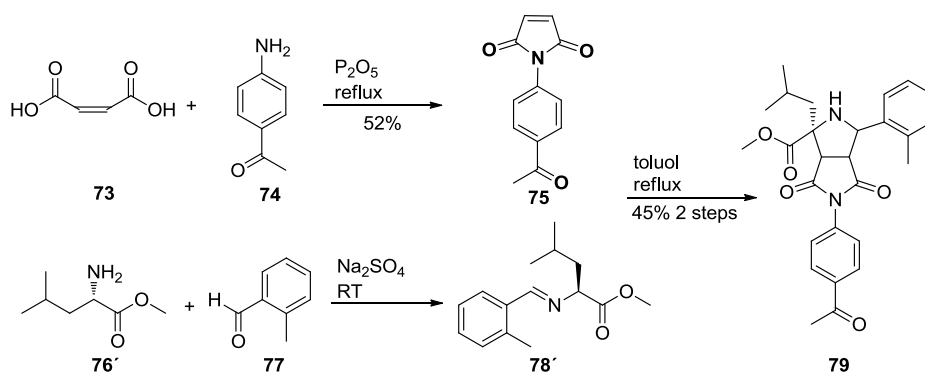
Table 6. Further N-substituted pyrrole derivatives

R-NH ₂	intermediate	final product
	 yield 82%	 52%
	 yield 86%	 45%
	 yield 96%	 29%  59%
	 yield 49%	 22%  35%
	 yield 69%	 21%  59%
	 yield 75%	 49%  68%
	 yield 80%	 45%
	 yield 41%	 37%

3.5 Synthesis of the bicyclic compounds and its derivatives

3.5.1 Synthesis of the lead structure of the bicyclic compounds

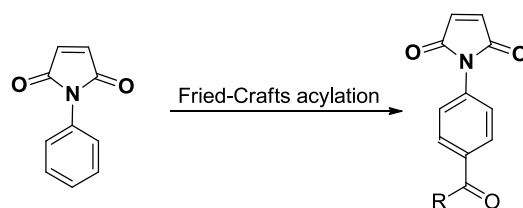
The formation of the methyl ester of lead structure **79** was straightforward, because all the required starting materials were commercially available. Starting with the synthesis of the under building block **78'**, it was easily formed through imide formation from maleic acid **73** and the (4-aminophenyl)ethanone (**74**) with phosphorus pentoxide to yield the cyclic imide **75** in 52% isolated yield.^[54] Followed by the condensation of the L-leucine methyl ester **76** with 2-methylbenzaldehyde (**77**) over 30 hours,^[53] the raw imine **78'** was then allowed to react with cyclic imide **75** to yield the bicyclic methyl ester **79** with an isolated yield of 45% over two steps (Scheme 51).^[55]



Scheme 51. Synthesis of the **79** of the bicyclic inhibitor.

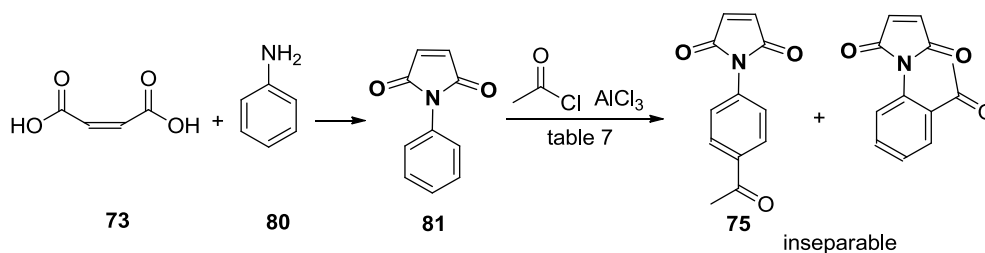
3.5.2 Derivatization at the *para*-position of the aniline

Instead of the commercial purchase, the derivatization of the *para*-position of aniline was about to be achieved by introduction of different moieties through the Friedel-Crafts acetylation. If the Friedel-Crafts acetylation worked specifically at the *para*-position, this method was capable of generation of a large number of *para*-aldehyde derivatives.



Scheme 52. Derivatization of the *para*-position through the Friedel-Crafts acylation

The first attempt was the synthesis of intermediate **75** from **81** through Friedel-Crafts acylation.



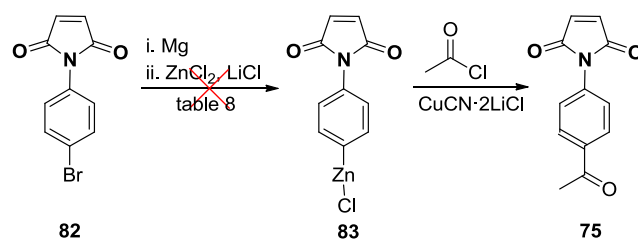
Scheme 53. Unselective Friedel-Crafts acylation.

Table 7. Friedel-Crafts acylation under various conditions.

entry	solvent	temperature	results
19	nitrobenzene	RT	no reaction
20	nitrobenzene	60 °C	<i>o</i> and <i>p</i> acetylated mixture
21	1,2-dichloroethene	RT	no reaction
22	1,2-dichloroethene	60 °C	<i>o</i> and <i>p</i> acetylated mixture

The acetylation of the aniline was tricky, at RT the acylation took place neither in nitrobenzene^[65] nor in 1,2-dichloroethene (Table 7. entry 19 and 21), unless the temperature reached 60 °C. Both *ortho*- and the *para*-positions were unspecifically acetylated (Table 7. entry 20 and 22) judged by the NMR analysis and even worth was that the resulted products had the identical polarity and it was impossible to separate both products through flash chromatography.

The direct *para*-Friedel-Crafts acylation failed, however the *para*-acetyl moiety might be obtained indirectly from some *para*-substituted precursors, such as the *para*-bromo precursor through the chemical manipulation. Theoretically, the bromine residue could be converted into the aryl-metallic bromides and then added to acetyl chloride to yield the desired *para*-acetyl compound. Two approaches hereby have been examined.



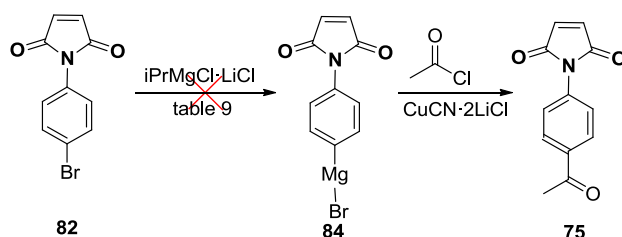
Scheme 54. Unsuccessful attempt of generation of **75** through *para*-organozinc compound **83**.

Table 8. Attempts to generate the organozinc compound **83** at two temperatures.

entry	temperature	result
23	RT	no reaction
24	40 °C	no reaction

The first experiment (Table 8, entry 23 and 24) was intended to convert the compound **82** into a highly active organozinc chloride **83** via Grignard reagent^[66] and organozinc chloride **83** was then expected to react with acetyl chloride with a Cu(I) catalyst. Unfortunately, the transmetalation did not take place, the elemental magnesium seems to be insufficient reactive to transform the starting material to the Grignard reagent.

In the second approach, it was intended to form the *para*-Grignard compound *in situ* through the transmetalation from a reactive Grignard isopropylmagnesium chloride lithium chloride complex **85**^[67] and then the *para*-Grignard intermediate **84** would be added to acetyl chloride along with a Cu(I) catalyst.



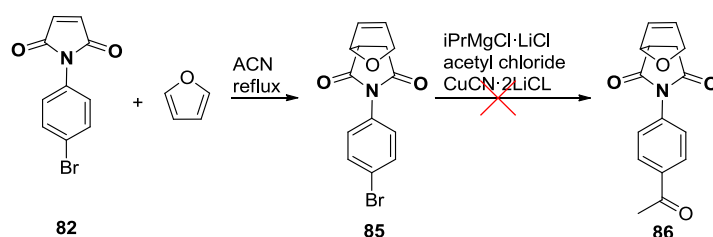
Scheme 55. Unsuccessful attempt to generate the *para*-acylated compound through a Grignard reaction

Table 9. Generation of the *para*-Grignard compound at different temperatures

entry	temperature	result
25	0 °C	decomposition
26	-60 °C	decomposition
27	-78 °C	no reaction

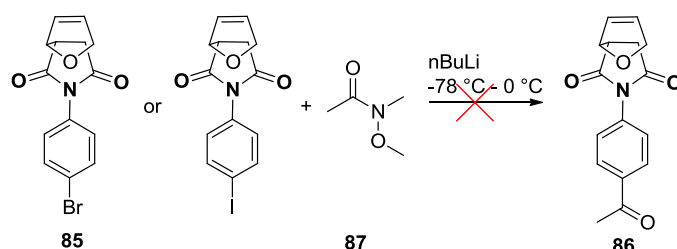
At -60 °C (Table 9. entry 25) and 0 °C (Table 9. entry 26), upon the addition of the isopropylmagnesium chloride lithium chloride complex solution into the compound **84**, the starting material was consumed within 5 min. but formed a polymeric substance (very high polarity observed at TLC). The isopropylmagnesium chloride may attack the double bond of the cyclic imide and trigger the polymerization. Oppositely, at -78 °C no reaction was observed (Table 9. entry 27).

In order to utilize the organometallic reagent, the double bond was deliberately masked by furan through a Diels-Alder reaction^[68] and the furan could be easily removed after the establishment of the *para*-acetyl compound through the retro Diels-Alder reaction. As expected, without the disturbance of the double bond the compound was more stable but showed very sparingly solubility in THF. Unfortunately at 0 °C after 8 hours no reaction happened between **86** and the isopropylmagnesium chloride lithium chloride complex (Scheme 56).

**Scheme 56.** Failed attempt of generation **86** through the protected intermediate **85**

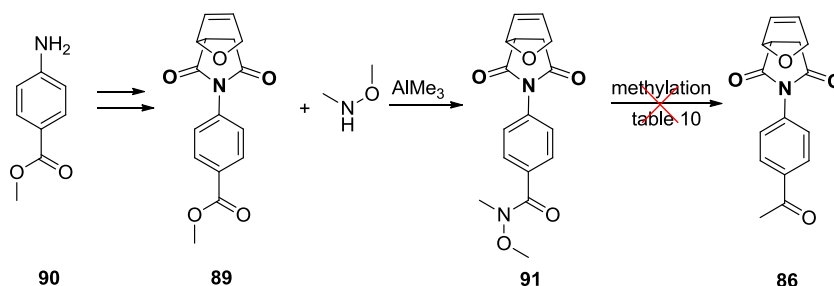
Acetylation through the organometallic compound was found to be very difficult in this case study, alternatively a sophisticated idea based on the Weinreb ketone synthesis was thereby tested. Starting with furan protected compound **85**, through a lithium-halogen exchange it was supposed to be transformed into an

organolithium intermediate, which was then allowed to react with the N-methoxy-N-methylacetamide **87** (Weinreb amide) and was expected to form the product **86**. Sadly this idea could not be realized since no reaction took place in a large range of temperatures ($-78\text{ }^{\circ}\text{C}$ – $0\text{ }^{\circ}\text{C}$).^[69] The iodo variation was also tested, but it did not change the outcome (Scheme 57). This was presumably again caused by the very limited THF solubility of the intermediate **85**.



Scheme 57. Unsuccessful attempt to generate **88** through the Weinreb ketone synthesis

Conversely, the ester **89** was synthesized in 2 steps from the starting material **90** and was successfully transformed into the Weinreb amide **91**,^[70] and followed by the methylation of this Weinreb amide to yield the product **86** (Scheme 58).



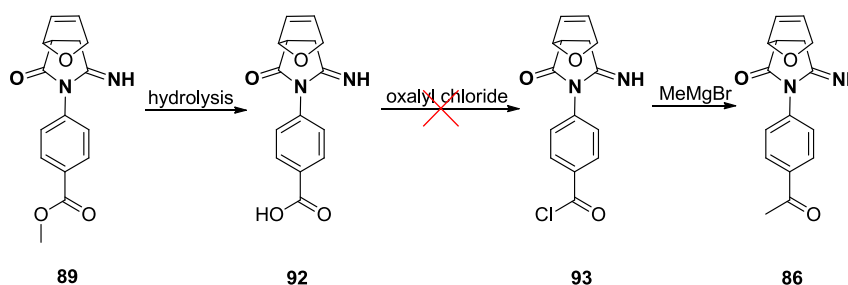
Scheme 58. Unsuccessful attempt to generate **86** via Weinreb amide **91**

Table 10. Methylation of **91** under different conditions

entry	methylation reagent	temperature	result
28	Mel	$0\text{ }^{\circ}\text{C}$	no product
29	Mel	$-30\text{ }^{\circ}\text{C}$	no product
30	Mel	$-78\text{ }^{\circ}\text{C}$	no product
31	MeMgBr	1h, $-78\text{ }^{\circ}\text{C}$, 1h $0\text{ }^{\circ}\text{C}$	no product

The Weinreb amide intermediate **91** was initially constructed after a few attempts, but unfortunately the intermediate **91** was still very limited soluble in THF and thus the methylation of **91** did not work by applying either MeI (Table 10. entry 28-30)^[71] or MeMgBr (Table 10. entry 31), no product was isolated, whereas most starting material remained unreacted.

The last attempt to achieve the *para*-acetyl residue was to turn the ester **89** firstly into the carboxylic acid **92** (Scheme 59), then the acid would be converted to acid chloride **93** with oxalyl chloride and finally methylated with methyl iodide. Unfortunately in practice the formed acid **92** was soluble neither in THF nor in DCM, therefore, the transformation of the acid **92** into acetyl chloride **93** failed.



Scheme 59. Unsuccessful attempt to generate **87** via acyl chloride **91**

The attempt to achieve the *para*-acetyl group in the compound **83** was neither successful directly through the Friedel-Crafts acylation nor indirectly through other *para*-substituted precursors. The double bond from the upper side was found to be vulnerable in the presence of strong nucleophile such as organometallic compound, however protection of the double bond with furan made the new compound very limited soluble in many organic solvents and it was believed that this sparingly solubility prevented further reactions. The introduction of the *para*-acetyl group of the particular compound **81** is highly challenging, further *para*-aldehyde derivatives might unlikely be generated in the manners, which were tested before, but rather by direct using commercially available chemicals.

4. Summary and conclusion

In this work the lead structure of the heterocyclic inhibitor has been synthesized. Since there is no stereo center, the synthesis in general was straightforward and encountered no problems. Furthermore 23 heterocyclic derivatives have also been generated by using the available starting materials, the derivatization was found in all four designated areas, which are outlined in the earlier chapter. The syntheses of these derivatives were mostly successful except the synthesis of **17**. The synthesis of the fluorine containing compound **40** was challenging. The trifluoromethyl group changed the electron density significantly, so that the Hantzsch method was no more applicable. Fortunately the compound **40** could still be achieved through the Paal-Knorr method but only obtained in poor yield (6%). Because the purpose of this work was to rapidly generate the library of the Cdc25A inhibitor for the biological assessment, no optimization of the yield has been performed.

According to the preliminary biological assessment, the thiophene group on the far right side is important for the biological activity, upon exchange of thiophene against other heterocyclic compounds like N-methyl pyrrole or N-methyl indole, the biological activity dropped. The replacement of the nitrogen atom of pyrrole also alters the biological activity. If the benzene residue was attached to the nitrogen atom via the CH₂ (benzyl), the biological activity was lower than the direct attachment of the aromatic ring system to the nitrogen atom. Moreover the fluorine substitution on the aromatic ring system enhanced the biological activity. Like expected the trifluoromethyl group at the 2-position instead of the methyl group also improved the biological activity.

The study of the bicyclic inhibitor didn't progress as deep as for the heterocyclic inhibitor, though the synthetic route towards the lead structure was nearly finished, the ester **79** only needs to be hydrolyzed to form the final product. By following the same synthetic strategy further derivatives could be prepared. The attempt of derivatization at the *para*-position of the aniline failed, the idea of the introduction of a *para*-acetyl group through the Friedel-Crafts acylation could not be executed due to the unselective acylation at three possible positions. The indirect conversion from other *para*-substituted precursors into the *para*-acetyl aniline was not successful either. Therefore this reduced the degree of the

derivatization at the *para*-position. Nevertheless, there are sufficient amount of commercially available *para*-substituted anilines, which could be converted into a large library for the SAR study.

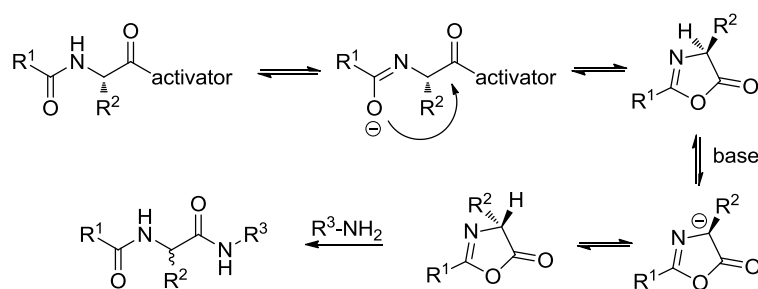
Part II. Development of solid phase synthesis of cyclic peptides

1 Introduction

1.1 Conventional and native chemical ligation methods of peptide synthesis

1.1.1 Conventional methods of peptide synthesis

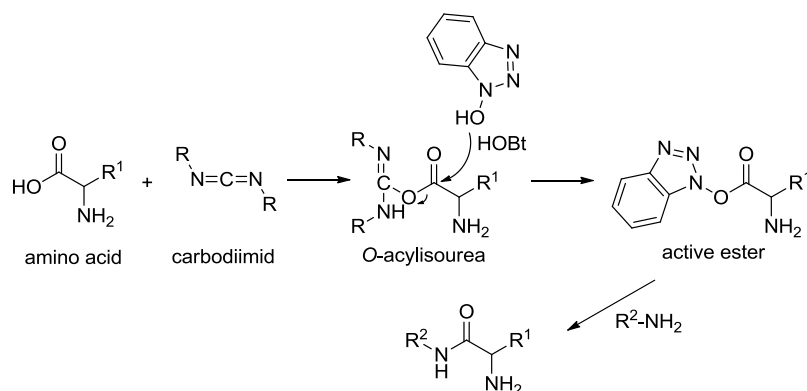
Conventionally the amide bonds of the peptide was formed through activation of the respective coupling reagent, for this purpose many activators have been tested, evaluated and applied in the past decades. Upon adding the coupling reagent, the carboxylic acid, which is involved in the amide bond formation, is converted into the active intermediate and followed by the sequential amide bond formation with other amino. Since fifty years the most important activators used for amide bond formation are the carbodiimides (*N,N'*-dicyclohexylcarbodiimide (DCC)^[72] and *N,N'*-diisopropylcarbodiimide (DIC)). Carbodiimids have been regularly applied to generate active esters and symmetrical anhydrides or for a direct coupling. Upon addition of the carbodiimides into the carboxyl acid, the carboxyl group is converted into the *O*-acylisourea, which is one of the most reactive acylating intermediates. In the presence of free amino groups, the *O*-acylisourea intermediate will be quickly converted into the respective amide compound and urea. But the *O*-acylisourea intermediate is highly reactive and often results in the racemization of formed product (Scheme 60).^[72]



Scheme 60. Racemization under basic conditions

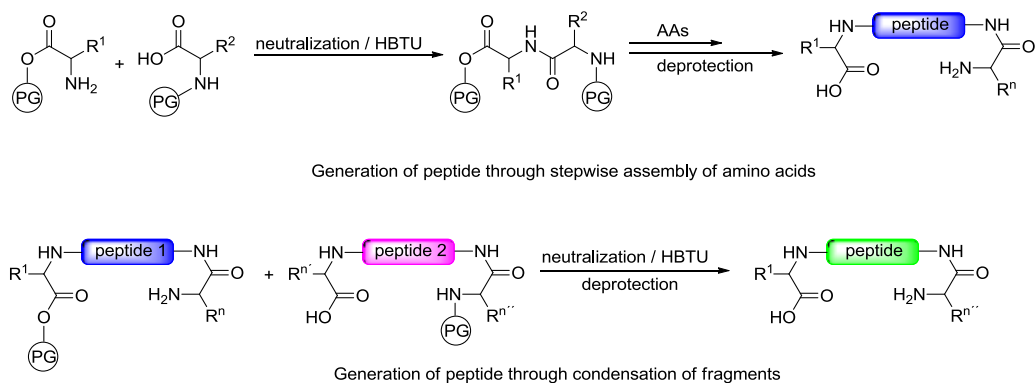
To reduce the extend of racemization, azolol additives (hydroxybenzotriazole (HOBt),^[73] *N,N,N',N'*-tetramethyl-*O*-(1*H*-benzotriazol-1-yl)uronium hexafluorophosphate (HBTU), 1-[Bis(dimethylamino)methylene]-1*H*-1,2,3-triazolo[4,5-*b*]pyridinium 3-oxid hexafluorophosphate (HATU), and *O*-(Benzotriazol-1-yl)-*N,N,N',N'*-tetramethyluronium tetrafluoroborate (TBTU) etc.) are introduced. Through *O*-acylisourea intermediates or directly, azolol forms

active ester intermediates with the carboxyl group and then this is converted into the amide with respective amine. The final product, which is constructed in this way, can be usually obtained in high yield with much lower degree of racemization (Scheme 61).



Scheme 61. Amide formation through active ester

By utilization of the coupling reagents, two methodologies were developed with the intention of generating the long chain peptides (Scheme 62). The former is the stepwise coupling of each amino acid by using the *in situ* neutralization / HBTU activation protocol in the given order. This approach is a long standing and reliable method but lacks flexibility and is also very time-consuming. The latter is the condensation of different pre-made fragments through an amide bond linkage, which is more flexible to generate derivatives. But applications of this method require a large excess of fragments and often cause enormous waste of materials and furthermore it can potentially lead to racemization. These setbacks sometimes limit their widespread use and therefore, a more efficient way to construct long peptide was investigated in the past.



Scheme 62. Two different ways of generation of peptides

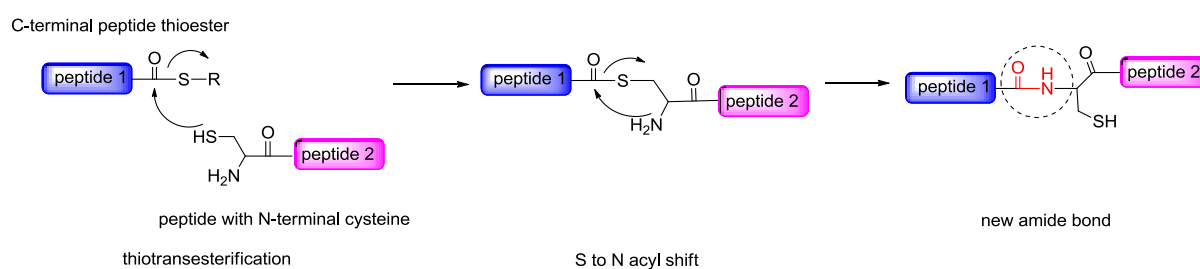
1.1.2 Native chemical ligation (NCL)

1.1.2.1 Birth and the main features of the NCL

Following Wieland's pioneering work on the activator-free formation of a unique valine and cysteine junction,^[74] many groups have worked on the development of practical methodologies for peptide and protein syntheses. In 1994 Dawson, Muir and Kent reported a novel native chemical ligation (NCL)^[75] and demonstrated the practical application of NCL through the synthesis of human interleukin 8 (IL-8), which is a 72-amino polypeptide bearing four cysteine residues.

The newly introduced native chemical ligation concept uses the idea of fragment condensation to generate long peptides. In this particular case the amide bond linkage of the fragments is achieved through a X-Cys junction and replacement with the thermodynamically stable amide bond.

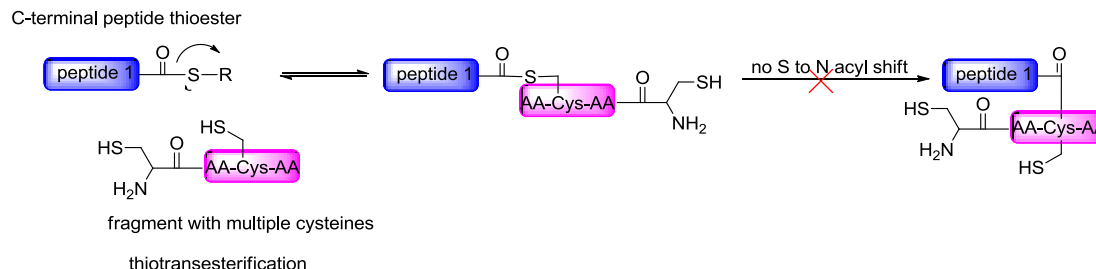
In order to successfully generate the peptide sequence by applying this methodology, at least one cysteine residue is required to be contained in the peptide sequence. The position, where the cysteine situated, is used as the junction point for the condensation. Along this X-Cys junction point the entire sequence can be broken into two peptidic fragments, which carry the C-terminal junction partner X (X could be a random amino acid) and the N-terminal cysteine. However, the fragment carrying the C-terminal junction partner, could not be used directly for the NCL, but rather synthesized as a C-terminal peptide thioester with an adequate thiol leaving group. Frequently, the ligation is carried out in buffered neutral (pH = 6.5 ~ 7.5) aqueous environment, which is also suitable for many biological processes and modifications. After two separately synthesized fragments are added into the buffered solution, a thioester-mediated amide formation will take place (Scheme 63).



Scheme 63. The native chemical ligation between two peptides

At first the sulfhydryl group of the N-terminal cysteine substitutes the C-terminal peptide thioester to construct a new thioester intermediate and then the nearby amino group of the N-terminal cysteine replaces the sulfhydryl group spontaneously to irreversibly generate a new amide bond and thus two fragments are linked.

The NCL proceeds always with high regioselectivity and chemoselectivity. The high regioselectivity means that this method tolerates sulfhydryl side chains in the proceeding fragments. Technically sulfhydryl groups of every cysteine could participate in the transthioesterification with C-terminal peptide thioester, but this process is reversible and both thioesters exist in balance. The follow-up spontaneous S–N acyl shift will break this balance and transform the thioester intermediate into the final amide product. The S–N acyl shift could specifically take place between the thioester intermediate and the free amino group of the N-terminal cysteine, therefore only the thioester intermediate at the junction point could be converted into the amide bond and thus appears as the sole final product (Scheme 64).



Scheme 64. NCL is regioselective.

The chemoselectivity means that the S–N acyl shift would take place only between thioester intermediate and the free amino group of the N-terminal cysteine, not the amino groups at other positions of the peptide sequence.

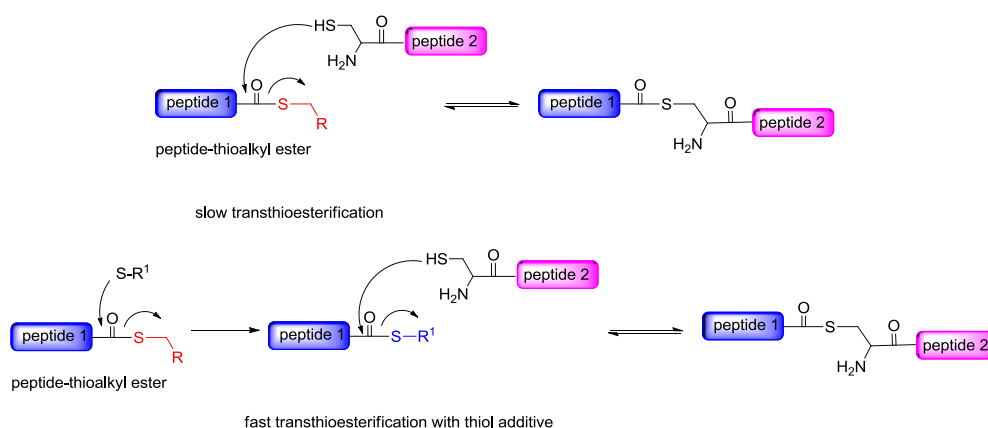
1.1.2.2 Limitation of the NCL

Since early 90s', the NCL methodology has been intensely investigated. In 1999, Dawson investigated the feasibility of NCL of cysteine with 20 other amino acids.^[76] In the investigation, a trityl-associated-mercaptopropionic acid-leucine (TAMPAL) resin was converted from the N^α -Boc-MBHA resin and S-trityl mercaptopropionic acid, and on this formed TAMPAL resin the C-terminal Leu-

Tyr-Arg-Ala-X thioester (X = 20 amino acids) was synthesized and after cleavage this fragment was allowed to ligate under the standard NCL condition with the fragment CRANK and the conversion rates of all 20 amino acids were constantly recorded. The X-Cys junction was observed in all cases afterwards, however the facility of X-Cys junction substantially depends on the ligation partner. Based on their effectiveness, the amino acids were then classified into four categories. The histidine, cysteine and glycine were found to be best suitable for the NCL, whereas the valine, isoleucine and proline were least favored for the NCL due to their β -branched side chain. The β -branched side chain severely hinders the progression of the NCL and thus the NCL proceeds slowly with the member of this group. After 48 hours, with none of these three amino acids a conversion of 50% could be achieved. These results were confirmed through the synthesis of hsPLA₂ and an enzymatic inactive hsPLA₂.^[76] Out of 20 amino acids, 17 are determined to be fully compatible with NCL, whereas valine, isoleucine and proline could only be used for this particular method with large limitation.

1.1.2.3 Promotion of NCL through thiol additives

The NCL is initialized by transthioesterification, through which the C-terminal peptide thioester is converted to a new thioester intermediate. The C-terminal peptide- α -thioalkyl ester is frequently used for the synthesis, but the thioalkyls are generally bad leaving groups and thus often insufficient reactive for the transthioesterification. Unfortunately, better leaving groups, such like 5-thio-2-nitrobenzoic acid^[77] are not easily accessible. The transthioesterification is the rate-limiting step and thus using the C-terminal peptide- α -thioalkyl ester significantly prolongs the reaction time. However, the less reactive thioalkyl residues can be replaced prior to the transthioesterification by reactive exogenous thiol additives *in situ* and results in highly reactive peptide thioester, consequentially the ligation rate will significantly rise. The thiol additive forms new thioester through substitution of original thioalkyl residue and this new thioester is much more reactive and can be much easier replaced by the sulfhydryl group of N-terminal cysteine than the inert predecessors (Scheme 65).



Scheme 65. Acceleration of the transthioesterification through thiol additive

The popular thiol additives are benzyl mercaptan / thiophenol mixture and alkanethiol sodium 2-sulfanylethanesulfonate (MESNa) (Figure 14). Dawson firstly investigated the influence of benzyl mercaptan / thiophenol additive on the ligation rate.^[78] At the beginning of the investigation, only benzyl mercaptan was added to replace the alkyl thioester, but the new formed peptide benzyl thioester was still not reactive enough, so additionally thiophenol was introduced and the peptide benzyl thioester intermediate was transformed further into peptide phenyl thioester, which is a highly reactive intermediate. By using this combination, the ligation time was substantially reduced.

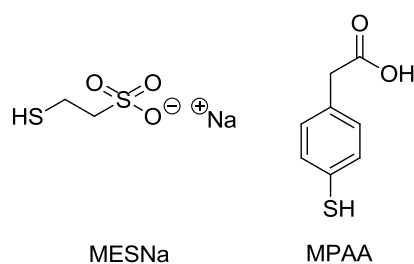


Figure 14. Two frequently used thiol additive

Sodium 2-sulfanylethanesulfonate (MESNa) is an alkanethiol additive,^[79] which is also regularly applied for the NCL, but in practice, MESNa was only found to have limited catalytic ability. Alternatively, Kent used thiophenol,^[80] which is a moderate leaving group and has been previously deployed for the NCL. Diverse electron withdrawing groups were intentionally introduced at the *para*-position of thiophenol in order to reduce the nucleophilicity of the sulfhydryl group and consequentially generate a perfect thiol leaving group. After a series of

experiments, the newly prepared (4-carboxymethyl)thiophenol (MPAA) was found to have the highest catalytic activity among all test subjects, besides it is good water soluble and thus it is very suitable for the native chemical ligation in buffered solution.

Additionally, utilization of the thiol additives are advantageous, because aside from being the promoter, they constantly keep the N-terminal cysteine in reduced form and eliminate the chance of unnecessary transthioesterification, which is caused by the sulfhydryl group of the internal cysteine residue.

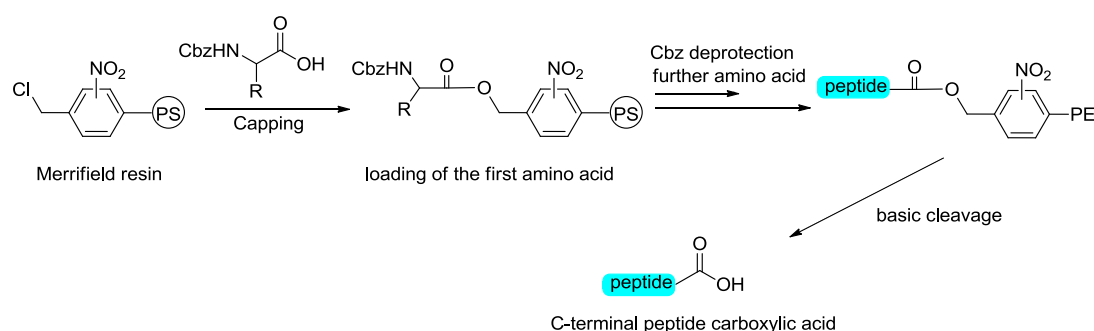
1.2 Development of the solid phase peptide synthesis (SPPS)

1.2.1 Development of the Merrifield resin

In the late 50's and early 60's, peptides emerged as important bioactive compounds and thus novel methodologies are highly desired to generate peptides. At that time synthesis of short chain peptides through various approaches have been published,^[81] however the synthesis of long size peptides was still an issue. Through elongation of the peptide chain, the solubility of the peptide in organic solvents decreased and the purification of the raw peptide *via* recrystallization and flash chromatography became difficult. Therefore, a suitable synthetic method to generate large size peptide was desired and since then various new ideas were tested. Unfortunately none of these ideas were practically applicable until Merrifield came up with the revolutionary invention.^[82]

The idea of Merrifield's novel methodology is to immobilize the first amino acid onto a polymer support *via* a covalent bond and the following amino acids are stepwise coupled to the first amino acid on the solid phase. The main chain remains on the solid phase throughout the synthesis and the excess reagents and soluble by-products are easily washed away, no work-up and purification steps are required after each coupling. The chloromethylated (or nitrated or brominated) copolymer of styrene (PS) was selected for the experiment, because it fulfilled all requirements of a proper polymer support (physical steadiness, insoluble in organic solvent and availability of a proper functionality (linker) to anchor the first amino acid). Then this polymeric support was practically deployed to generate a tetrapeptide (Scheme 65). The chloromethylated polymeric support was firstly treated with the triethylammonium salt of the first amino acid to form

the ester bond and then the unreacted chloromethyl groups were capped to avoid formation of by-products. The chain elongation proceeded with Cbz protected amino acids according to the deprotection / DCC activation / coupling and washing protocol. In order to achieve the quantitative coupling, an excess (10 folds) amount of Cbz-protected amino acid was added for each coupling. After the synthesis, the ester bond between the linker and peptide chain was hydrolyzed by strong base (NaOH or LiOH) and the peptide was subsequently liberated from the polymer support.



Scheme 66. First solid phase peptide synthesis on the Merrifield resin

This was the first practical application of solid phase peptide synthesis and the chloromethylated copolymer of styrene was named Merrifield resin. Merrifield resin was in the future frequently deployed as backbone resin to develop more advanced polymeric support.

This procedure had a major problem, because the stepwise Cbz group deprotection requires a hydrogen bromide / acetic acid mixture, which cleaves the peptide through hydrolysis of the ester bond. This setback could be reduced with nitrated or brominated polymer, however a considerable amount of the peptide went lost through the synthesis. Thereafter, Merrifield proposed a *tert*-butyloxycarbonyl (Boc) / benzyl (Bzl) protection / deprotection scheme for the solid phase peptide synthesis in order to overcome this issue.^[83] Boc group (Figure 15) was introduced by Carpino in 1957^[84] and deployed firstly in the peptide chemistry by McKay and Albertson.^[85] The Boc group is sensitive to the acid and can be easily removed in weak acidic condition (eg. 1 N HCl in acetic acid, 30 min.).

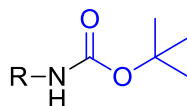


Figure 15. Boc protecting group

By deploying the new protocol, Merrifield demonstrated the synthesis of a natural product Bradykinin on Merrifield resin. The hydroxyl group of serine was protected by benzyl group, which is unaffected by the 1 N HCl treatment. After the synthesis the peptide was liberated from the resin by using HBr-TFA mixture, which also led concomitant benzyl deprotection.

In 1967 S. Sakakibara *et al.* showcased an effective cleavage of the peptide from Merrifield resin by using hydrogen fluoride.^[86] Along with scavenger (normally the anisole in 1:9 to HF) the resin containing peptide was placed in a sealed corrosion-resistant all-fluorocarbon reactor. New distilled anhydrous HF was introduced under cooling slowly into reactor, after one hour the HF was evaporated and the peptide was cleaved from the resin fully unprotected. But the handling of HF is extremely hazardous and the size of the special reactor limited the utilization of the HF cleavage in large scale.

1.2.2 Development of more advanced resins and methods

1.2.2.a Phenylacetamidomethyl (PAM) resin

Even with this new Boc / Bzl protection / deprotection protocol, the SPPS on the Merrifield resin still caused peptide loss after each coupling. When a medium- or large-sized peptide is generated in this way, the loss will be significant at the end of the synthesis. In 1976 Mitchell and Merrifield worked together and demonstrated an advanced linker strategy to deal with the prematurely release of the peptide through the acidic hydrolysis.^[87] An acidic stable phenylacetamidomethyl (PAM) bridge was introduced onto the unmodified Merrifield resin (Figure 16).

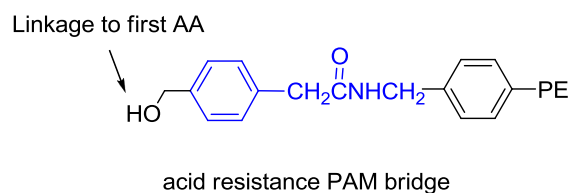
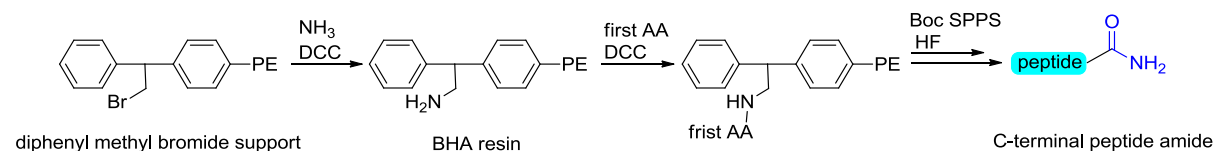


Figure 16. PAM linker

The PAM bridge is a strongly electron withdrawing moiety, and thus the ester bond which links the first amino acid and the PAM bridge is stable upon acidic treatment and could not be hydrolyzed easily. The isolated yield of peptide, which was synthesized through this way, significantly increased. Nowadays, the PAM resin is widely used for the synthesis of peptide within the frame of the Boc-SPPS.

1.2.2.b Benzydrylamine(BHA) and 4-methylbenzhydrylamine (MBHA) resin

In 1970, Pietta and Marshal introduced the BHA (Benzhydrylamine Hydrochloride Salt) resin,^[88] which's creation was entirely inspired by synthesis of a pentapeptide Gastrin. Gastrin is a C-terminal peptide amide, and unfortunately by using the Merrifield resin, the first amino acid is anchored to the resin through an ester bond and thus the cleaved peptide is obtainable only as the C-terminal peptide carboxylic acid. In order to generate Gastrin, the diphenylamine linker was developed from diphenylmethyl bromide or chloride support, which was used previously by Southward.^[89] The diphenylmethyl bromide was converted into the diphenylamine linker by using ammonia and DCC. The first amino acid could be coupled through an amide bond, which is stable to the acidic treatment during Boc SPPS procedure. After the synthesis, the peptide can be cleaved by anhydrous HF and obtained as peptide amide (Scheme 67).



Scheme 67. SPPS on the BHA resin

In middle 70's, Stewart and Matsueda modified this linker and introduced a *p*-methyl group onto the phenyl group to enhance its stability towards TFA and its sensitivity towards HF.^[90] This modified resin was accordingly called 4-methylbenzhydrylamine (MBHA) resin. In the present days, both BHA and MBHA

resins could be regularly found in use within the frame of Boc-SPPS chemistry for their good acidic and basic stabilities.

1.2.2.c 9-fluorenylmethoxycarbonyl (Fmoc) protecting group

In the same year, Carpino and Han^[91] developed the 9-fluorenylmethoxycarbonyl (Fmoc) protecting group (Figure 17). This group is stable under many conditions and only sensitive to bases. Upon exposure to a base, the β -elimination is triggered and the Fmoc protected amino group will be deprotected.

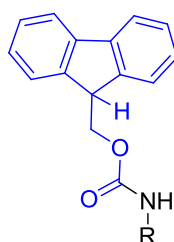
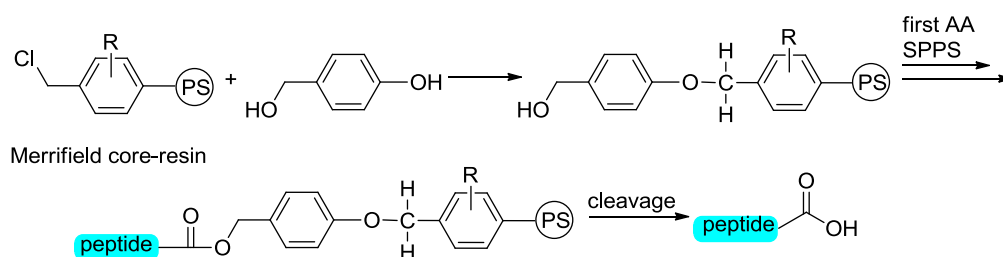


Figure 17. Fmoc protected amino group.

1.2.2.d Wang resin

Two years later Wang introduced a novel *p*-alkoxybenzyl alcohol resin,^[92] which was also converted from Merrifield resin. The first amino acid could be anchored to the resin through an ester bond (Scheme 68).



Scheme 68. Preparation of Wang resin and SPPS on Wang resin

On this resin Wang demonstrated the syntheses of a few peptides and after the syntheses, these peptides were isolated in high yield with very low degree of racemization of the first amino acid.

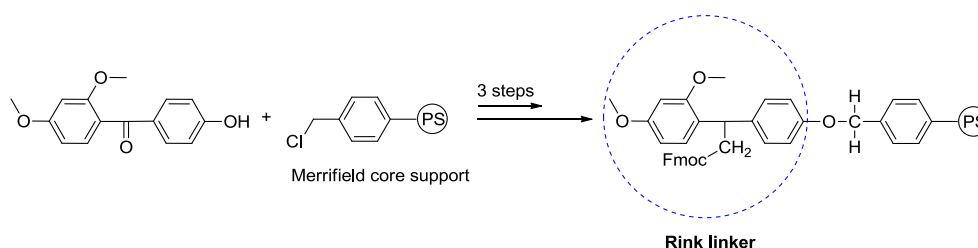
1.2.2.e Introduction of the Fmoc-SPPS chemistry

In 1978 Chang and Meienhofer outlined the Fmoc-SPPS protocol based on the Wang resin.^[93] The first amino acid was anchored^[93] to Wang resin *via* the ester bond and the Fmoc-protected amino acids were stepwise assembled and finally the sequence was acidic cleaved (generally concentrated TFA) from the resin.

Since then different versions of this protocol were developed, various coupling reagent (carbodiimide / HOBT^[94], Fmoc amino acid active ester,^{[95][96]} phosphonium and uronium / amidinium salts) have been examined, different Fmoc deprotection strategies have also been investigated^{[97][98][99]} as well as the investigation of diverse cleavage cocktails. Today, the Fmoc-SPPS protocol is more favored by peptide chemists than the Boc-SPPS for the absence of anhydrous HF.

1.2.2.f Rink linker

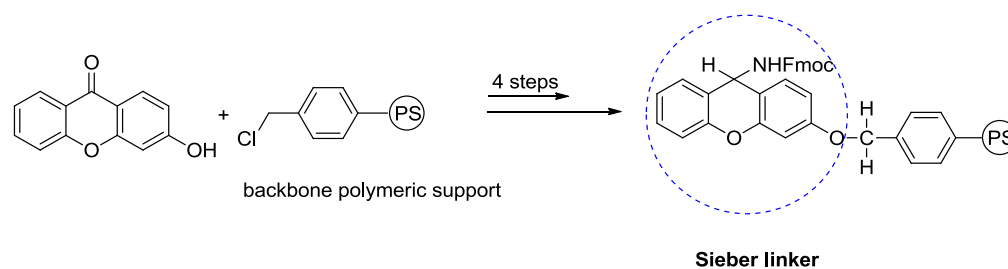
Within the scope of Fmoc-SPPS protocol, Rink developed a linker strategy to produce the unprotected peptide amide.^[100] The Rink linker was introduced to the Merrifield resin through chemical conversion. The first amino acid is attached to the Rink linker through an amide bond, which is stable to the basic treatment throughout Fmoc-SPPS. Due to the acidic sensitivity of the Rink linker the peptide can be easily cleaved by TFA / DCM = 1:1 mixture as peptide amide (Scheme 69).



Scheme 69. Preparation of the Rink linker

1.2.2.g Sieber linker

In the same year, Sieber also demonstrated a similar linker strategy,^[101] which is also fully compatible with the Fmoc-SPPS protocol. The intention of using this new strategy was to produce fully protected peptide amide. Similar to Rink's amide resin, this resin was converted from Merrifield resin as well. The first amino acid was also anchored to the Sieber linker through an amide bond. The Sieber linker is electron rich and thus extremely acidic sensitive. Consequentially the peptide can be cleaved as the peptide amide from the resin by 5% TFA treatment. Meanwhile under such mild acidic condition, most protecting groups still remain attached to the side-chains (Scheme 70).



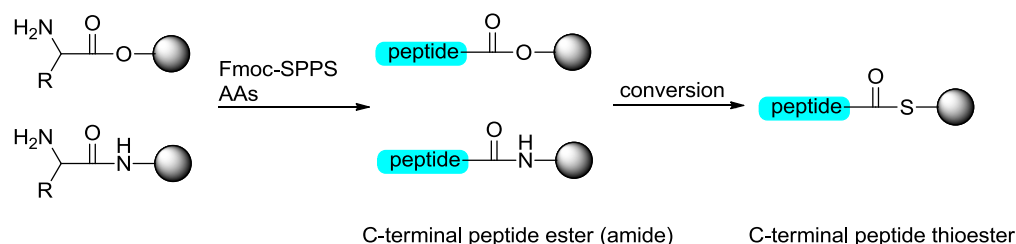
Scheme 70. Preparation of the Sieber linker

1.3 Latent thioester linker strategy

Since the birth of the native chemical ligation, the C-terminal peptide thioester fragment, which is required for the chemical ligation, is frequently generated on solid phase. Because the C-terminal peptide thioester is very sensitive to nucleophilic attack, the C-terminal peptide thioester could only be synthesized through Boc-SPPS protocol, but after Boc-SPPS the HF cleavage of the final peptide thioester is often inevitable. The use of HF is sometimes disadvantageous, because a large number of glycopeptides or proteins are sensitive to HF treatment.^[102] Moreover HF or trifluoromethanesulfonic acid (TFMSA) is incompatible with the post-translational modifications (PTM), which are required in many cases to enhance the biological activity of the original peptide or protein.

Unlike its counterpart, cleavage of peptide sequence after Fmoc-SPPS only requires concentrated TFA, which will not damage the glycopeptides or proteins. But unfortunately stepwise removal of Fmoc group needs nucleophilic reagents (DIPEA, piperidine), which could easily hydrolyze the thioester bond and release the peptide sequence prematurely. Therefore the Fmoc-SPPS is apparently unsuitable for the synthesis of the C-terminal peptide thioester.

In the hope of applying the Fmoc-SPPS despite the incompatibility of thioester linkage with Fmoc-SPPS, many latent thioester linker strategies were developed. According to these latent thioester linker strategies, usually the C-terminal peptide amide or ester, which are compatible with Fmoc-SPPS, are generated in advance through the Fmoc-SPPS. Then the desired C-terminal peptide thioester is converted from the corresponding C-terminal peptide ester or peptide amide either through O to S or N to S acyl transfer (Scheme 71).

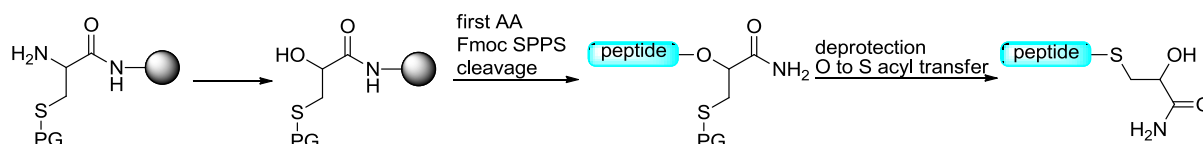


Scheme 71. Latent thioester linker strategy

1.3.1 O to S acyl transfer

1.3.1.a Botti's latent thioester linker strategy

Botti have developed a latent thioester linker strategy, which is based on the principle of O to S acyl transfer.^[103] The latent thioester linker was formed from Fmoc-Cys(StBu)-NH-Rink S RAM polymer, from which the amino group of cysteine was converted into a hydroxyl group. The first amino acid was anchored to the latent thioester linker through esterification and further amino acids were assembled through the Fmoc-SPPS. After the synthesis, the C-terminal peptide ester was cleaved off the resin and the sulfhydryl group of the linker was deprotected. A new thioester bond was formed *in situ* through O to S acyl transfer, then this new C-terminal peptide thioester was ligated with other N-terminal cysteine containing peptide fragment to construct new amide bond (Scheme 72).



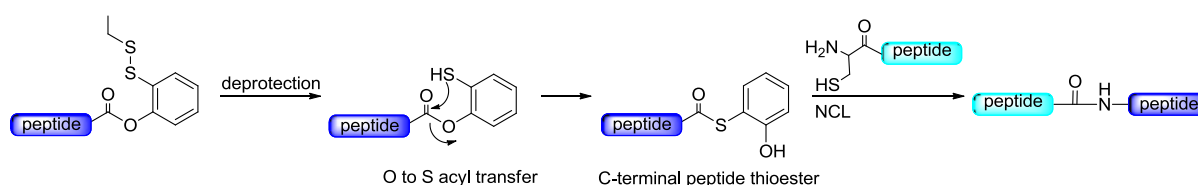
Scheme 72. Work-flow of the Botti's latent thioester linker

Disadvantageously by using this latent thioester linker in aqueous buffer medium, the hydrolysis of the C-terminal peptide ester also inevitably takes place. Thereafter Cheng *et al.* investigated a few latent thioester linkers of the same kind,^[104] and they stated that the Botti's latent thioester linker is suitable for O to S acyl shift and when NCL was performed at low temperature (ca. 10 °C), the ester bond would unlikely be hydrolyzed, whereas at higher temperature (RT or higher) the formation of hydrolyzed by-product was inevitable.

Muir reported the synthesis of thiol lactone inhibitors of *Staphylococcal virulence* by applying the Botti's linker strategy^[105] Instead of preparation of the latent thioester linker in solid phase, which resulted in poor yield, the same linker was prepared in solution phase with good yield, and by using this latent thioester linker they succeed in generation of a library of the thiol lactone inhibitors through intramolecular NCL cyclization.

1.3.1.b Danishefsky's latent thioester linker strategy

At the same time, another successful latent thioester linker strategy was introduced by Danishefsky.^{[106][107]} A simple latent thioester linker based on the 2-mercaptophenol was developed. The *ortho*-sulfhydryl group was in the beginning masked by a disulfide bond and the hydroxyl group was coupled through esterification to the C-terminal peptide carboxylic acid, which was synthesized on Wang resin through Fmoc-SPPS. Upon deprotection of the *ortho*-sulfhydryl group, a new C-terminal peptide thioester was formed *in situ* in the same manner of Botti's linker and through NCL this new C-terminal peptide thioester formed a new amide linkage with other suitable fragment (Scheme 73).



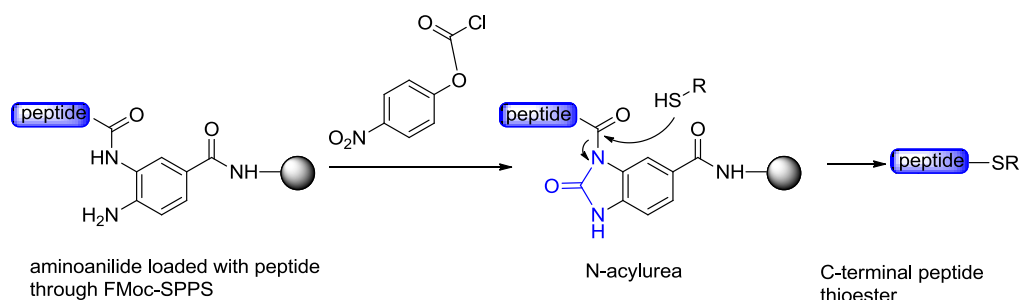
Scheme 73. NCL through Danishefsky's latent thioester linker

1.3.2 N to S acyl transfer

1.3.2.a Dawson's aminoanilide auxiliary strategy

The C-terminal peptide thioester fragment within the scope of Fmoc SPPS can be also accomplished through the N to S shift. Dawson *et al.* demonstrated a method by utilizing a novel acylation agent.^[108] At the beginning, a stable aminoanilide auxiliary was synthesized on the resin and the first amino acid was coupled to this auxiliary *via* an amide bond, then the designed sequence was assembled through Fmoc SPPS, after synthesis, the aminoanilide auxiliary was transformed into a N-acylurea functionality by adding *p*-nitrophenylchloroformate, then this peptide N-acylurea compound could be easily converted into the

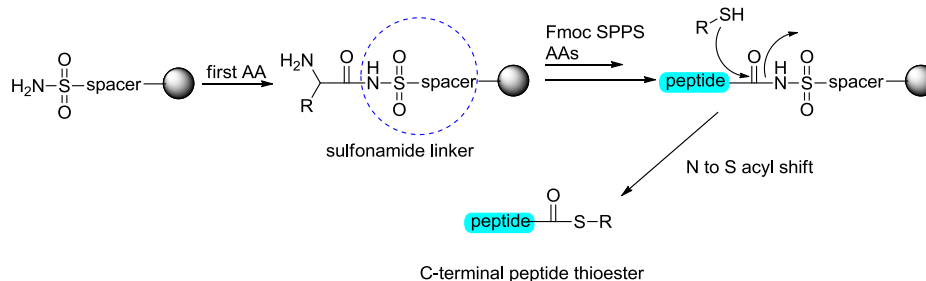
desired C-terminal peptide thioester by exposure to the thiol, because the N-acylurea moiety is an excellent leaving group (Scheme 74).



Scheme 74. N to S acyl transfer through Dawson's auxiliary

1.3.2.b Ingenito's sulfonamide latent thioester linker strategy

Another exceptional example was demonstrated by Ingenito.^[109] A sulfonamide linker was attached to the solid phase through a spacer and the first amino acid was anchored to this linker *via* an amide bond. Then the Fmoc-SPPS was performed to elongate the peptide chain. After the synthesis on the resin, this C-terminal peptide sulfonamide was simply treated with thiol and converted into respective C-terminal thioester through N to S acyl transfer (Scheme 75).



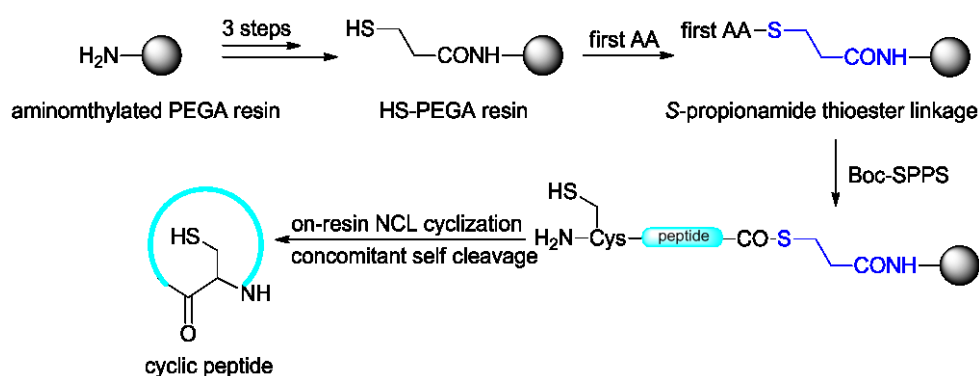
Scheme 75. N to S acyl transfer through sulfonamide linker

1.4 NCL cyclization in solution and solid phase

Tam conducted a series of experiments of the head-to-tail NCL cyclization^[110] and concluded that compared to the conventional cyclization with coupling reagent in solution phase, the NCL cyclization can be performed in solution phase with moderate concentration of the linear precursor without formation of dimers or oligomers.

Camello and Muir demonstrated the intermolecular and intramolecular NCL of unprotected peptides on the resin.^[111] The polyethylene glycol-poly-(*N,N*-

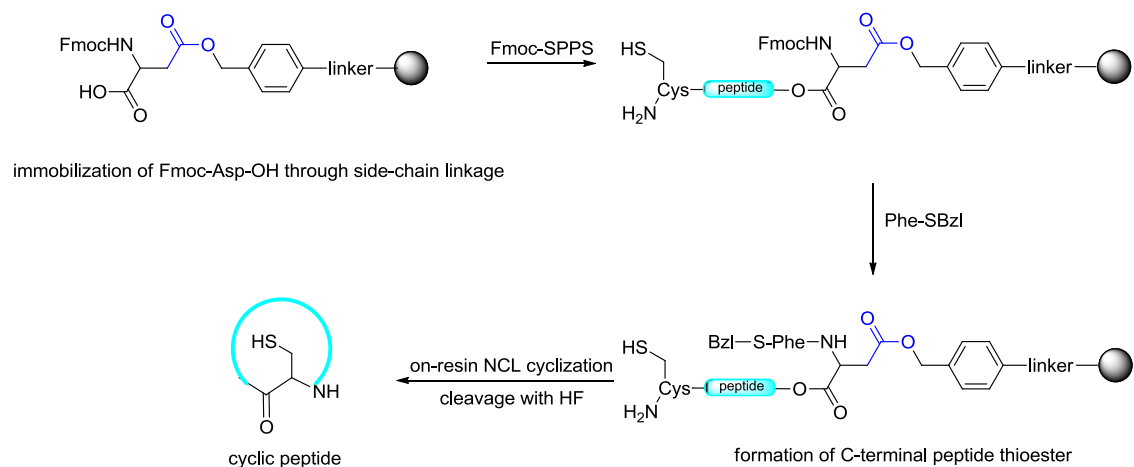
dimethylacrylamide) copolymer support (PEGA), which was developed by Meldal,^[112] was applied in this study. This solid support is compatible with Boc-SPPS and thus C-terminal peptide thioester can be directly synthesized on it. Moreover it has excellent swelling ability in aqueous medium, in which NCL reaction takes place. At the beginning, the commercially available aminomethylated PEGA was converted into the corresponding 3-mercaptopropionic acid PEGA (HS-PEGA) and the first amino acid was immobilized to the resin *via* a S-propionamide thioester linkage. This backbone anchor linkage is stable upon HF treatment, so the global deprotection after Boc-SPPS was achieved by using anhydrous HF in *p*-cresol without the cleavage of the peptide off the resin. The resin containing the linear precursor was then swollen in neutral phosphate buffer solution and the NCL cyclization took place with concomitant release from the resin. The isolated cyclic peptides were generally clean, however only in moderate yield (5 - 50%) (Scheme 76).



Scheme 76. On-resin NCL cyclization of C-terminal peptide thioester

Tulla-Puche and Barany reported the on-resin NCL cyclization from a side-chain linkage.^[113] The second C-terminal amino acid Fmoc-Asp-OAl was firstly immobilized onto the solid support through its side-chain *via* a *p*-alkoxybenzyl ester. The peptide chain was then elongated through Fmoc-SPPS, the C-terminal peptide thioester was formed at the late stage since the thioester bond did not withstand Fmoc-SPPS. After global deprotection under mild condition the NCL cyclization was performed in buffer solution followed by the cleavage of the cyclic peptide by anhydrous HF. Three kinds of polymer supports: PEGA, cross-linked ethoxylate acrylate resin (CLEAR) and poly(ethylene glycol)-polystyrene (PEG-

PS) were investigated in the study. Two out of three resins except PEG-PS resulted in good yield, due to PEG resin's sparingly swelling ability in water.



Scheme 77. On-resin NCL cyclization of C-terminal peptide thioester from a side chain linkage

1.5 Polymeric support

In the on-resin NCL study, the choice of suitable polymer support is crucial. There are many commercially available polymeric supports on the market but not all of them fulfill the criteria for the on-resin NCL study. The target polymeric support should possess adequate swelling property in the aqueous medium, which is commonly used in the NCL reaction. The most common resin in SPPS is the cross-linked-polystyrene resin, which was developed by Merrifield back in 1960s'.^[82] It is constructed from co-polymer of styrene-divinyl benzene with 1-2% cross-linkages (Figure 5) and it is chemical highly stable. It can be functionalized with different moieties, but its poor water swelling property limits its application in the on-resin NCL study,^[116] besides the PE resin with different functionalities are often commercially available in high loading (0.8 – 1.5 mmol / g), which is too dense for the on-resin NCL cyclization.

Another popular polymer support in peptide synthesis is polyacrylamide, which is constructed from the acrylamide monomer in simple chain or cross linked form (Figure 17).^[114] It mimics the peptide, which is attached to it and reduces the peptide-peptide-chain-interaction. It is a good water soluble resin but so far very few on-resin studies were tested on this basis.

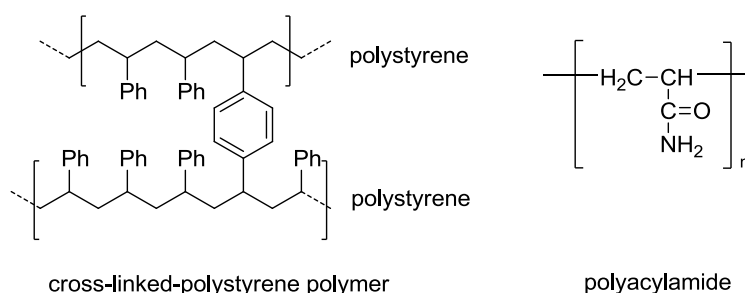


Figure 17. Polystyrene and polyacrylamide polymer

TentaGel is a polyethylene glycol-polystyrene (PS-POE) graft support, within which up to 70% polyethylene glycol (PEG) is attached to polystyrene (PS) matrix through an ethyl ether bond (Figure 18).^[115]

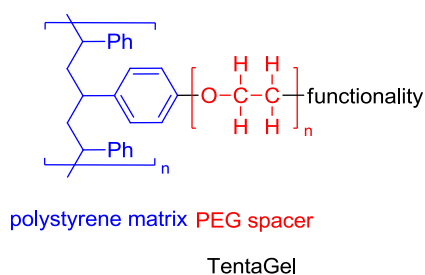


Figure 18. TentaGel polymer

It can be swollen well in a large number of protic and aprotic solvents^[116] and it mimics the conditions very similar to the solution phase, hence the peptide attached to it will behave very similar like in solution phase. This resin is usually available in relatively low (0.2 to 0.3 mmol / g), which is suitable for the on-resin NCL cyclization. Furthermore there are two more well-known polymeric supports, which are frequently used in SPPS and solid phase organic synthesis, The PEGA (poly[acryloyl-bis(aminopropyl)polyethylene glycol]) polymeric support presents excellent swelling property in aqueous medium^[113] and available in proper loading capacity (0.4 mmol / g), therefore this polymeric support is an ideal platform for the on-resin NCL study. Barany has already succeeded in on-resin NCL cyclization studies by deploying this resin.^[113] The cross-linked ethoxylate acrylate polymeric support (CLEAR) was introduced by Barany and Kempe (Figure 19).^[117] It was reported that CLEAR resin is an excellent polymeric support and suitable for many challenging syntheses, especially the on-resin ligation cyclization of the peptide.^[118] However, its availability is relatively limited

(not commercially available in Germany) in comparison to other polymers and thus could not be deployed regularly.

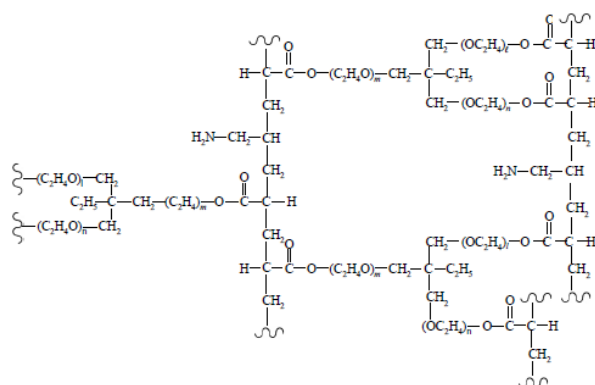


Figure 19. The network structure of the CLEAR resin^[119]

2. Plan for the prove-of-concept on-resin NCL cyclization study

2.1 Motivation of development of the methodology

This work was initially inspired by the synthesis of interesting bio-active naturally occurring cyclic peptides like argyrin and vioprolide (Figure 20), which contain thioazole and thioazoline residues within their ring structure.

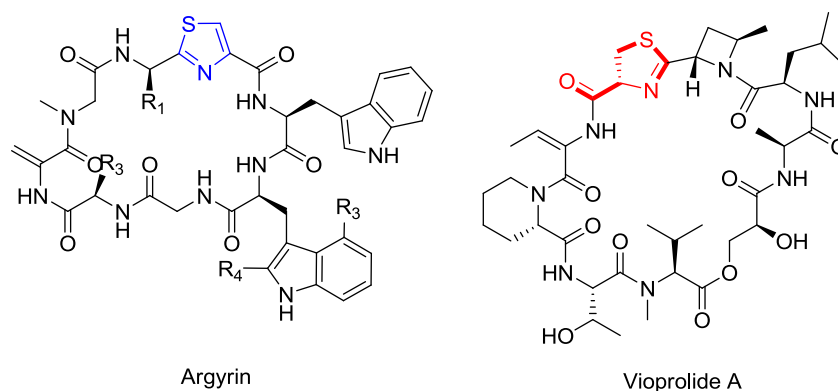
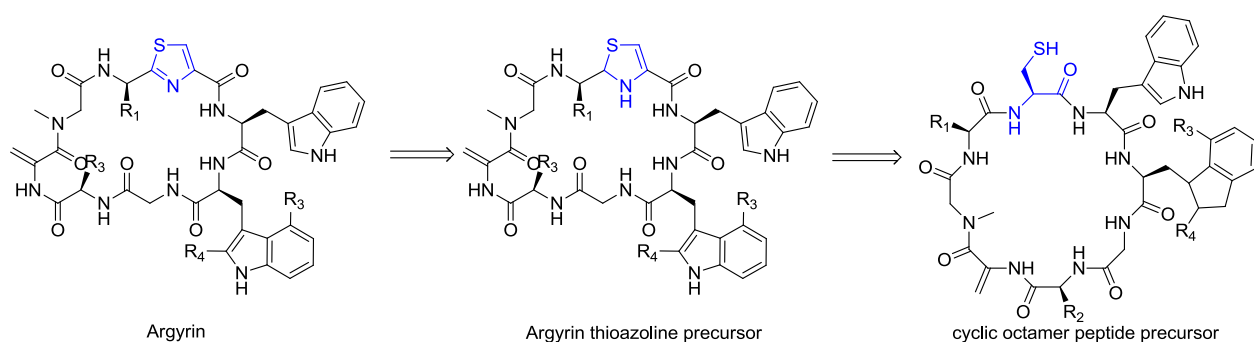


Figure 20. Argyrin and vioprolide

These natural products show enormous bio-activity and thus they are potential candidates for pharmaceutical research. But before advanced research of these compounds can be performed, their structure-activity relationship (SAR) studies need to be completed. For the SAR study, a library containing a large number of derivatives is required. In order to generate such library, a lot of work and time are needed through conventional organic synthetic chemistry. So far the conventional organic synthetic chemistry has already done plenty of efforts to yield these compounds. Ley *et al.*^[120] published the total synthesis of the argyrin B and Prof. Kalesse's group from University Hanover also dedicated themselves to generate some of the argyrin derivatives. In the case of the novel compound vioprolide and its derivatives, there is no published total synthesis so far. With intention of rapid establishment of the library of these cyclic peptides, in this work an efficient route will be developed.



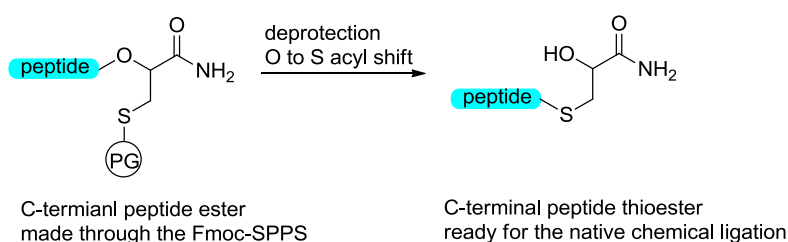
Scheme 78. Retro synthesis of the argyrin from the cyclic peptide precursor

All these cyclic peptide compounds mentioned before contain either thioazole or thioazoline residue, which could be converted from the cysteine containing cyclic peptide precursors through dehydration (and the sequentially oxidation in the case of thiazole, Scheme 78). The aim of this work is to establish a new methodology, which could rapidly generate cyclic cysteine-containing peptidic precursors. The design of the synthetic route will focus on the word “rapid”. In order to achieve the rapidity in the synthesis, all possible measures will be deployed to accelerate the synthetic procedure. Throughout this route the final product should be obtained in a short time. Synthesis of these compounds through the conventional organic synthesis in solution phase won't be considered in this study, because the stepwise elongation of the linear peptide chain and the purification in solution phase are often time-consuming. Alternatively, to the solution phase peptide synthesis, the solid phase peptide synthesis procedure is an alternative choice. It is fast and devoid of the troubles that occur at the purification and the increasing insolubility of the long chain peptide in the organic solvent. When this process is fully automated by using the SPPS synthesizer most short or medium size sequences could be generated within one day. Moreover on the synthesizer different derivatives could be conveniently synthesized parallel and this is more advantageous over the solution phase peptide synthesis. For all these reasons in this work the linear peptide will be assembled by SPPS procedure.

2.2 Cyclization through on-resin Native Chemical Ligation

In order to rapidly cyclize these cysteine-containing linear precursors, the ordinary head-to-tail lactam formation by using chemical coupling reagents will not be performed in this work. Instead the cysteine residue in sequences will be well used as the junction point. In order to generate the cyclic structure, a cysteine residue will be ligated within the scope of the native chemical ligation with a C-terminal amino acid X to construct the X-Cys junction and thus accomplish the head-to-tail cyclization. In practice, the cysteine residue would be placed on the N-terminus of the linear precursor, accordingly the C-terminal ligation partner X would be generated in C-terminus as a thioester.

Within the frame of the SPPS, these peptide C-terminal thioester linear precursors could only be straightforward obtainable through the Boc-SPPS. But Boc-SPPS requires special facility for the HF cleavage (see section 1.2.1), which restricts the use of the Boc-SPPS and in the present days the Fmoc-SPPS protocol is more favorable among the chemistry community. But the straightforward application of the Fmoc-SPPS for generation of these C-terminal peptide thioesters faces a major obstacle, because the C-terminal thioester residue is unstable in the presence of nucleophilic compounds (like piperidine), which are necessary for the Fmoc cleavage. A few solutions to solve this problem have been reported in the past years (see previous chapter), this work will concentrate on the latent thioester linker strategy, which was firstly introduced by Botti (Scheme 79).



Scheme 79. The latent thioester linker strategy

According to this strategy, a special linker will be required. The latent thioester linker in this work will be generated by standard organic synthesis in solution phase through a new designed synthetic route, which is time-saving but as efficient as the previous reported methods.

Upon completion of the special linker, it will be attached onto the polymeric support and the first amino acid could be coupled to the linker through an ester bond, which is supposed to be stable to the nucleophilic treatment through the Fmoc-SPPS. After all amino acids are properly assembled, the linear peptidic precursor bearing the special linker will remain on the solid phase. The protecting group of the sulfhydryl group next to the ester bond will be cleaved, and a new thioester bond will be generated *in situ* through the O to S acyl transfer. Afterwards the NCL cyclization of the linear precursor will progress directly on the resin whereas the cyclized product will be cleaved simultaneously from the resin and simply isolated through HPLC. The on-resin cyclization-cleavage concept will bypass the cleavage and the work-up steps and thus avoid the handling loss and saves time. But theoretically the linear precursor attached to the polymeric support is less reactive than in solution phase, so that a slow NCL cyclization rate will be expected in this case.

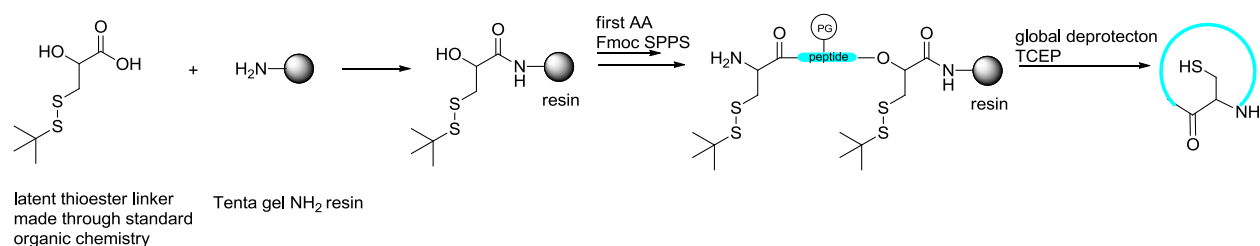
2.3 Choice of proper polymeric support and sulfhydryl protecting group

To successfully apply the NCL cyclization, the unprotected form of the linear precursor is often required because of the large steric hindrance of the side-chain protecting groups. In the present days, all side-chain protection groups are so designed, that their cleavage is accomplished coincidentally with cleavage of the sequence by TFA treatment. In order to perform the on-resin NCL cyclization of the unprotected linear precursor, only the polymeric support without cleavable linker will be used, because when the peptide sequence is anchored to the solid phase via the cleavable linker, the peptide sequence will be cleaved from the solid phase upon deprotection of the side chains through the concentrated THF.

In this study, the solid support TentaGel NH₂ resin, which is a PS-POE polymer without cleavable linker but a free NH₂ group, will be applied as the solid phase. The latent thioester linker will be anchored onto this resin through an amide bond. This amide bond is stable during the Fmoc-SPPS and the deprotection cocktail (concentrated.TFA:triisopropylsilane:water = 95%:2.5%:2.5%) treatment. With this resin, the linear precursor can be fully deprotected with TFA without cleavage of the sequence from the resin.

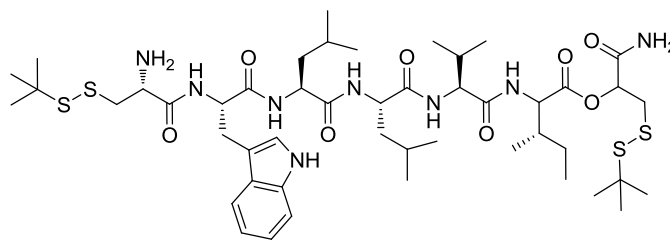
Furthermore the sulfhydryl protecting groups of the latent thioester linker and the N-terminal cysteine are unique in this model study. The common trityl protected cysteine will not be used because of its highly acidic lability. The trityl protected sulfhydryl group of N-terminal cysteine could be deprotected prematurely with other side-chain protecting groups through the TFA treatment and could lead to the undesired side-products. Instead both sulfhydryl groups are accordingly masked by the *tert*-butyl disulfide moiety, which will remain intact during the TFA global deprotection and can only be reductively cleaved. The *tert*-butyl disulfide protected cysteine is commercially available, the construction of the *tert*-butyl disulfide protected linker could be readily synthesized as well.

After the TFA global deprotection, the on-resin NCL cyclization is triggered by deprotection of both sulfhydryl groups. A handful of compounds have already been used to reduce the disulfide bond in the peptide and protein research. The frequently used compounds among them are dithiothreitol (DTT)^[121] and tris(2-carboxyethyl)phosphine (TCEP)^[122] TCEP is commercially available since 1992 and is more advantageous over the DTT. TCEP is more hydrophilic, efficient within a large range of pH values, odorless and more air oxidation resistant. It reduces the disulfide irreversibly while the DTT can form the new disulfide bond with the deprotected sulfhydryl group. Therefore the TCEP will be utilized in the model study. The general work-flow of the new methodology is as follows:



Scheme 80. Outline of the synthesis of the cysteine-containing cyclic peptide

At the beginning of the work, a model sequence (stBuS)Cys-Typ-Leu-Leu-Val-Ile-O-latent thioester linker (Figure 21) will be constructed and the feasibility of its NCL cyclization will be investigated.



14

Figure 21. The model sequence (stBuS)WLLVI-latent thioester linker **14**

This model sequence has its origin in a natural product and was isolated by J. Niggemann at the Helmholtz Center for Infection Research (HZI). It is a hexamer cyclic peptide and possesses the optimal configuration to form the ring structure.

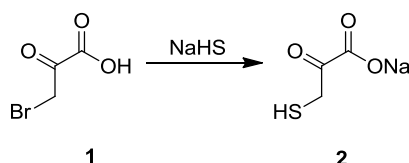
The aim of this study is to develop a methodology of the on-resin NCL cyclization. At the beginning of the model study, the NCL cyclization will not be performed directly on the polymeric support but rather in solution phase, because this latent thioester linker was never deployed on the solid phase to synthesize the cyclic peptide. In solution phase the progression of NCL cyclization can be monitored by analytical HPLC and if the NCL proceeds in the wrong way, these issues could be observed and identified, additionally the linear precursor can be cleaved and its quality can be examined prior to the NCL cyclization. The TentaGel S RAM resin, which bears a cleavable Rink linker, will be deployed for the solution phase model study. TentaGel S RAM resin allows the peptide sequence to be cleaved after synthesis, so that the quality of the linear precursor can be controlled. Through the solution phase model study, the optimal conditions for the NCL cyclization will be determined. Once the investigation of NCL cyclization in solution phase is completed, the model study will be performed on the solid phase by using these determined optimal conditions either directly or with slight modifications.

3. Results and discussion

3.1 Organic synthetic chemistry

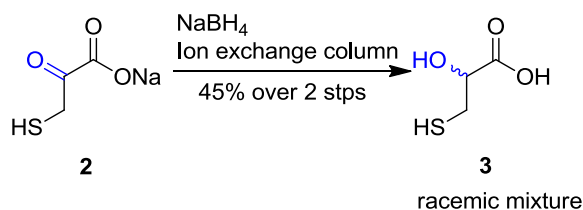
3.1.1 Initial attempt of generation of the latent thioester linker 4

Botti and Muir had already developed their own routes to generate the latent thioester linker.^{[103][105]} Here, a different strategy was developed to prepare this linker in a rapid and simple way.



Scheme 81. Synthesis of intermediate 2

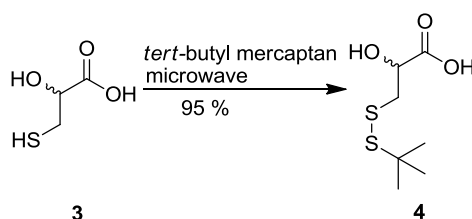
Starting with the bromopyruvate (1), bromine was replaced by the hydrogen sulfide at 0 °C through a S_N2 displacement and the raw product was collected as the sodium hydrogen sulfidepyruvate salt (2) without further purification.^[123] The raw product 2 was dried in *vacuo* over phosphorus pentoxide for 24 hours and directly used for the next step (Scheme 81).



Scheme 82. Synthesis of intermediate 3

Next selective reduction of the carbonyl group (in blue color) with sodium borohydride was carried out in aqueous medium.^[124] Sodium borohydride was good soluble in water and unlike expected, that it did not react spontaneously with water at neutral pH but rather reduced the carbonyl group, performed by adding small portions of sodium borohydride every 5 min., otherwise a less polar by-product was observed by TLC. Rapid introduction of the sodium borohydride resulted in a high concentration of sodium borohydride in the reaction flask, in this case the β -carbonyl group could not consume the large amount of sodium borohydride fast enough and thus the excess amount of sodium borohydride began to reduce the carboxylic carbonyl group and forms the fully reduced and

less polar by-product. After addition of sodium borohydride, the reduction was completed at RT after one hour. The purification was performed by direct passing of the reaction mixture through two ion exchange columns (first the cation exchange column, followed by the anion exchange column). The cation exchange column (pre-loaded with H^+) separated the product (still in sodium salt form) from other impurities and the anion exchange column (pre-loaded with acetate ion) acidified the sodium salt to yield the final product as a racemic mixture. The intermediate **3** was collected in 45% yield calculated over two steps (Scheme 82).



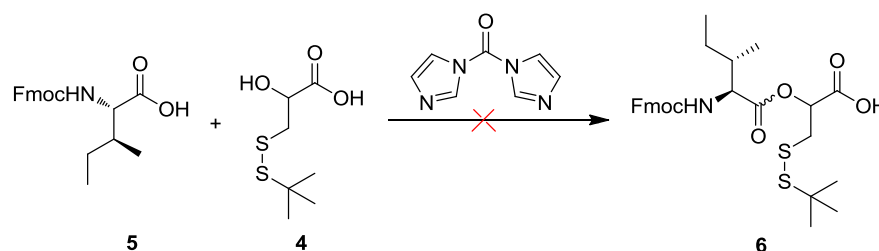
Scheme 83. Synthesis of intermediate **4**

The sulfhydryl group was then protected through the microwave-mediated disulfide formation (Scheme 83).^[125] **3** was dissolved in buffer solution (10 mM ammonium acetate solution in acetonitrile:water = 3 :2), which contains a large excess amount of *tert*-butyl mercaptane and DMSO. Afterwards, this mixture was allowed to react in a microwave synthesizer for 10 minutes (temperature 150 °C, power 150 W). This reaction progressed smoothly and fast. After 10 min. all starting material was completely consumed and a single product was formed as detected by TLC. After the reaction it was attempted to extract the product from the aqueous DMSO mixture with ethyl acetate. Unfortunately, the product was sparingly soluble in the organic phase, so alternatively the aqueous solvent and the leftover *tert*-butyl mercaptan were evaporated and the DMSO was removed by using the centrifuge evaporator. The purification of the raw product is optional for this step, because technically trace of DMSO and the ammonium chloride salt from the buffer solution would not interfere with the subsequent reactions. Otherwise the purification was conducted through RP-HPLC in 95% yield, because the DMSO residue in the raw product made the purification through the silica gel flash chromatography only in small scale possible.

3.1.2 Attempt of formation of depsi-peptide building block **6** in solution

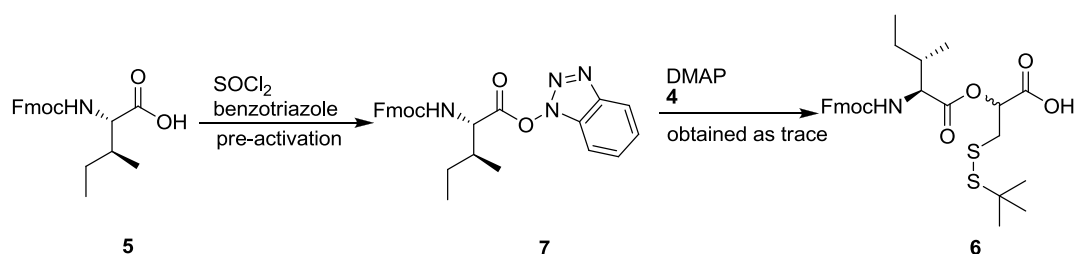
Initially the depsi-peptide building block **6** was formed from **4** and Fmoc-Ile-OH in solution phase, because the esterification on solid phase is generally considered to be more difficult, besides the formation of the product in solution phase is traceable. After building block **6** was completed, it is supposed to be coupled onto the resin through the standard HBTU activation protocol.

At first, carbonyldiimidazole (CDI) was deployed as the coupling reagent.^[126] Two equivalents of Fmoc-Ile-OH was activated in THF by CDI beforehand and then latent thioester linker **4** was added and the mixture was stirred at RT overnight. Surprisingly, nothing happened (Scheme 84). The mixed anhydride, which was formed from CDI and **4**, was presumably insufficient reactive for the esterification.



Scheme 84. Synthesis of depsi-peptide building block **6** through CDI

Alternatively, Fmoc-Ile-OH was pre-activated by thionyl chloride and benzotriazole (HBT) and converted into the active ester **7**.^[127] The active ester **7** was highly stable and separable *via* flash chromatography, then the isolated active ester **7** was added to thioester linker **4** in 7 exceed folds along with 10 folds of DMAP, after 24 hours thioester linker **4** was completely consumed as judged by TLC (Scheme 85).

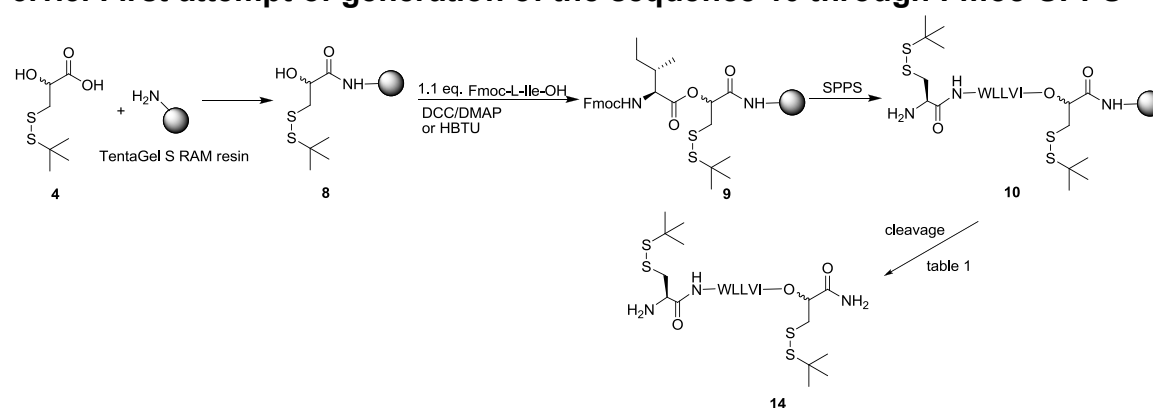


Scheme 85. Synthesis of **6** through benzotriazole and SOCl₂ activation.

This reaction generated a large number of products and after isolation of each single product through HPLC, the desired ester building block **6** (characterized by

HRMS) was found only existed as trace ($\leq 1\%$). The reaction was repeated with less active ester **7** (2.8 eq.) and DMAP (3.3 eq.), but this didn't result in the correct formation of the ester building block **6** either (still as trace). The generation of the desire ester building block **6** in solution phase could be achieved by neither of these methods, it was more difficult than estimated thus the esterification had to be performed on the resin after the immobilization of the linker **4**.^{[103][105]}

3.1.3. First attempt of generation of the sequence **10** through Fmoc-SPPS



Scheme 86 The synthetic route towards linear precursor **10** by using linker **4**

At the beginning, the latent thioester linker **4** was immobilized onto the TentaGel S RAM resin overnight in slight excess (1.1 equivalent) through HBTU activation, after the coupling the unreacted free amino groups of the resin remained uncapped, because in this particular case, capping of the free amino groups by ethyl acetic anhydride will also acylate the secondary alcohol of latent thioester linker **4**, which is supposedly to be coupled with the first amino acid. Fmoc-Ile-OH was then coupled to the latent thioester linker **4** through the esterification, which was carried out with either DCC activation or HBTU activation (Table 11, entry 1 and 2). After esterification, the coupling quality was determined by the Fmoc release UV assay (procedure see experimental section), the coupling was found highly efficient. In both cases the coupling achieved the high degree of loading (96% and 100%)

Table 11. Attempts of the synthesise of linear precursor **10** by using linker **4**

entry	equivalent of 4	coupling reagent of esterification	product 10 found
1	1.1	DCC / DMAP	no
2	1.1	HBTU	no

After coupling of Fmoc-Ile-OH, the sequence was elongated in the given order on the automated peptide synthesizer. The synthesizer was programmed to execute the Fmoc-SPPS protocol and the pre-loaded resin was filled in small syringes (suitable for up to 25 μmol batch) with filter, the peptide sequence was generated stepwise by following the batch flow-through principle.

One complete coupling cycle is comprised of following steps:

-Fmoc cleavage

The pre-loaded resin was treated twice with 20% piperidine / DMF solution (700 μL for each 2 min. and 8 min.) to liberate the amino group and then the resin washed with DMF thoroughly

-Activation and coupling

500 μL of the amino acid stock solution (0.5 M in NMP) is introduced into the small syringe and followed by 500 μL 0.5 M TBTU stock solution, then 500 μL DIPEA is also added. The small syringe is then incubated for one hour with occasional shake. After the coupling is completed the solution is drained, the resin is thoroughly washed with DMF and is ready for the next coupling.

According to this procedure the remaining amino acids of sequence **10** were assembled.

After the cleavage with the cleavage cocktail (TFA:triisopropylsilane:water = 95%:2.5%:2.5%), the LC-MS analysis of the crude product was rather disappointing (Figure 14).

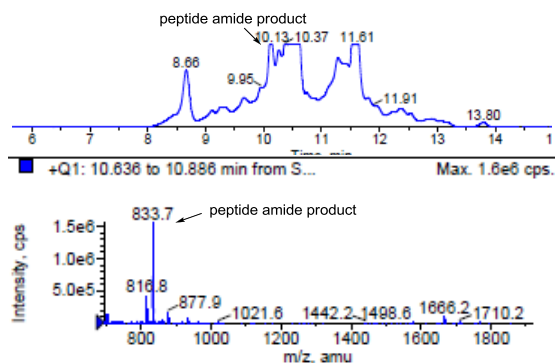


Figure 14 LC-MS analysis (UV: 190 – 600 nm) of the crude product mixture after cleavage

No trace of the desired linear product **10** was found, instead one main peak in the UV spectra (Figure 14) was then identified by its mass spectrum as the peptide amide product (Figure 15). None of mass of other peaks matched the desired product either.

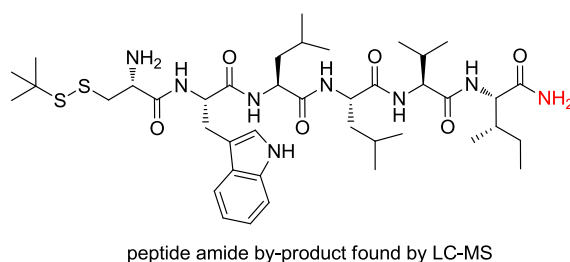
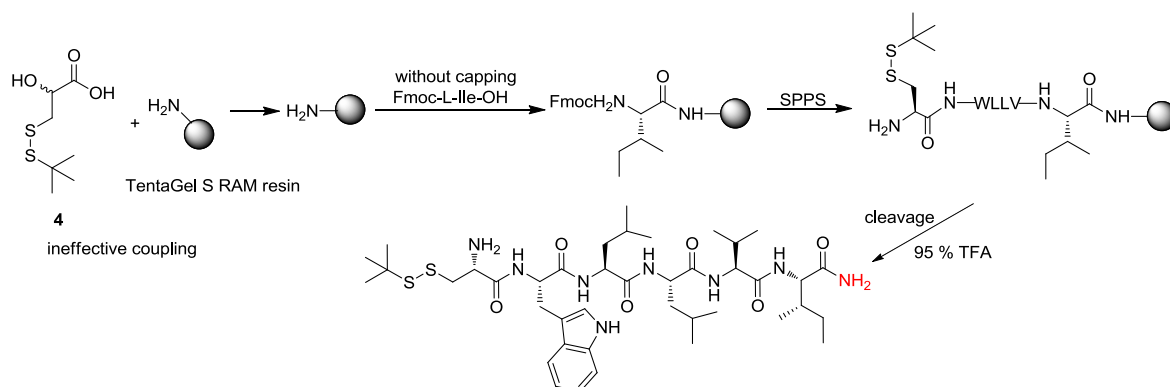


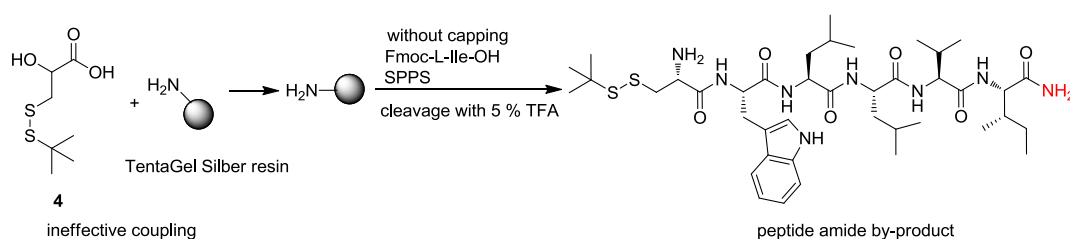
Figure 15. The detected sole peptide amide by-product

This peptide amide by-product could only exist, when Fmoc-Ile-OH bypassed the latent thioester linker **4** and was directly coupled to the TentaGel S RAM resin (Scheme 87).



Scheme 87. The emergence of the wrong product through the wrong pathway

Additionally, it could also be the case that the model sequence **10** decomposed during the concentrated TFA treatment. In order to validate this assumption, the influence of concentrated TFA on the model sequence **10** was examined. The model sequence **10** was then prepared again through the same procedure but on the Silber S RAM resin,^[101] the cleavage of the linear precursor was conducted by using 5% TFA in DCM, which should be compatible to the model sequence **10** (Scheme 88).



Scheme 88. Fmoc-SPPS on the Silber resin resulted in the same by-product.

After the cleavage, the LC-MS analysis of the crude product mixture identified the same by-product as the previous experiment. No trace of correct product was found and the by-product peptide amide remained one of the main products. But this result suggested that the concentrated TFA treatment was not responsible for the failed synthesis.

Based on these facts, the linker **4** was considered not to be suitable for the synthesis, because the standard SPPS protocol suggests that the first amino acid (in this case, the latent thioester linker **4**) should be coupled to the resin in a large

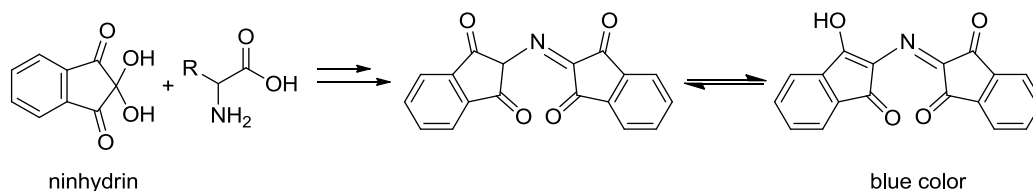
excess (3-5 equivalent), though the latent thioester linker **4** carries a free hydroxyl group, when the coupling of the linker **4** is carried out in high concentration (3-5 folds excess), the intermolecular esterification might become inevitable. Besides the acetylate (capping) of the unreacted free amino functionalities of the resin after the coupling is impossible as long as the free secondary hydroxyl group still exists.

Loading of 1.1 equivalent of the latent thioester linker **4** onto the resin might be highly insufficient and left a lot of unreacted free amino groups on the resin. Without capping, these free amino groups involved in the amide formation with Fmoc-Ile-OH under same esterification conditions. The quantitative loading of isoleucine (according to the Fmoc release UV assay) was deceiving, because the isoleucine was loaded directly onto the resin and falsified a perfect loading. That might be the reason, why after the cleavage the peptide amide instead of the desired product **10** was found as the main product.

To verify this hypothesis, the loading of the latent thioester **4** onto the resin was examined semi-quantitatively by the Kaiser test.

The Kaiser test is a color test,^[128] which allows to semi-quantitatively and if necessary quantitatively detect the presence of the terminal free amino groups, was regularly applied in the SPPS to assess the coupling quality.

At presence of the free amino group, the Kaiser reagent (mainly ninhydrin) will be converted into a blue dye molecule through a serial of the reactions between the ninhydrin and the terminal free amino group (Scheme 89).



Scheme 89 The Kaiser test

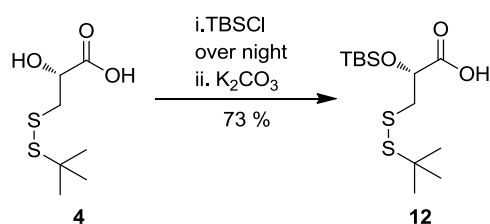
The Kaiser test works well with all natural amino acids with the only exception of proline, with which's secondary amino group, ninhydrin could not undergo the same process to form the blue dye molecule. The Kaiser test is extremely

sensitive and is applicable even when extremely low concentrations of free amino groups (5 μmol / mg) are present.

With the help of the Kaiser test (test procedure see experimental section), the loading of latent thioester linker **4** was determined and the color test was strongly positive. Both resin beads and the solution were intense blue and this proved that the coupling was totally failed. The loading of the linker **4** onto the resin with only an equimolar amount was ineffective thus the coupling did not proceed properly. Thereafter, the concentration of the linker **4** should be necessarily increased to achieve the proper loading, but the high concentration of the activated latent thioester linker **4** may also lead to the esterification between the linkers. In order to avoid this undesired esterification, the secondary hydroxyl group of latent thioester linker **4** should be masked before it can be used for the synthesis again. The protected secondary alcohol will allow the deployment of the high excess amount of the linker at the coupling step, moreover the capping will become feasible due to the absence of the free hydroxyl group.

3.1.4 Modification of the linker **4** and repeating of the Fmoc-SPPS

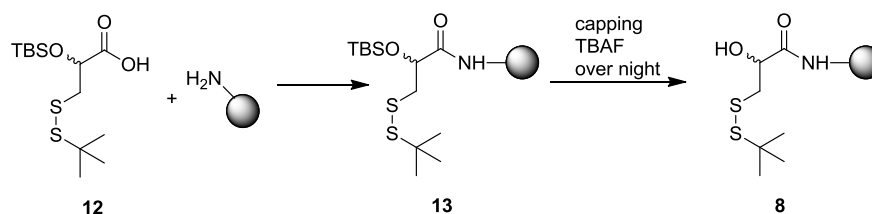
The protection of the hydroxyl group of the linker **4** was achieved through a one-step protection / deprotection procedure (scheme 90).^[129]



Scheme 90. The protection of **4** to generate the new linker **12**

The first step was the general protection of the latent thioester linker **4** with *tert*-butyldimethylsilyl chloride in the presence of the imidazole, in this step the free hydroxyl group was protected with TBDMS as well as the carboxylic acid. The determination of the completion of this reaction is difficult, because after the overall protection there were no UV active functionalities left and even worse was that the TLC plate could not be stained to become visible. Finally, the completion of the reaction was determined through the LC-MS analysis. The fully protected

intermediate was then treated with a weak base (K_2CO_3) to saponify the silyl carboxylic ester and left the primary silyl ether unaffected. The purification was easily performed through the flash chromatography and the final product **12** was obtained in 73% yield.



Scheme 91. Loading of the new linker **12** and the Fmoc-Ile-OH

The latent thioester linker **12** was unfortunately highly unstable, it can undergo decomposition at RT in a very short period (max. 3 hours) even under inert gas. At $-70\text{ }^\circ\text{C}$ this linker could only be kept no longer than one day. Each time this new latent thioester linker **12** had to be utilized immediately after the purification.

The new investigations started with the latent thioester linker **12** and the quality of the loading was controlled by Kaiser color test. At the beginning, an equimolar amount (1.1 eq.) of the latent thioester linker **12** was coupled onto the resin, but the color test failed and an intense blue color was shown both in the solution and on the resin beads. Then the introduced amount of the latent thioester linker **12** was deliberately increased ranged from 2 to 5 equivalents and separately coupled onto the resin. After each coupling, the shade of the blue color changed: the more the latent thioester linker **12** was charged at the beginning, the lighter the blue color became. From 3 equivalents onwards the blue color of the resin beads disappeared and the solution only showed a slight green grey color, which suggested that the coupling quality was improved. Then the TBDMS group was removed overnight on the resin by TBAF and Fmoc-Ile-OH was coupled (10 eq.) two times onto the linker **12** through the esterification by using the standard HBTU / DMAP activation protocol. The coupling quality of the first two steps was then quantitatively determined by Fmoc release UV assay.

Coupling of latent thioester linker **12** onto the resin with 1.1 equivalent amount only achieved a loading of 53% (Table 12, entry 3) and this reflected why an intense blue color was seen in both resin bead and the solution. With increasing amount of the latent thioester linker **12**, the loading of the first two steps increased accordingly. When doubling the initial charge of the latent thioester linker **14** (2 eq.), the loading increased by 30% and reached 82% (entry 4). With increasing amount over 2 eq. the loading increased only insignificantly and reached 93% when 3.5 equivalent amounts of the latent thioester linker **12** (entry 7) was utilized, beyond this point, further addition of latent thioester linker **12** has no substantial influence on the loading.

Table 12. The efficiency of the loading through various charges of linker **12**

entry	equivalent of the charged linker 12	loading after first two steps
3	1.1	53%
4	2	82%
5	2.5	85%
6	3	90%
7	3.5	93%
8	4	93%
9	5	94%

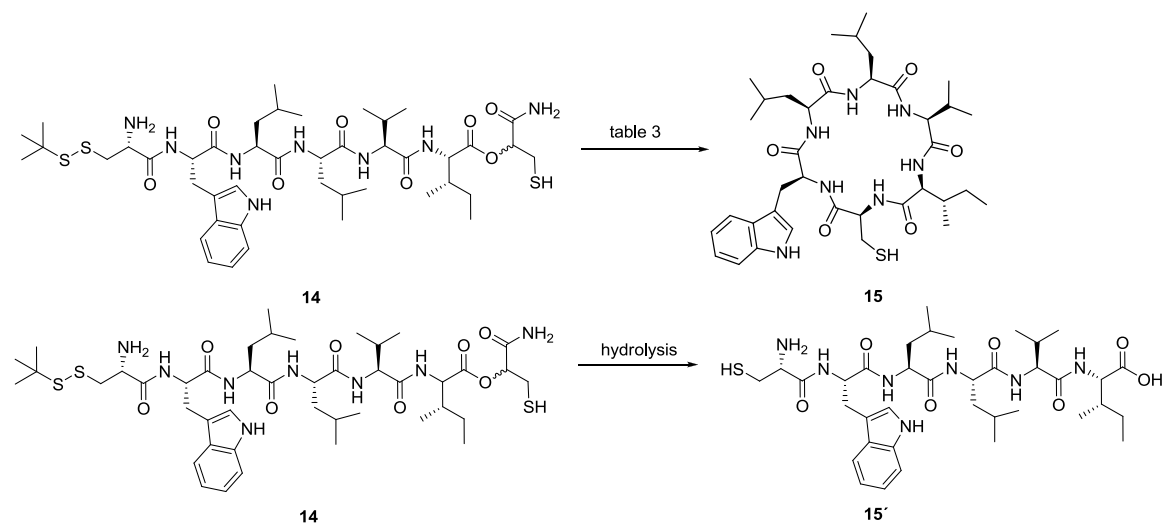
In all further studies, 3.5 eq. amounts of latent thioester linker **12** were uniformly applied at the beginning to achieve efficient coupling without unnecessary waste.

After Fmoc-Ile-OH was successfully anchored onto the linker, the rest amino acids (valine, leucine, leucine, tryptophan and cysteine) were consecutively assembled by the automated SPPS synthesizer. The linear peptide **14** was then cleaved and precipitated with MTB ether. The raw product **14** in a relatively clean condition was clearly characterized by the LC-MS analysis. No purification through HPLC was performed due to the high sensitivity of the ester bond to the water / ACN HPLC eluent.

3.2 Investigation of solution phase NCL cyclization

3.2.1 Investigation of solution phase NCL cyclization of **14**

The NCL cyclization of the linear precursor **14** was initially performed under the same conditions described by George *et al.*^[109]



Scheme 92. Two reactions compete against each other during the NCL cyclization

Table 13. The results of cyclization at various concentrations

entry	buffer mixture used	conc. of 14	denaturant (6 M GdmCl)	pH	product detected
10	20% ACN 80% phosphate buffer	0.2 mM	yes	6.79	hydrolyzed by-product
11	20% ACN 80% phosphate buffer	0.2 mM	yes	6.32	hydrolyzed by-product
12	20% ACN 80% phosphate buffer	1 mM	yes	7.0	hydrolyzed by-product
13	20% ACN 80% phosphate buffer	2 mM	yes	6.68	hydrolyzed by-product

The raw product **14** was at first dissolved in a small portion of ligation buffer solution mixture (20% ACN / 80% 0.1 M phosphate buffer containing 6 M guanidium chloride (GdmCl)) and was then diluted with a large amount of buffer mixture to a final concentration of 0.2 mM in order to avoid the dimerization or polymerization. The buffer mixture contained 350 folds of TCEP (70 mM), which allowed the rapid deprotection of the disulfide bonds. The pH value was adjusted to 6.79, which is common for the NCL reaction (Table 13, entry 10). The progression of the cyclization was monitored by analytical HPLC. The linear precursor **14** completely disappeared after four hours whereas a new peak constantly grew in the analytical HPLC. According to the LC-MS analysis, the new formed large peak was not the desired cyclic peptide **15** but the hydrolyzed by-product **15'** (Figure 16).

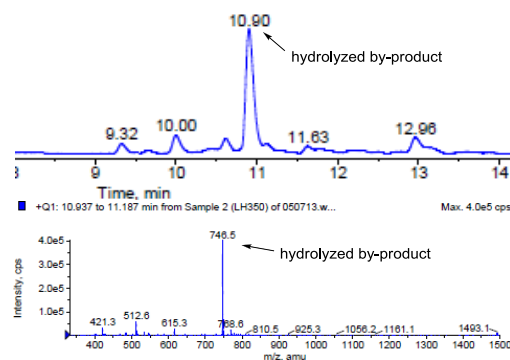
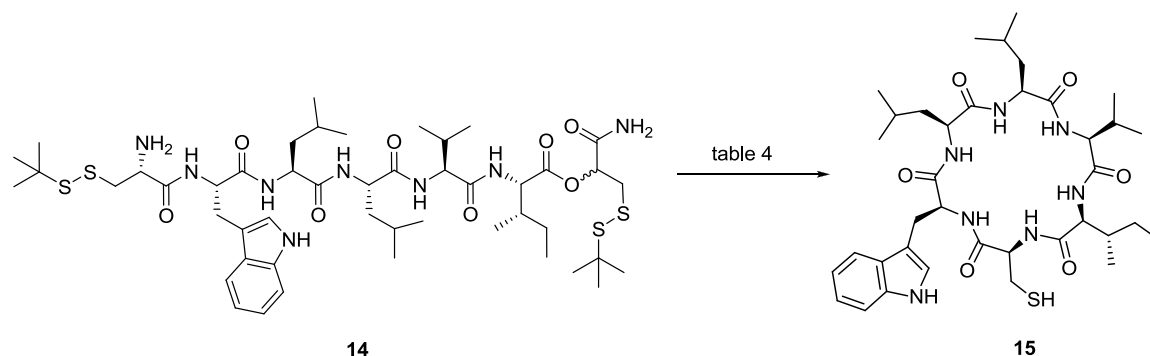


Figure 16. The hydrolyzed by-product was identified as the main product

Then the pH value was lowered to 6.3 (entry 11) in order to slow down the hydrolysis rate based on the statement of the literature,^[109] which claimed that the high pH value benefits the hydrolysis. The cyclization, which was repeated in this way, didn't change the outcome, the hydrolyzed by-product remained the sole detectable main peak in the LC-MS analysis. Then the concentration of the linear precursor **14** was intentionally increased to 1 mM and 2 mM (entry 12 and 13) to improve the chance of the head-to-tail contact (this may also lead to dimerisation or oligomerisation of the linear precursor). Again these attempts were unsuccessful, no cyclic products (monomer, dimer, or oligomer) was detected by LC-MS.

The failure of initial experiments indicated that the ester bond linkage is sensitive to the nucleophilic buffer solution. If the NCL cyclization could be performed in

pure aprotic polar organic solvent, without the disturbance of the nucleophile the cyclization might be working.^[130]



Scheme 93. The solution phase NCL of **14** in the modified buffer mixtures.

Table 14. The results of reactions in an organic solvent

entry	buffer mixture	pH value	concentration of TCEP	product detected
14	70% DMF	5.13	50 mM	no reaction
(RT → 40 °C)	30% phosphate buffer			
15	90% DMF	/	50 mM	no reaction
	10% phosphate buffer			
16	95% DMF	/	slightly soluble	no reaction
	5% phosphate buffer			
17	99% DMF	/	slightly soluble	no reaction
	1% phosphate buffer			
18	100% DMF	/	insoluble	no reaction

A series of organic solvent mixtures, which contain different ratios of the aqueous phosphate buffer solution were prepared and NCL cyclization of **14** was then performed in these mixtures. During these experiments, the presence of water in the model study was found very crucial, because the TCEP is only soluble in aqueous medium. When there was no or little water in the ligation mixture (Table 14, entry 16, 17 and 18), the TCEP was very limited dissolved. No reaction took

place in pure DMF after 24 hours (entry 18), the linear precursor **14** was intact judged by LC-MS. In experiments 16 and 17, after 24 hours, a small amount of TCEP was eventually dissolved and reduced one of two disulfide bonds or both of them. In these mixtures the linear precursor **14** existed in three different reduced forms: fully reduced and two partially reduced forms, no sign of the cyclic product was identified though (Figure 17).

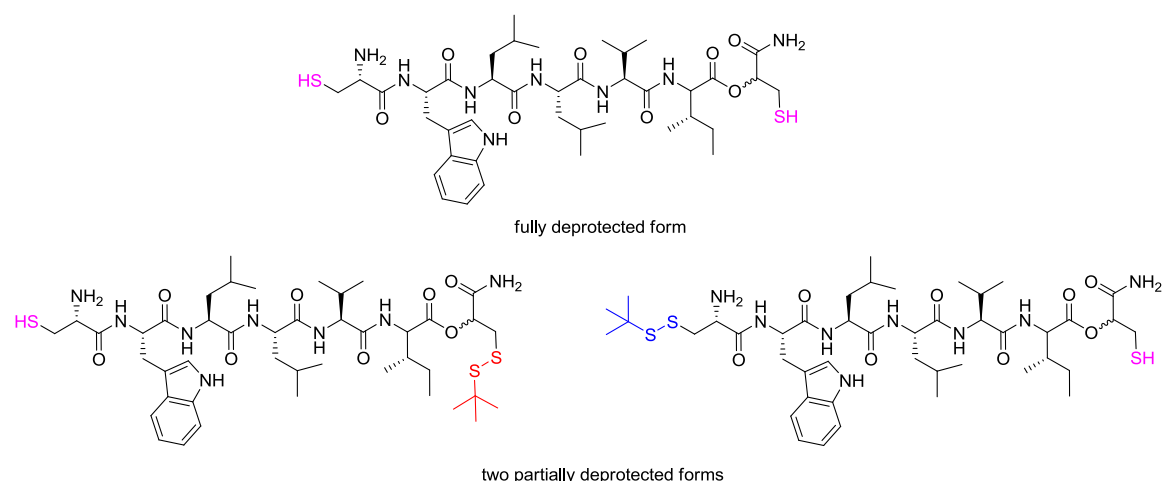


Figure 17. Three reduced forms detected by LC-MS

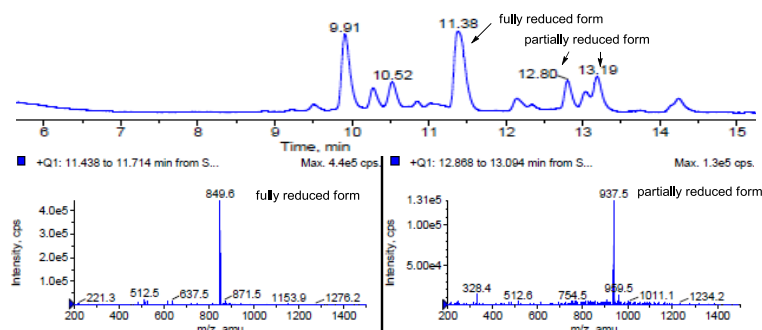


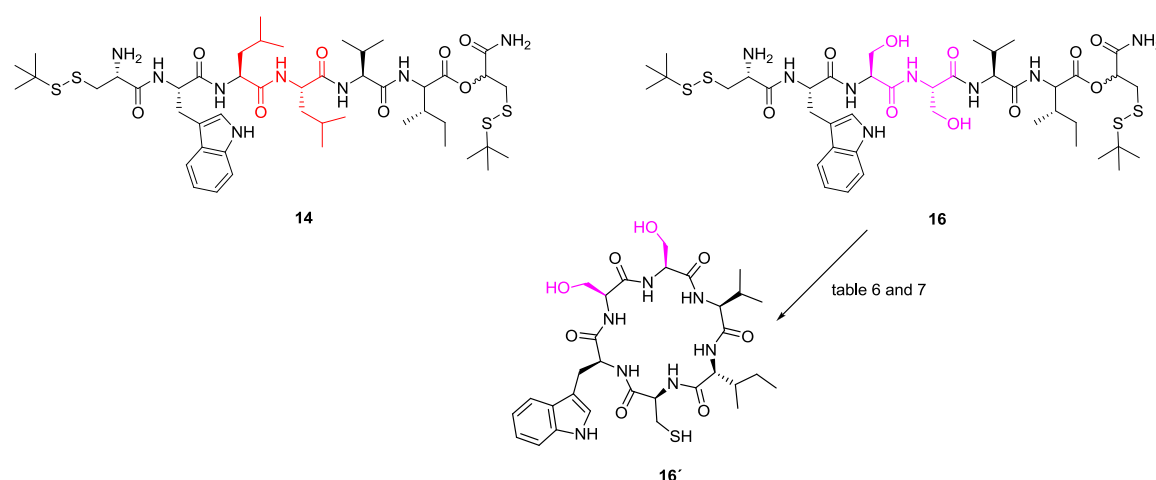
Figure 18. LC-MS analysis (UV: 190 – 600 nm) of entry 16 and 17

In the experiment 14 and 15, with higher percentage of water in the buffer mixture, the TCEP was easily soluble in the buffer mixture and in both cases, after 24 hours the linear precursor **14** was found existed in fully reduced form (entry 14 and 15). No ligation took place neither did the hydrolysis. The reaction mixture of the experiment 14 was then heated at 40 °C for 12 hours but the linear precursor **14** could still not be cyclized in organic solvent through NCL.

3.2.2 Modification of the sequence **14** and investigation of the new sequence **16**

The model sequence CWLLVI **14** was comprised of over 80% hydrophobic amino acids thus it presented a strong hydrophobic character and in the previous experiments it was found to be poor soluble in the aqueous medium. Each time, the model sequence **14** could not be directly dissolved in the 20% ACN / 80% phosphate buffer mixture but rather firstly dissolved in a small amount of DMF (30 μ L), then the aqueous buffer mixture was carefully added. The poor solubility of **14** in water might decelerate or even hinder the ligation and thus only the hydrolysis by-product was formed

With the purpose of verifying this speculation, the original model sequence CWLLVI **14** underwent some slight changes to increase its water solubility, thereby the leucines were deliberately replaced by two serines (Scheme 94).



Scheme 94 The modification of **14** into **16**

The modified sequence CWSSVI **16** was synthesized through the same procedure on the resin and after the synthesis it was cleaved and found to be very soluble in the aqueous buffer mixture. Then the NCL cyclization of the modified sequence **16** was investigated again under the previous conditions (20% ACN / 80% 0.1 M phosphate buffer, 6 M guanidium chloride, 50 mM TCEP, concentration: ca 1 mM in buffer mixture).

Table 15. Results of cyclization at different pH values

entry	pH value	product detected
19	6.32	by-product
20	6.55	by-product
21	6.71	by-product
22	6.95	by-product
23	7.08	by-product

In the beginning, a row of buffer mixtures of the pH values ranged between 6.32 and 7.08 (Table 15) were prepared and the NCL was performed in these mixtures. Surprisingly the NCL cyclization did not happen in none of these experiments. The hydrolyzed by-product remained the main detectable substance at LC-MS analysis, therefore, the pH value was determined not to be a crucial factor for the NCL cyclization, at least not in this model study. The problem remained and one question still needed to be answered, what is utmost essential factor for the NCL cyclization.

Camellio's previous investigation of the on-resin NCL cyclization^[111] has determined that the denaturant 6 M guanidium chloride considerably reduced the ligation rate, but in most cases the proteins and large peptides are ligated, the presence of denaturant is necessary. In this model study, the sequence **16** is a small peptide, which theoretically does not possess the secondary structure yet and thus the presence of the denaturant is redundant.

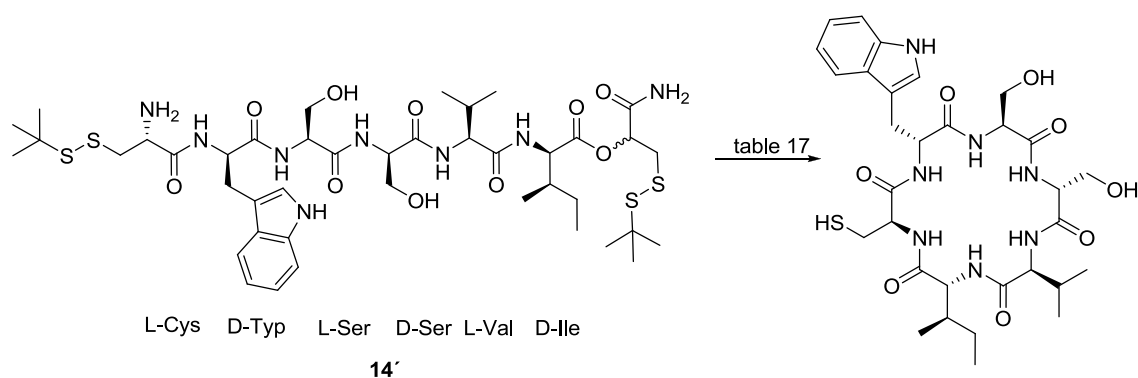
Table 16. Results of cyclization in the denaturant-free buffer mixture

experiment	pH value	product detected
24	6.8	by-product
25	7.0	by-product

Thereafter the solution phase NCL cyclization of **16** was carried out twice in the denaturant-free buffer mixtures and the previous problem remained (Table 16). As usual the linear precursor **16** was completely hydrolyzed. The denaturant might reduce the ligation rate, but in this case study there must be a more important fact, which obstructs the NCL cyclization of **16**.

3.2.3 Investigation of CWSSLI **16** with alternating stereochemistry

So far only the L-amino acids were used to construct the model sequence **14**, as a result there could be a possibility, that the side chains, which all situate on the same side of the sequence, caused a large steric blockade when the NCL cyclization progresses and under such circumstance the NCL cyclization might progress not fast enough to surpass the hydrolysis. In order to reduce the ring strain during the cyclization, half of the L-amino acids were thereafter replaced by D-amino acids and the resulted optimal geometrical configuration was expected to possess less steric hindrance and formation of the cyclic product should be eased. The NCL cyclization of **14'** was performed twice under the previous conditions (RT, standard buffer mixture).



Scheme 95. The cyclization of linear sequence CWSSLI **16** with alternating configurations

Table 17. Results of cyclization of the CWSSLI **15** with alternating stereochemistry

experiment	buffer mixture used	pH value	product detected
26	20% ACN 80% phosphate buffer	6.87	by-product
27	20% ACN 80% phosphate buffer	6.68	by-product

Unfortunately the NCL cyclization of linear CWSSLI **14'** with alternating configurations failed again (Table 17), the hydrolyzed by-product was still identified as the main product by LC-MS analysis.

3.2.5 Investigation of solution phase NCL cyclization of **16** with thiol additive

In the buffer mixture, upon reduction of the disulfide bond, the peptide- α -thioalkyl ester was formed *in situ* through the O to S acyl transfer and followed by the transthioesterification, which in the case of sequence **16** might be very slow and consequentially the cyclization was suppressed by the hydrolysis. According to the common knowledge, the transthioesterification rate can be improved by using promoters, thereby the influence of promoters (1% v/v benzy mercaptan with 3% v/v thiophenol and MESNa) on the NCL cyclization of **16** was investigated.

Table 18. Results of cyclization with thiol additives

entry	promoter	product detected
28	1% v/v benzy mercaptan and 3% v/v thiophenol	no
29	MESNa	no

The cyclization was performed under previous conditions but with additional thiol additives (Table 18). The cyclization did not take place in the buffer solution containing promoters, no sign of the product was detected after the reaction.

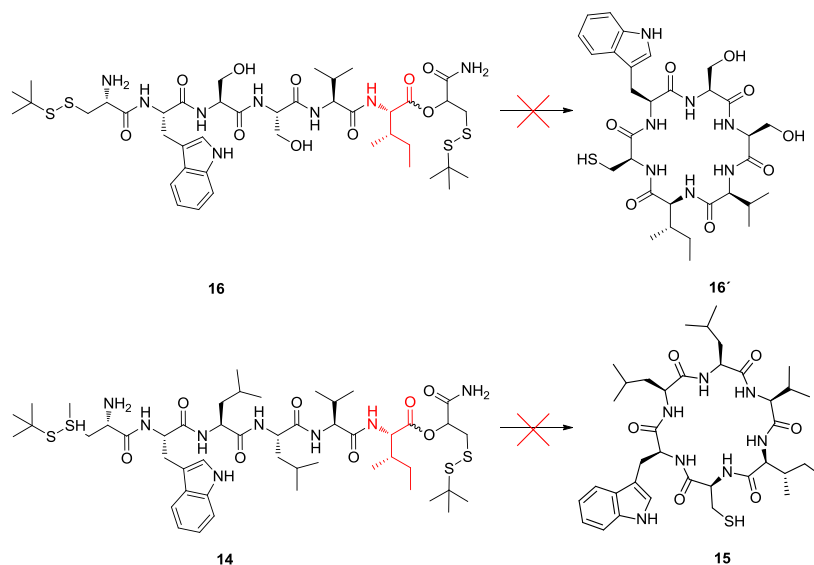
3.2.6 Reinvestigation of the solution phase NCL cyclization of **14** at low temperatures

The NCL cyclization of the initial model sequence CWLLVI **14** could be accomplished under no circumstances. Inspired by the research reports,^[104] which suggested that in the NCL reaction, the hydrolysis is the thermodynamic product and the NCL is the kinetically controlled product, the NCL cyclization of the sequence CWLLVI **14** was reexamined at low temperature.

Table 19. Results of cyclization at low temperature

entry	temperature	product detected
30	10 - 13 °C	by-product
31	0 °C	by-product

The new experiments were carried out under the same previous conditions but the temperature was lowered down to 10 – 13 °C and 0 °C (Table 19, entry 30 and 31) respectively. Disappointingly, even at the low temperature the ligation of the sequence **14** could still not surpass the hydrolysis to generate the correct cyclic product, after 16 hours the hydrolyzed by-product was again identified by LC-MS as the single main product in both cases, no trace of the cyclic product was found.



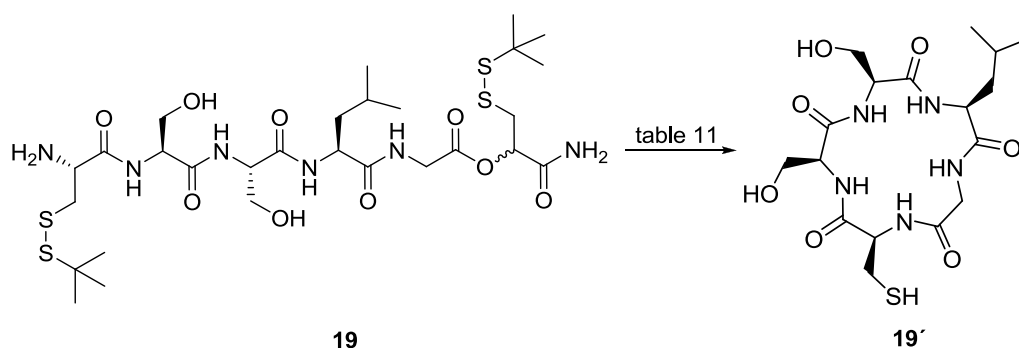
Scheme 96. The unsuccessful attempt of cyclization of linear sequence CWLLVI **14** and CWSSVI **16**

All attempts of the NCL cyclization with both model sequences CWLLVI **14** and CWSSVI **16** failed. None of them could be converted into the desired cyclic products due to vast steric hindrance of the C-terminal isoleucine. These results were in consistence with Dawson's publication^[78] and verified that the isoleucine is not suitable to be used as the ligation partner in the NCL reaction to generate the amide linkage. In the case of the NCL cyclization, the geometrical influence of the side chain of the C-terminal isoleucine is so high, that the ligation was severely hindered by the bulky side chain and consequentially the NCL cyclization progressed extremely slowly. Even with the promoters, neither of linear precursors **14** and **15** could be cyclized. The NCL cyclization could not be accomplished under previous conditions as long as isoleucine situates at the junction site.

3.2.6 Shift of the investigation subject to the sequence **19**

Since the further investigation of the model sequences CWLLVI **14** and CWSSVI **16** was pointless, a new model sequence CSSLG **19**, which was inspired by Muir's work,^[105] was constructed. Instead of the bulky isoleucine, glycine was in this case placed at the junction site. Formation of a Gly-Cys junction should confront the least steric barrier due to the absence of the side chain and the ligation rate should be predictably easier.^[78]

The new sequence **19** has the idea geometry at the junction site and is good soluble in water and thus it supposed to be a perfect model for the NCL cyclization study. The sequence **19** was generated by using the established synthetic route and was investigated under various conditions (Scheme 97).



Scheme 97. The cyclization of the new sequence **19** under previous conditions

Table 20. Initial results of the cyclization of the sequence **19**

entry	promoter	product detected
31	none	by-product
32	60 mM MESNa	strong MESNa peak

Initially, the investigation was carried under the original conditions (1mM in buffer solution, RT, neutral pH, 6 M Gdm·Cl and 70 mM TCEP) (Table 20, entry 31), after four hours the linear precursor **19** disappeared in the analytical HPLC, but unfortunately even with minimal steric hindrance at the ligation site, the NCL cyclization could not be accomplished. The hydrolyzed by-product emerged as the main product judged by the LC-MS analysis. Then the experiment was repeated with additional 60 mM MESNa (entry 32) in the buffer mixture and after 16 hours there was still no sign of the cyclic product **19**.

In previous experiments, the model sequence CWSSIV **14** was once cyclized at low temperatures. The linear precursor **19** was again investigated at low temperature, although the previous experiment was unsuccessful. Additionally, in order to achieve a higher ligation rate, the denaturant 6 M guanidium chloride was excluded from the buffer mixture and would not be used for the further investigations.^[111]

Table 21. Results of cyclization of **19** at low temperature

entry	temperature	product detected
33	10 - 13 °C	by-product and product co-existed
34	0 °C	yes
35 (50 mM MPAA)	0 °C	yes

The reactions at lower temperature progressed slower than at RT, after four hours the starting material **19** still existed in a large amount (analytical HPLC) and thus the sequence **19** was allowed to react overnight and after 16 hours the

starting material **19** was found completely consumed by LC-MS. After the reaction performed at 10 – 13 °C for 16 hours the desired cyclic product **19'** was finally detected by LC-MS (Table 21, entry 33), despite the majority of the linear precursor **19** was still hydrolyzed in a ratio of approximately 5:1 (LC-MS, calculated through integration of the UV chromatogram, Figure 19) to the cyclic product **19'**. At this temperature, formation of the by-product was still more favored.

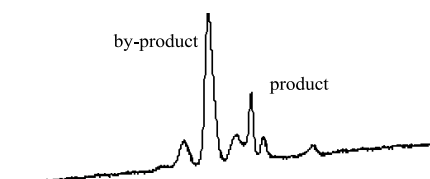


Figure 19. LC-MS analysis (UV: 190 – 600 nm) of the solution phase NCL cyclization of **19** at 10 °C

Finally, at 0 °C (entry 34) no more hydrolyzed by-product could be observed by LC-MS and the cyclic product **19** existed as the sole main product. Furthermore, the influence of the promoter MPAA (50 mM) was also investigated at 0 °C and it was found that at 0 °C with or without promoter the cyclic product **19'** could be cleanly formed. Besides, utilization of a large amount of MPAA was disadvantageous, because its high UV absorption created a significant signal in the UV spectrum, which overlaps many small peaks including the cyclic product **19'** (Figure 20). Consequently, all further experiments were carried out without promoter.

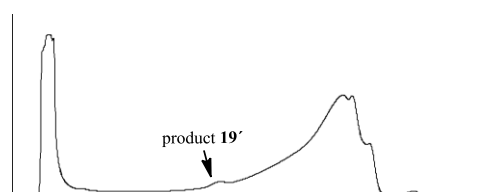


Figure 20. UV spectrum of LC-MC analysis (UV: 190 – 600 nm) of the reaction mixture using a large amount of MPAA additive

3.2.7 Determination of the ideal TCEP concentration in the buffer mixture

Theoretically the concentration of TCEP in the buffer mixture does not participate in the NCL cyclization, because its only function is to reduce the disulfide bonds. However in practice, after the reaction, the solvent will be removed and the cyclic product will be directly isolated from the reaction mixture through HPLC. High concentrations of TCEP in the buffer mixture resulted in a large amount of TCEP residue in the solid mixture. The isolation of the product from the large amount of leftover TCEP requires multiple HPLC runs because of the limited loading capacity of the HPLC column, as a result this cause considerable handling loss of the cyclic product.

For this particular reason, the amount of TCEP in the buffer solution should be reduced to a proper level for the convenient purification and the reduction of the handling loss, meanwhile this lower TCEP concentration must be still capable of efficient reducing the disulfide bonds.

Table 22. Cyclization of **19** in buffer mixture with different TCEP concentrations

entry	conc. of TCEP
36	50 mM
37	30 mM
38	10 mM

In order to determine the ideal TCEP concentration in the buffer mixture, the linear precursor **19** was allowed to be cyclized in the buffer mixtures containing different amount of TCEP (Table 22). The cyclization in these buffer mixtures showed that at 0 °C the cyclization in the buffer solution containing 10 mM TCEP (entry 38) was accomplished qualitatively as good as in the buffer solution containing 50 mM TCEP (entry 36) and no by-product was identified by LC-MS in all three cases. This means, efficient reduction of the disulfide bond required no more than 10 mM TCEP in the buffer mixture, it is unnecessary to utilize a large amount of the TCEP in this case study. The investigation of the cyclization in buffer solution containing lower than 10 mM TCEP was not carried out, although

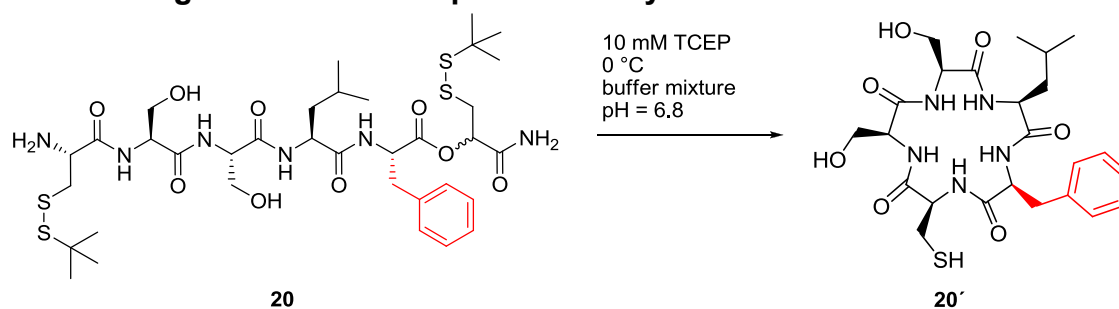
in some publications the deprotection in solution phase was performed with mere two equivalent amount of TCEP (in this case equals 2 mM TCEP in buffer solution). Maintaining of such relatively high concentration of TCEP in buffer solution is based on the following basis, because in the further on-resin experiments, the immobilized disulfide bond are much less reactive and reachable and thus the rapid reduction of the disulfide bond in solid phase should require a relatively high level of TCEP concentration.

The initial investigation of solution phase NCL cyclization of the model sequence **19** was concluded. The preliminary optimal conditions, which were determined through the previous experiments, were summarized here:

Table 23. The optimal conditions for the solution phase NCL cyclization

conc. of the linear precursor	1 mM
temperature	0 – 5 °C
denaturant	none
promoter	none
conc. of TCEP	10 mM
buffer mixture solution	20% ACN / 80% 0.1 M phosphate buffer
pH value	6.8 – 7.0

3.2.8 Investigation of solution phase NCL cyclization of **20**



Scheme 98. Cyclization of the linear sequence **20** in the solution phase

In order to validate that the established conditions are not specifically applicable for the cyclization of the sequence **19**, the NCL cyclization of the new sequence CWLLF **20** was investigated under the same conditions as well (Scheme 98).

The linear precursor **20**, which contains a C-terminal phenylalanine, was prepared through the previous established route and cyclized. While cyclizing sequence **20**, large steric blockade was expected due to the benzyl residue of the C-terminal phenylalanine. But in fact in solution phase and at 0 °C the benzyl residue did not have influence on the NCL cyclization, and like its predecessor **19** the cyclization of sequence **20** resulted in the clean cyclic product **20'**.

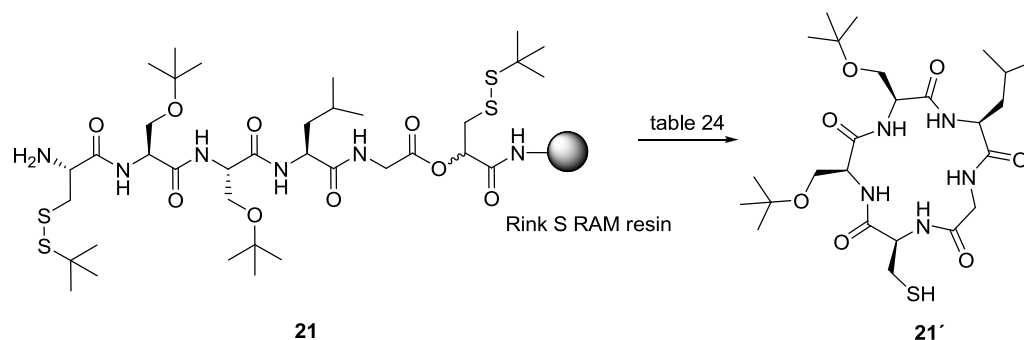
Through this experiment the established reaction conditions were proven applicable and the NCL cyclization of linear peptide by applying this latent thioester linker strategy was feasible at least in these cases.

Based on these conditions, which were developed for the solution phase NCL cyclization, the following work is going to investigate the NCL cyclization of various peptides in solid phase.

3.3 Investigation of on-resin NCL cyclization

3.3.1 On-resin NCL cyclization of fully protected sequence 21

At the beginning of the investigation, the model sequence **21**, which is the fully protected sequence **19**, was generated on the TentaGel S RAM resin and directly cyclized on the resin under the established conditions. The reason, why a fully protected peptide sequence was used, was that under the deprotection condition (concentrated TFA treatment), the immobilized peptide sequence will be concomitantly cleaved due to the acidic sensitive Rink linker thus no on-resin investigations could be conducted (Scheme 99).



Scheme 99. The on-resin cyclization of fully protected **21**

Table 24. Results of on-resin cyclization of **21** at various temperatures

entry	temperature	product detected
39	0 - 5 °C	no reaction
40	10 - 15 °C	no reaction
41	RT	trace, mostly hydrolyzed
42	40 °C	hydrolyzed

Not so surprisingly, the immobilized linear precursor **21** was much less reactive than in solution phase, hence the low temperature was inappropriate for the on-resin NCL cyclization. At low temperature (Table 15, entry 39 and 40), after 16 hours neither the hydrolyzed by-product nor the NCL cyclic product was observed by LC-MS. At RT the cyclization progressed very slowly, after 16 hours the cyclic product **21'** existed only as trace while the majority of the linear precursor was hydrolyzed (entry 41). The higher temperature was not beneficial for the cyclization either, because the test at 40 °C showed that after 4 hours only the hydrolyzed by-product was detected in the buffer mixture (entry 42). These facts indicated that the cyclization on the resin didn't take place until the temperature reached RT and the side chain protecting groups must be removed prior to the cyclization, otherwise the NCL cyclization confronts the large steric barrier and the hydrolyzed by-product was preferentially formed.

3.3.2 Investigation of on-resin NCL cyclization of sequence **19**

In order to deprotect the side chains with concentrated TFA without from the resin, the same sequence was generated on the TentaGel NH₂ resin instead of the previously used TentaGel S RAM resin. The TentaGel NH₂ resin is similar to the TentaGel Rink S RAM resin in terms of the core copolymer but it does not carry the cleavable Rink linker (Figure 21).

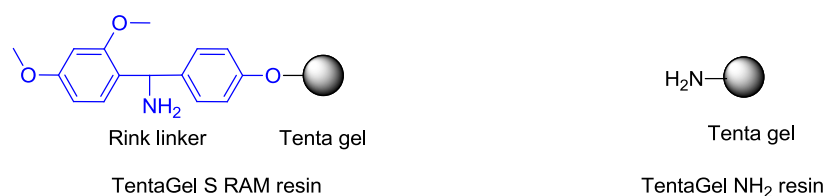
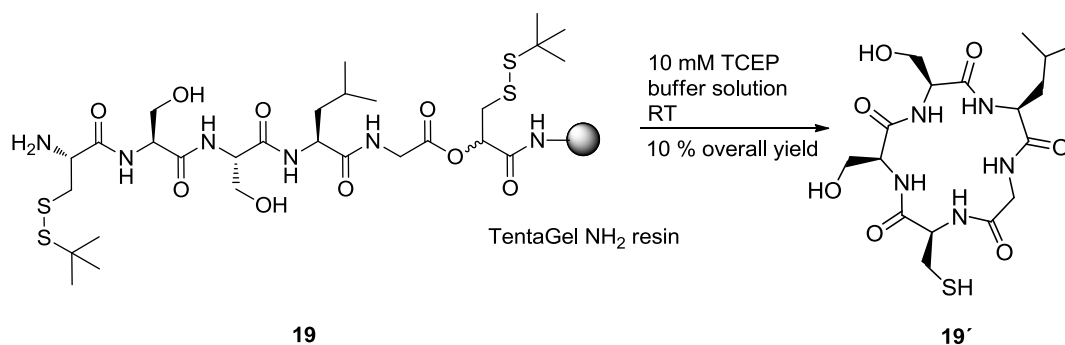


Figure 21. Difference between two resins

The linkage between the latent thioester linker **12** and the TentaGel NH₂ resin is achieved through an amide bond, which is highly stable upon treatment with concentrated TFA thus it allows the attached sequence **19** to be deprotected with concentrate TFA without the risk of cleavage of the linear sequence. By following the established route, the linear precursor **19** was generated on the TentaGel NH₂ resin and after the synthesis, the sequence was deprotected with cleavage cocktail (concentrate TFA:triisopropylsilane:water = 95%:2.5%:2.5%) on the resin (in this case all side chain protecting groups except the *tert*-butyl mercapto groups were cleaved). No linear sequence was prematurely released as peptide amide during the TFA treatment judged by the LC-MS analysis of the cleavage cocktail. After the resin was washed and dried, it was allowed to be swollen in the buffer mixture at RT for 16 hours (Scheme 100).



Scheme 100. The on-resin cyclization of **19**

After 16 hours the cyclic product **19'** was detected as the main product (LC-MS), furthermore the solution after the NCL cyclization was relatively clean and none of these small peaks were identified as the hydrolyzed by-product (Figure 22).

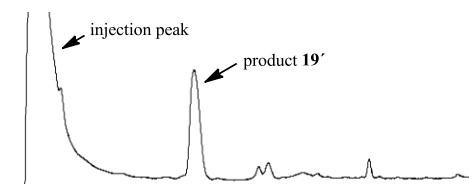


Figure 22. LC-MS analysis (UV: 190 – 600 nm) of successful on-resin NCL cyclization of sequence **19**

This successful experiment indicated that the previously established conditions, except the low temperature, were fully adoptable for the on-resin NCL cyclization. The purification of product **19'** was performed through semi-prep HPLC in 10% overall yield. The overall yield was calculated through comparison of the amount of the substance between deployed resin at the beginning of the SPPS and the isolated cyclic product at the end.

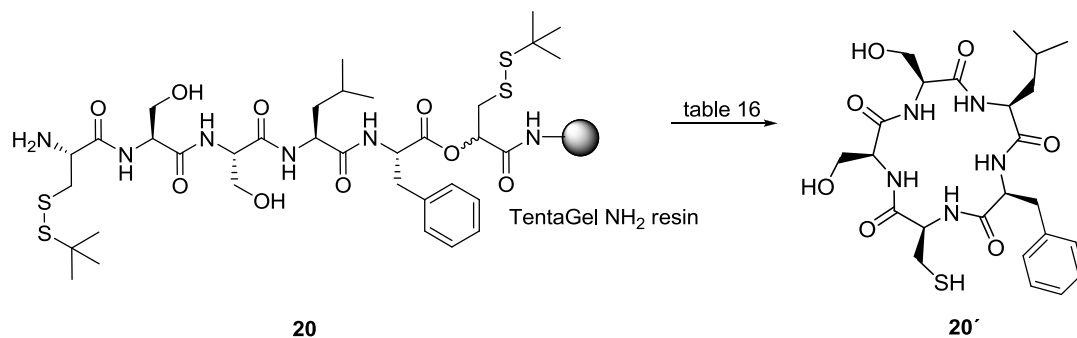
The cyclic product **19'** was only isolated in modest overall yield (10%) but it was relatively clean and could be easily purified. However, the yield might be improved by using modified buffer mixture based on the following consideration: The TentaGel NH₂ resin, which was used in the model study, only has moderate swelling property in water, therefore, the resin may not be properly swollen in the 20% ACN / 80% phosphate buffer mixture. In this case, a large number of linear precursors may still be wrapped underneath the resin and could not participate in the NCL cyclization. With higher percentage of the polar, aprotic organic solvent in the buffer solution, the swelling ability of the TentaGel might be improved and possibly result in higher yield. Thereafter the buffer mixture was adjusted to contain more acetonitrile (50%) and the NCL cyclization of the sequence **19** was investigated in this mixture again. After 16 hours the cyclic product **19'** was isolated through HPLC but the overall yield showed no improvement.

3.3.3 Investigation of on-resin NCL cyclization of further model sequences

3.3.3.1 Investigation on-resin NCL cyclization of further 5 membered peptides

3.3.3.1a On-resin NCL cyclization of sequence **20**

In order to check the general feasibility of the on-resin NCL cyclization, a few further sequences were examined under the established conditions (Scheme 101).



Scheme 101. The on-resin cyclization of **20**

Table 25. Results of on-resin cyclization of **20** at two temperatures

entry	temperature	product detected
42	RT	yes
43	15 °C	no reaction after 16 h

The TentaGel NH₂ resin loaded with the linear precursor **20** was allowed to be swollen at RT for 16 hours and was then examined by LC-MS.

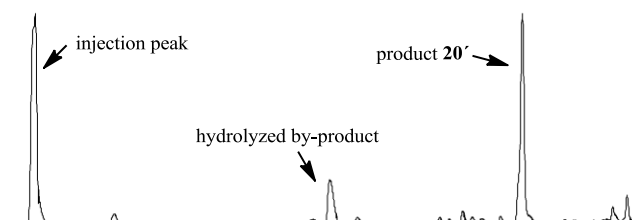


Figure 23. LC-MS analysis (UV: 190 – 600 nm) of on-resin NCL cyclization of sequence **20**

Due to the bulky benzyl moiety of the C-terminal phenylalanine, the ligation progressed slower than the cyclization of CSSLG **19**. The ligation was unable to completely suppress the hydrolysis, a small portion (29% of the cyclic product, LC-MS analysis calculated through integration of the UV chromatogram, Table 16, entry 42) of the linear precursor **20** was hydrolyzed (Figure 19). The isolated overall yield of CSSLF **20'** was 6%, which dropped around 40% in contrast to the cyclic product **19'**.

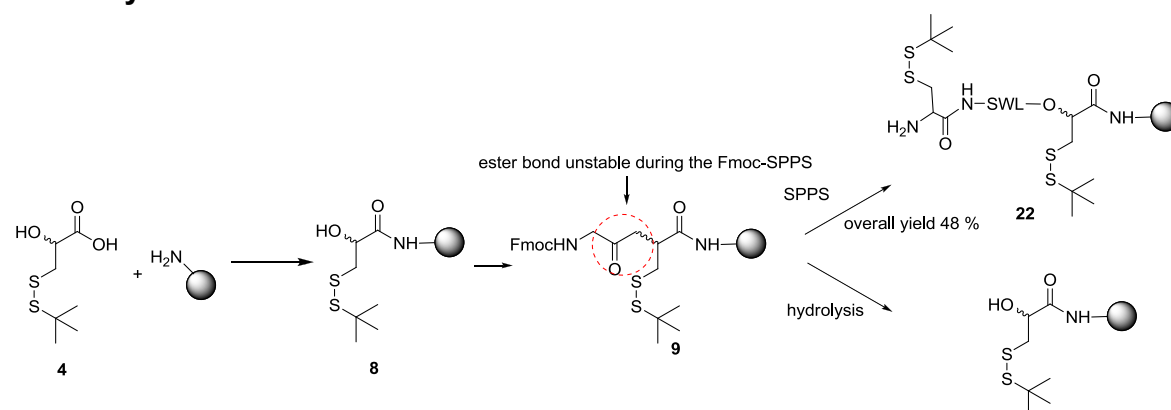
In order to eliminate the hydrolyzed by-product, the cyclization of **20** was carried out at 15 °C (Table 25, entry 43), despite the previous unsuccessful attempts at low temperature. With no exception, the on-resin NCL cyclization did not take place at 15 °C after 16 hours. Lowering of the pH value may not be a right solution either, because the low pH value only slows down the cyclization.^[105] The promoters (MPAA or MESNa) were not considered to be used in the model studies for the particular reason, which was described before (section 3.2.6). All further on-resin studies were uniformly carried out under the exact conditions, which were applied for the on-resin cyclization of sequence **19** without any modification.

3.3.3.1b On-resin NCL cyclization of sequence 22

In the previous investigations, the consumption of the linear precursor on the resin was not monitored due to the immobilized nature of the starting material, so when the on-resin cyclization concludes was still unknown. In order to determine the real reaction duration, the formation of the cyclic product must be quantitatively tracked. Tryptophan has specific UV absorption because of the indole residue. When the tryptophan moiety is incorporated into the linear peptide precursor and after the formation of the cyclic product, the UV absorbance of the tryptophan in the solution could be measured by spectrophotometer thus the concentration change of the cyclic product could be monitored this way.

In order to determine kinetic progression of the on-resin NCL cyclization, the sequence CSWLG **22** was prepared on the TentaGel NH₂ resin.

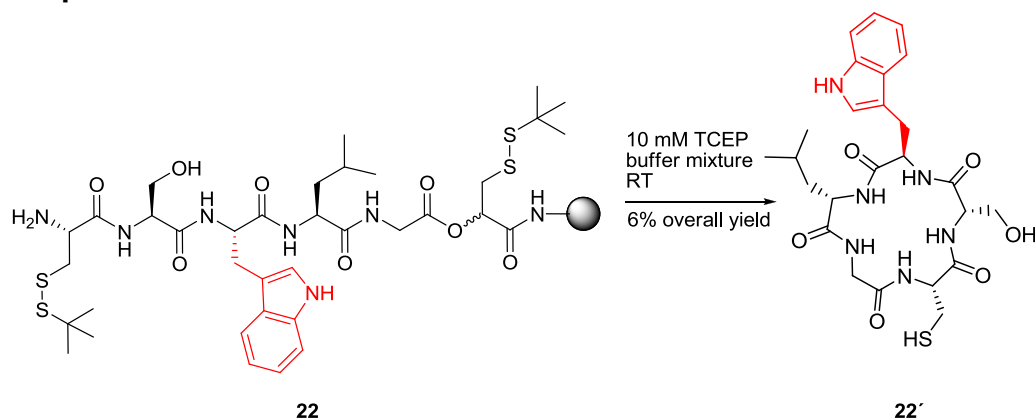
3.3.3.1b (a) Quantitative quality assessment of the linear sequence **22** prior to the cyclization



Scheme 102. The hydrolysis of the ester bond during Fmoc-SPPS

After the SPPS, the loading of the sequence **22** on the resin was determined through Fmoc release UV assay and this was calculated as 48% overall yield of the linear precursor **22** prior to cyclization. This calculated overall yield indicated that the C-terminal peptide ester was not completely stable to the piperidine treatment (Scheme 35). A substantial amount of the ester bond was hydrolyzed for each coupling and the halfway finished linear peptide precursor was prematurely released in its peptide carboxylic acid form from the resin after each coupling. Fortunately, the freed hydroxyl group of the latent linker could unlikely form the new amide bond with any preceding amino acid under the TBTU / DIPEA activation and avoid the formation of a large number of products. Later on a test reaction was carried out, in which a random Fmoc protected amino acid was coupled twice to the linker through the TBTU / DIPEA activation (without DMAP). After the coupling the Fmoc release UV assay showed that only very few of the amino acids were successfully linked to the linker and this result validated the previous hypothesis.

3.3.3.1b (b) The on-resin NCL cyclization of **22** under the monitor of the spectrophotometer



Scheme 103. The on-resin cyclization of **22**

After the pre-cyclization investigation, the resin bearing the linear precursor **22** was swollen in the buffer mixture under the previous conditions. The UV absorbance of the formed cyclic product **22'** in the solution was recorded for 32 hours by spectrophotometer at wavelength of 280 nm. After the recording, according to the Lambert-Beer law the concentration of the cyclic product **22'** was calculated from the recorded UV absorbance:

$$A = \varepsilon * c * l$$

A = absorbance

ε ($L \cdot \text{mol}^{-1} \cdot \text{cm}^{-1}$) = molar absorption coefficient

c = molar concentration

l = path length of the cuvette (1 cm)

The ε of the tryptophan is $5500 L \cdot \text{mol}^{-1} \cdot \text{cm}^{-1}$ at 280 nm.

With the calculated dates, the kinetic diagram of the on-resin NCL cyclization was hereby created.

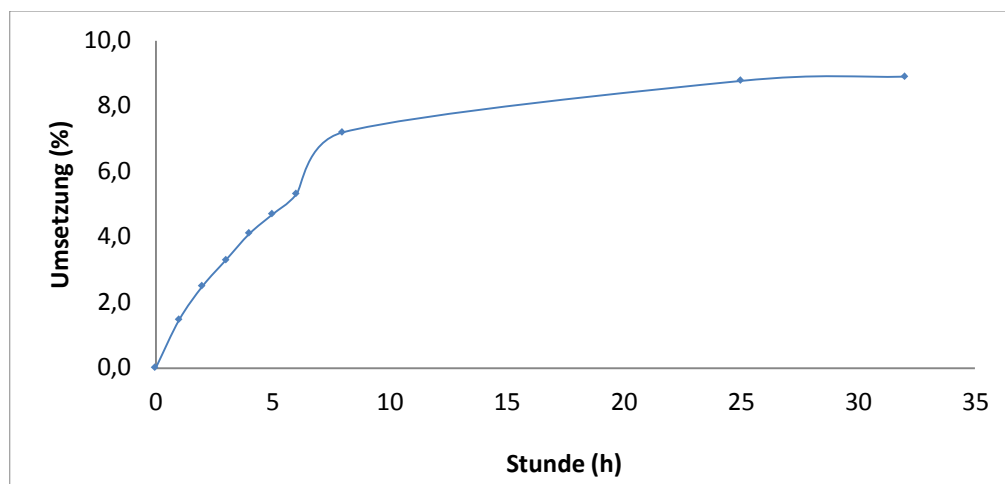


Figure 24. The kinetic diagram of the NCL cyclization

The kinetic diagram (Figure 24) showed that the on-resin cyclization of **22** progressed erratically within the first 10 hours, then the concentration elevation slowed down and after approximately 24 hours the cyclization completely ceased. In the old buffer mixture the reductant TCEP after 36 hours might be wore out due to the oxidization and lost its reactivity, after the reaction the old buffer mixture containing the cyclic product **22'** was drained and the freshly prepared buffer mixture containing 10 mM TCEP was then added to the reaction vessel to ensure no unreacted linear precursor remains on the resin. In the fresh prepared buffer solution, the resin was swollen for additional 16 hours and after the reaction only very weak UV absorbance of the solution was measured by the spectrophotometer. This indicated that in the fresh buffer solution no more cyclic product was formed and the on-resin cyclization of the sequence **22** has already concluded within the first 24 hours thus the prolonged reaction time was unnecessary. The LC-MS analysis showed that under previous conditions the on-resin cyclization of **22** has achieved a very similar result as the sequence **20**, again a small part of the linear precursor was hydrolyzed (29% of the cyclic product, LC-MS, calculated through integration of the UV chromatogram, Figure 25).

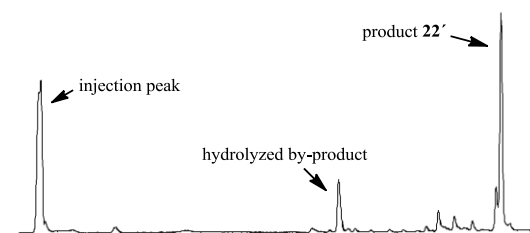


Figure 25. LC-MS analysis (UV: 190 – 600 nm) of the on-resin NCL cyclization of the sequence **22**

After the cyclization of **22**, the concentration of the cyclic product **22'** regardless of the existence of the hydrolyzed by-product was calculated from the UV absorbance and resulted in a concentration of $0.1787 \text{ mmol L}^{-1}$. In 5 mL buffer mixture, the theoretic amount of the cyclic product **22'** contained in the buffer mixture was:

$$m = 0.1787 \frac{\text{mmol}}{\text{L}} \times 5 \text{ mL} \times 546.64 \frac{\text{g}}{\text{mol}} = 0.49 \text{ mg}$$

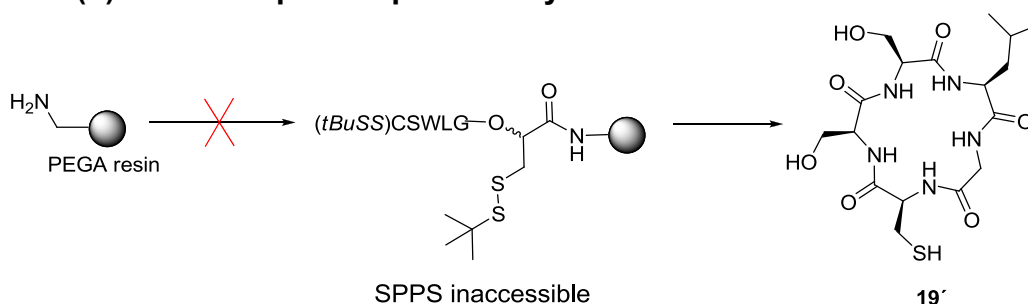
After the isolation, 0.33 mg cyclic product **22'** was recovered. This figure indicated that roughly 34% of the cyclic product **22'** was lost during the HPLC purification. The final isolated overall yield was 6%, which suggested that out of 8 linear precursors on the resin only one has been successfully cyclized and isolated. (Comparison of the overall yields before and after the cyclization. 48%:6% \approx 8:1)

3.3.3.1b (c) The attempt to improve the yield on ultrasound bath

As described in the previous chapter, the TentaGel resin could be only limited swollen in the aqueous medium and this is presumably the reason, why in the previous experiments all products were isolated in poor yields. When this resin was insufficient swollen, the surface of the polymer might still entangle with each other and a large amount of linear precursors loaded on the resin was not allowed to react. If the entangled polymer surface could be unscrewed by ultrasound, the chained linear precursor might be liberated and will participate in NCL cyclization. The linear sequence **22** was again allowed to be cyclized on the resin but this time the reaction vessel was placed in an ultrasound bath. The reaction vessel was kept in the ultrasound bath for eight hours and the warm water in the ultrasound bath, which was caused by the ultrasound effect, was

replaced by cold water each 20 min. The UV absorbance of the buffer mixture was monitored by spectrophotometer: under the effect of ultrasound, the UV absorbance rose erratically in the first two hours and after 8 hours the reaction concluded. Sadly the LC-MS analysis of the buffer mixture showed that the linear sequence **22** or the resin was completely destroyed by ultrasound and resulted in a large number of fragments, therefore, no cyclic product **22'** was isolated afterwards. The UV absorption of the buffer solution was not caused by the cyclic product **22'** but by these fragments, which contain tryptophan moiety.

3.3.3.1b (d) The attempt to improve the yield on the PEGA resin



Scheme 104. The failed Fmoc-SPPS on the PEGA resin

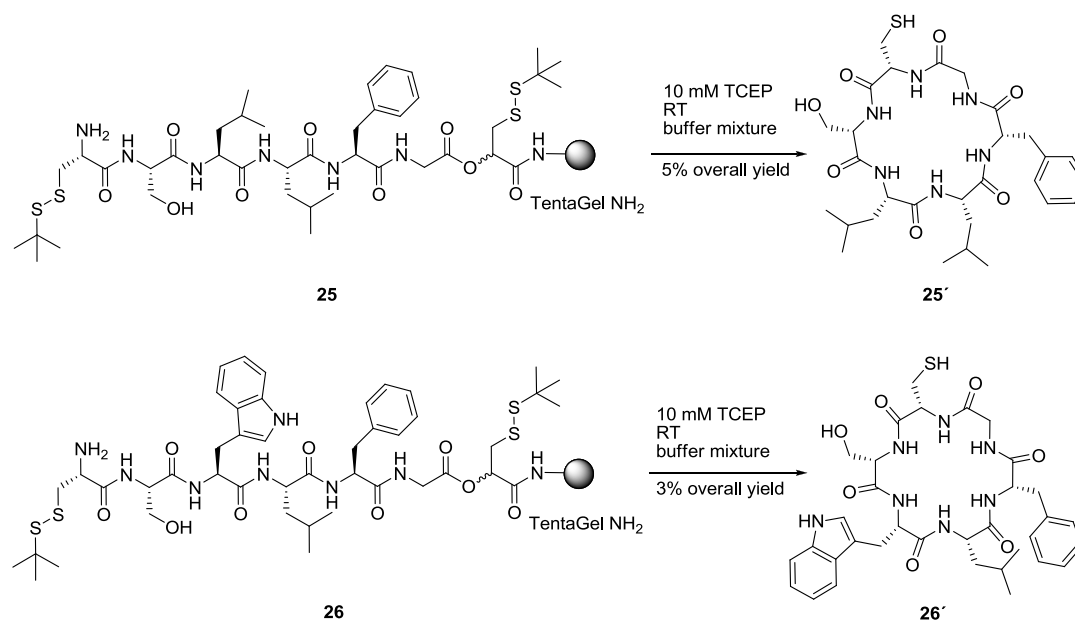
Since the NCL cyclization on the TentaGel NH_2 resin always results in the poor yield, the PEGA resin, which has excellent water swelling ability,^{[113][118]} was chosen as the solid phase for the on-resin NCL cyclization investigation. In this case study, the PEGA NH_2 resin was used to synthesize the sequence **22**. The PEGA NH_2 resin is basically the PEGA backbone polymer with the NH_2 handle, the latent thioester linker **12** was anchored onto the PEGA resin through a stable amide bond. The loading of the linker **12** onto the PEGA resin was as good as on the TentaGel NH_2 resin judged by the Kaiser test and the TBDMS group was then removed overnight by TBAF solution followed by the coupling of Fmoc-Gly-OH. The Fmoc release UV assay showed that in comparison with previous experiments the coupling of Fmoc-Gly-OH on the PEGA NH_2 resin achieved a comparable loading. Unfortunately the PEGA polymer was too fragile to resist the external mechanical force, when the coupling was carried out with slightest stirring, only after first two steps the resin beads were completely “grinded” thus became very muddy and jammed the filter of the syringe. Under this circumstance, assemble of the further amino acids through the batch-flow

through process was no more possible. This plan was thereafter abandoned and no further experiments on this basis were attempted.

3.3.3.1c On-resin NCL cyclization of sequence CAALG 24

Since none of these previous experiments had successfully improved the yield, no more efforts to improve the yield would be made, instead the further experiments focused on the investigation of the NCL cyclization of the different model sequences. So far the model sequences CSSLG **19**, CSSLF **20** and CSWLG **22** have been investigated and based on these initial studies the NCL cyclization was determined to be strongly affected by ligation partner and side chains. Among three sequences only the sequence CSSLG **19** could achieve a satisfactory NCL cyclization, otherwise the cyclization of both CSSLF **20** and CSWLG **22** led to the hydrolyzed product in different degrees. In the case of the sequence **20**, the additional benzyl residue at the ligation site disturbed the NCL cyclization and resulted in a 30% yield decline in contrast to the CSSLG **19**. In the case of the sequence CSWLG **22**, a serine in the middle of the sequence **19** was replaced by tryptophan and this modification also caused around 30% reduction of the isolated yield. According to these preliminary results, the outcome of the on-resin NCL cyclization might be forecasted like follows: the NCL cyclization of the slim linear peptides may progress faster and results in better yield than the bulky peptide sequences. In order to validate this prediction, the on-resin NCL cyclization of the sequence CAALG **24** was tested. Serines of the previous sequence CSSLG **19** were replaced by alanines and thus the resulted sequence **24** is more slim than **19**. Therefore, this new sequence was expected to achieve the same or even better yield than the sequence CSSLG **19** did.

The resin loaded with sequence CAALG **24** was allowed to be cyclized for 24 hours under the established conditions, but after the reaction, the isolated overall yield was only 5%.



Scheme 106. The on-resin cyclization of the **25** and **26**

The sequence **25**, **26** and **27** all carry the C-terminal glycine, which is ideal for the NCL cyclization according to the previous results, besides the six-membered sequence **25** and **26** theoretically might cause less ring strain during the ring closure thus they were ideal models for the on-resin NCL cyclization study.

However with an additional phenylalanine, the cyclization quality of the sequence CSSLFG **25** could not catch up with the CSSLG **19**, though 5% overall yield was still comparable with the sequence CSSLF **20**. The additional benzyl moiety slowed down the cyclization and allowed the formation of the hydrolyzed by-product (32% of the cyclic product, LC-MS, calculated through integration of the UV chromatogram, Figure 26). In the case of sequence CSWLFG **26**, with increasing number of the bulky side chain, the NCL cyclization was further obstructed, as a result more linear precursor was hydrolyzed (52% of the cyclic product, LC-MS calculated through integration of the UV chromatogram, Figure 21) and the overall yield (3%) has dropped by around 40% in comparison with CSSLFG **25**.

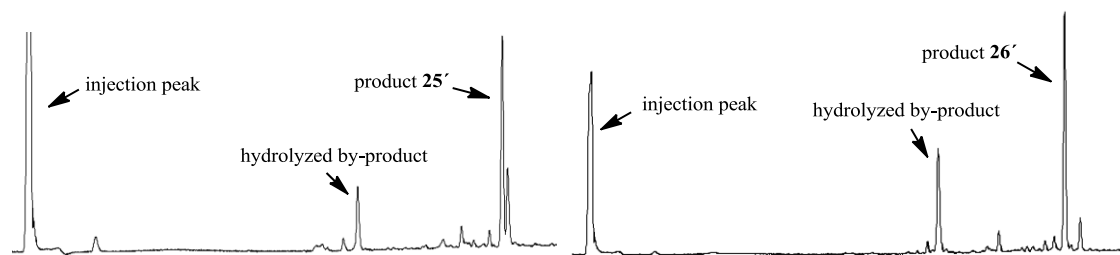
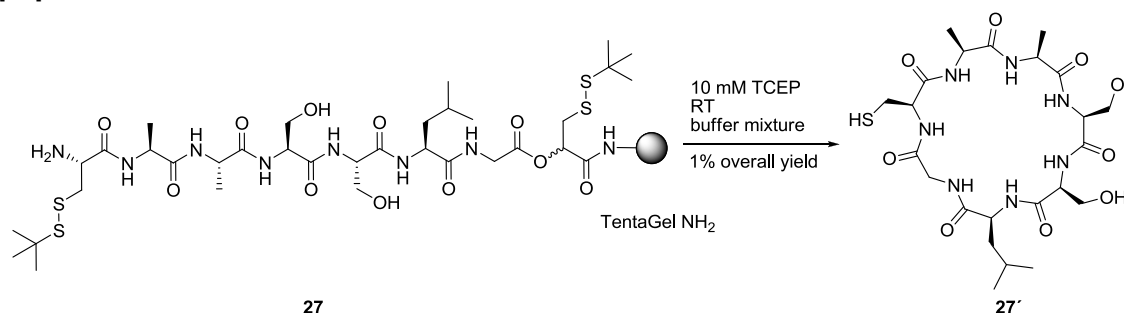


Figure 26. LC-MS analysis (UV: 190 – 600 nm) of on-resin NCL cyclization of sequence **25** and **26**

3.3.3.3 Investigation of the on-resin NCL cyclization of seven-membered peptide **27**

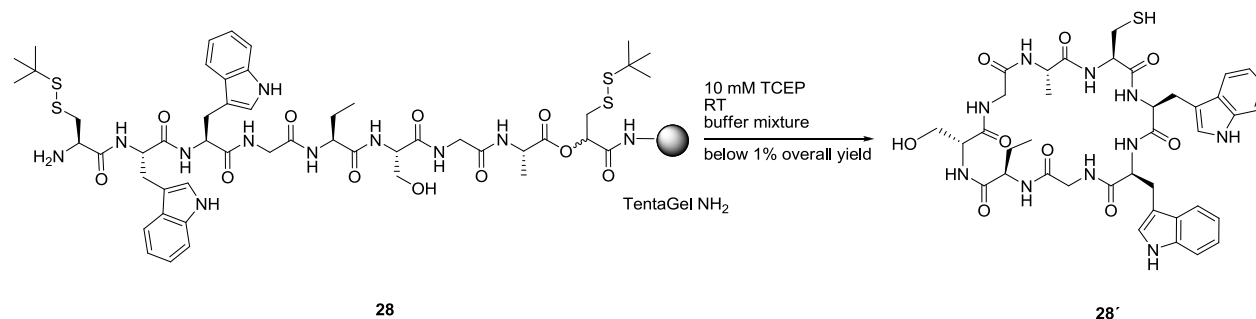


Scheme 107. The on-resin cyclization of CAASSLG **27**

The heptapeptide CAASSLG **27** carries no bulky side chains and it is predictably hydrophilic, so it was expected to achieve good result. However, the NCL cyclization of **27** achieved the worst yield (1%) so far. This poor yield might not be caused only by NCL cyclization itself but also by Fmoc-SPPS. In the previous experiment (section **3.3.2**) the ester bond, which links the main sequence and the linker **12**, was found not highly stable upon the piperidine treatment, the ester bond was partially hydrolyzed when each time piperidine was introduced, the synthesis of sequence CAASSLG **27** needed two additional coupling steps than the synthesis of pentapeptide **19**, **20** and **22**, thus the ester bond was longer exposed to piperidine and consequentially more ester bond was hydrolyzed. This led to a larger loss of the linear precursor prior to the cyclization and thus the final yield was worse. Besides with increasing size of the peptide sequence, the head-to-tail NCL cyclization became more difficult to be achieved than previous experiments.

3.3.3.4 Investigation of the on-resin NCL cyclization of eight-membered peptide **28**

At the end of this work, the feasibility of NCL cyclization of the octapeptide **28** was examined.



Scheme 108. The on-resin cyclization of CWWG(Abu)SGA **28**

The octapeptide CWWG(Abu)SGA **28** was an argyrin B linear precursor analogous, which carries some features of the argyrin B linear precursor. After 24 hours the cyclic product **28'** was clearly identified by LC-MS (Figure 27), but after HPLC purification no considerable amount of the cyclic product **28'** was obtained. The overall yield was below 1%, the cyclic product **28'** was only obtainable as the trace. The poor result might be explained by the same reasons, which caused the poor yield of the cyclic CAASSLG **27'**.

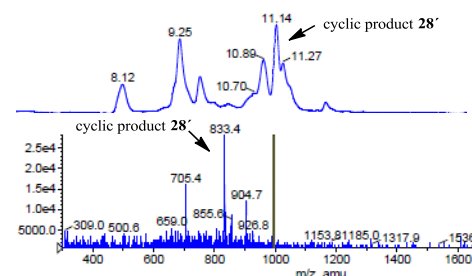


Figure 27. LC-MS identification of cyclic product **28'**

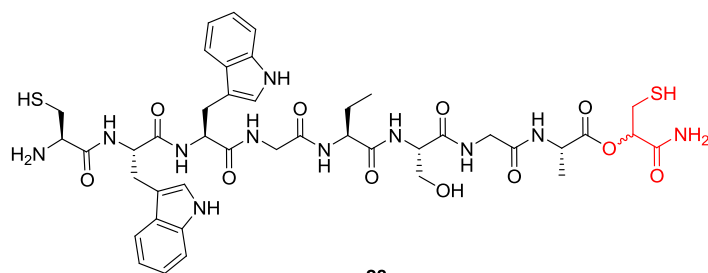
In order to verify this explanation, the linear precursor **28** was synthesized on the TentaGel S RAM resin and, after cleavage, the desired linear sequence CWWG(Abu)SGA **28** was identified only as a minor product by LC-MS (Table 26, entry 44). This means that after eight coupling steps, a large number of the ester bonds were hydrolyzed and thus only few linear precursor CWWG(Abu)SGA **28** was still attached to the resin. For comparison the backbone sequence CWWG(Abu)SGA without the latent thioester linker **29** (Figure 23) was generated through the standard Fmoc-SPPS on the TentaGel S RAM resin. Surprisingly

after the cleavage, the backbone sequence CWWG(Abu)SGA without the latent thioester linker **29** was identified as the main product in LC-MS analysis (Table 26, entry 45).

Table 26.

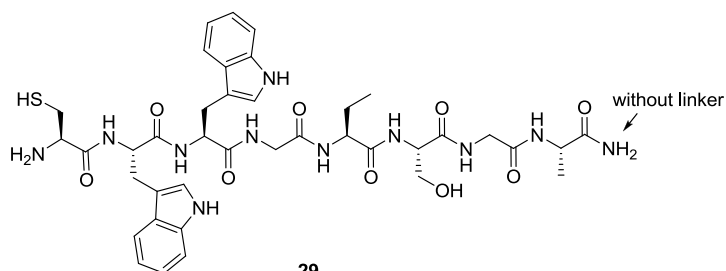
entry	compound	result after cleavage
44	28	minor product
45	29	main product

This comparison reflected the fact that the backbone model sequences were fully compatible with the Fmoc-SPPS, however with the additional latent thioester linker the immobilized sequence did not well survive the Fmoc-SPPS. Nonetheless the NCL cyclization of the sequence CWWG(Abu)SGA **28** was proven feasible, except the very low isolated yield.



28

linear sequence obtained from Fmoc SPP minor product in LC-MS



29

backbone sequence without latent thioester linker obtained from Fmoc-SPPS, main product in LC-MS

Figure 28. Sequence CWWG(Abu)SGA with linker **28** and the sequence CWWG(Abu)SGA without linker **29**

4. Summary and outlook

In this work, the on-resin NCL cyclization of a few model sequences has been investigated in every respect. By using the latent thioester linker strategy the linear precursor was generated through the standard Fmoc-SPPS protocol and the NCL cyclization was directly carried out on the resin.

In the beginning, the designed latent thioester linker **4** was synthesized straightforward, but the initial idea of the formation of the depsipeptide building block **6** in solution phase from the latent thioester linker **4** and Fmoc-Ile-OH failed. Alternatively the latent thioester linker **4** was directly immobilized to the resin and the first amino acid was linked onto it *via* an ester bond. The preliminary test showed that the coupling of the latent thioester linker **4** onto the resin was not successful by charging equimolar amount of the linker **4**, however utilization of large amount of the linker **4** might potentially cause the esterification between themselves. So the free hydroxyl group of the linker **4** was then protected by TBDMS silyl ether to construct the new latent thioester linker **12**. The coupling of the linker **12** was proven efficient, when 3.5 equivalent amount of the linker **12** was charged.

The latent thioester linker **12** can be readily synthesized from bromopyruvate **1** in four steps in 32% overall yield. The synthetic route could be up-scaled trouble-free, but the linker **12** was highly sensitive. It is vulnerable under almost all conditions, so it could not be synthesized in a large amount and stored, but rather be freshly generated from its stable precursor prior to the coupling. After the latent thioester linker **12** was successfully synthesized and coupled onto the resin, the model sequence **14** and **16** was generated on the resin through the Fmoc-SPPS and cleaved. The NCL cyclization was firstly examined in solution phase to determine the optimal conditions, which could be applied directly or with slight modification for the on-resin NCL cyclization. All attempts with **14** and **16** were failed, despite all relevant factors (temperature, pH, promoter and buffer mixture) have been changed, modified and tested. Due to the bulky geometry of the C-terminal isoleucine at the junction point, the NCL cyclization was hardly applicable on these model sequences. This result was also found to be in consistence with Dawson's report.^[75]

Nevertheless when two simpler model sequences **19** and **20** were tested in the solution and at low temperature (0 – 5°C), the NCL cyclization was found well applicable. By testing these two sequences in solution phase the initial ideal conditions were determined.

Based on these established conditions, the on-resin NCL cyclization of these model sequences was then performed. The sequences immobilized on the resin were less reactive, therefore the NCL cyclization could only take place at RT in contrast to the cyclization in solution phase. The ligation rate on the resin was slower than in the solution, so the hydrolysis could not be suppressed entirely in most of the cases. Eight model sequences (CSSLG **19**, CSSLF **20**, CSWLG **24**, CAALG **22**, CSLLFG **25**, CSWLFG **26**, CAASSLG **27** and CWWG(Abu)SGA) **28** were investigated. During the experiments the ester bond linkage was found to be unstable during the Fmoc-SPPS, after each coupling step, a considerable amount of linear sequence went lost. The longer the sequence is, the bigger the loss will be. The general poor yield reflects this problem. Aside from the substance loss, which was caused by Fmoc-SPPS, the on-resin NCL cyclization itself was affected by various factors (Table 27).

Table 27. Importance of the different factors

factor	importance
ligation partner	decisive
side-chain	essential
sequence size	essential
temperature	semi-essential
reaction duration	semi-essential
buffer mixture	non-essential
pH value	non-essential
resin	not confirmed

The decisive factor, which dominates the ligation, is the geometry of the ligation partner. The more bulky the ligation partner is, the slower the ligation progresses. Second to the ligation partner the side-chain geometry as well as the sequence size also significantly affected NCL cyclization. The bulky side chains could block the head-to-tail interaction and slow down the ligation rate. The cyclization of the large sequences met stronger ring-strain resistance than the shorter sequence. Temperature is an important factor, it should be kept at ambient temperature at all times, below or above RT only leads the reaction to the wrong way. The preliminary experiment confirmed that the complete on-resin cyclization required up to 24 hours, prolonged reaction time is unnecessary. The NCL ligation could be performed in a relatively wide range of pH values (6.5 – 7.5), some slight alternation didn't change the outcome of the NCL cyclization and the composition of the buffer mixture only played a subordinate roll throughout the entire NCL cyclization study.

The model studies showed that the rapid establishment of a library of the cyclic peptides by using this new on-resin strategy was possible but with some limitations. The isolated overall yield of all these model sequences were generally poor, but as the prove-of-concept experiments, further optimization are definitively required.

So far, no promoter (MPAA, MESNa) has been used in large excess for the on-resin studies in order to avoid complexity at the HPLC purification, but maybe equimolar amount or slight excess amount of promoter already has the ability to accelerate the NCL without disturbing the HPLC purification. This should be tested in the further investigation. The denaturant 6 M guanidium chloride was generally not used because of its side effect, which reduces the ligation rate, but in the case of cyclization of the longer sequence (heptamer, octamer), which might begin to construct the secondary structure and hinder the cyclization, the influence of additional denaturant on the cyclization should be tested. Moreover the on-resin study was only performed on the TentaGel resin, which is a PS-POE polymer and has moderate swelling properties in the aqueous medium. The investigation of the sequence CSWLG **22** has showed that only around 12% of all immobilized linear precursors were cyclized from the TentaGel resin.

The PEGA resin with excellent swelling properties was also test, but the synthesis of the linear precursor on the PEGA resin was unsuccessful because of high fragility of the PEGA resin, if the PEGA resin could be stirred by nitrogen vortex instead of the magnetic stirrer bar, the practical problems may be overcome and the on-resin NCL cyclization on the PEGA resin might be examined. The CLEAR resin was reported to have an excellent performance for the on-resin NCL, so this resin should be tested as well.

Experimental section

Part I. Development of synthetic strategies for libraries of heterocyclic and bicyclic inhibitors of Cdc25A

1. General details

Reactions and materials

All reactions were carried out at RT (unless otherwise specified) without inert gas atmosphere

All solvent and reagents used were obtained from Sigma-Aldrich, Acros, Fluka, TCI (Tokyo Chemical industry Co.,Ltd), or J.T Baker and were used as received without further purification.

Thin layer and flash chromatography

Analytic TLC was run on aluminium sheets coated with silica gel 60 F₂₅₄ (Merck KGaA). The analysis of the TLC plate was conducted under ultraviolet lamp ($\lambda = 254 \text{ nm}$) and consecutively the TLC plate was dipped into color reagents (potassium permanganate or Cer(IV) reagent) to visualize the spots.

The flash chromatography was carried out under slight pressure on the flash chromatography column loaded with silica gel 60 (Merck, 40–60 μm , 60 \AA).

Nuclear magnetic resonance and mass spectrometry

Proton nuclear magnetic resonances (^1H NMR) and carbon nuclear magnetic resonances (^{13}C NMR) were recorded on a 300 Hz Bruker DPX300 at 298 K, and the chemical shifts are reported in parts per million (δ) from an internal standard of residual chloroform (7.26 ppm, 77.2 ppm), or methanol (3.31 ppm, 4.78 ppm, 49.0 ppm).

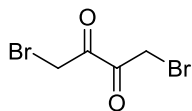
Proton NMR signals multiplicity is reported as follows: s = singlet, d = doublet, t = triplet, q = quartett, m = multiplet, b = broad. Carbon NMR signals multiplicity is reported as: s = singlet, d = doublet, t = triplet, q = quartett.

High-resolution mass spectra (HRMS) were measured on a Bruker maXis HD by using the electron spray ionization (ESI) mode, from the department of the chemical biology, Helmholtz Centre for Infection Research, Braunschweig, Germany.

Most of the synthesis has only been performed once thus all yields reported are not optimized.

2. Synthesis of the lead structure 13 and its amide derivatives 20 and 21 through Hantzsch method

2.1. 1,4-dibromobutane-2,3-dione (10)



2.58 g 2,3-Butanedione (0.03 mmol) was dissolved in 5.2 mL chloroform in a round flask, 3.2 mL bromine (10 g, 0.06 mmol) was dissolved in 5.2 mL chloroform and added dropwise at RT over 2.5 hours to the round flask. After the introduction, the reaction was heated at 45 °C until no more gas emerged. Then the mixture was cooled to the RT and the round flask was cooled in the refrigerator overnight. The precipitation was filtered and washed 3 times with chloroform (3 × 10 mL). Finally, the raw product was subject to the recrystallization from toluene to yield a pale yellow solid. (776 mg, 11%)

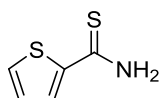
$R_f = 0.7$ (PE:EtOAc = 8 :1)

$^1\text{H NMR}$ (300 MHz, CDCl_3): δ_{H} 4.32 (s, 4H, CH_2)

$^{13}\text{C NMR}$ (75 MHz, CDCl_3): δ_{C} 188.0 (q, 2C, CO), 28.4 (d, 2C, CH_2).

The NMR data is in consistence with that reported in literature.^[46]

2.2 Thiophene-2-carbothioamide (6)



500 mg thiophene (5.94 mmol) was charged into a brown round flask and dissolved carefully at 0 °C with 9 mL methanesulfonic acid. Then this solution was slowly added into a second round flask, which was already loaded with 662 mg potassium thiocyanate (6.83 mmol) at 0 °C. After the addition the mixture was stirred at RT for 4.5 hours. After the starting material was completely consumed (TLC, DCM:MeOH = 20:1), the mixture was poured in ice water and the precipitation was then filtered. The precipitation was washed with ice water a few times afterwards and the aqueous layer was then extracted three times with

DCM (3 × 20 mL), then the organic layer was dried over sodium sulfate and the DCM was removed through rotation evaporator and resulted in a brown crystal. This brown crystal was then combined with other precipitation and purified through the flash chromatography (DCM:MeOH = 40:1) and yield a pale brown crystal. (409 mg, 48%)

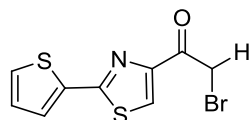
$R_f = 0.57$ (DCM:MeOH = 20 :1).

$^1\text{H NMR}$ (300 MHz, CDCl_3): δ_{H} 7.52 (d, $J = 3.83$ Hz, 1H, thiophene), 7.49 (d, $J = 3.83$ Hz, 1H, thiophene), 7.07 (dd, $J = 4.23, 5.24$, 1H, thiophene).

$^{13}\text{C NMR}$ (75 MHz, CDCl_3): δ_{C} 192.1 (q, SC), 144.7 (q, thiophene), 133.9 (t, thiophene), 128.3 (t, thiophene), 126.9 (t, thiophene).

The $^{13}\text{C NMR}$ was identical with that reported in literature.^[44]

2.3. 2-bromo-1-(2-(thiophen-2-yl)thiazol-4-yl)ethanone (2)



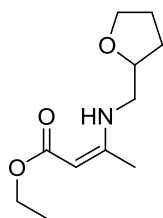
100 mg thiophene-2-carbothioamide (**2**) (0.7 mmol) was dissolved in a flask with 2.2 mL abs. ethanol. 510 mg 1,4-dibromobutane-2,3-dione (**10**) was dissolved in 10 mL abs. ethanol and slowly added to the flask charged with the thiophene-2-carbothioamide (**2**). The mixture was then allowed to be stirred at first for 1 hour at RT and followed by 3 hours stir under reflux. The reaction was monitored by the TLC (DCM :PE = 3 :1) and after the starting materials were completely gone the solvent was simply removed by evaporation. The solid was then added to 30 mL saturated sodium hydrogen carbonate solution and extracted 3 times with chloroform (3 × 20 mL). The organic layer was dried over sodium sulfate and concentrated. The raw product was then subject to the flash chromatography (PE:EtOAc = 20 :1) to yield a pale white crystal. (99 mg, 49%)

$R_f = 0.16$ (PE:EtOAc = 20 :1).

¹H NMR (300 MHz, CDCl₃): δ_H 8.17 (s, 1H, thiazole), 7.56 (d, *J* = 3.7 Hz, 1H, thiophene), 7.46 (d, *J* = 4.78 Hz, 1H, thiophene), 7.10 (dd, *J* = 3.78, 5.43 Hz, 1H, thiophene), 4.72 (s, 2H, CH₂).

¹³C NMR (75 MHz, CDCl₃): δ_C 185.9 (q, CO), 162.2 (q, thiazole), 152.3 (q, thiazole), 136.1 (q, thiophene), 129.0 (t, thiophene), 128.1 (t, thiophene), 127.8 (t, thiophene), 125.9 (t, thiazole), 33.7 (d, CH₂).

2.4 (Z)-ethyl 3-(((tetrahydrofuran-2-yl)methyl)amino)but-2-enoate (12)



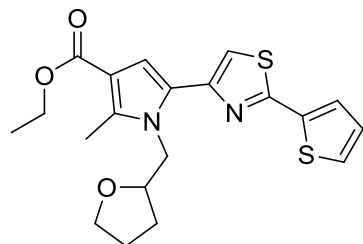
1 g ethyl 3-oxobutanoate (**11**) (3.8 mmol) and 931.5 mg (tetrahydrofuran-2-yl)methanamine (**4**) (4.6 mmol) were mixed in a round flask and was allowed to react for 3 hours at RT and was monitored by the TLC (PE:EE = 4 :1). After the reaction, the raw product was purified by the flash chromatography (PE:EtOAc = 8 :1) to yield 667 mg clear oily substance (82%)

R_f = 0.44 (PE:EtOAc = 8:1).

¹H NMR (300 MHz, CDCl₃): δ_H 4.44 (s, 1H, enamine), 4.08 (q, *J* = 7.49 Hz, 2H, CH₂, COOEt), 3.98 (m, 1H, THF), 3.88 (q, *J* = 7.49 Hz, 1H, THF), 3.76 (q, *J* = 7.93 Hz, 1H, CH₂), 3.38 -3.20 (m, 2H, CH₂ and THF), 2.05 – 1.98 (m, 2H, THF), 1.92 (s, 3H, CH₃, COOEt), 1.94 -1.85 (m, 1H, THF), 1.67 – 1.57 (m, 1H, THF).

¹³C NMR (75 MHz, CDCl₃): δ_C 170.5 (q, CO), 161.7 (q, alkene), 82.6 (t, alkene), 78.0 (t, THF), 68.4 (d, THF), 58.2 (d, CH₂, OEt), 46.9 (d, CH₂), 28.8 (d, THF), 25.8 (d, THF), 19.5 (s, CH₃, Me), 14.6 (s, CH₃, OEt).

2.5 Ethyl 2-methyl-1-((tetrahydrofuran-2-yl)methyl)-5-(2-(thiophen-2-yl)thiazol-4-yl)-1H-pyrrole-3-carboxylate (13)



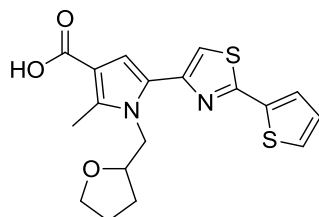
46.4 mg 2-bromo-1-(2-(thiophen-2-yl)thiazol-4-yl)ethanone (**2**) (0.16 mmol) was dissolved with 0.75 mL dimethoxyethane (DME) in a round flask. 58.4 mg (Z)-ethyl 3-(((tetrahydrofuran-2-yl)methyl)amino)but-2-enoate (**12**) (0.26 mmol) was dissolved in 0.75 mL DME and slowly added to the round flask. The mixture was allowed to react overnight under reflux (85 °C). After 12 hours, the 2-bromo-1-(2-(thiophen-2-yl)thiazol-4-yl)ethanone (**2**) was completely consumed as judged by the TLC (PE:EtOAc = 8:1) and the mixture was poured into 30 mL saturated sodium hydrogen carbonate solution. The aqueous layer was then extracted 3 times with ethyl acetate (3 × 15 mL) and the combined organic layer was washed 3 times with saturated brine solution (3 × 30 mL) and dried over sodium sulfate. Finally, the solvent was removed and the raw product was then subjected to the flash chromatography (PE:EE = 15 :1) to yield a white crystal. (26.5 mg, 43%)

$R_f = 0.25$ (PE:EtOAc = 15:1).

¹H NMR (300 MHz, CDCl₃): δ_H 7.5 (d, $J = 3.2$ Hz, thiophene 1H), 7.37 (d, $J = 5.42$ Hz, thiophene, 1H), 7.2 (s, thiazole, 1H), 7.07 (t, thiophene 1H), 6.85 (s, pyrrole, 1H), 4.63 (dd, $J = 2.46$ Hz, 13.3 Hz, 1H, THF), 4.27 (q, $J = 7.20$ Hz, 2H, CH₂, OEt), 4.32 – 4.21 (m, 2H, CH₂), 3.81 – 3.62 (m, THF 2H), 2.65 (s, CH₃ 3H), 2.02 – 1.92 (m, THF, 1H), 1.86 – 1.75 (m, THF, 2H), 1.59 – 1.48 (m, THF, 1H), 1.34 (t, $J = 7.20$ Hz, 3H, CH₃, OEt).

¹³C NMR (75 MHz, CDCl₃): δ_C 165.4 (q, CO), 160.9 (q, thiazole), 149.0 (q, thiazole), 138.6 (q, thiophene), 137.5 (q, pyrrole), 128.9 (t, thiophene), 126.6 (t, thiophene), 126.4 (t, thiophene), 126.3 (q, pyrrole), 113.2 (t, thiazole), 112.1 (q, pyrrole), 111.1 (t, pyrrole), 79.4 (t, THF), 68.4 (d, THF), 59.7 (d, CH₂, OEt), 49.1 (d, CH₂), 29.4 (d, THF), 26.0 (d, THF), 15.0 (s, CH₃, OEt), 12.2 (s, CH₃).

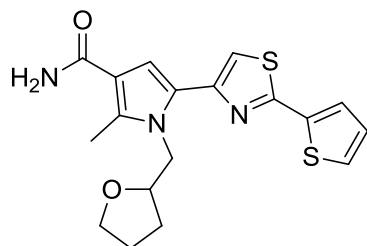
2.6 2-methyl-1-((tetrahydrofuran-2-yl)methyl)-5-(2-(thiophen-2-yl)thiazol-4-yl)-1H-pyrrole-3-carboxylic acid (**18**)



95.9 mg ethyl 2-methyl-1-((tetrahydrofuran-2-yl)methyl)-5-(2-(thiophen-2-yl)thiazol-4-yl)-1H-pyrrole-3-carboxylate (**13**) (0.24 mmol) was dissolved in 0.7 mL ethanol and 776 μ L 10% KOH ethanol solution (1.2 mmol) was introduced to this solution. The mixture was allowed to react under reflux overnight. After 12 hours, the starting material was gone as judged by the TLC (DCM:EtOAc = 20:1 with 0.2% acetic acid), then the mixture was neutralized with saturated ammonium chloride solution. The aqueous layer was then extracted 3 times with chloroform (3 \times 10 mL) and the combined organic layer was dried over sodium sulfate. The solvent was subsequently removed and the raw product was then deployed without purification for the next conversion.

R_f = 0.39 (DCM:EtOAc = 20:1 with 0.2% acetic acid).

2.7 2-methyl-1-((tetrahydrofuran-2-yl)methyl)-5-(2-(thiophen-2-yl)thiazol-4-yl)-1H-pyrrole-3-carboxamide (**19**)



44.1 mg raw starting material 2-methyl-1-((tetrahydrofuran-2-yl)methyl)-5-(2-(thiophen-2-yl)thiazol-4-yl)-1H-pyrrole-3-carboxylic acid (**18**) (0.12 mmol), 90.3 mg EDC·HCl (0.48 mmol) and 28.8 mg DMAP (0.24 mmol) were loaded in a round flask and dissolved under inert gas in 1.6 mL anhydrous DCM. 700 μ L NH_3 solution 0.5 M in dioxane (1.4 mmol) was then introduced to the flask and the mixture was stirred at RT for 6 hours. After the starting material was completely consumed (TLC, (DCM:EtOAc = 20 :1 with 0.1% acetic acid) the mixture was

diluted with 3 mL DCM. The organic layer was washed by the 1 M HCl solution twice (2 × 5 mL) and followed by 10 mL saturated sodium hydrogen carbonate solution. Afterwards, the organic layer was dried over sodium sulfate and concentrated in *vacuo*. The raw product was purified by the flash chromatography (DCM:EtOAc = 15:1) to yield a white crystal. (11.5 mg, 26% over two steps)

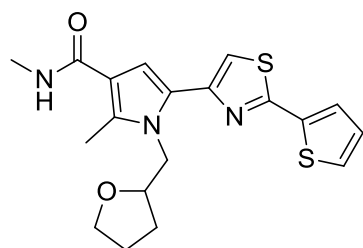
$R_f = 0.42$ (DCM:EtOAc = 15 :1).

$^1\text{H NMR}$ (300 MHz, CDCl_3): δ_{H} 7.50 (d, $J = 3.55$ Hz, 1H, thiophene), 7.38 (d, $J = 4.98$ Hz, 1H, thiophene), 7.23 (s, 1H, thiazole), 7.08 (t, 1H, thiophene), 6.90 (s, 1H, pyrrole), 4.64 (d, $J = 11.37$ Hz, 2.46 Hz, 1H, THF), 4.33 – 4.20 (m, 2H, CH_2), 3.80 -3.68 (m, 2H, THF), 2.69 (s, 3H, Me), 2.03 – 1.95 (m, 1H, THF), 1.89 – 1.75 (m, 2H, THF), 1.61 – 1.47 (m, 1H, THF).

$^{13}\text{C NMR}$ (75 MHz, CDCl_3): δ_{C} 161.2 (q, CO), 161.0 (q, thiazole), 148.6 (q, thiazole), 141.4 (q, thiophene), 137.5 (q, pyrrole), 128.0 (t, thiophene), 127.7 (t, thiophene) 126.8 (q, pyrrole), 126.5 (t, thiophene), 113.9 (t, thiazole), 111.7 (t, pyrrole), 111.3 (q, pyrrole), 78.9 (t, THF), 68.0 (d, THF), 49.0 (d, CH_2), 29.1 (d, THF), 25.6 (d, THF), 12.1 (s, Me).

HRMS m/z calcd for $\text{C}_{18}\text{H}_{20}\text{N}_3\text{O}_2\text{S}_2$ $[\text{M} + \text{H}]^+$, 374.0991; found, 374.0988.

2.8 *N*,2-dimethyl-1-((tetrahydrofuran-2-yl)methyl)-5-(2-(thiophen-2-yl)thiazol-4-yl)-1H-pyrrole-3-carboxamide (20)



53.3 mg raw starting material 2-methyl-1-((tetrahydrofuran-2-yl)methyl)-5-(2-(thiophen-2-yl)thiazol-4-yl)-1H-pyrrole-3-carboxylic acid (**18**) (0.14 mmol), 109.1 mg EDC·HCl (0.57 mmol) and 35.5 mg DMAP (0.28 mmol) were loaded in a round flask and dissolved under inert gas in 2 mL anhydrous DCM. 30.5 mg methylamine hydrogenchloride (0.21 mmol) was then added to the flask and the mixture was allowed to be stirred at RT and monitored by the TLC (DCM:EtOAc = 8 :1 with 0.1% acetic acid). After 24 hours the reaction was completed and the

mixture was diluted with 3 mL DCM. Then the organic layer was washed twice with 1 M HCl solution (2 × 5 mL) and followed by 10 mL saturated sodium hydrogen carbonate solution. The combined organic layer was dried over sodium sulfate and the solvent was removed. The raw product was then subject to the flash chromatography (DCM:MeOH = 30 :1) to yield a white crystal. (14.5 mg, 26.3% over two steps)

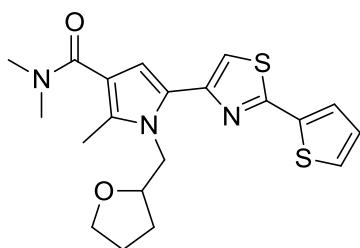
$R_f = 0.31$ (DCM:MeOH = 30:1).

$^1\text{H NMR}$ (300 MHz, CDCl_3): δ_{H} 7.50 (d, $J = 3.83$ Hz, 1H, thiophene), 7.38 (d, $J = 5.03$ Hz, 1H, thiophene), 7.14 (s, 1H, thiazole), 7.07 (dd, $J = 3.87, 5.3$, 1H, thiophene), 6.52 (s, 1H, pyrrole), 5.76 (b, 1H, NH), 4.54 (dd, $J = 3.23, 13.99$ Hz, 1H, CH, THF), 4.30 – 4.14 (m, 2H, CH_2), 3.77 – 3.59 (m, 2H, THF), 2.92 (d, $J = 4.78$, 3H, NHCH_3), 2.65 (s, 3H, Me), 2.03 – 1.89 (m, 1H, THF), 1.87 – 1.74 (m, 2H, THF), 1.59 – 1.45 (m, 1H, THF).

$^{13}\text{C NMR}$ (75 MHz, CDCl_3): δ_{C} 166.3 (q, CO), 160.7 (q, thiazole), 148.8 (q, thiazole), 137.3 (t, thiophene), 135.5 (t, thiophene), 126.2 (t, thiophene), 125.9 (q, pyrrole), 114.9 (q, pyrrole), 112.7 (t, thiazole), 107.4 (t, pyrrole), 78.7 (t, THF), 67.7 (d, THF), 48.3 (d, CH_2), 28.8 (d, THF), 25.9 (s, NHCH_3), 25.3 (d, THF), 11.4 (s, Me).

HRMS m/z calcd for $\text{C}_{19}\text{H}_{22}\text{N}_3\text{O}_2\text{S}_2$ [$\text{M} + \text{H}$] $^+$, 388.1148; found, 388.1149.

2.9 *N,N*,2-trimethyl-1-((tetrahydrofuran-2-yl)methyl)-5-(2-(thiophen-2-yl)thiazol-4-yl)-1H-pyrrole-3-carboxamide (21)



This compound was prepared by using the same procedure of synthesis of the compound 20.

Isolated substance: 12 mg, 21% over two steps.

$R_f = 0.35$ (DCM:MeOH = 20:1).

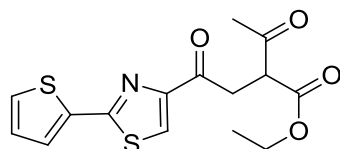
$^1\text{H NMR}$ (300 MHz, CDCl_3): δ_{H} 7.50 (d, $J = 3.77$ Hz, 1H, thiophene), 7.37 (d, $J = 5.09$ Hz, 1H, thiophene), 7.13 (s, 1H, thiazole), 7.07 (dd, $J = 3.77, 5.92$ Hz, 1H, thiophene), 6.41 (s, 1H, pyrrole), 4.62 – 4.48 (m, 1H, CH, THF), 4.29 – 4.15 (m, 2H, CH_2), 3.80 – 3.61 (m, 2H, THF), 3.07 (s, 6H, CH_3 , Me_2NH), 2.41 (s, 3h, Me), 2.05 – 1.90 (m, 1H, THF), 1.87 – 1.72 (m, 2H, THF), 1.59 - 1.45 (m, 1H, THF).

$^{13}\text{C NMR}$ (75 MHz, CDCl_3): δ_{C} 168.8 (q, CO), 16.8 (q, thiazole), 149.3 (q, thiazole), 137.6 (q, thiophen), 133.2 (q, pyrrole), 127.9 (t, thiophene), 127.5 (t, thiophene), 126.3 (t, thiophene), 125.7 (q, pyrrole), 115.8 (q, pyrrole), 112.7 (t, thiazole), 109.3 (t, pyrrole), 79.2 (t, THF), 67.9 (d, THF), 48.7 (d, CH_2), 29.1 (d, THF), 25.5 (d, THF), 11.7 (s, Me).

HRMS m/z calcd for $\text{C}_{20}\text{H}_{24}\text{N}_3\text{O}_2\text{S}_2$ [$\text{M} + \text{H}$] $^+$, 402.1304; found, 398.1308.

3 Syntheses of N-substituted pyrrole derivatives through the Paar-Knorr pyrrole synthesis route

3.1 Ethyl 2-acetyl-4-oxo-4-(2-(thiophen-2-yl)thiazol-4-yl)butanoate (14)



22.5 mg sodium hydrid (60% dispersed in mineral oil) (0.56 mmolL) was washed twice under inert gas by pentane and dried in *vacuo*. Dried sodium hydrid was then dispersed in 0.7 mL absolute THF. 90 μL ethyl 3-oxobutanoate (**11**) (0.47 mmolL) was introduced to the sodium hydrid suspension at 0 °C and after 5 min., 150 mg 2-bromo-1-(2-(thiophen-2-yl)thiazol-4-yl)ethanone (**2**) (0.52 mmolL in 1 mL absolute THF) was added to this mixture. The mixture was then allowed to react at 0 °C for 10 min. and the reaction concluded as judged by the TLC (DCM:PE = 3:1). After the reaction, the mixture was poured to the phosphate buffer solution (pH = 7.4) and the aqueous layer was extracted 3 times with DCM (3 \times 5 mL). Then the combined organic layer was wash twice with saturated brine solution (2 \times 10 mL) and dried over sodium sulfate. The solvent was then removed and the raw product was then purified by the flash chromatography (DCM \rightarrow DCM:EtOAc = 20 :1) to yield a white crystal. (66.8 mg, 42%)

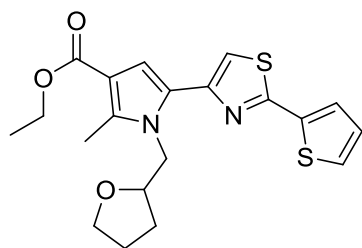
$R_f = 0.19$ (DCM).

$^1\text{H NMR}$ (300 MHz, CDCl_3): δ_{H} 8.03 (s, 1H, thiazole), 8.03 (s, 1H, thiazole), 7.55 (d, $J = 3.42$ Hz, 1H, thiophene), 7.44 (d, $J = 4.79$, 1H, thiophene), 7.09 (d, $J = 5.48$ Hz, 1H, thiophene), 4.22 (q, $J = 7.24$ Hz, 2H, CH_2 , COOEt), 4.20 – 4.14, (m, 1H, CH), 3.75 (dq, $J = 50.44, 8.24$ Hz, 2H, CH_2), 2.41 (s, 3H, Me), 1.29 (t, $J = 7.49$ Hz, 3H, CH_3 , COOEt).

$^{13}\text{C NMR}$ (75 MHz, CDCl_3): δ_{C} 202.3 (q, COMe), 192.1 (q, CO), 169.0 (q, CO, COOEt), 162.0 (q, thiazole), 154.2 (q, thiazole), 136.4 (q, thiophene), 128.7 (t, thiophene), 128.0 (t, thiophene), 127.6 (t, thiophene), 124.6 (t, thiazole), 61.7 (d, CH_2 , OEt), 53.9 (t, CH), 39.0 (d, CH_2), 30.0 (s, CH_3 , Me), 14.1 (s, CH_3 , Oet).

General procedure of generation of N-substituted pyrrole derivatives

3.2 Ethyl 2-methyl-1-((tetrahydrofuran-2-yl)methyl)-5-(2-(thiophen-2-yl)thiazol-4-yl)-1H-pyrrole-3-carboxylate (**13**)

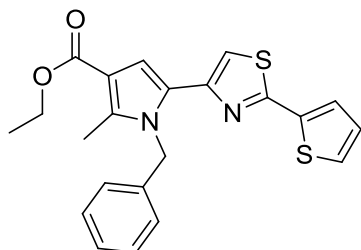


29.6 mg ethyl 2-acetyl-4-oxo-4-(2-(thiophen-2-yl)thiazol-4-yl)butanoate (**14**) (0.088 mmol) was dissolved in 0.8 mL absolute ethanol. 9 μL (tetrahydrofuran-2-yl)methanamine (**4**) (0.088 mmol) was added to this solution and followed by 1 drop of acetic acid. The mixture was then stirred under reflux for 2 hours and monitored by the TLC (DCM:EEtOAc = 20:1). After the starting material was completely gone, the mixture was diluted with 5 mL ethyl acetate, and the organic layer was sequentially washed 10 mL with saturated sodium hydrogen carbonate solution and 10 mL water. Afterwards, the organic layer was dried over sodium sulfate and concentrated. The raw product was then subjected to the flash chromatography (DCM:EtOAc = 20 :1) to yield a white crystal. (13.7 mg, 38.9%)

All analytic data of **13** made from Paar-Knorr method are identical to **13**, which was made from previous method.

The compounds **15**, **16**, **51** – **58** were prepared by following the same procedure of synthesis of the compound **13**.

3.3 Ethyl 1-benzyl-2-methyl-5-(2-(thiophen-2-yl)thiazol-4-yl)-1H-pyrrole-3-carboxylate (**15**)



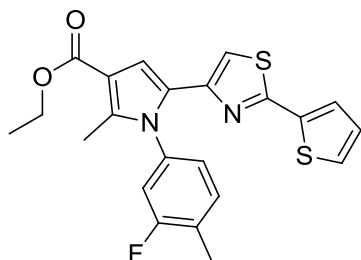
Isolated yield 54%

R_f = 0.45 (DCM)

$^1\text{H NMR}$ (300 MHz, CDCl_3): δ_{H} 7.43 (d, J = 4.05 Hz, 1H, thiophene), 7.33 (d, J = 5.39 Hz, 1H, thiophene), 7.29 – 7.18 (m, 3H, H_{Ar}), 7.09 (s, 1H, thiazole), 7.03 (dd, J = 4.05, 5.06 Hz, 1H, thiophene), 7.00 – 6.95 (m, 2H, H_{Ar}), 6.94 (s, 1H, pyrrole), 5.59 (s, 2H, CH_2), 4.30 (q, J = 6.38 Hz, 2H, CH_2 , OEt), 2.52 (s, 3H, Me), 1.37 (t, J = 8.10 Hz, 3H, CH_3 , OEt).

$^{13}\text{C NMR}$ (75 MHz, CDCl_3): δ_{C} 165.7 (q, CO), 161.3 (q, thiazole). 148.6 (q, thiazole), 138.3 (q, thiophene), 138.3 (q, C_{Ar}), 137.1 (q, pyrrole), 128.9 (t, 2C, C_{Ar}), 128.0 (t, 2C, thiophene), 127.3 (q, pyrrole), 126.7 (t, thiophene), 126.4 (t, 2C, C_{Ar}), 113.7 (t, thiazole), 112.8 (q, pyrrole), 111.3 (t, pyrrole), 59.8 (d, CH_2 , OEt), 48.6 (d, CH_2), 14.8 (s, CH_3 , OEt), 11.7 (s, Me).

3.4 Ethyl 1-(3-fluoro-4-methylphenyl)-2-methyl-5-(2-(thiophen-2-yl)thiazol-4-yl)-1H-pyrrole-3-carboxylate (**16**)



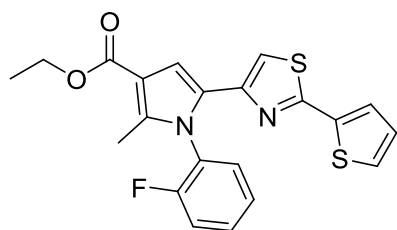
Isolated yield 70%

R_f = 0.5 (DCM)

¹H NMR (300 MHz, CDCl₃): δ_H 7.40 (d, *J* = 3.52 Hz, 1H, thiophene), 7.33 (d, *J* = 5.46 Hz, 1H, thiophene), 7.28 (t, *J* = 8.10 Hz, 1H, H_{Ar}), 7.18 (s, 1H, thiazole), 7.01 (dd, *J* = 3.88, 5.29 Hz, 1H, thiophene), 6.99 – 6.93 (m, 2H, H_{Ar}), 6.24 (s, 1H, pyrrole), 4.32 (q, *J* = 7.05 Hz, 2H, CH₂, OEt), 2.36 (s, 6H, Ar-Me and Me), 1.37 (t, *J* = 6.87 Hz, 3H, CH₃, OEt).

¹³C NMR (75 MHz, CDCl₃): δ_C 165.7 (q, CO), 162.6 (q, C_{Ar}), 160.6 (q, thiazole), 160.1 (q, C_{Ar}), 147.7 (q, thiazole), 138.9 (q, thiophene), 137.6 (q, pyrrole), 137.4 (q, d, *J* = 10.53 Hz, C_{Ar}, F coupling), 132.2 (t, d, *J* = 6.70 Hz, C_{Ar}, F coupling), 128.6 (q, pyrrole), 128.0 (t, thiophene), 128.0 (t, thiophene), 126.7 (t, thiophene), 126.5 (q, C_{Ar}), 126.3 (q, C_{Ar}), 124.5 (t, C_{Ar}), 116.2 (t, C_{Ar}), 116.0 (t, C_{Ar}), 113.2 (q, Pyrrole), 111.8 (t, thiazole), 111.2 (t, pyrrole), 59.9 (d, CH₂, OEt), 14.8 (s, CH₃, OEt), 14.8 (s, CH₃, Ar-Me), 12.1 (s, Me).

3.5 Ethyl 1-(2-fluorophenyl)-2-methyl-5-(2-(thiophen-2-yl)thiazol-4-yl)-1H-pyrrole-3-carboxylate (51)



Isolated yield 82%

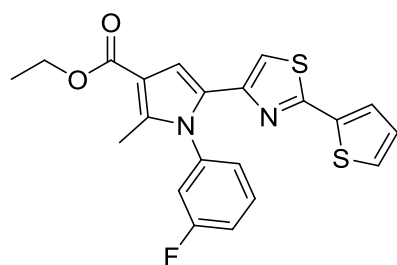
R_f = 0.93 (DCM).

¹H NMR (300 MHz, CDCl₃): δ_H 7.57 – 7.51 (m, 1H, H_{Ar}), 7.43 (d, *J* = 2.54 Hz, 1H, thiophene), 7.38 (d, *J* = 3.56 Hz, 1H, thiophene), 7.37 – 7.28 (m, 3H, H_{Ar}), 7.25 (s, 1H, thiazole), 7.06 (dd, *J* = 3.56, 5.11 Hz, 1H, thiophene), 6.55 (s, 1H, pyrrole), 4.40 (q, *J* = 7.12 Hz, 2H, CH₂, OEt), 2.44 (s, 3H, Me), 1.46 (t, *J* = 7.12 Hz, CH₃, OEt).

¹³C NMR (75 MHz, CDCl₃): δ_C 165.7 (q, CO), 160.8 (q, thiazole), 160.6 (q, C_{Ar}), 157.3 (q, C_{Ar}), 147.8 (q, thiazole), 139.3 (q, thiophene), 137.7 (q, C_{Ar}), 131.3 (t, d, *J* = 7.86 Hz, C_{Ar}, F coupling), 131.1 (t, C_{Ar}), 128.6 (q, pyrrole), 128.1 (t, thiophene), 128.0 (t, thiophene), 126.8 (t, thiophene), 126.6 (q, pyrrole), 125.0 (t, d, *J* = 4.05 Hz, C_{Ar}, F coupling), 117.2 (t, d, *J* = 19.70 Hz, C_{Ar}, F coupling), 113.6 (q, pyrrole),

111.8 (t, thiazole), 111.3 (t, pyrrole), 60.0 (d, CH₂, OEt), 15.0 (s, CH₃, OEt), 12.2 (s, Me).

3.6 Ethyl 1-(3-fluorophenyl)-2-methyl-5-(2-(thiophen-2-yl)thiazol-4-yl)-1H-pyrrole-3-carboxylate (52)



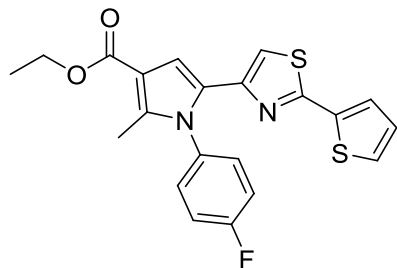
Isolated yield 86%

R_f = 0.67 (DCM).

¹H NMR (300 MHz, CDCl₃): δ_H 7.54 (q, *J* = 7.74 Hz, 1H, H_{Ar}), 7.48 (d, *J* = 5.24 Hz, 1H, Thiophene), 7.42 (d, *J* = 5.24 Hz, 1H, Thiophene), 7.28 (td, *J* = 8.73, 2.25 Hz, 1H, H_{Ar}), 7.18 – 7.16 (m, 1H, H_{Ar}), 7.16 – 7.13 (m, 1H, H_{Ar}), 7.11 (s, 1H, Thiazole), 7.10 (dd, *J* = 4.24, 5.24 Hz, 1H, Thiophene), 6.43 (s, 1H, Pyrrole), 4.41 (q, *J* = 7.24 Hz, 2H, CH₂, OEt), 2.46 (s, 3H, Me), 1.47 (t, *J* = 6.99 Hz, 3H, CH₃, OEt).

¹³C NMR (75 MHz, CDCl₃): δ_C 165.3 (q, CO), 164.4 (q, C_{Ar}), 161.1 (q, C_{Ar}), 160.4 (q, thiazole), 147.3 (q, thiazole), 139.7 (q, C_{Ar}), 138.4 (q, thiophene), 137.1 (q, pyrrole), 130.4 (t, d, *J* = 8.73 Hz, C_{Ar}, F coupling), 128.1 (q, pyrrole), 127.7 (q, thiophene), 127.6 (q, thiophene), 126.4 (t, thiophene), 124.6 (t, d, *J* = 3.54 Hz, C_{Ar}, F coupling), 116.5 (t, C_{Ar}), 116.2 (t, C_{Ar}), 113.1 (q, pyrrole), 111.5 (t, thiazole), 111.2 (t, pyrrole), 59.6 (d, CH₂, OEt), 14.5 (s, CH₃, OEt), 12.2 (s, Me).

3.7 Ethyl 1-(4-fluorophenyl)-2-methyl-5-(2-(thiophen-2-yl)thiazol-4-yl)-1H-pyrrole-3-carboxylate (53)



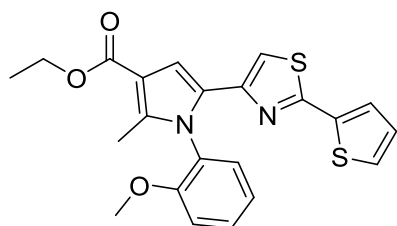
Isolated yield 96%

$R_f = 0.49$ (DCM).

$^1\text{H NMR}$ (300 MHz, CDCl_3): δ_{H} 7.46 (d, $J = 3.51$, 1H, thiophene), 7.41 (d, $J = 5.41$, 1H, thiophene), 7.36 – 7.29 (m, 2H, H_{Ar}), 7.27 (s, 1H, thiazole), 7.09 (dd, $J = 3.51$, 5.40, 1H, thiophene), 6.91 (t, $J = 8.83$ Hz, 1H, H_{Ar}), 6.67 (q, $J = 4.53$ Hz, 1H, H_{Ar}), 6.35 (s, 1H, pyrrole), 4.40 (q, $J = 6.97$ Hz, 2H, CH_2 , OEt), 2.43 (s, 3H, Me), 1.45 (t, $J = 7.21$ Hz, 3H, CH_3 , OEt).

$^{13}\text{C NMR}$ (75 MHz, CDCl_3): δ_{C} 165.3 (q, CO), 164.1 (q, C_{Ar}), 160.8 (q, thiazole), 160.3 (q, C_{Ar}), 147.4 (q, thiazole), 138.6 (q, thiophene), 137.1 (q, pyrrole), 134.3 (q, d, $J = 3.67$ Hz, C_{Ar} , F coupling), 130.4 (q, pyrrole), 130.4 (t, d, $J = 8.43$ Hz, 2C, C_{Ar} , F coupling), 128.3 (q, pyrrole), 127.7 (t, thiophene), 127.6 (t, thiophene), 126.4 (t, thiophene), 116.4 (t, d, $J = 22.58$ Hz, 2C, C_{Ar} , F coupling), 112.9 (q, pyrrole), 111.4 (t, thiazole), 111.0 (t, pyrrole), 59.5 (d, CH_2 , OEt), 14.5 (s, CH_3 , OEt), 12.2 (s, Me).

3.8 Ethyl 1-(2-methoxyphenyl)-2-methyl-5-(2-(thiophen-2-yl)thiazol-4-yl)-1H-pyrrole-3-carboxylate (54)



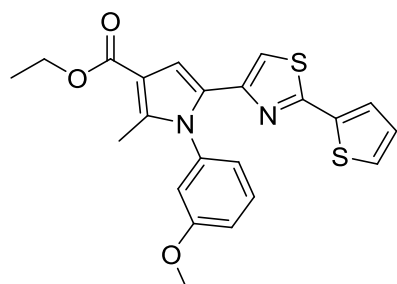
Isolated yield 49%

$R_f = 0,55$ (DCM).

$^1\text{H NMR}$ (300 MHz, CDCl_3): δ_{H} 7.46 (t, $J = 7.97$ Hz, 1H, H_{Ar}), 7.38 (d, $J = 3.45$ Hz, 1H, thiophene), 7.32 (d, $J = 4.47$ Hz, 1H, thiophene), 7.24 (s, 1H, thiazole), 7.19 (dd, $J = 7.72, 1.22$ Hz, 1H, H_{Ar}), 7.07 (d, $J = 2.23$ Hz, 1H, H_{Ar}), 7.04 (dd, $J = 5.89, 8.53$ Hz, 1H H_{Ar}), 7.00 (dd, $J = 3.66, 4.27$ Hz, 1H, thiophene), 6.13 (s, 1H, pyrrole), 4.32 (q, $J = 6.90$ Hz, 2H, OEt), 3.72 (s, 3H, OMe), 2.31 (s, 3H, Me), 1.37 (t, $J = 6.90$ Hz, 3H, OEt).

$^{13}\text{C NMR}$ (75 MHz, CDCl_3): δ_{C} 165.6 (q, CO), 160.0 (q, thiazole), 156.0 (q, C_{Ar}), 147.9 (q, thiazole), 139.3 (q, thiophene), 137.4 (q, pyrrole), 130.6 (t, C_{Ar}), 130.1 (t, C_{Ar}), 128.2 (q, pyrrole), 127.6 (t, thiazole), 127.6 (t, thiazole), 127.0 (q, C_{Ar}), 126.3 (t, thiophene), 120.9 (t, C_{Ar}), 112.5 (q, pyrrole), 112.3 (t, C_{Ar}), 111.2 (t, thiophene), 109.7 (t, pyrrole), 59.4 (d, CH_2 , OEt), 55.8 (s, OMe), 14.6 (s, CH_3 , OEt), 11.8 (s, Me).

3.9 Ethyl 1-(3-methoxyphenyl)-2-methyl-5-(2-(thiophen-2-yl)thiazol-4-yl)-1H-pyrrole-3-carboxylate (55)



Isolated yield 69%

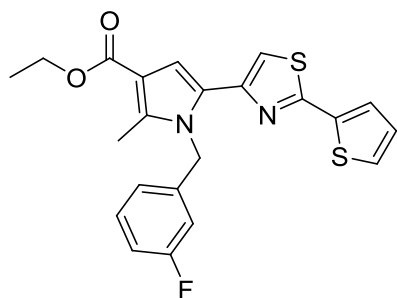
$R_f = 0,53$ (DCM)

$^1\text{H NMR}$ (300 MHz, CDCl_3): δ_{H} 7.47 (d, $J = 2.89$ Hz, 1H, thiophene), 7.39 (t, $J = 8.02$ Hz, 1H, H_{Ar}), 7.34 (d, $J = 5.13$ Hz, 1H, thiophene), 7.04 (dd, $J = 1.21, 2.65$ Hz, thiophene), 7.03 – 7.00 (m, 1H, H_{Ar}), 6.87 (dq, $J = 7.96, 0.72$ Hz, 1H, H_{Ar}), 6.80 (t, $J = 2.29$ Hz, 1H, H_{Ar}), 6.08 (s, 1H, pyrrole), 4.32 (q, $J = 7.47$ Hz, 2H, CH_2 , OEt), 3.79 (s, CH_3 , OMe), 2.37 (s, CH_3 , Me), 1.37 (t, $J = 7.23$ Hz, 3H, CH_3 , OEt).

$^{13}\text{C NMR}$ (75 MHz, CDCl_3): δ_{C} 165.4 (q, CO), 160.4 (q, thiazole), 160.2 (q, C_{Ar}), 147.4 (q, thiazole), 139.3 (q, thiophene), 138.7 (q, C_{Ar}), 137.2 (q, pyrrole), 130.11 (t, C_{Ar}), 128.3 (q, pyrrole), 127.6 (t, 2C, thiophene), 126.5 (t, thiophene), 120.8 (t,

C_{Ar}), 115.0 (t, C_{Ar}), 114.2 (t, C_{Ar}), 112.7 (q, pyrrole), 111.5 (t, thiazole), 110.4 (t, pyrrole), 59.5 (d, CH_2 , OEt), 55.5 (s, CH_3 , OMe), 14.6 (s, CH_3 , OEt), 12.2 (s, Me).

3.11 Ethyl 1-(3-fluorobenzyl)-2-methyl-5-(2-(thiophen-2-yl)thiazol-4-yl)-1H-pyrrole-3-carboxylate (57)

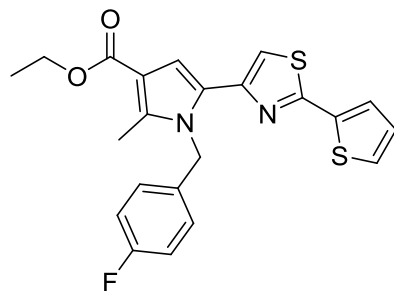


Isolated yield 80%

R_f = 0,63 (DCM).

1H NMR (300 MHz, $CDCl_3$): δ_H 7.42 (d, J = 3.63 Hz, 1H, thiophene), 7.33 (d, J = 4.98 Hz, 1H, thiophene), 7.20 (t, J = 7.72 Hz, 1H, H_{Ar}), 7.02 (t, J = 3.96 Hz, 1H, thiophene), 6.93 (s, 1H, pyrrole), 6.88 (t, J = 10.74 Hz, 1H, H_{Ar}), 6.77 (d, J = 7.72 Hz, 1H, H_{Ar}), 6.69 (d, J = 9.8 Hz, 1H, H_{Ar}), 5.59 (s, 2H, CH_2), 4.30 (q, J = 6.97 Hz, 2H, CH_2 , OEt), 2.51 (s, 3H, Me), 1.36 (t, J = 7.16 Hz, 3H, CH_3 , OEt).

^{13}C NMR (75 MHz, $CDCl_3$): δ_C 165.3 (q, CO), 164.7 (q, C_{Ar}), 161.4 (q, C_{Ar}), 161.1 (q, thiazole), 148.1 (q, thiazole), 140.6 (q, thiophene), 137.8 (q, pyrrole), 137.3 (q, C_{Ar}), 130.1 (t, d, J = 8.06 Hz, C_{Ar} F coupling), 127.8 (t, 2C, thiophene), 126.8 (q, pyrrole), 126.4 (t, thiophene), 121.6 (t, d, J = 2.46 Hz, C_{Ar} , F coupling), 113.9 (t, d, J = 20.74 Hz, C_{Ar} , F, coupling), 113.4 (t, thiazole), 113.0 (t, d, J = 22.16 Hz, C_{Ar} , F coupling), 112.7 (q, pyrrole), 111.0 (t, pyrrole), 59.5 (d, CH_2 , OEt), 47.9 (d, CH_2), 14.5 (s, CH_3 , OEt), 11.4 (s, Me).

3.12 Ethyl 1-(4-fluorobenzyl)-2-methyl-5-(2-(thiophen-2-yl)thiazol-4-yl)-1H-pyrrole-3-carboxylate (58)

Isolated yield 41%

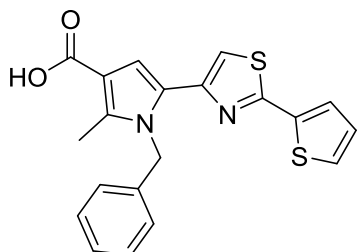
$R_f = 0,63$ (DCM).

$^1\text{H NMR}$ (300 MHz, CDCl_3): δ_{H} 7.43 (d, $J = 3.77$ Hz, 1H, thiophene), 7.34 (d, $J = 5.09$ Hz, 1H, thiophene), 7.12 (s, 1H, thiazole), 7.03 (dd, $J = 3.58, 5.39$ Hz, 1H, thiophene), 6.98- 6.92 (m, 4H, H_{Ar}), 6.91 (s, 1H, pyrrole), 5.54 (s, 2H, CH_2), 4.29 (q, $J = 7.16$ Hz, CH_2 , OEt), 2.51 (s, 3H, Me), 1.36 (t, $J = 6.97$ Hz, 3H, CH_3 , OEt).

$^{13}\text{C NMR}$ (75 MHz, CDCl_3): δ_{C} 165.3 (q, CO), 163.5 (q, C_{Ar}), 161.1 (q, thiazole), 160.2 (q, C_{Ar}), 148.2 (q, thiazole), 137.8 (q, thiophene), 137.3 (q, pyrrole), 133.5 (q, d, $J = 6.38$ Hz, C_{Ar} , F coupling), 127.8 (t, d, $J = 6.75$ Hz, 2C, C_{Ar} , F coupling), 127.7 (t, 2C, thiophene), , 126.8 (q, pyrrole), 126.5 (t, thiohene), 115.5 (t, d, $J = 21.01$ Hz, 2C, C_{Ar} , F coupling), 113.5 (t, thiazole), 112.6 (q, pyrrole), 111.0 (t, pyrrole), 59.5 (d, CH_2 , OEt), 47.7 (d, CH_2), 14.5 (s, CH_3 , OEt), 11.4 (s, Me).

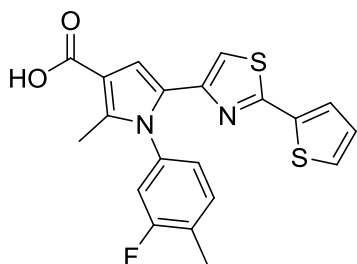
Compounds **15**, **16**, **51** – **58** were hydrolyzed according to the same procedure of generation of **18** to their respective carboxylic acid intermediate without purification.

3.13 1-benzyl-2-methyl-5-(2-(thiophen-2-yl)thiazol-4-yl)-1*H*-pyrrole-3-carboxylic acid (**15'**)



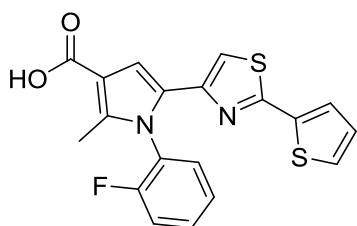
$R_f = 0,26$ (DCM:EtOAc = 20:1 with 0.2% acetic acid).

3.14 1-(3-fluoro-4-methylphenyl)-2-methyl-5-(2-(thiophen-2-yl)thiazol-4-yl)-1*H*-pyrrole-3-carboxylic acid (**16'**)

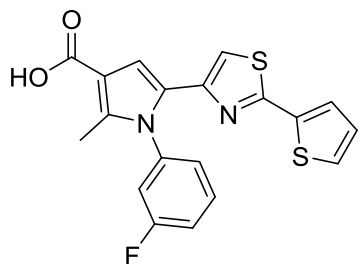


$R_f = 0,21$ (DCM:EtOAc = 20:1 with 0.2% acetic acid).

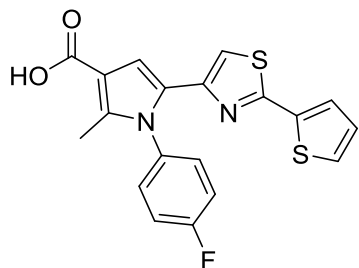
3.15 1-(2-fluorophenyl)-2-methyl-5-(2-(thiophen-2-yl)thiazol-4-yl)-1*H*-pyrrole-3-carboxylic acid (**51'**)



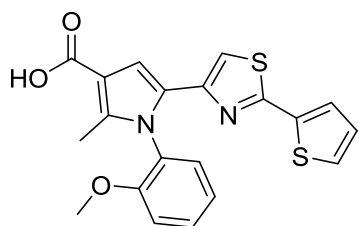
$R_f = 0,28$ (DCM:EE = 40:1 with 0.1% acetic acid).

3.16 1-(3-fluorophenyl)-2-methyl-5-(2-(thiophen-2-yl)thiazol-4-yl)-1*H*-pyrrole-3-carboxylic acid (52')

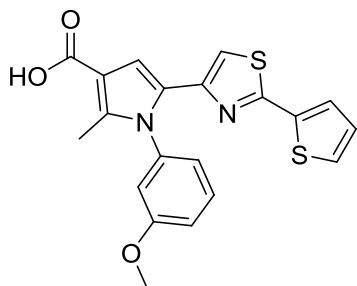
$R_f = 0.26$ (DCM:EtOAc = 40:1 with 0.1% acetic acid).

3.17 1-(4-fluorophenyl)-2-methyl-5-(2-(thiophen-2-yl)thiazol-4-yl)-1*H*-pyrrole-3-carboxylic acid (53')

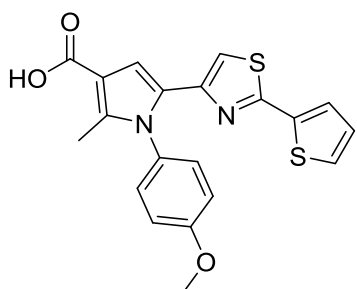
$R_f = 0.22$ (DCM:EtOAc = 40:1 with 0.1% acetic acid).

3.18 1-(2-methoxyphenyl)-2-methyl-5-(2-(thiophen-2-yl)thiazol-4-yl)-1*H*-pyrrole-3-carboxylic acid (54')

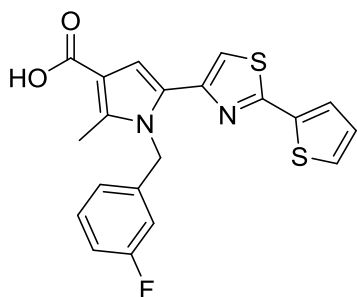
$R_f = 0.26$ (DCM:EtOAc = 40:1 with 0.1% acetic acid).

3.19 1-(3-methoxyphenyl)-2-methyl-5-(2-(thiophen-2-yl)thiazol-4-yl)-1H-pyrrole-3-carboxylic acid (55')

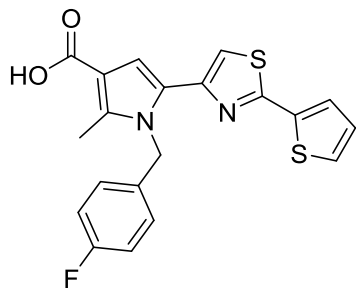
$R_f = 0.27$ (DCM:EtOAc = 40:1 with 0.1% acetic acid).

3.20 1-(4-methoxyphenyl)-2-methyl-5-(2-(thiophen-2-yl)thiazol-4-yl)-1H-pyrrole-3-carboxylic acid (56')

$R_f = 0.23$ (DCM:EtOAc = 40:1 with 0.1% acetic acid).

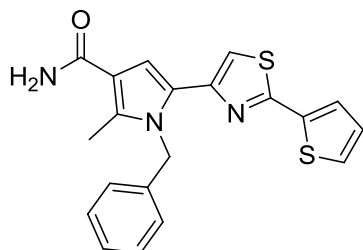
3.21 1-(3-fluorobenzyl)-2-methyl-5-(2-(thiophen-2-yl)thiazol-4-yl)-1H-pyrrole-3-carboxylic acid (57')

$R_f = 0.30$ (DCM:EtOAc = 40:1 with 0.1% acetic acid).

3.22 1-(4-fluorobenzyl)-2-methyl-5-(2-(thiophen-2-yl)thiazol-4-yl)-1H-pyrrole-3-carboxylic acid (58')

$R_f = 0.34$ (DCM:EtOAc = 40:1 with 0.1% acetic acid).

Compounds **15'**, **16'**, **51'** – **58'** were then converted into the primary or secondary amides according to the same procedures of generation of **19** and **20**.

3.23 1-benzyl-2-methyl-5-(2-(thiophen-2-yl)thiazol-4-yl)-1H-pyrrole-3-carboxamide (23)

Isolated yield 28% over two steps

$R_f = 0.25$ (DCM)

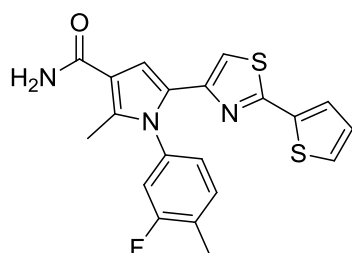
$^1\text{H NMR}$ (300 MHz, CDCl_3): δ_{H} 7.44 (d, $J = 3.81$ Hz, 1H, thiophene), 7.35 (d, $J = 4.57$ Hz, 1H, thiophene), 7.30 -7.20 (m, 3H, H_{Ar}), 7.13 (s, 1H, thiazole), 7.04 (dd, $J = 3.55, 5.33$ Hz, 1H, thiophene), 7.00 (d, $J = 1.62$ Hz, 1H, H_{Ar}), 6.99 (s, 1H, pyrrole), 6.99 – 6.97 (m, 1H, H_{Ar}), 5.86 (b, 2H, NH_2), 5.61 (s, 2H, CH_2), 2.59 (s, 3H, Me).

$^{13}\text{C NMR}$ (75 MHz, CDCl_3): δ_{C} 161.6 (q, CO), 161.5 (q, thiazole), 148.2 (q, thiazole), 141.3 (q, thiophene), 137.7 (q, pyrrole), 137.7 (q, C_{Ar}), 129.1 (t, 2C, C_{Ar}), 128.3 (t, thiophen), 128.2 (t, thiophene), 127.9 (q, pyrrole), 127.6 (t, thiophene),

127.0 (t, C_{Ar}), 126.5 (t, 2C, C_{Ar}), 114.6 (t, thiazole), 112.1(t, pyrrole), 48.9 (d, CH₂), 12.1 (s, Me).

HRMS *m/z* calcd for C₂₀H₁₈N₃OS₂ [M + H]⁺, 380.0886; found, 380.0874.

3.24 1-(3-fluoro-4-methylphenyl)-2-methyl-5-(2-(thiophen-2-yl)thiazol-4-yl)-1H-pyrrole-3-carboxamide (24)



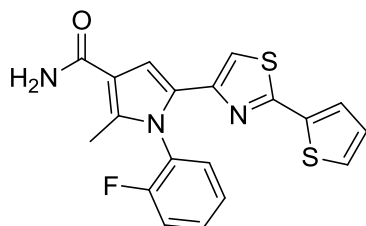
Isolated yield 21% over two steps

R_f = 0.27 (DCM:PE = 10:1).

¹H NMR (300 MHz, CDCl₃): δ_H 7.41 (d, *J* = 3.30 Hz, 1H, thiophene), 7.33 (d, *J* = 4.76 Hz, 1H, thiophene), 7.31 (t, *J* = 8.42 Hz, 1H, H_{Ar}), 7.04 – 6.98 (m, 1H, thiophene and 2H, H_{Ar}), 6.35 (s, 1H, pyrrole), 5.78 (b, 2H, NH₂), 2.45 (s, 3H, Ar-Me), 2.37 (s, Me).

¹³C NMR (75 MHz, CDCl₃): δ_C 162.3 (q, CO), 161.2 (q, C_{Ar}), 160.5 (q, thiazole), 159.8 (q, C_{Ar}), 147.1 (q, thiazole), 141.5 (q, thiophene), 137.2 (q, pyrrole), 136.7 (q, d, *J* = 10.46 Hz, C_{Ar} F coupling), 132.0 (q, d, *J* = 5.78 Hz, C_{Ar} F coupling), 128.8 (t, C_{Ar}), 127.8 (t, thiophene), 127.7 (t, thiophene), 126.5 (t, thiophene), 126.3 (q, pyrrole), 124.1 (t, d, *J* = 4.07 Hz, C_{Ar}, F coupling), 115.8 (t, d, *J* = 17.62 Hz, C_{Ar}, F coupling), 112.1 (q, pyrrole), 111.9 (t, thiazole), 111.7 (t, pyrrole), 14.5 (s, Me-Ar), 12.5 (s, Me).

HRMS *m/z* calcd for C₂₀H₁₇FN₃OS₂ [M + H]⁺, 398.0792; found, 380.0782.

3.25 1-(2-fluorophenyl)-2-methyl-5-(2-(thiophen-2-yl)thiazol-4-yl)-1H-pyrrole-3-carboxamide (59)

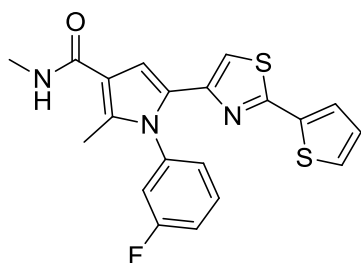
Isolated yield 52% over two steps

R_f = 0.55 (DCM).

$^1\text{H NMR}$ (300 MHz, CDCl_3): δ_{H} 7.49 (q, 1H, H_{Ar}), 7.36 (d, $J = 3.94$, 1H, thiophene), 7.33 (t, 1H, H_{Ar}), 7.31 (s, 1H, thiazole), 7.30 – 7.25 (m, 2H, H_{Ar} ; 1H, thiophene), 6.99 (t, 1H, thiophene), 6.60 (s, 1H, pyrrole), 5.89 (b, 2H, NH_2), 2.45 (s, 3H, Me).

$^{13}\text{C NMR}$ (75 MHz, CDCl_3): δ_{C} 161.0 (q, CO), 160.6 (q, thiazole), 159.7 (q, C_{Ar}), 157.2 (q, C_{Ar}), 147.1 (q, thiazole), 141.9 (q, thiophene), 137.2 (q, pyrrole), 131.1 (t, d, $J = 8.35$ Hz, C_{Ar} , F coupling), 130.6 (t, C_{Ar}), 128.7 (q, pyrrole), 127.7 (t, thiophene), 127.6 (t, thiophene), 126.4 (t, thiophene), 126.1 (q, d, $J = 12.77$ Hz, C_{Ar} , F coupling), 124.7 (t, d, $J = 3.94$ Hz, C_{Ar} , F coupling), 116.8 (t, C_{Ar}), 116.6 (t, thiazole), 112.4 (q, pyrrole), 111.7 (t, pyrrole), 12.1 (s, Me).

HRMS m/z calcd for $\text{C}_{19}\text{H}_{15}\text{FN}_3\text{OS}_2$ $[\text{M} + \text{H}]^+$, 384.0635; found, 384.0640.

3.26 1-(3-fluorophenyl)-*N*,2-dimethyl-5-(2-(thiophen-2-yl)thiazol-4-yl)-1H-pyrrole-3-carboxamide (60)

Isolated yield 45% over two steps

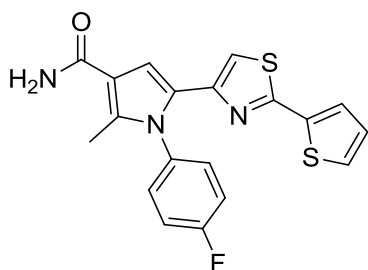
R_f = 0.19 (DCM:MeOH = 40 : 1).

¹H NMR (300 MHz, CDCl₃): δ_H 7.46 (dd, *J* = 1.6, 8.31, 1H, H_{Ar}), 7.43 (d, *J* = 3.52, 1H, thiophene), 7.36 (d, *J* = 4.79, 1H, thiophene), 7.21 (t, 1H, H_{Ar}), 7.08 (d, *J* = 7.67, 1H, H_{Ar}), 7.03 (t, 1H, H_{Ar}), 7.02 (dd, *J* = 3.84, 8.95, 1H, thiophene), 6.94 (s, 1H, thiazole), 6.07 (s, 1H, pyrrole), 5.96 (b, 1H, NH), 2.97 (s, 3H, NHCH₃), 2.38 (s, 3H, Me).

¹³C NMR (75 MHz, CDCl₃): δ_C 166.5 (q, CO), 164.4 (q, C_{Ar}), 161.9 (q, C_{Ar}), 160.9 (q, thiazole), 147.5 (q, thiazole), 140.1 (q, pyrrole), 139.8 (q, d, *J* = 10.13 Hz, C_{Ar}, F coupling), 137.3 (q, thiophene), 136.9 (q, pyrrole), 130.7 (t, d, *J* = 9.49 Hz, C_{Ar}, F coupling), 128.3 (q, pyrrole), 128.2 (t, thiophene), 128.1 (t, thiophene), 127.0 (t, thiophene), 124.7 (t, d, *J* = 22.76 Hz, C_{Ar}, F coupling C_{Ar}), 116.3 (t, d, *J* = 21.77 Hz, C_{Ar}, F coupling), 116.1 (t, d, *J* = 21.26 Hz, C_{Ar}, F coupling), 116.1 (q, pyrrole), 110.8 (t, thiazole), 108.0 (t, pyrrole), 25.5 (s, NHCH₃), 12.3 (s, Me).

HRMS *m/z* calcd for C₂₀H₁₇FN₃OS₂ [M + H]⁺, 398.0792; found, 398.0760.

3.27 1-(4-fluorophenyl)-2-methyl-5-(2-(thiophen-2-yl)thiazol-4-yl)-1H-pyrrole-3-carboxamide (63)



Isolated yield 29% over two steps

R_f = 0.75 (DCM:EE = 40:1 with 0.1% AcOH).

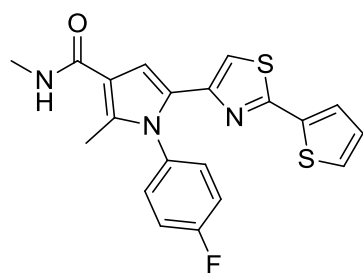
¹H NMR (300 MHz, CDCl₃): δ_H 7.40 (d, *J* = 3.90 Hz, 1H, thiophene), 7.33 (d, *J* = 4.48 Hz, 1H, thiophene), 7.31 – 7.26 (m, 2H, H_{Ar}), 7.25 (s, 1H, thiazole), 7.23 – 7.16 (m, 2H, H_{Ar}), 7.07 (dd, *J* = 3.7, 5.07, 1H, thiophene), 6.38 (s, 1H, Pyrrole), 2.44 (s, 1H, Me).

¹³C NMR (75 MHz, CDCl₃): δ_C 164.3 (q, CO), 161.1 (q, Thiazole), 161.0 (q, C_{Ar}), 160.6 (q, C_{Ar}), 147.1 (q, thiazole), 141.5 (q, thiophene), 137.1 (q, pyrrole), 134.0

(q, d, $J = 3.05$ Hz, C_{Ar} , F coupling), 130.4 (t, d, $J = 7.74$ Hz, 2C, C_{Ar} , F coupling), 128.9 (q, pyrrole), 127.9 (t, thiophene), 127.7 (t, Thiophene), 126.5 (t, thiophene), 116.6 (t, d, $J = 17.40$ Hz, 2C, C_{Ar} , F coupling), 112.1 (q, pyrrole), 111.9 (t, thiazole), 111.8 (t, pyrrole), 12.5 (s, Me).

HRMS m/z calcd for $C_{19}H_{15}FN_3OS_2$ $[M + H]^+$, 384.0635; found, 384.0635.

3.28 1-(4-fluorophenyl)-*N*,2-dimethyl-5-(2-(thiophen-2-yl)thiazol-4-yl)-1*H*-pyrrole-3-carboxamide (64)



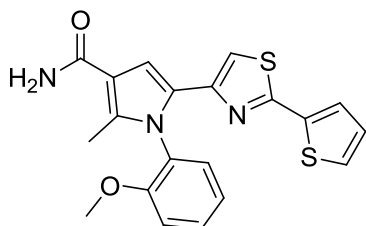
Isolated yield 59% over two steps

$R_f = 0.26$ (DCM:MeOH = 40 :1).

1H NMR (300 MHz, $CDCl_3$): δ_H 7.43 (d, $J = 3.87$ Hz, 1H, thiophene), 7.36 (d, $J = 5.09$ Hz, 1H, thiophene), 7.29 – 7.14 (m, 4H, H_{Ar}), 7.03 (dd, $J = 3.67, 5.09$ Hz, 1H, thiophene), 6.94 (s, 1H, thiazole), 6.02 (s, 1H, pyrrole), 5.94 (b, 1H, NH), 2.97 (d, $J = 1.47$ Hz, 3H, $NHCH_3$), 2.36 (s, 3H, Me).

^{13}C NMR (75 MHz, $CDCl_3$): δ_C 166.7 (q, CO), 161.6 (q, thiazole), 161.3 (q, C_{Ar}), 160.9 (q, C_{Ar}), 147.7 (q, thiazole), 137.4 (q, thiophene), 137.2 (q, pyrrole), 134.7 (q, d, $J = 2.89$ Hz, C_{Ar} , F coupling), 130.9 (t, d, $J = 8.09$ Hz, 2C, C_{Ar} , F coupling), 128.6 (q, pyrrole), 128.3 (t, thiophene), 128.2 (t, thiophene), 127.1 (t, thiophene), 116.9 (t, d, $J = 22.42$ Hz, 2C, C_{Ar} , F coupling), 116.1 (q, pyrrole), 110.7 (t, thiazole), 108.7 (t, pyrrole), 26.6 (s, $CH_3, NHCH_3$), 12.4 (s, Me).

HRMS m/z calcd for $C_{20}H_{17}FN_3OS_2$ $[M + H]^+$, 398.0792; found, 398.0768.

3.29 (1-(2-methoxyphenyl)-2-methyl-5-(2-(thiophen-2-yl)thiazol-4-yl)-1H-pyrrole-3-carboxamide (65)

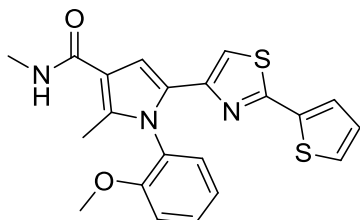
Isolated yield 22% over two steps

$R_f = 0.50$ (DCM).

$^1\text{H NMR}$ (300 MHz, CDCl_3): δ_{H} 7.48 (t, 1H, H_{Ar}), 7.39 (d, $J = 3.78$ Hz, 1H, thiophene), 7.33 (s, 1H, thiazole), 7.30 (d, $J = 5.11$ Hz, 1H, thiophene), 7.23 (d, $J = 7.95$, 1H, H_{Ar}), 7.09 (d, $J = 3.22$, H_{Ar}), 7.06 (t, 1H, H_{Ar}), 7.00 (dd, $J = 3.78$, 5.3 Hz, thiophene), 6.25 (s, 1H, pyrrole), 5.78 (b, 2H, NH_2), 3.76 (s, 3H, OMe), 2.40 (s, 3H, Me).

$^{13}\text{C NMR}$ (75 MHz, CDCl_3): δ_{C} 161.4 (q, CO), 160.1 (q, thiazole), 155.9 (q, C_{Ar}), 147.6 (q, thiazole), 142.2 (q, thiophene), 137.4 (q, C_{Ar}), 130.8 (t, C_{Ar}), 130.0 (t, C_{Ar}), 128.6 (q, pyrrole), 127.6 (t, 2C, thiophene), 126.8 (q, pyrrole), 126.4 (t, thiophene), 120.9 (t, C_{Ar}), 112.3 (t, C_{Ar}), 111.9 (q, pyrrole), 111.7 (t, thiazole), 110.5 (t, pyrrole), 55.9 (s, OMe), 12.1 (s, Me).

HRMS m/z calcd for $\text{C}_{20}\text{H}_{18}\text{N}_3\text{O}_2\text{S}_2$ [$\text{M} + \text{H}$] $^+$, 396.0835; found, 396.0838.

3.30 1-(2-methoxyphenyl)-*N*,2-dimethyl-5-(2-(thiophen-2-yl)thiazol-4-yl)-1H-pyrrole-3-carboxamide (66)

Isolated yield 35% over two steps

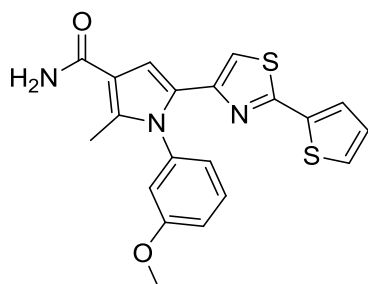
$R_f = 0.19$ (DCM:MeOH = 40:1).

¹H NMR (300 MHz, CDCl₃): δ_H 7.47 (t, *J* = 8.14 Hz, 1H, H_{Ar}), 7.43 (d, *J* = 3.56 Hz, 1H, thiophene), 7.35 (d, *J* = 5.09 Hz, 1H, thiophene), 7.20 (d, *J* = 7.63 Hz, 1H, H_{Ar}), 7.09 – 7.03 (m, 2H, H_{Ar}), 7.03 (dd, *J* = 3.56, 5.14 Hz, 1H, thiophene), 7.00 (s, 1H, thiazole), 5.94 (b, 1H, NH), 5.93 (s, 1H, pyrrole), 3.72 (s, 3H, CH₃, OMe), 2.97 (d, *J* = 3.56 Hz, 3H, NHCH₃), 2.32 (s, 3H, Me).

¹³C NMR (75 MHz, CDCl₃): δ_C 166.5 (q, CO), 160.2 (q, thiazole), 156.0 (q, C_{Ar}), 147.7 (q, thiazole), 137.3 (q, thiophene), 137.2 (q, pyrrole), 130.7 (t, C_{Ar}), 130.3 (t, C_{Ar}), 128.0 (q, C_{Ar}), 127.7 (t, thiophene), 127.7 (t, thiophene), 127.0 (q, pyrrole), 126.6 (t, thiophene), 121.0 (t, C_{Ar}), 115.2 (q, pyrrole), 108.9 (t, Thiazole), 180.0 (t, pyrrole), 55.8 (s, CH₃, OMe), 26.1 (s, CH₃, NHCH₃), 11.6 (s, Me).

HRMS *m/z* calcd for C₂₁H₂₀N₃O₂S₂ [M + H]⁺, 410.0991; found, 410.0968.

3.31 1-(3-methoxyphenyl)-2-methyl-5-(2-(thiophen-2-yl)thiazol-4-yl)-1H-pyrrole-3-carboxamide (67)



Isolated yield 21% over two steps

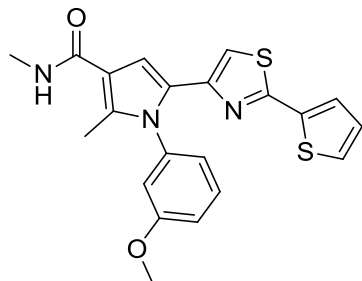
R_f = 0.24 (DCM:PE = 3 : 1).

¹H NMR (300 MHz, CDCl₃): δ_H 7.45 – 7.38 (m, 1H, thiophene, 1H, H_{Ar}), 7.34 - 7.30 (m, 1H, thiophene, 1H, thiazole), 7.05 (dd, *J* = 2.63, 8.46 Hz, 1H, H_{Ar}), 7.01 (dd, *J* = 3.76, 4.70 Hz, 1H, thiophene), 6.91 (d, *J* = 7.71, 1H, H_{Ar}), 6.84 (t, 1H, H_{Ar}), 6.78 (s, 1H, pyrrole), 5.76 (b, 2H, NH₂), 3.81 (s, 3H, OMe), 2.46 (s, 3H, Me).

¹³C NMR (75 MHz, CDCl₃): δ_C 161.3 (q, CO), 160.5 (q, thiazole), 160.3 (q, C_{Ar}), 147.1 (q, thiazole), 141.5 (q, thiophene), 139.0 (q, C_{Ar}), 137.2 (q, pyrrole), 130.2 (t, C_{Ar}), 128.8 (q, pyrrole), 127.8 (t, thiophene), 127.7 (t, thiophene), 126.5 (t, thiophene), 120.8 (t, C_{Ar}), 115.3 (t, C_{Ar}), 114.0 (t, C_{Ar}), 112.0 (t, thiazole), 112.0 (q, pyrrole), 111.2 (t, pyrrole), 55.8 (s, OMe), 12.5 (s, Me).

HRMS m/z calcd for $C_{20}H_{18}N_3O_2S_2$ $[M + H]^+$, 396.0835; found, 396.0830.

3.32 1-(3-methoxyphenyl)-*N*,2-dimethyl-5-(2-(thiophen-2-yl)thiazol-4-yl)-1*H*-pyrrole-3-carboxamide (68)



Isolated yield 59% over two steps

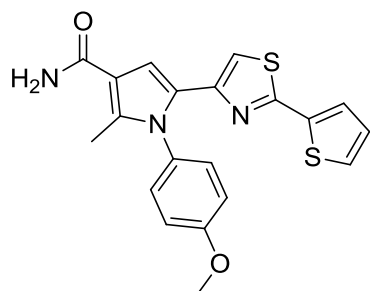
0.25 (DCM:MeOH = 40 :1).

1H NMR (300 MHz, $CDCl_3$): δ_H 7.44 (d, $J = 3.68$, 1H, thiophene), 7.40 (t, 1H, H_{Ar}), 7.36 (d, $J = 5.14$, 1H, thiophene), 7.04 (dq, $J = 7.61$, 1H, thiophene), 7.04 (dd, $J = 3.79$, 5.29, 1H, H_{Ar}), 6.99 (s, 1H, thiazole), 6.87 (dq, $J = 7.59$, 1H, H_{Ar}), 6.80 (t, 1H, H_{Ar}), 5.96 (b, 1H, NH), 5.92 (s, 1H, pyrrole), 3.80 (s, 3H, OMe), 2.97 (d, $J = 3.92$, 3H, $NHCH_3$), 2.39 (s, 3H, Me).

^{13}C NMR (75 MHz, $CDCl_3$): δ_C 166.8 (q. CO), 160.9 (q, thiazole), 160.7 (q, C_{Ar}), 147.7 (q. thiazole), 139.8 (q, C_{Ar}), 137.5 (q. thiophene), 137.2 (q, pyrrole), 130.7 (t, C_{Ar}), 128.5 (q. pyrrole), 128.2 (t, 2C, thiophene), 127.1 (t, Thiophene), 121.3 (t, C_{Ar}), 115.9 (q. pyrrole), 115.5 (t, C_{Ar}), 114.6 (t, C_{Ar}), 110.3 (t, thiazole), 108.3 (t, pyrrole), 56.0 (s, OMe), 26.6 (s, $NHCH_3$), 12.4 (s, Me).

HRMS m/z calcd for $C_{21}H_{20}N_3O_2S_2$ $[M + H]^+$, 410.0991; found, 410.0968.

3.33 1-(4-methoxyphenyl)-2-methyl-5-(2-(thiophen-2-yl)thiazol-4-yl)-1*H*-pyrrole-3-carboxamide (69)



Isolated yield 49% over two steps

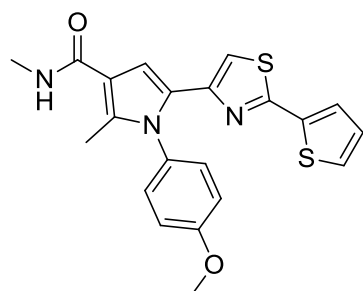
$R_f = 0.63$ (DCM:EE = 40 :1).

$^1\text{H NMR}$ (300 MHz, CDCl_3): δ_{H} 7.43 (d, $J = 3.86$ Hz, 1H, thiophene), 7.32 (d, $J = 4.54$, 1H, thiophene), 7.32 (s, 1H, thiazole), 7.23 (d, $J = 9.07$, 2H, H_{Ar}), 7.02 (d, $J = 9.53$, 2H, H_{Ar}), 7.01 (dd, $J = 3.86, 4.99$, 1H, thiophene), 6.12 (s, 1H, pyrrole), 5.77 (b, 2H, NH_2), 3.88 (s, 3H, OMe), 2.43 (s, 3H, Me).

$^{13}\text{C NMR}$ (75 MHz, CDCl_3): δ_{C} 161.4 (q, CO), 160.3 (q, thiazole), 160.0 (q, C_{Ar}), 147.3 (q, thiazole), 141.9 (q, thiophene), 137.3 (q, C_{Ar}), 130.6 (q, pyrrole), 129.6 (t, 2C, C_{Ar}), 129.1, (q, pyrrole), 127.7 (t, thiophene), 127.6 (t, thiophene), 126.5 (t, thiophene), 114.7 (t, 2C, C_{Ar}), 111.9 (t, thiazole), 111.8 (q, pyrrole), 111.1 (t, pyrrole), 55.6 (s, OMe), 12.5 (s, Me).

HRMS m/z calcd for $\text{C}_{20}\text{H}_{18}\text{N}_3\text{O}_2\text{S}_2$ $[\text{M} + \text{H}]^+$, 396.0835; found, 396.0807.

3.3.4 1-(4-methoxyphenyl)-*N*,2-dimethyl-5-(2-(thiophen-2-yl)thiazol-4-yl)-1*H*-pyrrole-3-carboxamide (70)



Isolated yield 68% over two steps.

$R_f = 0.25$ (DCM:MeOH = 40 :1).

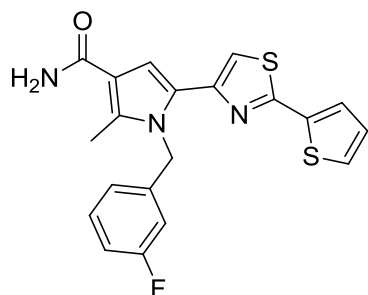
$^1\text{H NMR}$ (300 MHz, CDCl_3): δ_{H} 7.43 (d, $J = 3.60$, 1H, thiophene), 7.35 (d, $J = 4.98$, 1H, thiophene), 7.17 (d, $J = 6.37$, 2H, H_{Ar}), 7.03 (dd, $J = 3.60, 4.71$, 1H, thiophene), 6.99 (d, $J = 6.65$, 2H, H_{Ar}), 6.98 (s, 1H, thiazole), 5.99 (b, 1H, NH), 5.84 (s, 1H, pyrrole), 3.87 (s, 3H, OMe), 2.96 (d, $J = 4.15$, 3H, NHCH_3), 2.35 (s, 3H, Me).

$^{13}\text{C NMR}$ (75 MHz, CDCl_3): δ_{C} 166.8 (q, CO), 160.6 (q, thiazole), 160.2 (q, C_{Ar}), 147.9 (q, thiazole), 137.5 (q, thiophene), 137.5 (q, pyrrole), 131.3 (q, C_{Ar}), 130.1 (t, 2C, C_{Ar}), 128.8 (q, pyrrole), 128.1 (t, 2C, thiophene), 127.0 (t, thiophene), 115.7

(q, pyrrole), 115.1 (t, 2C, C_{Ar}), 110.1 (t, thiazole), 108.5 (t, pyrrole), 56.0 (s, CH₃, OMe), 26.5 (s, CH₃. NHCH₃), 12.4 (s, Me).

HRMS *m/z* calcd for C₂₁H₂₀N₃O₂S₂ [M + H]⁺, 410.0991; found, 410.0970.

3.3.5 1-(3-fluorobenzyl)-2-methyl-5-(2-(thiophen-2-yl)thiazol-4-yl)-1H-pyrrole-3-carboxamide (71)



Isolated yield 45% over two steps

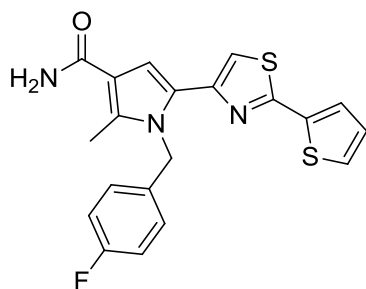
R_f = 0.25 (DCM).

¹H NMR (300 MHz, CDCl₃): δ_H 7.43 (d, *J* = 3.77, 1H, thiophene), 7.35 (d, *J* = 4.80, 1H, thiophene), 7.23 (q, 1H, H_{Ar}), 7.17 (s, 1H, thiazole), 7.04 (dd, *J* = 3.74, 5.18, 1H, thiophene), 6.98 (s, 1H, pyrrole), 6.91 (t, 1H, H_{Ar}), 6.78 (d, *J* = 8.25, 1H, H_{Ar}), 6.73 (d, *J* = 9.06, 1H, H_{Ar}), 5.88 (b, 2H, NH₂), 5.61 (s, 2H, CH₂), 2.58 (s, 3H, Me).

¹³C NMR (75 MHz, CDCl₃): δ_C 164.3 (q, CO), 161.9 (q, C_{Ar}), 161.3 (q, thiazole), 161.0 (q, C_{Ar}), 147.6 (q, thiazole), 140.7 (q, thiophene), 140.0 (q, d, *J* = 7.29 Hz, C_{Ar}, F coupling), 137.2 (q, pyrrole), 130.2 (t, d, *J* = 8.06 Hz, C_{Ar}, F coupling), 127.9 (t, thiophene), 127.9 (t, thiophene), 127.4 (q, pyrrole), 126.6 (t, thiophene), 121.7 (t, d, *J* = 3.04 HZ, C_{Ar}, F coupling), 114.2 (t, thiophene), 114.1 (t, d, *J* = 21.09 HZ, C_{Ar}, F coupling), 113.2 (t, d, *J* = 22.76 HZ, C_{Ar}, F coupling), 111.8 (q, pyrrole), 111.6 (t, pyrrole), 48.1 (d, CH₂), 11.6 (s, Me).

HRMS *m/z* calcd for C₂₀H₁₇FN₃OS₂ [M + H]⁺, 398.0792; found, 398.0800.

3.3.6 1-(4-fluorobenzyl)-2-methyl-5-(2-(thiophen-2-yl)thiazol-4-yl)-1*H*-pyrrole-3-carboxamide (72)



Isolated yield 37% over two steps

$R_f = 0.29$ (DCM).

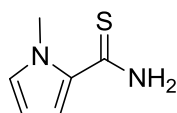
$^1\text{H NMR}$ (300 MHz, CDCl_3): δ_{H} 7.44 (d, $J = 3.56$ Hz, 1H, thiophene), 7.35 (d, $J = 4.07$ Hz, 1H, thiophene), 7.14 (s, 1H, thiazole), 7.04 (dd, $J = 3.56, 5.22$ Hz, 1H, thiophene), 7.00 – 6.93 (m, 3H, H_{Ar}), 6.96 (s, 1H, pyrrole), 6.96 – 6.93 (m, 1H, H_{Ar}), 5.79 (b, 2H, NH_2), 5.56 (s, 2H, CH_2), 2.58 (s, 3H, Me).

$^{13}\text{C NMR}$ (75 MHz, CDCl_3): δ_{C} 163.5 (q, CO), 161.6 (q, C_{Ar}), 161.4 (q, C_{Ar}), 161.1 (q, thiazole), 148.0 (q, thiazole), 141.0 (q, thiophen), 137.5 (q, pyrrole), 133.3 (q, d, $J = 3.01$ Hz, C_{Ar} , F coupling), 128.2 (t, d, $J = 8.02$ Hz, 2C C_{Ar} , F coupling), 128.2 (t, 2C, thiophene), 127.7 (q, pyrrole), 126.9 (t, thiophen), , 115.8 (t, d, $J = 21.67$ Hz, 2C, C_{Ar} , F coupling), 114.6 (t, thiazole), 112.1 (q, pyrrole), 111.9 (t, pyrrole), 48.2 (d, CH_2), 12.0 (s, Me).

HRMS m/z calcd for $\text{C}_{20}\text{H}_{17}\text{FN}_3\text{OS}_2$ $[\text{M} + \text{H}]^+$, 398.0792; found, 398.0799.

4 Synthesis of the derivative with N-methyl pyrrole on the right side.

4.1 1-methyl-1*H*-pyrrole-2-carbothioamide (26)



This compound was prepared by the same synthetic method of generation of thiophene-2-carbothioamide (**6**).

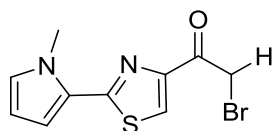
The raw product was clean judged by TLC hence no purification: collected yield 59%.

$R_f = 0.76$ (DCM:MeOH = 20 :1).

$^1\text{H NMR}$ (300 MHz, MeOD): δ_{H} 6.93 (t, 1H, pyrrole), 6.73 (dd, $J = 1.75, 4.02$, 1H, pyrrole), 6.10 (dd, $J = 2.63, 4.16$, 1H, pyrrole), 4.05 (s, 3H, Me).

$^{13}\text{C NMR}$ (75 MHz, MeOD): δ_{C} 192.0 (q, CS), 133.8 (q, pyrrole), 131.9 (t, pyrrole), 113.6 (t, pyrrole), 108.2 (t, pyrrole), 37.9 (s, Me).

4.2 2-bromo-1-(2-(1-methyl-1H-pyrrol-2-yl)thiazol-4-yl)ethanone (29)



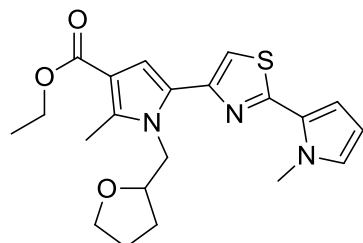
1.2 g 1,4-dibromobutane-2,3-dione (**10**) (4.96 mmol) was dissolved in 9 mL anhydrous THF, 312.8 mg 1-methyl-1H-pyrrole-2-carbothioamide (**26**) was also dissolved in 9 mL anhydrous THF and this solution was slowly introduced to 1,4-dibromobutane-2,3-dione (**10**) THF solution and followed by 0.4 mL DIPEA (2.48 mmol). This mixture was allowed to be stirred at RT for 15 min. and the starting material is completely consumed (TLC, DCM:PE = 5:1). After the reaction, the mixture was poured into 30 mL saturated sodium hydrogen carbonate solution, and the aqueous layer was extracted 3 times with chloroform (3 × 20 mL). The combined organic layer was then dried over sodium sulfate and the solvent was removed. The raw material was then subject to the flash chromatography (DCM:PE = 2 :1) to yield a slight red crystal. (287.6 mg, 41%)

$R_f = 0.63$ (DCM:PE = 5:1).

$^1\text{H NMR}$ (300 MHz, CDCl_3): δ_{H} 8.06 (s, 1H, thiazole), 6.78 (t, $J = 1.88$ Hz, 1H, pyrrole), 6.71 (t, $J = 3.96$ Hz, 1H, pyrrole), 6.16 (dd, $J = 2.64, 3.88$ Hz, 1H, pyrrole), 4.61 (s, 2H, CH_2), 4.05 (s, 3H, Me).

¹³C NMR (75 MHz, MeOD): δ_{C} 185.8 (q, CO), 161.4 (q, thiazole), 151.8 (q, thiazole), 127.6 (t, thiazole), 125.5 (q, pyrrole), 124.6 (t, pyrrole), 113.7 (t, pyrrole), 108.7 (t, pyrrole), 36.9 (s, Me), 33.1 (d, CH₂).

4.3 Ethyl 2-methyl-5-(2-(1-methyl-1*H*-pyrrol-2-yl)thiazol-4-yl)-1-((tetrahydrofuran-2-yl)methyl)-1*H*-pyrrole-3-carboxylate (31)



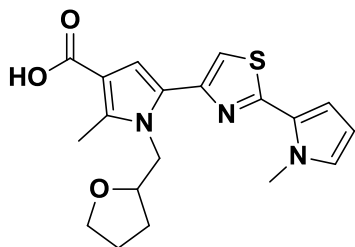
This compound was prepared through the same method of generation ethyl 2-methyl-1-((tetrahydrofuran-2-yl)methyl)-5-(2-(thiophen-2-yl)thiazol-4-yl)-1*H*-pyrrole-3-carboxylate (**13**) and was isolated in 37% yield as a pink solid.

$R_f = 0.56$ (DCM:EtOAc = 40 :1).

¹H NMR (300 MHz, CDCl₃): δ_{H} 7.39 (s, 1H, thiazole), 6.96 (s, 1H, pyrrole), 6.87 (t, $J = 2.03$ Hz, 1H, *N*-methyl pyrrole), 6.83 (dd, $J = 3.05, 4.07$ Hz, 1H, *N*-methyl pyrrole), 6.30 (dd, $J = 3.05, 3.56$ Hz, 1H, pyrrole), 4.69 (dd, $J = 4.58, 14.50$ Hz, 1H, CH, THF), 4.50 (dd, $J = 7.12, 14.54$ Hz, 1H, CH₂), 4.41 (q, $J = 7.12$ Hz, 2H, CH₂, OEt), 4.21 – 4.15 (m, 1H, CH₂), 4.14 (s, 3H, CH₃, *N*-methyl pyrrole), 3.89 – 3.73 (m, 2H, THF), 2.78 (s, 3H, Me), 1.97 – 1.84 (m, 3H, THF), 1.62 – 1.52 (m, 1H, THF), 1.48 (t, $J = 7.12$ Hz, 3H, CH₃, OEt).

¹³C NMR (75 MHz, MeOD): δ_{C} 164.6 (q, CO), 58.7 (q, thiazole), 148.4 (q, thiazole), 138.1 (q, pyrrole), 126.9 (q, pyrrole), 126.7 (q, *N*-methyl pyrrole), 126.6 (t, *N*-methyl pyrrole), 126.6 (t, thiazole), 112.3 (t, *N*-methyl pyrrole), 112.0 (q, pyrrole), 111.1 (t, *N*-methyl pyrrole), 108.3 (t, pyrrole), 78.4 (t, THF), 67.9 (d, THF), 59.3 (d, CH₂, OEt), 48.1 (d, CH₂), 36.8 (s, CH₃, *N*-methyl pyrrole), 28.9 (d, THF), 25.4 (d, THF), 14.5 (s, CH₃, OEt), 11.7 (s, Me).

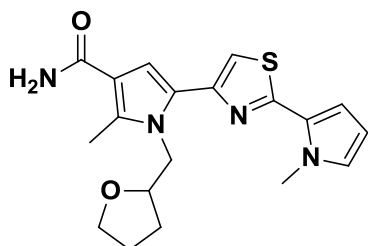
4.4 2-methyl-5-(2-(1-methyl-1*H*-pyrrol-2-yl)thiazol-4-yl)-1-((tetrahydrofuran-2-yl)methyl)-1*H*-pyrrole-3-carboxylic acid (**33**)



37.8 mg ethyl 2-methyl-5-(2-(1-methyl-1*H*-pyrrol-2-yl)thiazol-4-yl)-1-((tetrahydrofuran-2-yl)methyl)-1*H*-pyrrole-3-carboxylate (**31**) (0.095 mmol) was dissolved in a flask with 0.3 mL ethanol. 0.6 mL 10% KOH ethanol solution (0.93 mmol) was then added to the flask then the mixture was allowed to react under reflux for 48 hours and monitored by the TLC. (TLC, DCM :EtOAc = 20 : 1 with 0.1% acetic acid). After the reaction, the mixture was neutralized by 10 mL 1 M HCl solution and the aqueous layer was extracted 3 times with chloroform (3 × 5 mL). The combined organic layer was then dried over sodium sulfate and concentrated to give the pink raw product. The raw product was then utilized for the amide formation without purification.

$R_f = 0.42$ (DCM:EtOAc = 20 : 1 : 1 with 0.1% AcOH)

4.5 2-methyl-5-(2-(1-methyl-1*H*-pyrrol-2-yl)thiazol-4-yl)-1-((tetrahydrofuran-2-yl)methyl)-1*H*-pyrrole-3-carboxamide (**35**)



This compound was prepared by following the same procedure of generation of 2-methyl-1-((tetrahydrofuran-2-yl)methyl)-5-(2-(thiophen-2-yl)thiazol-4-yl)-1*H*-pyrrole-3-carboxamide (**19**) in 39% yield over 2 steps as the pale red crystal.

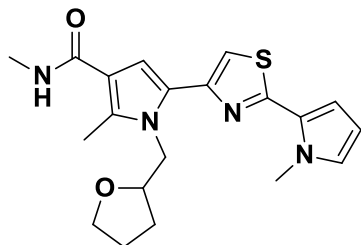
$R_f = 0.3$ (DCM:EtOAc = 40 : 1).

¹H NMR (300 MHz, CDCl₃): δ_H 7.13 (s, 1H, thiazole), 6.86 (s, 1H, pyrrole), 6.74 (t, *J* = 2.03 Hz, 1H, *N*-methyl pyrrole), 6.70 (dd, *J* = 1.53, 5.59 Hz, 1H, *N*-methyl pyrrole), 6.16 (dd, *J* = 2.54, 4.07 Hz, 1H, *N*-methyl pyrrole), 5.92 (b, 2H, NH₂), 4.56 (dd, *J* = 4.58, 14.24 Hz, 1H, CH, THF), 4.38 (dd, *J* = 7.63, 14.24 Hz, 1H, CH₂), 4.08 – 4.02 (m, 1H, CH₂), 4.00 (s, CH₃, *N*-methyl pyrrole), 3.75 – 3.61 (m, 2H, THF), 2.69 (s, 3H, Me), 1.86 – 1.72 (m, 3H, THF), 1.49 – 1.39 (m, 1H, THF).

¹³C NMR (75 MHz, CDCl₃): δ_C 161.0 (q, CO), 160.5 (q, thiazole), 147.8 (q, Thiazole), 140.8 (q, pyrrole), 127.2 (q, *N*-methyl pyrrole), 126.5 (t, *N*-methyl pyrrole), 126.5 (q, pyrrole), 112.8 (t, *N*-methyl pyrrole), 112.5 (t, *N*-methyl pyrrole), 111.5 (t, thiazole), 111.1 (q, pyrrole), 108.2 (t, pyrrole), 78.2 (t, THF), 67.8 (t, THF), 48.2 (d, CH₂), 36.7 (d, THF), 28.8 (d, THF), 25.3 (d, THF), 11.8 (s, Me).

HRMS *m/z* calcd for C₁₉H₂₅N₄O₂S [M + H]⁺, 371.1536; found, 371.1614.

4.6 *N*,2-dimethyl-5-(2-(1-methyl-1H-pyrrol-2-yl)thiazol-4-yl)-1-((tetrahydrofuran-2-yl)methyl)-1H-pyrrole-3-carboxamide (**36**)



This compound was prepared by following the same procedure of generation of *N*,2-dimethyl-1-((tetrahydrofuran-2-yl)methyl)-5-(2-(thiophen-2-yl)thiazol-4-yl)-1H-pyrrole-3-carboxamide (**20**) in 52% yield over 2 steps as the pale red crystal.

R_f = 0.21 (DCM:MeOH = 30:1).

¹H NMR (300 MHz, MeOD): δ_H 7.05 (s, 1H, thiazole), 6.73 (t, *J* = 2.07 Hz, 1H, *N*-methyl pyrrole), 6.69 (dd, *J* = 1.70, 3.77 Hz, 1H, *N*-methyl pyrrole), 6.48 (s, 1H, pyrrole), 6.16 (dd, *J* = 2.64, 3.77 Hz, 1H, pyrrole), 5.77 (b, 1H, NH), 4.48 (dd, *J* = 5.09, 14.06 Hz, 1H, CH, THF), 4.34 (dd, *J* = 6.97, 14.65 Hz, 1H, CH₂), 4.07 – 4.02 (m, 1H, CH₂), 4.00 (s, 3H, Me, *N*-methyl pyrrole), 3.78 – 3.56 (m, 2H, THF),

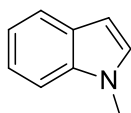
2.92 (s, 3H, CH₃, NHCH₃), 2.65 (s, 3H, Me), 1.81 – 1.71 (m, 3H, THF), 1.50 – 1.35 (m, 1H, THF).

¹³C NMR (75 MHz, CDCl₃): δ_C 166.5 (q, CO), 160.5 (q, thiazole), 148.4 (q, Thiazole), 135.7 (q, pyrrole), 126.8 (q, pyrrole), 126.6 (t, *N*-methyl pyrrole), 126.6 (q, *N*-methyl pyrrole), 112.6 (t, *N*-methyl pyrrole), 111.9 (t, *N*-methyl pyrrole), 108.4 (t, thiazole), 107.6 (t, pyrrole), 78.3 (t, THF), 67.9 (d, THF), 48.0 (d, CH₂), 36.9 (s, CH₃, *N*-methyl pyrrole), 29.0 (d, THF), 26.1 (s, CH₃, NHCH₃), 11.5 (s, Me).

HRMS *m/z* calcd for C₂₀H₂₅N₄O₂S [M + H]⁺, 385.1693; found, 371.1694.

5 Synthesis of derivative with *N*-methyl indole on the right side.

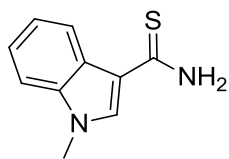
5.1 1-methyl-1*H*-indole (27)



3.02 g sodium hydride (60% dispersed in mineral oil) (75 mmol) was loaded in a flask and washed twice under inert gas with pentane and then dried in *vacuo*. The dry sodium hydride was dispersed in 5 mL anhydrous THF. 5.82 g Indole (50 mmol) was dissolved at 0 °C in 15 mL anhydrous THF and slowly introduced into the flask loaded with sodium hydride. The mixture was allowed to be stirred at 0 °C for 10 min. then 4.2 mL methyl iodide (67 mmol) was slowly added. The temperature was warmed to RT and the mixture was stirred at this temperature for 2 hours. After the starting material was consumed as judged by the TLC (PE:EtOAc = 10 :1), the mixture was again cooled to the 0 °C and 30 mL saturated ammonium chloride solution was added. The aqueous layer was then extracted 3 times with ethyl acetate (3 × 20 mL) and the combined organic layer was washed sequentially with 20 mL 1 M HCl solution, 20 mL saturated ammonium chloride solution and 20 mL saturated brine. Then the organic layer was dried over sodium sulfate and the solvent was completely removed. The resulted raw product (colorless liquid) was utilized without further purification for the next step.

R_f = 0.78 (PE:EtOAc = 10 :1).

5.2 1-methyl-1H-indole-3-carbothioamide (**28**)



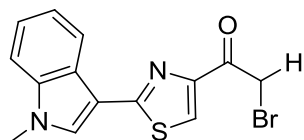
1.5 g unpurified 1-methyl-1H-indole (**27**) (11.4 mmol) was carefully dissolved at 0 °C in 17 mL methyl sulfonic acid (263 mmol) and 2.56 g potassium thiocyanate (26.3 mmol) was added to this mixture. The mixture was stirred at RT for 30 hours and monitored by the TLC (DCM:EtOAc = 15 :1). After the reaction, the reaction mixture was poured into the ice water and the red precipitation was then filtered and washed with very little amount of ethyl acetate. The precipitation was then dried in *vacuo* and subject to the flash chromatography to yield the pale red solid. (685.9 mg, 32%)

$R_f = 0.3$ (DCM:EE = 15 :1)

mp: 136 °C

The melting point is in consistence with the reference.^[44]

5.3 2-bromo-1-(2-(1-methyl-1H-indol-3-yl)thiazol-4-yl)ethanone (**30**)



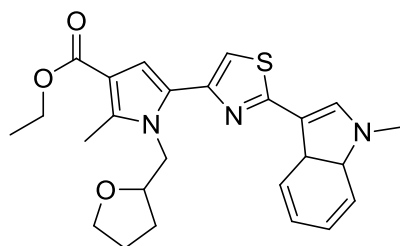
100 mg 1-methyl-1H-indole-3-carbothioamide (**28**) (0.57 mmol) was dissolved in 9 mL absolute ethanol and 281.3 mg 1,4-dibromobutane-2,3-dione (**10**) (1.14 mmol dissolved in 9 mL absolute ethanol) was slowly introduced to this solution. The mixture was stirred at RT for 30 min. and the reaction was concluded as judged by the TLC (TLC, DCM:EtOAc = 30 :1). After the reaction, the ethanol was evaporated and 15 mL saturated sodium hydrogen carbonate solution was added. The aqueous layer was then extracted 3 times with chloroform (3 × 10 mL) and the combined organic layer was dried over sodium sulfate. After evaporation of the solvent, the raw product was subject to the flash chromatography (DCM:EtOAc = 30:1) to yield the pale red crystal. (54.5 mg, 29%)

$R_f = 0.35$ (DCM:EtOAc 30:1).

$^1\text{H NMR}$ (300 MHz, MeOD): δ_{H} 8.30 – 8.24 (m, 1H, H_{Ar}), 8.09 (s, 1H, thiazole), 7.69 (s, 1H, pyrrole (indole)), 7.38 – 7.30 (m, 3H, H_{Ar}), 4.78 (s, 2H, CH_2), 3.84 (s, 3H, Me).

$^{13}\text{C NMR}$ (75 MHz, MeOD): δ_{C} 168.5 (q, CO), 163.9 (q, thiazole), 152.2 (q, thiazole), 137.7 (q, C_{Ar}), 130.0 (t, pyrrole), 125.5 (q, C_{Ar}), 124.0 (t, thiazole), 123.6 (t, C_{Ar}), 122.0 (t, C_{Ar}), 121.3 (t, C_{Ar}), 110.4 (q, pyrrole), 110.3 (t, C_{Ar}), 34.3 (s, CH_3 , *N*-methyl), 33.7 (d, CH_2).

5.4 Ethyl 2-methyl-5-(2-(1-methyl-3a,7a-dihydro-1*H*-indol-3-yl)thiazol-4-yl)-1-((tetrahydrofuran-2-yl)methyl)-1*H*-pyrrole-3-carboxylate (**32**)



This compound was prepared through the same procedure of generation of ethyl 2-methyl-1-((tetrahydrofuran-2-yl)methyl)-5-(2-(thiophen-2-yl)thiazol-4-yl)-1*H*-pyrrole-3-carboxylate (**13**) in 41 % yield as the pale red solid.

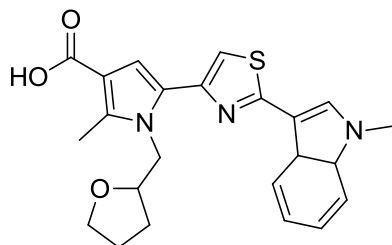
$R_f = 0.2$ (DCM:EtOAc = 30 :1).

$^1\text{H NMR}$ (300 MHz, CDCl_3): δ_{H} 8.24 (d, $J = 7.99$, 1H, H_{Ar}), 7.70 (s, 1H, thiazole), 7.36 (t, 1H, H_{Ar}), 7.34 – 7.26 (m, 2H, H_{Ar}), 7.15 (s, 1H, pyrrole (indole)), 6.86 (s, 1H, H_{Ar}), 4.72 (dd, $J = 3.73, 12.25$, 1H, THF), 4.41 (q, 1H, THF), 4.28 (q, 2H, CH_2 , OEt), 4.21 – 4.11 (m, 1H, THF), 3.85 (s, 3H, *N* – methyl), 3.67 (dq, $J = 31.97$, 2H, THF), 2.67 (s, 3H, Me), 1.86 – 1.75 (m, 1H, THF), 1.75 – 1.69 (m, 2H, THF), 1.52 – 1.41 (m, 1H, THF), 1.35 (t, 3H, CH_3 , OEt).

$^{13}\text{C NMR}$ (75 MHz, CDCl_3): δ_{C} 165.5 (q, CO), 162.3 (q, thiazole), 148.3 (q, thiazole), 138.2 (q, C_{Ar}), 137.3 (q, pyrrole), 129.1 (t, pyrrole (indole)), 127.1 (q, pyrrole), 125.1 (q, C_{Ar}), 122.8 (t, C_{Ar}), 121.1 (t, C_{Ar}), 120.9 (t, C_{Ar}), 112.0 (q, pyrrole), 111.3 (t, thiazole), 111.1 (q, pyrrole (indole)), 110.9 (t, C_{Ar}), 109.8 (t,

pyrrole), 78.7 (t, THF), 67.9 (d, THF), 59.2 (d, CH₂, OEt), 48.4 (d, CH₂), 33.2 (s, CH₃, *N*-methyl), 28.9 (d, THF), 25.4 (d, THF), 14.6 (s, CH₃, OEt), 11.8 (s, Me).

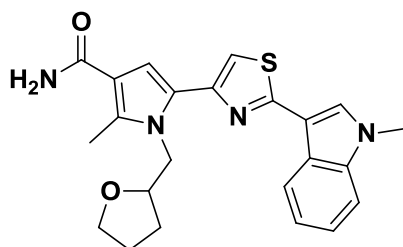
5.5 2-methyl-5-(2-(1-methyl-3a,7a-dihydro-1*H*-indol-3-yl)thiazol-4-yl)-1-((tetrahydrofuran-2-yl)methyl)-1*H*-pyrrole-3-carboxylic acid (34)



20.6 mg ethyl 2-methyl-5-(2-(1-methyl-3a,7a-dihydro-1*H*-indol-3-yl)thiazol-4-yl)-1-((tetrahydrofuran-2-yl)methyl)-1*H*-pyrrole-3-carboxylate (**32**) (0.05 mmol) was dissolved in a *t*-Butyl alcohol / methanol mixture (2 mL:2 mL). Under inert gas 1 mL 10% KOH ethanol solution (1.6 mmol) was introduced to this solution. The mixture was then stirred at 60 °C and monitored by the TLC (DCM:EtOAc:MeOH = 20 :1:1 with 0.1% acetic acid). After 36 hours the reaction concluded, then the mixture was acidified with 1M HCL solution and the aqueous layer was extracted 3 times with chloroform (3 × 10 mL). The combined organic layer was dried over sodium sulfate and concentrated in *vacuo*. The raw product was used for the amide formation without further purification.

$R_f = 0.38$ (DCM:EtOAc: MeOH = 20 : 1 : 1 with 0.1% AcOH)

5.6 2-methyl-5-(2-(1-methyl-3a,7a-dihydro-1*H*-indol-3-yl)thiazol-4-yl)-1-((tetrahydrofuran-2-yl)methyl)-1*H*-pyrrole-3-carboxamide (37)



This compound was prepared through the same procedure of generation of 2-methyl-1-((tetrahydrofuran-2-yl)methyl)-5-(2-(thiophen-2-yl)thiazol-4-yl)-1*H*-pyrrole-3-carboxamide (**19**) in 62% yield over 2 steps as the pale red solid.

$R_f = 0.21$ (DCM:EE = 8 : 1).

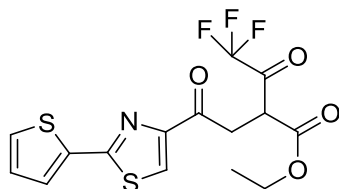
¹H NMR (300 MHz, CDCl₃): δ_H 8.24 (d, *J* = 7.93, 1H, H_{Ar}), 7.71 (s, 1H, thiazole), 7.32 (t, 2H, H_{Ar}), 7.18 (s, 1H, pyrrole (indole)), 6.92 (s, 1H, pyrrole), 5.77 (b, 2H, NH₂), 4.73 (dd, *J* = 4.20, 15.11, 1H, THF), 4.44 (q, 1H, THF), 4.23 – 4.14 (m, 1H, THF), 3.86 (s, 3H, CH₃, *N*-methyl), 3.76 – 3.60 (m, 2H, THF), 3.73 (s, Me), 1.88 – 1.79 (m, 1H, THF), 1.79 – 1.68 (m, 2H, THF), 1.53 – 1.44 (m, 1H, THF).

¹³C NMR (75 MHz, CDCl₃): δ_C 162.5 (q, CO), 161.3 (q, thiazole), 147.9 (q, thiazole), 141.0 (q, C_{Ar}), 137.3 (q, pyrrole), 129.1 (t, pyrrole (indole)), 127.6 (q, pyrrole), 125.2 (q, C_{Ar}), 122.8 (t, C_{Ar}), 121.2 (t, C_{Ar}), 120.9 (t, C_{Ar}), 111.9 (t, Thiazole), 111.6 (t, C_{Ar}), 111.3 (q, pyrrole), 111.1 (q, pyrrole (indole)), 109.8 (t, pyrrole), 78.6 (t, THF), 68.0 (d, THF), 48.6 (d, THF), 33.2 (s, CH₃; *N*-methyl), 29.0 (d, THF), 25.5 (d, THF), 12.0 (s, Me).

HRMS *m/z* calcd for C₂₃H₂₅N₄O₂S [M + H]⁺, 421.1693; found, 421.1663.

6 Synthesis of 2-trifluoromethyl pyrrole derivative.

6.1 Ethyl 4,4,4-trifluoro-3-oxo-2-(2-oxo-2-(2-(thiophen-2-yl)thiazol-4-yl)ethyl)butanoate (41)

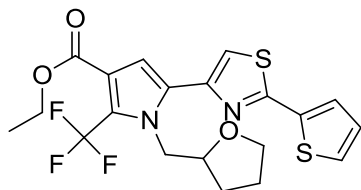


30.4 mg sodium hydride (60% dispersed in mineral oil, 0.72 mmol) was washed twice under inert gas with pentane and then dried in *vacuo*. Dry sodium hydride was dispersed in 1.4 mL dimethoxyethane afterwards and 102 μL ethyl 4,4,4-trifluoro-3-oxobutanoate (**38**) (0.34 mmol) was dropwise added to the dispersion at 0 °C. The mixture was stirred at 0 °C for 10 min. and 100 mg 2-bromo-1-(2-(thiophen-2-yl)thiazol-4-yl)ethanone (**2**) (0.34 mmol in 2 mL dimethoxyethane) was slowly introduced at the same temperature. The temperature was then warmed to the RT and the mixture was then stirred under reflux overnight. After the starting material was completely consumed (TLC, DCM:PE = 3 :1), the mixture was poured to 4 mL water and the aqueous layer was adjusted to about pH = 2 with 2M HCl solution. The aqueous layer was then extracted 3 times with ethyl acetate (3 × 10 mL) and the combined organic layer was dried over sodium

sulfate and concentrated in vacuo. The resulted raw product (162 mg) was used without purification for the next step.

$R_f = 0.25$ (DCM:PE = 3 :1).

6.2 Ethyl 1-((tetrahydrofuran-2-yl)methyl)-5-(2-(thiophen-2-yl)thiazol-4-yl)-2-(trifluoromethyl)-1H-pyrrole-3-carboxylate (**40**)



The raw starting material 4,4,4-trifluoro-3-oxo-2-(2-oxo-2-(2-(thiophen-2-yl)thiazol-4-yl)ethyl)butanoate (**41**) (162 mg 0.41 mmol) was dissolved in 4 mL absolute ethanol, to this solution 40 μ L furan-2-ylmethanamine (**4**) (0.41 mmol) was then slowly introduced and followed by 4 drops of acetic acid. The mixture was stirred under reflux for 3 hours until the starting material was completely consumed. (TLC, DCM:PE = 3:1 \rightarrow DCM). After the reaction the mixture was diluted with 5 mL ethyl acetate and washed sequentially with 10 mL saturated sodium hydrogen carbonate solution and 10 mL water. The organic layer was then dried over sodium sulfate and the solvent was removed. The raw product was then subject to the flash chromatography (DCM \rightarrow DCM:EtOAc = 40:1) to yield the white crystal. (29.9 mg, 16% over 2 steps)

$R_f = 0.28$ (DCM).

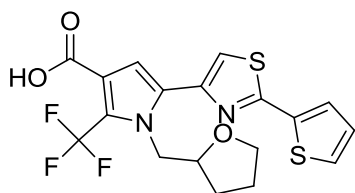
$^1\text{H NMR}$ (300 MHz, CDCl_3): δ_{H} 7.54 (d, $J = 3.66$, 1H, thiophene), 7.41 (d, $J = 4.97$, 1H, thiophene), 7.35 (s, 1H, thiazole), 7.09 (dd, $J = 3.79, 4.97$, 1H, THF), 6.86 (s, 1H, pyrrole), 4.70 (q, 1H, THF), 4.58 (dd, $J = 3.93, 14.92$, 1H, THF), 4.30 (q, $J = 7.03$ Hz, 2H, CH_2 , OEt), 4.19 – 4.13 (m, 1H, THF), 3.64 – 3.56 (m, 1H, THF), 3.53 – 3.44 (m, 1H, THF), 1.97 – 1.87 (m, 1H, THF), 1.80 – 1.71 (m, 2H, THF), 1.56, 1.46 (m, 1H, THF), 1.34 (t, $J = 7.32$ Hz, 3H, CH_3 , OEt).

$^{13}\text{C NMR}$ (75 MHz, CDCl_3): δ_{C} 163.5 (q, CO), 161.9 (q, thiazole), 148.0 (q, thiazole), 137.4 (q, thiophene), 131.1 (q, pyrrole), 128.5 (t, thiophene), 128.4 (t,

thiophene), 127.3 (t, thiophene), 123.2 (q, pyrrole), 119.1 (q, pyrrole), 117.1 (t, thiazole), 113.6 (t, pyrrole), 78.7 (t, THF), 68.4 (d, THF), 51.2 (d, CH₂), 29.5 (d, THF), 25.9 (d, THF), 14.6 (s, Me).

CF₃ is invisible in ¹³C spectrum

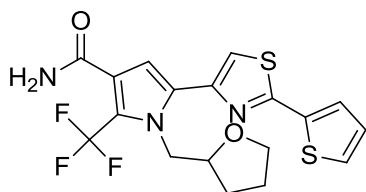
6.3 1-((tetrahydrofuran-2-yl)methyl)-5-(2-(thiophen-2-yl)thiazol-4-yl)-2-(trifluoromethyl)-1*H*-pyrrole-3-carboxylic acid (**42**)



21.2 mg ethyl 1-((tetrahydrofuran-2-yl)methyl)-5-(2-(thiophen-2-yl)thiazol-4-yl)-2-(trifluoromethyl)-1*H*-pyrrole-3-carboxylate (**40**) (0.05 mmol) was dissolved in 0.4 mL ethanol and 0.4 mL 10% KOH ethanol solution (0.62 mmol) was also added. The mixture was stirred under reflux for 2 hours until the starting material was completely consumed (TLC, DCM:EtOAc = 40:1 with 0.1% acetic acid). After the reaction, the mixture was neutralized with 1 M HCl solution. The aqueous layer was then extracted 3 times with chloroform (3 × 10 mL). The combined organic layer was then dried over sodium sulfate and the solvent was removed. The raw product was then deployed for the next step without purification.

R_f = 0.28 (DCM:EtOAc = 40 :1 with 0.1% AcOH).

6.4 1-((tetrahydrofuran-2-yl)methyl)-5-(2-(thiophen-2-yl)thiazol-4-yl)-2-(trifluoromethyl)-1*H*-pyrrole-3-carboxamide (**43**)



28.9 mg unpurified raw product 1-((tetrahydrofuran-2-yl)methyl)-5-(2-(thiophen-2-yl)thiazol-4-yl)-2-(trifluoromethyl)-1*H*-pyrrole-3-carboxylic acid (**42**) (0.07 mmol), 20.9 mg HOBt·H₂O (0.14 mmol) and 26.1 mg EDC·HCl (0.14 mmol) were

loaded in a round flask and dissolved in 0.8 mL DMF at 0 °C, 3 mL 2 M NH₃ dioxan solution (1.6 mmol) was then added to the solution and the mixture was stirred at 60 °C for 2 hours. After the starting material was completely consumed (TLC, DCM:MeOH = 40 :1), the mixture was poured into 30 mL saturated sodium hydrogen carbonate solution. The aqueous layer was then extracted 3 times with ethyl acetate (3 × 15mL) and the combined organic layer was dried over sodium sulfate. Then the solvent was removed and the raw product was then purified by the flash chromatography to yield the pale white solid. (7.5 mg, 26% over 2 steps)

R_f = 0.17 (DCM:MeOH = 40 :1).

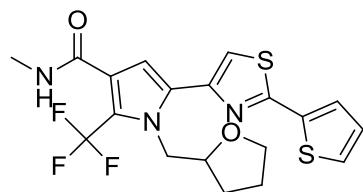
¹H NMR (300 MHz, CDCl₃): δ_H 7.54 (d, *J* = 2.54 Hz, 1H, thiophene), 7.41 (d, *J* = 5.09 Hz, 1H, thiophene), 7.34 (s, 1H, thiazole), 7.10 (dd, *J* = 3.56, 5.09 Hz, 1H, thiophene), 6.68 (s, 1H, pyrrole), 5.76 (b, 2H, NH₂) 4.67 (dd, *J* = 8.65, 14.85 Hz, 1H, THF), 4.53 (dd, *J* = 3.56, 14.85 Hz, 1H, CH₂), 4.20 – 4.13 (m, 1H, CH₂), 3.63 – 3.44 (m, 2H, THF), 2.00 – 1.89 (m, 1H, THF), 1.82 – 1.71 (m, 2H, THF), 1.57 – 1.47 (m, 1H, THF).

¹³C NMR (75 MHz, CDCl₃): δ_C 166.0 (q, CO), 161.6 (q, thiazole), 147.5 (q, thiazole), 137.0 (q, thiophene), 131.2 (q, pyrrole), 128.1 (t, thiophene), 128.0 (t, thiophene), 126.9 (t, thiophene), 122.5 (q, pyrrole), 119.8 (q, pyrrole), 116.4 (t, thiazole), 111.1 (t, pyrrole), 78.3 (t, THF), 68.0 (d, THF), 50.6 (d, CH₂), 29.1 (d, THF), 25.5 (d, THF).

CF₃ is invisible in ¹³C spectrum

HRMS *m/z* calcd for C₁₈H₁₇ F₃N₃O₂S₂ [M + H]⁺, 428.0709; found, 428.0709.

6.5 *N*-methyl-1-((tetrahydrofuran-2-yl)methyl)-5-(2-(thiophen-2-yl)thiazol-4-yl)-2-(trifluoromethyl)-1*H*-pyrrole-3-carboxamide (**44**)



26.4 mg unpurified 1-((tetrahydrofuran-2-yl)methyl)-5-(2-(thiophen-2-yl)thiazol-4-yl)-2-(trifluoromethyl)-1*H*-pyrrole-3-carboxylic acid (**42**) (0.06 mmol), 18.5 mg

HOBt·H₂O (0.12 mmol) and 23.6 mg EDC·HCl (0.12 mmol) were loaded in a flask and dissolved at 0 °C in 0.4 mL DMF. 25.6 methylamine hydrochloride (0.37 mmol) was then introduced to the flask and the mixture was allowed to react for 1 hour at RT and then overnight at 60 °C. After the starting material was gone (TLC DCM:EE = 40:1 with 0.1% acetic acid), 10 mL saturated sodium hydrogen carbonate solution was added. The aqueous layer was then extracted 3 times with ethyl acetate (3 × 10 mL) and the combined organic layer was dried over sodium sulfate and concentrated in *vacuo*. The raw product was purified by flash chromatography (DCM:MeOH = 80 :1 → 40:1) to yield the white crystal. (3.5 mg, 13% over 2 steps)

R_f = 0.35 (DCM:EE = 40:1).

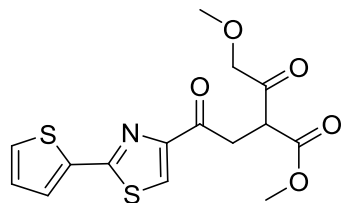
¹H NMR (300 MHz, CDCl₃): δ_H 7.54 (d, *J* = 3.80, 1H, thiophene), 3.41 (d, *J* = 5.02, 1H, thiophene), 7.33 (s, 1H, thiazole), 7.10 (dd, *J* = 3.71, 5.24, 1H, THF), 6.60 (s, 1H, pyrrole), 5.78 (b, 1H, NH), 4.65 (q, 1H, THF), 4.50 (dd, *J* = 3.49, 15.07, 1H, THF), 4.20 – 4.12 (m 1H, THF), 3.53 (dq, *J* = 39.75, 2H, THF), 2.95 (d, *J* = 5.68, CH₃, NHCH₃), 1.98 – 1.88 (m, 1H, THF), 1.82 – 1.71 (m, 2H, THF), 1.56 – 1.47 (m, 1H, THF).

¹³C NMR (75 MHz, CDCl₃): δ_C 165.2 (q, CO), 161.5 (q, thiazole), 147.7. (q, thiazole), 137.0 (q, thiophene), 131.2 (q, pyrrole), 128.1 (t, thiophene), 128.0 (t, thiophene), 127.0 (q, pyrrole), 126.9 (t, thiophene), 123.5 (q, pyrrole), 116.2. (t, thiazole), 110.6 (t, pyrrole), 78.3 (t, THF), 67.9 (d, THF), 50.5 (d, CH₂), 29.1 (d, THF), 26.8 (s, CH₃, NHCH₃), 25.5 (d, THF).

CF₃ and the nearby quartet carbon are invisible in ¹³C NMR spectrum.

7 Synthesis of 2-methoxymethyl pyrrole derivative

7.1 Ethyl 4-methoxy-3-oxo-2-(2-oxo-2-(2-(thiophen-2-yl)thiazol-4-yl)ethyl)butanoate (46)



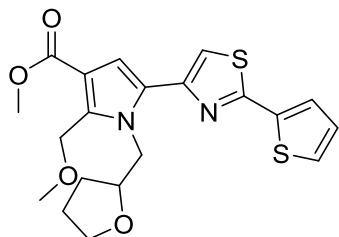
8.3 mg sodium hydride (60% dispersed in mineral oil, 0.2mmol) was washed under inert gas with pentane and dried in *vacuo*. Dry sodium hydride was then dispersed in 0.4 absolute THF. 22 μ L ethyl 4-methoxy-3-oxobutanoate (**45**) (0.17 mmol) was added at 0 °C and the mixture was stirred at the same temperature for 10 min. 52.6 mg 2-bromo-1-(2-(thiophen-2-yl)thiazol-4-yl)ethanone (**2**) was dissolved in 1 mL absolute THF and added at 0 °C, then mixture was warmed to RT and stirred for 3.5 hours. After the reaction (TLC DCM:EE = 40:1), the mixture was poured to 20 mL saturated ammonium chloride solution and the aqueous layer was extracted 3 times with DCM (3 \times 10 mL). The combined organic layer was then washed by the saturated brine solution and dried over sodium sulfate. The solvent was then removed and the raw product was subject to the flash chromatography (DCM \rightarrow DCM:EE = 40 :1) to yield white solid. (21 mg, 36%)

R_f = 0.11 (DCM).

^1H NMR (300 MHz, CDCl_3): δ_{H} 8.02 (s, thiazole), 7.54 (d, J = 4.07 Hz, 1H, thiophene), 7.44 (d, J = 5.09 Hz, 1H, thiophene), 7.08 (dd, J = 4.07, 5.09 Hz, 1H, thiophene), 4.32 (s, 2H, CH_2 , COCH_2OMe), 4.29 (q, J = 5.09 Hz, CH), 3.90 (dd, J = 8.65, 19.33 Hz, 1H, CH_2), 3.75 (s, 3H, CH_3 , COCH_2OMe), 3.71 (dd, J = 5.09, 19.15 Hz, 1H, CH_2), 3.46 (s, 3H, COOMe).

^{13}C NMR (75 MHz, CDCl_3): δ_{C} 203.1 (q, CO, COCH_2OMe), 192.1 (q, CO, COOMe), 169.5 (q, CO), 162.3 (q, thiazole), 154.2 (q, thiazole), 136.6 (q, thiophene), 129.1 (t, thiophene), 128.2 (t, thiophene), 127.9 (t, thiophene), 125.0 (t, thiazole), 77.5 (d, CH_2 , COCH_2OMe), 59.7 (s, CH_3 , COCH_2OMe), 53.0 (t, C), 49.2 (s, CH_3 , COOMe), 39.1 (d, CH_2).

7.2 Ethyl 2-(methoxymethyl)-1-((tetrahydrofuran-2-yl)methyl)-5-(2-(thiophen-2-yl)thiazol-4-yl)-1H-pyrrole-3-carboxylate (47)



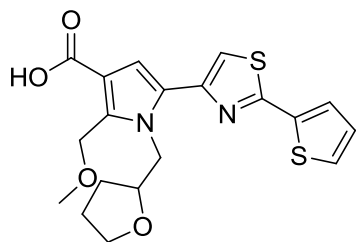
This compound was prepared by following the same procedure of generation of ethyl 1-((tetrahydrofuran-2-yl)methyl)-5-(2-(thiophen-2-yl)thiazol-4-yl)-2-(trifluoromethyl)-1H-pyrrole-3-carboxylate (**40**) in 82% yield.

$R_f = 0.46$ (DCM:EE = 40 :1).

$^1\text{H NMR}$ (300 MHz, CDCl_3): δ_{H} 7.51 (d, $J = 3.56$ Hz, 1H, thiophene), 7.38 (d, $J = 5.09$ Hz, 1H, thiophene), 7.25 (s, 1H, thiazole), 7.08 (dd, $J = 4.07, 5.09$ Hz, 1H, thiophene), 6.87 (s, 1H, pyrrole), 5.02 (dd, $J = 12.72, 66.12$ Hz, 2H, CH_2 , CH_2OMe), 4.48 (dd, $J = 8.65, 14.24$ Hz, 1H, CH_2), 4.29 – 4.21 (m, 1H, CH_2), 3.81 (s, CH_3 , OMe), 3.75 – 3.63 (m, 2H; THF), 3.36 (s, 3H, CH_3 , CH_2OMe), 2.06 – 1.97 (m, 1H, THF), 1.86 – 1.76 (m, 2H, THF), 1.58 – 1.50 (m, 1H, THF).

$^{13}\text{C NMR}$ (75 MHz, CDCl_3): δ_{C} 165.6 (q, CO), 161.3 (q, thiazole), 148.9 (q, thiazole), 137.7 (q, thiophene), 136.6 (q, pyrrole), 136.6 (q, pyrrole), 128.2 (t, thiophene), 128.0 (t, thiophene), 126.8 (t, thiophene), 114.7 (q, pyrrole), 114.3 (t, thiazole), 111.4 (t, pyrrole), 79.5 (t, THF), 68.3 (d, THF), 63.3 (d, CH_2 , CH_2OMe), 57.8 (s, CH_3 , CH_2OMe), 51.2 (s, CH_3 , OMe), 49.8 (d, CH_2), 29.4 (d, THF), 25.9 (d, THF).

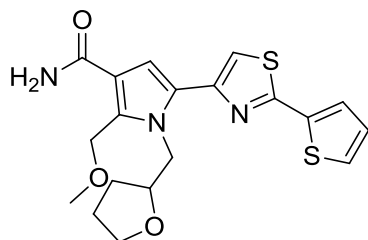
7.3 Ethyl 2-(methoxymethyl)-1-((tetrahydrofuran-2-yl)methyl)-5-(2-(thiophen-2-yl)thiazol-4-yl)-1*H*-pyrrole-3-carboxylate (**48**)



This compound was prepared through the same procedure of synthesis of 1-((tetrahydrofuran-2-yl)methyl)-5-(2-(thiophen-2-yl)thiazol-4-yl)-2-(trifluoromethyl)-1*H*-pyrrole-3-carboxylic acid (**42**). The resulted raw product was used for the next step without any purification.

$R_f = 0.2$ (DCM:EtOAc = 40 :1 with 0.1% AcOH).

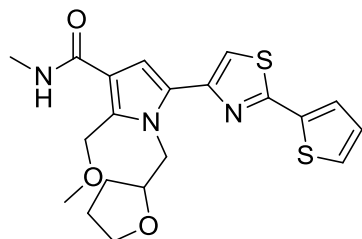
7.4 2-(methoxymethyl)-1-((tetrahydrofuran-2-yl)methyl)-5-(2-(thiophen-2-yl)thiazol-4-yl)-1*H*-pyrrole-3-carboxamide (**49**)



This compound was prepared through the same procedure of generation of 1-((tetrahydrofuran-2-yl)methyl)-5-(2-(thiophen-2-yl)thiazol-4-yl)-2-(trifluoromethyl)-1*H*-pyrrole-3-carboxamide (**43**) in 7% yield over two steps.

$^1\text{H NMR}$ (300 MHz, CDCl_3): δ_{H} 7.55 (d, $J = 3.72$ Hz, 1H, thiophene), 7.42 (d $J = 5.84$ Hz, 1H; thiophene), 7.38 (s, 1H, thiazole), 7.22 (s, 1H, pyrrole), 7.11 (dd, $J = 3.72, 5.38$ Hz, 1H, thiophene), 5.01 (q, $J = 12.66$ Hz, 2H, $\text{CH}_2, \text{CH}_2\text{OMe}$), 4.81 (dd, $J = 2.81, 14.48$ Hz, 1H, CH, THF), 4.54 (dd, $J = 8.87, 14.25$ Hz, 1H, CH_2), 4.39-4.29 (m, 1H, CH_2), 3.81-3.68 (m, 2H, THF), 3.36 (s, 3H, $\text{CH}_3, \text{CH}_2\text{OMe}$), 2.16-2.05 (m, 1H, THF), 1.95-1.81 (m, 2H, THF), 1.65-1.58 (m, 1H, THF).

HRMS m/z calcd for $\text{C}_{19}\text{H}_{21}\text{N}_3\text{O}_3\text{S}_2\text{Na}$ $[\text{M} + \text{Na}]^+$, 426.0917; found, 426.0916.

7.5 2-(methoxymethyl)-N-methyl-1-((tetrahydrofuran-2-yl)methyl)-5-(2-(thiophen-2-yl)thiazol-4-yl)-1H-pyrrole-3-carboxamide (50)

This compound was prepared through the same procedure of generation of N-methyl-1-((tetrahydrofuran-2-yl)methyl)-5-(2-(thiophen-2-yl)thiazol-4-yl)-2-(trifluoromethyl)-1H-pyrrole-3-carboxamide (**44**) in 61% yield over two steps.

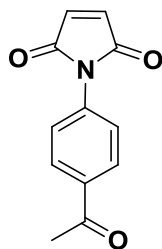
$R_f = 0.14$ (DCM:EtOAc = 40 :1 with 0.1% AcOH).

$^1\text{H NMR}$ (300 MHz, CDCl_3): δ_{H} 7.51 (d, $J = 4.06$ Hz, 1H, thiophene), 7.38 (d, $J = 5.47$ Hz, 1H, thiophene), 7.22 (s, 1H, thiazole), 7.08 (dd, $J = 3.24, 5.47$ Hz, 1H, thiophene), 6.71 (s, 1H, pyrrole), 6.51 (b, 1H, NH), 4.87 (dd, $J = 13.18, 49.07$ Hz, 2H, $\text{CH}_2, \text{CH}_2\text{OMe}$), 4.68 (dd, $J = 2.84, 15.00$ Hz, 1H, CH, THF), 4.46 (dd, $J = 7.50, 14.60$ Hz, 1H, CH_2), 4.25 – 4.16 (m, 1H, CH_2), 3.74 -3.62 (m, 2H, THF), 3.40 (s, 3H, CH_3, OMe), 2.93 (d, $J = 5.07$ Hz, 3H, $\text{CH}_3, \text{NHCH}_3$), 2.04 – 1.96 (m, 1H, THF), 1.83 – 1.75 (m, 2H, THF), 1.55 – 1.48 (m, 1H, THF).

$^{13}\text{C NMR}$ (75 MHz, CDCl_3): δ_{C} 165.6 (q, CO), 160.7 (q, thiazole), 148.4 (q, thiazole), 137.1 (q, thiophene), 132.2 (q, pyrrole), 127.6 (t, thiophene), 127.4 (t, thiophene), 127.4 (q, pyrrole), 126.2 (t, thiophene), 119.1 (q, pyrrole), 113.8 (t, thiazole), 108.9 (t, pyrrole), 78.9 (t, THF), 67.7 (d, THF), 63.3 (d, CH_2), 57.1 (s, OMe), 48.7 (d, $\text{CH}_2, \text{MeOCH}_2$), 28.6 (d, THF), 26.0 (s, NHCH_3), 25.3 (d, THF).

8 Synthesis of the lead structure of the bicyclic inhibitor

8.1 1-(4-acetylphenyl)-1H-pyrrole-2,5-dione (75)



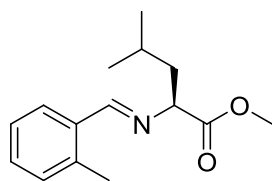
1 g 1-(4-aminophenyl)ethanone (**74**) (7.4 mmol) was dissolved in 15 mL dioxane and the solution was cooled to 0 °C, at this temperature 2.1 g phosphorus pentoxide (14.8 mmol) was slowly added and followed by 858.8 mg maleic acid (**73**) (7.4 mmol). The mixture was stirred under reflux for 1 hour and the both starting materials were completely consumed (TLC: DCM:EtOAc = 40:1). After the reaction, the mixture was poured to 50 mL ice water. Then the aqueous layer was extracted 3 times with chloroform (3 × 30 mL). The combined organic layer was dried over sodium sulfate and the solvent was then removed. The raw product was purified through the flash chromatography (DCM:EtOAc = 40 :1) in 52% yield (827 mg) as the white solid.

$R_f = 0.25$ (DCM:EtOAc = 40 :1)

¹H NMR (300 MHz, CDCl₃): δ_H 8.05 (d, $J = 8.38$ Hz, 2H, H_{Ar}), 7.52 (d, $J = 8.69$ Hz, 2H, H_{Ar}), 6.88 (s, 2H, alkene), 6.21 (s, 3H, CH₃).

¹³C NMR (75 MHz, CDCl₃): 197.0 (q, CO), 168.9 (q, 2C, CO, imide), 135.9 (q, C_{Ar}), 135.5 (q, C_{Ar}), 134.3 (t, 2C, alkene), 129.2 (t, 2C, C_{Ar}), 125.4 (t, 2C, C_{Ar}), 26.6 (s, CH₃).

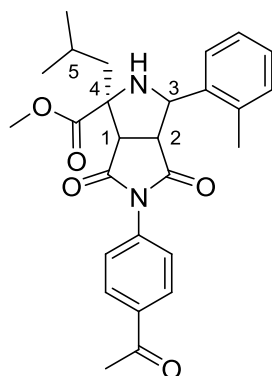
8.2 (S,E)-methyl 4-methyl-2-(2-methylbenzylideneamino)pentanoate (78)



1 g L-leucine methyl ester hydrochloride (**76**) (5.5 mmol) was dissolved in 9 mL absolute DCM, 1.05 g anhydrous sodium sulfate (7.36 mmol) was then added to this solution. 890 μ L triethylamine (6.44 mmol) was then dropwise introduced to this mixture and the mixture was stirred at RT for 1 h. After 1 h, 530 μ L 2-methylbenzaldehyde (**77**) (4.49 mmol) was added to the mixture and the mixture was allowed to react for 3 days. After 3 days, the starting materials were found to be completely consumed (TLC: DCM), the sodium sulfate was subsequently filtered and the solution was concentrated to yield a white solid. The solid was then washed with petroleum ether twice (2×30 mL) and followed by 10 mL chloroform. Then the white solid was dried *in vacuo* and used for the next step without further purification.

$R_f = 0.21$ (DCM)

8.3 (1S)-methyl 5-(4-acetylphenyl)-1-isobutyl-4,6-dioxo-3-oxotolyloctahydropyrrolo[3,4-c]pyrrole-1-carboxylate (79)



320 mg 1-(4-acetylphenyl)-1H-pyrrole-2,5-dione (**75**) (1.5 mmol) was dispersed in 13 mL toluene. 1.1 g unpurified (S,E)-methyl 4-methyl-2-(2-methylbenzylideneamino)pentanoate (**78**) (4.5 mmol) was then added to the suspension and the mixture was stirred under reflux for 3 days. After 3 days, the

reaction was accomplished (TLC: DCM), the solvent was removed and the raw product was subjected to the flash chromatography (DCM) to yield 312.5 mg product (45% yield over two steps) as the white solid.

$R_f = 0.14$ (DCM)

^1H NMR (300 MHz, MeOD): δ_{H} 7.82 (d, $J = 8.12$ Hz, 2H, H_{Ar}), 7.62-7.57 (m, 1H, H_{Ar}), 7.34 (d, $J = 8.23$ Hz, 2H, H_{Ar}), 7.15-7.16 (m, 3H, H_{Ar}), 4.79 (d, $J = 7.06$ Hz, 1H, H_3), 3.80 (s, 3H, CH_3 , COOMe), 3.70 (t, $J = 7.64$ Hz, 1H, H_2), 3.47 (d, $J = 8.23$ Hz, 1H, H_1), 2.53 (s, 3H, CH_3 , COMe), 2.44 (s, 3H, CH_3 , Ar-Me), 2.25-2.15 (m, 1H, H_5), 1.95-1.74 (m, 2H, CH_2), 1.04 (d, $J = 6.12$ Hz, CH_3), 0.96 (d, $J = 6.59$ Hz, CH_3).

^{13}C NMR (75 MHz, MeOD): δ_{C} 199.4 (q, CO, COMe), 177.0 (q, CO, COOMe), 172.2 (q, 2C, CO, imide), 144.1 (q, C_{Ar}), 136.9 (q, C_{Ar}), 136.6 (q, C_{Ar}), 133.5 (q, C_{Ar}), 131.3 (t, C_{Ar}), 130.3 (t, 2C, C_{Ar}), 128.3 (t, C_{Ar}), 127.1 (t, C_{Ar}), 126.7 (t, C_{Ar}), 120.6 (t, 2C, C_{Ar}), 71.6 (q, C_4), 62.5 (t, C_3), 60.9 (t, C_1), 54.0 (t, C_2), 52.8 (s, Me, COOMe), 48.4 (d, CH_2 visible in DEPT), 26.4 (s, CH_3), 26.2 (s, CH_3), 25.1 (s, CH_3 , COMe), 23.7 (t, C_5), 19.8 (s, CH_3 , Ar-Me)

Part II. Development of solid phase synthesis of cyclic peptides

1 General details

Materials. Sodium hydrogen sulfide, potassium carbonate anhydrous and bromopyruvic acid were purchased from Abcr GmbH, 2-(1*H*-benzotriazol-1-yl)-1,1,3,3-tetramethyluronium hexafluorophosphate (HBTU), *N,N*-diisopropylethylamine (DIPEA), trifluoroacetic acid (TFA), tris-(2-carboxyethyl)-phosphine hydrochloride (TCEP), piperidine and dimethylformamide (DMF) were obtained from Carl Roth GmbH. Fmoc-Gly-OH, Fmoc-Leu-OH, Fmoc-Val-OH, Fmoc-Ser-OH, Fmoc-Trp-OH, Fmoc-Ile-OH, Fmoc-Ala-OH, Fmoc-Phe-OH and 2-(1*H*-benzotriazole-1-yl)-1,1,3,3-tetramethylaminium tetrafluoroborate (TBTU) were obtained from Fa. Gerhardt (Wolfhagen, DE). Fmoc-Abu-OH and Fmoc-Cys(StBu)-OH were obtained from Nova Biochem. TentaGel S RAM resin was obtained from Iris Biotech GmbH (Marktredwitz, DE), TentaGel S NH₂ resin was obtained from RAPP Polymere GmbH (Tübingen, DE). Sodium borohydride powder, 2-methyl-2-propanethiol, 4-mercaptophenylacetic acid (MPAA), Ion exchange resin Dowex 1×2 (Cl⁻) form (200-400 mesh), formic acid, triisopropylsilane, methanol anhydrous and dichloromethan (DCM) were obtained from Sigma Aldrich. Ion exchange resin Dowex 50×2 (H⁺) from (200-400 mesh) was obtained from Alfa Aesar. Tetrabutylammonium fluoride trihydrate (TBAF) and 4-(dimethylamino)pyridine (DMAP) were obtained from Acros organics. 1-Methyl-2-pyrrolidinone (NMP) was obtained from Biosolve BV (Valkenswaard, NL). 1-Butanol was obtained from Th. Geyer (Renningen, DE). Acetonitrile HPLC grade, methanol and chloroform were purchased from J.T.Baker (Avantor performance materials, Deventer, NL). *tert*-butyl(chloro)-dimethylsilane was obtained from Fluorochem Ltd. (Hadfield, USA). Imidazole was obtained from Fluka.

Thin layer and flash chromatography

Analytic TLC was run on aluminium sheets coated with silica gel 60 F₂₅₄. The flash chromatography was carried out under slight pressure on the flash chromatography column loaded with silica gel 60 (Merck, 40 – 60 μm, 60 Å).

Analytic and preparative HPLC

A Merck Hitachi D-7000 HPLC instrument with a Phenomenex C₅ column (5 μ m, 50 \times 2.00 mm) at flow rate 0.7 mL / min was used for analytic HPLC. Semi-preparative HPLC was performed by using a Thermo scientific UltiMate 3000 instrument with a Phenomenex C₁₈ column (5 μ m, 250 \times 21 mm) at a flow rate of 10 mL / min.

Nuclear magnetic resonance

All NMR sample were dissolved either in CD₃OD (Sigma Aldrich) or DMSO-d₆ (Deutero GmbH, Kastellaun, DE) and spectra were recorded at 298K.

Proton nuclear magnetic resonances (¹H NMR) and carbon nuclear magnetic resonances (¹³C NMR) were recorded on 700 Hz and 500 Hz Bruker NMR spectrometers (Ascend 700 / Avance III HD, Ultrashield 500 Plus / Avance III 500) at 298 K, and the chemical shifts are reported in *parts per million* (δ) from an internal standard of residual chloroform (7.24 ppm, 77.0 ppm), methanol (3.31 ppm, 4.78 ppm, 49.0 ppm) and DMSO-d₆ (2.49 ppm, 39.7 ppm). Proton NMR signals multiplicity is reported as follows: s = singlet, d = doublet, t = triplet, q = quartett, m = multiplet, b = broad.

LC-MS and high-resolution mass spectroscopy

LC-MS was carried out on an Agilent Technologies 1100 series device. A Phenomenex column (2.6 μ m, 50 \times 2.1 mm) and a flow rate 10 mL / min is used for the LC-MS. High-resolution mass spectra (HRMS) were obtained on a Bruker MaXis mass spectrometer by using electron spray ionization (ESI) from the department of microbial drugs, Helmholtz Centre for Infection Research, Braunschweig, Germany.

Microwave and automated SPPS synthesizer

The microwave assisted disulfide formation was performed in a CEM Discover S-class microwave synthesizer with microwave suitable glass vessel.

The automatic peptide synthesis was carried out on a MultiSyn tech's Syro peptide synthesizer.

2 Procedure of preparing ion exchange column

2.1 Preparation of (H⁺) exchange column

15 g commercially purchased Dowex 50×2 (H⁺) form resin was soaked in 4 M HCl and swollen for 1Hour. The resin was then loaded in a chromatography column (20 × 1 cm), washed slowly with 4 M HCl for 1Hour and followed by the deionized water until it was neutral.

2.2 Preparation of (CH₃COO⁻) exchange column

20 g commercially purchased Dowex 1×2 (Cl⁻) resin was soaked in 1 M NaOH and swollen for 1 hour. The resin was then loaded in a chromatography column (20 ×1 cm) and washed slowly with 1 M NaOH for 1 additional hour and followed by the deionized water until pH was neutral. Afterward the column was slowly washed with 3 M sodium acetate solution for 1 hour to load the acetate ion into the resin, the rest sodium acetate solution was then washed out by deionized water. The column was ready for the ion exchange as soon as the pH value reaches 7.

3 Procedure of Kaiser test to determine the free amino groups

10 mg resin was picked up from the syringe and washed a few times with DMF followed by DCM and dried under vacuum. To the resin beads, three drops of each reagent A (5 g ninhydrin in 100 ml ethanol), reagent B (80 g phenol in 20 ml ethanol) and reagent C (2 ml 0.00 1 M aqueous KCN in 98 ml pyridine)^[128] were added and this mixture was heated at 120 °C for 3 min. Based on the following chart, the progress of reaction could be qualitatively estimated.

solution	bead	completeness of reaction
colorless	colorless	completed
light blue to blue	colorless	nearly completed, capping of unreacted amino group
light blue	dark blue	Incomplete, recoupling required
dark blue	dark blue	coupling failed

4 Determination of the loading through Fmoc release UV assay

After coupling of the first amino acid, the resin was washed a few times with DMF followed by the DCM and completely dried under vacuum. Between 5 to 10 mg resin would be taken into a vial. 1 mL 20% piperidine / DMF solution was then added to the vial and shaken for 20 min. Afterwards, two aliquots of each 100 μ L piperidine / DMF solution from the vial were diluted with 10 mL DMF in the flasks. The UV absorbance of the Fmoc group was measured on the UV spectrometer at 280 nm, while the pure DMF was taken as the blank sample. The final loading was then calculated by using the following equation:

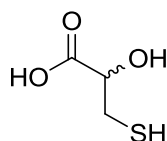
$$\text{Loading} = \frac{101 \times A}{7.8 \times W}$$

A = Fmoc absorbance

W = weight of the resin

5 Preparation of the latent thioester linker 12

5.1 2-hydroxy-3-mercaptoacetic acid (3)



Anhydrous sodium hydrogen sulfide (1 g, 17.8 mmol) was dissolved in 5 mL anhydrous methanol and this solution was introduced into the reaction vessel loaded with bromopyruvic acid (1.5 g, 8.9 mmol) in 10 mL anhydrous methanol over 90 min at 0 °C. During the addition a white precipitation was formed gradually. After the addition of the sodium hydrogen sulfide the reaction mixture was stirred at RT for further 20 min and the vessel was added with 5 mL ethanol afterwards. The precipitation was then filtered and washed three times with absolute ethanol and dried under vacuum. The white powder was then dissolved in a mixture of 9 mL mL 0.1 M HCl and 15 mL ethanol and recrystallized in the fridge overnight. The newly grew white crystal was filtered and washed three times with 5 mL absolute ethanol each then followed by two times each of 2 mL 75% ethanol and the raw product was dried for one day over phosphorus pentoxide in an evacuated desiccator. 997 mg raw intermediate (5.6 mmol) was dissolved in 7 mL deionized water and 275 mg sodium hydride (7.3 mmol) was

slowly added at RT under stirring. After the introduction of sodium hydride, the mixture was stirred for one further hour. After the starting material was completely consumed (TLC, n-butanol:formic acid:water = 75%:15%:10%) the solution was directly loaded into the cation exchange column, and slowly eluted with 150 mL deionized water. The fractions were collected and concentrated to dryness by rotation evaporator. The white powder was again dissolved in 2 mL deionized water and the pH value was adjusted to around 6 by using the 28% ammonium hydroxide solution, then the solution was loaded in the anion exchange column and eluted firstly with 100 mL deionized water and followed by 200 mL 1 M formic acid. The fractions were collected and dried under vacuum to yield a white fine powder (489 mg, 45%)

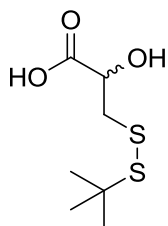
$R_f = 0.79$ (n-butanol:formic acid :water = 75%:15%:10%)

$^1\text{H NMR}$ (500 MHz, MeOD): δ_{H} 4.32 (t, $J = 4.68$ Hz, 1H), 2.92 (dd, $J = 13.45, 4.09$ Hz, 1H), 2.83 (dd, $J = 13.74, 5.85$ Hz, 1H).

$^{13}\text{C NMR}$ (125 MHz, MeOD): δ_{C} 175.75, 72.71, 29.41.

HRMS m/z : calcd for $\text{C}_3\text{H}_5\text{O}_3\text{S} [\text{M} - \text{H}]^-$, 120.9959, found 120.9956.

5.2 3-(tert-butylsulfanyl)-2-hydroxypropanoic acid (**4**)



150 mg 2-hydroxy-3-mercaptopropanoic acid (**3**) (1.2 mmol) was dissolved in 15 mL buffer solution (10 mM ammonium acetate solution in acetonitrile:water = 3:2) in a microwave suitable glass tube (diameter 2.5 cm), 1.35 mL 2-methyl-2-propanethiol (12 mmol) and 0.85 mL DMSO (12 mmol) were subsequently added into this. The tube was sealed and placed into a CEM microwave and stirred under following configurations (power = 150 W, $T_{\text{max}} = 150$ °C) for 10 min. After all the starting material disappeared (TLC, n-butanol:formic acid:water = 75%:15%:10%), the mixture was transferred into a round bottomed flask and

concentrated to about 5 mL by rotation evaporator. The DMSO and water residue was subsequently removed by a centrifugal evaporator (Christ, RVC 2–25 CD plus) at 40 °C and the raw product was finally purified through the preparative HPLC (water:acetonitrile, gradient 5%–95%, 30 min.) to yield a white fine powder. (240 mg, 95%)

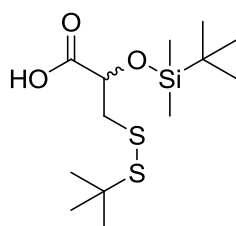
$R_f = 0.91$ (n-butanol:formic acid:water = 75%:15%:10%)

$^1\text{H NMR}$ (500 MHz, MeOD): δ_{H} 4.40 (q, $J = 3.97$ Hz, 1H), 3.19 (dd, $J = 13.39, 3.93$ Hz, 1H), 2.98 (dd, $J = 13.35, 7.93$ Hz, 1H), 1.38 (s, 9H).

$^{13}\text{C NMR}$ (125 MHz, MeOD): δ_{C} 175.94, 70.54, 48.57, 46.35, 30.23 (3C).

HRMS m/z : calcd for $\text{C}_7\text{H}_{13}\text{O}_3\text{S}_2\text{Na}$ [$\text{M} - \text{H}$] $^-$, 233.0282, found 233.0274.

5.3 2-(tert-butyldimethylsilyloxy)-3-(tert-butylsulfanyl)propanoic acid (**12**)



240 mg 3-(tert-butylsulfanyl)-2-hydroxypropanoic acid (**4**) (1.14 mmol) was dissolved in 2.5 mL anhydrous DMF, 372 mg imidazole (5.4 mmol) and 416 mg *tert*-butyldimethylsilyl chloride (2.7 mmol) were added too. The mixture was stirred at RT overnight and then diluted with 8 mL (ethyl acetate:toluene = 1:1) solvent. The organic layer was then sequentially washed with each 15 mL of 10% citric acid, saturated sodium hydrogen carbonate solution, water and saturated brine solution and dried over sodium sulfate. The solvent was then evaporated to give a pale yellow oily substance. All yellow oily substance was dissolved in 22 mL methanol, 690 mg potassium carbonate (5 mmol) was then added and followed by 7.2 mL water at 0 °C. The mixture was warmed up to RT and stirred overnight. After the reaction is finished (TLC: DCM:MeOH = 20:1) the mixture was slowly acidified with 10% citric acid. At pH = 3 white solids were precipitated and these were extracted 3 times with ethyl acetate (3 × 10 mL). The organic layer was then dried over sodium sulfate and the solvent was evaporated. The raw product was subjected to the flash chromatography (100 mL fractions DCM

followed by 200 mL DCM:MeOH = 40:1) to yield the pale yellow oily substance (277 mg, 75%) and this was utilized immediately in the next step due to its high instability.

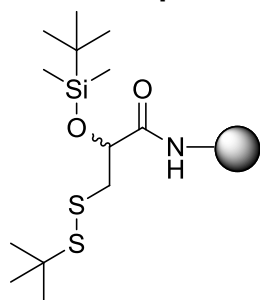
$R_f = 0.18$ (DCM:MeOH = 20 :1)

$^1\text{H NMR}$ (500 MHz, CDCl_3): δ_{H} 4.49 (q, $J = 3.64$ Hz, 1H), 3.15 (dd, $J = 13.57, 3.54$ Hz, 1H), 2.95 (dd, $J = 13.58, 7.36$ Hz, 1H), 1.33 (s, 9H), 0.94 (s, 9H), 0.19 (s, 3H), 0.15 (s, 3H).

$^{13}\text{C NMR}$ (125 MHz, CDCl_3): δ_{C} 172.91, 71.32, 48.34, 45.64, 29.89 (3C), 25.72 (3C), -4.54.

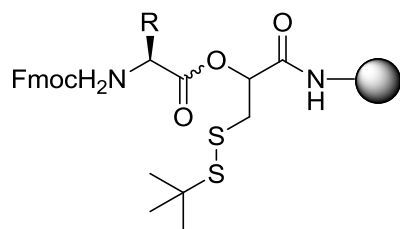
HRMS m/z : calcd for $\text{C}_{13}\text{H}_{27}\text{O}_3\text{S}_2\text{Si}$ [$\text{M} - \text{H}$] $^-$, 323.1171, found 323.1181.

6 General procedure of loading of the linker 12 onto the Tentagel NH_2 resin



486.7 mg TentaGel S NH_2 resin (loading: 0.27 mmol / g) was swollen in DMF in a syringe with filter for 30 min and then drained to dryness. 150 mg linker (0.46 mmol) was dissolved under inert gas in 0.5 mL anhydrous DMF and injected into a HBTU solution 174.5 mg HBTU (0.46 mmol) was dissolved under inert gas in 0.5 mL anhydrous DMF) 156 μL DIPEA (0.92 mmol) was then added into this and the mixture was pre activated for 5 min. before it was injected into the syringe loaded with resin. The resin was shaken under inert gas overnight on an orbital shaker and 20 mg of the resin was taken and tested with Kaiser reagent. Judged by the very pale blue color of the test solution and the colorless beads the reaction was nearly completed and the rest solution was drained. The resin was washed a few times with DMF followed by DCM and dried in *vacuo*. The unreacted free amino groups were capped twice for each 15 min. with acetylation mixture (DMF:acetic anhydride:water = 8:1 :1).

7 TBAF deprotection and the coupling of the first amino acid through the esterification



The resin was swollen in anhydrous THF for 15 min and then the solvent was drained, 5 mL fresh prepared 1 M TBAF THF solution was added. The TBAF group was deprotected overnight and the TBAF solution was drained. 10 fold first amino acid was dissolved in 0.5 mL DMF and added into the HBTU solution (10 folds HBTU dissolved in 0.5 mL DMF) the amino acid was pre-activated for 5 min with additional 20 folds of DIPEA. After the pre-activation the mixture was injected into the syringe loaded with the resin. Additionally 1 fold of DMAP was added into this syringe as well. The resin was shaken for 2 hours and washed a few times with DMF. Then the coupling of the first amino acid was repeated under the same condition for one additional hour. After the coupling was completed, the resin was washed with DMF, tested with Fmoc release UV assay (loading: 93%) and the following amino acids were allowed to be assembled by the automated Fmoc-SPPS.

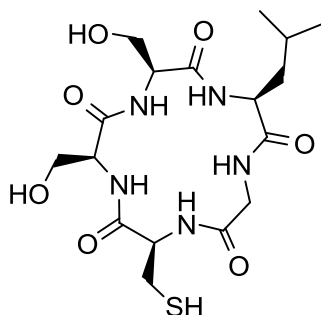
8 Post SPPS work-up and deprotection of the various protecting groups

After the automated Fmoc-SPPS was done, the resin was washed a few times with DMF followed by the DCM and completely dried under vacuum. The deprotecting cocktail (TFA:triisopropylsilane:water = 9.5:0.5:0.5 (in case the sequence contains tryptophan, the cocktail mixture was changed to TFA:phenol:dimethyl sulfide:water = 8.5:0.5:0.5 :0.5) was added then the deprotection mixture was covered with aluminum sheet and with occasionally shake for two hours. After the deprotection, the deprotecting cocktail was drained and the resin was washed a couple of times with DMF and DCM then dried under vacuum and the cyclization will be carried out.

9 General procedure of the on-resin NCL cyclization

100 mg resin was swollen in cyclization buffer solution (0.1 M sodium phosphate buffer solution: acetonitrile = 4:1, containing 10 mM TCEP, pH = 6.7 ~ 6.8) and shaken under inert gas for 24 hours, after the cyclization the buffer solution was drained and the resin was wash a few times with mixture water:acetonitrile = 4:1, the filtrate was combined with the buffer solution and was directly freeze-dried. The raw product was subjected to semi-preparative HPLC to yield the white and hygroscopic substance.

9.1 Cyclo Cys-Ser-Ser-Leu-Gly (19')



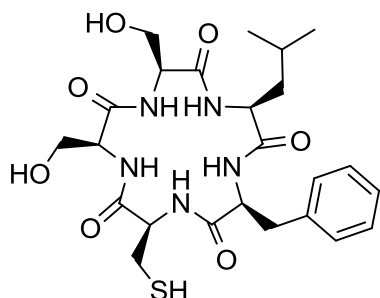
HPLC purification: $t_R = 20.87$ min, UV = 205 nm, gradient: ACN / water = 0% - 70%, 90 min.

$^1\text{H NMR}$ (700 MHz, DMSO): δ_{H} 8.74 (t, $J = 5.47$ Hz, 1H), 8.2 (d, $J = 8.62$ Hz, 1H), 8.07 (d, $J = 6.61$ Hz, 1H), 7.69 (d, $J = 9.02$ Hz, 1H), 7.5 (d, $J = 8.62$ Hz, 1H), 5.32 (b, 2H), 4.3 (m, 1H), 4.28 (m, 1H), 4.26 (m, 1H), 4.01 (m, 1H), 3.94 (m, 1H), 3.67 (m, 2H), 3.65 (m, 2 H), 3.60 (m, 1H), 2.87 (m, 1H), 2.74 (m, 1H), 2.55 (t, $J = 8.43$ Hz, 1H), 1.55 (m, 1H), 1.45 (m, 2H), 0.88 (d, $J = 5.07$ Hz, 3H), 0.87 (d, $J = 5.07$ Hz, 3H).

$^{13}\text{C NMR}$ (175 MHz, DMSO): δ_{C} 172.84, 170.11, 169.93, 169.37, 169.18, 60.47, 60.28, 56.75, 56.68, 54.64, 50.91, 43.54, 41.10, 25.44, 24.35, 22.83, 21.92.

HRMS m/z : calcd for $\text{C}_{17}\text{H}_{30}\text{N}_5\text{O}_7\text{S}$ $[\text{M} + \text{H}]^+$, 448.1866; found 448.1858.

9.2 Cyclo Cys-Ser-Ser-Leu-Phe (20')



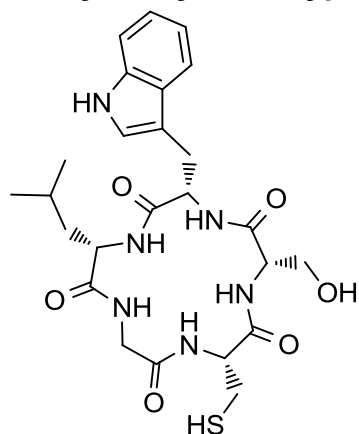
HPLC purification: t_R = 36.65 min., UV = 220 nm, gradient: ACN / water = 5% - 95%, 70 min.

^1H NMR (700 MHz, DMSO): δ_H 8.17 (d, J = 8.28 Hz, 1H), 8.04 (d, J = 8.69 Hz, 1H), 7.87 (d, J = 8.28 Hz, 1H), 7.74 (d, J = 7.86 Hz, 1H), 7.68 (d, J = 8.69 Hz, 1H), 7.28 (t, J = 7.86 Hz, 2H), 7.22 (d, J = 7.86 Hz, 3H), 5.36 (broad, 1H), 5.24 (b, 1H), 4.36 (m, 1H), 4.2 (m, 1H), 4.16 (m, 1H), 4.12 (m, 1H), 4.08 (m, 1H), 3.70 (m, 2H), 3.62 (m, 2H), 3.08 (m, 1H), 3.02 (m, 1H), 2.4 (t, J = 8.26 Hz, 1H), 1.45 (m, 1H), 1.32 (m, 2H), 0.80 (d, J = 6.09 Hz, 3H), 0.77 (d, J = 6.09 Hz, 3H).

^{13}C NMR (175 MHz, DMSO): δ_C 171.35, 170.70, 169.83, 169.71, 169.18, 137.28, 129.06 (2C), 128.23 (2C), 126.48, 60.40, 60.35, 57.49, 56.32, 55.95, 55.49, 52.97, 40.58, 36.73, 24.88, 24.10, 22.39, 21.98.

HRMS m/z : calcd for $\text{C}_{17}\text{H}_{30}\text{N}_5\text{O}_7\text{S}$ [$\text{M} + \text{H}$] $^+$, 538.2335; found 538.2340.

9.3 Cyclo Cys-Ser-Typ-Leu-Gly (22')



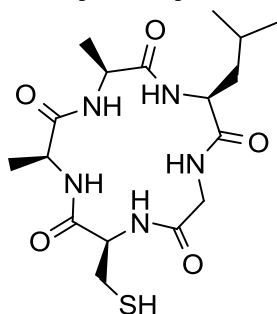
HPLC purification: t_R = 38.78 min., UV = 220 nm, gradient: ACN / water = 5% - 95%, 70 min.

¹H NMR (700 MHz, DMSO): δ_{H} 10.88 (d, $J = 1.83$ Hz, 1H), 8.8 (t, $J = 5.7$ Hz, 1H), 8.38 (d, $J = 8.16$ Hz, 1H), 8.12 (d, $J = 6.78$ Hz, 1H), 7.74 (d, $J = 8.50$ Hz, 1H), 7.58 (d, $J = 8.62$ Hz, 1H), 7.53 (d, $J = 7.93$ Hz, 1H), 7.33 (d, $J = 8.44$ Hz, 1H), 7.14 (d, $J = 2.07$ Hz, 1H), 7.07 (td, $J = 7.56, 0.89$ Hz, 1H), 6.98 (td, $J = 7.34, 0.78$ Hz, 1H), 5.26 (t, $J = 4.76$ Hz, 1H), 4.27 (m, 1H), 4.23 (m, 2H), 4.14 (m, 1H), 3.90 (m, 1H), 3.69 (m, 1H), 3.54 (m, 1H), 3.38 (m, 1H), 3.18 (m, 2H), 2.86 (m, 1H), 2.54 (t, $J = 8.50$ Hz, 1H), 2.74 (m, 1H), 1.45 (m, 2H), 1.39 (m, 1H), 0.86 (d, $J = 6.54$ Hz, 3H), 0.84 (d, $J = 6.54$ Hz, 3H).

¹³C NMR (175 MHz, DMSO): δ_{C} 173.33, 171.46, 170.00, 169.47, 169.28, 136.10, 127.01, 123.56, 120.99, 118.37, 118.15, 111.37, 109.58, 60.37, 57.14, 56.66, 54.70, 50.77, 43.62, 40.97, 26.32, 25.37, 24.38, 22.90, 21.75.

HRMS m/z : calcd for $\text{C}_{25}\text{H}_{35}\text{N}_6\text{O}_6\text{S}$ $[\text{M} + \text{H}]^+$, 547.2339; found 547.2336.

9.4 Cyclo Cys-Ala-Ala-Leu-Gly (24')

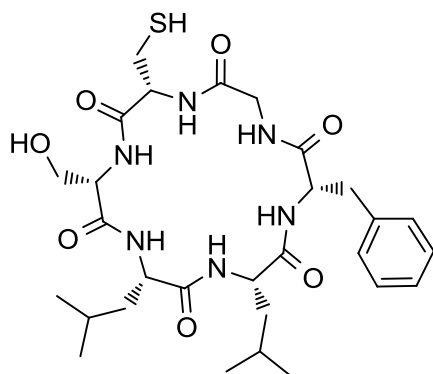


HPLC purification: $t_{\text{R}} = 26.6$ min., UV = 205 nm, gradient: ACN / water = 5% - 95%, 70 min.

¹H NMR (700 MHz, DMSO): δ_{H} 8.89 (t, $J = 8.03$ Hz, 1H), 8.36 (d, $J = 7.9$ Hz, 1H), 8.03 (d, $J = 6.6$ Hz, 1H), 7.69 (d, $J = 8.5$ Hz, 1H), 7.36 (d, $J = 8.64$ Hz, 1H), 4.27 (m, 2H), 4.24 (m, 1H), 3.92 (m, 2H), 3.37 (m, 1H), 2.90 (m, 2H), 2.42 (t, $J = 8.92$ Hz, 1H), 1.53 (m, 1H), 1.44 (m, 2H), 1.33 (m, 3H), 1.32 (m, 3H), 0.89 (d, $J = 7.20$ Hz, 3H), 0.88 (d, $J = 7.0$ Hz, 3H).

¹³C NMR (175 MHz, DMSO): δ_{C} 173.49, 172.77, 171.24, 169.52, 168.94, 56.33, 51.72, 50.56, 48.87, 43.70, 41.25, 25.29, 24.49, 22.95, 21.77, 16.93, 16.54.

HRMS m/z : calcd for $\text{C}_{17}\text{H}_{30}\text{N}_5\text{O}_5\text{S}$ $[\text{M} + \text{H}]^+$, 416.1968, found 416.1962.

9.5 Cyclo Cys-Ser-Leu-Leu-Phe-Gly (25')

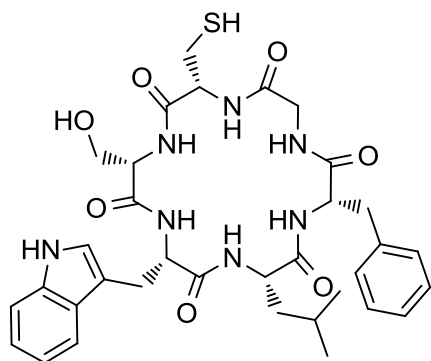
HPLC purification: $t_R = 44.14$ min., UV = 220 nm, gradient: ACN / water = 5% - 95%, 70 min.

$^1\text{H NMR}$ (700 MHz, DMSO): δ_H 8.82 (t, $J = 5.36$ Hz, 1H), 8.48 (d, $J = 8.66$ Hz, 1H), 7.88 (d, $J = 5.78$ Hz, 1H), 7.83 (d, $J = 8.25$ Hz, 1H), 7.74 (d, $J = 8.25$ Hz, 1H), 7.38 (d, $J = 5.78$ Hz, 1H), 7.25 (t, $J = 7.43$ Hz, 2H), 7.20 (t, $J = 7.01$ Hz, 1H), 7.12 (d, $J = 7.01$ Hz, 2H), 5.36 (t, $J = 6.48$ Hz, 1H), 4.37 (m, 1H), 4.35 (m, 1H), 4.31 (m, 1H), 3.98 (m, 1H), 3.81 (m, 2H), 3.69 (m, 1H), 3.45 (m, 1H), 2.97 (m, 2H), 2.93 (m, 1H), 2.76 (m, 1H), 2.41 (t, $J = 8.51$ Hz, 1H), 1.62 (m, 1H), 1.49 (m, 2H), 1.44 (m, 1H), 1.43 (m, 1H), 1.36 (m, 1H), 0.89 (d, $J = 6.77$ Hz, 3H), 0.84 (d, $J = 6.21$ Hz, 3H), 0.83 (d, $J = 6.7$ Hz, 3H), 0.79 (d, $J = 6.21$ Hz, 3H).

$^{13}\text{C NMR}$ (175 MHz, DMSO): δ_C 171.92, 171.53, 169.90, 169.64, 169.39, 169.20, 136.99, 129.16 (2C), 128.01 (2C), 126.39, 61.49, 55.66, 54.20, 53.95, 53.20, 51.89, 43.47, 40.59, 40.15, 37.56, 25.01, 24.19 (2C), 22.86, 22.80, 21.48, 21.28.

HRMS m/z : calcd for $\text{C}_{29}\text{H}_{45}\text{N}_6\text{O}_7\text{S}$ $[\text{M} + \text{H}]^+$, 621.3070, found 621.3072.

9.6 Cyclo Cys-Ser-Trp-Leu-Phe-Gly (26')

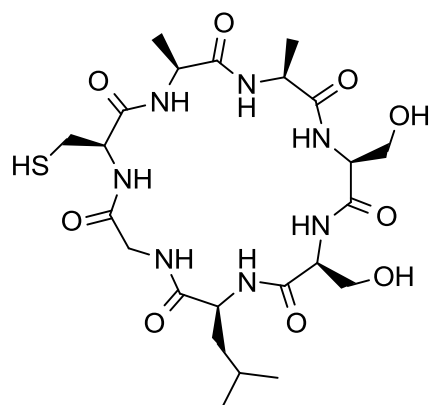


HPLC purification: $t_R = 45.43$ min., UV = 220 nm, gradient: ACN / water = 5% – 95%, 70 min.

$^1\text{H NMR}$ (700 MHz, DMSO): δ_{H} 10.89 (s, 1H), 8.8 (t, $J = 5.5.2$ Hz, 1H), 8.47 (d, $J = 7.73$ Hz, 1H), 7.98 (d, $J = 6.35$ Hz, 1H), 7.86 (d, $J = 8.55$ Hz, 1H), 7.71 (d, $J = 7.73$ Hz, 1H), 7.5 (d, $J = 7.73$ Hz, 1H), 7.36 (d, $J = 5.93$ Hz, 1H), 7.33 (d, $J = 8.03$ Hz, 1H), 7.24 (m, 2H), 7.18 (m, 2H), 7.10 (d, $J = 8.01$ Hz, 2H), 7.07 (t, $J = 8.41$ Hz, 1H), 6.98 (t, $J = 7.61$ Hz, 1H), 5.35 (t, $J = 5.91$ Hz, 1H), 4.40 (m, 1H), 4.30 (m, 1H), 4.28 (m, 1H), 4.26 (m, 1H), 4.03 (m, 1H), 3.76 (m, 2H), 3.69 (m, 1H), 3.44 (m, 1H), 3.10 (m, 2H), 2.93 (m, 2H), 2.75 (m, 1H), 2.42 (t, $J = 8.50$ Hz, 1H), 1.27 (m, 2H), 1.23 (m, 1H), 0.76 (d, $J = 5.81$ Hz, 3H), 0.69 (d, $J = 5.81$ Hz, 3H).

$^{13}\text{C NMR}$ (175 MHz, DMSO): δ_{C} 171.49, 171.44, 171.20, 169.88, 169.52, 169.16, 137.01, 136.06, 129.12 (2C), 127.96 (2C), 127.10, 126.32, 123.55, 120.95, 118.34, 118.08, 111.33, 109.36, 61.49, 55.47, 54.18, 53.74, 52.35, 52.14, 43.58, 40.43, 37.58, 28.97, 26.85, 23.92, 22.53, 21.48.

HRMS m/z : calcd for $\text{C}_{34}\text{H}_{44}\text{N}_7\text{O}_7\text{S}$ $[\text{M} + \text{H}]^+$, 694.3022, found 694.3043.

9.7 Cyclo Cys-Ala-Ala-Ser-Ser-Leu-Gly (27')

HPLC purification: t_R = 23.56 min., UV = 205 nm, gradient: ACN / water = 5% - 95%, 70 min.

^1H NMR (700 MHz, DMSO): δ H 8.33 (d, J = 5.80 Hz, 1H), 8.13 (t, J = 8.13 Hz, 1H), 8.08 (d, J = 6.69 Hz, 1H), 8.05 (d, J = 7.14 Hz, 1H), 7.94 (d, J = 7.14 Hz, 1H), 7.91 (d, J = 7.14 Hz, 1H), 7.78 (d, J = 8.13 Hz, 1H), 5.32 (t, J = 5.01 Hz, 2H), 4.35 (m, 1H), 4.20 (m, 2H), 4.16 (m, 1H), 4.08 (m, 1H), 4.03 (m, 1H), 3.94 (m, 1H), 3.72 (m, 2H), 3.62 (m, 2 H), 3.55 (m, 1H), 2.86 (m, 1H), 2.81 (m, 1H), 2.29 (t, J = 8.46 Hz, 1H), 1.58 (m, 1H), 1.53 (m, 2H), 1.27 (t, J = 7.24 Hz, 6H), 0.87 (d, J = 6.43 Hz, 3H), 0.83 (d, J = 6.43 Hz, 3H).

^{13}C NMR (175 MHz, DMSO): δ C 172.26, 171.99, 171.86, 170.36, 169.70, 169.50, 168.87, 61.20, 61.08, 56.05, 55.82, 55.01, 51.91, 46.68, 49.07, 42.62, 40.48, 25.87, 24.11, 22.88, 21.50, 16.98, 16.93.

HRMS m/z : calcd for $\text{C}_{23}\text{H}_{40}\text{N}_7\text{O}_9\text{S}$ [$\text{M} + \text{H}$] $^+$, 590.2608, found 590.2596.

C. Reference list

- [1]. *Heterocyclic chemistry*, 1st Edn, Sainsbury M., **2002**, Wiley-RSC.
- [2]. Selvam T. P., James C. R., Dniandev P. V., Valzita S. K., *Research in Pharmacy*. **2009**, 2, 1–9.
- [3]. *Heterocyclic Compounds: An introduction*, Alvarez-Builla J. and Barlugenga J, *moderen Heterocyclic Chemistry* First Edn, **2011**, Wiley- VCH Verlag.
- [4]. Powell W. H., *Pure Appl. Chem.* **1983** 55, 409–416.
- [5]. *Heterocyclic chemistry* 5th Edn, Joule J. A. and Mills K., **2010** Blackwell Publishing Ltd. Oxford.
- [6]. Hanzsch A., *Ber. Dtsch. Chem. Ges.* **1890**, 23, 1474.
- [7]. Knorr L., *Ber. Dtsch. Chem. Ges.* **1884**, 17, 1635.
- [8]. Paar C, *Ber. Dtsch. Chem. Ges.* **1884**, 17, 2756.
- [9]. Campaigne E., Foye W.O., *J. Org. Chem.***1952**, 17, 1405–1412.
- [10]. Hanzsch A., *Ber. Dtsch. Chem. Ges.* **1887**, 20, 3118.
- [11]. Robinson R., *J. Chem. Soc.* **1909**, 95, 2167.
- [12]. Cook A. H.; Heilbron I.; MacDonald S. F.; Mahadera A. P., *J. Chem. Soc.***1949**, 14, 1064.
- [13]. Sivakumar K.; Xie F.; Cash B. M.; Long S.; Barnhill H. H.; Wang Q., *Org. Lett.*,**2004**, 6, 4603.
- [14]. Ye C. F.; Gawd G. L.; Winter R. W., Syvret R.G.; Twamleg B.; Shreve J. M., *Org. Lett.* **2007**, 9, 3841–3844.
- [15]. Fisher E, Jourdan F, *Ber. Dtsch. Chem. Ges.* **1886**, 16, 2241–2245.
- [16]. Batcho, A. D., Leimgruber, W., *Org. Synth.* **1985**, 63, 214–220.
- [17]. Rongveg P., Kirsch G., Bouaziz Z., Le Borgne M., *Eur J Med Chem.* **2013**, 69, 465–479..
- [18]. Marshall J. Wallace E. M., A., Bartley G. S., *J. Org. Chem.* **1996**, 61, 5729–5735.
- [19]. Neubauer M., Bach G. L., *Fortschr Med.* **1983**, 101, 1014–1016.
- [20]. Bonuso S., Di Stasio E., Marano E., Covelli V., Testa N., Tetto A., Buscaisno G. A., *Acta Neurol.***1994**, 16, 1–10.
- [21]. Li X., Brown N., Chau A. S., Lopez-Ribot J. L., Ruesga M. T., Quindos G., Mendrick C.A., Hare R. S., Loebenberg D., DiDomenico B., McNicholas P. M, *J. Antimicrob. Chemother.* **2004**, 53, 74–80.
- [22]. Das S. N., *antiseptic* **1946**, 43, 486.
- [23]. Houghton R. A., Pinnila L., Blondelle S. E., Dooley C. T.; Cuero J. H., *Nature* **1991**, 351, 84–86.
- [24]. Geysen H. M., Meloen R. H., Barteling S. J., *Proc. Natl. Acad. Sci. USA***1984**, 81, 3998.
- [25]. Furka A.; Sebestyen F.; Asgedom M.; Diba G., *Int. J. Pept. Protein Res.* **1991**, 37, 487–439.
- [26]. Gordon E. M.; Barrete R. W.; Dower W. J.; Fodor S. P. A.; Gallop M.

- A., *J. Med. Chem.* **1994**, *37*, 1385.
- [27]. Ballante F., Ragno R., *J. Chem. Inf. Model.* **2012**, *52*, 1674–1685.
- [28]. *Medicinal Chemistry*, 1st Edn. Thomas G., **2003**, Wiley-VCH Verlag.
- [29]. World cancer report 2014, World Health Organization.
- [30]. Timofeev O., Cizmecioglu O., Settele F., Kempf T., Hoffmann I., *J. Bio. Chem.* **2010**, *285*, 16978–16990.
- [31]. Tumurbaatar I., Cizmecioglu O., Hoffmann I., Grummt I., Voit R., *PLOS ONE* **2011**, *6*, 14711.
- [32]. Barr F. A., Sillje H. H. W., Nigg E. A., *Nat. Rev. Mol. Cell Bio.* **2004**, *5*, 429–441.
- [33]. Malumbres M., Barbacid M., *Trends Biochem. Sci.* **2005**, *30*, 630–641.
- [34]. Boutros R., Lobjois V., Ducommun B., *Nat. Rev. Cancer.* **2007**, *7*, 495–507.
- [35]. Lindqvist A., Kallstrom H., Lundgren A., Barsoum E., Rosenthal C. K., *J. Cell Biol.* **2005**, *171*, 35–45.
- [36]. Sadhu K., Reed S. I., Richardson H., Russel P., *Proc. Nati. Acad. Sci. USA* **1990**, *87*, 5139–5143.
- [37]. Galaktionov K., Beach D., *Cell* **1991**, *67*, 1181–1194.
- [38]. Lazo J.S., Nemoto K., Pestell K. E., Cooley K., Southwick E. C., Mitchell D. A., Furey W., Gussio R., Zaharevitz D. W., Joo B., Wipf P., *Mol Pharmacol.* **2002**, *61*, 720–728.
- [39]. Lazo J.S., Aslan D.C., Southwick E.C., Cooley K.A., Ducruet A.P., Joo B., Vogt A., Wipf P., *J Med Chem.* **2002**, *44*, 4042–4049.
- [40]. Kar S., Wang M, Wilcox C. S., Carr B. I., *Carcinogenesis* **2003**, *24*, 411–416.
- [41]. Pu L., Amoscato A. A., Bier M. E., Lazo J. S., *J Bio Chem.* **2002**, *277*, 46877–46885.
- [42]. Nören-Müller A., Reis-Corrêa I. Jr, Prinz H., Rosenbaum C., Saxena K., Schwalbe H. J., Vestweber D., Cagna G., Schunk S., Schwarz O., Schiewe H., Waldmann H., *Proc. Nati. Acad. Sci. USA* **2006**, *103*, 10606–10611.
- [43]. Matulenko M. D., Lee C. H., Jiang M., Frey R. R., Cowart M. D., Bayburt E. K., Didimenico S., Gfresser G. A., Gomtsyan A., Zheng G. Z., McKie J. A., Stewart A. O., Yu H., Kohlhaas K. L., Alexander K. M., McGaraughty S., Wissmer C. T., Mikusa J., Marsh K. C., Snyder R. D., Diehl M. S., Kowaluk E. A., Jarvis M. F., Bhagwat S. S., *Bioorg. Med. Chem.* **2005**, *13*, 3705–3720.
- [44]. Aki S., Fujioka T., Ishigami M., Minamikawa J., *Bioorganic medicinal chem letters* **2002**, *12*, 2317–2320.
- [45]. Rice C. R., Baylies C. J., Clayton H. J., Jeffery J. C., Paul R. L., Ward M. D., *Inorg. Chim. Acta.* **2003**, *351*, 207–216.
- [46]. Zou Y., Wang M., Sang G., Ye M., Li Y., *Adv. Funct. Mater.* **2008**, *18*, 2724–2732.

- [47]. Kato T., Chiba T., Sasaki M., Kamo M., *J Pharm Soc. Japan* **1981**, *101*, 40–47.
- [48]. Kameswaran V., Jiang B., *Synthesis* **1996**, *5*, 530–532.
- [49]. Menichincheri M., Albanese C., Alli C., Ballinari D., Bargiotti A., Caldarelli M., Ciavolella A., Cirila A., Colombo M., Colotta F., Croci V., D'Alessio R., D'Anello M., Ermoli A., Fiorentini F., Forte B., Galvani A., Giordano P., Isacchi A., Martina K., Molinari A., Moll J. K., Montagnoli A., Orsini P., Orzi F., Pesenti E., Pillan A., Roletto F., Scolaro A., Tato M., Tibolla M., Valsasina B., Varasi M., Vianello P., Volpi D., Santocanale C., Vanotti E., *J. Med. Chem.* **2010**, *53*, 7296–7315.
- [50]. Shen Q., Warshawsky A. M., Yee Y. K., United States Patent Application Publication, Pub. N. US 2008 / 0119407 A, **2008**, 14.
- [51]. Alhamadsheh M. M., Gupta S., Hudson R. A., Perera L., Tillekeratne L. M.V., *Chem. Eur. J.* **2008**, *14*, 570–581.
- [52]. (a) Lapina I. M.m Pevzner L. M., Prekhin A. A., *Russ. J. Gen. Chem.* **2007**, *77*, 923–925. (b) Gluzok S., Frederick R., Foulon C., Klupsch F., Supuran C. T., Vullo D., Scozzafava A., Goossens J., Masereel B., Depreux P. Goossens L., *Bioorg. Med. Chem.* **2010**, *18*, 7392–7401.
- [53]. Thomas G. L., Spandl R. J., Glansdorp F. G., Welch M., Bender A., Cockfield J., Lindsay J. A., Bryant C., Brown D. F. J., Loiseleur O., Rudyk H., Ladlow M., Spring D. R., *Angew. Chem. Int. Ed.* **2008**, *15*, 2802–2812.
- [54]. Alagic A., Koprianiuk A., Kluger R., *J. Am. Chem. Soc.* **2005**, *127*, 8036–8043.
- [55]. Kitti A., Ronald G., Nimal G. H. Q., James K., Visuvanathar S., *J. Chem. Soc., Perkin Trans. 1: Organic and Bio-Organic Chemistry (1972-1999)* **1987**, *10*, 2285–2296.
- [56]. Pyne J., Bonnefous C., Symons K.t., Nguyen P. M., Sablad M., Rozenkrants N., Zhang Y., Wang L., Yazdani N., Shiau A. K., Noble S. A., Rix P., Rao T. S., Hassig C. A., Smith N., D., *J Med Chem.* **2010**, *53*, 7739–7755.
- [57]. Kameswaren V., United States Patent, Patent Nr. 5,128,485, **1992**,
- [58]. Herath A., Cosford N. D. P., *Org. Lett.* **2010**, *12*, 5182–5185.
- [59]. Kareswaren V, Jiang B., *Synthesis* **1997**, *5*, 530–532.
- [60]. Poot A. J., Van Ameijde J., Slijper M., Van den Berg A., Hilhorst R., Ruijtenbeek R., Rijkers D. T. S., Liskamp R. M.J., *ChemBioChem* **2009**, *10*, 2042–2051.
- [61]. Dai Q., Yang W., Zhang X., *Org. Lett.* **2005**, *7*, 5343–5345.
- [62]. Aubert C., Begue J., Charpentier-Morize M., Nee G., Langlois B., *J. Fluor. Chem.* **1989**, *44*, 361–376.
- [63]. Roth B. D., Ortwine D. F., Hoefle M. L., Stratton C. D., Sliskovic D. R., Wilson M. W., Newton R. S., *J. Med. Chem.* **1990**, *33*, 21–31.

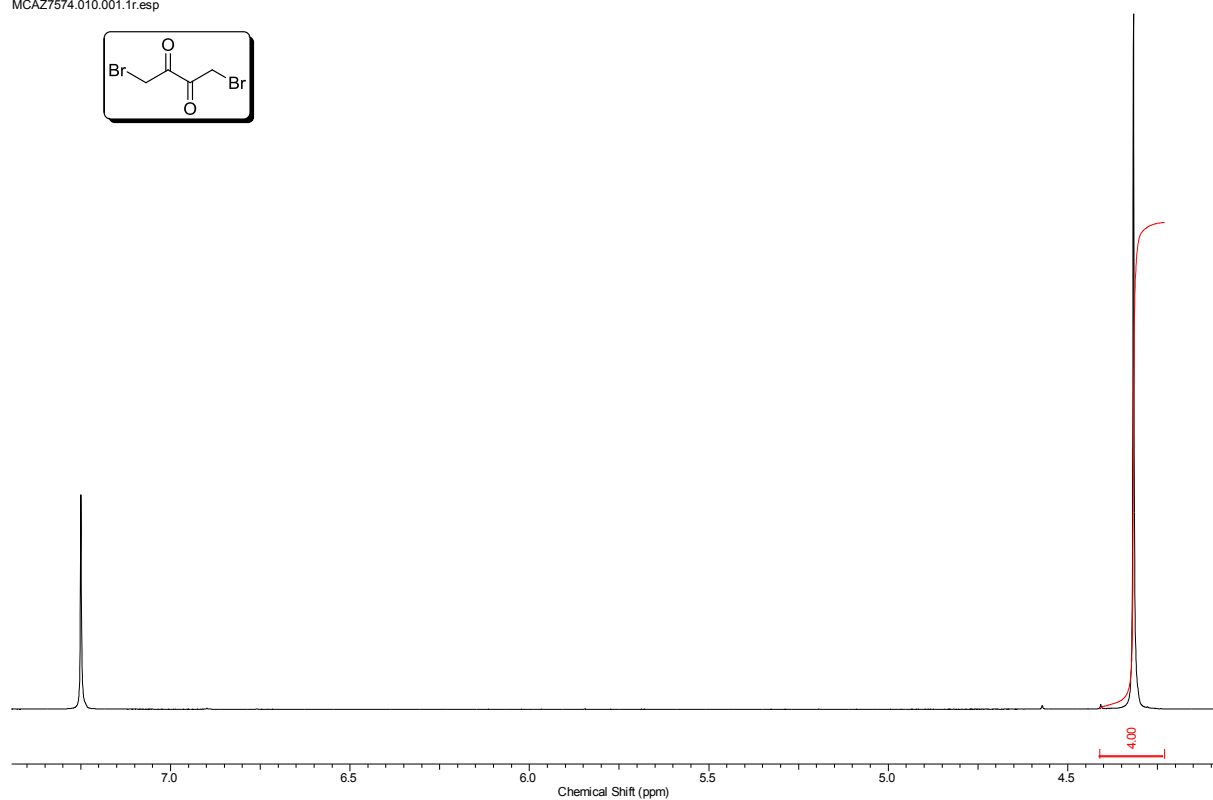
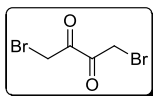
- [64]. Pinto D. J. P., Quan M. L., Smith L. M., II, Orwat M. J., Gilligan P. J., PCT Int. Appl., WO2008157162, **2008**, 168–169.
- [65]. Sanzhizhapov D. B., Mognonov D. M., Khakhinov V. V., Erdyneev N. S., *Izvestiya Akademii Nauk SSSR, Seriya Khimicheskaya* **1983**, 7, 1685.
- [66]. (a) Piller F. M., Appukkuttan P., Gavryushin A., Helm M., Knochel P., *Angew. Chem. Int. Ed.* **2008**, 47, 6802 – 6806. (b) Clososki G. C., Rohbogner C. J., Knochel P., *Angew. Chem. Int. Ed.* **2007**, 46, 7681–7684.
- [67]. Liu C., Knochel P., *J. Org. Chem.* **2007**, 72, 7106–7115.
- [68]. Celik C., Kulu I., Ocal N., Kaufmann D. E., *Helv. Chim. Acta.* **2009**, 92, 1092–1011.
- [69]. Brown W., Johnstone S., Labrecque D., PCT Int. Appl., WO2008018827, **2008**, 136.
- [70]. St.Jean D. J. Jr., Cheng E. P., Bercot E. A., *Tetrahedron Lett.* **2006**, 2006, 47, 6225–6227.
- [71]. Etayo P., Badorrey R., Diaz-de-Villegas M. D., Galvez J. A., *J. Org. Chem.* **2007**, 72, 1005–1008.
- [72]. Sheehan J. C., Hess G. P., *J. Am. Chem. Soc.* **1955**, 77, 1067–1068.
- [73]. König W., Geiger R., *Chem. Ber.* **1970**, 103, 788.
- [74]. Wieland T., Bokelmann E., Bauer L.; Lang H. U., Lau H.; *Liebigs Ann. Chem.* **1953**, 583, 129–149.
- [75]. Dawson P. E., Kent S. B. H., Muir T. W., *Science* **1994**, 266, 776–149.
- [76]. Hackeng T. M.; Griffin G. F.; Dawson P.E.; *Proc. Natl. Acad. Sci. USA* **1999**, 96, 10068–10073.
- [77]. Dawson P. E.; Muir T. W.; Kent S. B. H., PCT Int. Appl. WO 1996034878 A1, **1996**.
- [78]. Dawson P. E.; Churchill M. J.; Ghadiri. M. R.; Kent S. B. H. *J. Am. Chem. Soc.* **1997**, 119, 4325–4329.
- [79]. Evans T. C. Jr, Benner J., Xu M-Q., *Protein Sci.* **1998**, 7, 2256–2264.
- [80]. Johnson E. C. B.; Kent S. B. H., *J. Am. Chem. Soc.* **2006**, 126, 6640–6646.
- [81]. (a) Du Vigneaud V., Ressler C., Swan J. M., Roberts C. W., Katsoyannis P. G., Gordon S., *J. Am. Chem. Soc.* **1953**, 75, 4897. (b) Hofmann K., Yajima H., Yanaihara N., Liu T., Land S., *J. Am. Chem. Soc.* **1961**, 88, 487. (c) Boissonas R. A., Guttman S., Jaquenoud P. A., *Helv. Chim. Acta.* **1960**, 43, 1349.
- [82]. Merrifield R. B., *J. Am. Chem. Soc.* **1963**, 85, 2149–2154.
- [83]. Merrifield R. B., *J. Am. Chem. Soc.* **1964**, 86, 304–305.
- [84]. Carpino L. A., *J. Am. Chem. Soc.* **1957**, 79, 98–101.

- [85]. McKay F. C.; Albertson N. F., *J. Am. Chem. Soc.* **1957**, *79*, 4686–4690.
- [86]. Sakakibara S.; Shimonishi Y.; Kishida Y.; Okada M.; Sagihara H., *Bull. Chem. Soc. Jpn.* **1976**, *40*, 2164.
- [87]. Mitchell A. R.; Erickson B. W.; Ryabtser M. N.; Hodges R. S.; Merrifield R. B., *J. Am. Chem. Soc.* **1976**, *98*, 7357–7362.
- [88]. Pietta P. G.; Marshall G. R., *J. Chem. Soc. Chem. Comm.* **1970**, 650.
- [89]. Southard S. L., Brooke G. R., Pettee J. M., *Tetrahedron Letters*, **1969**, *10*, 3505–3508.
- [90]. Matsaeda G. R.; Stewart J. M., *Peptides* **1981**, *2*, 45.
- [91]. Carpino L. A.; Han G. Y., *J. Am. Chem. Soc.* **1970**, *92*, 5748–5749.
- [92]. Wang S. S., *J. Am. Chem. Soc.*, **1973**, *95*, 1328–1333.
- [93]. Chang C. D.; Meienhofer J., *Int. J. Pep. Protein Res.* **1978**, *3*, 246–249.
- [94]. Merrifield R. B., *Biochemistry* **1960**, *3*, 1385–1390.
- [95]. Kisfaludy L.; Schön I., *Synthesis* **1983**, 325.
- [96]. Atherton E.; Cameron L. R.; Sheppard R. C., *Tetrahedron* **1988**, *44*, 843–857.
- [97]. Wade J. D.; Bedford J.; Sheppard R. C.; Tregear G. W., *Pep. Res.* **1991**, *4*, 194–199.
- [98]. Liebe B.; Kunze K., *Ange. Chem. Int. Ed.* **1997**, *36*, 618–621.
- [99]. Larsin B. D.; Holm A.; *Int. J. Pept. Protein Res.* **1994**, *43*, 1–9.
- [100]. Rink H., *Tetrahedron Lett.* **1987**, *28*, 3787–3790.
- [101]. Sieber P., *Tetrahedron Lett.* **1987**, *28*, 2107–2110.
- [102]. Chen G.; Wan Q.; Tan Z.; Kan C.; Hua Z.; Ranganathan K.; Danishefsky S. J., *Ange. Chem. Int. Ed.* **2007**, *46*, 7383–7387.
- [103]. Botti P.; Vilan M.; Manganiello S.; Gaertner H., *Org. Lett.* **2004**, *6*, 4861–4864.
- [104]. (a). Zheng J-S., Chang H-N., Shi J., Liu L., *Science China. Chemistry* **2011**, *55*, 64–69. (b). Zheng J-S., Cui H-K., Fang G-M., Xi W-X., Liu L., *ChemBioChem.* **2010**, *11*, 511–518.
- [105]. George E. A.; Norrick R. P.; Muir T. W., *J. Am. Chem. Soc.* **2008**, *130*, 4914–4924.
- [106]. Warren J. D.; Miller J. S., Keding S. J., Danishefsky S. J., *J. Am. Chem. Soc.* **2004**, *126*, 6576–6578.
- [107]. Chen j., Warren J. D.; Wu B., Chen G.; Wan Q.; Danishefsky S. J., *Tetrahedron Lett.* **2006**, *47*, 1969–1972.
- [108]. Blanco-Canosa J. B.; Dawson P. E., *Ange. Chem. Int. Ed.* **2008**, *47*, 6851–6855.
- [109]. Ingenito R.; Bianchi E.; Fattori D.; Pessi A., *J. Am. Chem. Soc.* **1999**, *121*, 11369–11374.
- [110]. Zhang L. S.; Tam J. P., *J. Am. Chem. Soc.* **1997**, *119*, 2363–2370.

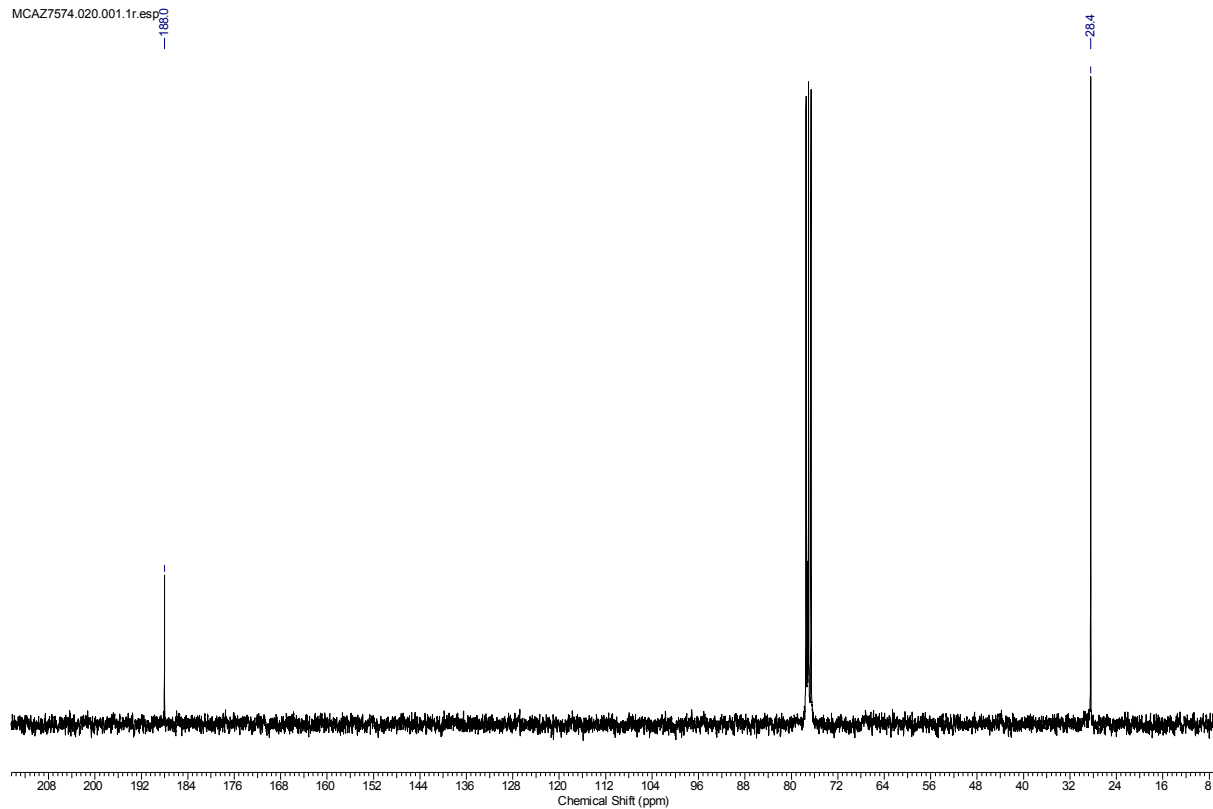
- [111]. Camarero J. A., Cotton G. J.; Adera A.; Muir T. W., *J. Peptide Res.* **1998**, *51*, 303–316.
- [112]. Melda M., *Tetrahedron Lett.* **1992**, *33*, 3077–3080.
- [113]. Tulla-Puche J., Barany G., *J. Org. Chem.* **2004**, *69*, 4101–4107.
- [114]. Seifert S., Oppermann W., Saalwächter K., *Polymer* **2007**, *48*, 5599–5611.
- [115]. TentaGel is a registered trademark of Rapp Polymere GmbH., D-72072 Tübingen, the technical descriptions are from the product brochure and the company website.
- [116]. *Synthesis of Peptides and Peptidomimetics*, Houben Weyl, Eds. Goodman M., Felix A., Moroder L., Toniolo C., Georg Thieme Verlag Stuttgart, New York, 2002, 22, 676.
- [117]. Kempe M.; Barang G., *J. Am. Chem. Soc.* **1996**, *118*, 7083–7093.
- [118]. Albericio F., Martin F. G., *Chimica Oggi / CHEMISTRY TODAY* **2008**, *26*, 29–34.
- [119]. Darlak K., Barany G., United States Patent Application Publication, Pub. Nr. US2006/0047105 A1, **2006**.
- [120]. Ley S. V., Priour A., Heusser C., *Org. Lett.* **2002**, *4*, 711–714.
- [121]. Cleland W. W., *Biochemistry* **1964**, *3*, 480–482.
- [122]. Burns J. A.; Button J. C.; Moran J.; Whitesides G. M., *J. Org. Chem.* **1991**, *58*, 2648–2650.
- [123]. Tanabe S.; Ogarsawara Y.; Nawata M.; Kawanabe K.; *Chem. Pharm. Bull.* **1989**, *37*, 2843–2845.
- [124]. Costa M.; Peusa B.; Lavarone C.; Cavallini D., *Prep. Biochem.* **1982**, *12*, 417–427.
- [125]. Görmer K.; Waldmann H.; Triola G., *J. Org. Chem.* **2010**, *75*, 1181–1183.
- [126]. Pedras M, Soledade C., Chumala P. B., Quail J. W., *Org. Lett.* **2004**, *6*, 4615–4617.
- [127]. Avan I., Tala S. R., Steel P. J., Katritzky A. R., *J. Org. Chem.* **2011**, *76*, 4884–4893.
- [128]. Kaiser E.; Colescott R. L.; Bossinger C. D.; Cook P. I., *Analytical Biochemistry* **1970**, *34*, 595–598.
- [129]. Menche D., Hassfeld J., Li J., Mayer K., Rudolph S., *J. Org. Chem.* **2009**, *74*, 7220–7229.
- [130]. (a). Dittmann M., Sauermann J., Seidel R., Zimmermann W., Engelhard M., *J. Pept. Sci.* **2010**, *16*, 558–562. (b). Dittmann M., Sadek M., Seidel R., Engelhard M., *J. Pept. Sci.* **2012**, *18*, 312–316.

D. Appendix

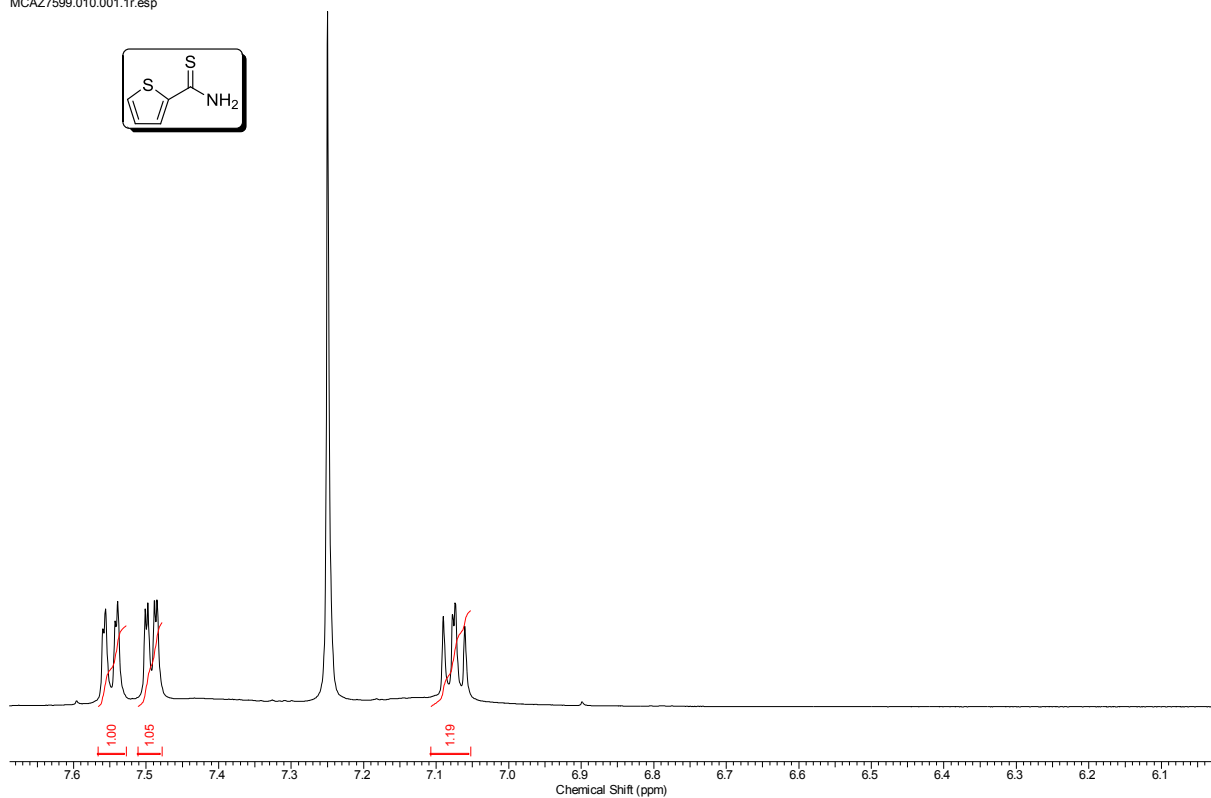
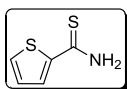
MCAZ7574.010.001.1r.esp



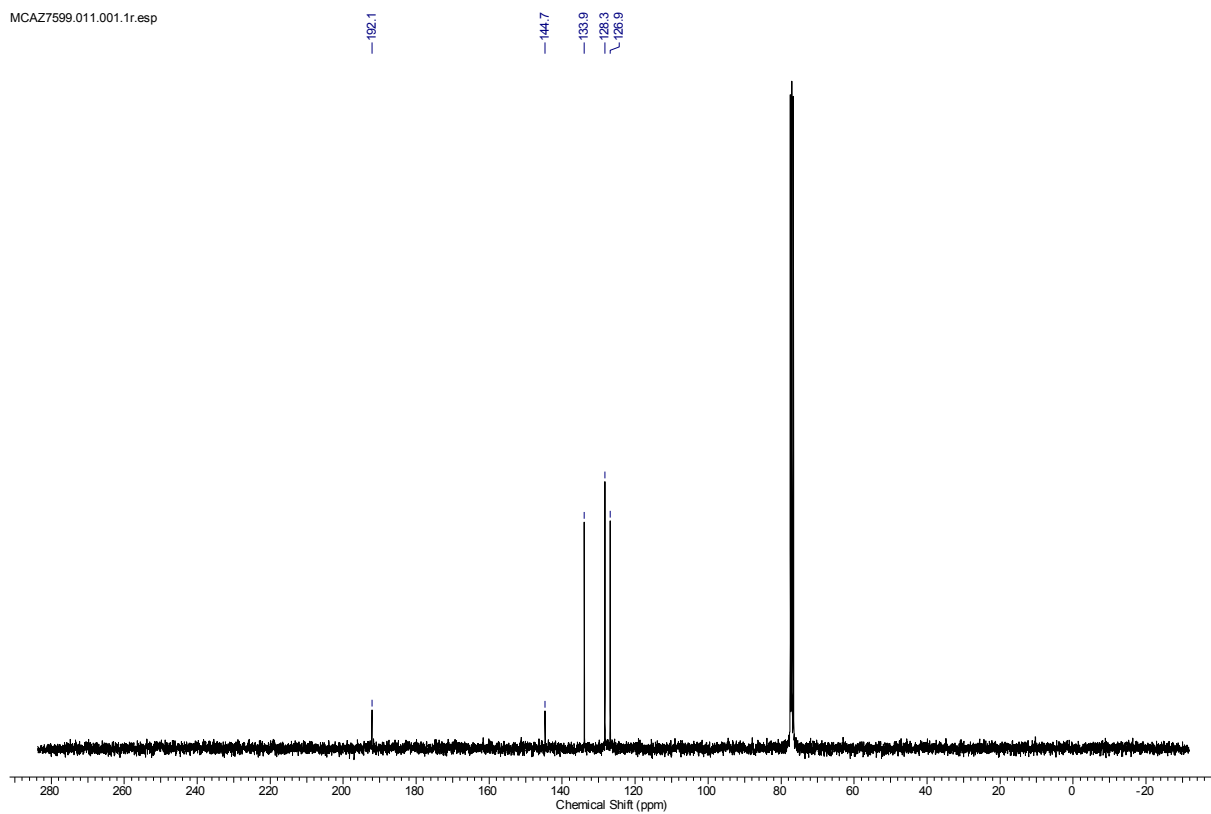
MCAZ7574.020.001.1r.esp



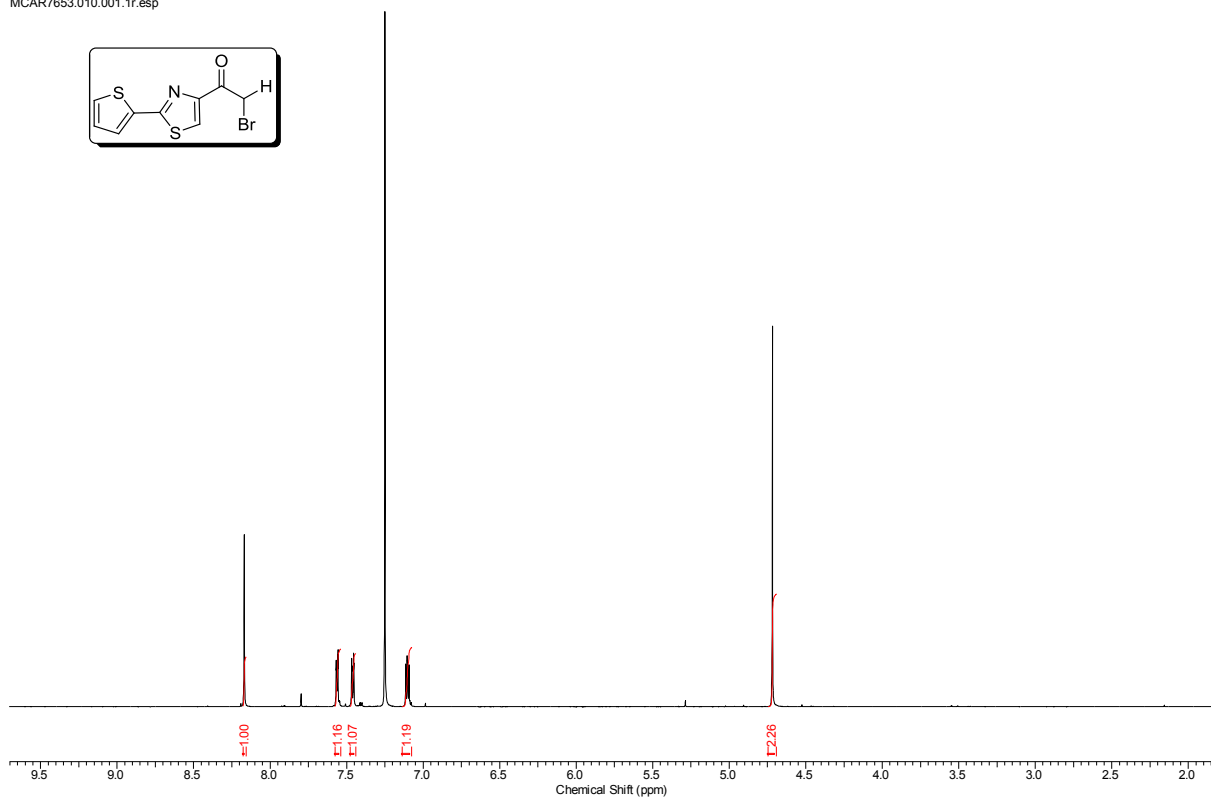
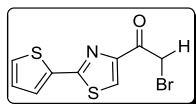
MCAZ7599.010.001.1r.esp



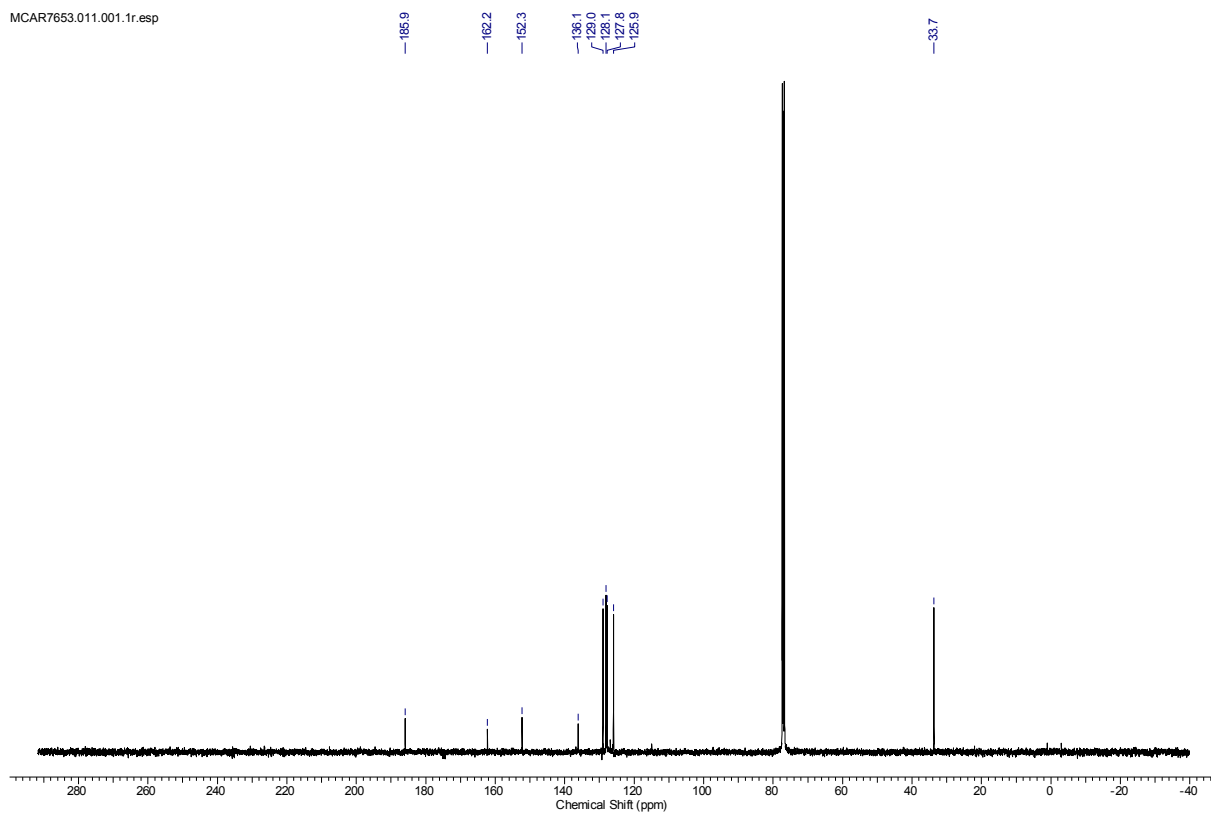
MCAZ7599.011.001.1r.esp



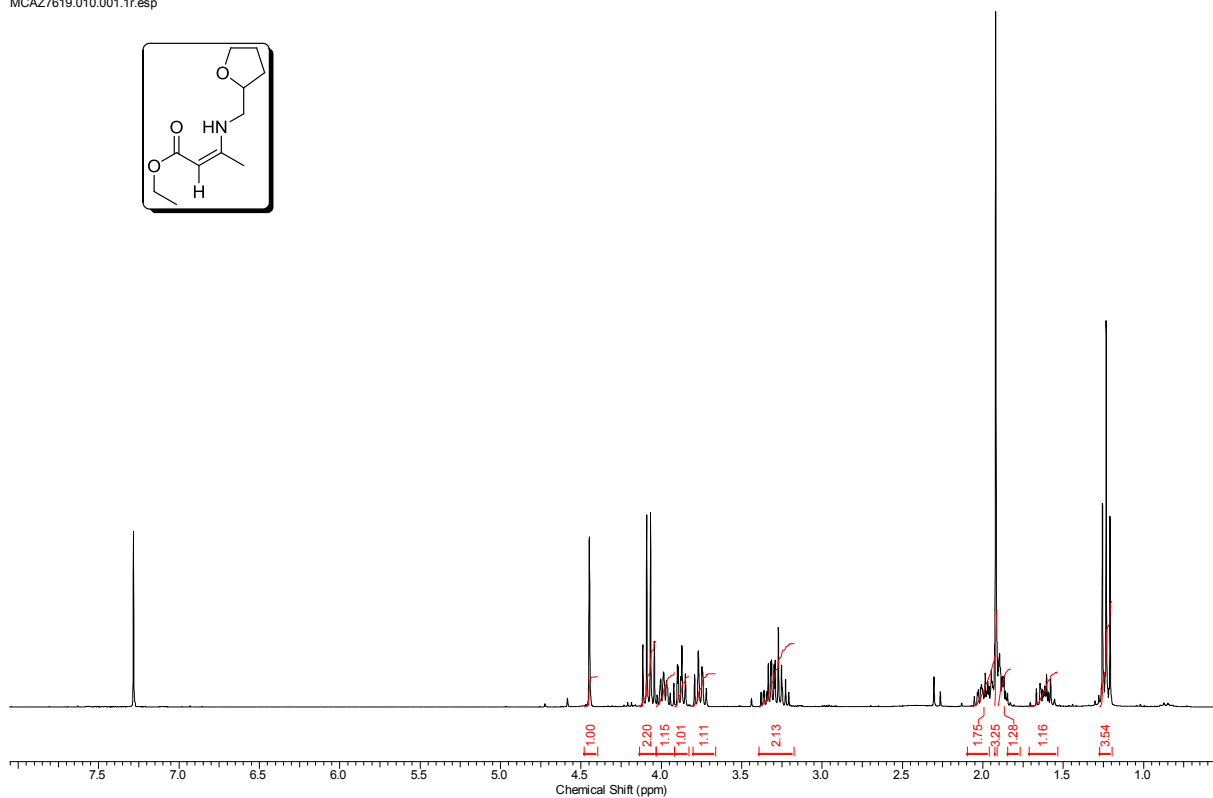
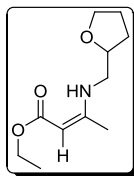
MCAR7653.010.001.1r.esp



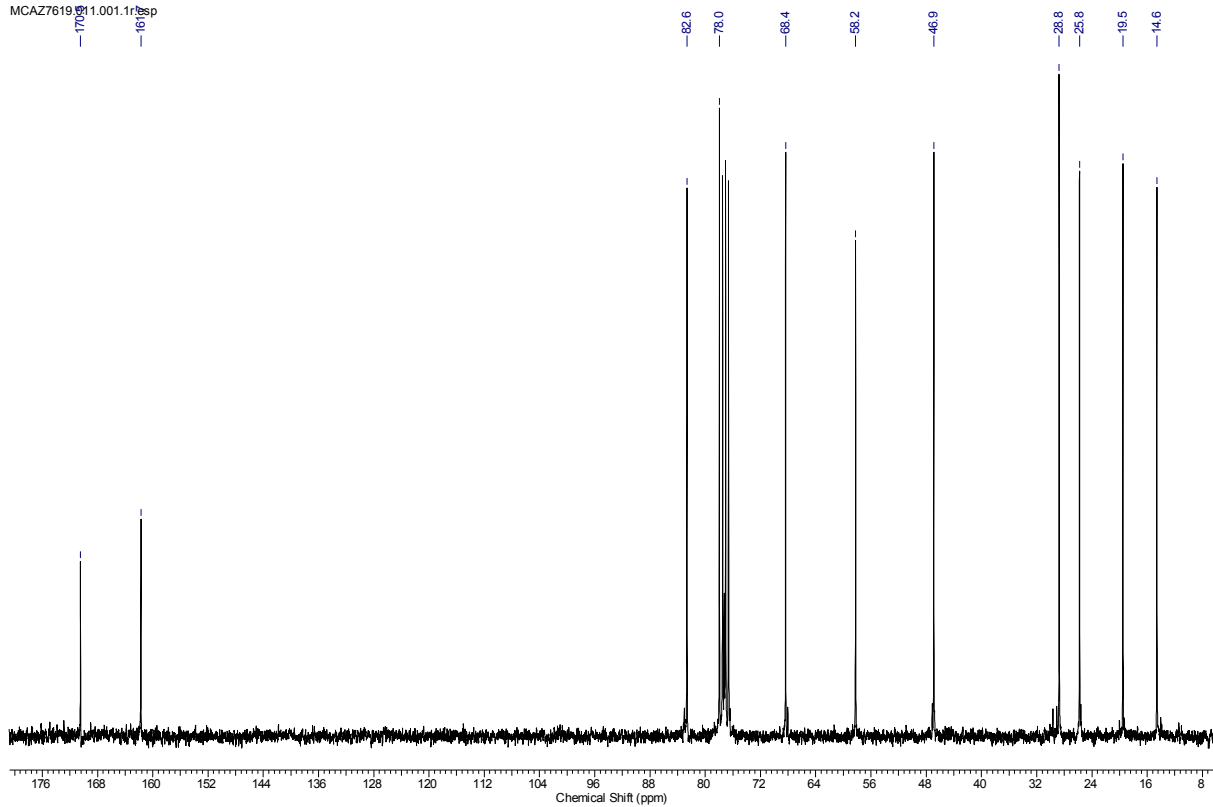
MCAR7653.011.001.1r.esp



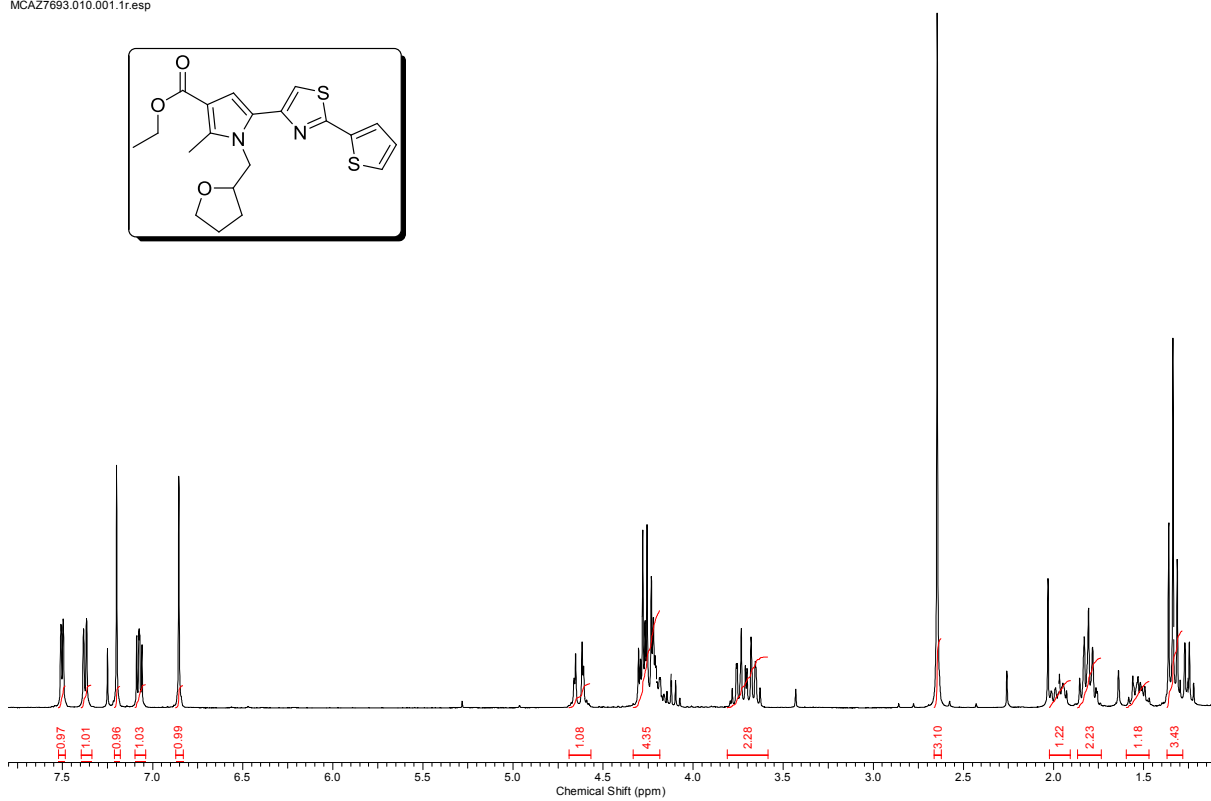
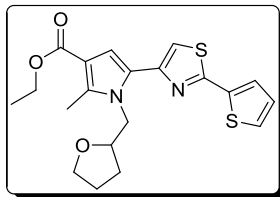
MCAZ7619.010.001.1r.esp



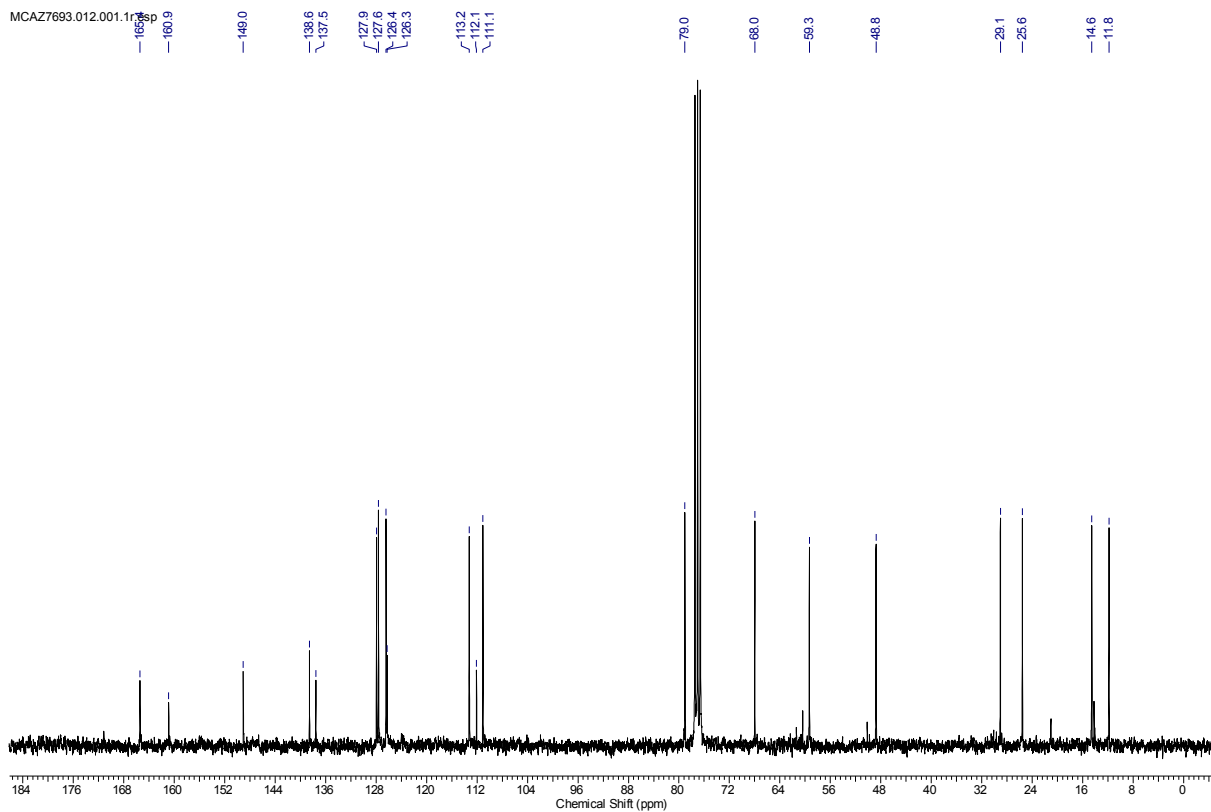
MCAZ7619.010.001.1r.esp



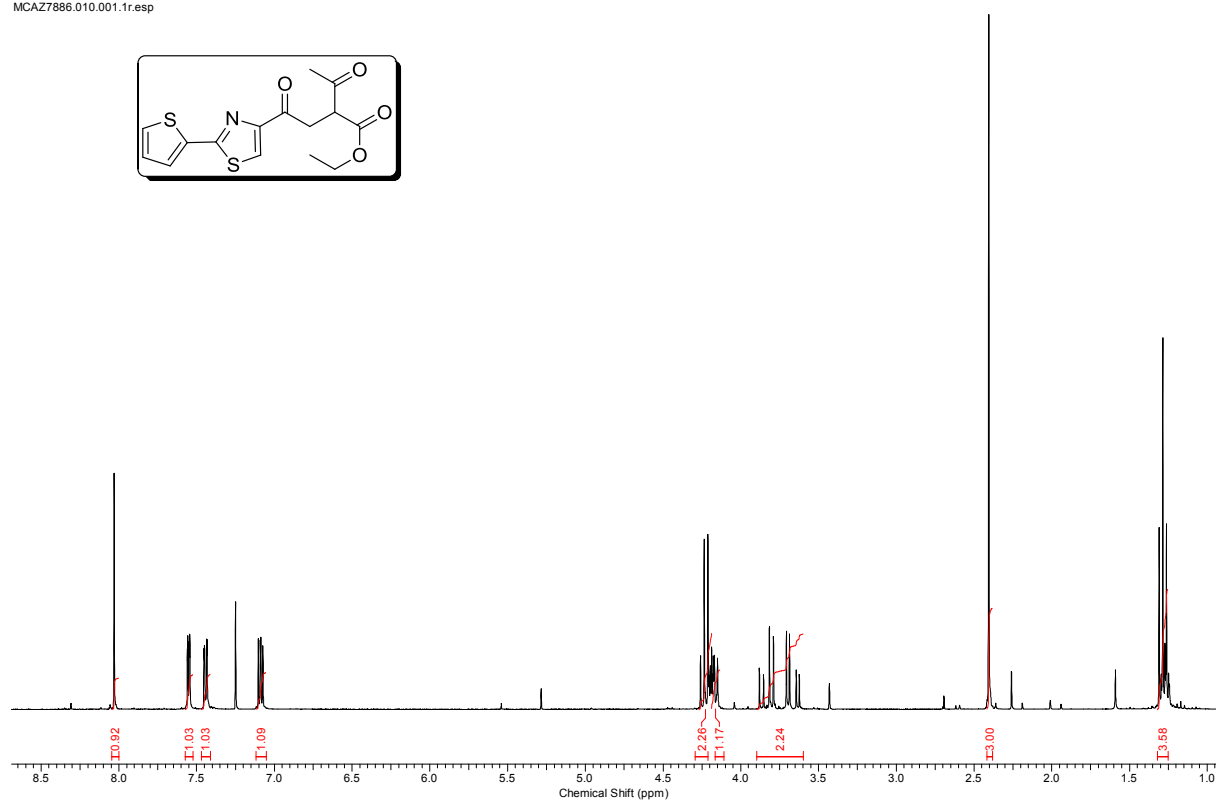
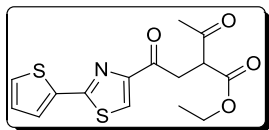
MCAZ7693.010.001.1r.esp



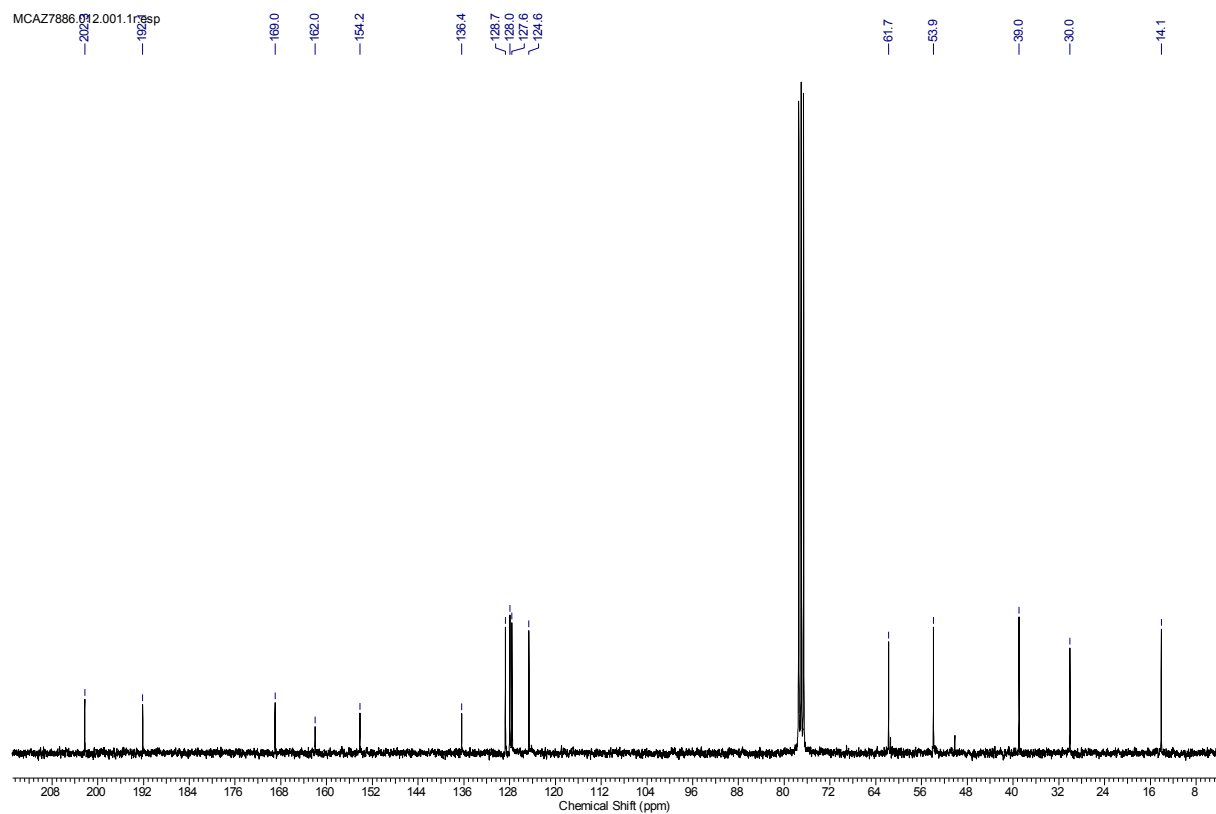
MCAZ7693.012.001.1r.esp



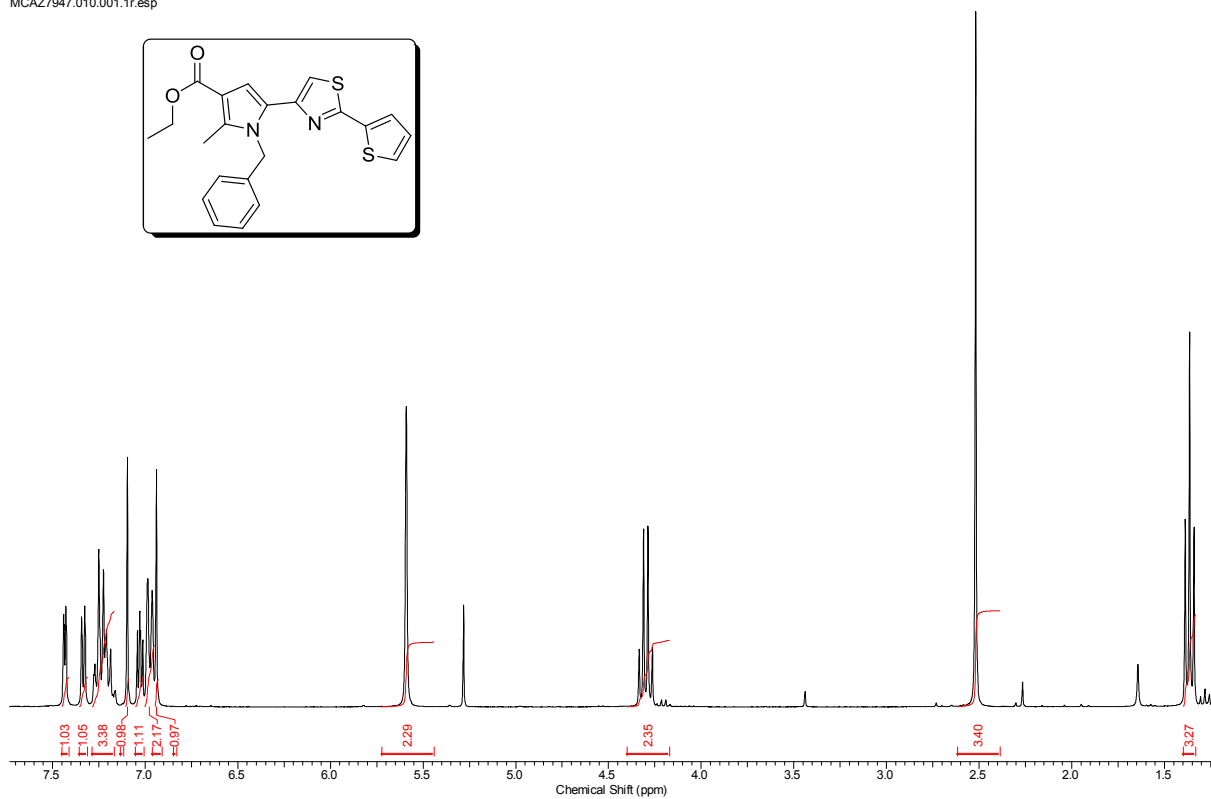
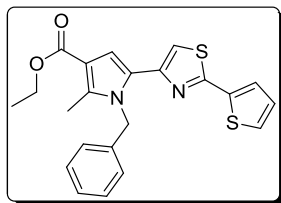
MCAZ7886.010.001.1r.esp



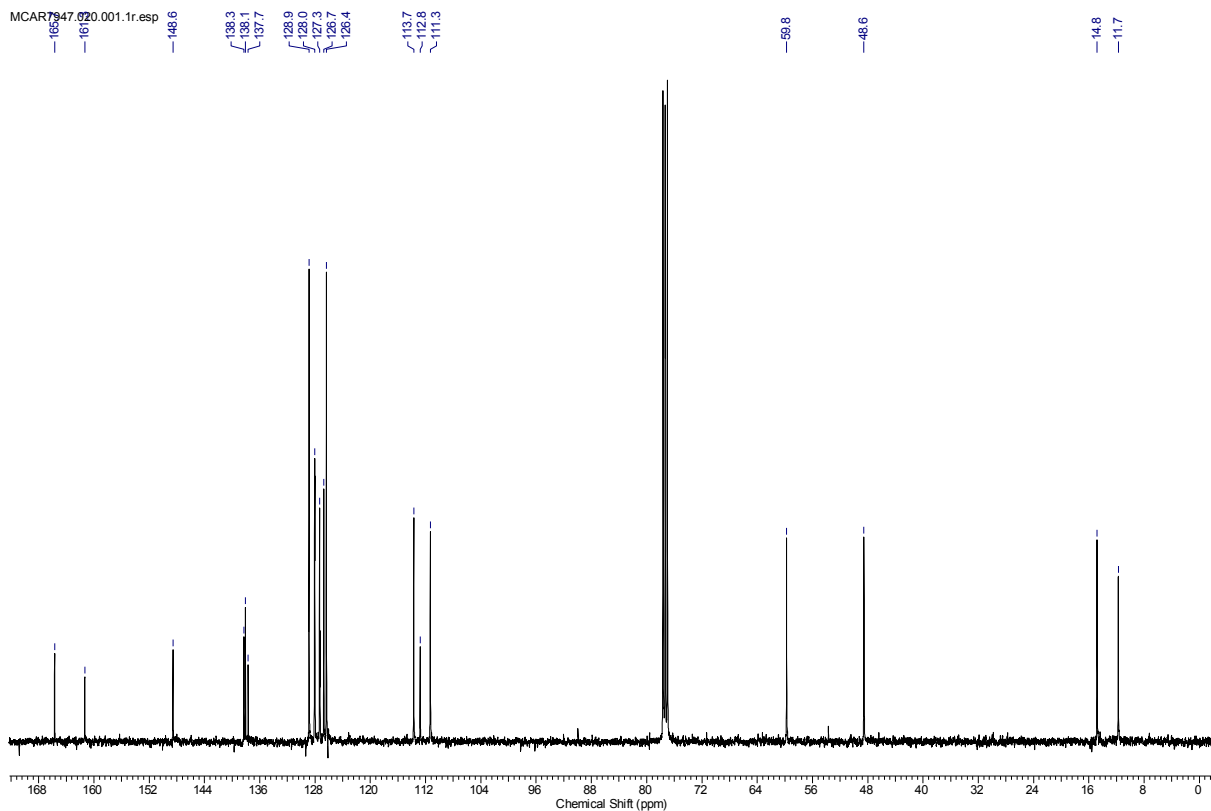
MCAZ7886.012.001.1r.esp



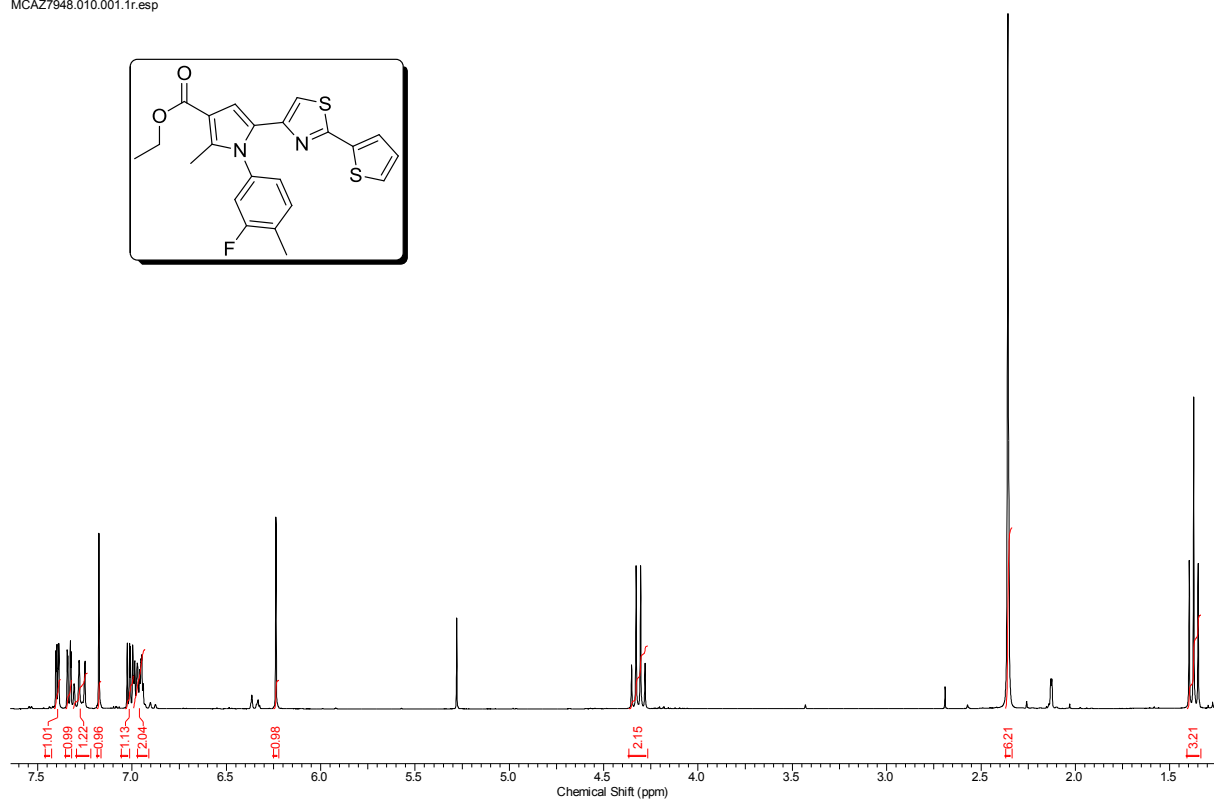
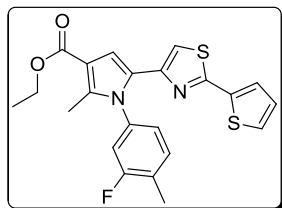
MCAZ7947.010.001.1r.esp



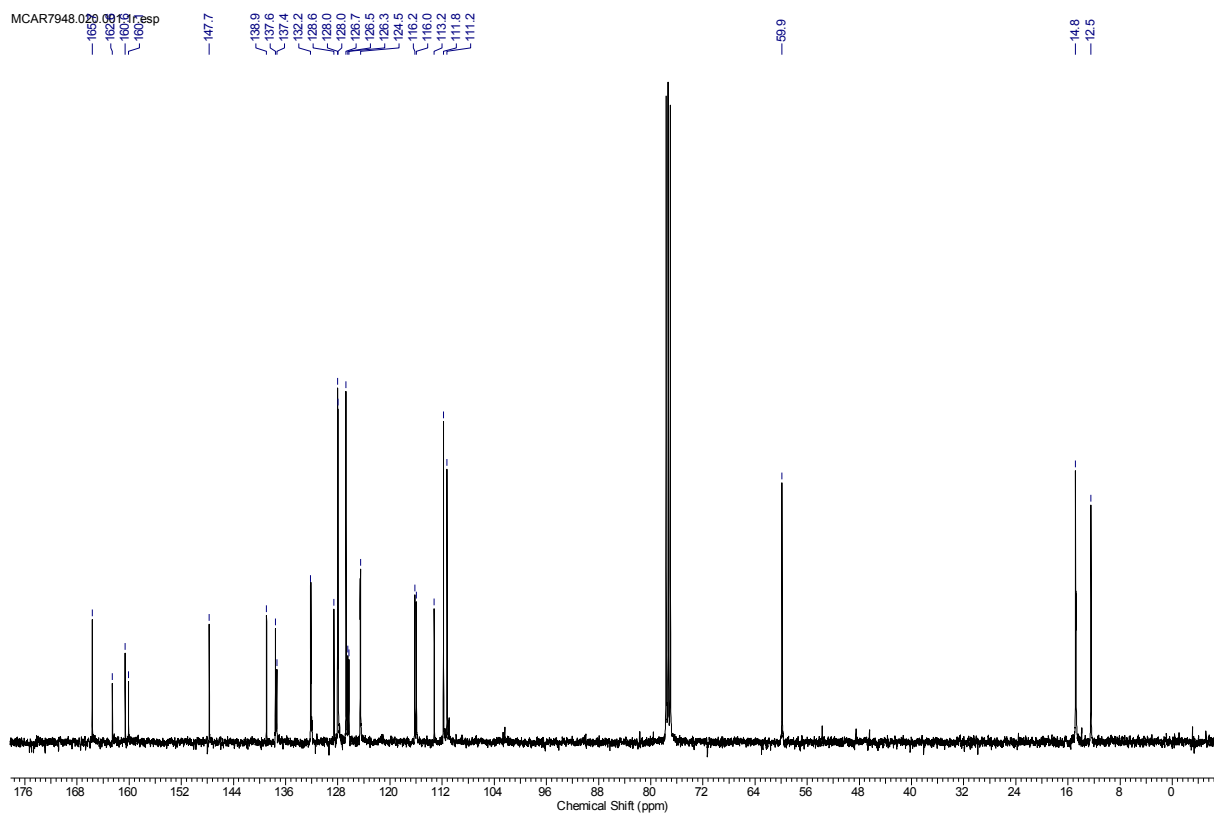
MCAZ7947.020.001.1r.esp



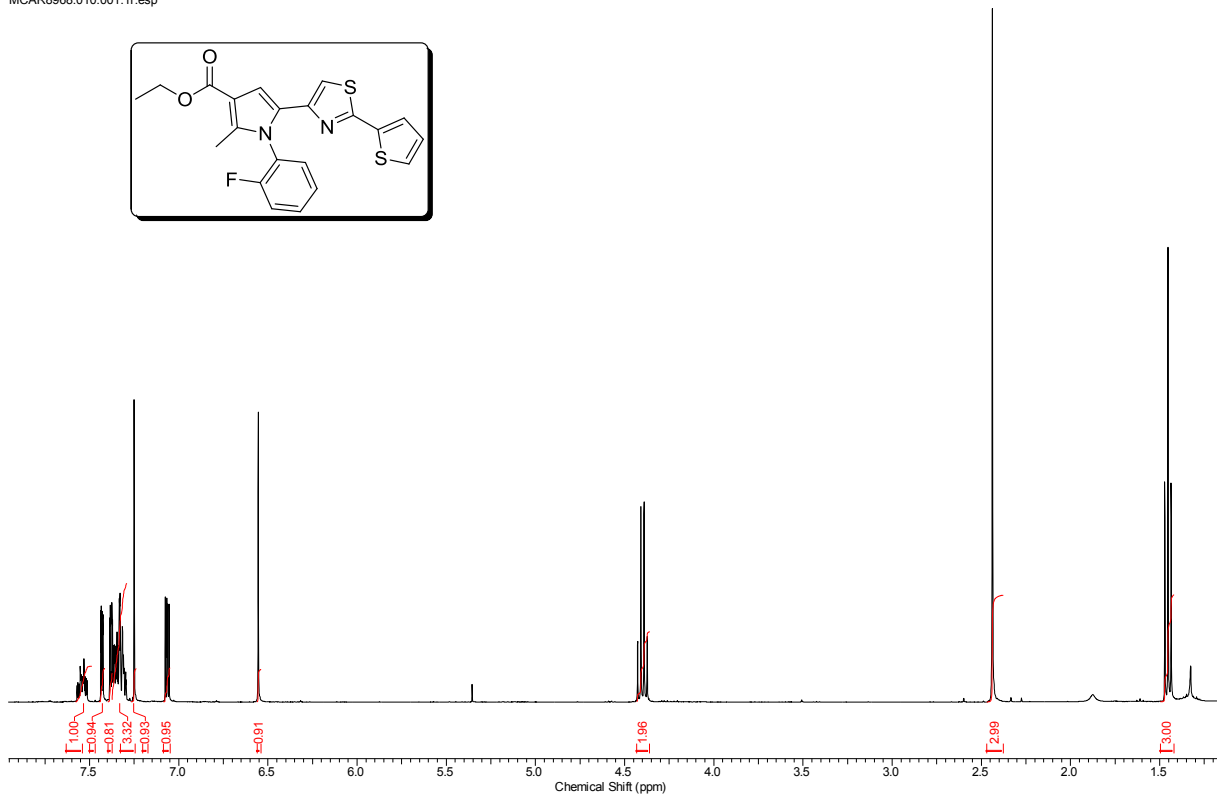
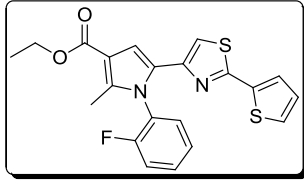
MCAZ7948.010.001.1r.esp



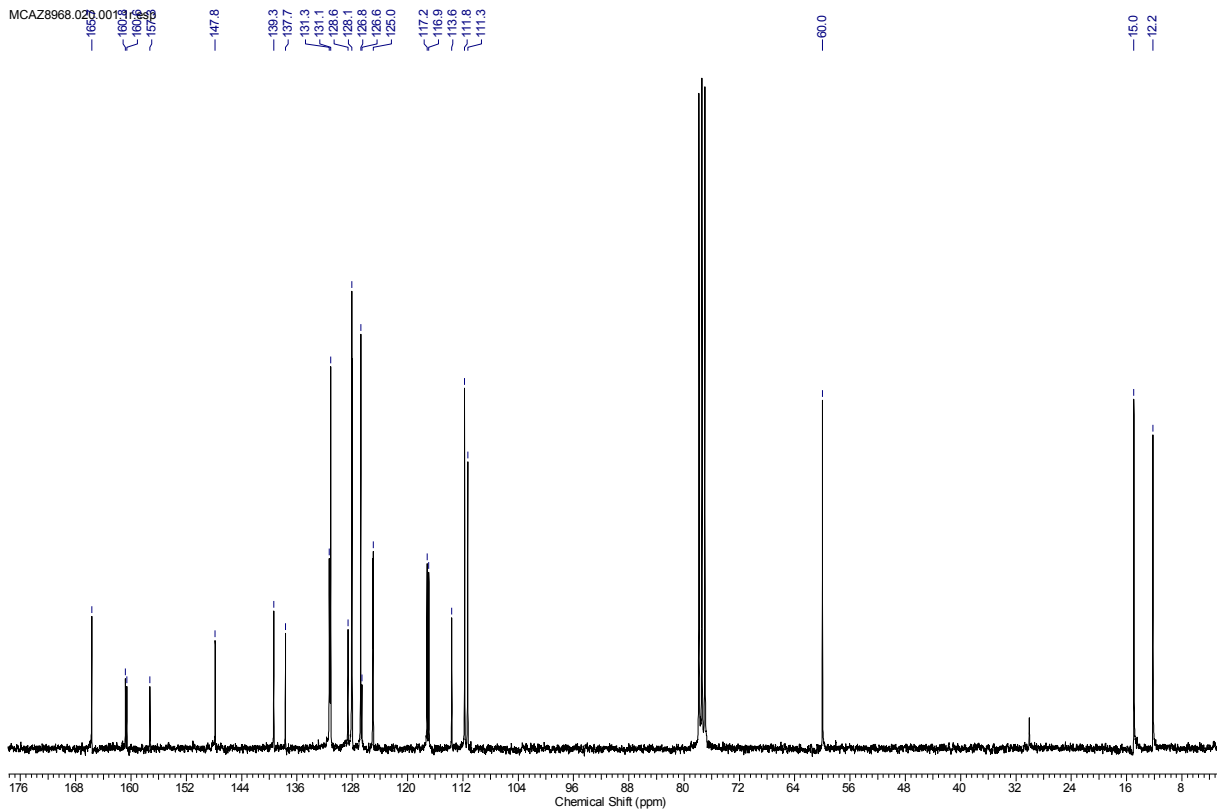
MCAZ7948.020.001.1r.esp



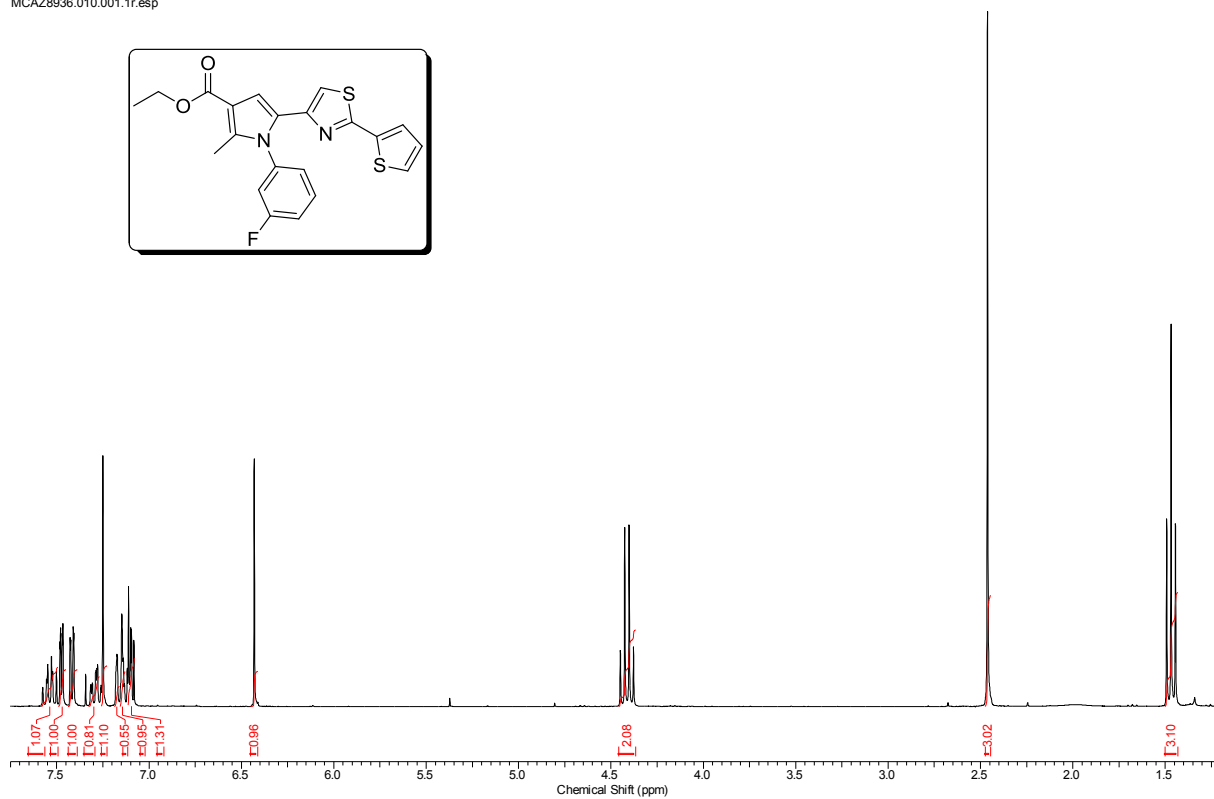
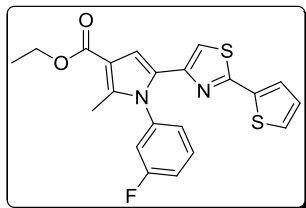
MCAZ8968.010.001.1r.esp



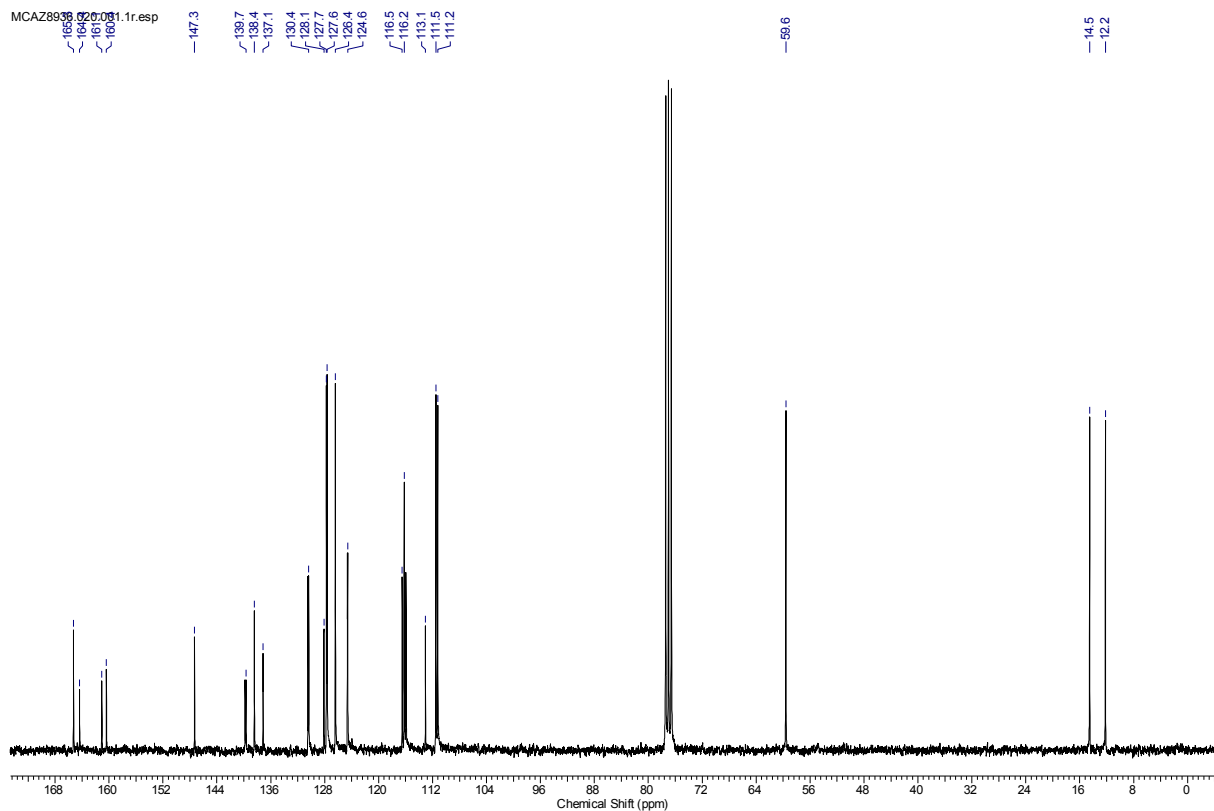
MCAZ8968.020.001.1r.esp



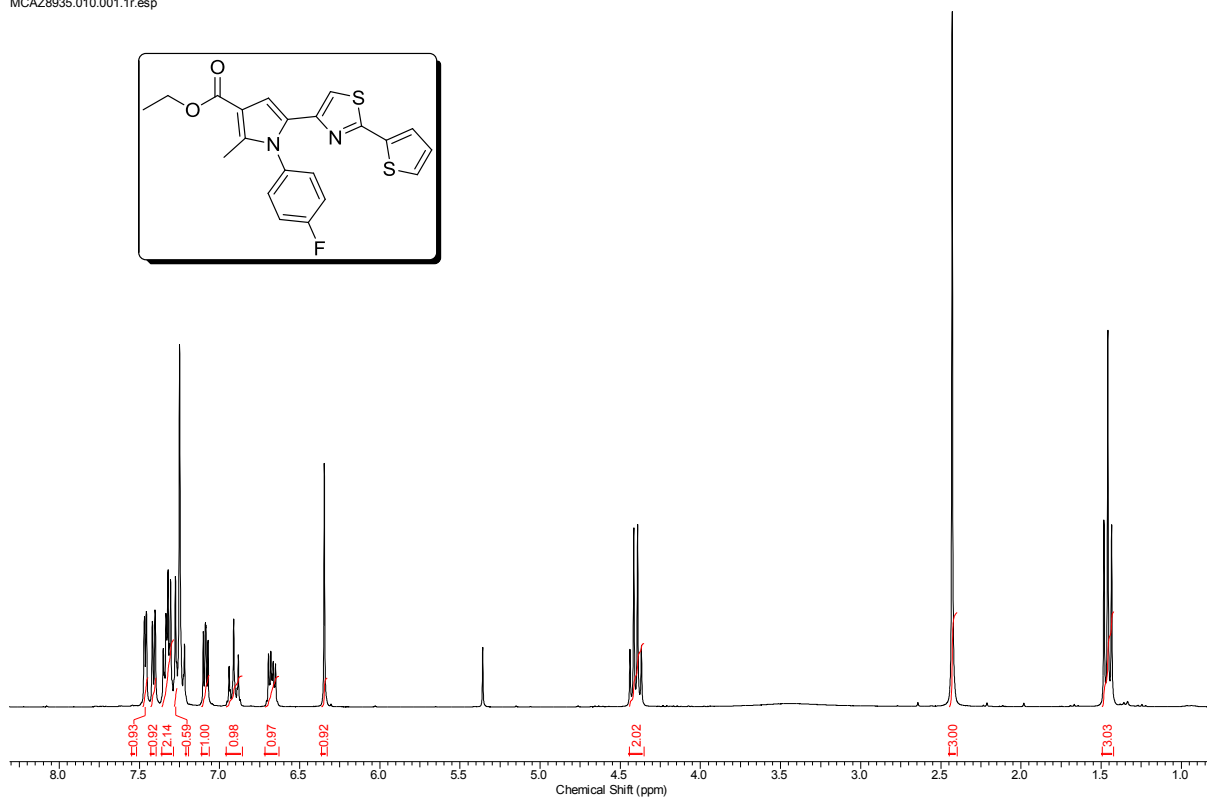
MCAZ8936.010.001.1r.esp



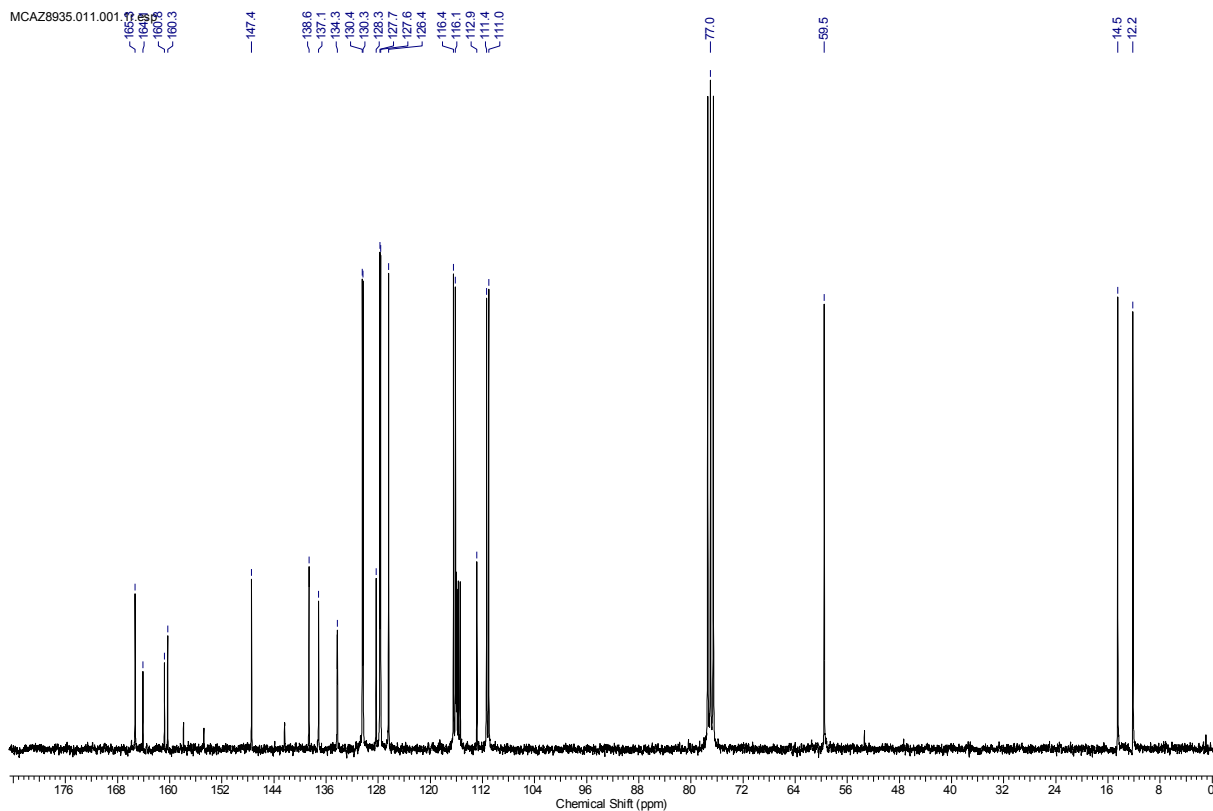
MCAZ8936.020.001.1r.esp



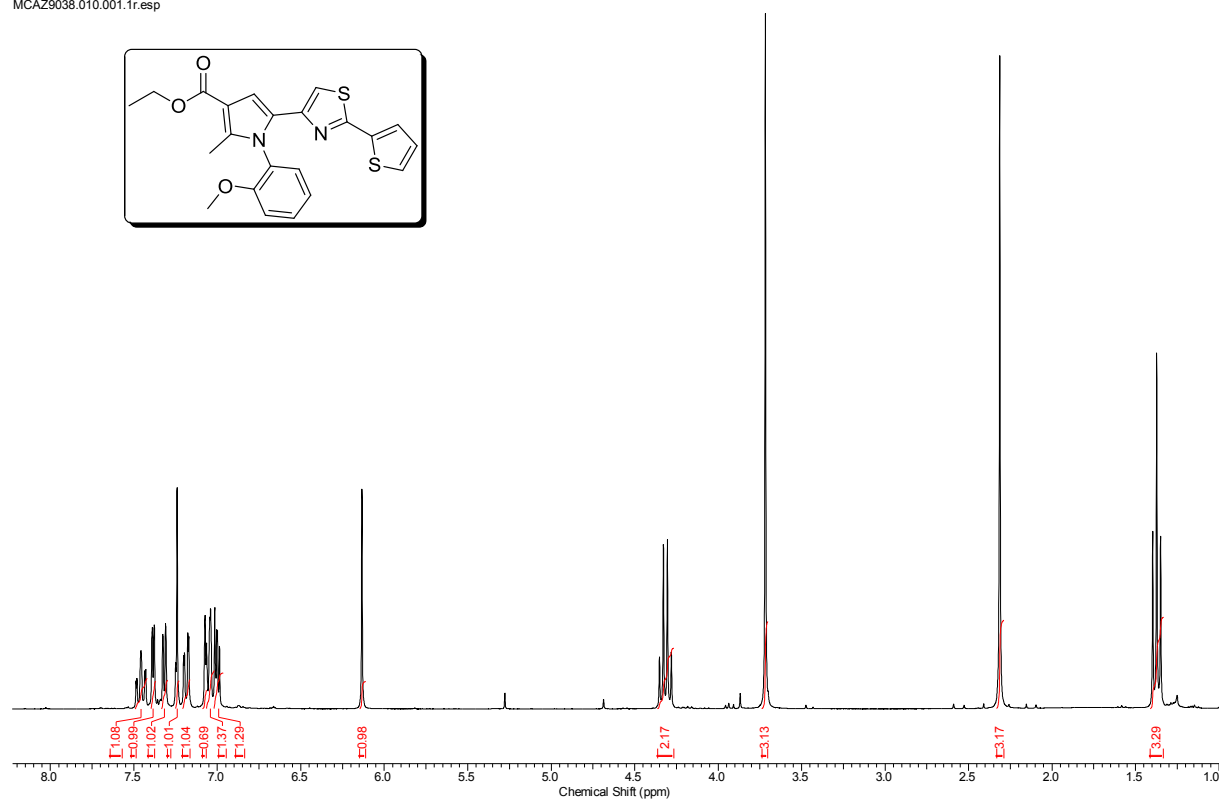
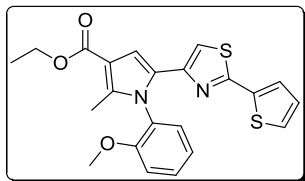
MCAZ8935.010.001.1r.esp



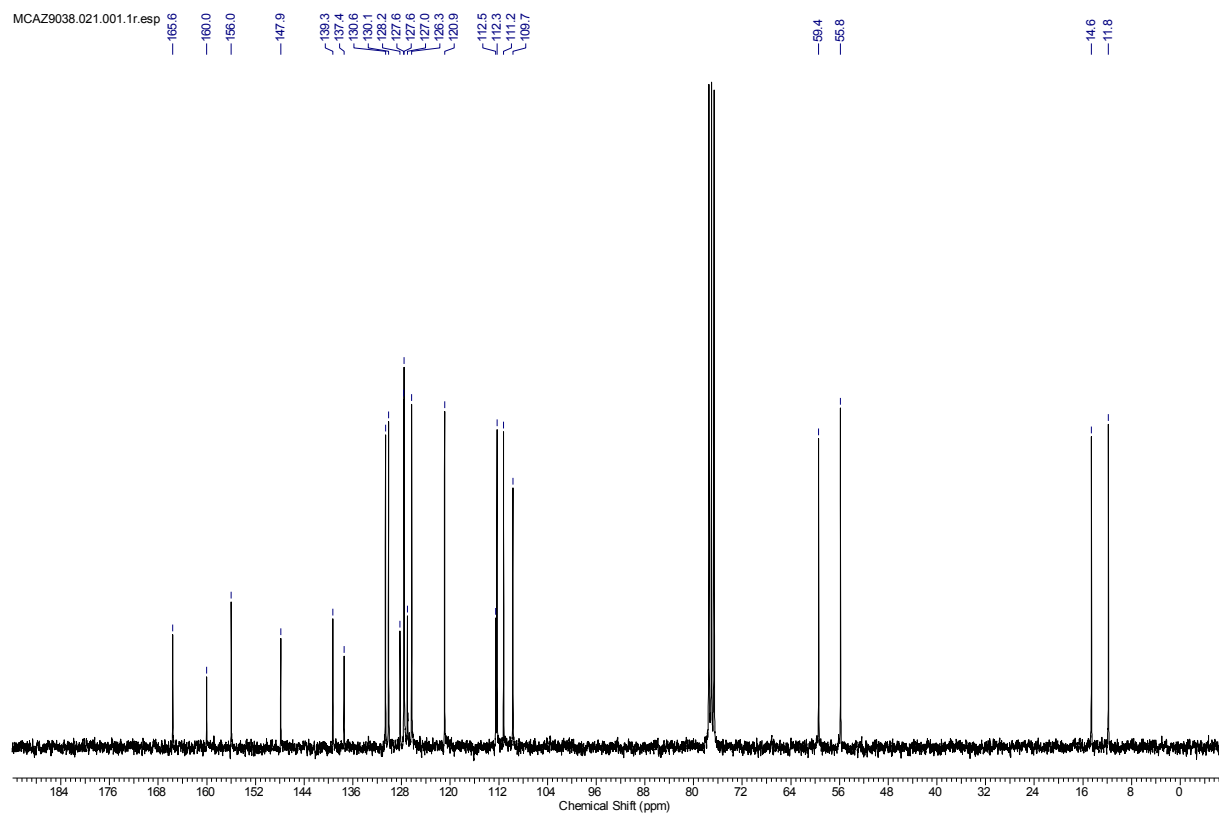
MCAZ8935.011.001



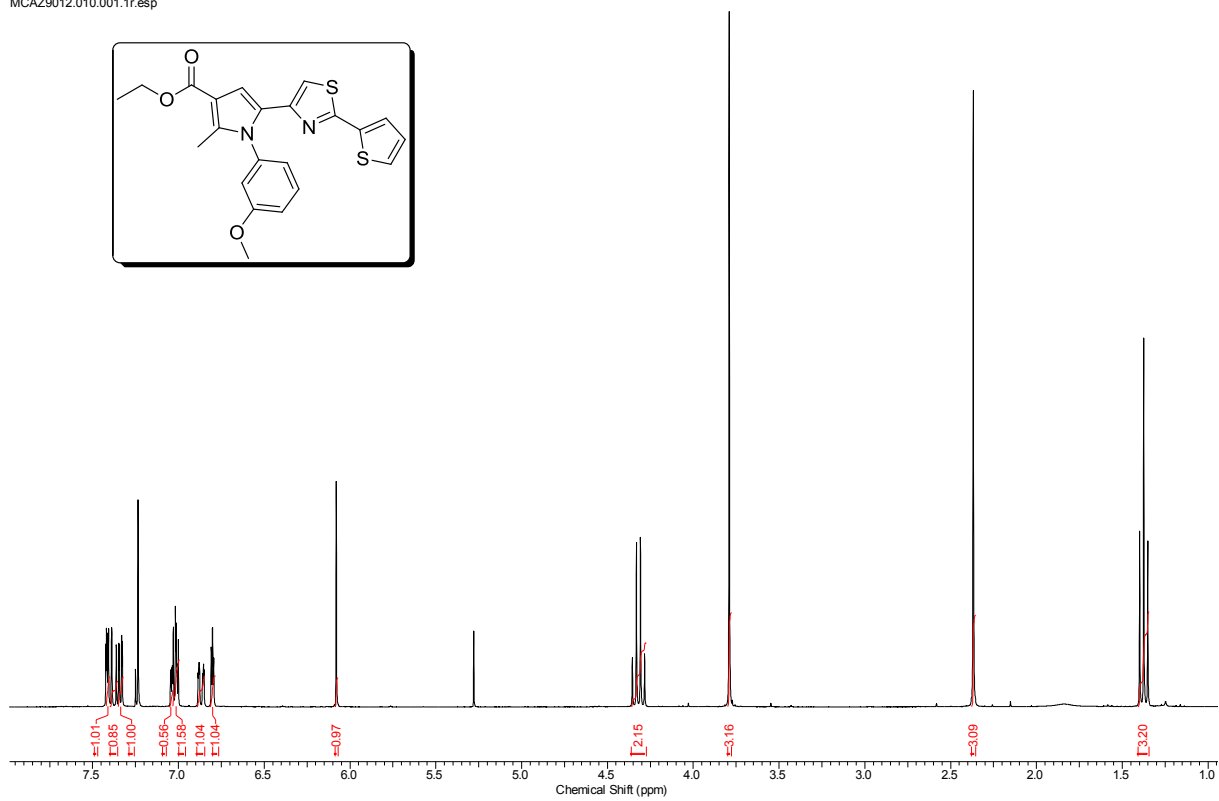
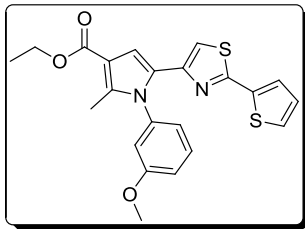
MCAZ9038.010.001.1r.esp



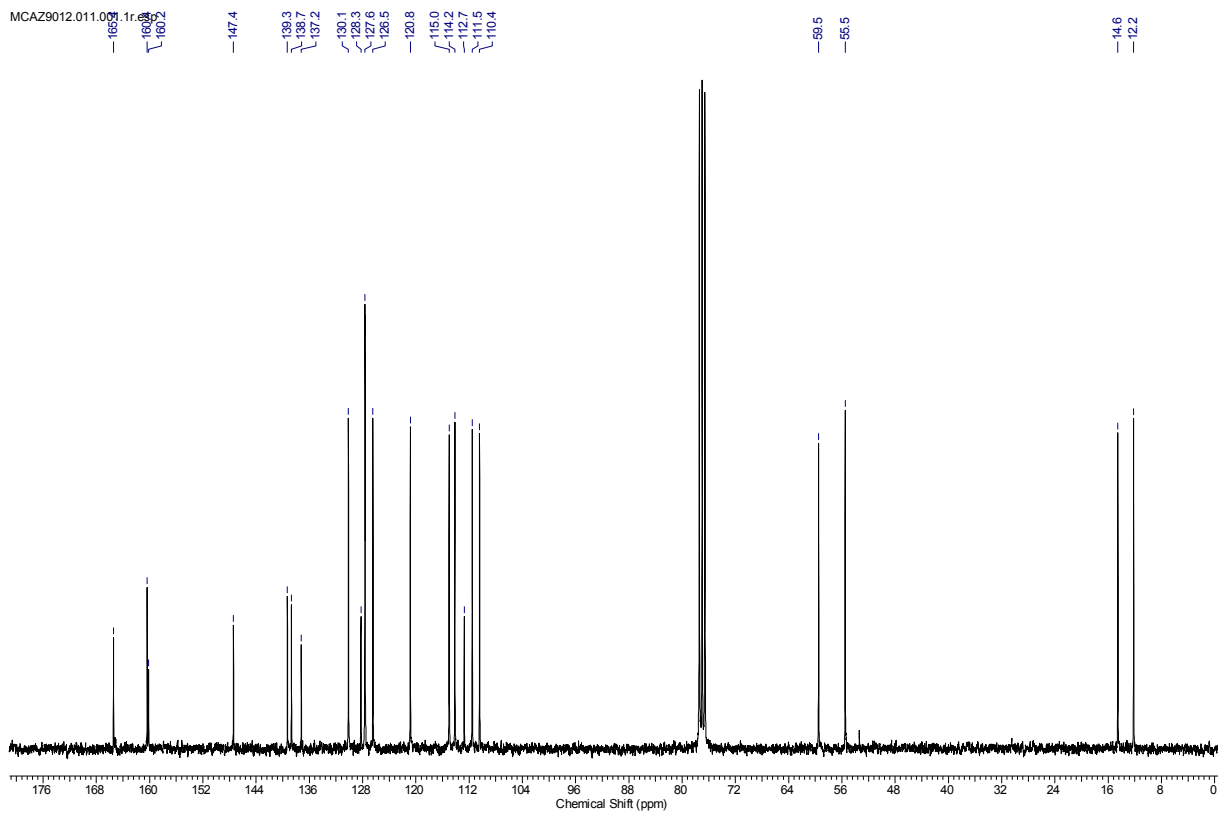
MCAZ9038.021.001.1r.esp



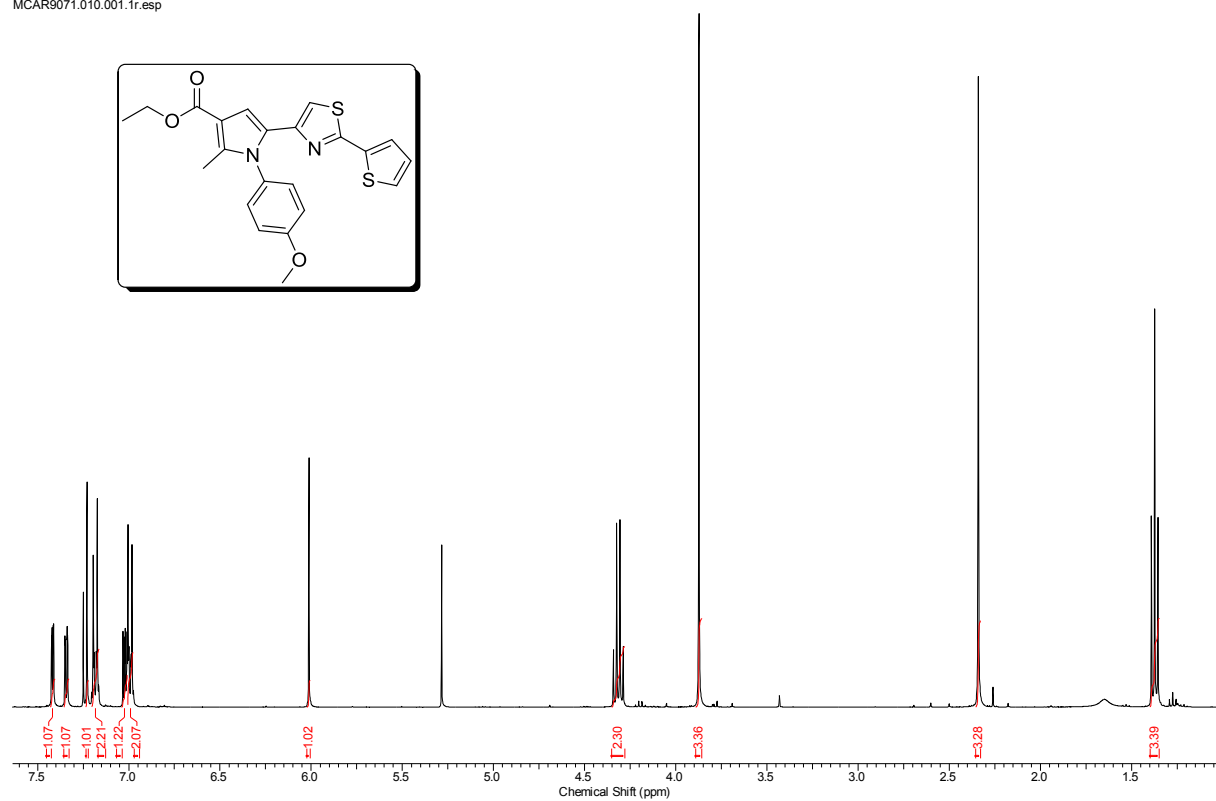
MCAZ9012.010.001.1r.esp



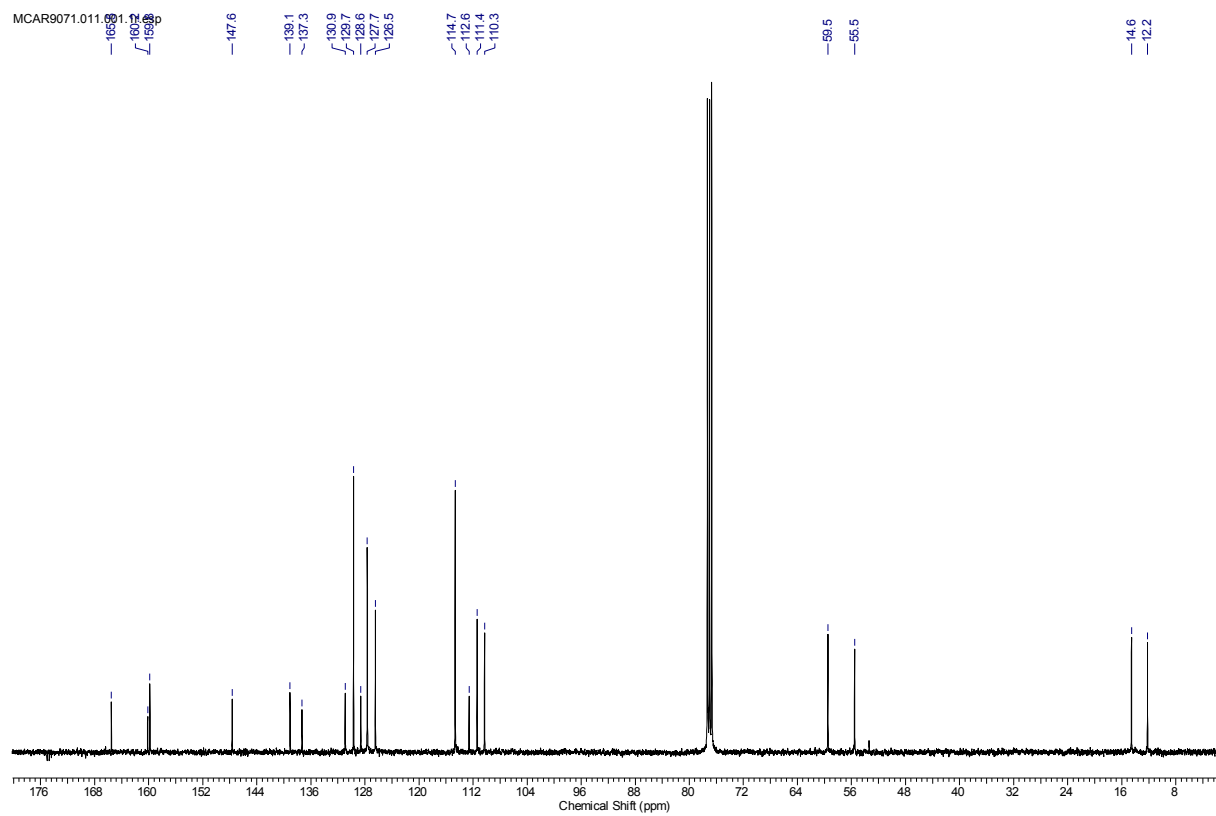
MCAZ9012.011.001.1r



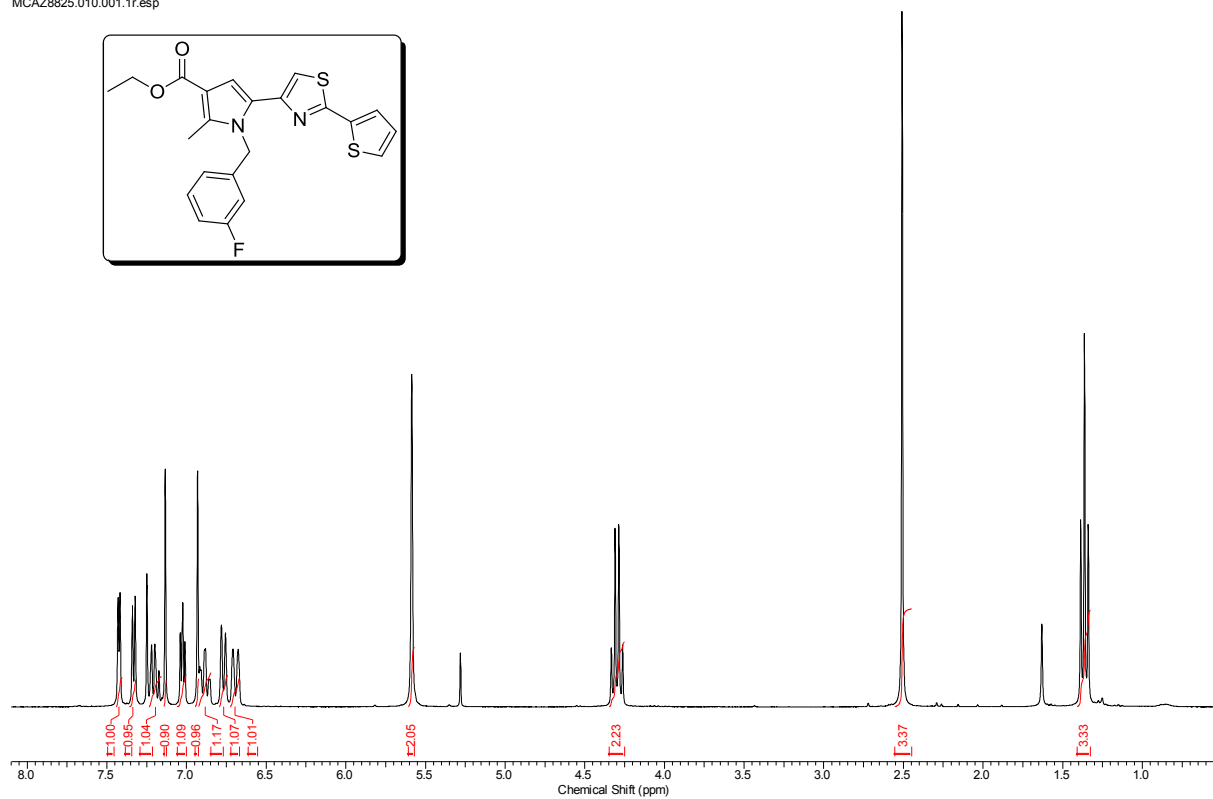
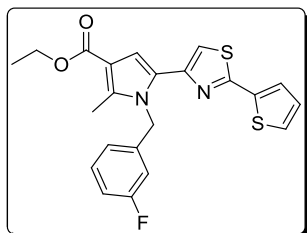
MCAR9071.010.001.1r.esp



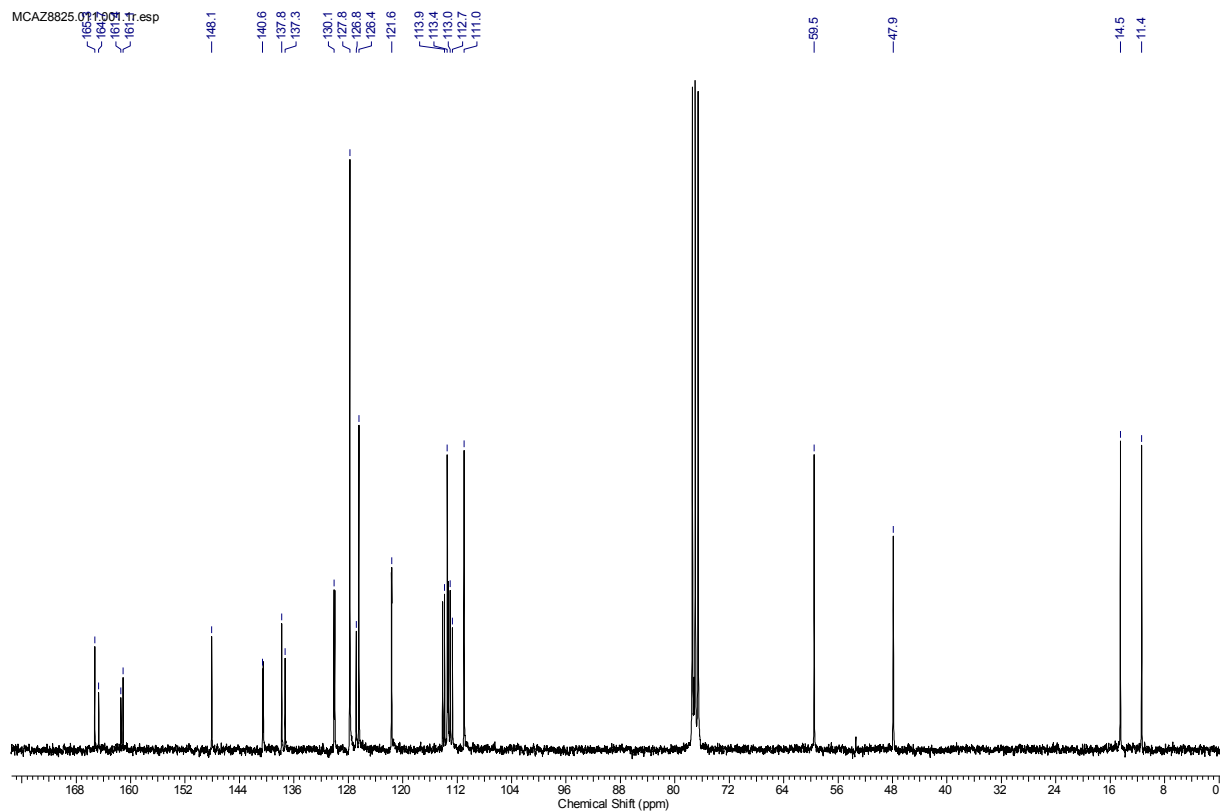
MCAR9071.011.001.1r.esp



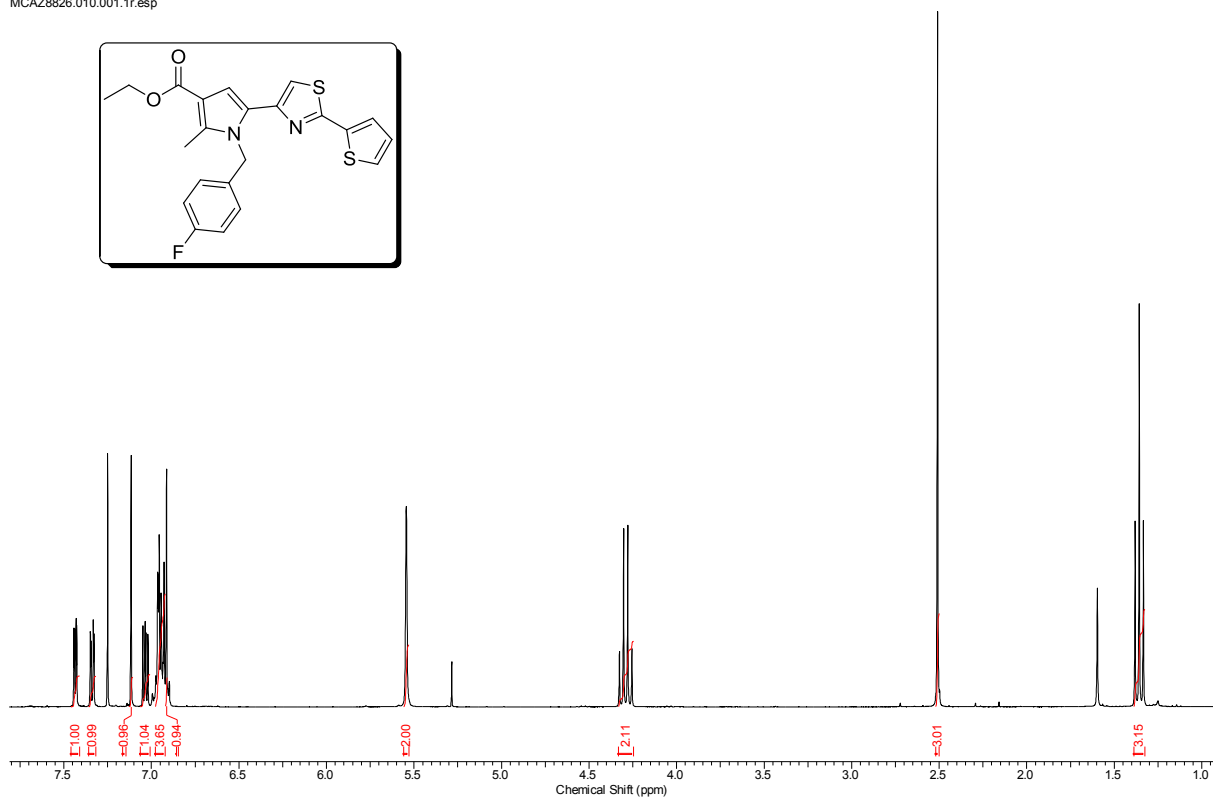
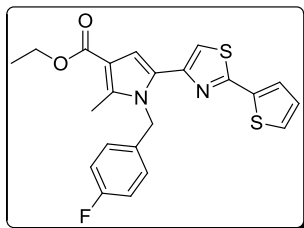
MCAZ8825.010.001.1r.esp



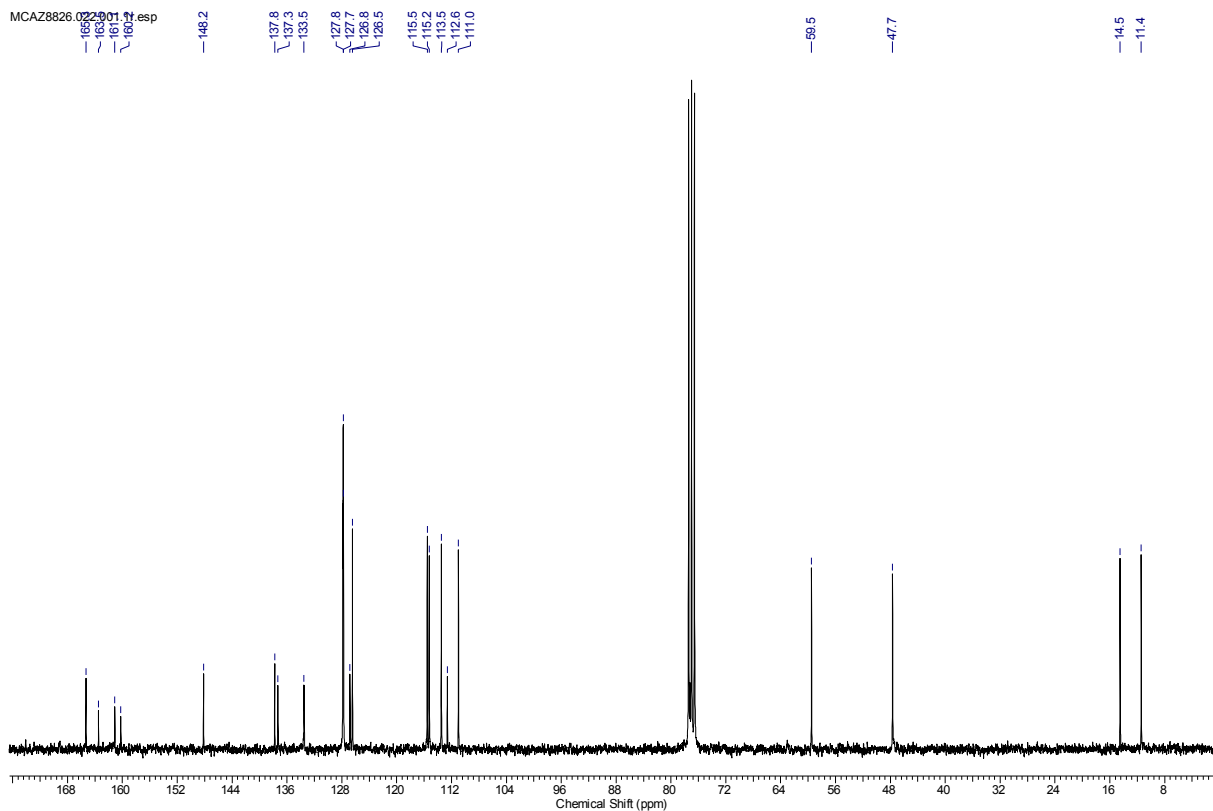
MCAZ8825.010.001.1r.esp



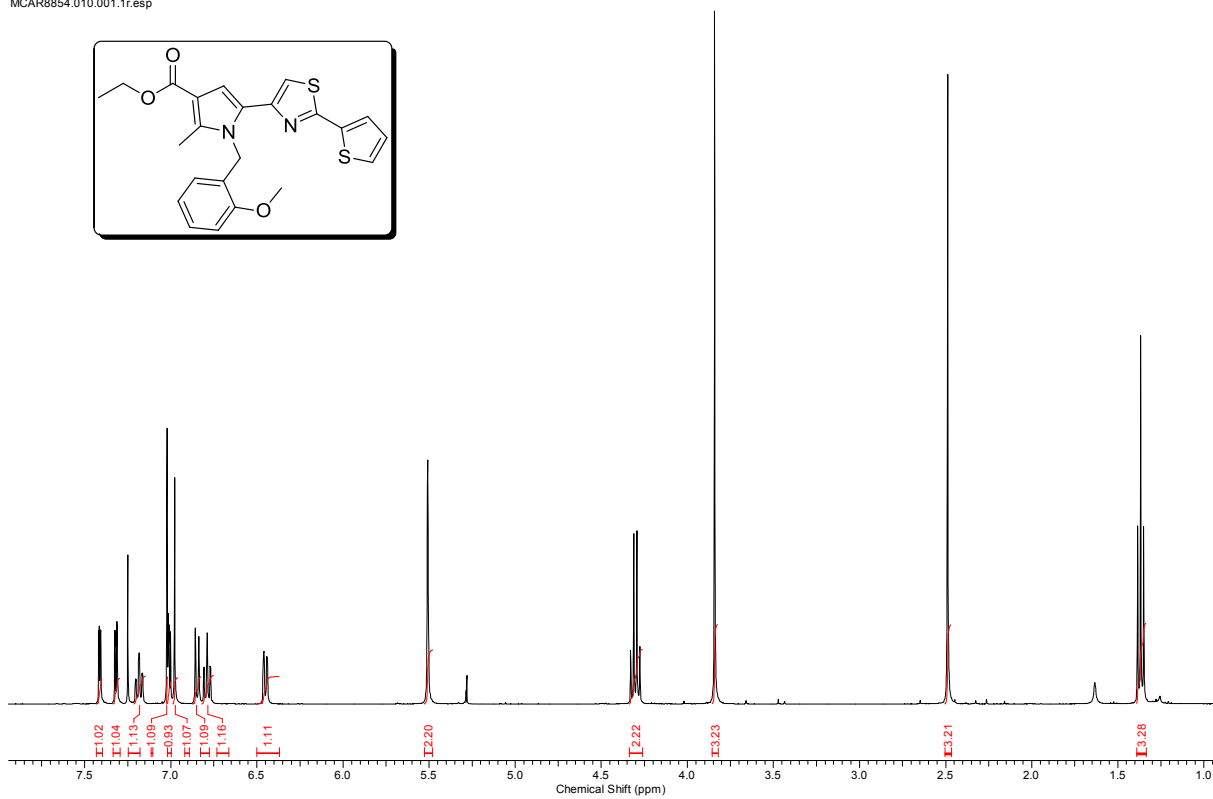
MCAZ8826.010.001.1r.esp



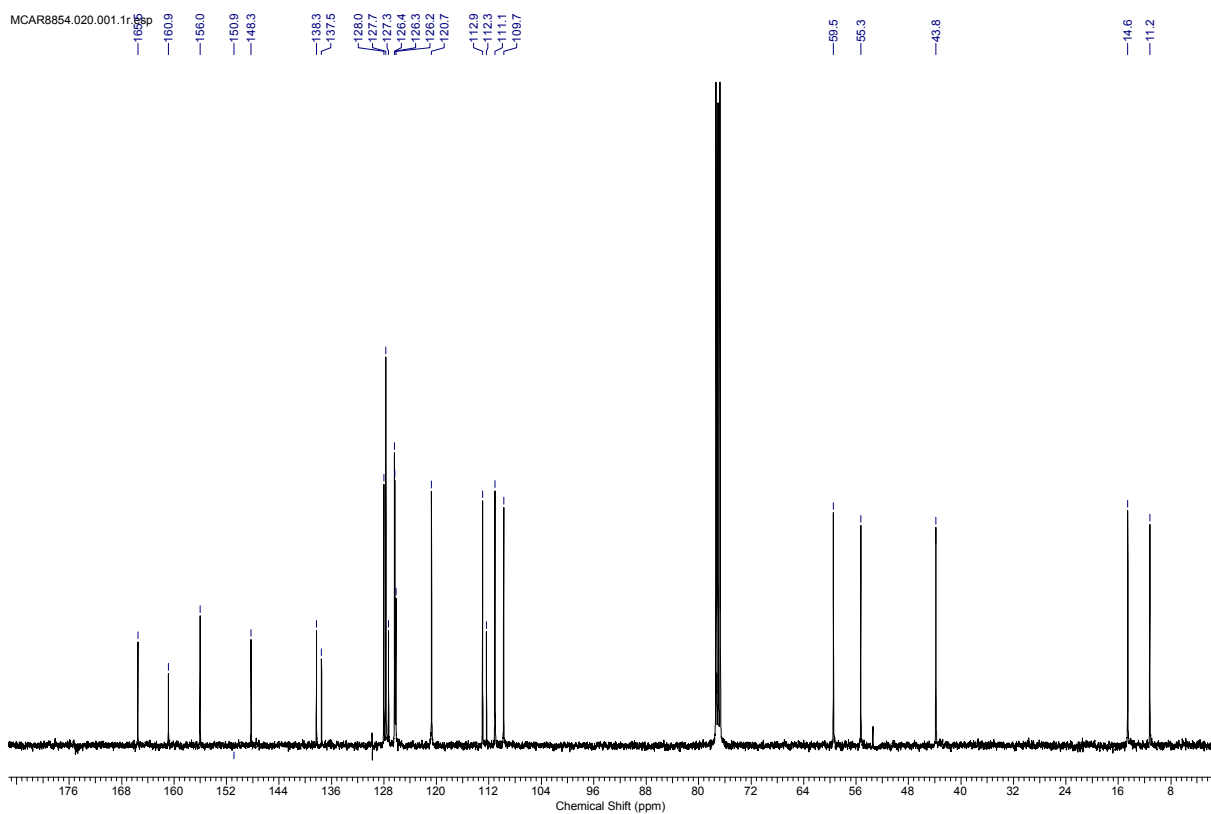
MCAZ8826.022.001.2r.esp



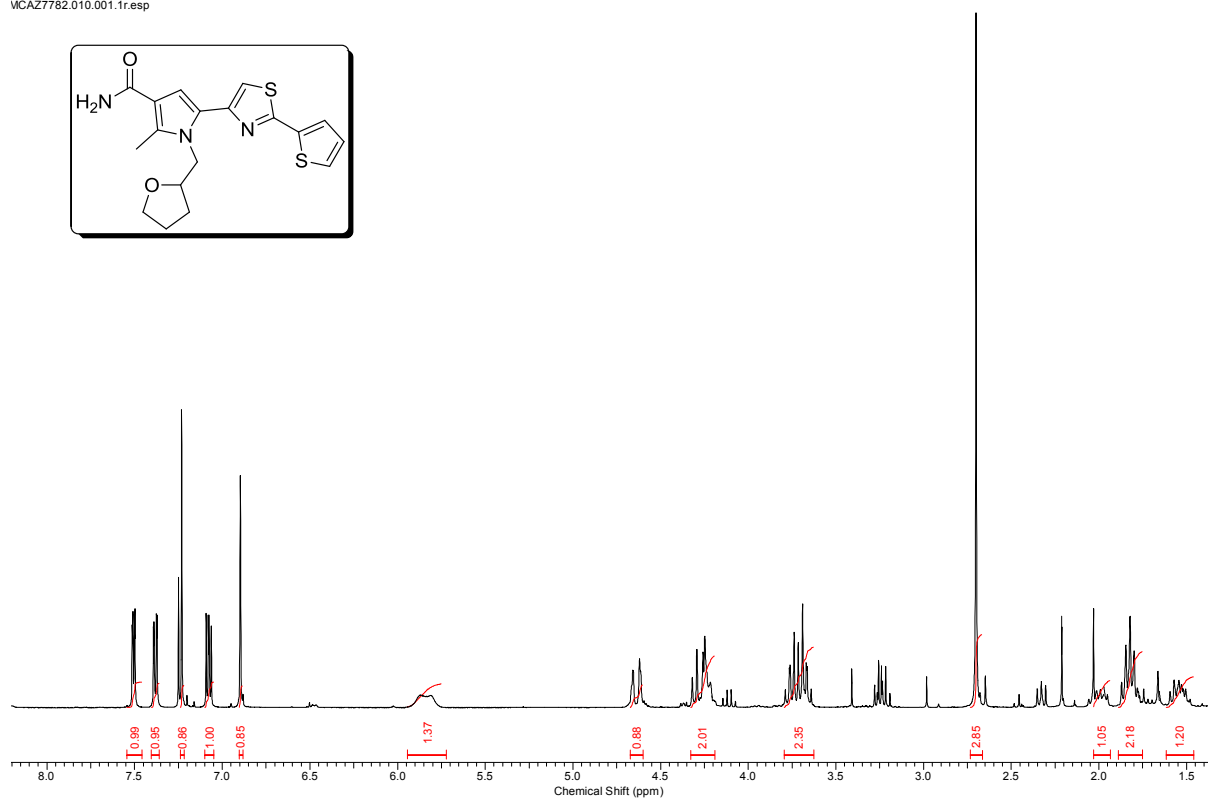
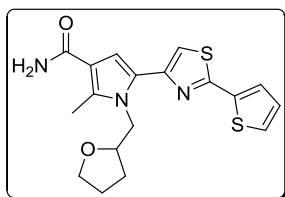
MCA8854.010.001.1r.esp



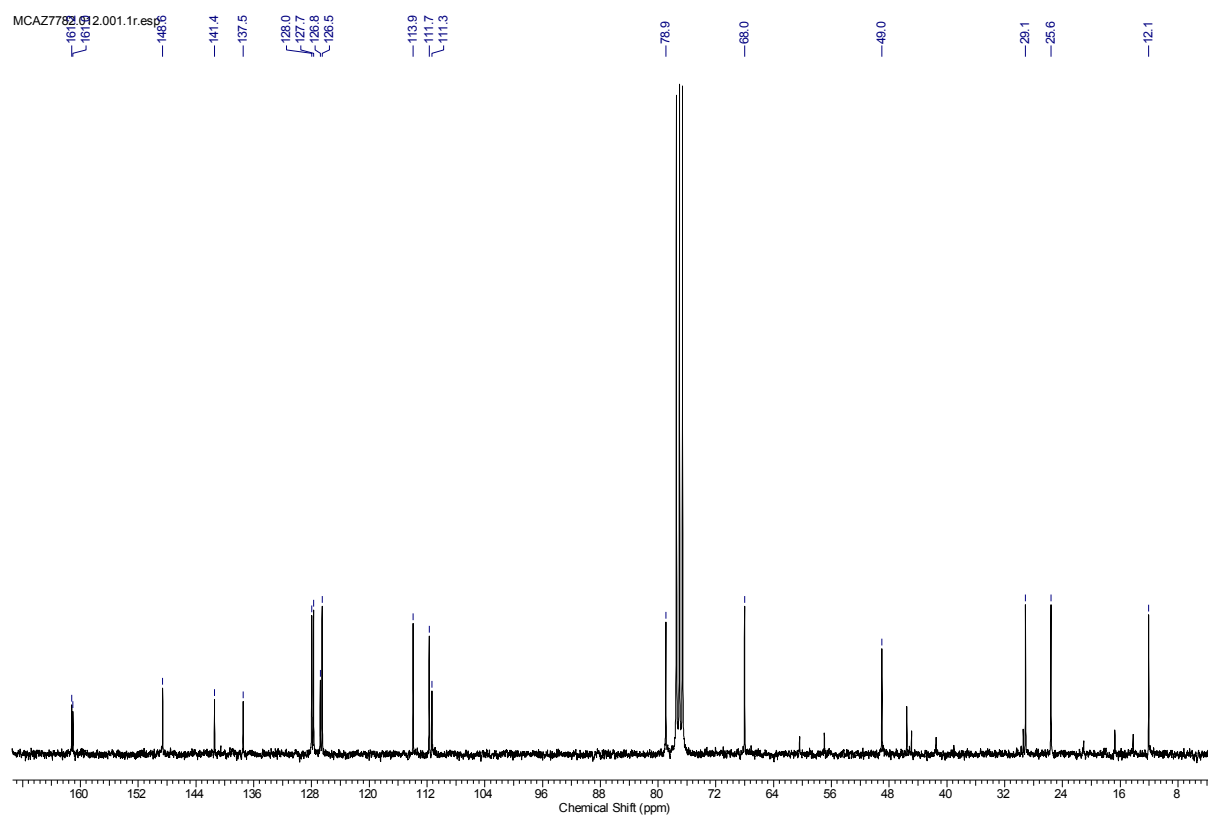
MCA8854.020.001.1r.esp



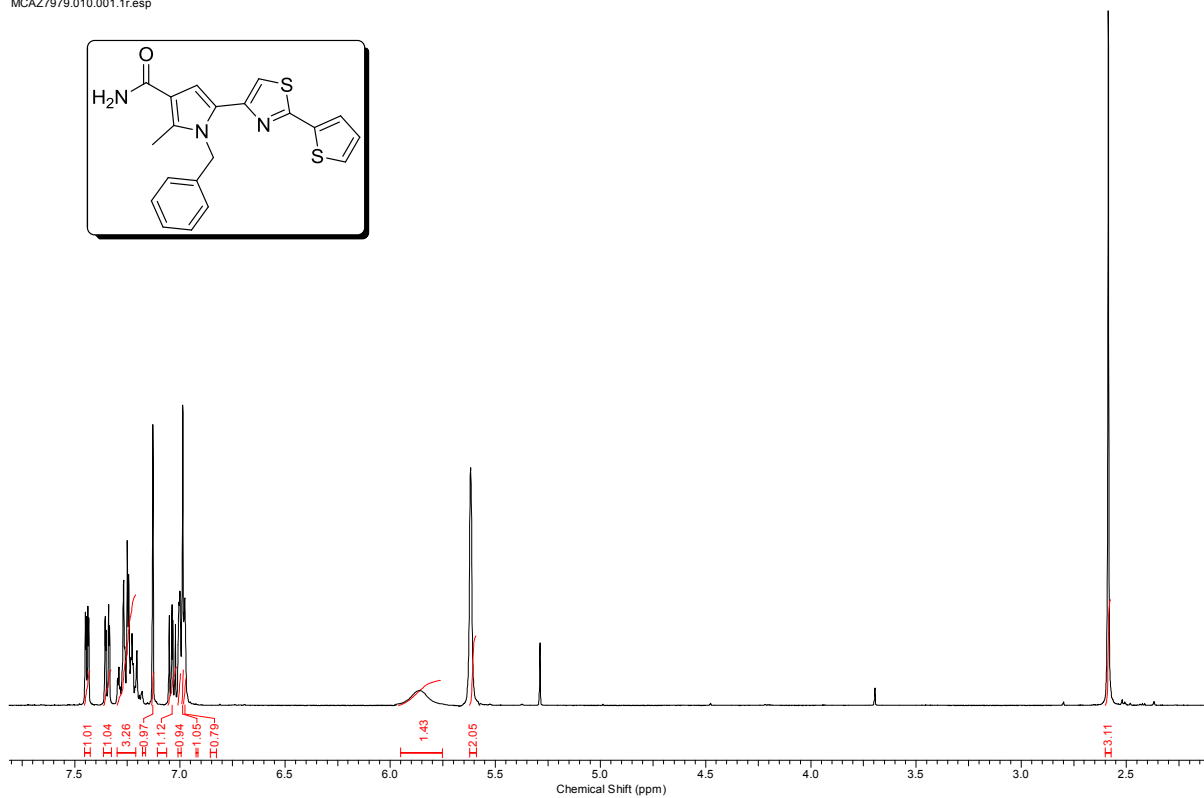
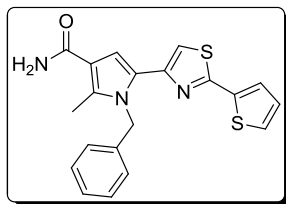
MCAZ7782.010.001.1r.esp



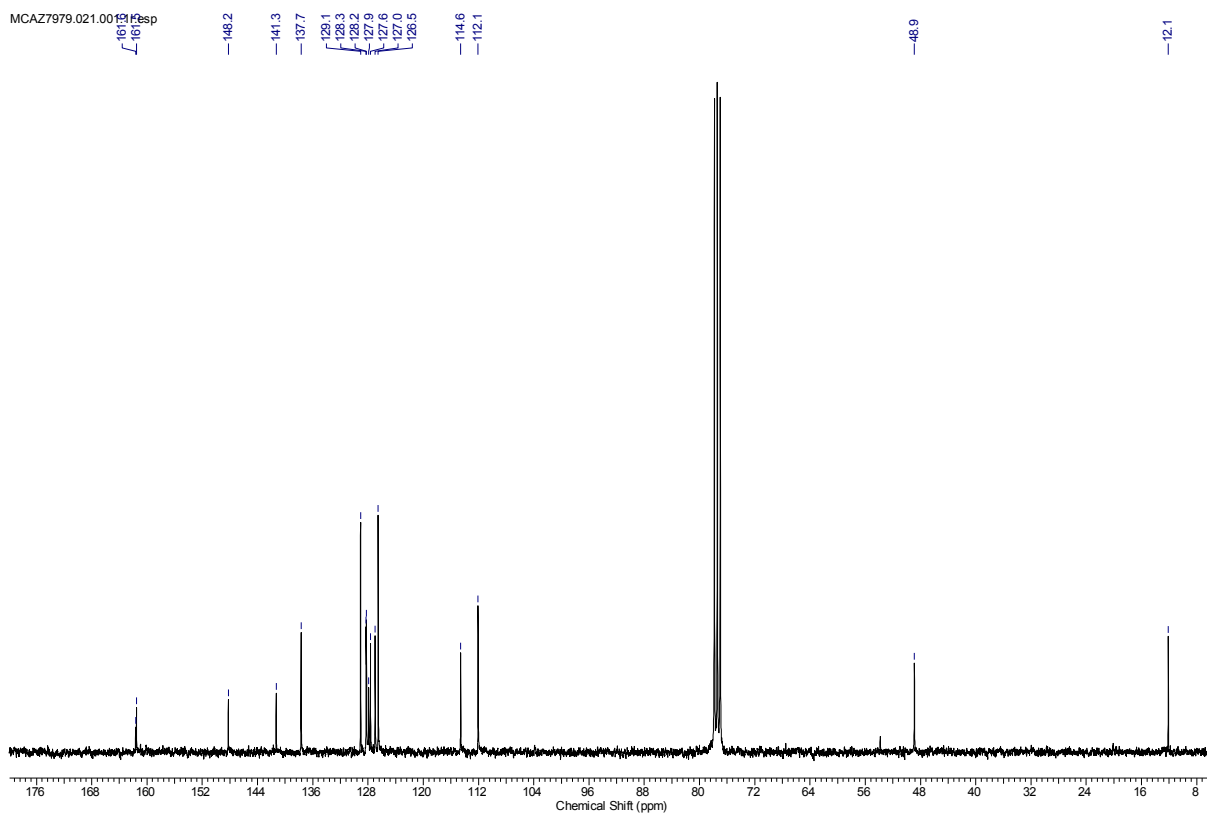
MCAZ7782.010.001.1r.esp



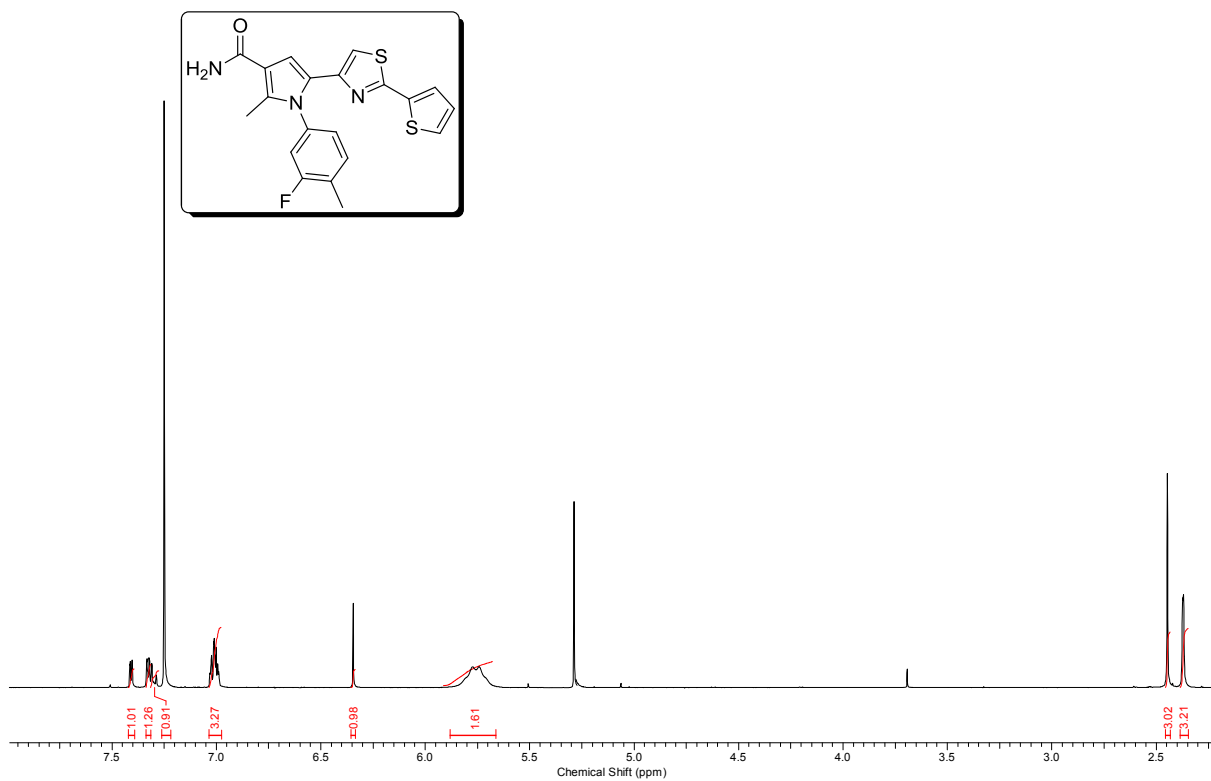
MCAZ7979.010.001.1r.esp



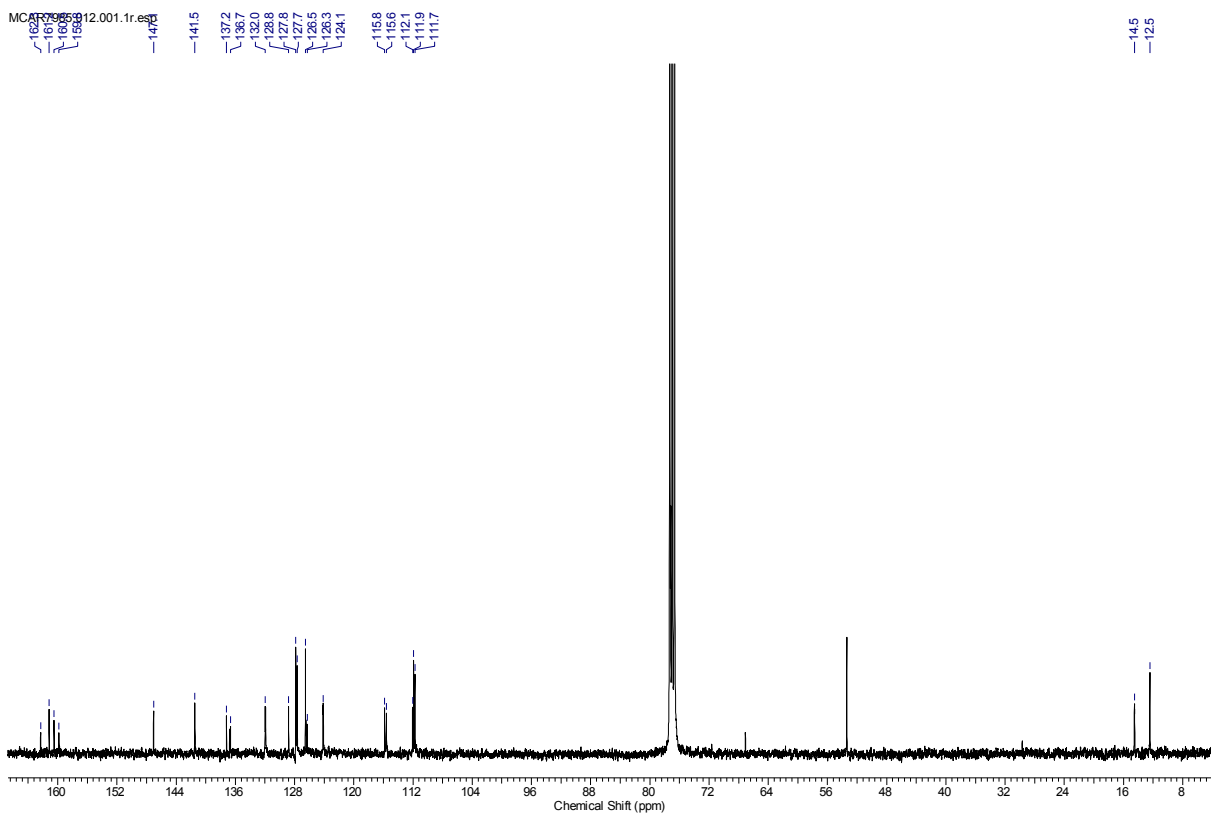
MCAZ7979.021.001.1r.esp



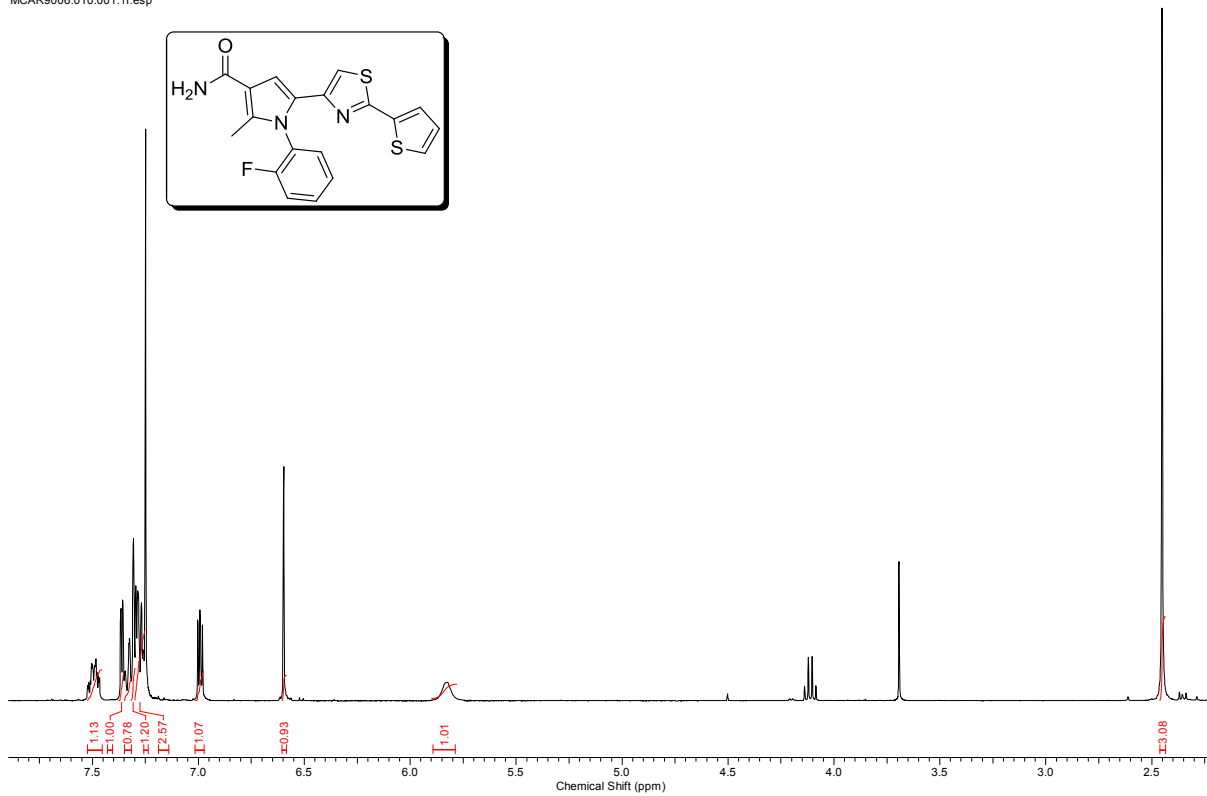
MCAR7985.010.001.1r.esp



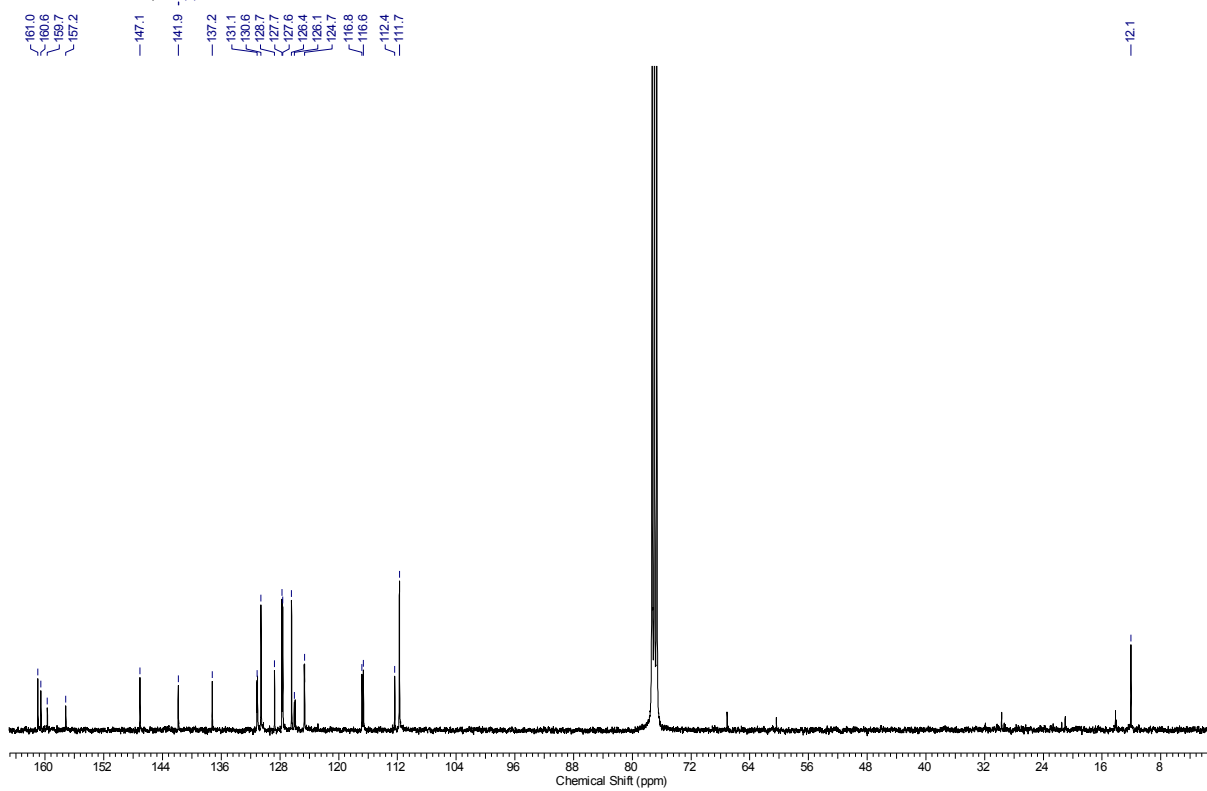
MCAR7985.012.001.1r.esp



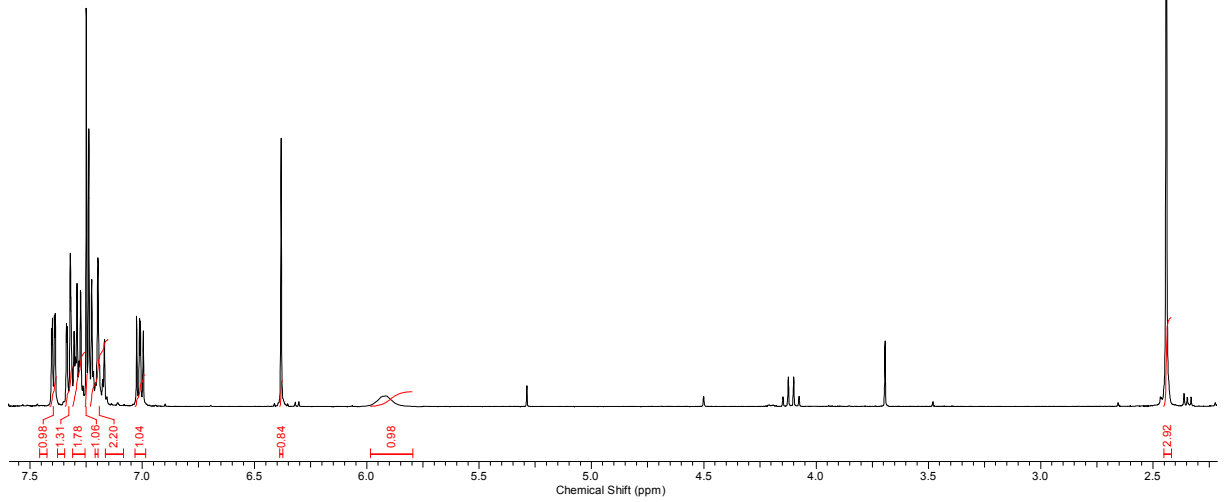
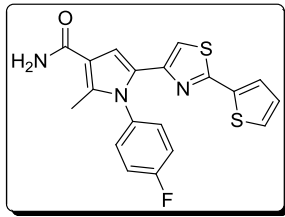
MCAR9006.010.001.1r.esp



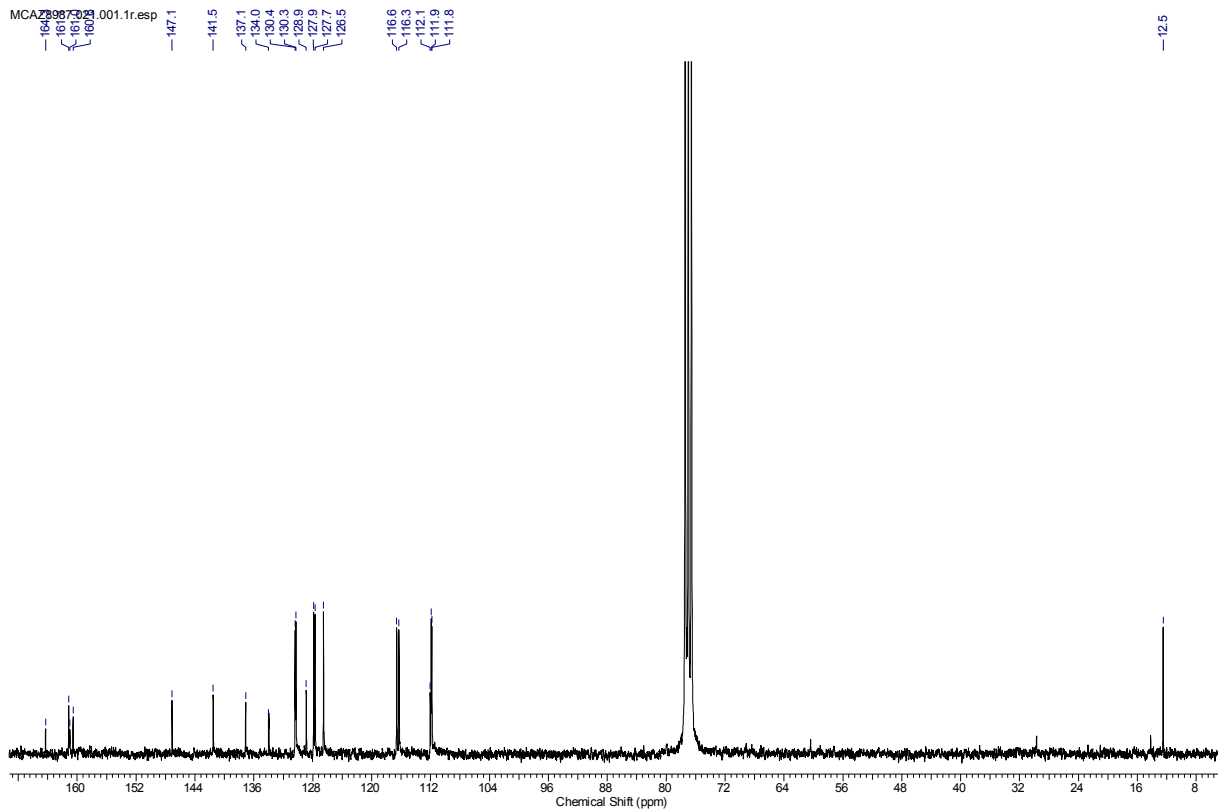
MCAR9006.021.001.1r.espM01(s)



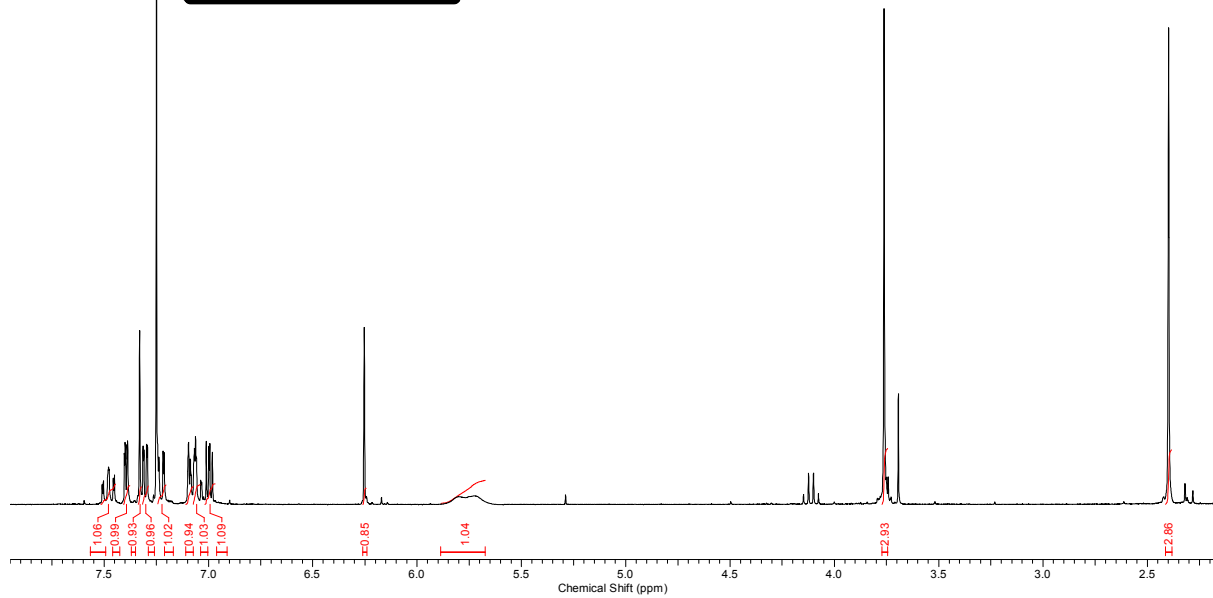
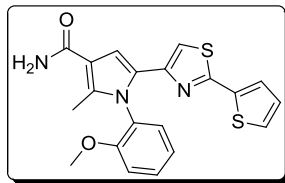
MCAZ8987.010.001.1r.esp



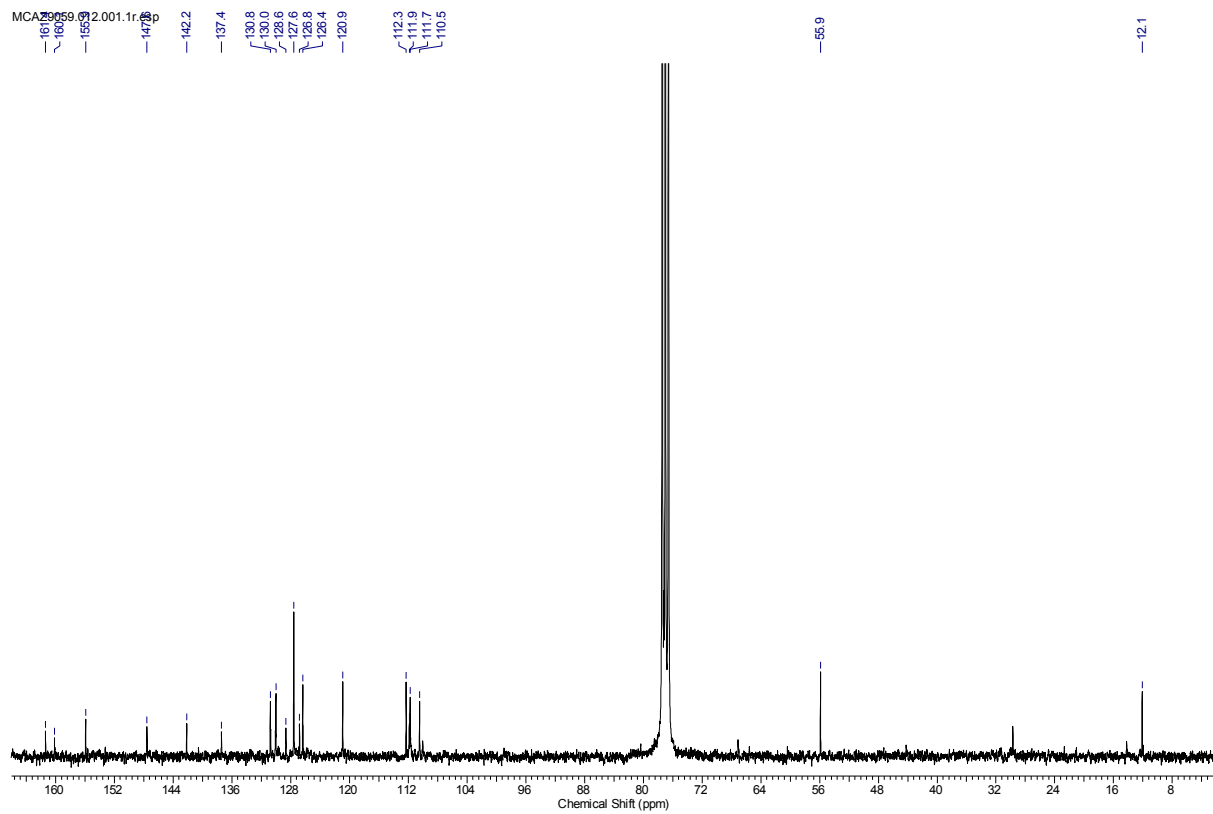
MCAZ8987.010.001.1r.esp



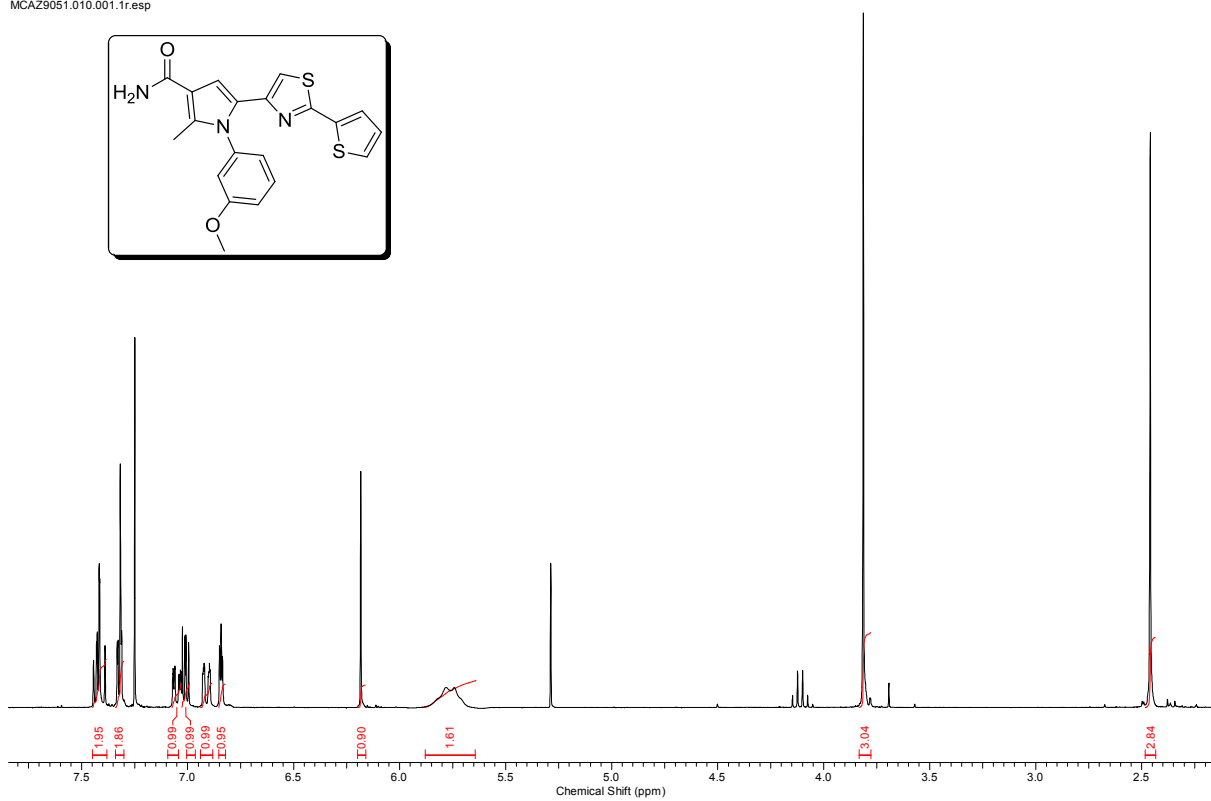
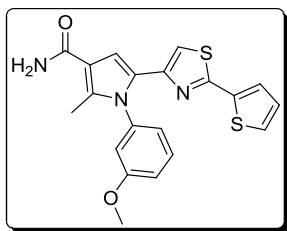
MCAZ9059.010.001.1r.esp



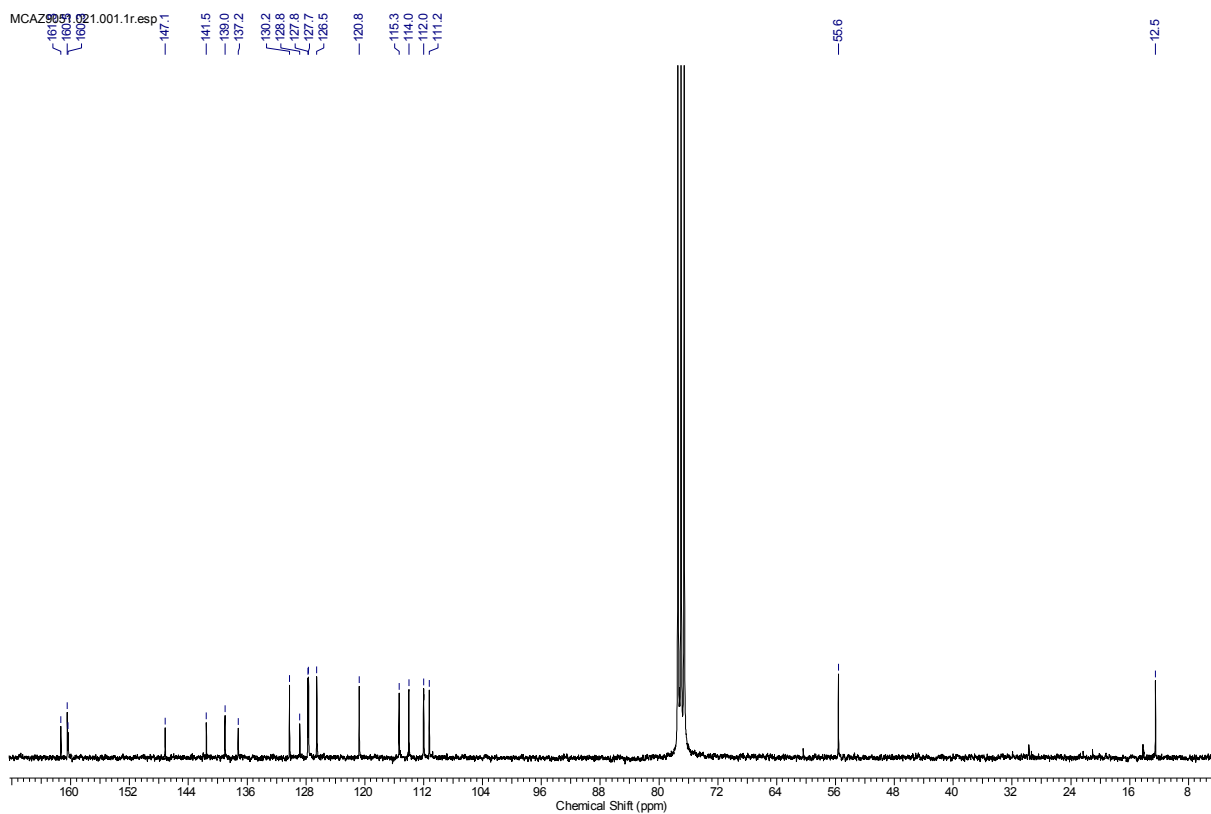
MCAZ9059.010.001.1r.esp



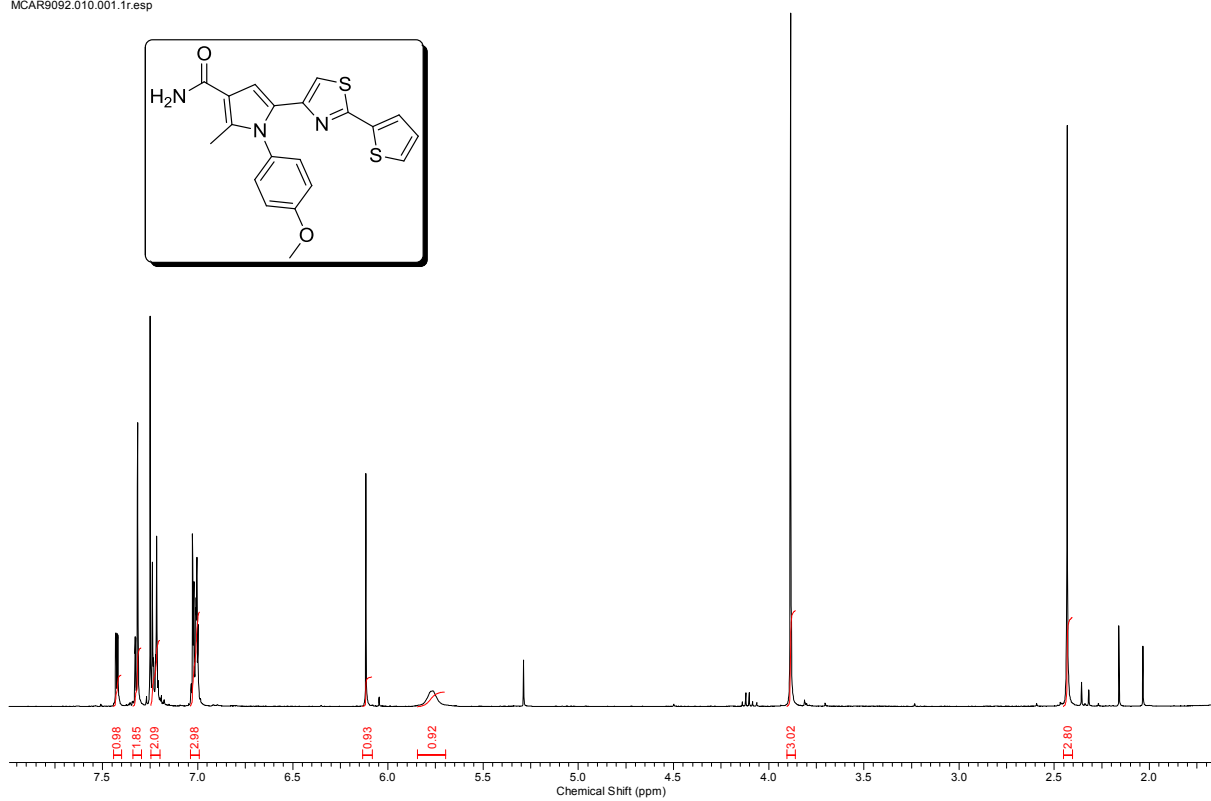
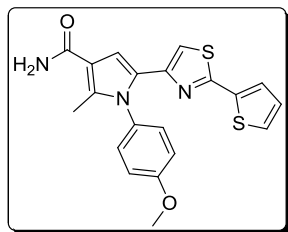
MCAZ9051.010.001.1r.esp



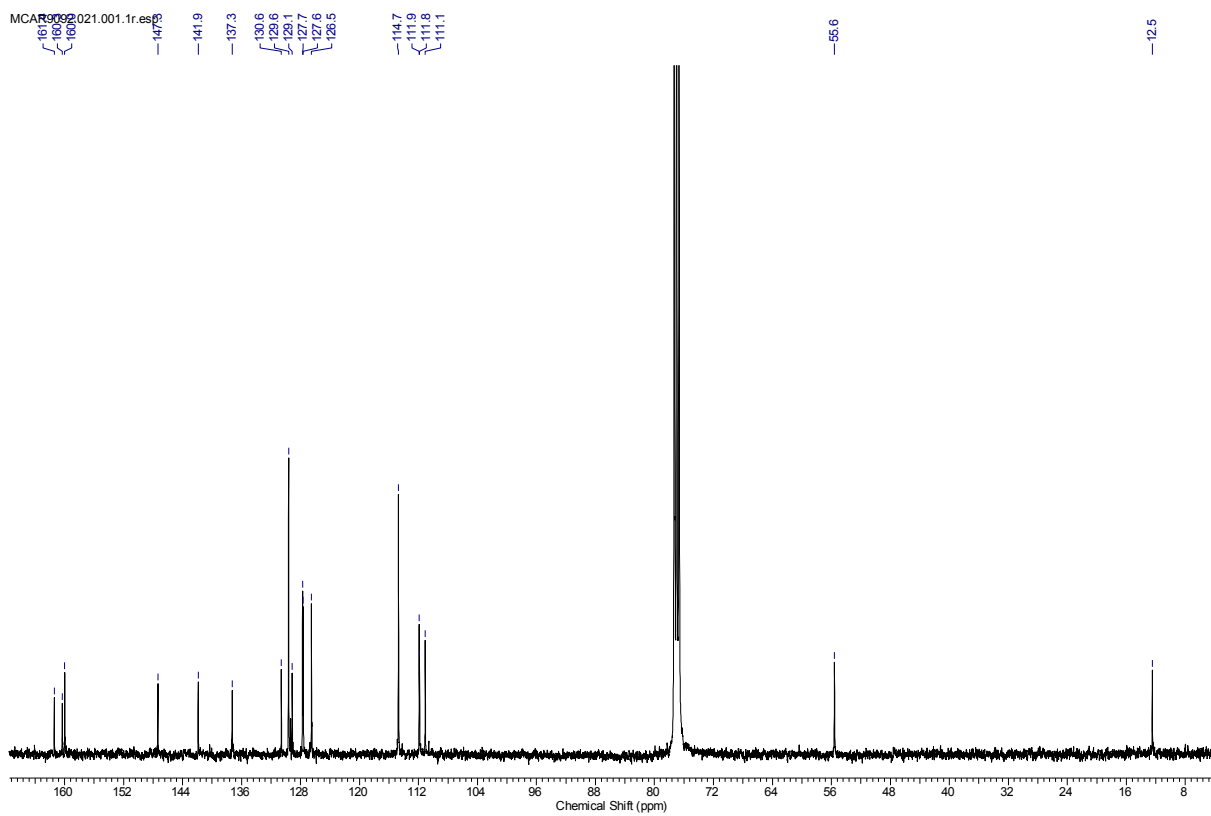
MCAZ9051.010.001.1r.esp



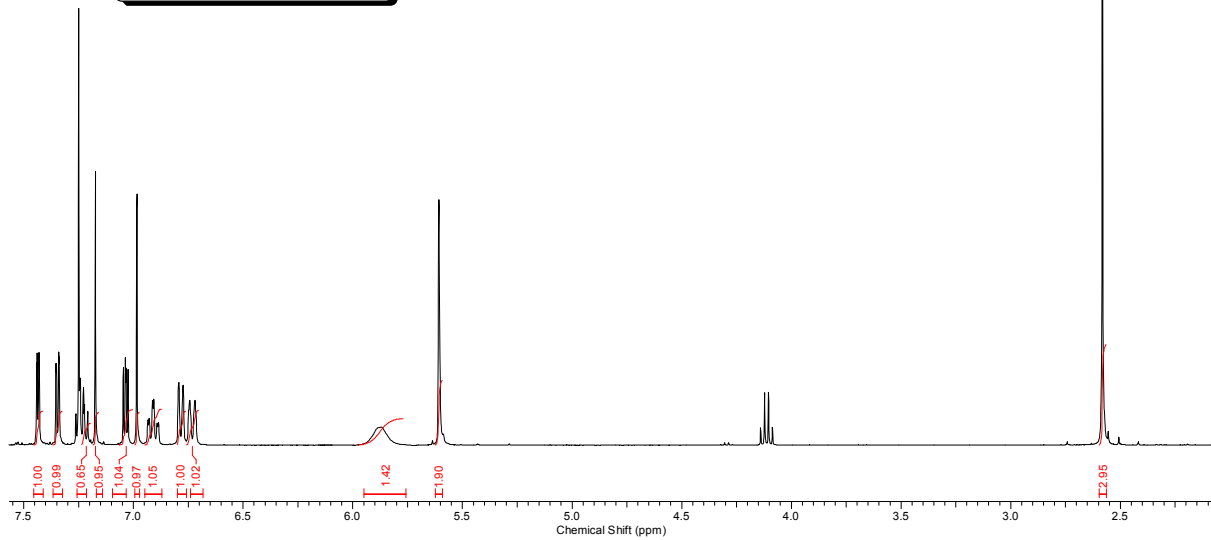
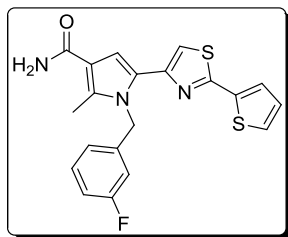
MCAR9092.010.001.1r.esp



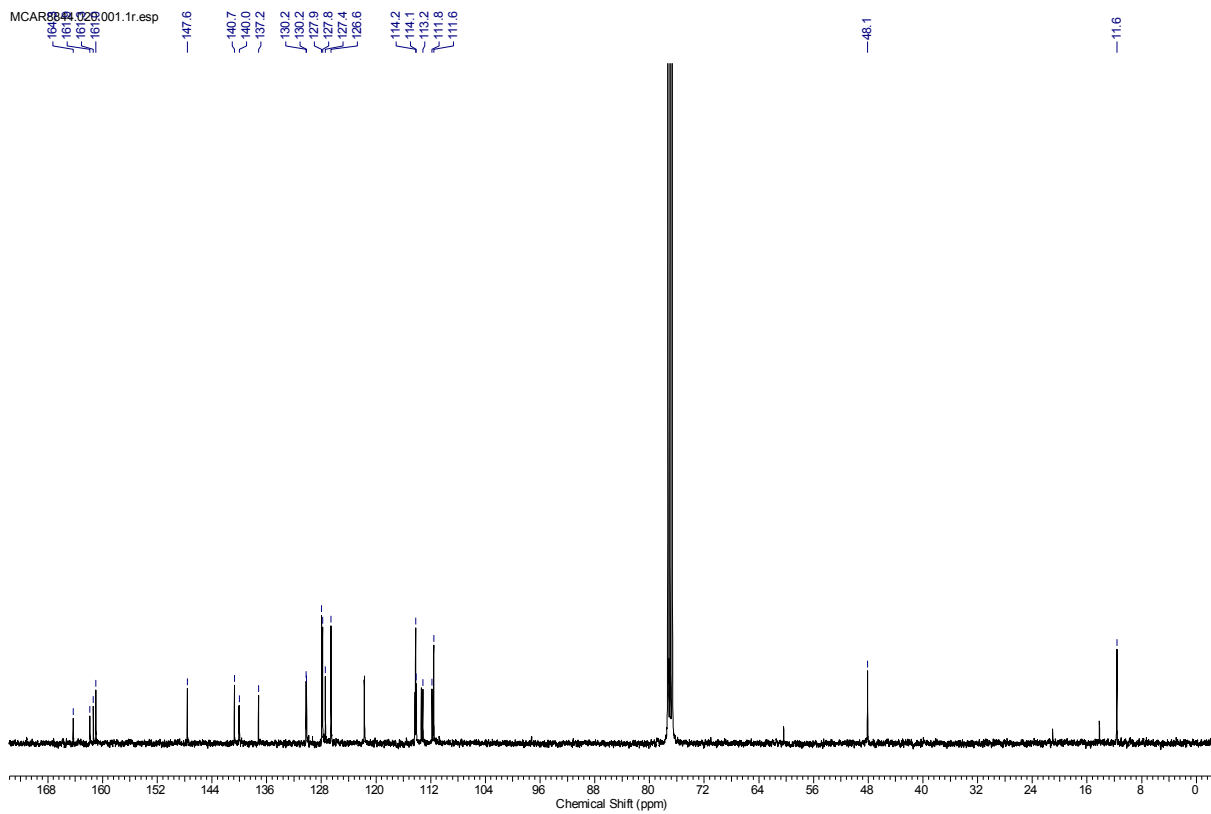
MCAR9092.021.001.1r.esp



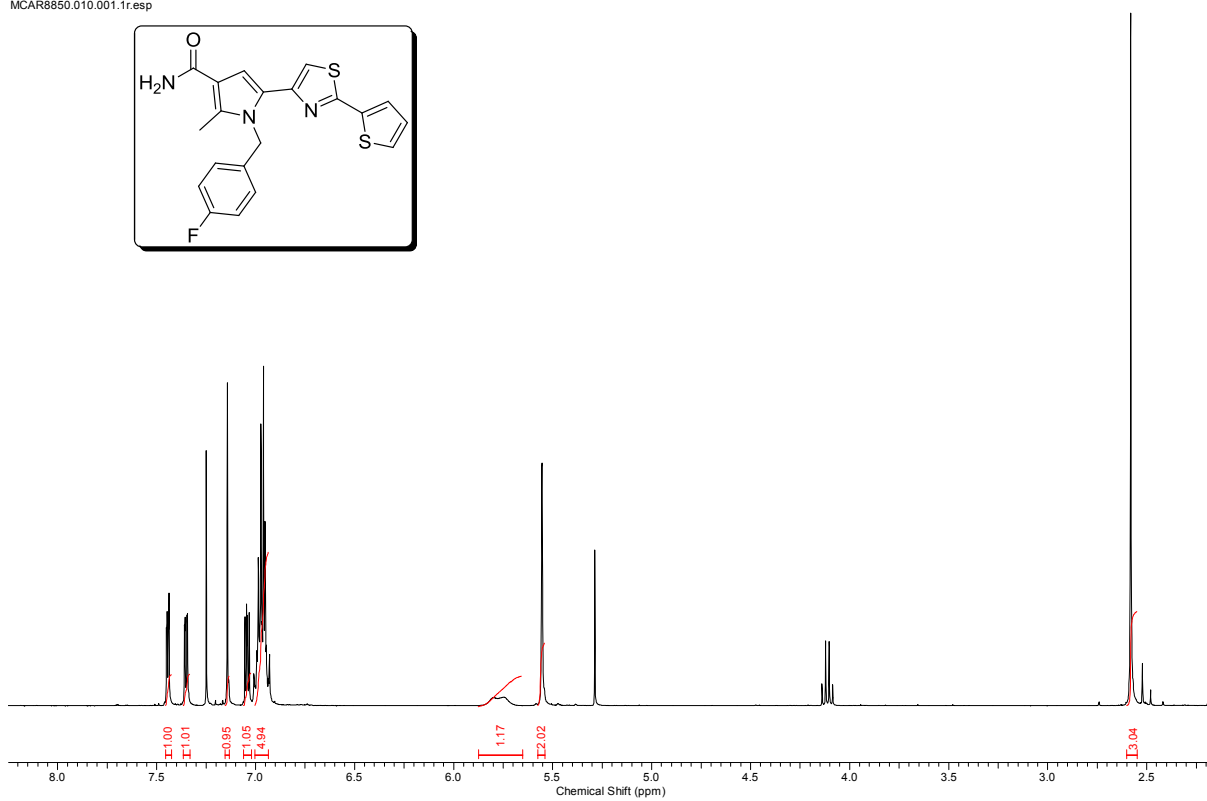
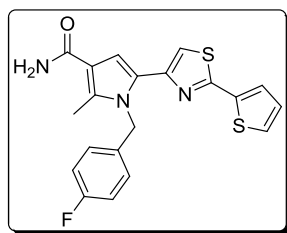
MCAR8844.010.001.1r.esp



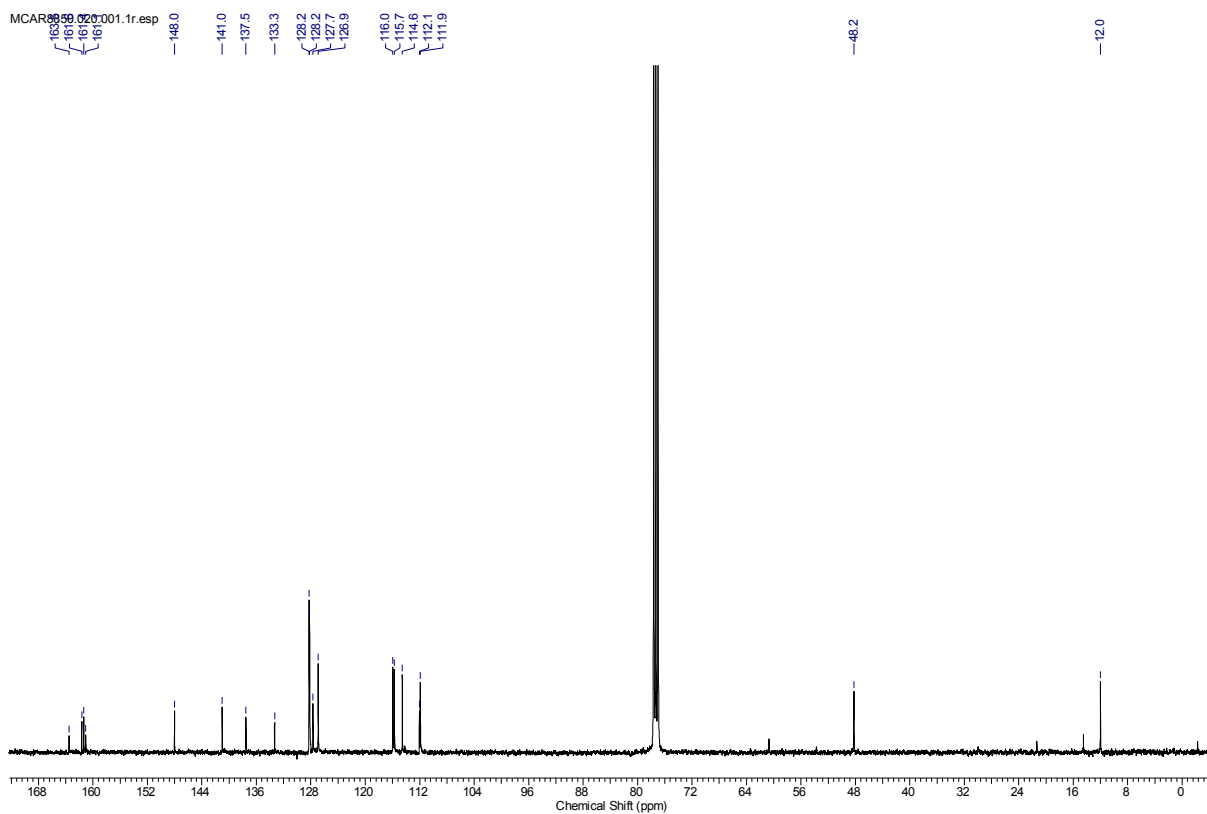
MCAR8844.010.001.1r.esp



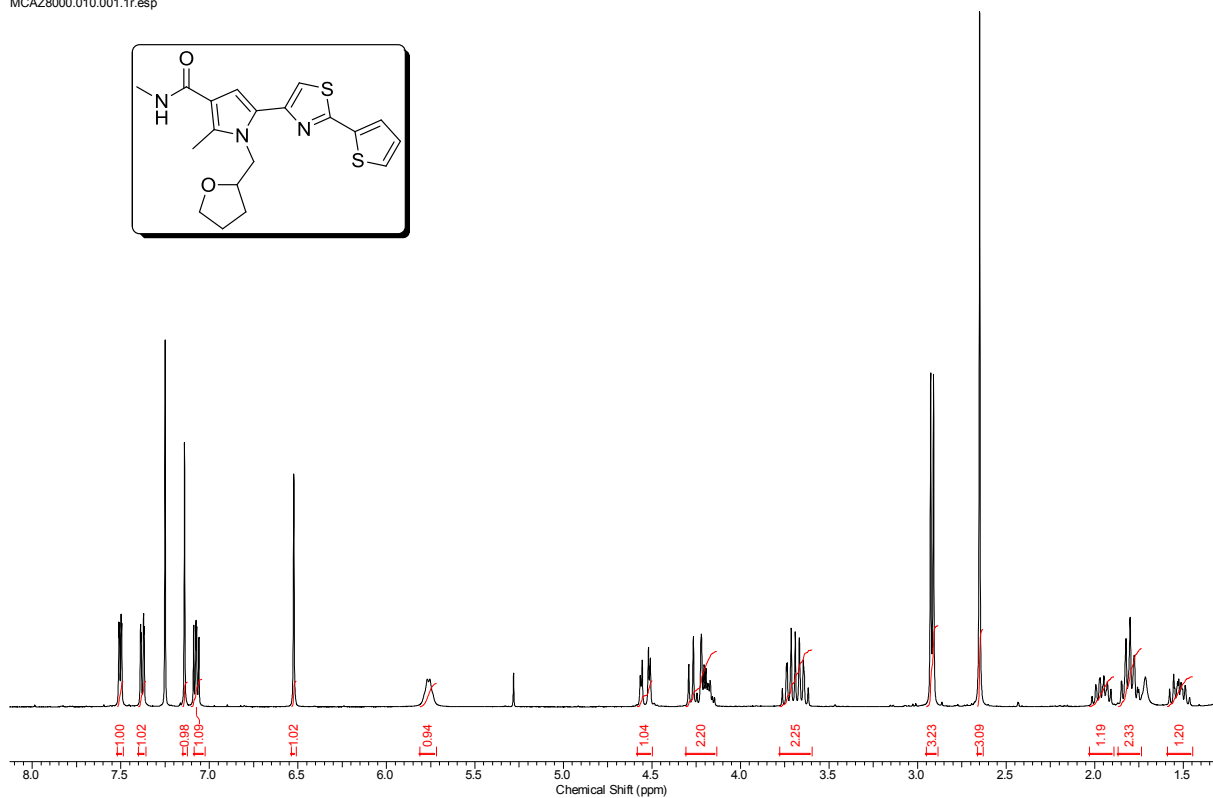
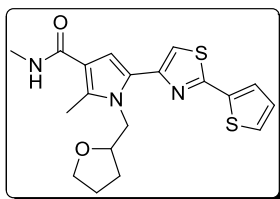
MCAR8850.010.001.1r.esp



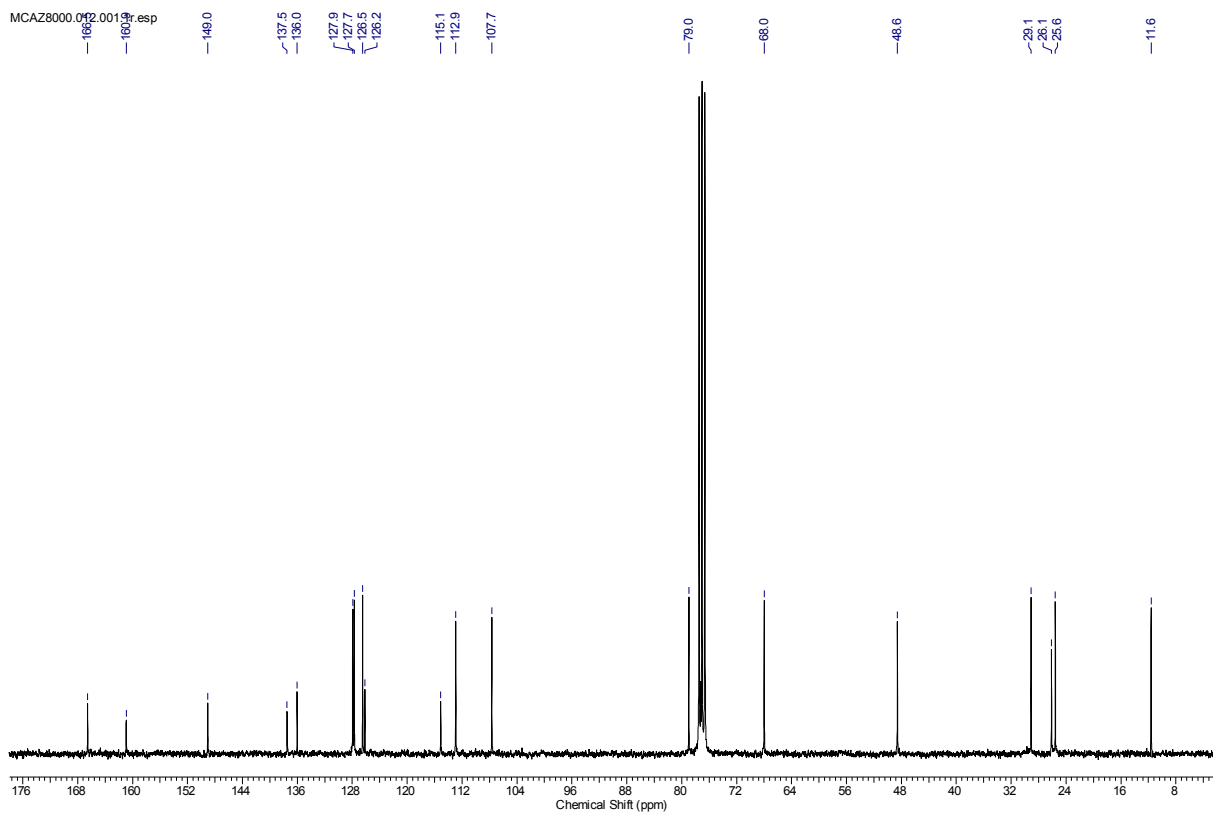
MCAR8850.020.001.1r.esp



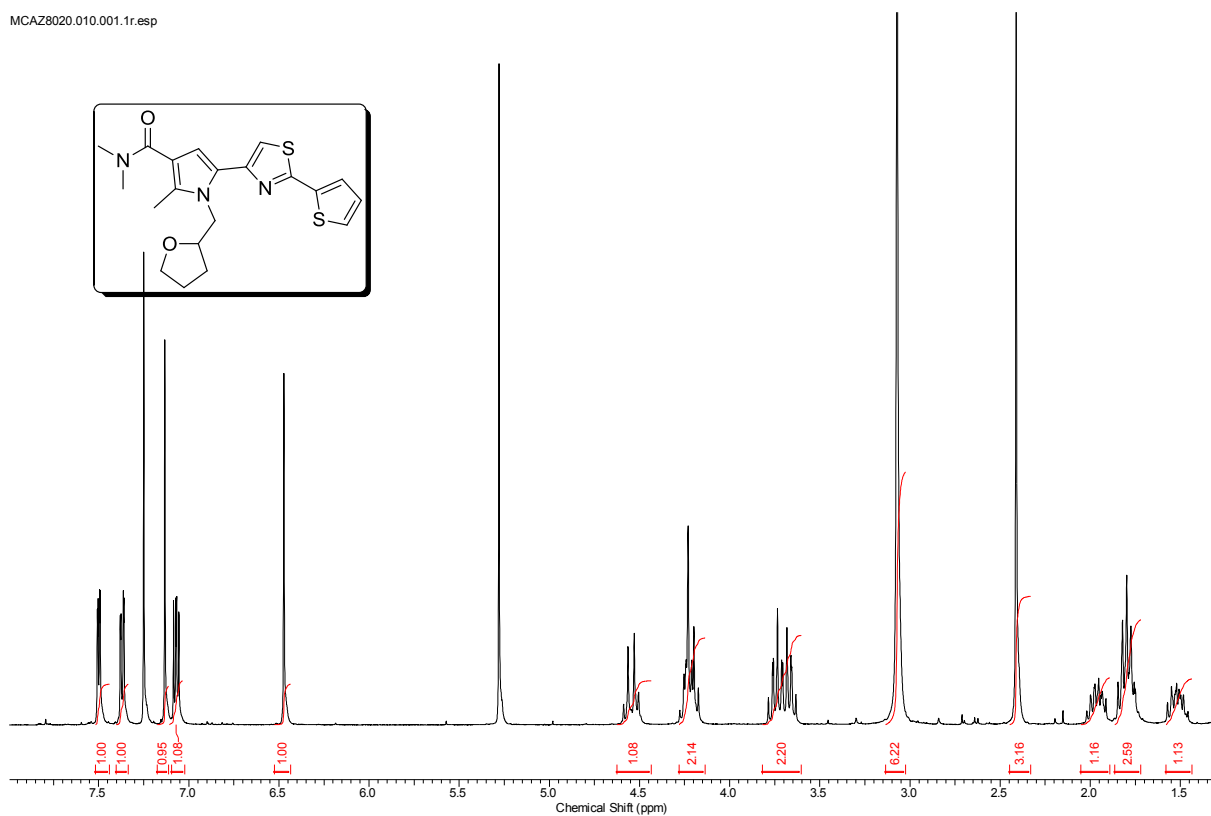
MCAZ8000.010.001.1r.esp



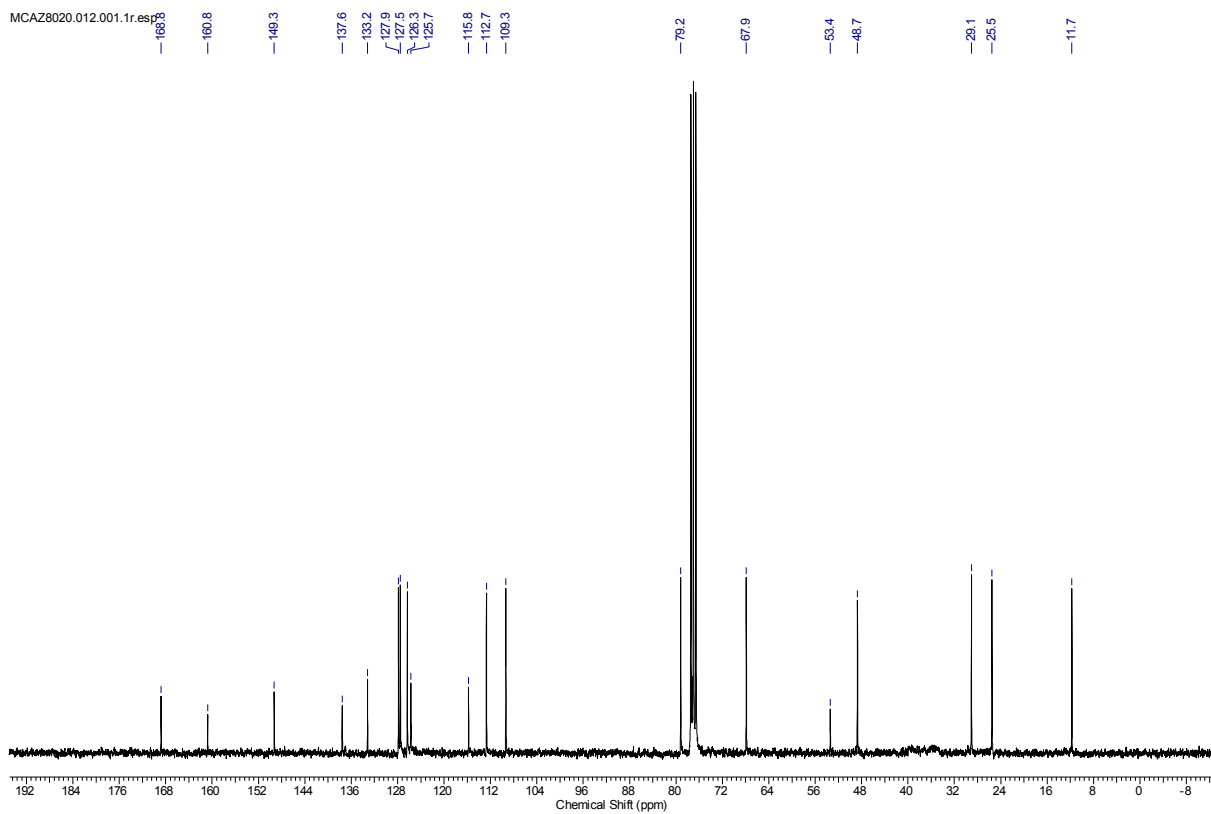
MCAZ8000.010.001.1r.esp



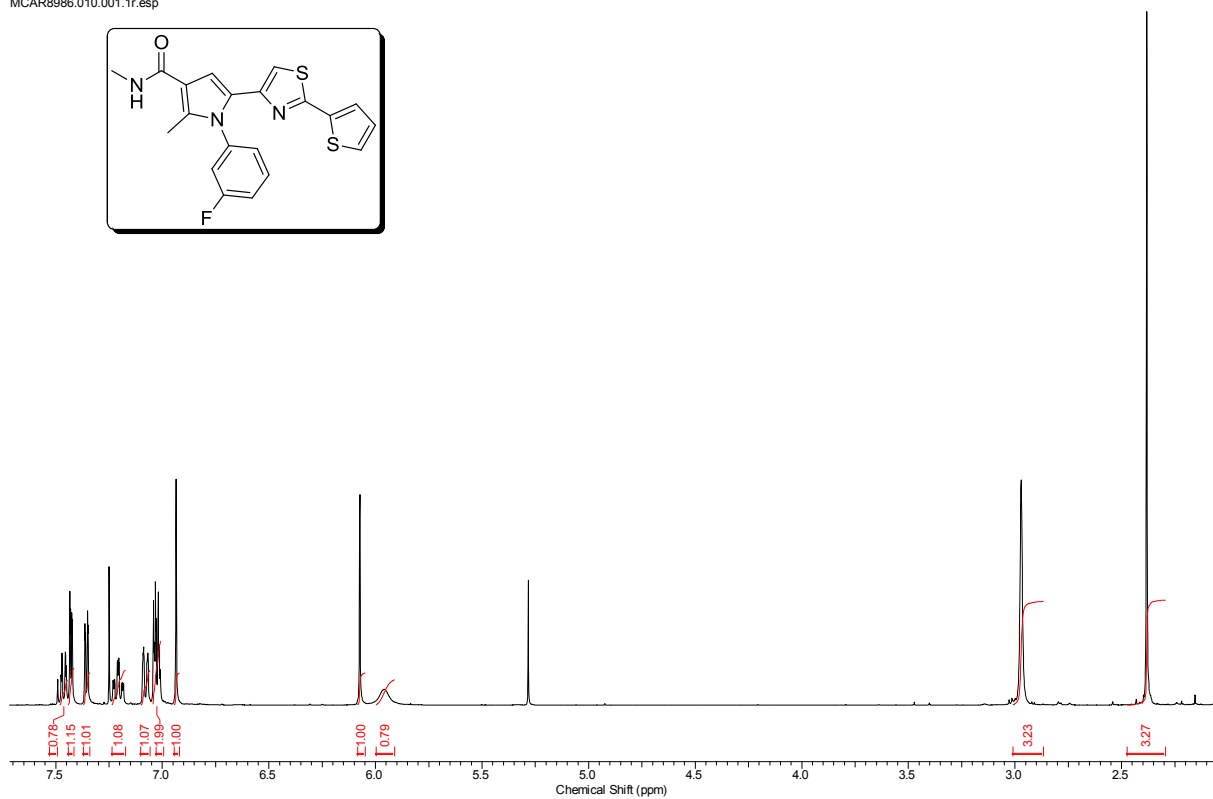
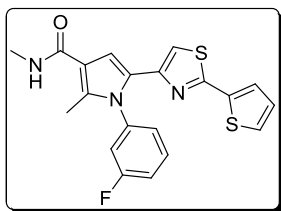
MCAZ8020.010.001.1r.esp



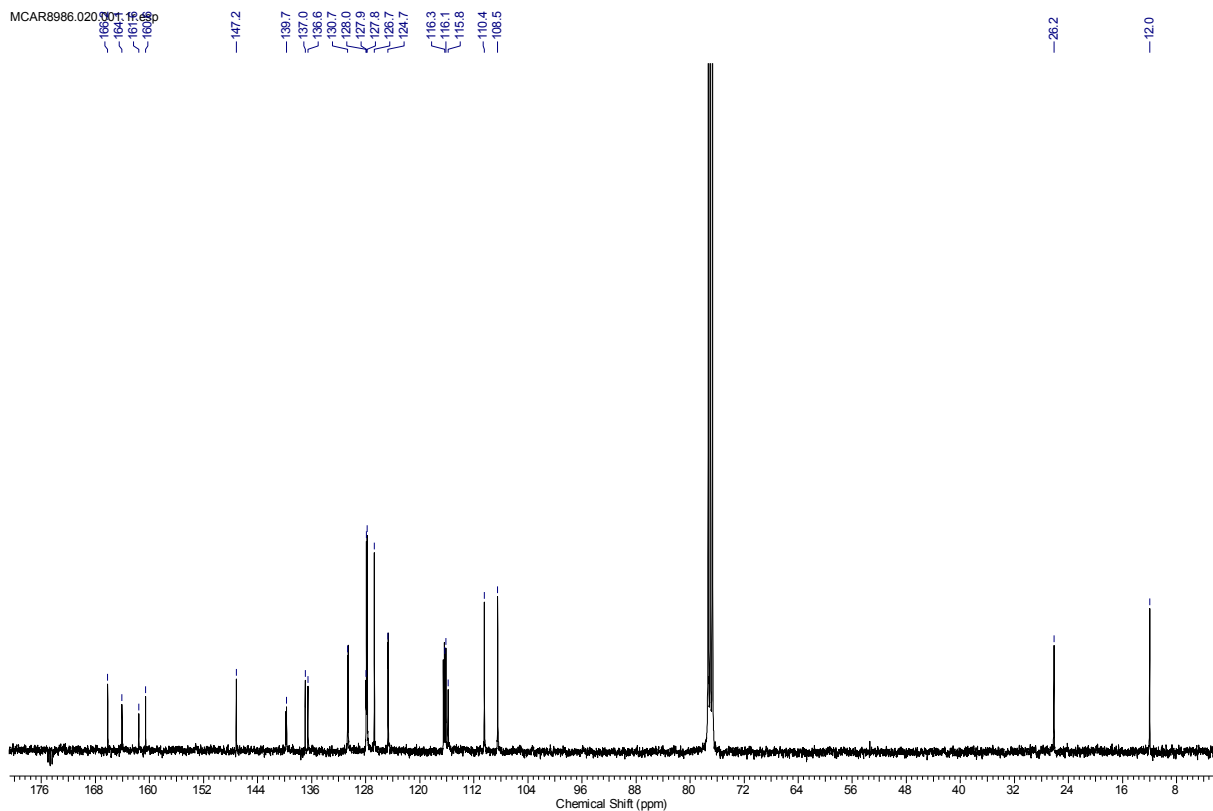
MCAZ8020.012.001.1r.esp



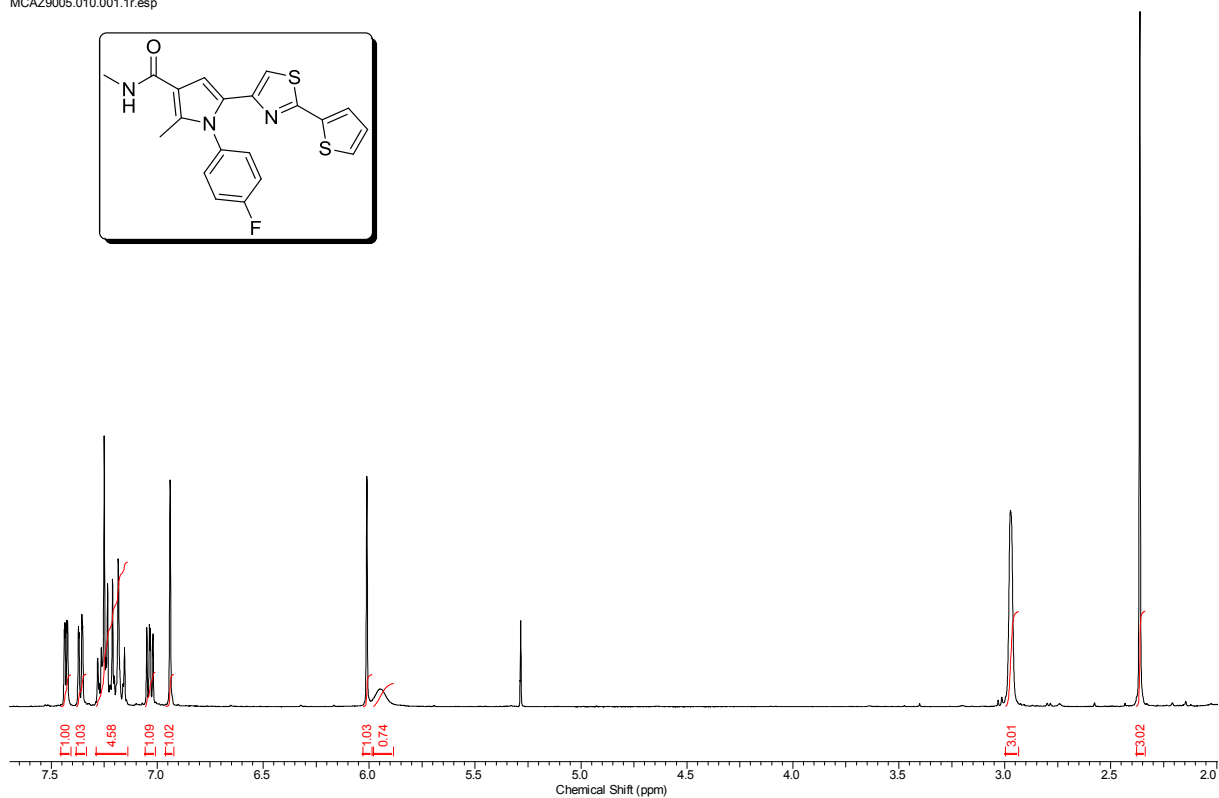
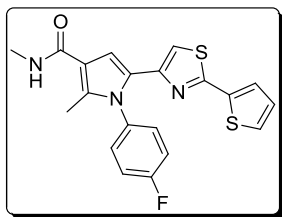
MCA8986.010.001.1r.esp



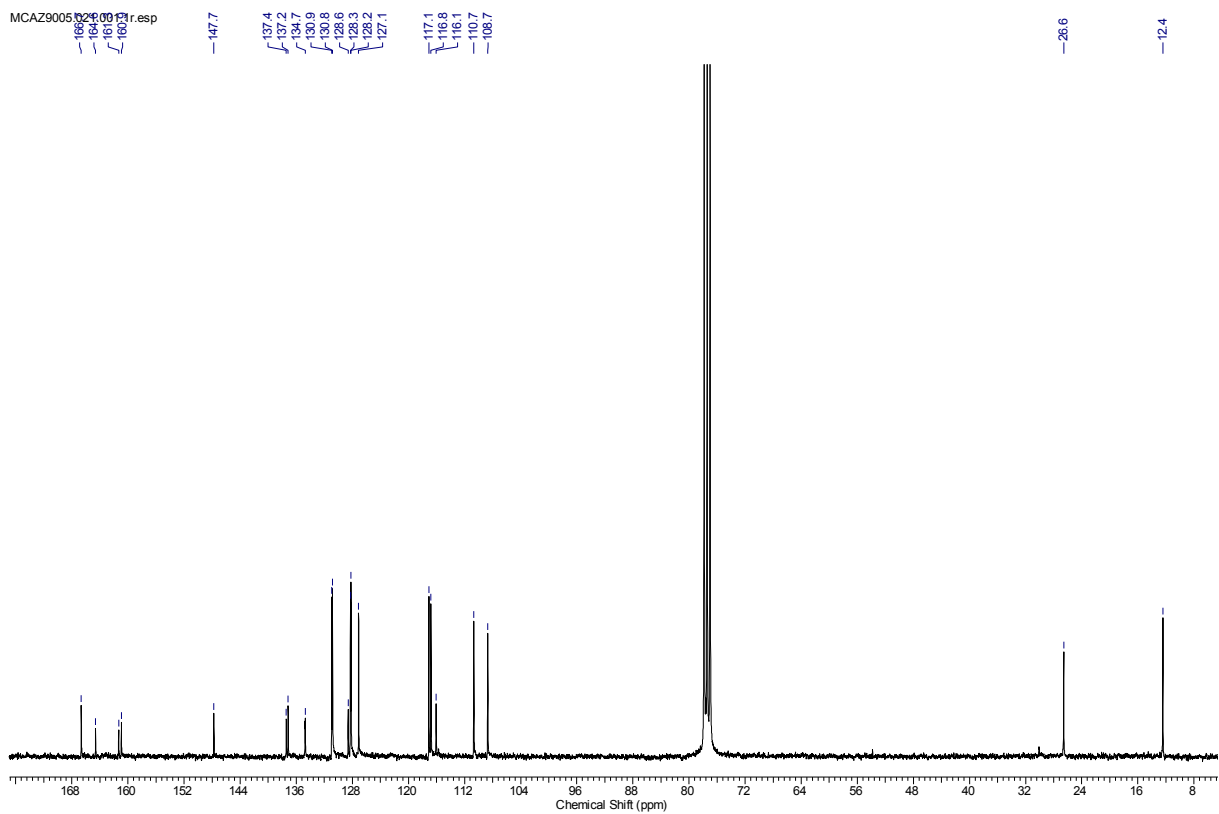
MCA8986.020.001.1r.esp



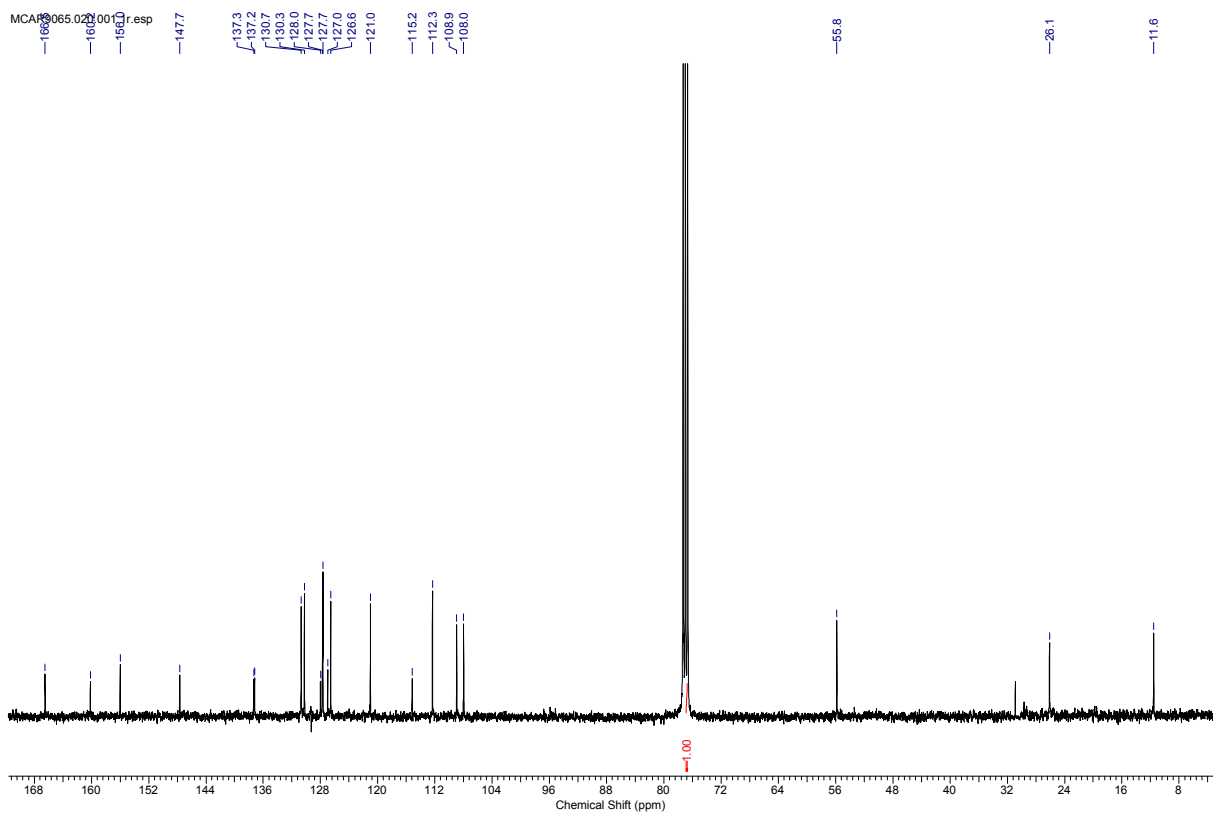
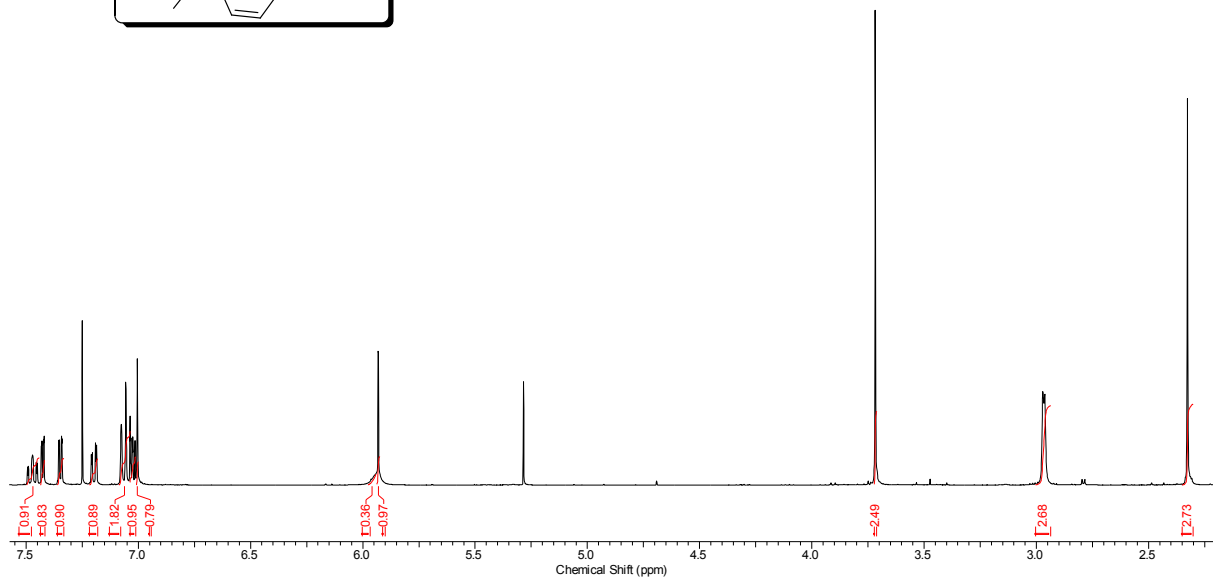
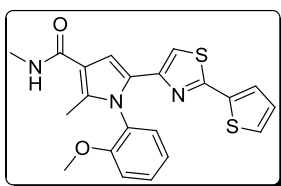
MCAZ9005.010.001.1r.esp



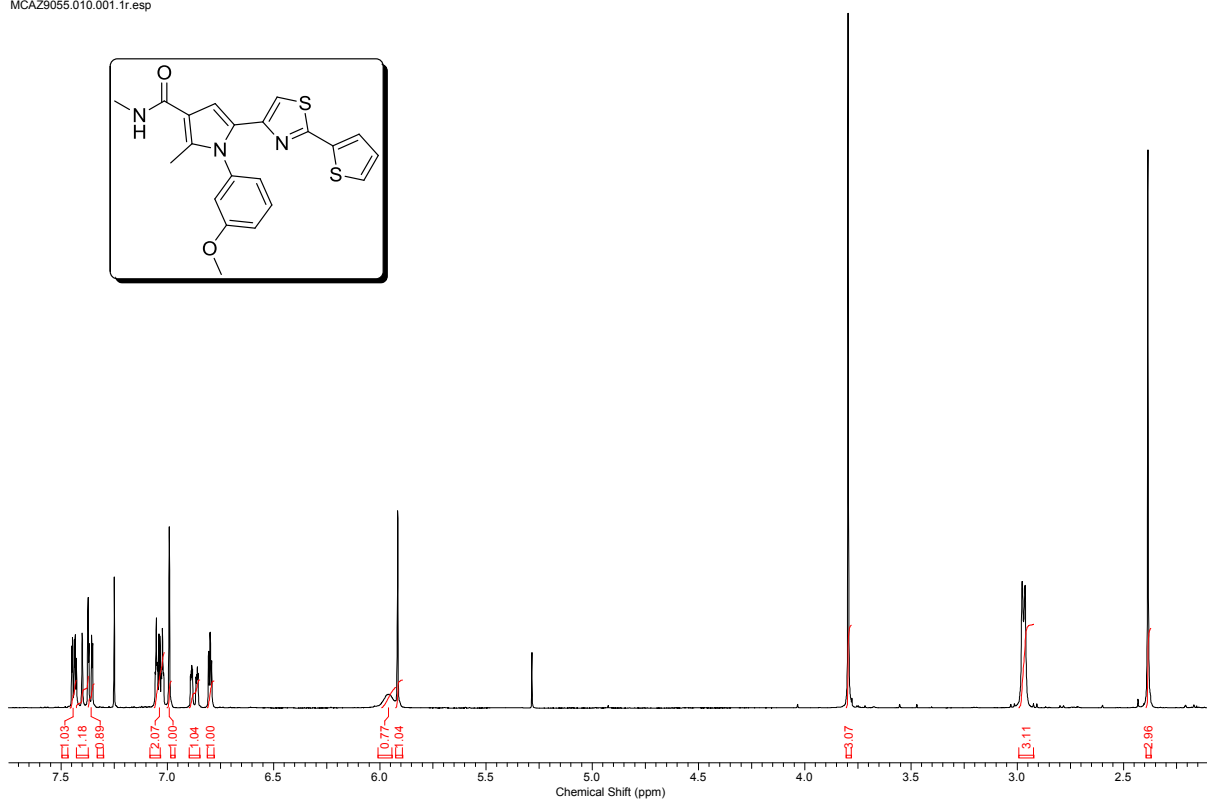
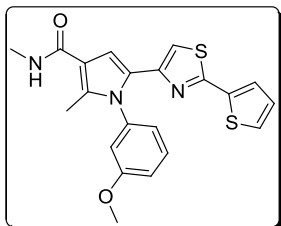
MCAZ9005.010.001.1r.esp



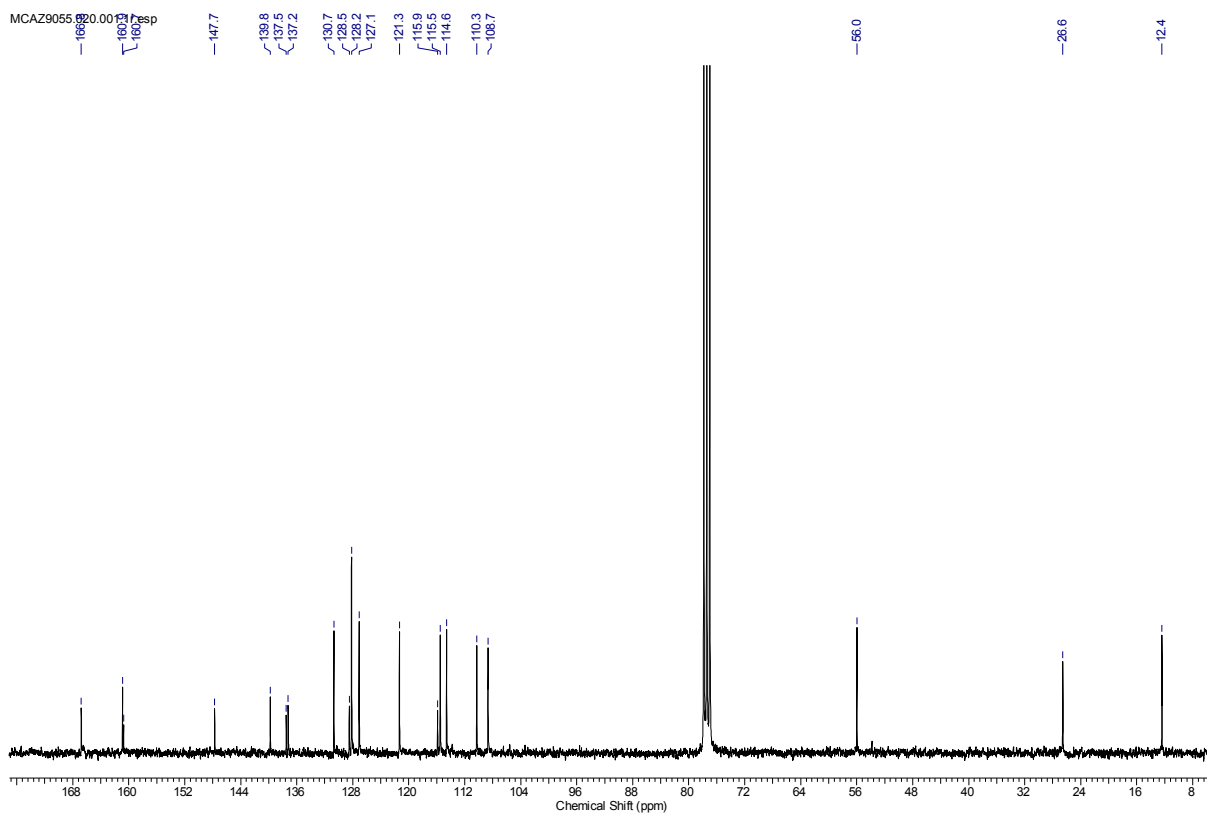
MCAR9065.010.001.1r.esp



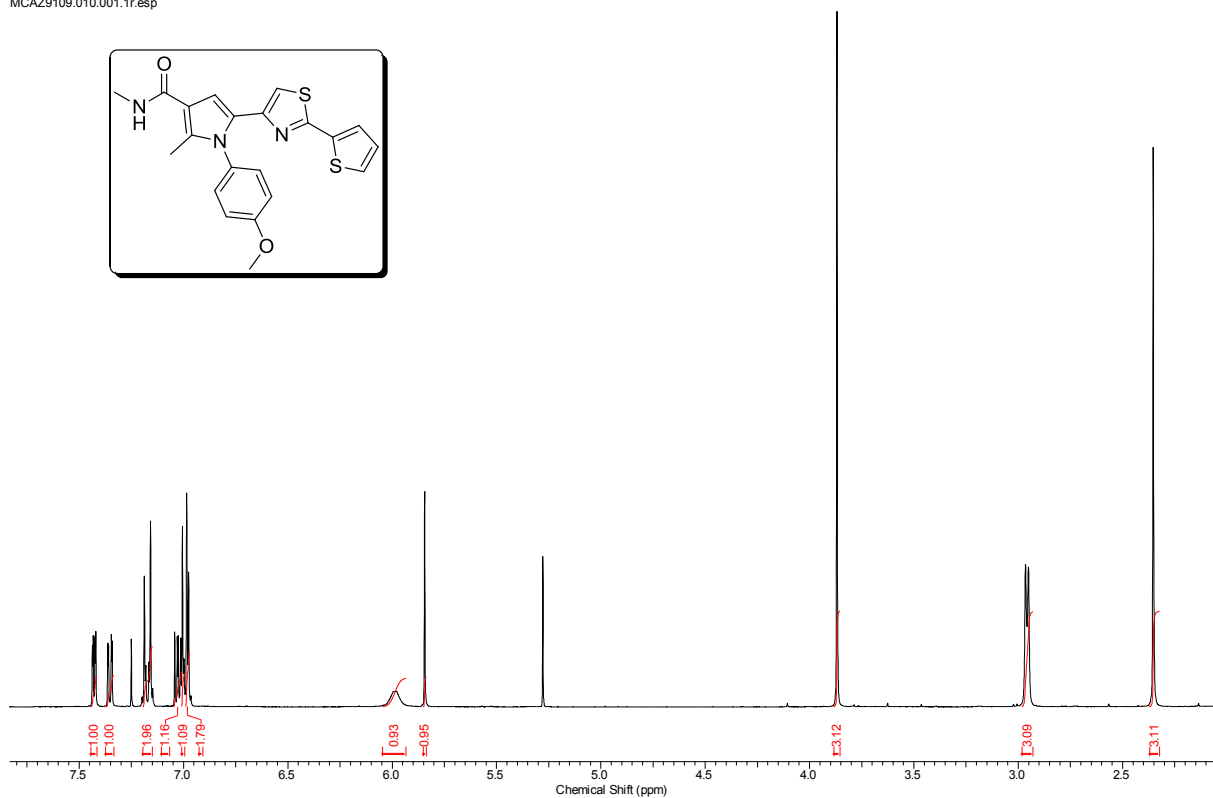
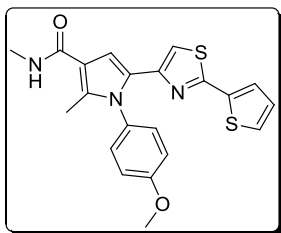
MCAZ9055.010.001.1r.esp



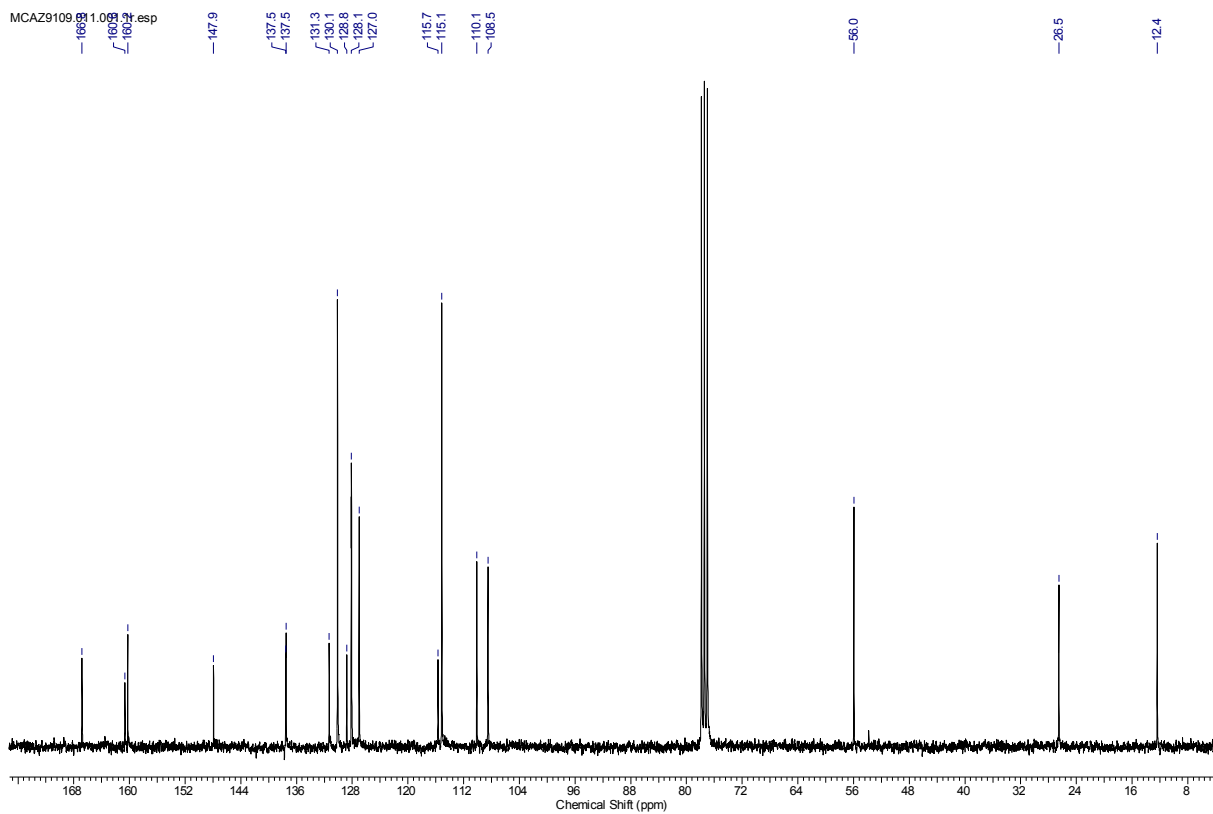
MCAZ9055.020.001.1r.esp



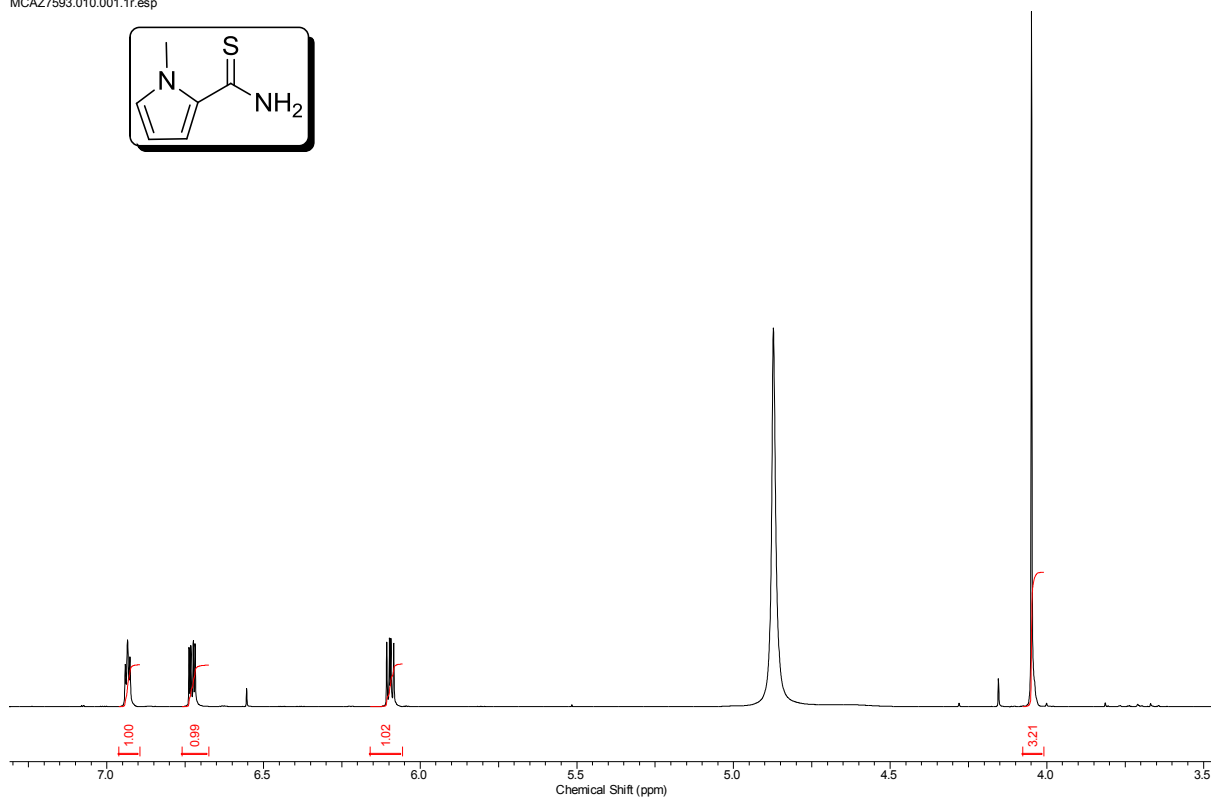
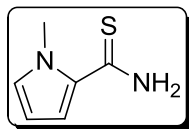
MCAZ9109.010.001.1r.esp



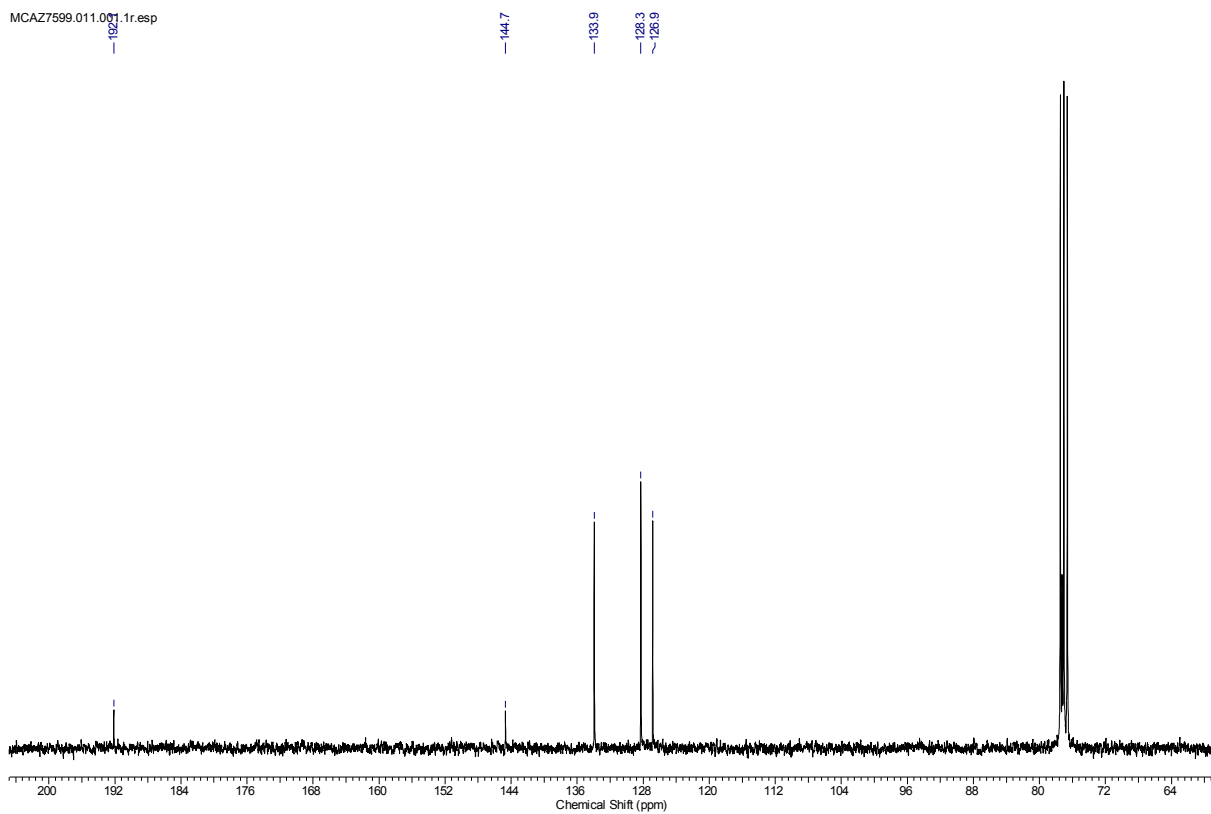
MCAZ9109.010.001.1r.esp



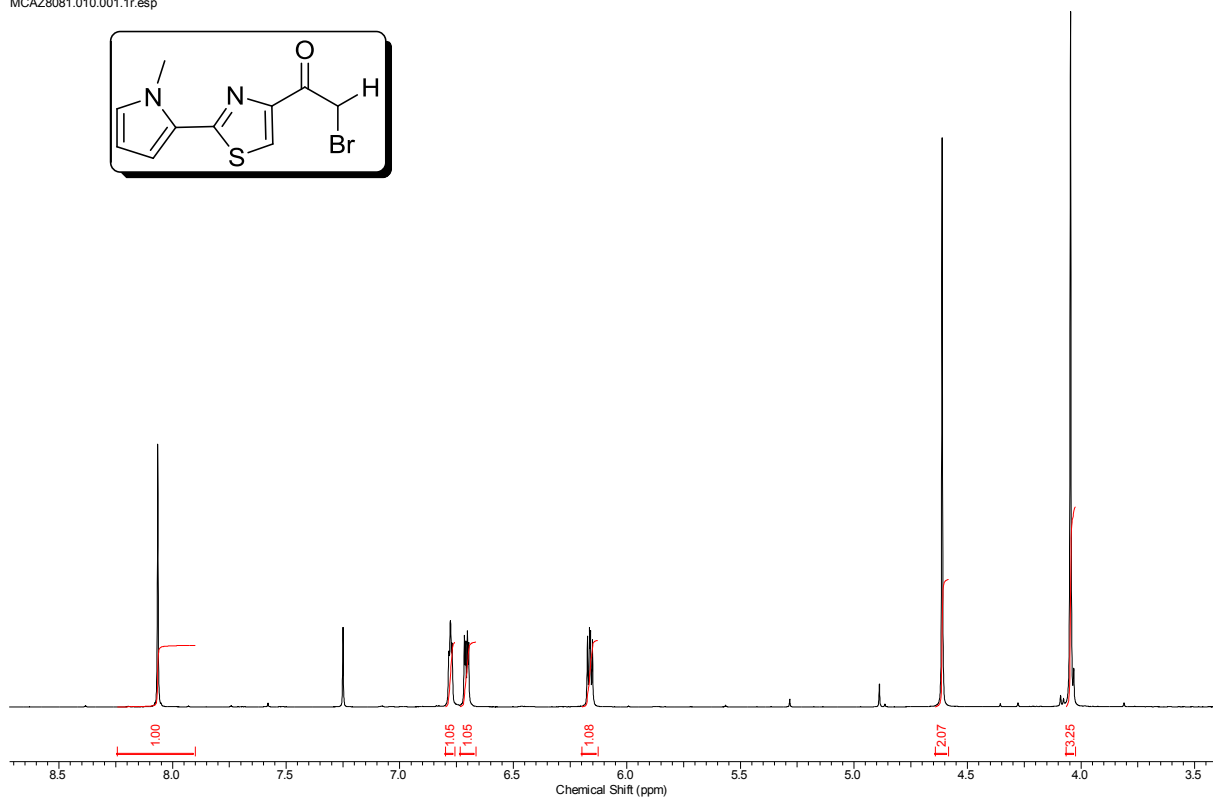
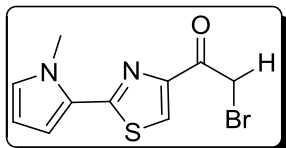
MCAZ7593.010.001.1r.esp



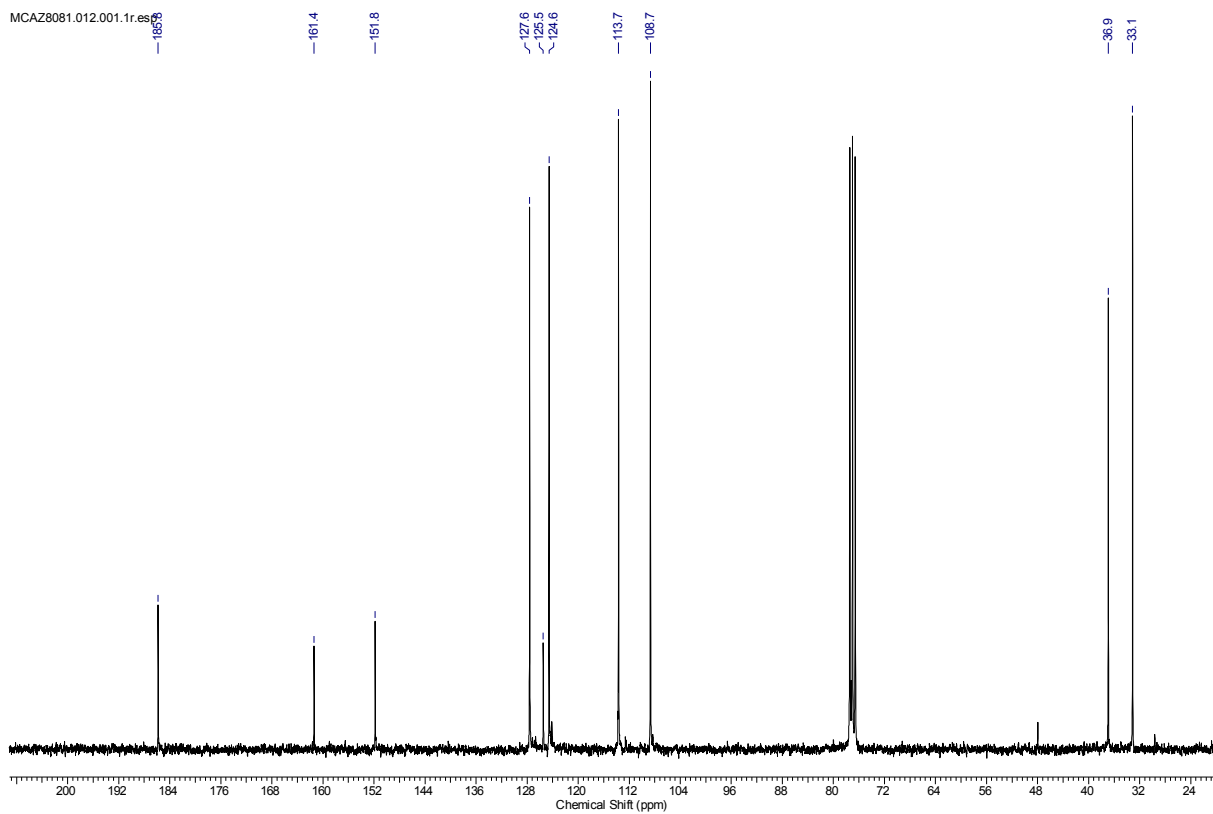
MCAZ7599.011.001.1r.esp



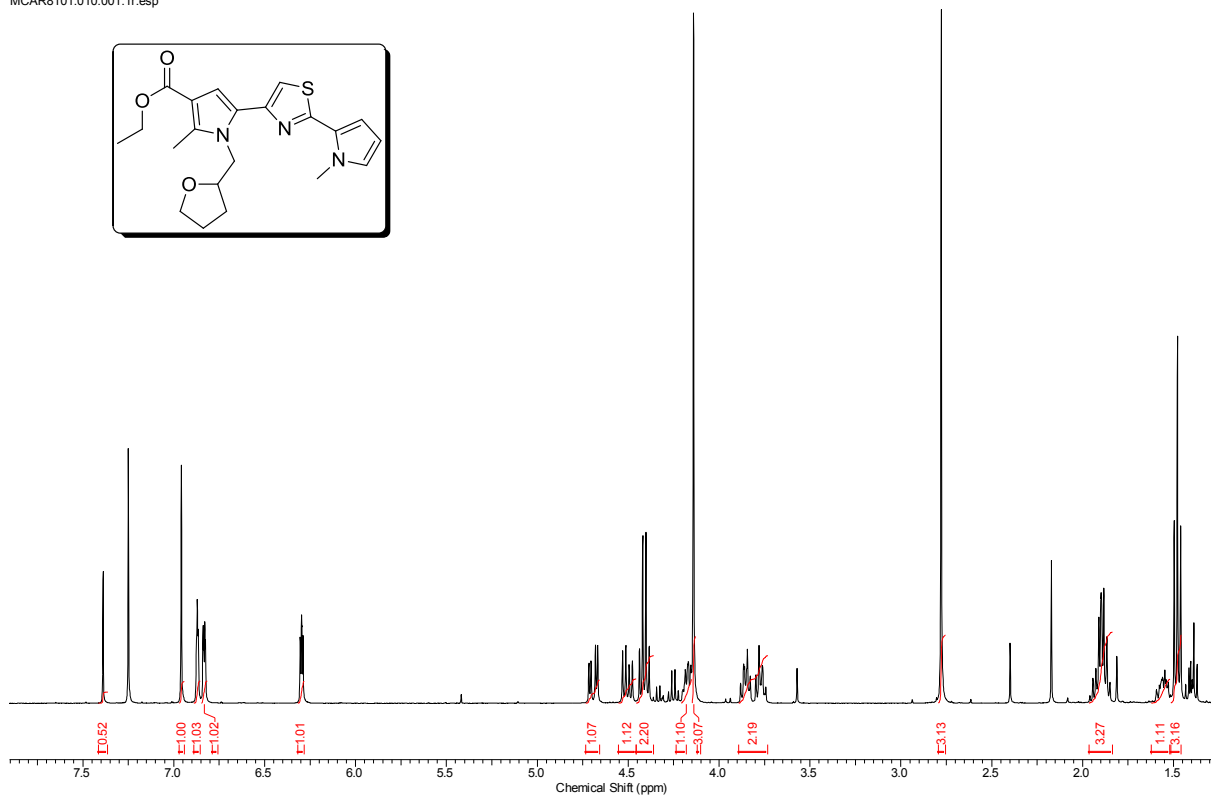
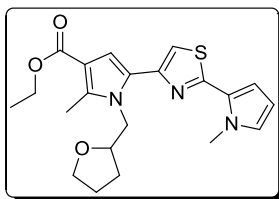
MCAZ8081.010.001.1r.esp



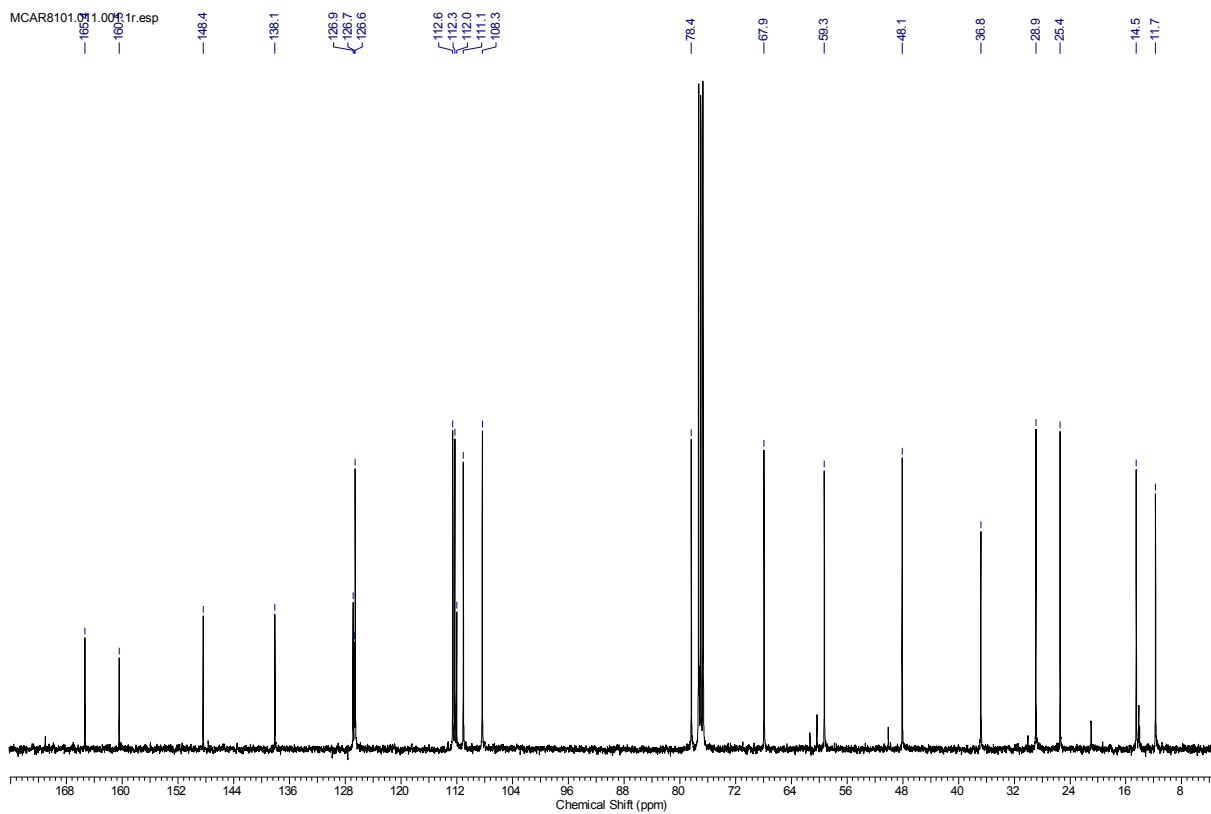
MCAZ8081.012.001.1r.es



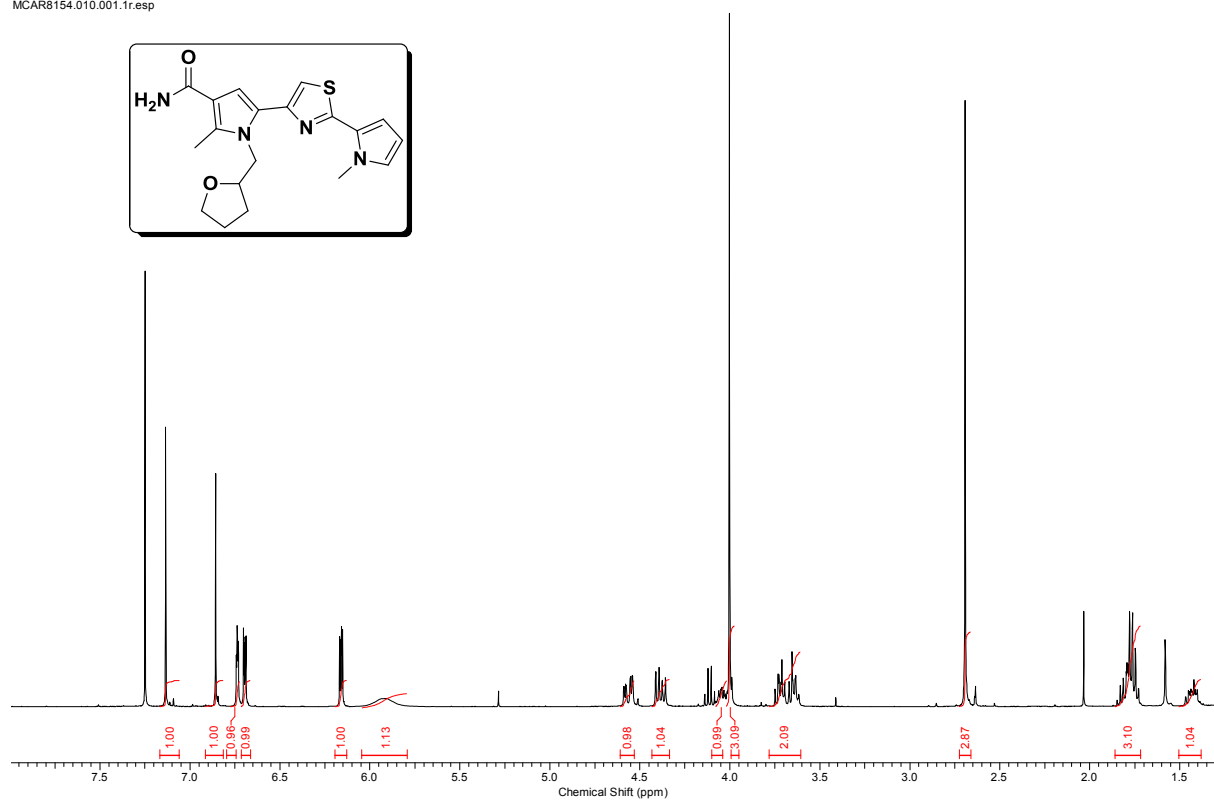
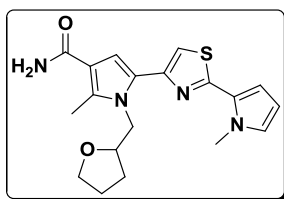
MCR8101.010.001.1r.esp



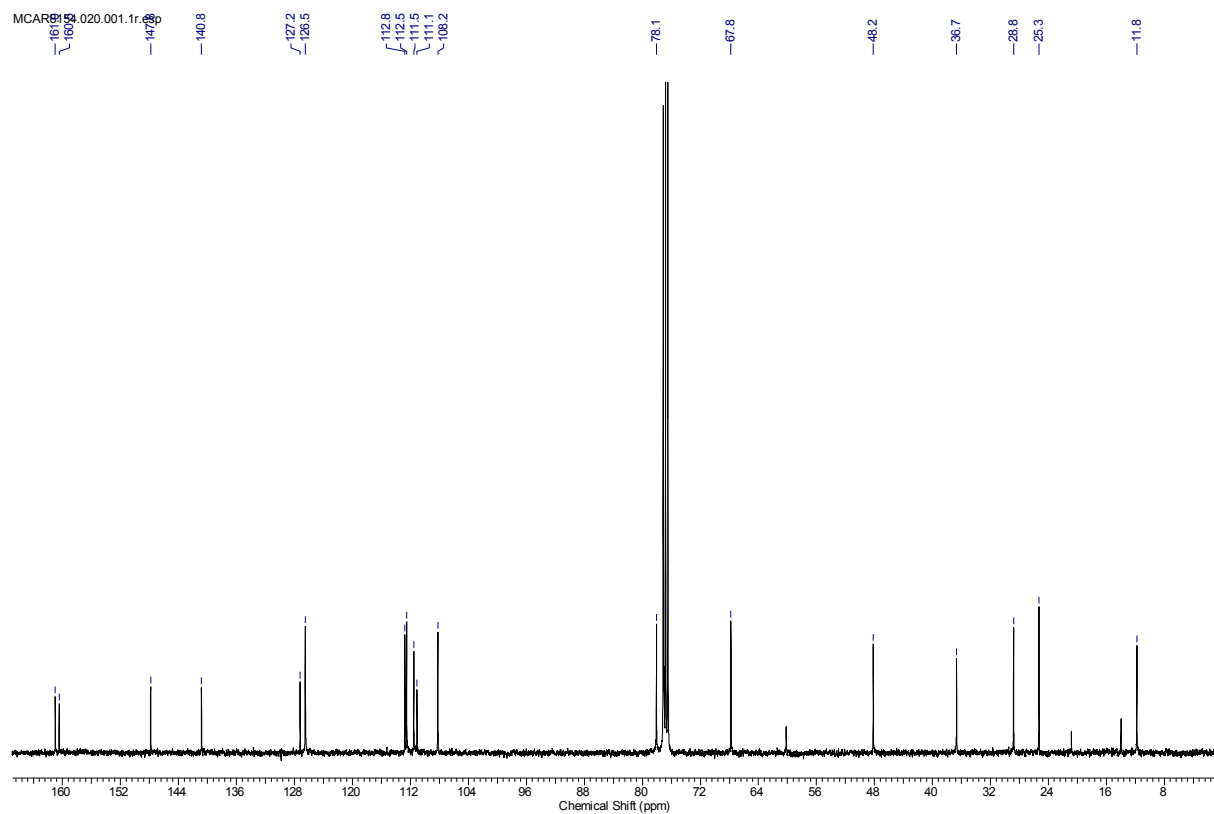
MCR8101.010.001.1r.esp



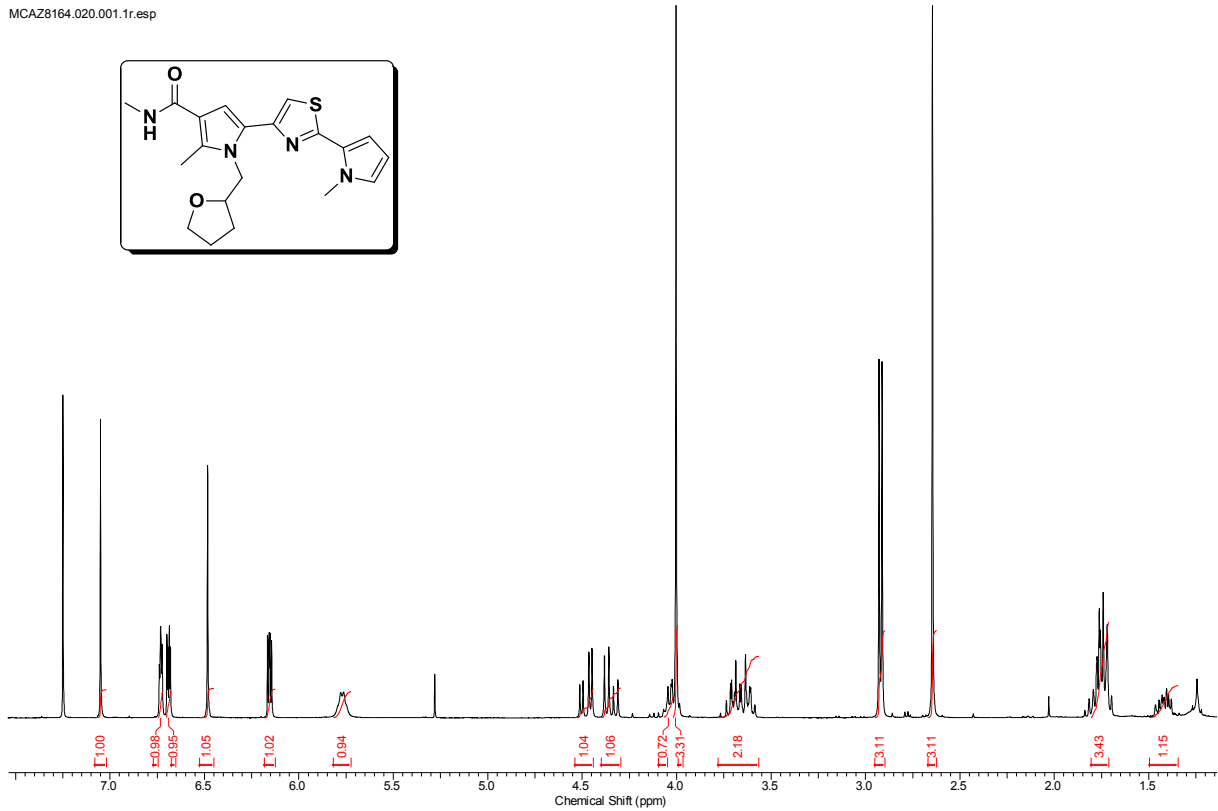
MCAR8154.010.001.1r.esp



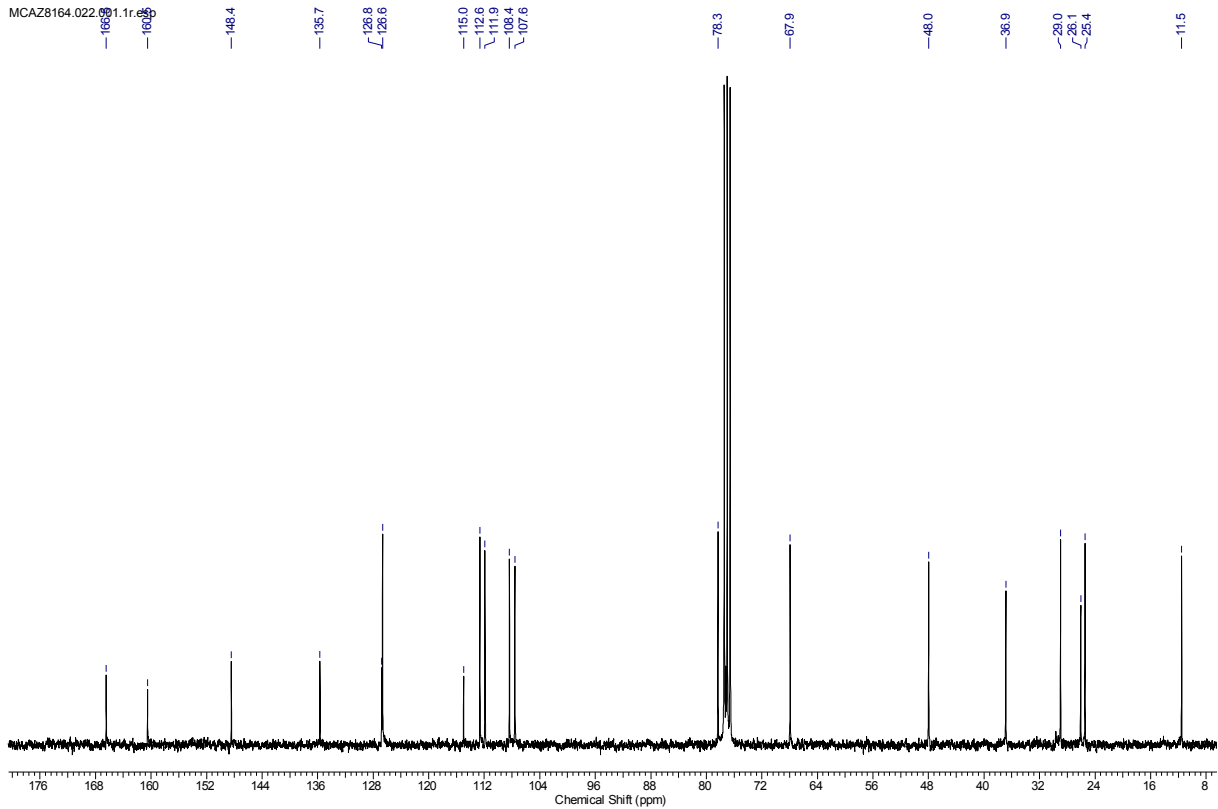
MCAR8154.020.001.1r.esp



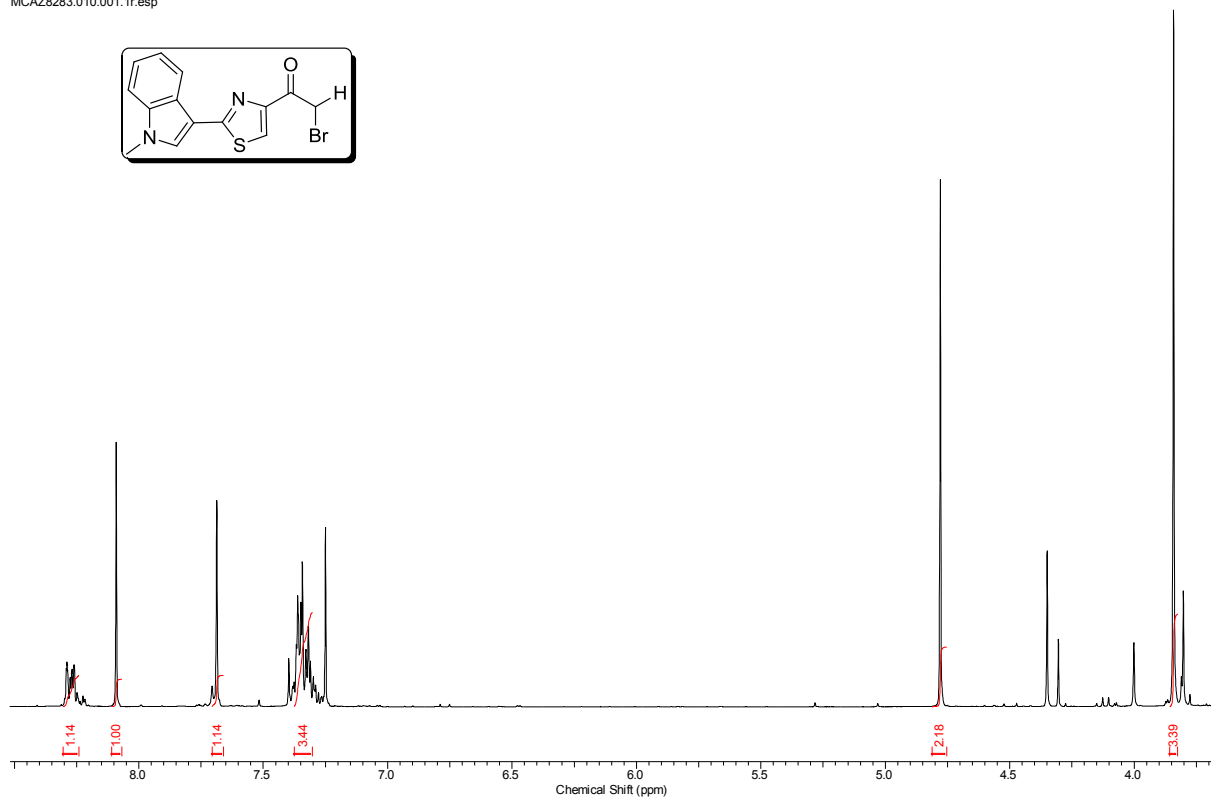
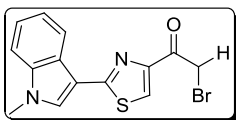
MCAZ8164.020.001.1r.esp



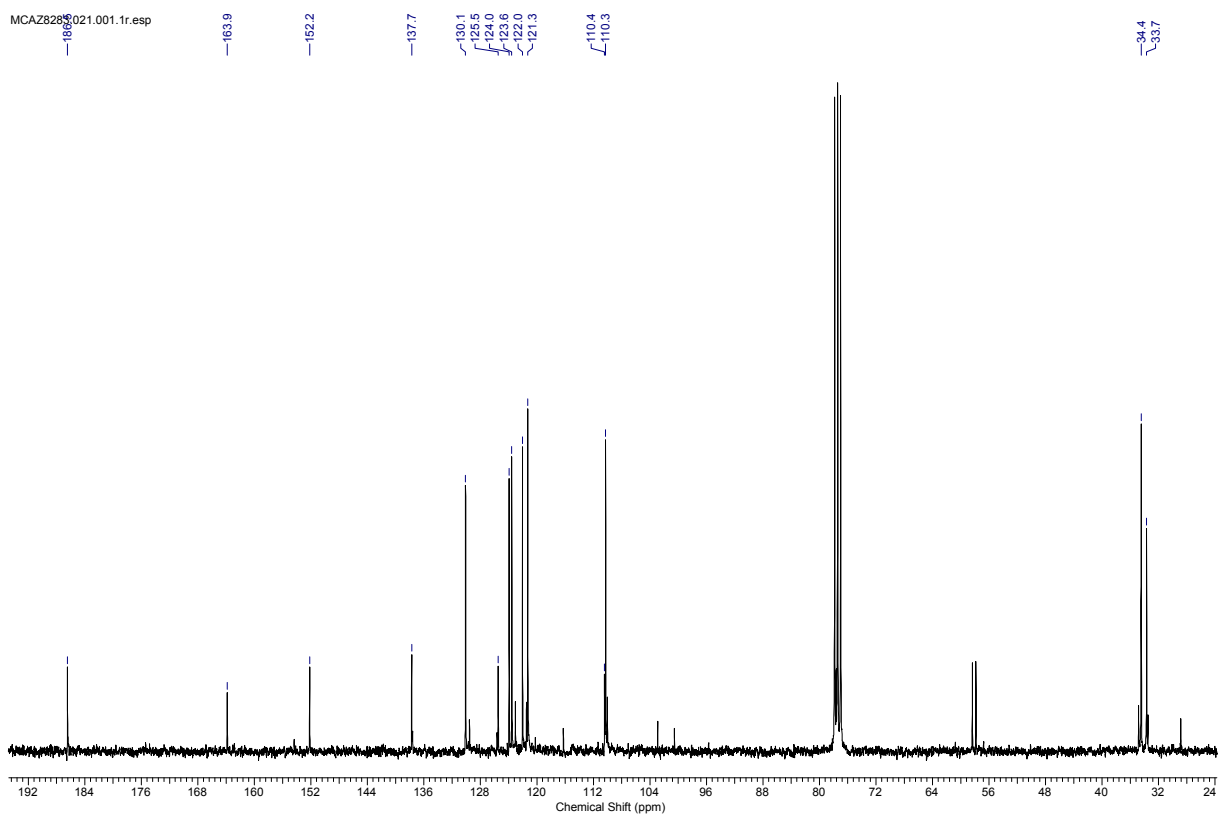
MCAZ8164.022.001.1r.esp



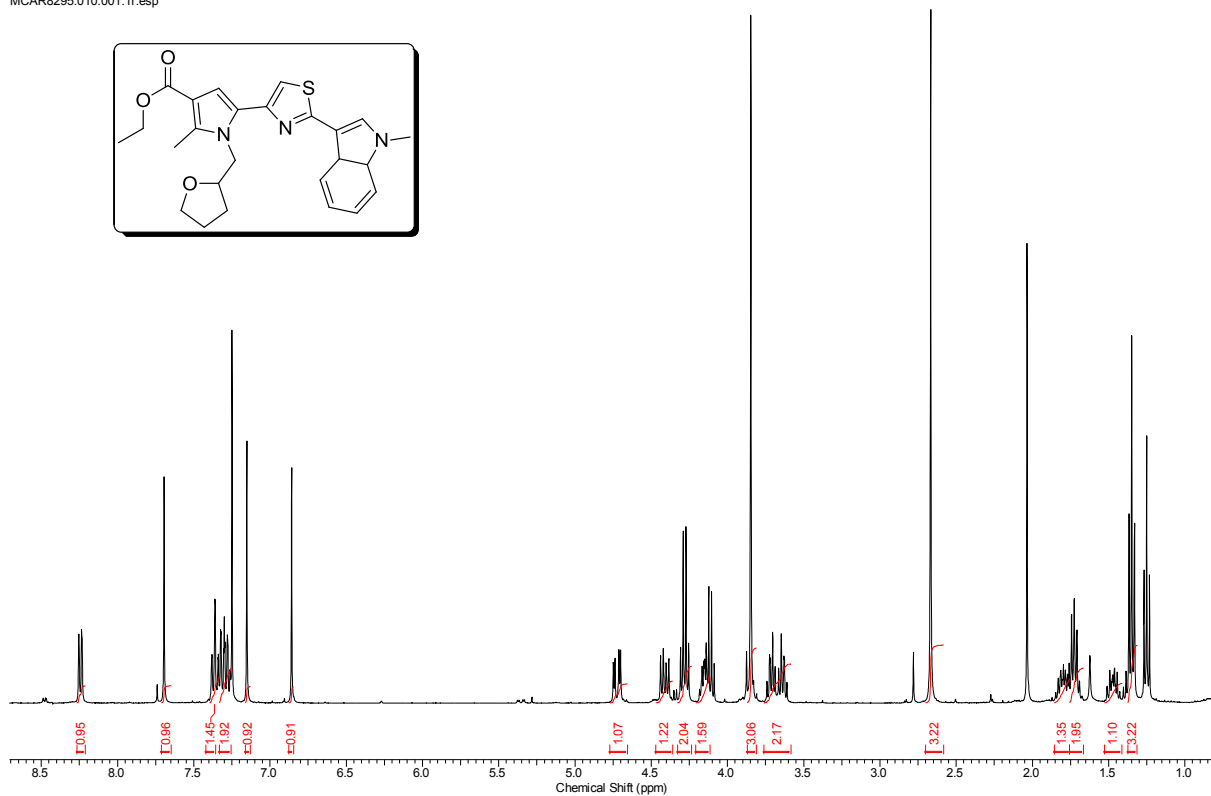
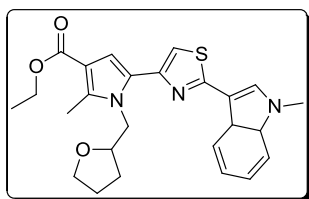
MCAZ6283.010.001.1r.esp



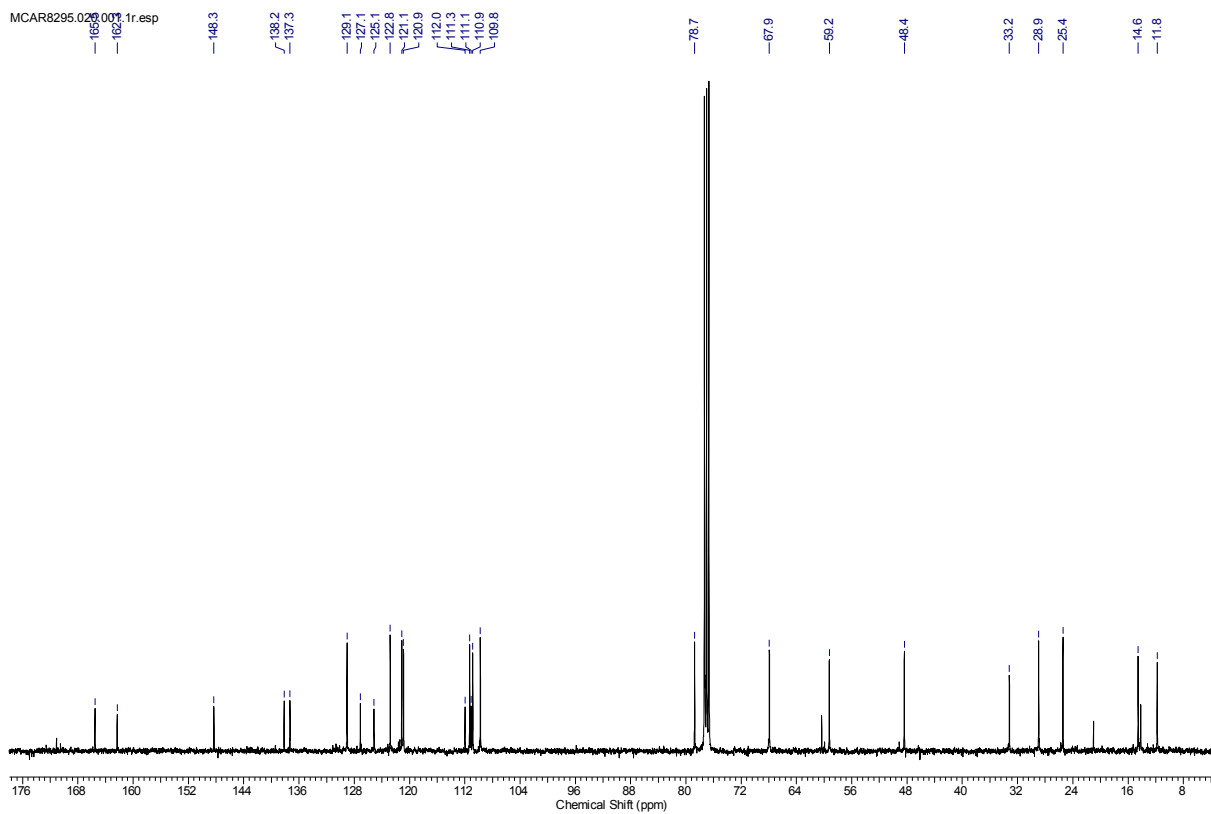
MCAZ6283.021.001.1r.esp

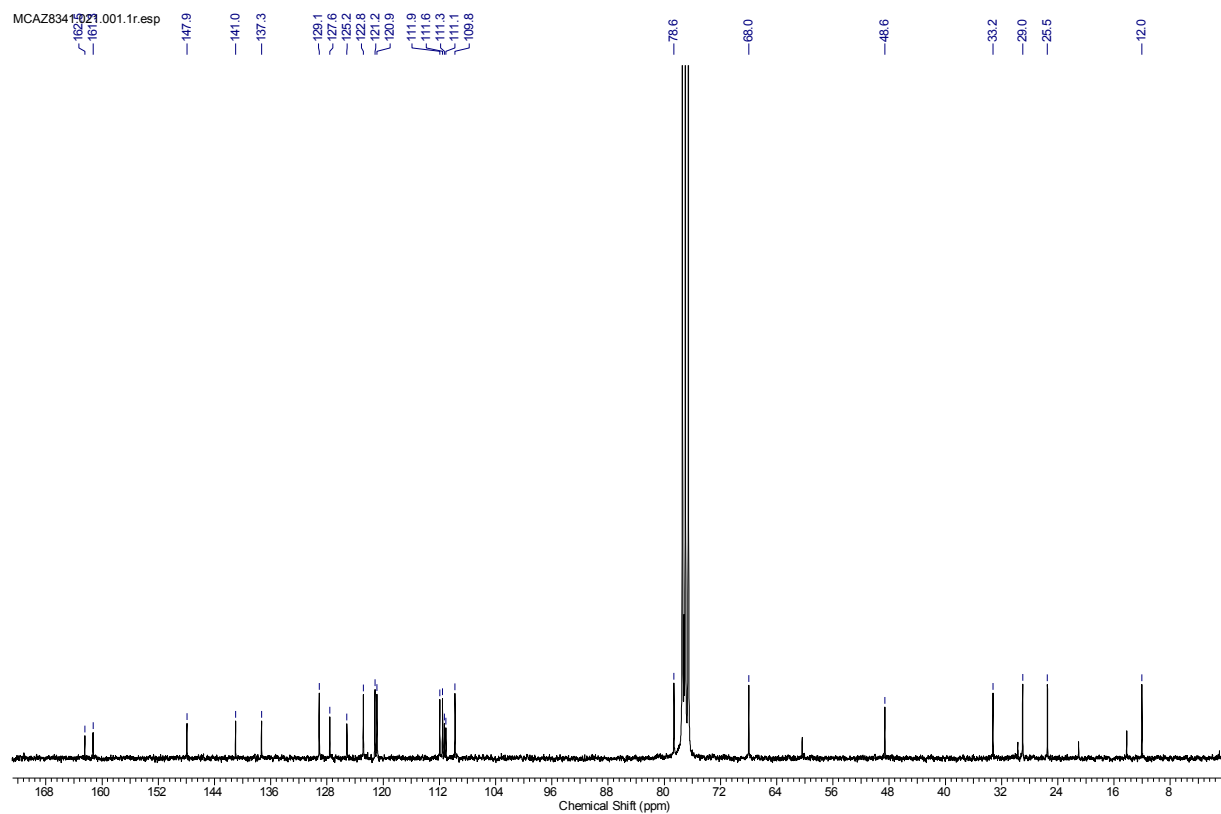
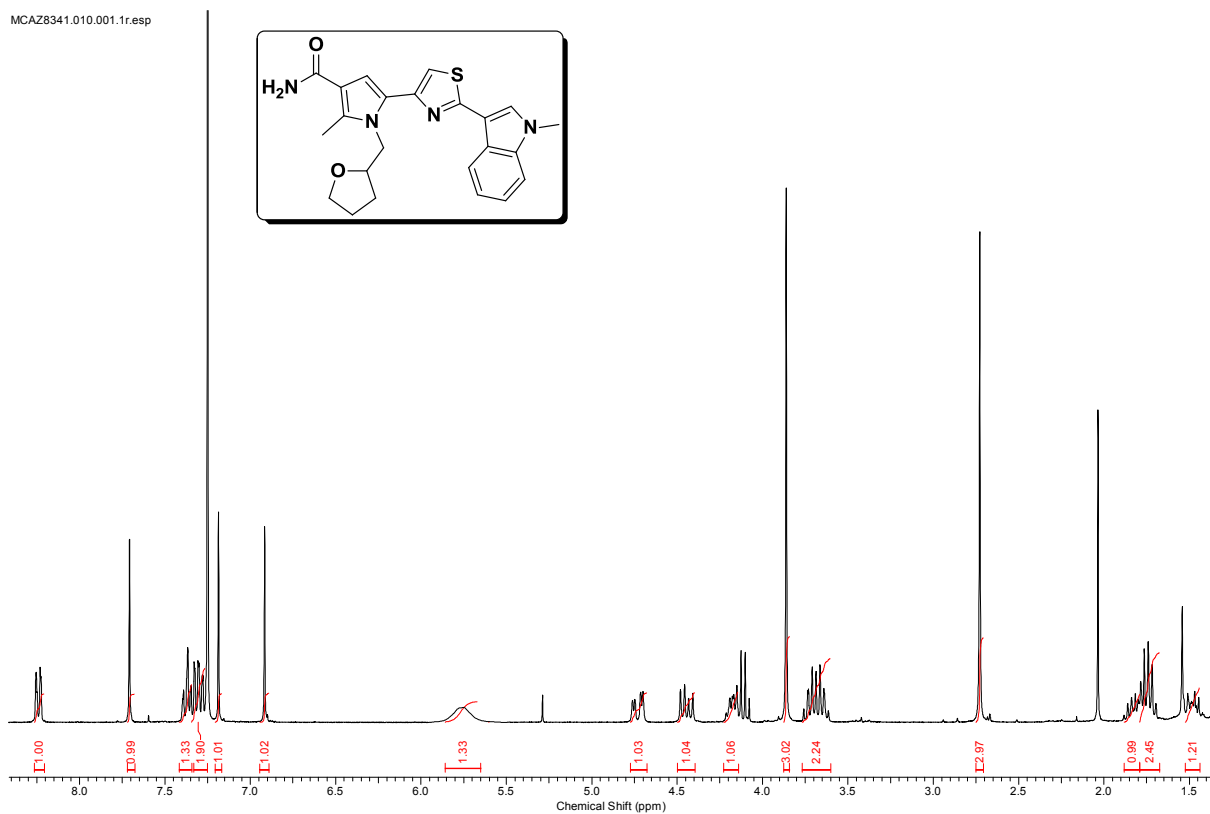


MCAR8295.010.001.1r.esp

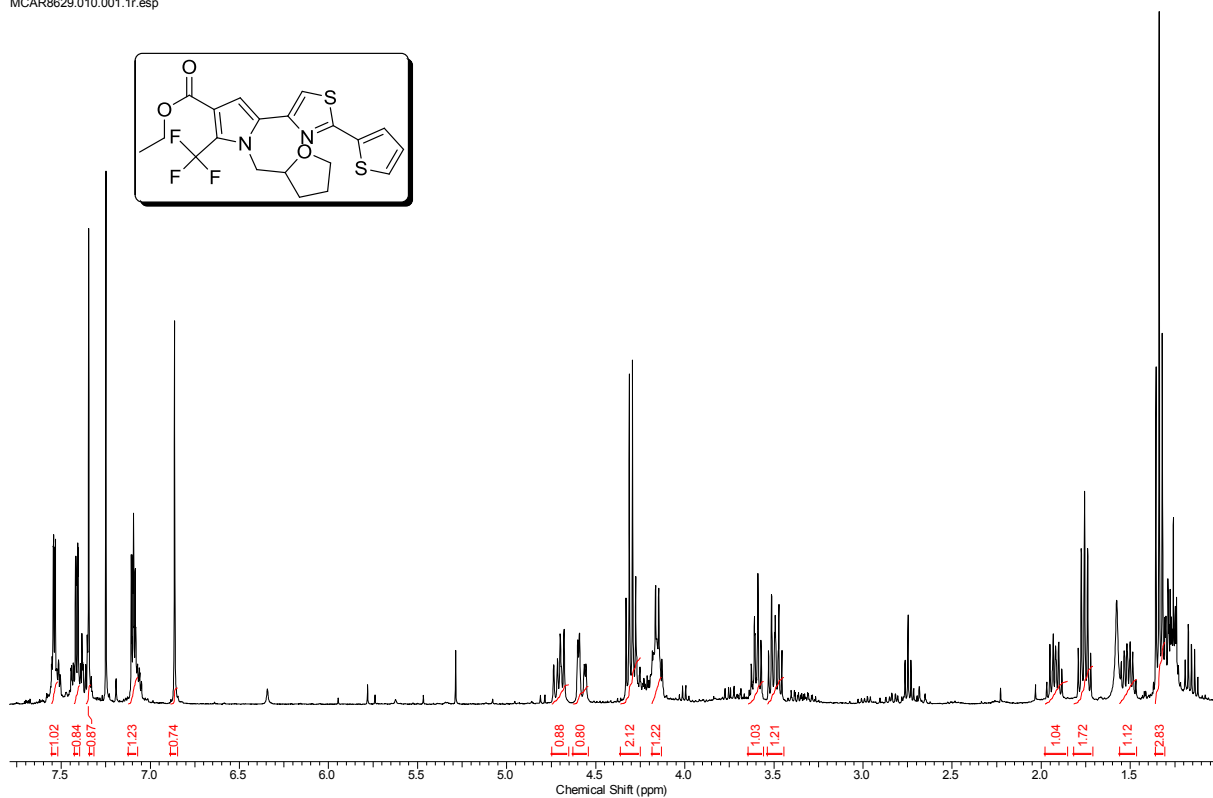


MCAR8295.020.001.1r.esp

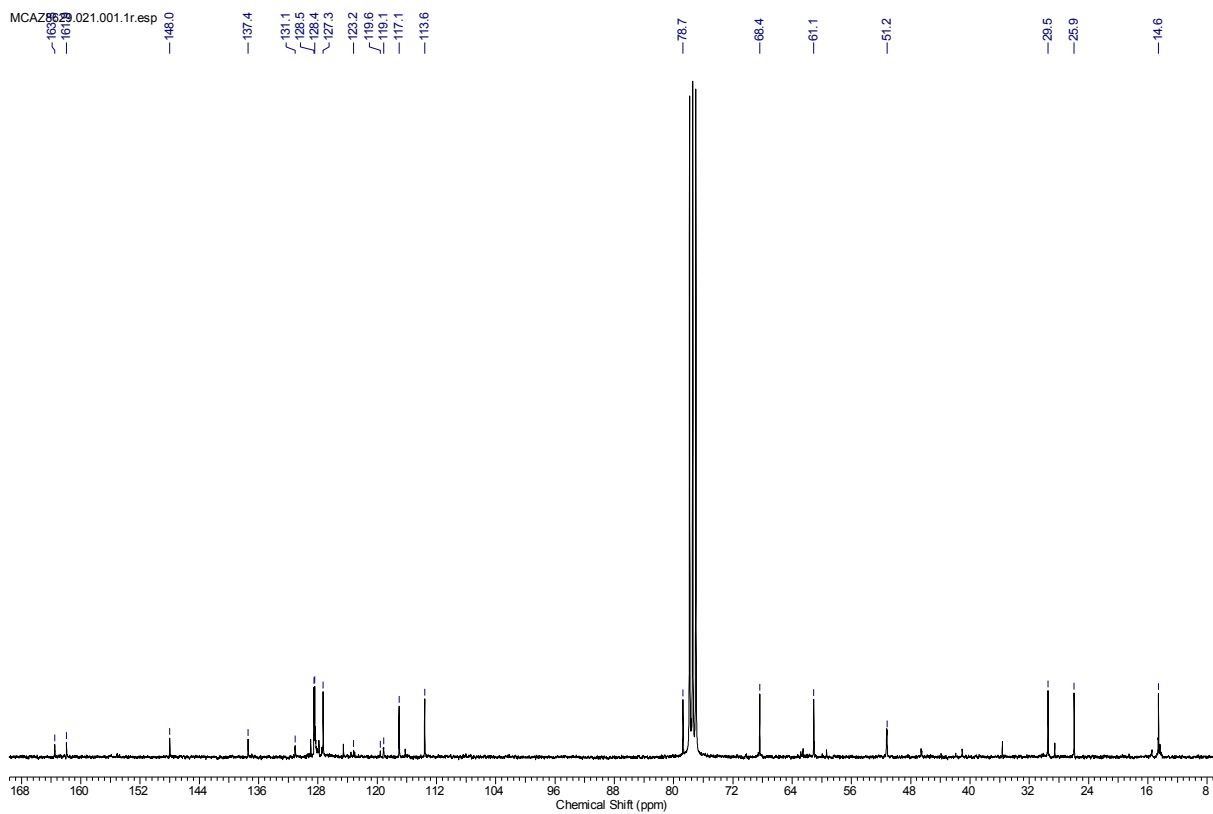


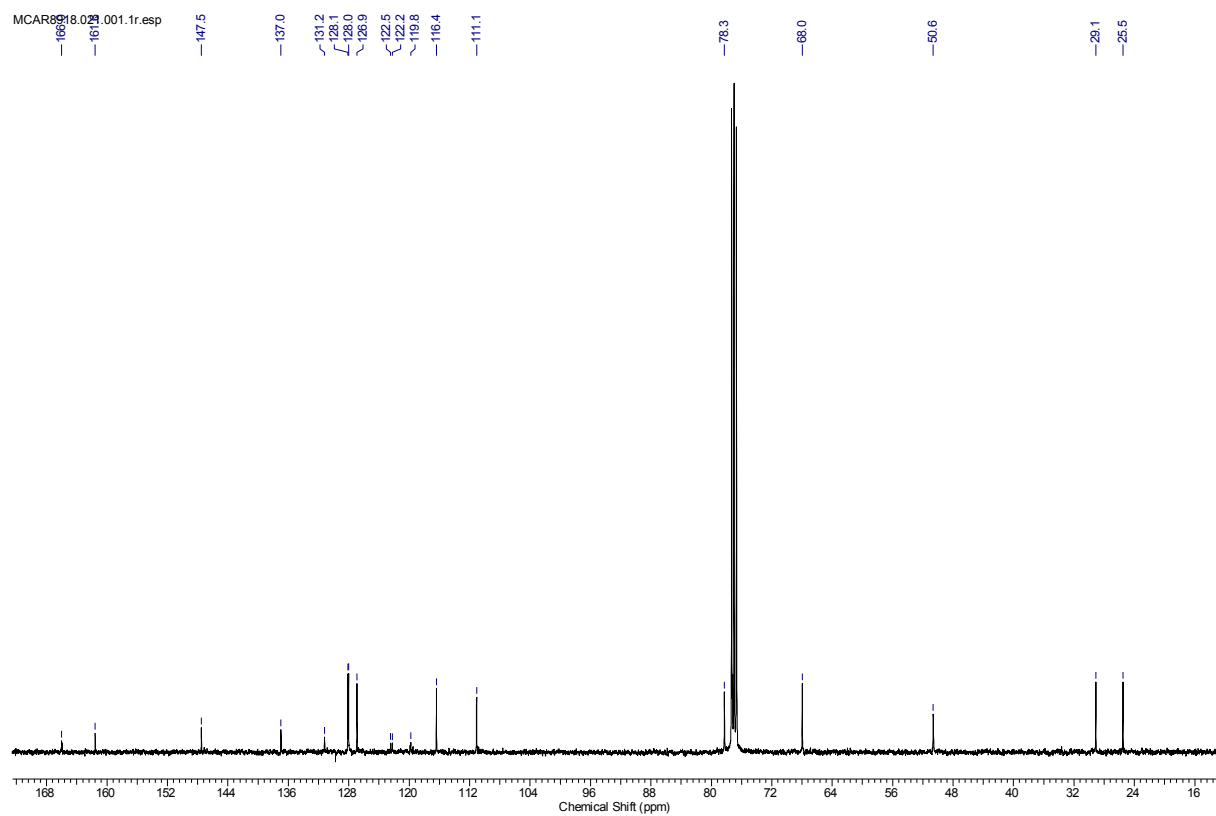
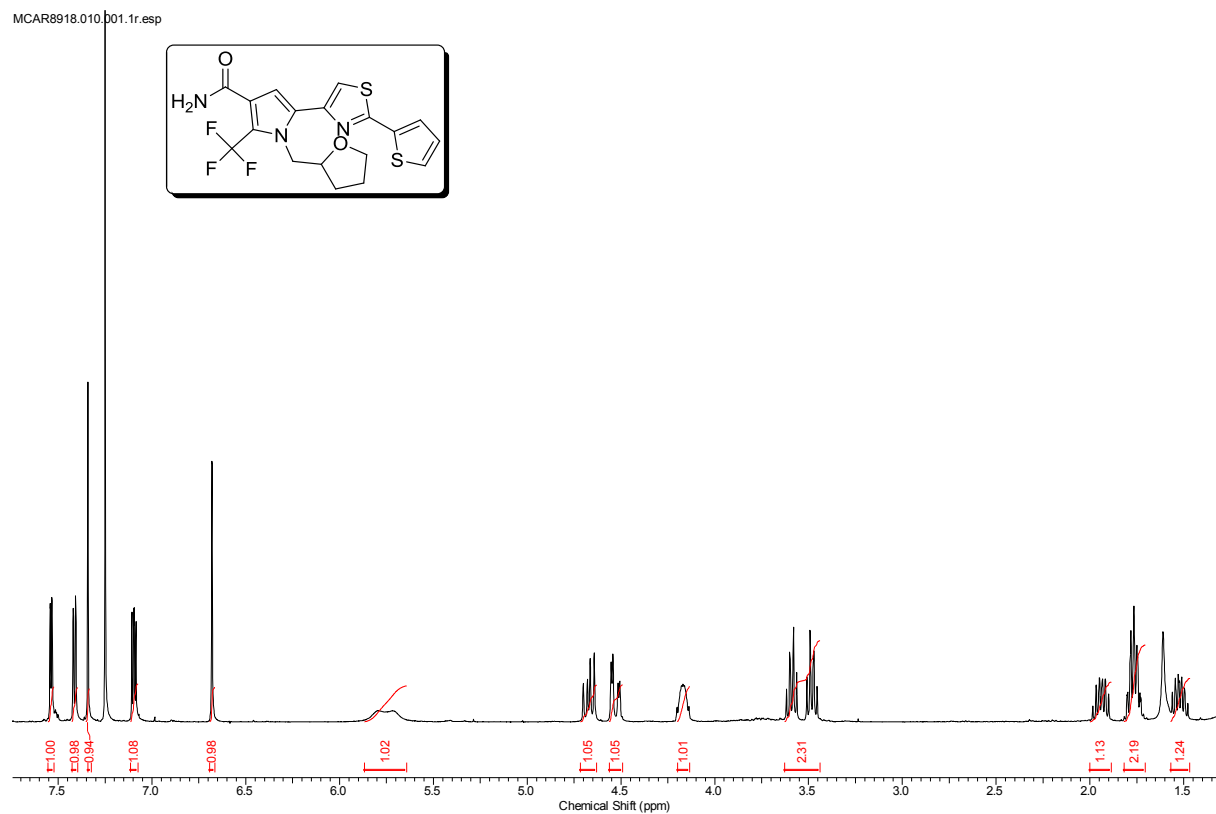


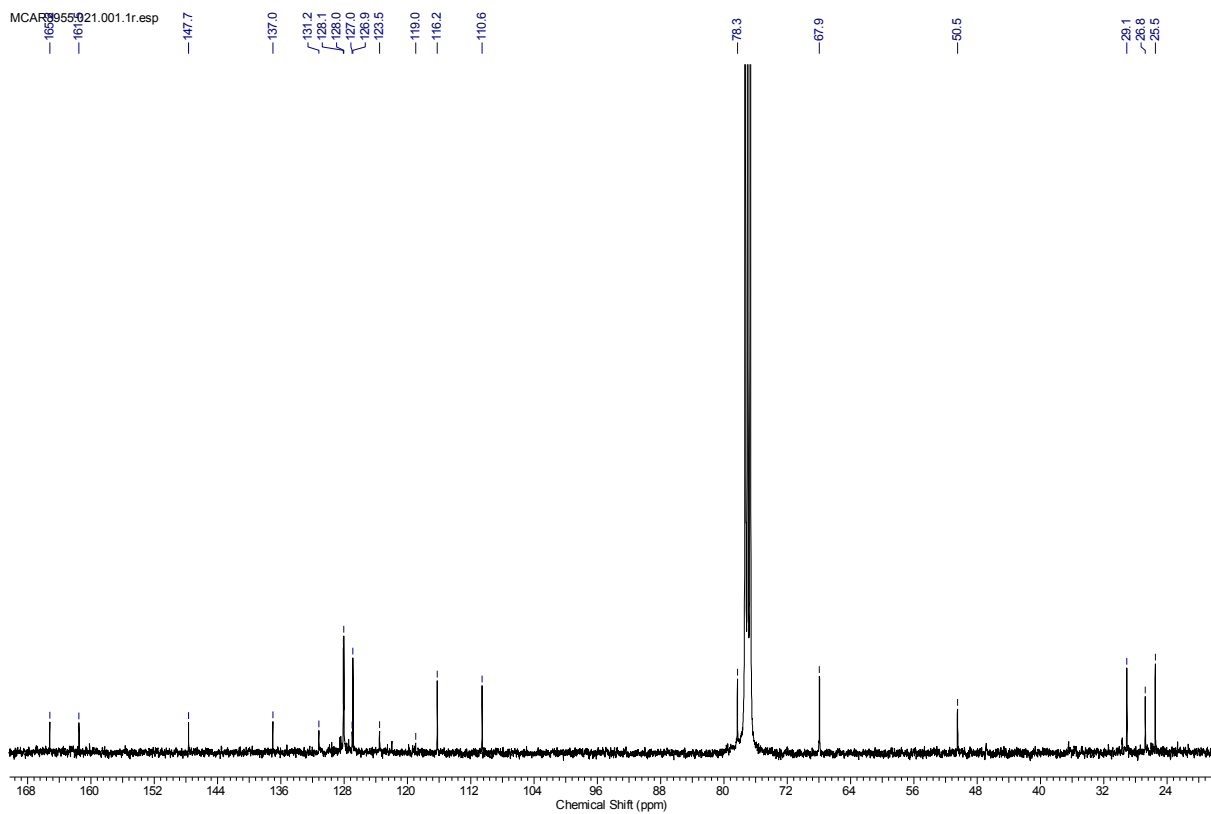
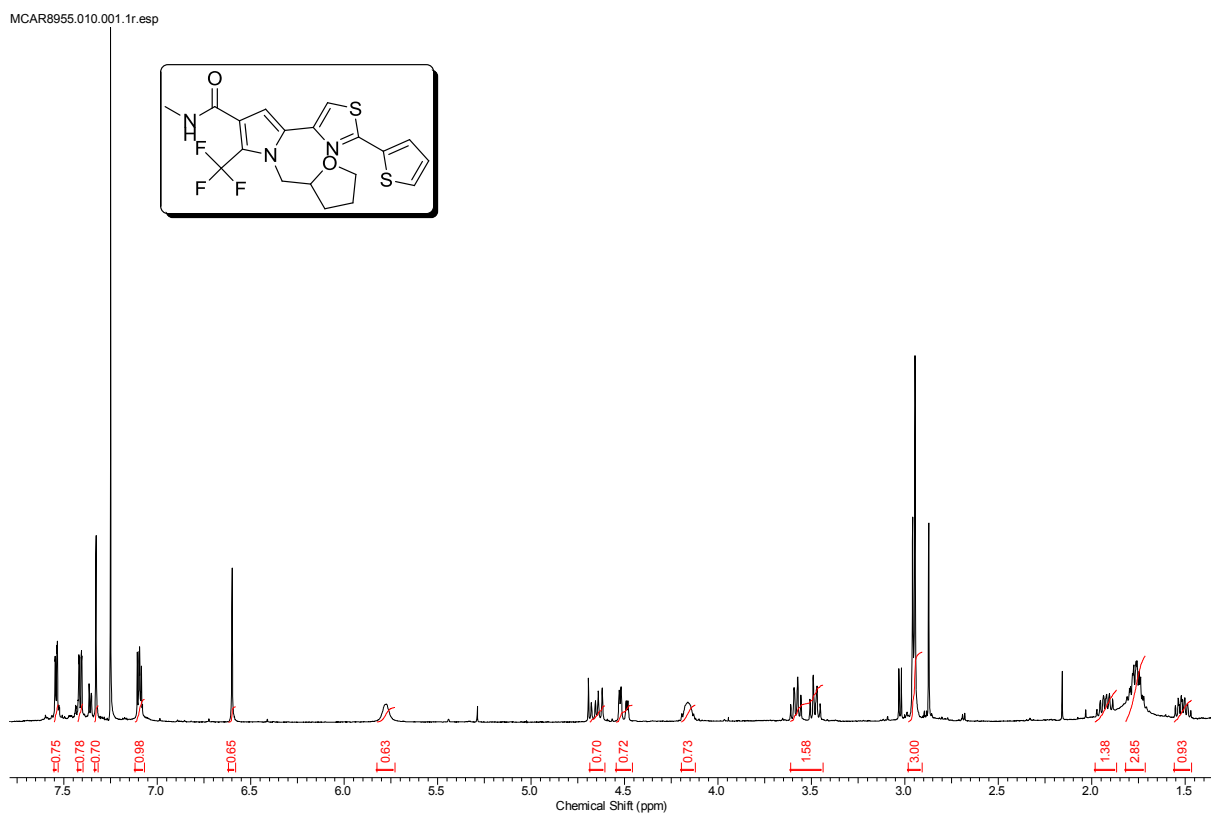
MCAZ8629.010.001.1r.esp



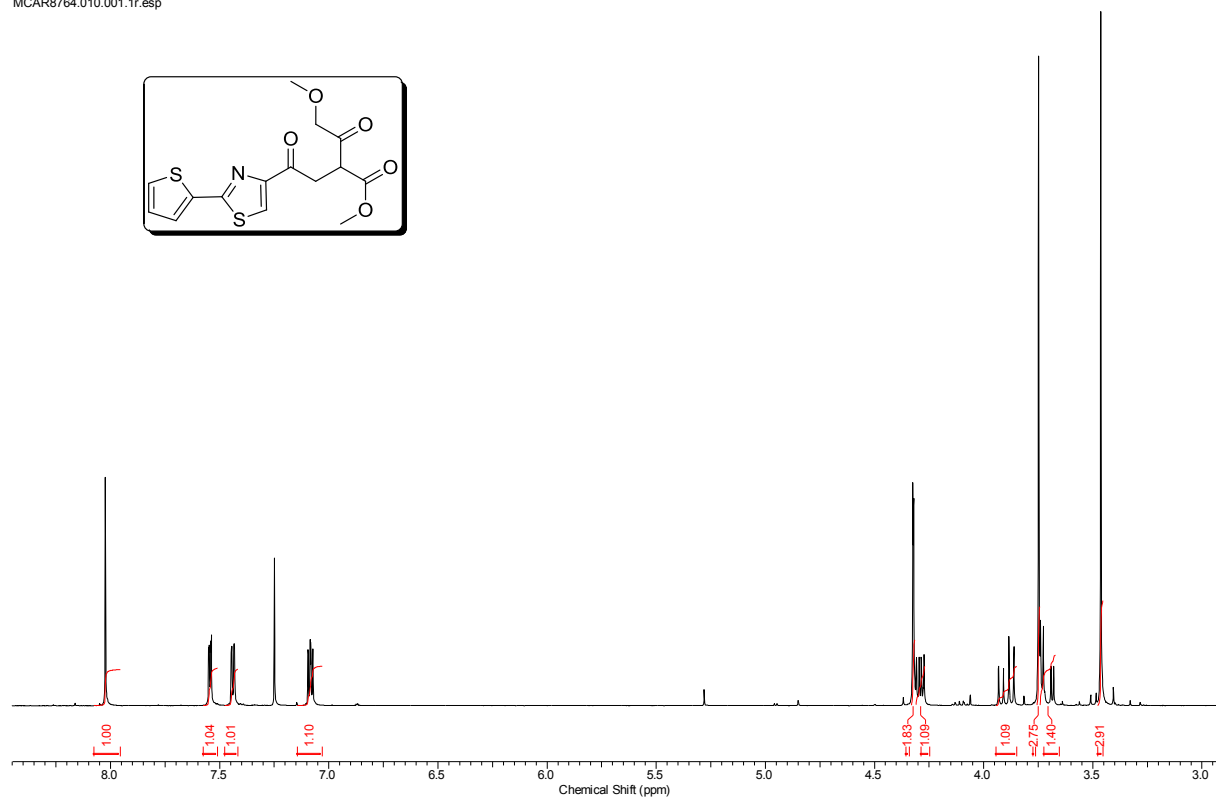
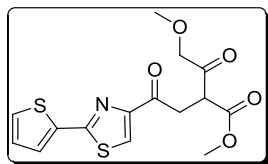
MCAZ8629.021.001.1r.esp



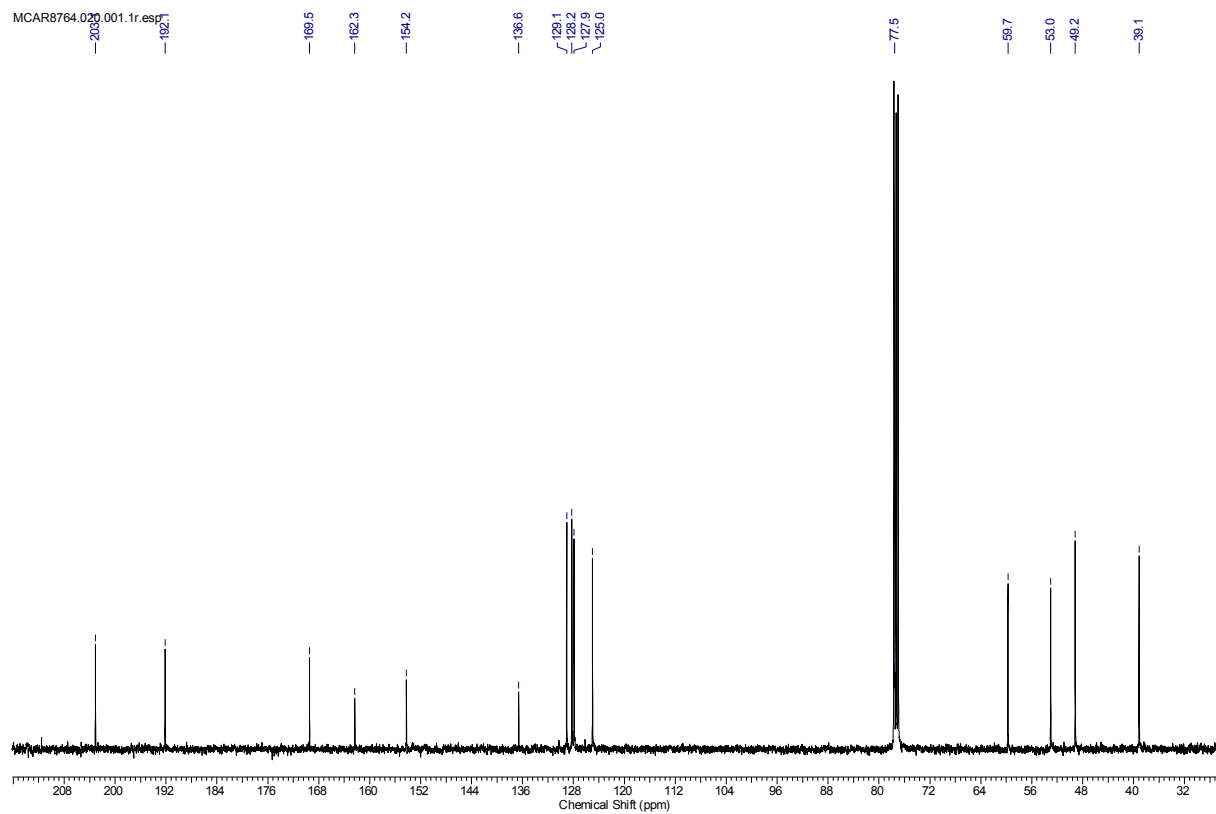




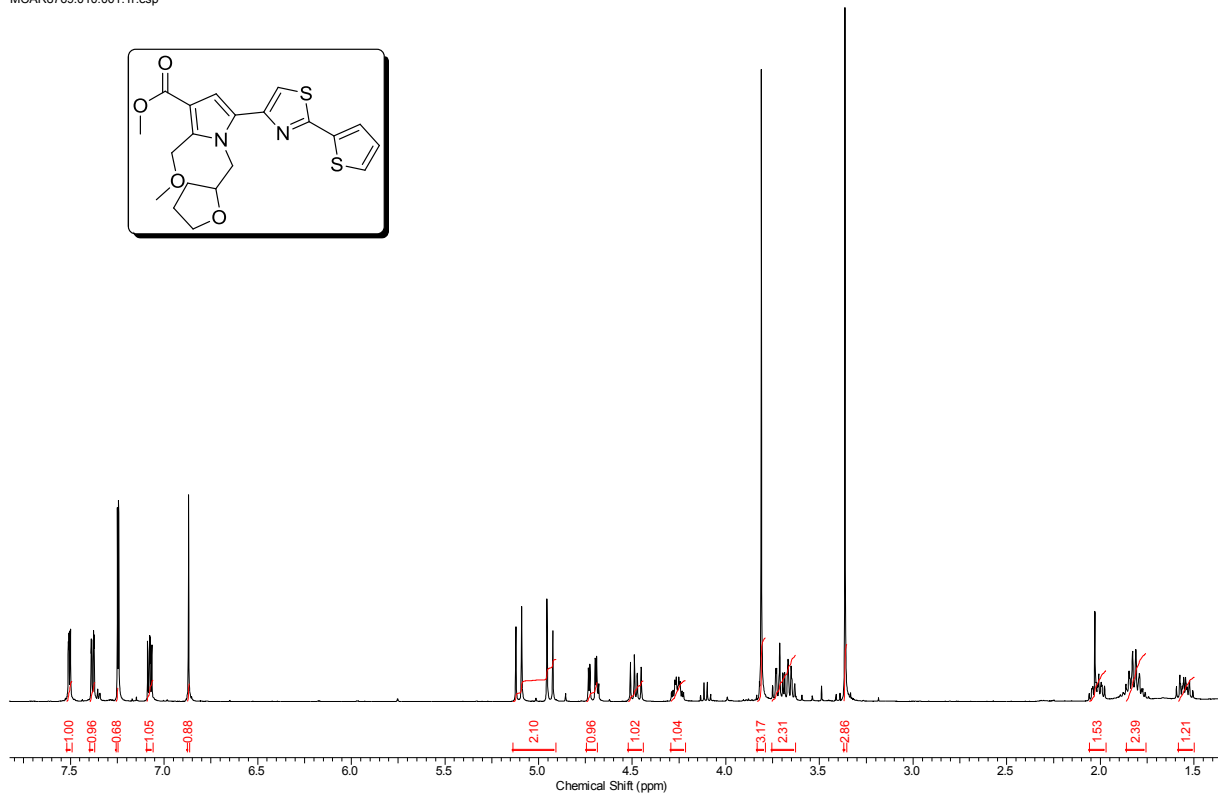
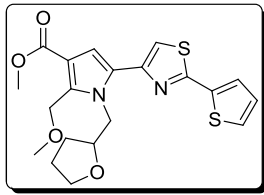
MCAR8764.010.001.1r.esp



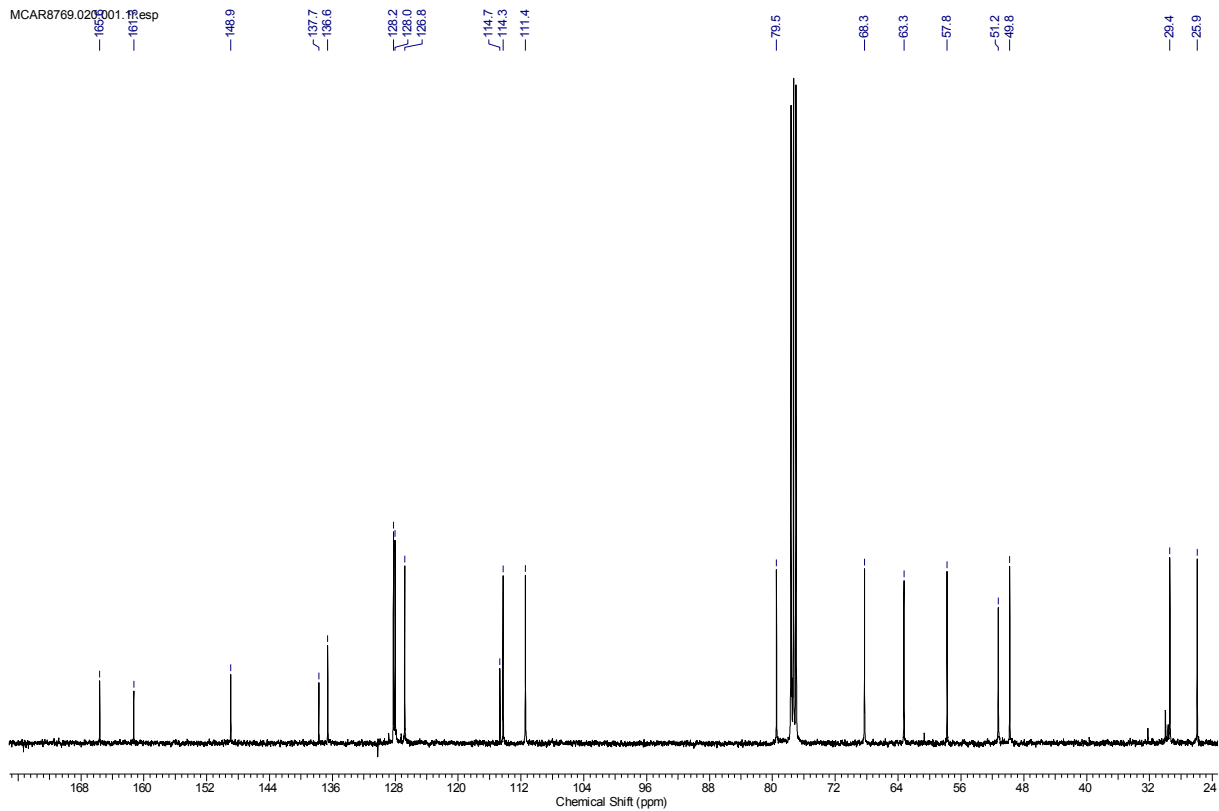
MCAR8764.020.001.1r.esp



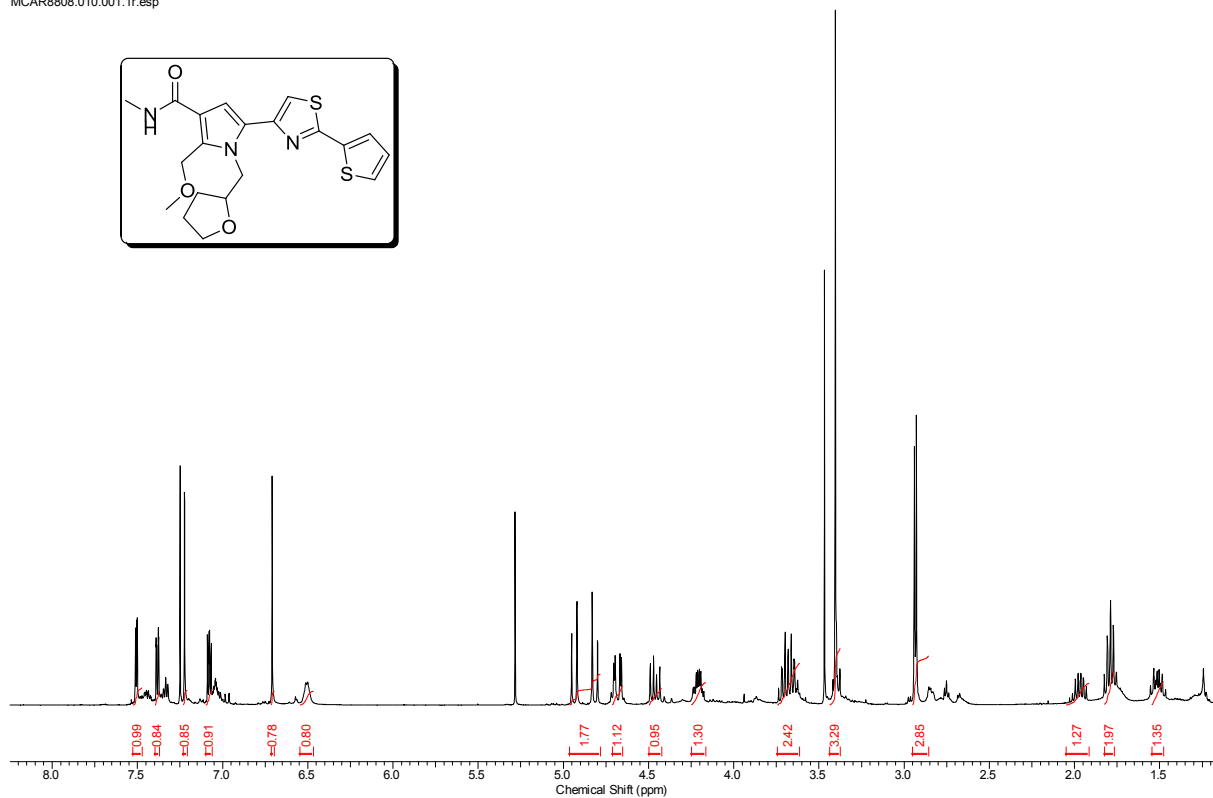
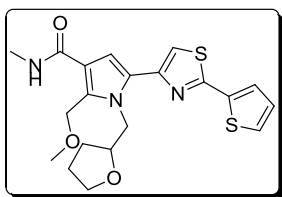
MCAR8769.010.001.1r.esp



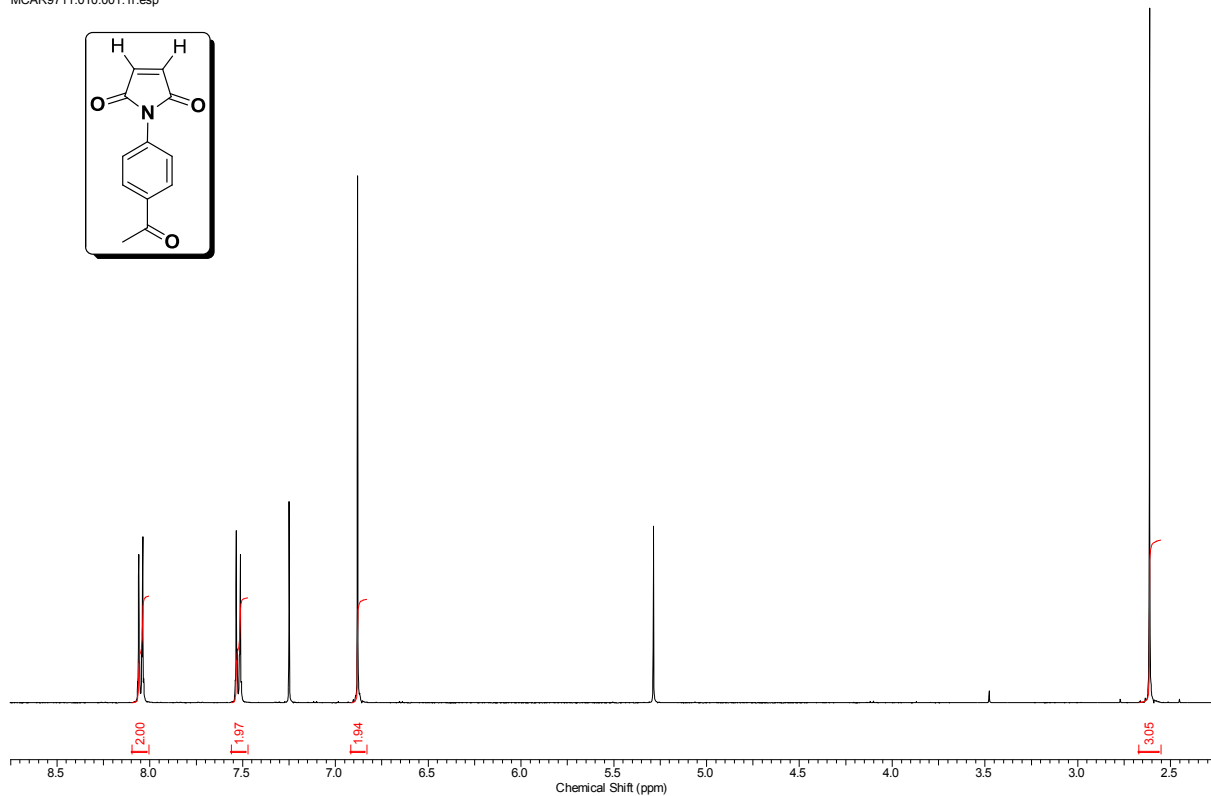
MCAR8769.020.001.1r.esp



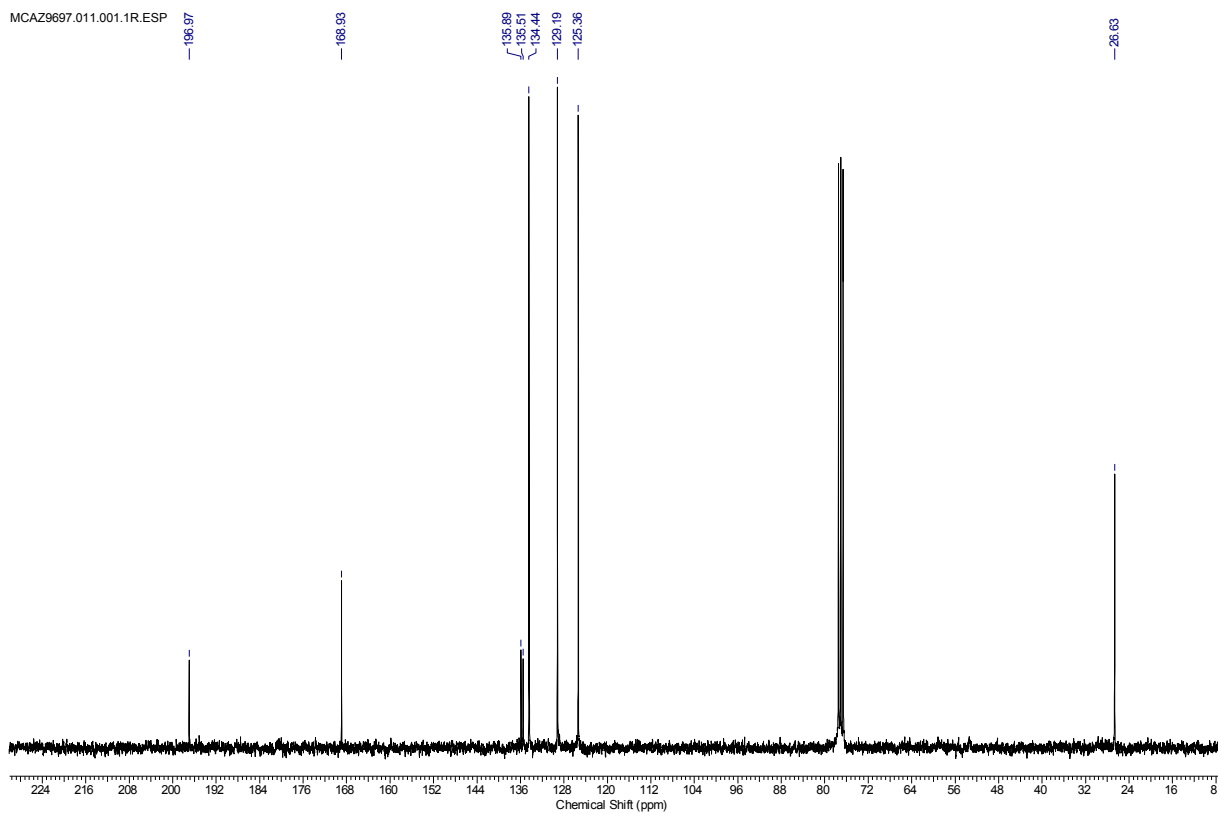
MCAR8808.010.001.1r.esp



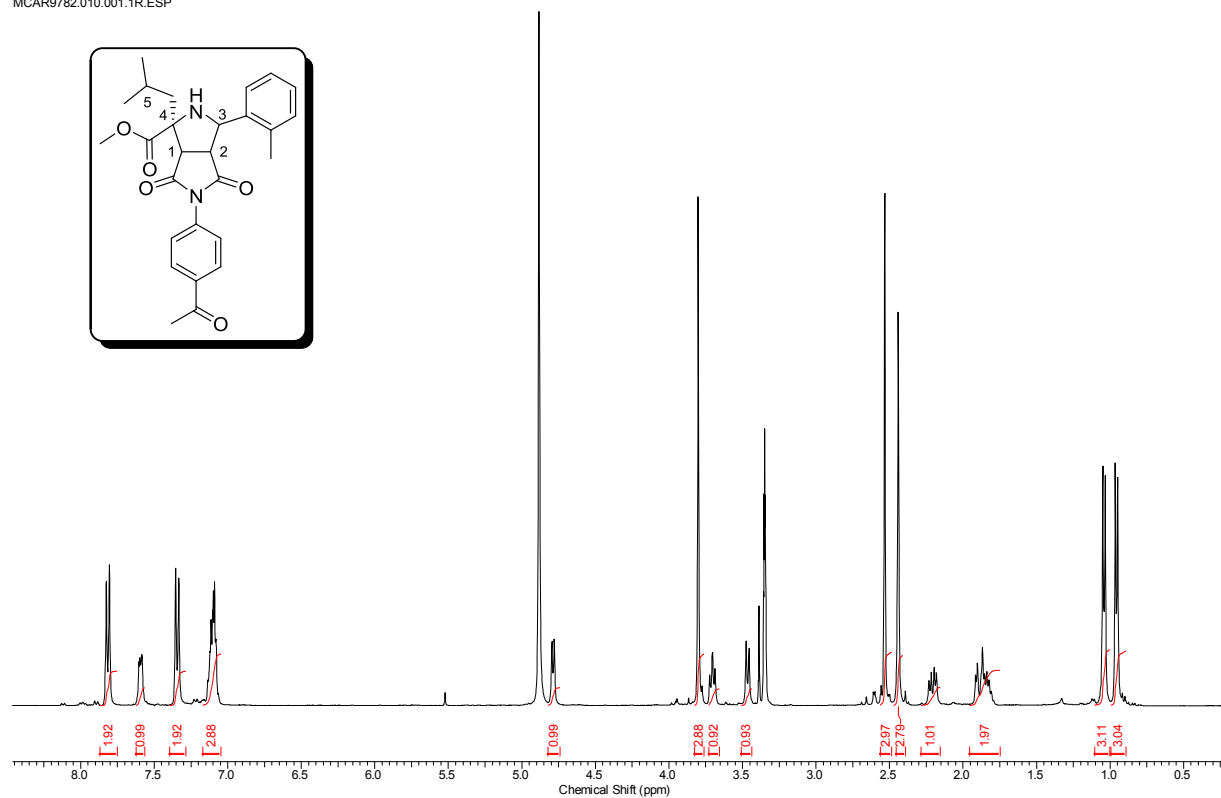
MCAR9711.010.001.1r.esp



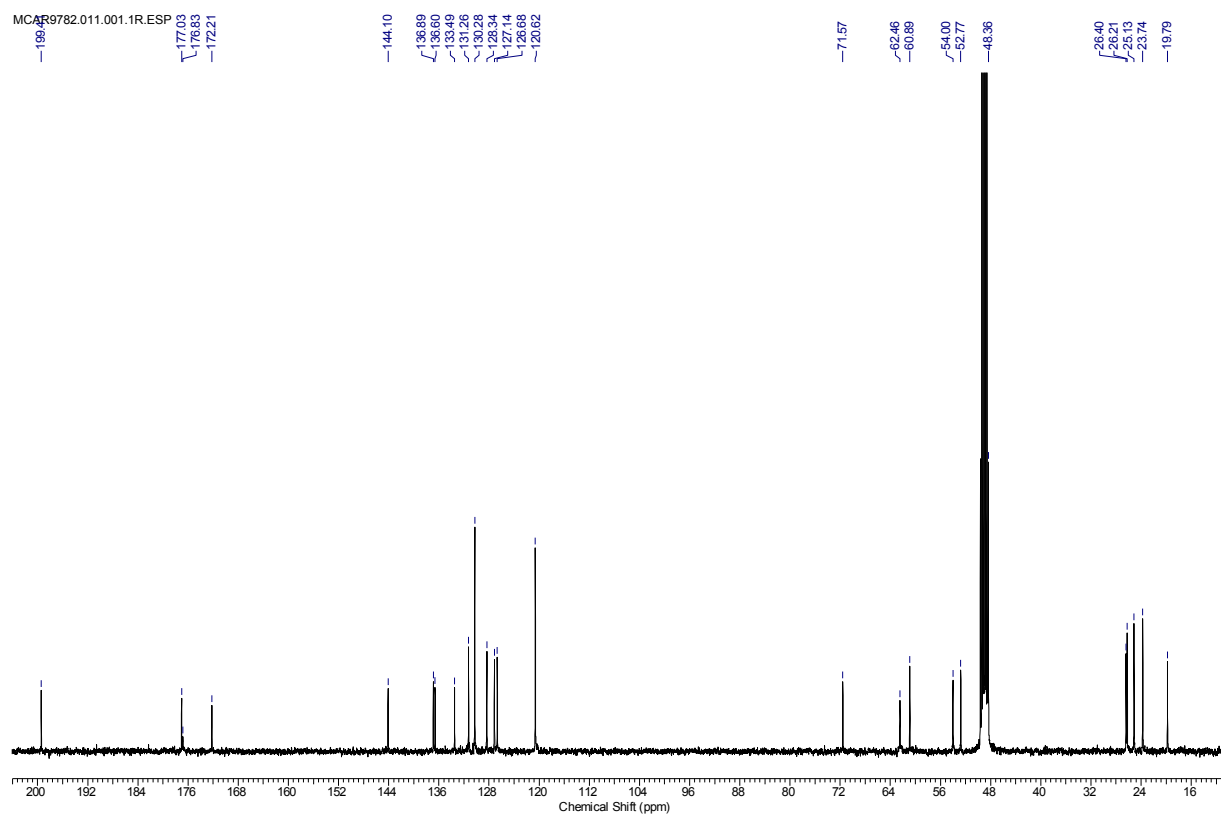
MCAZ9697.011.001.1R.ESP



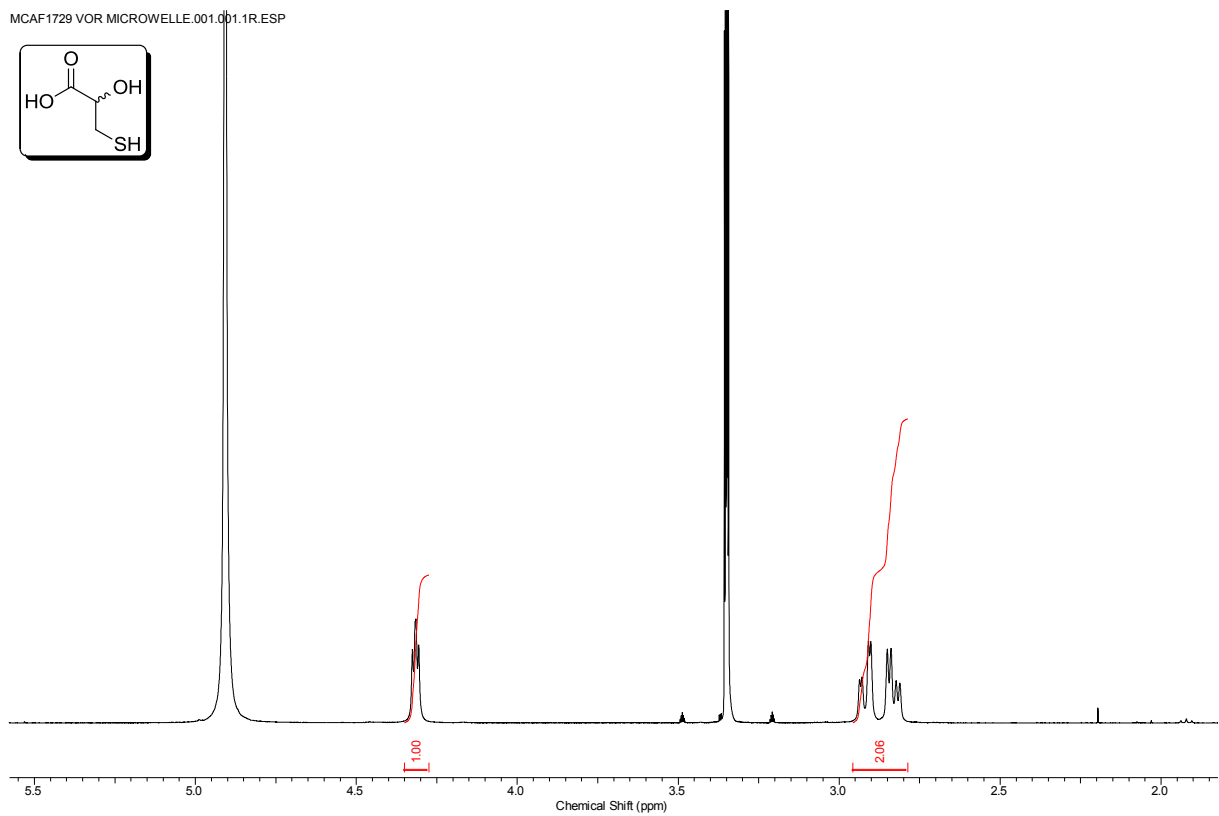
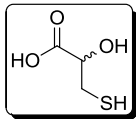
MCAR9782.010.001.1R.ESP



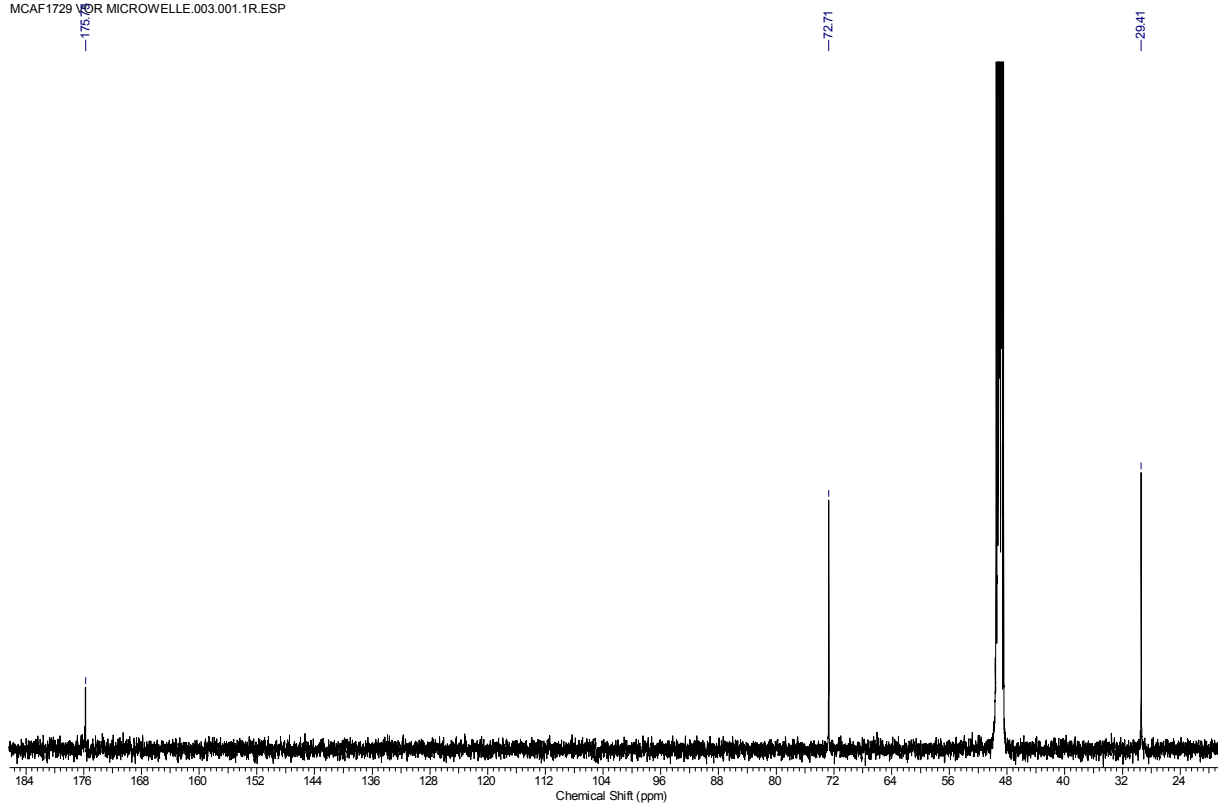
MCAR9782.011.001.1R.ESP



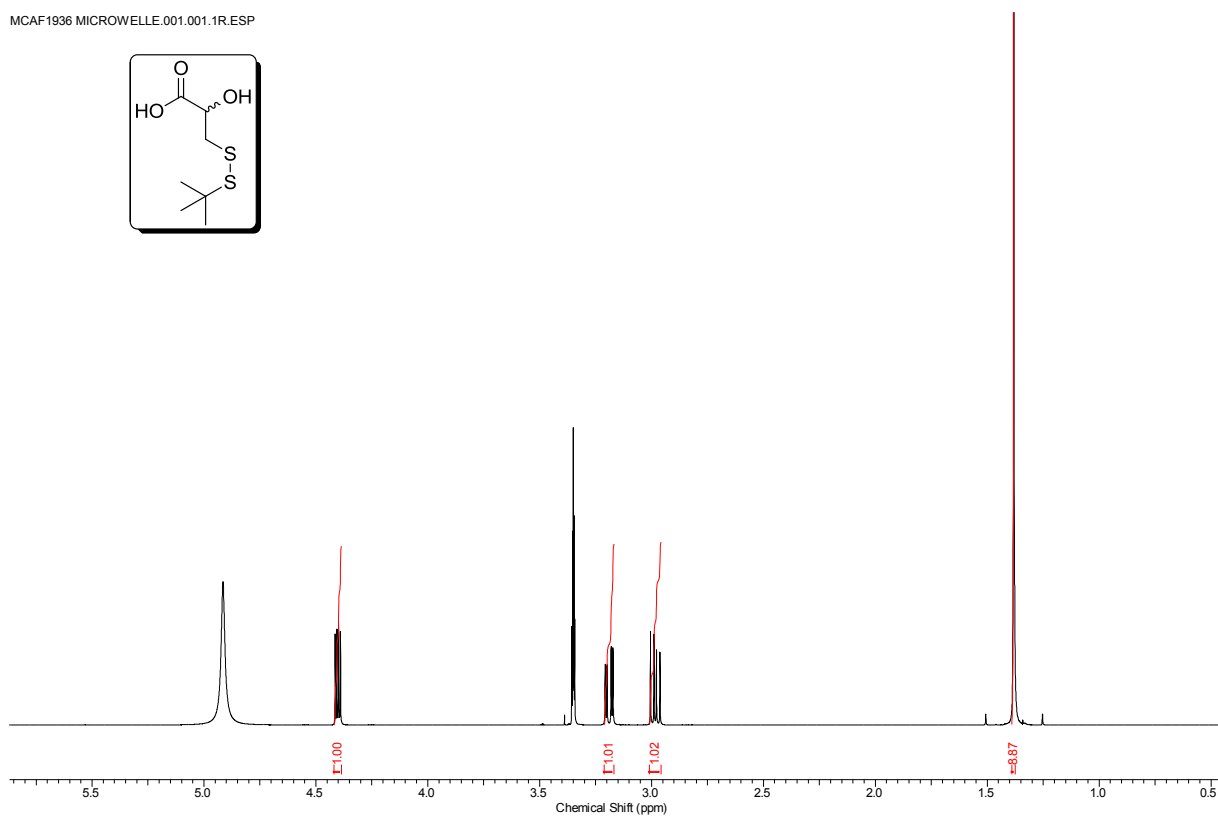
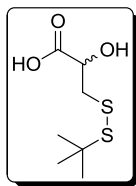
MCAF-1729 VOR MICROWELLE.001.001.1R.ESP



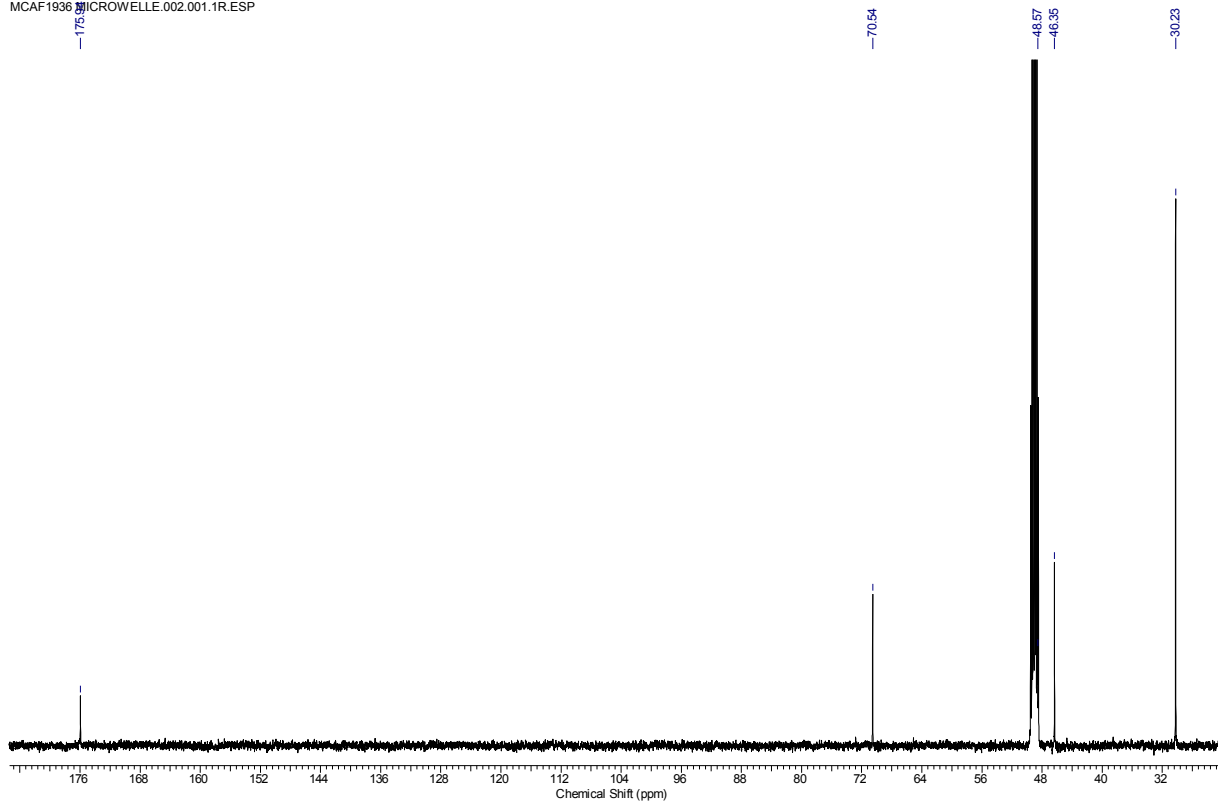
MCAF-1729 VOR MICROWELLE.003.001.1R.ESP



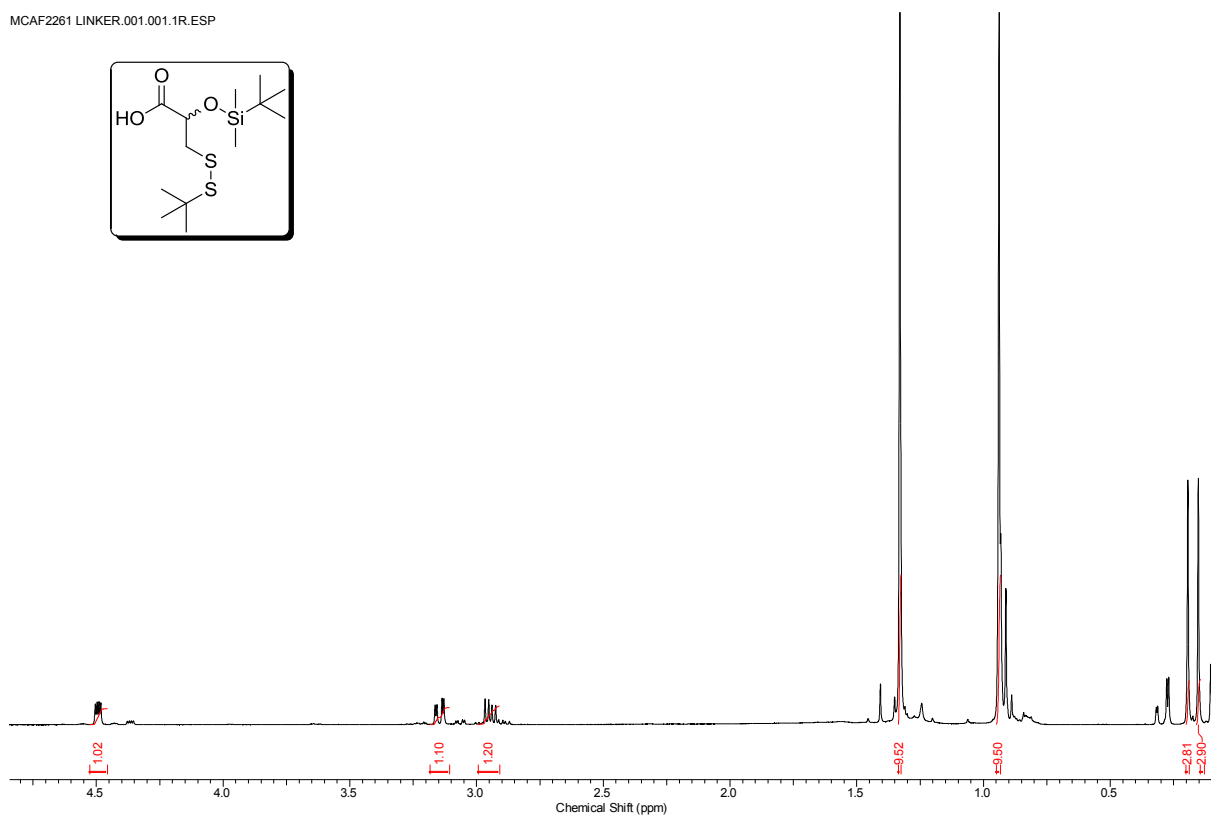
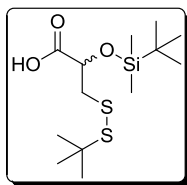
MCAF1936 MICROWELLE.001.001.1R.ESP



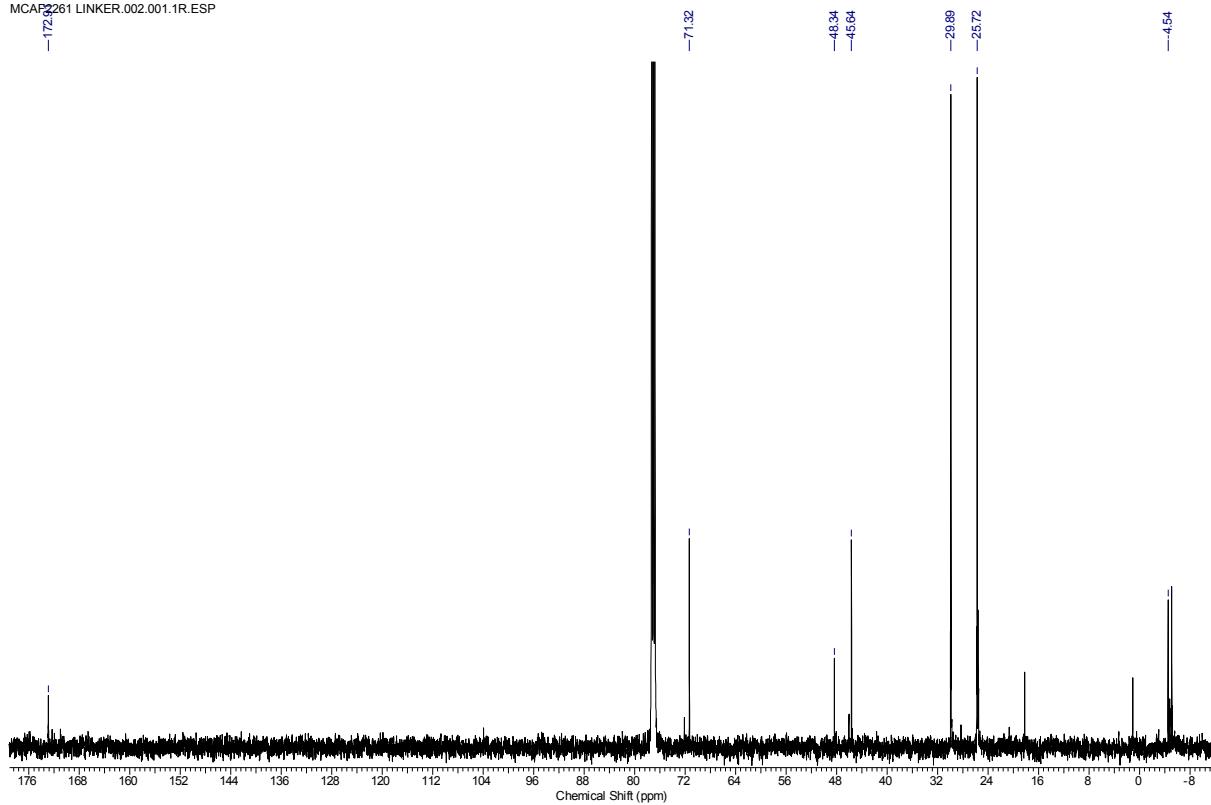
MCAF1936 MICROWELLE.002.001.1R.ESP



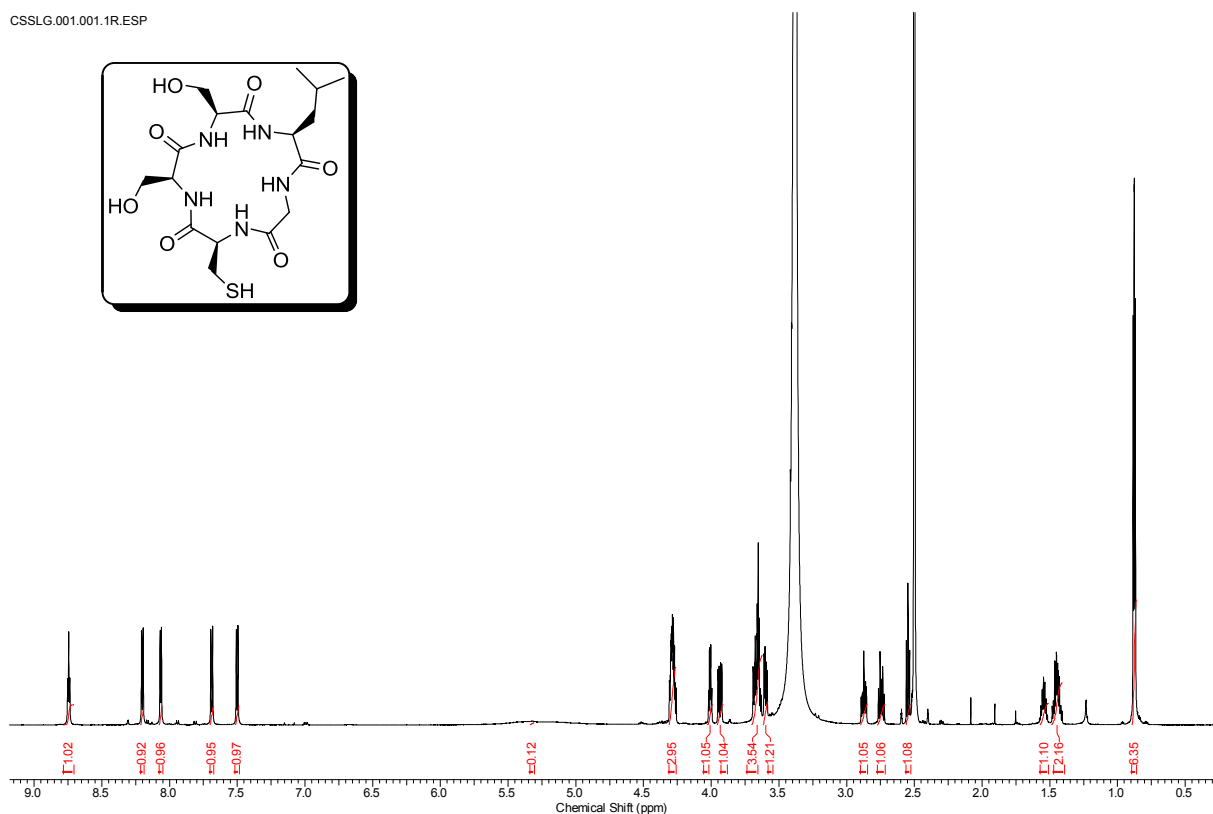
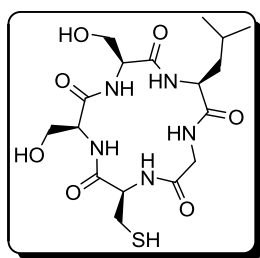
MCAF2261 LINKER.001.001.1R.ESP



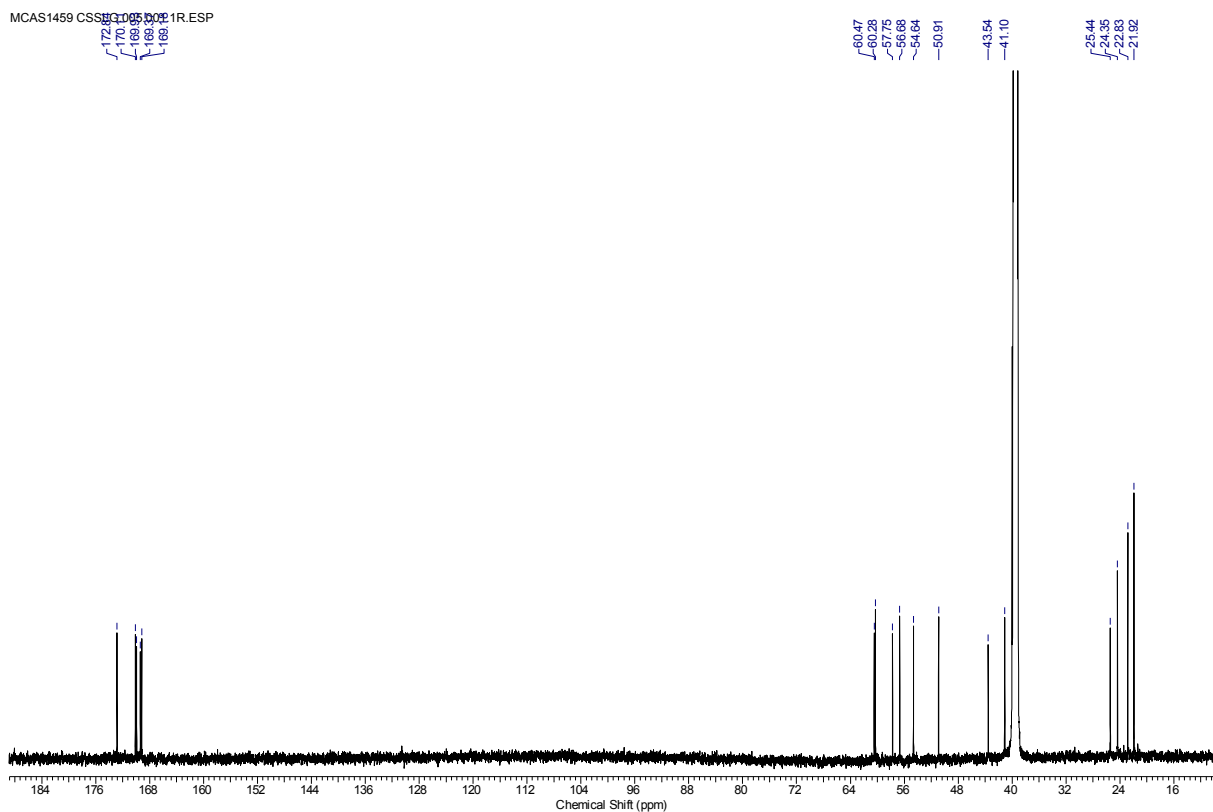
MCAF2261 LINKER.002.001.1R.ESP



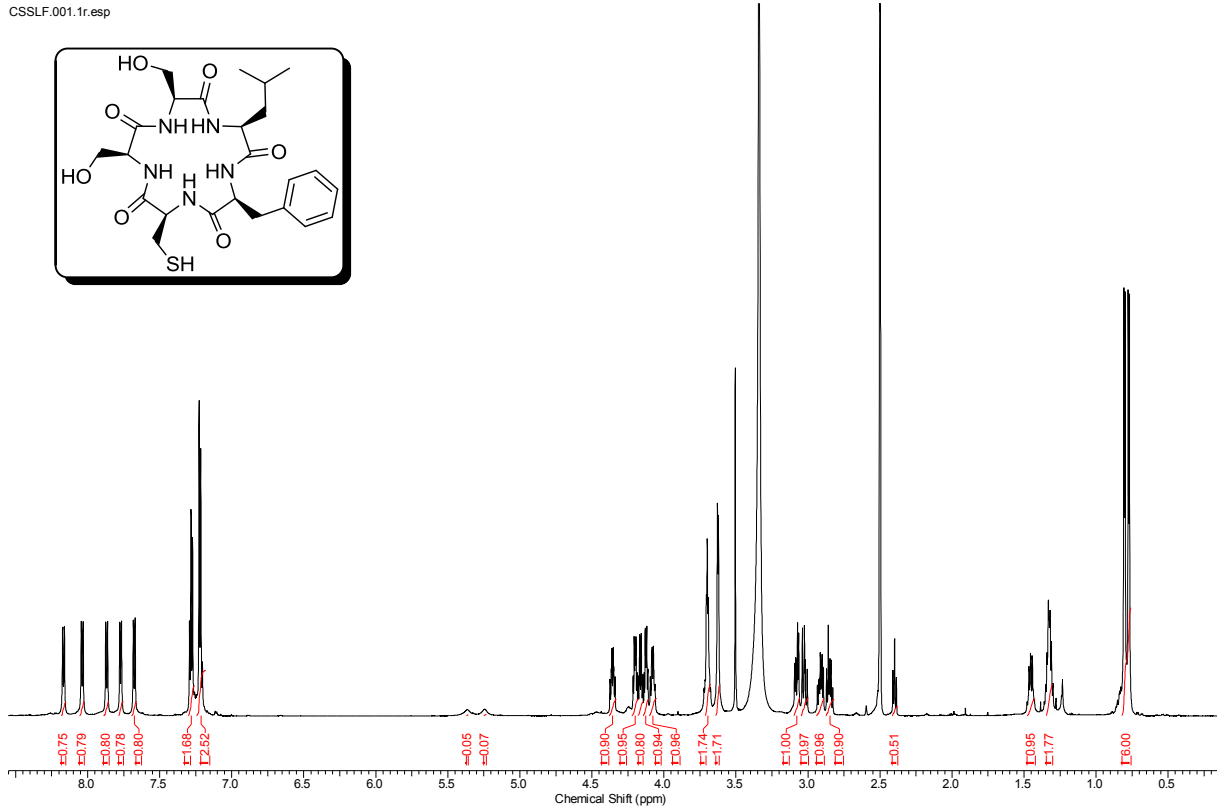
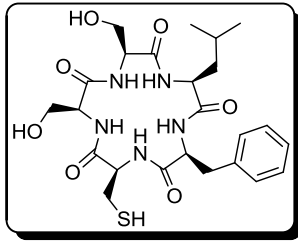
CSSLG.001.001.1R.ESP



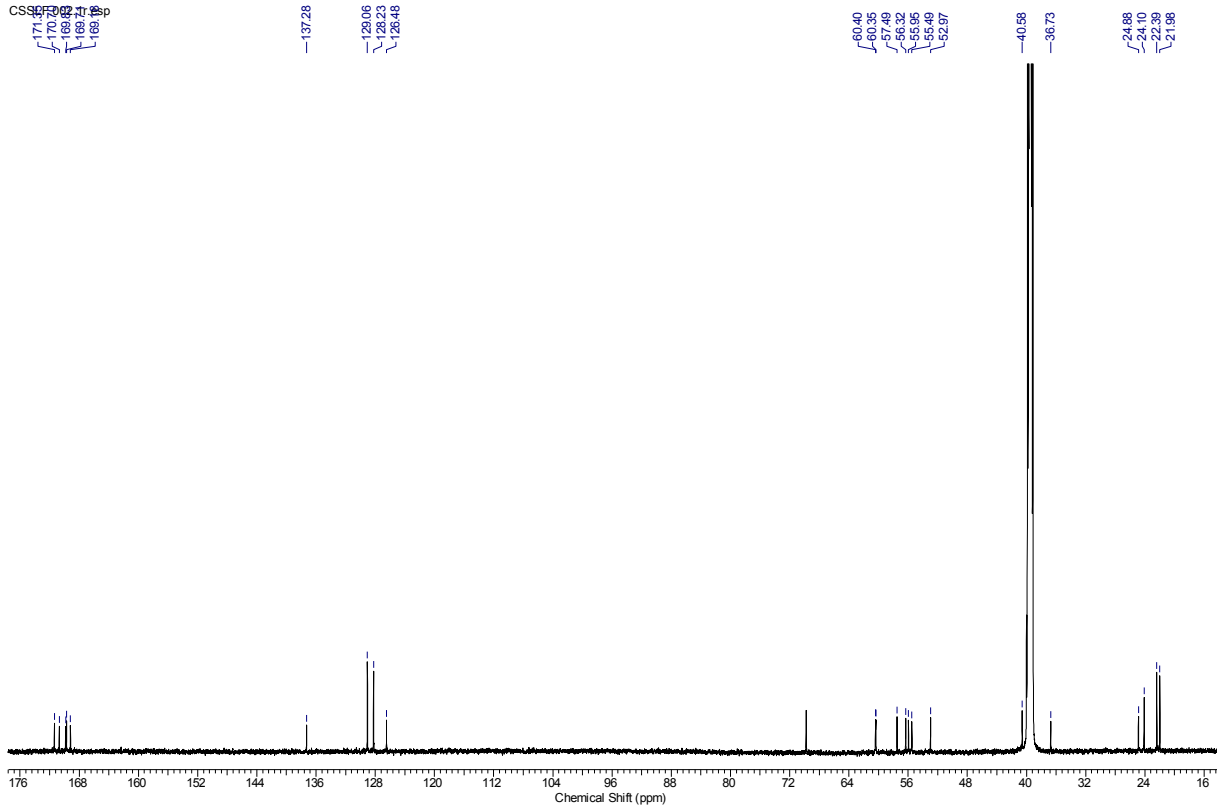
MCAS1459 CSSLG.001.001.1R.ESP



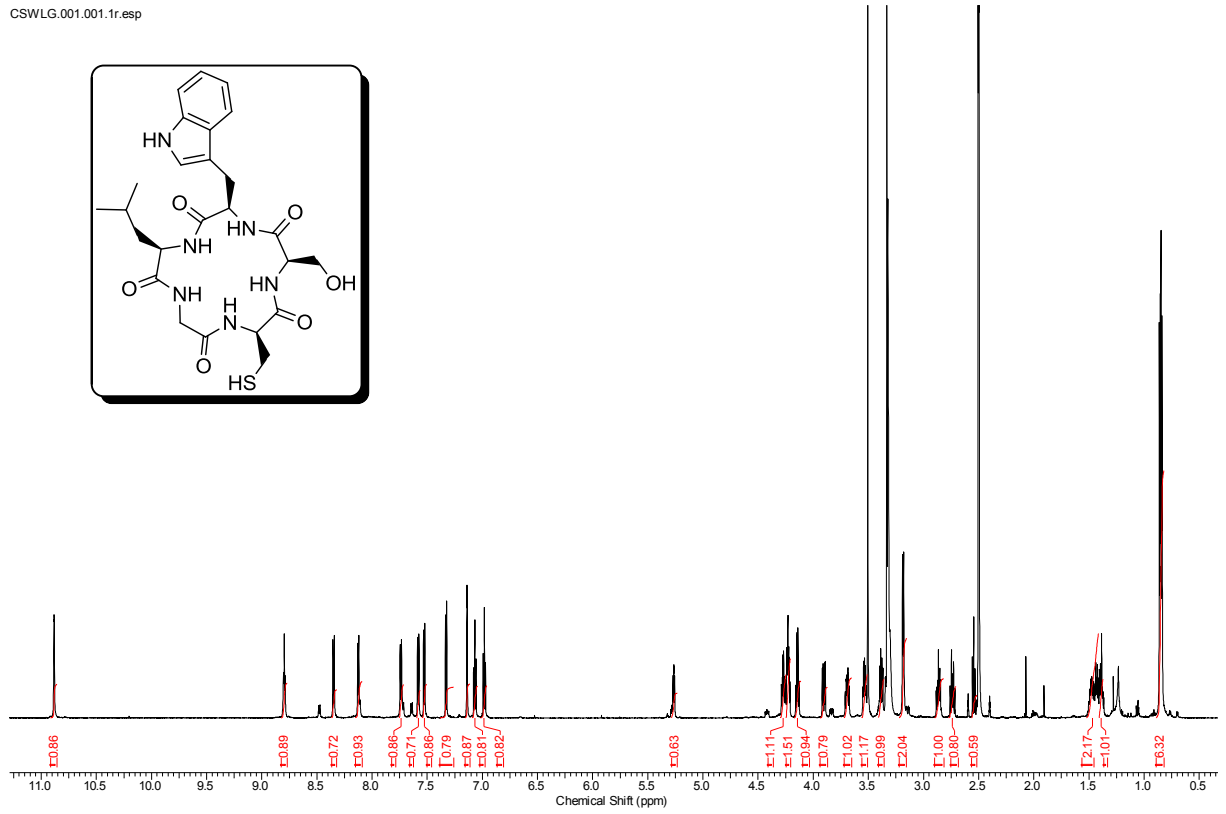
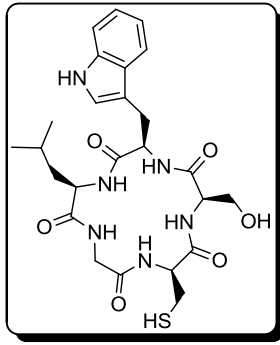
CSSLF.001.1r.esp



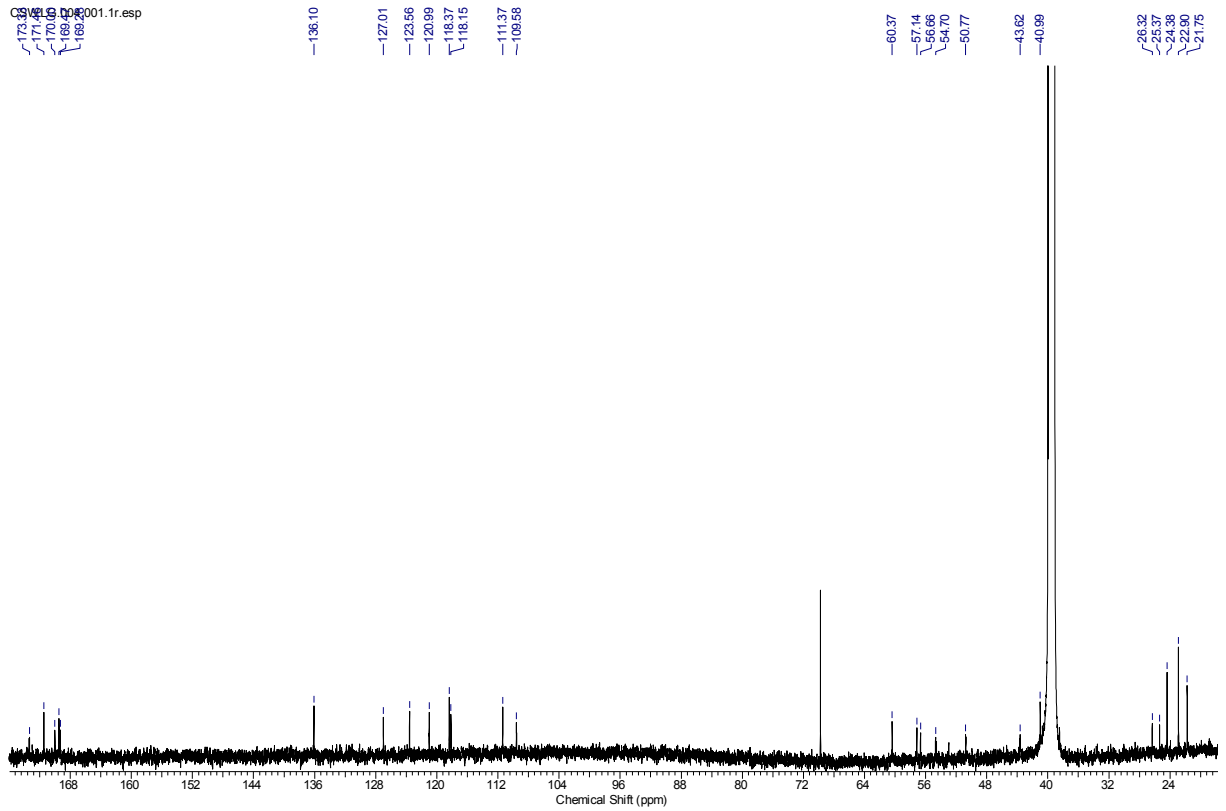
CSSLF.001.1r.esp



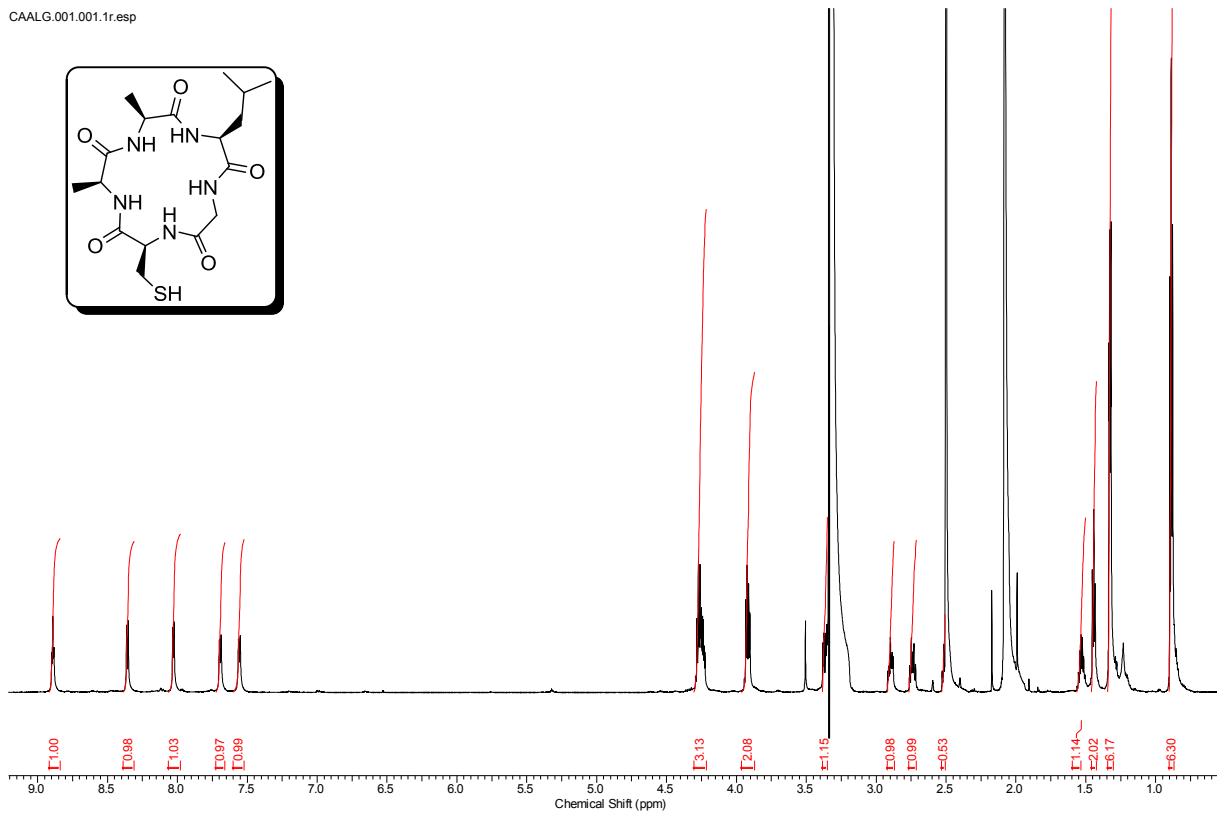
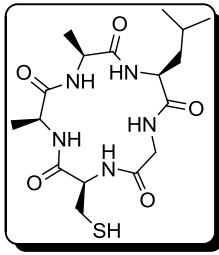
CSWLG.001.001.1r.esp



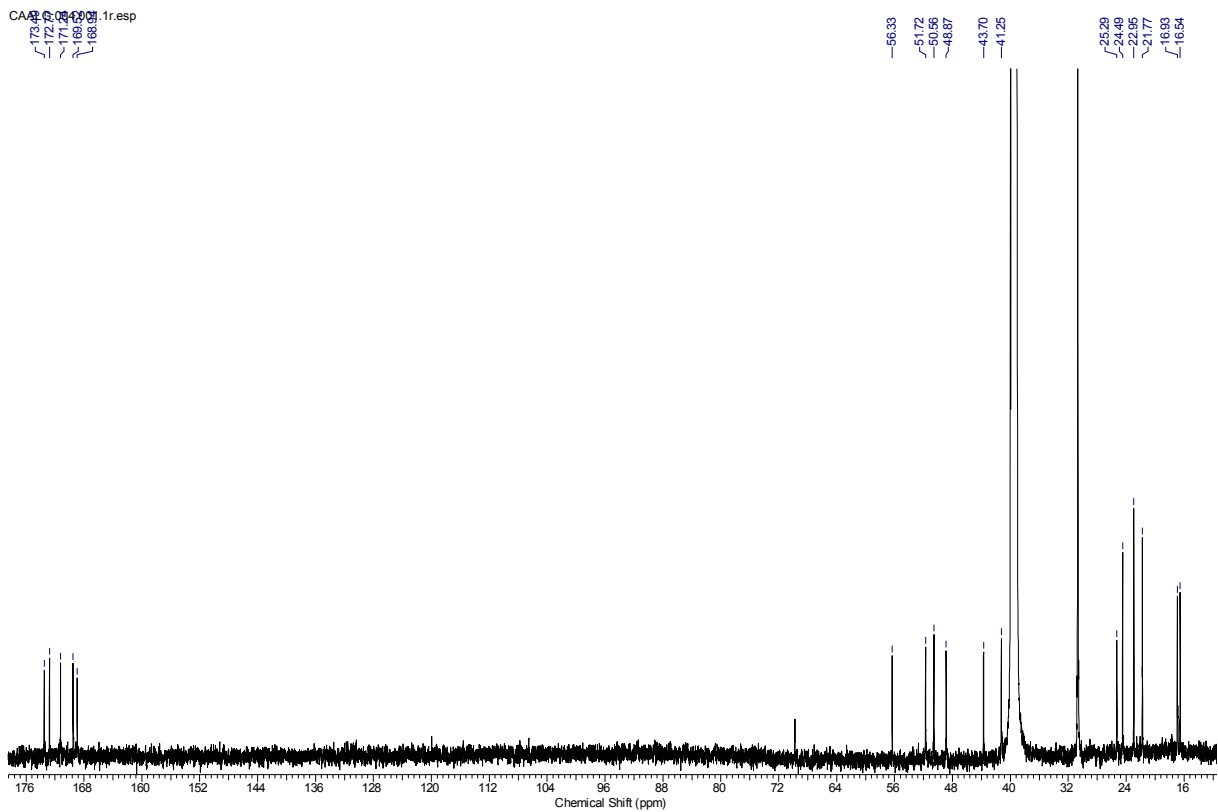
CSWLG.001.001.1r.esp



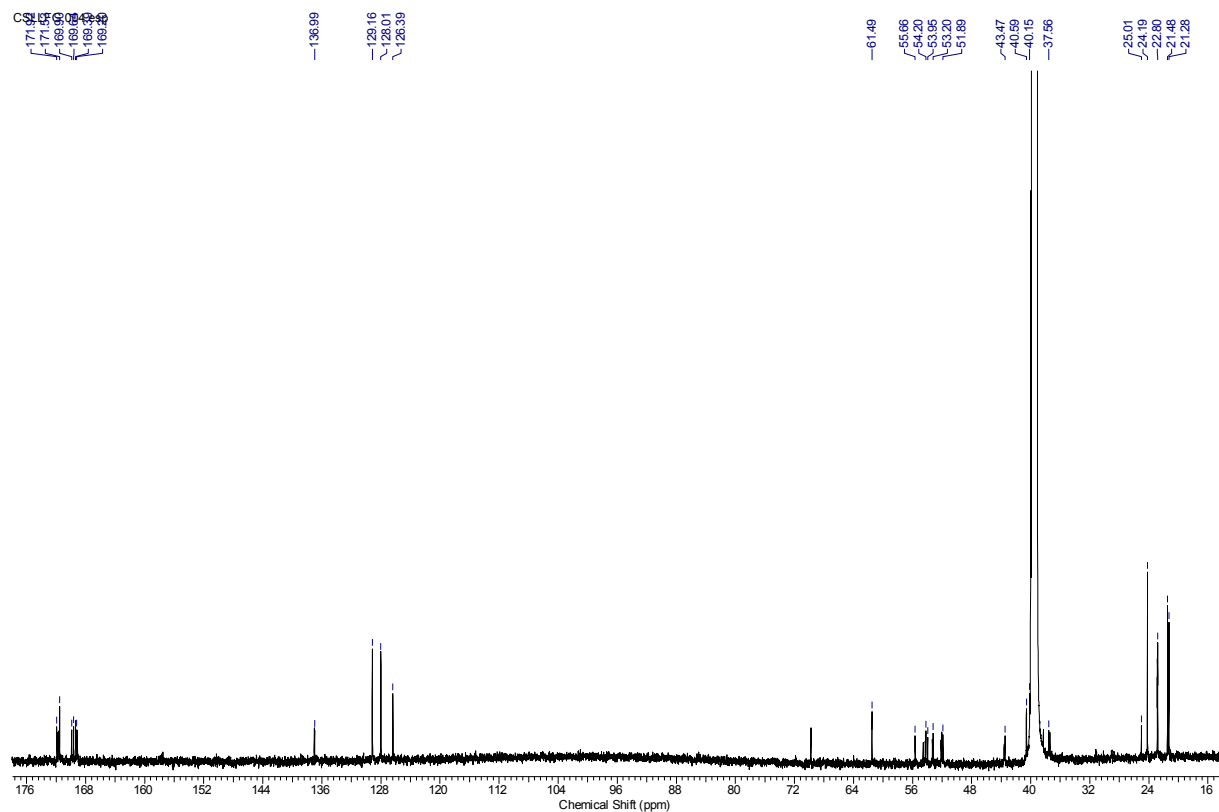
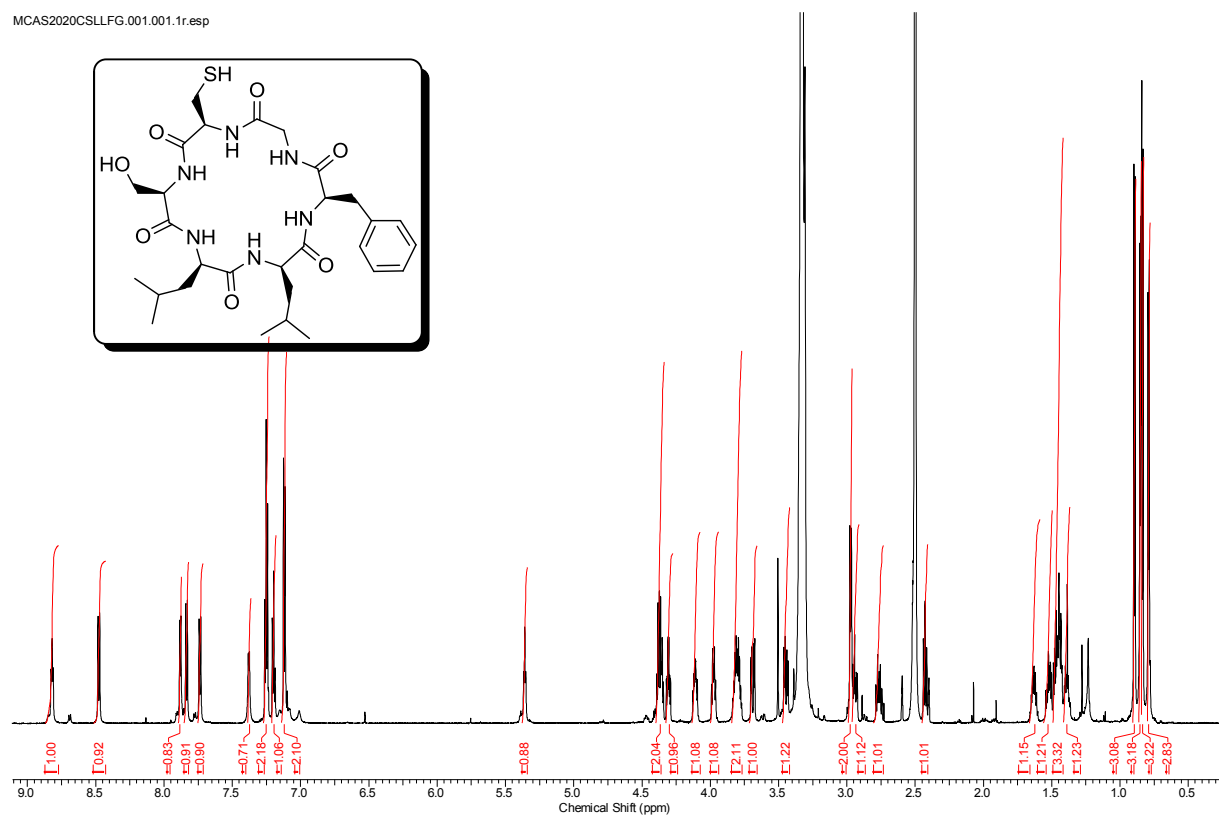
CAALG.001.001.1r.esp



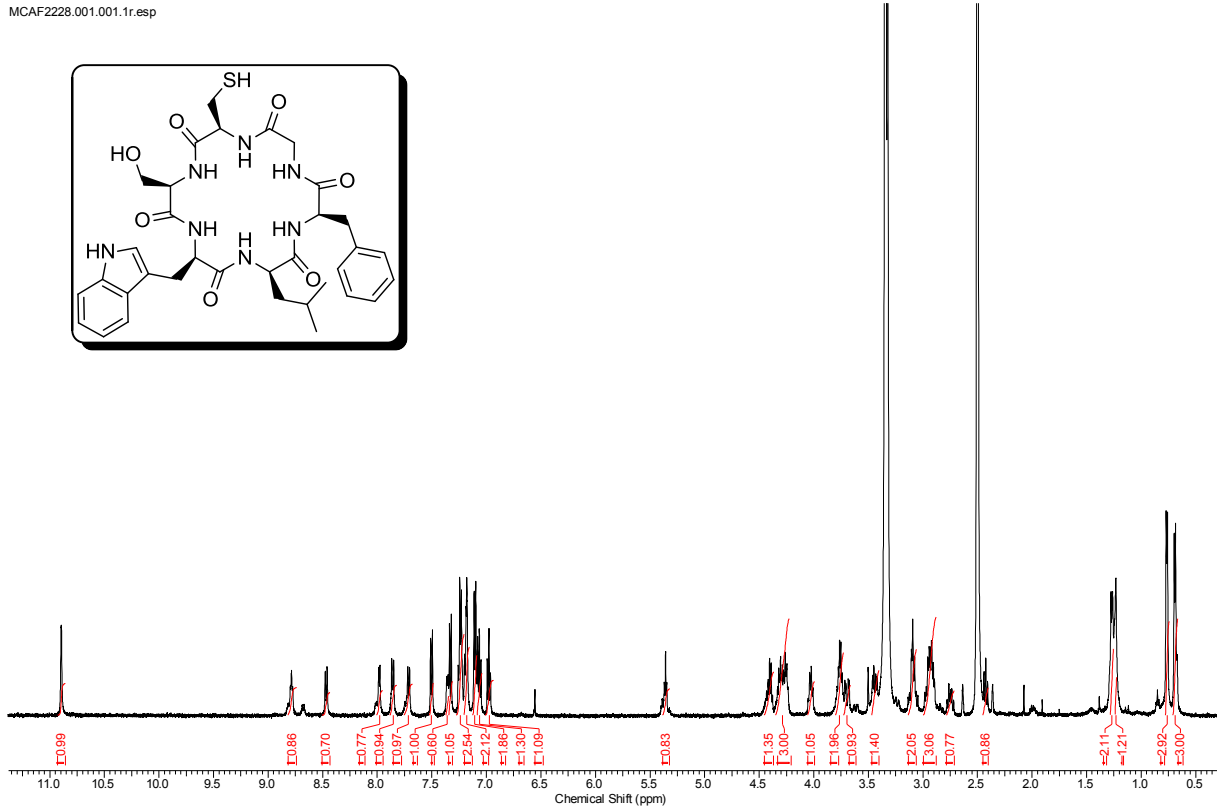
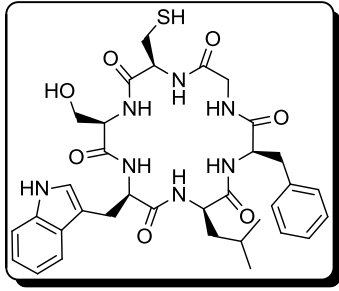
CAALG.001.001.1r.esp



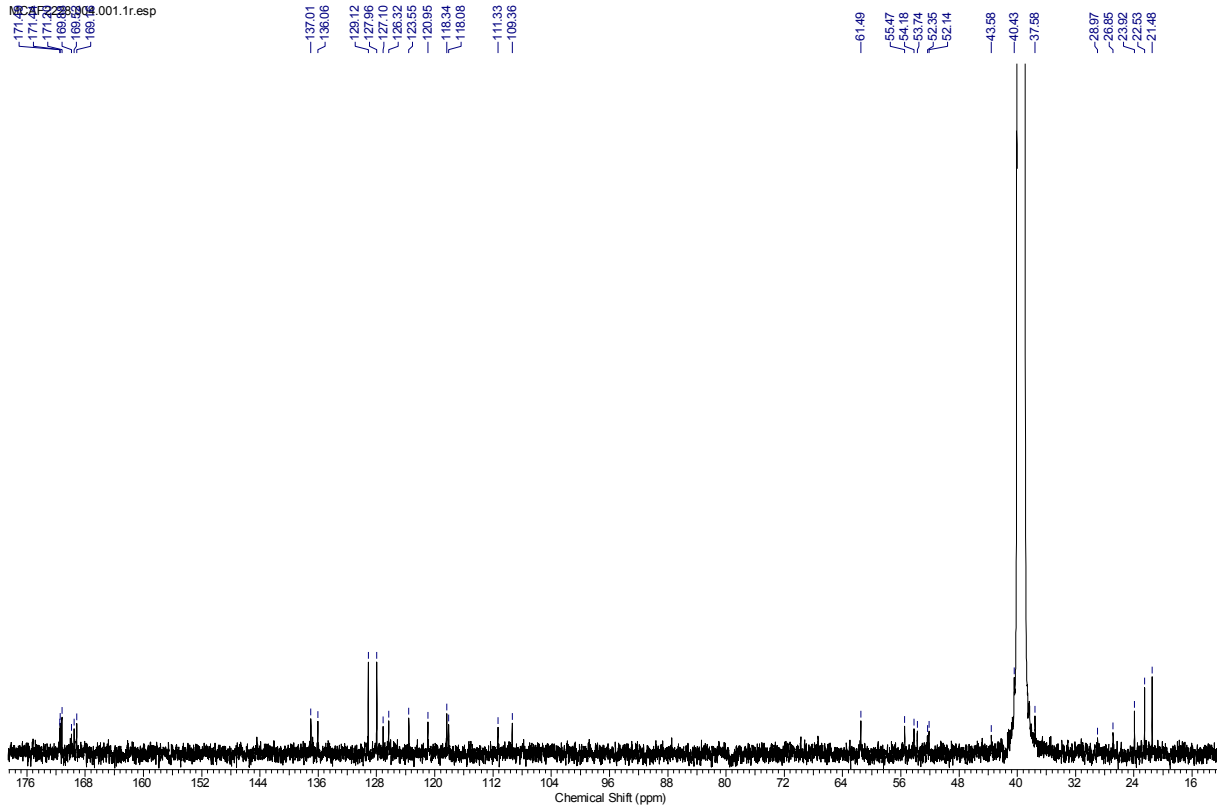
MCAS2020CSLLFG.001.001.1r.esp



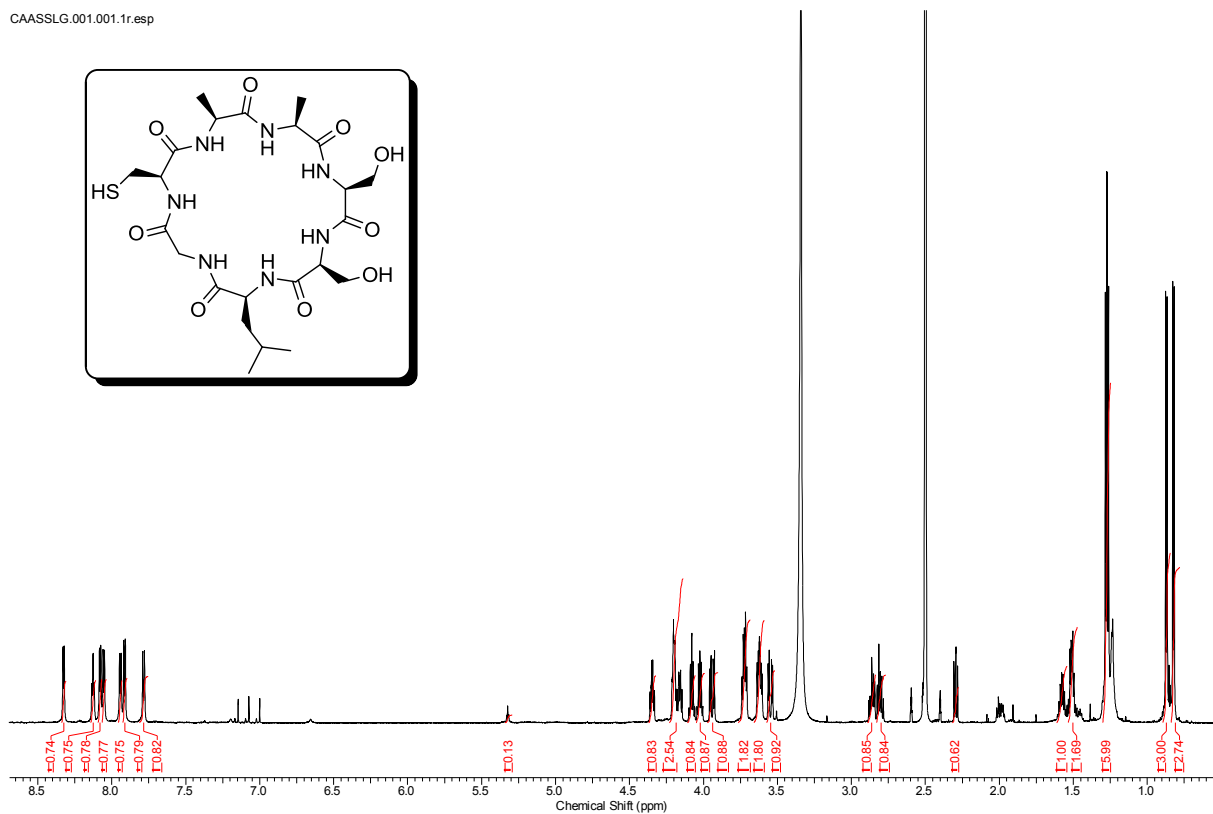
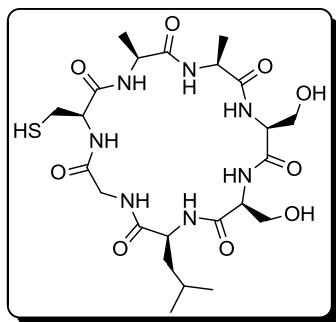
MCAF2228.001.001.1r.esp



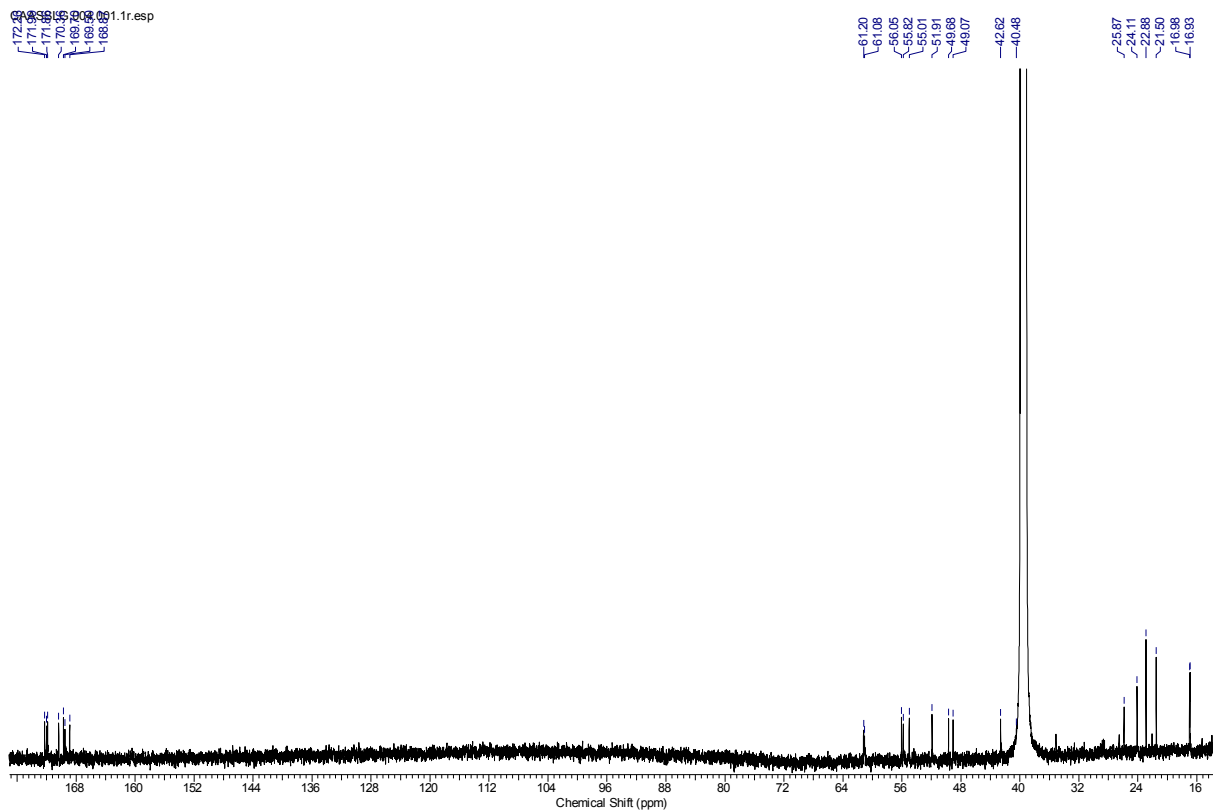
MCAF2228.001.001.1r.esp



CAASSLG.001.001.1r.esp



CAASSLG.001.001.1r.esp



Acknowledgments

First and foremost, I would like to express my deepest gratitude to my supervisor Prof. Dr Markus Kalesse for giving me the opportunity to work on these exciting projects. I appreciate his vast knowledge and skill in many areas and his assistance in writing this thesis. I would like to extend my gratitude to my own group medicinal chemistry of Helmholtz Centre for Infection Research (HZI) for their generous support and numerous help in matter of organic synthesis.

I also owe my gratitude to Prof. Dr. Andreas Kirschning for his willingness for being the co-supervisor and Prof. Dr. Carla Vogt for her willingness to complete the thesis committee.

I am also grateful to Dr. Werner Tegge, Dr. Raimo Franke, Brigitte Kornek from the department of the chemical biology (HZI) for their assistance in the solid phase peptide synthesis and countless valuable advices. .

My special thanks goes to two dear friends: Dr. Georg Bender and Dr. Nico Krauße for taking time out from their busy schedule to serve as my external readers.

Ulrike Beutling, Aliien Teichmann and Christel Kakoschke from the Helmholtz Centre for Infection Research are also appreciated for all NMR and mass spectrometry measurements.

Financial support from the University of Hanover and the international graduate school of the Helmholtz Centre for Infection Research is hereby gratefully acknowledged.

Last, but not least, I have to thank my parents for their love and support throughout my life. Thank you both to give me strength to chase my own dream.

Curriculum Vitae

Personal data

Name: Hao Luo
Gender: male
Date of birth: 06. 15. 1982
Place of birth: Chongqing, P.R.China
Nationality: Chinese

School education

09/1989 – 07/2001 Primary and high school in Chongqing, P.R.China.
07/2001 High-school diploma.

Academic education

09/2001 – 07/2002 Bachelor studies at the Beijing institute of petrochemical technology.
Subject: process equipment and control engineering (leaving without a certificate).
09/2004 – 02/2005 Pre-study education in Hanover, Germany (Das Niedersächsische Studienkolleg).
09/2005 – 09/2010 Chemistry studies at the Leibniz University of Hanover (LUH).
10/2010 – 03/2011 Diploma at the Helmholtz Centre for Infection Research (HZI) in the group of Prof. Dr. Markus Kalesse; Diploma thesis: „Synthesis of cyclic diadenosine 3´-5´ monophosphate“.
05/2011 – 10/2014 Ph.D. student in the group of Prof. Dr. Markus Kalesse, HZI. Ph.D thesis: „Development of synthetic strategies towards libraries of heterocyclic and bicyclic inhibitors of Cdc25A & Development of solid phase synthesis of cyclic peptides“.